

3270



Library

**LIBRARY
JAWAHARLAL NEHRU CENTRE
FOR ADVANCED SCIENTIFIC RESEARCH
JAKKUR POST
BANGALORE - 560 064**

JNCASR LIBRARY
3270



546.3 P03

1971-1972
1973-1974
1975-1976
1977-1978
1979-1980
1981-1982
1983-1984
1985-1986
1987-1988
1989-1990
1991-1992
1993-1994
1995-1996
1997-1998
1999-2000
2001-2002
2003-2004
2005-2006
2007-2008
2009-2010
2011-2012
2013-2014
2015-2016
2017-2018
2019-2020
2021-2022
2023-2024
2025-2026
2027-2028
2029-2030
2031-2032
2033-2034
2035-2036
2037-2038
2039-2040
2041-2042
2043-2044
2045-2046
2047-2048
2049-2050
2051-2052
2053-2054
2055-2056
2057-2058
2059-2060
2061-2062
2063-2064
2065-2066
2067-2068
2069-2070
2071-2072
2073-2074
2075-2076
2077-2078
2079-2080
2081-2082
2083-2084
2085-2086
2087-2088
2089-2090
2091-2092
2093-2094
2095-2096
2097-2098
2099-2100

546.3
P03 Thesis

LIBRARY
JAWAHARLAL NEHRU CENTRE
FOR ADVANCED SCIENTIFIC RESEARCH
JAKKUR POST
BANGALORE-560 064

Metal Carboxylates with Open Architectures

**A Thesis submitted in partial fulfillment
of the requirements of the degree of
Doctor of Philosophy**

**By
R. Vaidhyanathan**



**Chemistry and Physics of Materials Unit
Jawaharlal Nehru Centre for Advanced Scientific Research
(A Deemed University)
Bangalore - 560 064 (INDIA)
June 2003**

Dedicated to my parents

DECLARATION

I hereby declare that the matter embodied in this thesis entitled “Metal Carboxylates with Open Architectures” is the result of investigations carried out by me in the Chemistry and Physics of Materials Unit, Jawaharlal Nehru Centre for Advanced Scientific Research, Jakkur, Bangalore, India, under the Supervision of Professor C. N. R. Rao and Prof. S. Natarajan.

In keeping with the general practice of reporting scientific observations, due acknowledgements has been made whenever the work described has been based on the findings of the other investigators. Any omission which might have occurred by oversight or error of misjudgment is regretted.



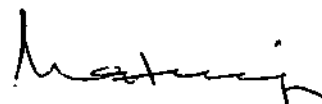
R. Vaidhyathan

CERTIFICATE

Certified that the work described in the thesis entitled “Metal Carboxylates With Open Architectures” is the result of investigations carried out by Mr. R. Vaidhyanathan in the Chemistry and Physics of Materials Unit, Jawaharlal Nehru Centre for Advanced Scientific Research, Jakkur, Bangalore 560 064 under our supervision.



Prof. C. N. R. Rao



Prof. S. Natarajan

ACKNOWLEDGEMENTS

I wish to express my sincere gratitude to Prof. C. N. R. Rao, FRS for suggesting the problems, invaluable guidance and encouragement throughout my research and also for the enormous moral support and confidence he has provided. He has showered fatherly affection on me and has transformed me from an excited boy to a more composed scientist. His passion and commitment to everything he does has been a real source of inspiration to me and has developed a desire in me to strive hard to be the best in everything that I do. He has imparted knowledge on various aspects of chemistry through the small, thought-provoking comments and hints, and has taught me how to analyze and organize the results. With the various skills that I have gained under his guidance and the training I have undergone, I am sure of making a successful research career.

I would like to acknowledge my thanks and regards to Prof. S. Natarajan who has guided me on my research work. He has taught and trained me in crystallography and has been of enormous help and support in tackling the various problems I faced during my work. He has appreciated and welcomed me whenever I approached him with my ideas and findings. In addition to the knowledge of inorganic chemistry, he has given me valuable advises and tips which have been so useful in shaping me as a disciplined and focussed man, thereby has helped to a great deal in various aspects of my research career.

I am thankful to all the faculty members of JNCASR and IISc who have imparted all the knowledge in me and exposed me to various new aspects of science by way of courses. In particular I would like to thank Profs. S. Chandrasekharan, Madyashtha, J. Chandrasekhar, D. D. Sarma, B. R. Jagirdar, K. L. Sebastian, S. Ramasesha, S. Vasudevan, K. J. Rao, J. Gopalakrishnan, T. N. Guru Row, G. U. Kulkarni, A. R. Raju, K. S. Narayanan, Drs. Shobhana Narasimhan, Chandrabhas, S. Sastry, Umesh Waghmare, S. Balasubramaniam, Swapan Pati and V. R. Peddi reddy.

I thank all my labmates and collaborators, Dr. Neeraj, Dr. A. Choudhury, Sandip Chakraborty, S. Mandal, Thiru Murugan, Ganeshan and Jayaraman. I am deeply indebted to them for the various help and support that they have offered me.

Apart from the lab mates I would like to thank all my friends of JNC who have made my life in the campus and in the hostel so wonderful, especially Rajesh, Krishnan, Ram Shankar, Gargi Raina, Meenakshi, Anupama, Kavitha, KSiva, John, Sachin, Pattu, Jaya, Dr. Murugavel, Sudhee, Dr. Govindraj, Gautam, Leo, Vinod, Manoj, Biru, Dr. Vijay Sharma, Manashi and all my IISc friends.

I would like to acknowledge the sincere efforts by all the staff of JNCASR, especially Srinivas, Srinath, Anil and Vasu, who have been so helpful and understanding in various experimental activities and Mr. Ram Prasad from IISc. I thank all the members of the computer lab who have

been enormously helpful and understanding to me throughout. I thank the library staff for all the help they have offered.

I thank the office staff of JNCASR and CSIR-COE. They have been so nice and helpful to me and have been very understanding whenever I approached them. I am obliged to Jawaharlal Nehru Center for the financial assistance to carry out this venture.

Finally, I would like to thank my parents who have showered so much love and affection on me and their prayers and blessings has given me all the success and happiness that I carry with me. I dedicate my thesis to my parents who mean everything to me.

CONTENTS

DECLARATION	i
CERTIFICATE	iii
ACKNOWLEDGEMENTS	v
PREFACE	ix
SUMMARY	xi
1. OVERVIEW OF MICROPOROUS OPEN-FRAMEWORK STRUCTURES	
1.1. Inorganic open-framework materials.....	1
1.1.1. Zeolites.....	1
1.1.2. Zeolite framework structures.....	2
1.1.3. Isomorphous substitution in zeolites.....	3
1.1.4. Extra-large pore framework solids.....	8
1.1.5. Synthesis of inorganic framework structures.....	8
1.1.6. Amine-phosphate as intermediates in the formation of open- framework zinc phosphates.....	10
1.1.7. Application of inorganic microporous framework materials.....	10
1.2. Inorganic open-frameworks with organic ligands.....	13
1.2.1. Monocarboxylates.....	13
1.2.2. Oxalates.....	17
1.2.3. Higher dicarboxylates.....	30
1.2.4. Hybrid compounds.....	40
1.2.5. Carboxylates with additional binding sites.....	48
1.2.6. Future prospects.....	50
References.....	52
2. SCOPE OF THE PRESENT INVESTIGATIONS	
2.1. Organic amine oxalates.....	68
2.2. Metal oxalates.....	69

2.3.	Open-framework metal dicarboxylates, $M(O_2C(CH_2)_nCO_2)$ ($M = Cd, Mn, Nd; n = 1, 2, 3, 4$).....	71
2.4.	Hybrid Organic-inorganic structures –Cadmium oxalate host frameworks incorporating alkali halides.....	72
	References.....	73
3.	EXPERIMENTAL	
3.1.	Hydro/solvothermal synthesis.....	77
3.2.	Synthesis.....	81
3.2.1.	Synthesis of zinc oxalates.....	81
3.2.2.	Synthesis and characterization of amine oxalates.....	81
3.2.3.	Reaction of amine oxalates with Zn^{II} ions.....	82
3.2.4.	Synthesis of cadmium oxalates.....	83
3.2.5.	Synthesis of rare-earth metal oxalates.....	84
3.2.6.	Synthesis of tin(II) oxalate.....	85
3.2.7.	Syntheses of cadmium malonate and manganese glutarate.....	87
3.2.8.	Synthesis of cadmium succinates.....	87
3.2.9.	Synthesis of manganese adipate.....	88
3.2.10.	Alkali halide structures incorporated in cadmium oxalate host lattices.....	90
3.3.	Characterization.....	91
	References.....	119
4.	RESULTS AND DISCUSSION	
4.1.	Hydrogen bonded structures in amine oxalates.....	120
4.2.	Open-framework zinc oxalates.....	133
4.3.	Reactions of Amine Oxalate with Zn^{II} ions.....	151
4.4.	Open-framework cadmium oxalates.....	161
4.5.	Three-dimensional rare-earth oxalates.....	182
4.6.	Open-framework tin(II) oxalate.....	204
4.7.	Cadmium malonate and Manganese glutarate.....	211
4.8.	Open-framework cadmium succinates of different dimensionalities...	220
4.9.	Cadmium succinates with XCd_4O_{24} ($X = Cl, Br$) tetrahedral clusters...	243

4.10. Manganese adipate.....	252
4.11. Hybrid Structures - Alkali halides incorporated in metal oxalate frameworks.....	255
4.11.1. Three-dimensional alkali halide lattices stabilized in host cadmium oxalate frameworks.....	255
4.11.2. Cadmium oxalate hosts incorporating layered alkali halide lattices...	260
4.11.3. Oxalate hosts incorporating one-dimensional alkali halide structures..	269
References.....	285

PREFACE

Metal organic compounds with framework structures capable of mimicking zeolitic structures and exhibiting interesting properties has been a topic of intense research in the recent years. This thesis deals with the results of investigations of open-framework metal carboxylates in the presence of structure-directing agents such as organic amines, under hydro/solvothermal conditions.

Several new open-framework metal carboxylates have been synthesized under hydrothermal conditions in the presence of structure directing or templating organic amines and characterized. The carboxylic acids employed include oxalic and other higher aliphatic dicarboxylic acids. The metal oxalate structures exhibit different dimensionalities ranging from zero- to three-dimensions. The zero-dimensional structures are mono- and dinuclear species, while the one-dimensional ones are chain structures, two-dimensional ones are generally honeycomb like structures and the three-dimensional structures have honeycomb-like layers cross-linked by an *out-of-plane* oxalate into three-dimensional structures with channels. The three-dimensional metal oxalates exhibit adsorption properties and the channels are functionalized by organic functional groups in some of them. An important contribution is the identification of amine-oxalates as possible intermediates in the formation of open-framework zinc oxalates. Reactions of amine-oxalates with Zn^{2+} ions under hydrothermal conditions yielded zinc oxalate structures of varying dimensionality, with a hierarchical structural relationship among them. The three-dimensional cadmium oxalates comprise of channels occupied by alkali cations, and show feeble ionic conductivity.

The compounds formed employing the higher dicarboxylic acids exhibit interesting structural features: a three-dimensional cadmium malonate formed

entirely from corner-sharing of cadmium polyhedra and possess hydrophobic channels, the cadmium succinates exhibit some well-known interpenetrated structures. Three-dimensional manganese glutarate and adipate, and neodymium succinate have also been made. We have rationalized the connectivities present in these structures and their possible mode of formation and represented them with suitable schematic illustrations.

In our pursuit to form hybrid inorganic-organic structures, we have synthesized and characterized novel cadmium oxalate host structures incorporating alkali halide structures of different dimensionalities. The three-dimensional cadmium oxalate framework contains three-dimensional alkali halide structures with rock salt like topology but with expanded lattice parameters. The two-dimensional framework incorporates graphite like alkali halide layers and the one-dimensional alkali halides have helical topology. These inorganic-organic hybrid compounds can be considered as nanocomposites with the presence of regularly alternating inorganic and organic units within the structure.

METAL CARBOXYLATES WITH OPEN ARCHITECTURES

SUMMARY

The area of inorganic open-framework materials has become one of intense research activity in the past several years. While one of the objectives of research in open-framework solids is to find materials possessing channels and other features which make them porous, thereby imparting potential catalytic and sorption properties, the discovery of fascinating architectures of different dimensionalities has been equally exciting. In an attempt to design materials exhibiting features otherwise unknown in traditional zeolites and related inorganic structures, there has been much interest in designing hybrid materials containing inorganic and organic linkers. This has resulted in the design of novel structures involving both organic and inorganic components by employing novel synthetic tools as well as supramolecular chemistry. In the design of hybrid structures, one takes advantage of metal-coordination as well as the functionalities of the organic components, the flexibility of the organic linkers rendering such open architectures attractive. Metal carboxylates are particularly interesting as even simple metal carboxylates such as formates and acetates are known to crystallize in unusual polymeric structures under different conditions, the carboxylate moieties exhibiting different binding modes in these compounds. However, systematic studies involving variation in the nature of the reactants or the synthetic conditions and carrying out reactions in the presence of additives such as organic amines, under hydro/solvothermal conditions, are scarce. In order to investigate these possibilities, a systematic study of open-framework metal carboxylates has been carried out.

In our pursuit to form new open-framework metal carboxylates in the presence/absence of structure directing or templating agents under hydro/solvothermal conditions, we have formed a variety of metal carboxylate compounds. In this study, different metals and carboxylic acids, including oxalic and other higher aliphatic dicarboxylic acids have been employed. Thus, new open-framework zinc oxalates have been prepared by hydrothermal methods in the presence of structure-directing organic amines. In the linkages between the Zn and oxalate units gives rise to layered as well as three-dimensional structures. Whilst the layered materials are characterized by 12-membered (6 Zn and 6 oxalates) honeycomb-like apertures wherein the extra-framework guest species are located, the three-dimensional Zn-oxalate has layers cross-linked by another oxalate unit distinct channels where the amine and water molecules reside. The largest aperture in the 3D Zn oxalate contains a 20-membered ring (10 Zn and 10 oxalates). One of the 2D zinc oxalates has pseudo one-dimensional tunnels as in zeolitic structures. The 3D Zn oxalate exhibit interesting reversible dehydration/hydration properties.

Oxalates of n-propylamine, n-butylamine, ethylenediamine, 1,4-butanediamine, piperazine, guanidine and 1,4-diazabicyclo[2,2,2]octane (DABCO) have been synthesized and characterized. Hydrogen bonded structures of these oxalates have been investigated and their thermal stability has been related to the strengths of the networks. A systematic study was carried out in order to explore the possible role of these amine oxalates as a precursor in the formation of open-framework zinc oxalates. Thus the reaction of the amine oxalates with Zn^{II} ions gave rise to hierarchy of novel zinc oxalates including monomers and dimers. The Zn oxalates obtained by us are composed of a network of ZnO_6 octahedra and oxalate units, and possess zero-, one-, two- and three-dimensional structures. The monomer, dimer, and chain zinc oxalates are the first members of the hierarchy of structures.

Two and three-dimensional zinc oxalates have also been isolated. Relationships amongst these various oxalate structures are noteworthy and give indications as to the manner in which these structures are formed. Thus, the three-dimensional structure can be formed by the linking of layers, and the layer structure by the condensation of linear chains.

Cadmium oxalates, $M_4Cd_2(C_2O_4)_4 \cdot 4H_2O$, $M = Na(I)$ and $K(II)$ with open architectures have been synthesized hydrothermally. The Cd atoms have the unusual eight-coordination with respect to the oxalate oxygens. The connectivity between the Cd and oxalate units forms layers with 12-membered apertures (six Cd and six oxalate units), with the layers interpenetrating to give rise to three-dimensional structures possessing 8-membered channels (four Cd and four oxalate units) wherein the Na^+ and K^+ ions are nestled. The Na^+ ion conductivity in the sodium compound is rather low, but the activation energy for conduction is comparable to those in glasses. The metathetic reaction between $CdCl_2 \cdot 2H_2O$ and sodium oxalate in n-hexanol solvent under solvothermal conditions, yields a hybrid compound of the formula $Cd_2(C_2O_4)_{0.5}Cl_3NaCl \cdot 4H_2O$. It consists of one-dimensional chains formed by Cd and Cl atoms, containing $\mu_2(Cl)$ and $\mu_3(Cl)$ bridges, and cross-linked by oxalate units to give a layered structure. The Na^+ ions and water molecules occupy the interlamellar spaces. The structure of this layered cadmium oxalate has been compared with some of the known metal carboxylates and a rational understanding has been developed explaining the formation of these compounds.

As a part of our investigations on the ability of rare-earth metal ions to form open-framework structures we have made new open-framework yttrium and neodymium oxalates, for the first time, employing hydrothermal methods in the presence of organic amines. The metal atom is 8- or 9-coordinated with square anti-prism or D_{3h} triply-capped trigonal prism geometry. The three-dimensional

framework structures of these rare-earth oxalates are built up by in-plane linkages between the metal atom and the oxalate moieties forming layers with 12-membered honeycomb-like apertures, pillared by another oxalate in an out-of-plane manner. Adsorption studies indicate that water and methanol can be reversibly adsorbed in one of the yttrium oxalates. The use of formic and acetic acids along with the organic amines, namely the 1,2-diaminopropane (1,2-DAP) and 1,3-diaminopropane (1,3-DAP), has given rise to some interesting features. In one of the yttrium oxalates, the reaction between the acetic acid and the 1,3-DAP has resulted in the in situ generation of new organic amine in the reaction medium. Similarly, in one of the neodymium oxalates also the reaction between the 1,2-DAP and the acetic acid has in situ generated the amide species, namely N-(2-aminopropyl acetimide). Another noteworthy feature is the presence of dangling formate group in addition to the disordered amine molecule, and the *in-situ* generated N-(2-aminopropyl acetimide) molecules, within the 12-membered channels of the Nd oxalates. The accessibility of the formate and N-(2-aminopropyl acetimide) functional groups uniformly distributed within the channels enables chemical manipulation.

An open-framework tin(II) oxalate with a layered architecture was also made in the presence of N,N,N',N'-tetramethyl ethylenediamine. The connectivities between the SnO_6 units [with pseudo-pentagonal bi-pyramidal geometry, assuming that one of the vertices is occupied by the lone-pair of electrons] and C_2O_4 moieties, forms puckered sheets containing 8- and 12-membered apertures. The organic amine resides in the 12-membered pores along with water molecules and these pores penetrate the entire structure in a direction perpendicular to the sheets, yielding a solid with uni-dimensional channels.

The use of higher dicarboxylic acids with different metals gave rise to open-framework structures with some possessing unique features. Thus, three-dimensional

open-framework cadmium malonate and manganese glutarate possessing channels with a hydrophobic environment have been synthesized. The three-dimensional structure of the cadmium malonate is attained through infinite Cd-O-Cd corner-linkages. On the other hand, the glutarate compound contains Mn-O-Mn layers cross-linked by MnO₆ octahedra and glutarate moieties.

Open-framework cadmium succinates of different dimensionalities have been synthesized by hydrothermal procedure by employing two different strategies, one involving the reaction of Cd salts with organic-amine succinates and the other involving the hydrothermal reaction of Cd salts with a mixture of succinic acid and the organic amine. While the latter procedure yields structures without any amine in them, the former gives rise to amine templated cadmium succinates with open-architectures. By employing guanidinium succinate we have obtained one- and three-dimensional structures, with piperazinium succinate we got two- and three-dimensional structures. The cadmium succinates without incorporation of amine also possess layered and three-dimensional structures. The three-dimensional structures exhibit interpenetration similar to that in diamondoid and α -polonium type structures respectively.

By carrying out a metathetic reaction between sodium succinate and CdCl₂ or CdBr₂ in a n-butanol-water mixture, two novel open-framework cadmium succinates, possessing interpenetrating three-dimensional open-framework structures have been obtained. They have tetrahedral Cl(Br)Cd₄O₂₄ clusters connected by succinate linkages, with the tetrahedral cluster itself being formed of four CdO₆ octahedra surrounding a halogen atom. The three-dimensional cadmium succinate framework incorporates sodium ions. Four sodiums surround the second nearest neighbor halogen atom, forming a Na₄Cl(Br) tetrahedron. Reaction between adipic acid and Mn²⁺ ions under solvothermal conditions, in the presence of piperazine, resulted in a

new manganese adipate, wherein the amine performs a dual role of being a ligand as well as a template. The presence of five-coordinated Mn^{2+} ions in a trigonal bipyramidal arrangement in this structure is an unusual feature in such open-framework carboxylates.

In pursuit of synthesizing novel hybrid structures, unusual inorganic-organic nano-composites containing extended alkali halide structures, present as layers or as three-dimensional units, have been synthesized by a metathetic reaction carried out under hydrothermal conditions. These compounds, with cadmium oxalate host lattices and the alkali halide structures as guests, have the compositions, Whilst the three-dimensional alkali halide structures with a super rock-salt cell, having expanded lattice parameters have been stabilized in three-dimensional cadmium oxalate framework with connectivities resembling chevrel phases. The two dimensional alkali halide layers containing six- and eight-membered rings resembling cyclohexane and cyclooctane have been stabilized in two and three-dimensional cadmium oxalate frameworks. The hydrothermal reaction between rubidium oxalate and $CdCl_2$ in the presence of NO_3^- ions gives a structure having cadmium chloro-oxalate layers. The Rb^+ ions present between the layers interact with the Cl atoms to form a one-dimensional $RbCl$ chain decorated by NO_3^- groups. Linear KCl and KBr chains have been incorporated into three-dimensional cadmium and manganese oxalate frameworks. The manganese oxalate framework possesses interesting monodentate linking by the oxalate units giving rise to the three-dimensional structure.

Papers based on this work have appeared in *Chem. Mater.* (1999), *Chem. Mater.* (1999), *Angew Chem.* (2000), *Chem. Mater.* (2001), *J. Chem. Soc. Dalton Trans.* (2001), *Chem. Mater.* (2001), *J. Solid State Chem.* (2001), *J. Mol. Struct.* (2002), *J. Solid State Chem.* (2002), *Inorg. Chem.* (2002), *Inorg. Chem.* (2002), *Solid State Sci.* (2002), *Cryst. Growth & Des.* (2003), *J. Chem. Soc. Dalton Trans.* (2003), *Eur. J. Inorg. Chem.* (2003), *Mater. Res. Bull.* (2003), *Angew. Chem.* (2003).

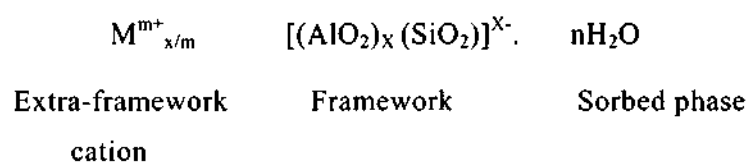
1. OVERVIEW OF MICROPOROUS OPEN-FRAMEWORK STRUCTURES

1.1. Inorganic open-framework materials

1.1.1. Zeolites

The discovery of aluminosilicates, well known as zeolites, was by Cronstedt and dates back to as early as 1756.^[1] However, the development of the field of microporous materials occurred after the first synthesis of the artificial zeolites in 1948, by Barrer.^[2] Since then numerous compounds with zeolitic structures have been prepared and characterized. The growth in this area can be evidenced from the number of reviews and related articles published in the literature.^[3-9]

Zeolites are a class of crystalline aluminosilicate materials that are characterized by their open-structures. The structure of zeolite itself can be realized to arise from the replacement of silicon in the neutral SiO₂ framework by Aluminium. Thus, the aluminosilicates are made up of TO₄ tetrahedra (where T is a tetrahedron, Si, Al), which are linked together through apical O-atoms to form an infinite three-dimensional framework structure with windows, channels and cages of molecular dimensions. The TO₄ tetrahedra in the zeolite are close to being regular, but the T-O-T angles about the apical O-atoms can accommodate values ranging from ~125° to 180° which is one reason why so many different structures are known.^[3,6] The general formula of an aluminosilicate zeolite is:



The framework has a O/T ratio of 2 and the presence of Al atom in the framework gives rise to a net negative charge that can be varied by changing the

Si/Al ratio. Many zeolites have Si/Al ratio ≥ 1 and satisfy the *Lowenstein's Rule*, which states that Al-O-Al type linkages are not favored.^[10] The negative charge of the framework is neutralized by the presence of extra-framework metal or organic cations or protons. The extra-framework cations located in the pore system can be exchanged by treatment in a suitable salt solution or molten salt. The third component is the sorbed phase. This can be any solvent species like H₂O, organics like benzene or alcohol etc. The organic amine cation can act as a template involved in the formation of these framework structures in more ways than one. While it is difficult to pin point the exact manner in which the amines participate in the formation of these inorganic structures, it is generally believed that their size and shape are crucial in determining the pore structure. The sorbed phase may be removed from the crystalline zeolite by heating under reduced pressure without destruction of the framework structure. The three components of the zeolite structure – the framework, the extra-framework cations and the sorbed phases – are each of interest and play a role of varying importance in the applications.

1.1.2. Zeolite framework structures

Diversity in the zeolite properties arise mainly due to the particular characteristics of their individual structures and it is this different crystal structures that may be used as a means of differentiating between the various zeolites. There are ~85 unique zeolite framework topologies that are known. These zeolites consist of primary building unit, the TO₄ tetrahedra, but similarities and relationships between the different structures become apparent only when larger building units are considered. Some of the more useful ways to describe how the zeolite structure is constructed from are by considering the zeolites to be built up from secondary building units, polyhedral building units or by stacking of layers.

Secondary building units

Secondary building units (SBU) are the 16 units proposed by Meier that can be linked to construct the most of the different zeolite framework topologies.^[3a] The 16 units consist of 4 to 16 T atoms and are shown in Figure 1.1. Individual combinations of SBUs can be used to form a particular zeolite structure. For example, the zeolites, ferrierite, mordenite and ZSM-5 all have frameworks based on the 5-1 SBU (5-ring) while that of faujasite is based on the 6-6 and 6-2 SBUs. Two simple zeolitic structures built up of 4-, 5- and 6- membered SBUs is shown in Figure 1.2.

Polyhedral building units and stacking of layers

Certain zeolite frameworks may be considered as being built up of specific polyhedral building units. One such polyhedral building unit is the β or sodalite cage which is a truncated octahedron consisting of 4- and 6-membered rings. Linkages of the sodalite cages through their rings produce the structures of sodalite, zeolite-A and faujasite as depicted in Figure 1.3. Many zeolite structures can be constructed from 2- and 3- connected nets, as is illustrated for the zeolite gmelinite in Figure 1.4.^[1] The fourth connection of the tetrahedra is directed either up or down and is used to join these 2-dimensional 3-connected nets to form a 3-dimensional 4-connected net. This method of constructing zeolitic topologies is particularly useful for the pentasil zeolites like ferrierite, mordenite, ZSM-5 and zeolite - β . The use of net topology is extremely useful when trying to visualize structures containing stacking faults.

1.1.3. Isomorphous substitution in zeolites

Barrer proposed that gallium, germanium, beryllium, boron, iron, chromium, phosphorous, magnesium can replace the Si isomorphously in many zeolites.^[3a] In

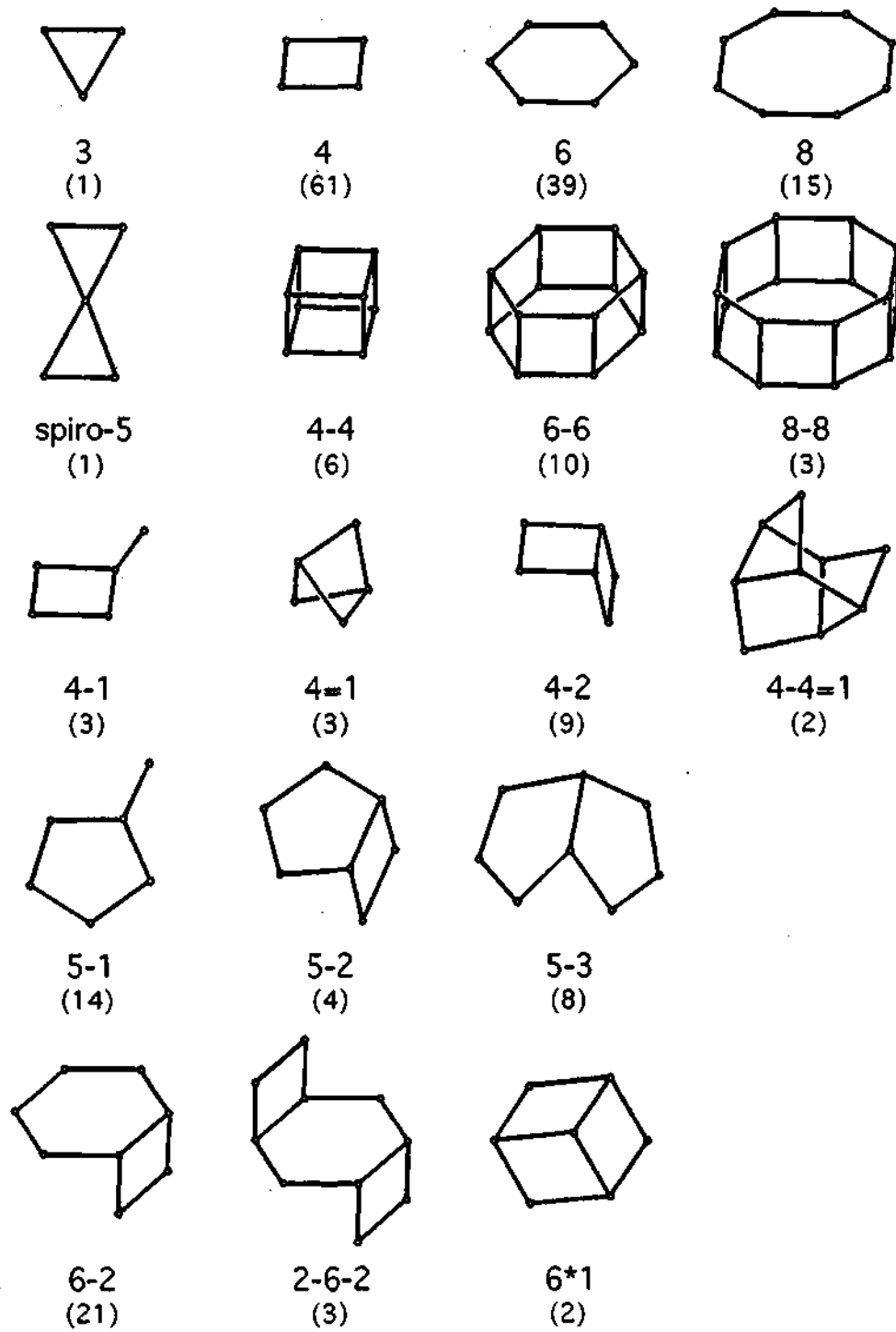
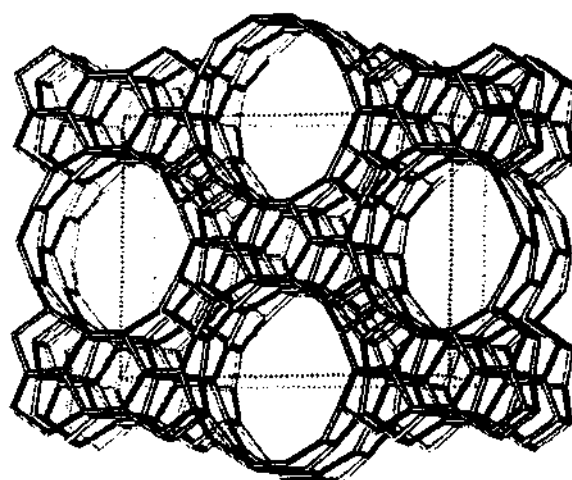
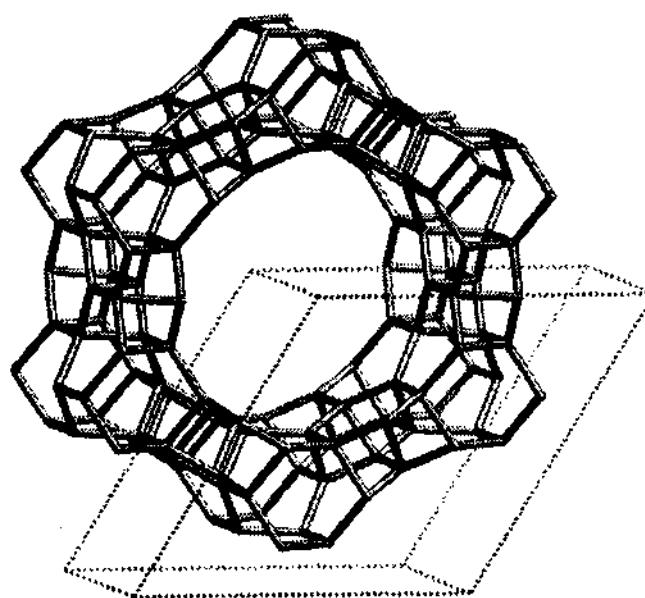


Fig. 1.1. The secondary building units found in the aluminosilicates with the legends indicating the type of ring present in the unit.



(a)



(b)

Fig. 1.2. Two simple zeolitic structures built up of 4-, 5- and 6- membered SBUs.
(a) Framework structure of UTD-1, showing large 14-membered channels (8.1 x 8.2 Å) present along the *b*-axis. (b) Framework structure of VPI-5, showing large 18 membered circular channels (12.7 x 12.7 Å) present along the *c*-axis.

fact, many naturally occurring minerals demonstrate this replacement. For example, the composition of helvine, $\text{Mn}_6[\text{Be}_6\text{Si}_6\text{O}_{24}]\text{MnS}$, and sodalite demonstrate the isomorphous replacement: $\text{Na}^+\text{Al}^{3+} = \text{Mn}^{2+} \text{Be}^{2+}$, while those of tugtupite, $\text{Na}_6[\text{Al}_2\text{Be}_2\text{Si}_8\text{O}_{24}]\text{Na}(\text{Cl},\text{S}_{1/2})$, and sodalite correspond to: $2\text{Al}^{3+} = \text{Be}^{2+}\text{Si}^{4+}$. Following this, many metal substituted aluminophosphates were made.^[3c,d,5,6c]

Taking into account the electroneutrality between the silica (SiO_2) and the aluminophosphate (AlPO_4), $2\text{Si}^{4+}\text{O}_2 = \text{Al}^{3+}\text{P}^{5+}\text{O}_4$, and also the fact that the crystalline silicas are indeed imitated by neutral AlPO_4 :

SiO_2	AlPO_4

Quartz	Berlinite
↓↑ 867°	↓↑ 815°±4°
Tridymite	Tridymite type
↓↑ 1470°	↓↑ 1025°±50°
Crystobalite	Crystobalite type

it was realized that AlPO_4 with neutral frameworks, having strictly alternating $[\text{AlO}_2]^-$ and $[\text{PO}_2]^+$, can also be made. Following this, a series of aluminophosphates designated as $\text{AlPO}_4\text{-n}$ were synthesized and characterized.^[12,13] These aluminium phosphates were synthesized by employing hydrothermal methods in the temperature range of 100°- 250°C, and using amines or quaternary ammonium salts as templates. About 20 novel structures were reported with the general composition $\text{AlPO}_4 \cdot x\text{R} \cdot y\text{H}_2\text{O}$, where R = organic template; x and y represent the number of template and water molecules needed to fill the intra-crystalline voids respectively. This opened up a new avenue in the field of open-framework solids.

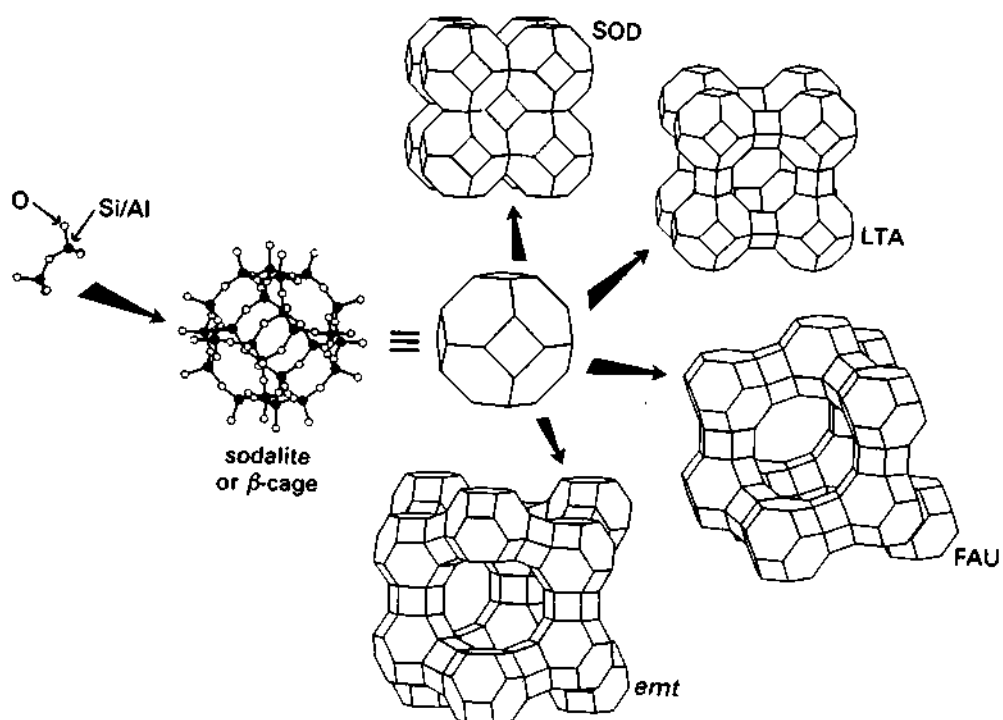


Fig. 1.3. Figure shows the secondary building unit (SBU) formed by the four- and six-membered rings in aluminosilicate framework and the formation of different framework structures with cages from this SBU.

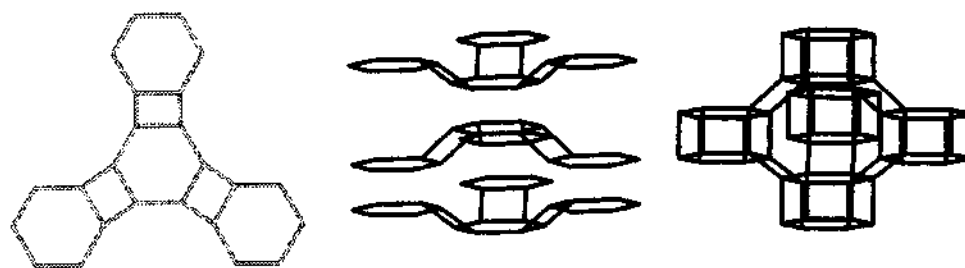


Fig. 1.4. zeolite structures can be constructed from 2- and 3- connected nets, as is illustrated for the zeolite gmelenite

Catalytic exchange capacity and the possibility of acidity can be introduced by partial substitution, generally for phosphorous as $M^{m+}_{x/m}[(Si_xP_{1-x}AlO_4)](SiO_2) \cdot yR \cdot nH_2O$, where R is any organic template. This substitution by silicon gives rise to a family of silicoaluminophosphates (SAPO-n) with novel structure and properties. Incorporation other metal cations in place of Al, or in addition to silicon has also been reported, the materials being termed, by analogy, MeAPO-n and MeAPSO-n, respectively, where Me can be any monovalent or divalent, trivalent metal.^[3a,7]

1.1.4. Extra-large pore framework solids

The preparation of the aluminophosphate VPI-5 - the crystalline microporous material with uniform pores larger than 1.0 nm - opened up the area of extra-large pore crystalline materials.^[14] Extra-large pores are obtained if more than 12 oxygen atoms span the circumference of the pore, and the resultant pore size allows practical applications for which materials with smaller pores are not suitable. In VPI-5, the circular one-dimensional channels have a uniform diameter of 1.2 nm and endow ~30% of the total volume as void.^[14a] Numerous extra-large pore materials were synthesized with some of them exhibiting significant stability upon the removal of the guest species.^[15]

1.1.5. Synthesis of inorganic framework structures

All the open-framework materials with zeolitic structures have been synthesized by exploiting the kinetic stability of their various metastable phases. Just like the metastable diamond phase being stabilized, under high pressure and temperature over the thermodynamically favored allotrope graphite, under geothermal conditions. Most of the open-framework structures have been made by hydrothermal methods, because, all these open-frameworks must be stabilized during growth by "templating" them with guest molecules. Although there is no

complete understanding, one assumes that the synthesis follows the following stages.

Reactants → Reactant gel → Precursors → Nucleation → Crystal growth

Therefore in these open-framework materials the pores can be designed to form in ordered fashion and also the pore size and shape can be controlled, by employing molecular units or hydrates of alkali or alkaline earth cations or amines/diamines as templates or structure directing agents (SDA). Thus, different framework structures are formed by the same amine, and the same framework structure is also formed by the use of different amines. Such observations have prompted investigations into the role of the amines in the formation of these structures. According to Davis and Lobo^[16] the amine acts as a template if the framework is flexible and as a SDA if the framework is related to the structure of the cation molecule. In hydrothermal synthesis, alkaline salt medium, water and salts may compete as “stabilizers”, so that each may be present in the intracrystalline pores.^[17] Some authors have sought to draw a distinction between *templating* and *structure direction*.^[16,18] In this context, templating refers to the process, in which a unique template leads to the formation of a unique structure which reflects the geometrical and electronic structure of the template. Whereas structure direction describes a more subtle effect in which the use of a particular organic amine leads to the synthesis of a particular structure *via* a combination factors such as pH, solubility and electrostatic interaction with solubilized inorganic species, like mineralizers.^[4d]

There are mechanistic considerations pertinent to the understanding of zeolite formation. These pertain to the solution-mediated transport and the solid hydrogel transformation. The solution-mediated process involves the dissolution of

the reagents in the solution phases followed by the transport of the dissolved species to the nucleation sites. The solid hydrogel transformation is the reorganization of solid phase from an initial amorphous phase to one with long range order. A schematic description of these processes is presented in Figure 1.5. Various methods have been developed to understand the processes that take place during the hydrothermal reactions, of which, the *in-situ* XRD studies appear to be prominent.^[19]

1.1.6. Amine-phosphate as intermediates in the formation of open-framework zinc phosphates

During the hydrothermal synthesis of metal phosphates, amine phosphates are often obtained as additional products. It has been shown recently that the reaction of amine phosphates with metal ions under hydrothermal conditions, in the absence of additional phosphoric acid, gives rise to open-framework metal phosphates.^[20,21] The amine phosphates react with metal ions under mild conditions (even at room temperatures) to yield materials with open-framework structures.

1.1.7. Application of inorganic microporous framework materials

Catalysis

Zeolites have been employed as catalysts for many chemical reactions. An important class of reactions is that catalyzed by hydrogen-exchanged zeolites, whose framework-bound protons give rise to very high acidity. This is exploited in many organic reactions, including crude oil cracking, isomerisation and fuel synthesis. Zeolites can also serve as oxidation or reduction catalysts, often after metals have been introduced into the framework. Examples are the use of titanium ZSM-5 in the production of caprolactam, and copper zeolites in NO_x decomposition. Underpinning these reactions is the unique microporous nature of zeolites where the shape and size of the pore system exerts steric influence on the

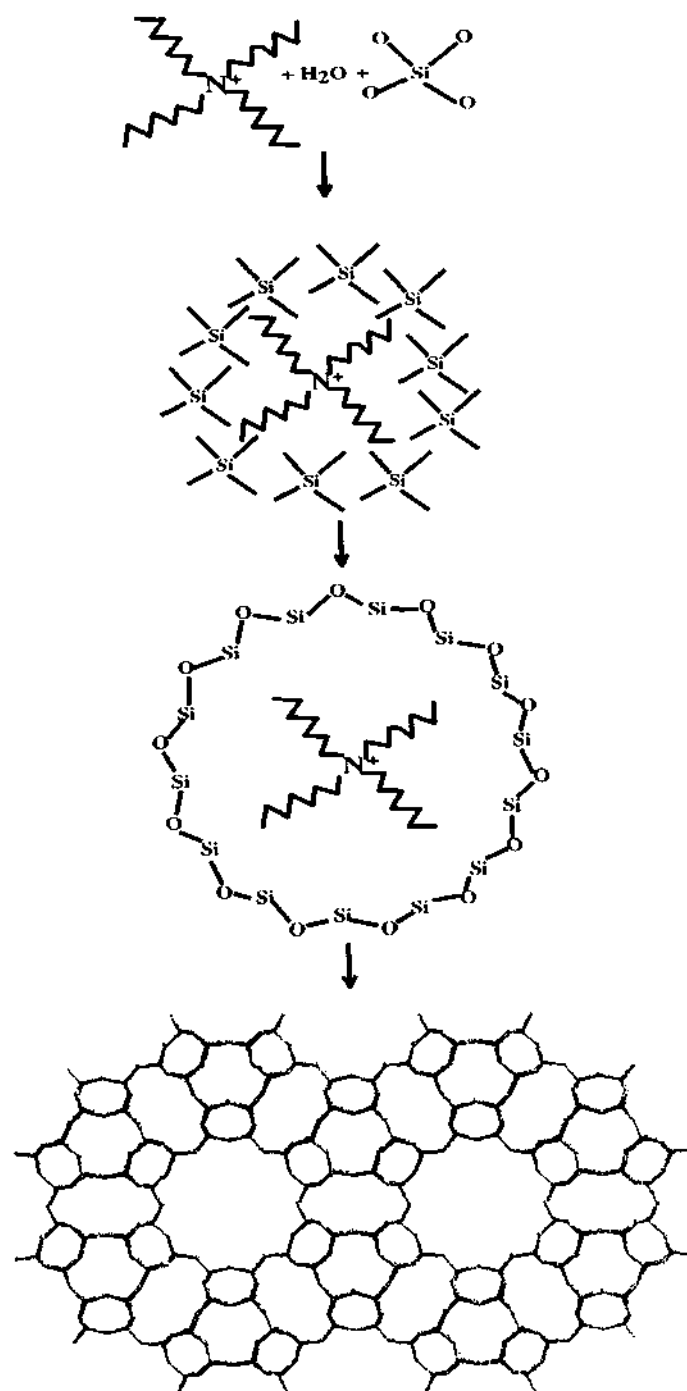


Fig. 1.5. A schematic representation of the solid hydrogel transformation involving the reorganization of solid phase from an initial amorphous phase to one with long range order

reaction, controlling the access of reactants and products. Some of the catalytic applications of inorganic microporous solids are listed in Table 1.1.

Table 1.1. Some important applications of aluminosilicate zeolites

Well-established:
ion-exchange with hydrated zeolites detergency (e.g. zeolites Na-A and Na-P) water softeners animal feeds radwaste remediation (e.g. Cs, Sr with clinoptilolite)
molecular sieving with dehydrated zeolites air separation (N ₂ from O ₂ with Li-LSX) drying agents (e.g. double glazing, air conditioning) sulfur removal from natural gas separation of HFCs (CFC substitutes)
catalysis with dehydrated zeolites catalytic cracking (gasoline production)–zeolite-Y derivatives xylene isomerization (for polyesters)–H-ZSM-5 butene isomerization–H-FER methanol to gasoline–H-ZSM-5 phenol to hydroquinone–titanosilicates denox reactions–Cu-ZSM-5, Co-FER
Future possibilities include:
nano-composites for electro-opticals sensors with zeolite thin films stereoselective polymerization contrast enhancement in MRI (e.g. Gd-Y)

Adsorption and Separation

The ability to preferentially adsorb certain molecules, while excluding others, has opened up many molecular sieving applications, as in the purification of para-

xylene by silicalite. Cation-containing zeolites are extensively used as desiccants due to their high affinity for water, and also find application in gas separation, where molecules are differentiated on the basis of their electrostatic interactions with the metal ions. Conversely, hydrophobic silica zeolites preferentially absorb organic solvents.

Ion Exchange

The loosely bound nature of extra-framework metal ions (e.g. zeolite NaA) enables their exchange for other types of metal, when in aqueous solution. This is exploited in water softening, where alkali metal ions, Na^+ or K^+ , in the zeolite, exchange with the Ca^{2+} and Mg^{2+} ions from the water. Commercial wastewater containing heavy metals and nuclear effluents can also be cleaned up using zeolites.

1.2. Inorganic open-Frameworks with organic ligands

A limitation with metal phosphates/silicates is that the structures comprise rigid polyhedra such as tetrahedra and octahedra, which constitute the primary building units,^[4c,d,22] and there has been much interest in designing hybrid materials containing inorganic and organic linkers.^[23-30] In the design of hybrid structures, one takes advantage of metal-coordination, the functionalities of the organic components as well as the flexibility of the organic linkers to give rise to open-framework structures.^[23-30] The metal carboxylates are particularly interesting in that they not only form open-framework structures resulting from the presence of carboxylate itself but also from the carboxylate acting as a linker between inorganic moieties. Another interesting variety is where the carboxylate unit co-exists with a phosphate or an arsenate to give rise to hybrid structures.

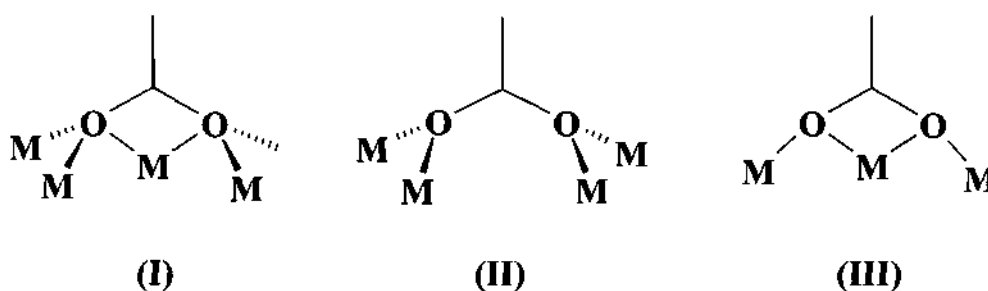
1.2.1. Monocarboxylates

Systematic investigations of open-framework monocarboxylate structures are rather limited, but some of the metal monocarboxylates coexist with other

ligands to form extended lattices of different dimensionalities.^[31-33] Thus, copper formate tetrahydrate has two-dimensional copper formate layers,^[34] separated by water molecules, while bismuth formate has a 1D chain structure.^[35] Monocarboxylates of alkali metals, exhibit several polymorphic modifications.^[36] Metal acetates tend to form dimers,^[31-33,37] the classic example being copper diacetate, which gets connected by other ligands into an infinite array.^[38] A layered copper acetate based compound is $[\{\text{Cu}_2(\text{O}_2\text{CCH}_3)_4\}(\text{tpt})_2] \cdot 2\text{MeOH}$, (tpt = 2,4,6-tri(4-pyridyl-1,3,5-triazine), with large pores, where the metal acetate dimers are linked by N-donor ligands is known (Fig.1.6).^[39] The organic linker, tpt, connects the acetate dimers, and avoids interpenetration through inter-layer π - π interactions, which also stabilizes the structure. Cotton et al.,^[40] have employed cyanide ligands to connect metal acetate dimers to form molecular boxes and layered structures, thus providing a new avenue for the construction of neutral frameworks. Thus, $[\text{Rh}_2(\text{O}_2\text{CCCF}_3)_4]_2(\text{TCNE})(\text{C}_6\text{H}_6)_2$ (TCNE = tetracyanoethylene) contains non-interpenetrating sheets formed by quasi-rectangular 30-membered rings. The sheets are, again, stabilized by significant π - π interactions between the $\text{Rh}_2(\text{O}_2\text{CCCF}_3)_4$ and $\text{C}_2(\text{CN})_4$ moieties.^[40] The TCNE units themselves are linked via $\text{Rh}_2(\text{O}_2\text{CCCF}_3)_4$ moieties, thereby demonstrating the bridging role of the rhodium carboxylate complexes. Harrison and Jacobson^[41] have prepared $\text{K}_3\text{Co}(\text{CN})_6 \cdot 2\text{Rh}(\text{O}_2\text{CMe})_4$ wherein the $\text{Rh}_2(\text{O}_2\text{CMe})_4$ dimers are linked through the octahedral $\text{Co}(\text{CN})_6$ unit, forming a two-dimensional structure with large windows.

High-nuclearity inorganic clusters formed by acetate ligands give rise to novel structures with interesting properties. They represent a bridge between molecular chemistry and solid state chemistry, providing a means to understand the size-dependant physical properties.^[42] In preparing new nanoscopic compounds with

such clusters, hydroxy, oxo and carboxylate groups are used, with hydrophilic groups lying within the core and hydrophobic groups at the periphery.^[43] High-nuclearity clusters are also assembled into infinite coordination polymers.^[44] A three-dimensional framework based on Ba_9 clusters, $Ba_9(CH_3CO_2)_{14}(ClO_4)_4$ reported by Dong et al (Fig. 1.7).^[45] The structure consists of $Ba_9(CH_3CO_2)_{14}(ClO_4)_4$, as an I-center tetragonal prism, connected by acetate and perchlorate bridges. The framework has the $\mu_5-\eta^3:\eta^3-$, $\mu_4-\eta^2:\eta^2-$ and $\mu_3-\eta^2:\eta^2$ -bridging modes shown below:



The μ_5 coordination mode being the largest ligation that an anion can form with the neighboring metal centers in its complexes.^[46] Meyer and co-workers, have prepared and characterized heteronuclear rare-earth trichloroacetates, possessing polymeric structures, exhibiting interesting optical properties.^[47] In most of the metal monocarboxylates, extensive hydrogen bond networks generally stabilize the structures.^[12c,35,39,47,48]

Microporous metal hydroxyacetates exhibiting ion-exchange behavior has also been reported.^[49] A cobalt hydroxyacetate, $Co_5(OH)_2(O_2CCH_3)_8 \cdot 2H_2O$, with a three-dimensional structure, built up entirely through edge-sharing cobalt-oxygen octahedra has been prepared.^[50] The acetate ligands, generated *in-situ via* oxidative

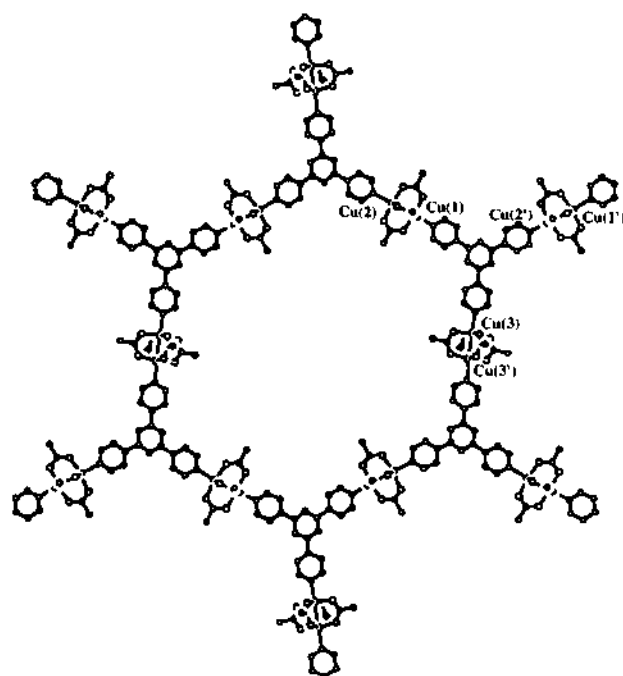


Fig. 1.6. Hexagonal window in the (6,3) sheets of $[\{\text{Cu}_2(\text{O}_2\text{CCH}_3)_4\}_3(\text{tpt})_2] \cdot 2\text{MeOH}$ (tpt = 2,4,6-tri(4-pyridyl)-1,3,5-triazine). The ring 'diagonals' are ca. 34-37 Å.

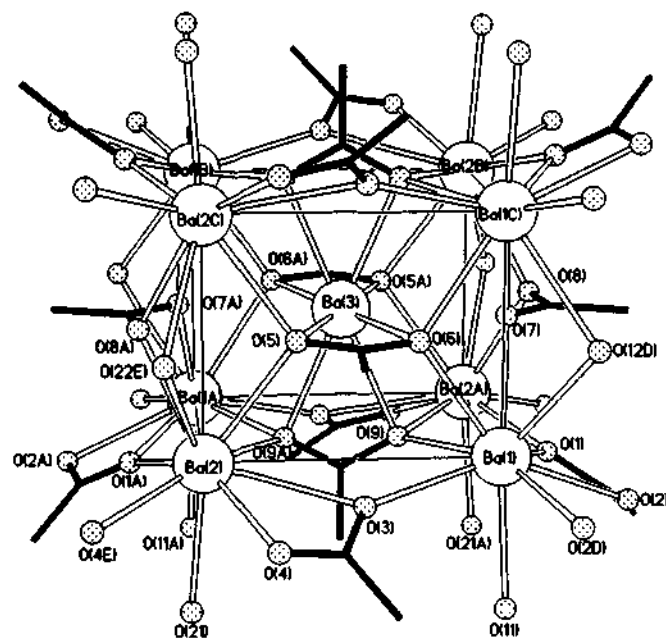


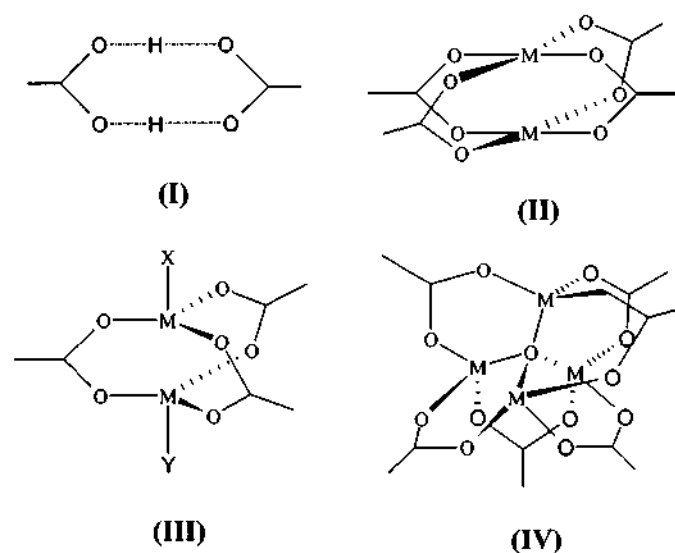
Fig. 1.7. *I*-centered Ba_9 cores in $[\text{Ba}_9(\text{CH}_3\text{CO}_2)_{14}(\text{ClO}_4)_4]_\infty$ formed by acetate bridges.

hydrolytic cleavage of the acetylacetonate ligand, exhibit $\eta_1:\eta_2$ and $\eta_2:\eta_2$ coordination, the latter being unusual. A two-dimensional copper acetate, $[\text{Cu}(\text{CH}_3\text{CO}_2)(\text{CH}_3\text{O})]_n$, with acetate ligands involving three-coordinated oxygens along with bridging methoxo groups has been reported recently.^[51] In $(\text{pipzH}_2)(\text{H}_3\text{O})[\text{Al}_{15}(\mu_3\text{-O})_4(\mu_3\text{-OH})_6(\mu\text{-OH})_{14}(\text{hpdtA})_4].\text{pipz}.41\text{H}_2\text{O}$, (pipz = piperazine, H_3hpdtA = 2-hydroxypropane-1,3-diamine- N,N,N',N' -tetraacetic acid),^[52] Al_{15} aggregates involving aluminium oxyhydroxide (brucite type) cores assembled through hpdtA linkers are observed.

Several structural motifs based on or related to carboxylates are profitably employed in the design of new solids with open structures (Scheme 1.1).^[53] Amongst the many structural motifs commonly used in supramolecular chemistry,^[53c] the simplest is the hydrogen bonded dimer (a in Scheme 1.1). The replacement of the proton in the dimer by metal acetate dimer or inorganic node facilitates the assembly into three-dimensional supramolecular networks through out-of-plane linkages. The use of the acetate dimer as a secondary building unit (SBU) in the design of rigid three-dimensional metal-organic frameworks is described in the later in sections. Paddle-wheel metal acetate clusters have been used to assemble encoded organic nodes (Fig. 1.8).^[54] This gives rise to “inverted” metal-organic framework with compartmentalized cavities and walls that are accessible for further functionalization of the channels.

1.2.2. Oxalates

The oxalate unit acts as a rigid bidentate ligand facilitating the formation of extended structures by bridging metal centers. Many metal oxalate structures are reported in the literature, including those occurring naturally as minerals.^[55] A specific characteristic of the oxalate that has been of interest is its ability to mediate



Scheme 1.1. Scheme illustrating the two-connected linear $R_2^2(8)$ dimer (a) in Carboxylate dimers and the secondary building units (SBUs) based upon $M(II)$ carboxylates providing square-planar (b), trigonal (c) and octahedral (d) nodes for the construction coordination networks and assemblies. Note that the higher connectivity of the metal carboxylate SBUs is facilitated in part by the replacement of the H^+ ions by higher charge M^{2+} ions.

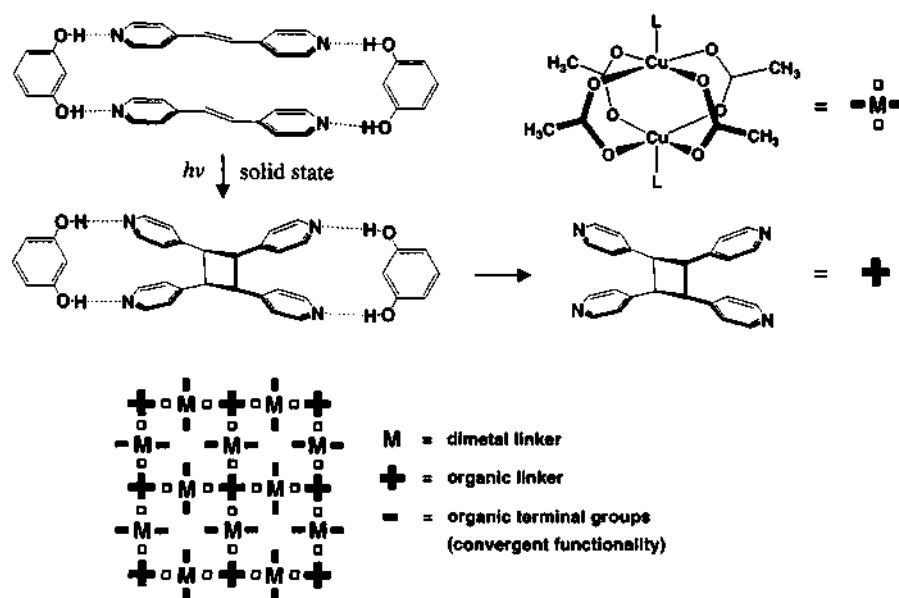


Fig. 1.8. Construction of an open-framework inverted metal-organic framework (IMOF) using copper acetate dimers as linkers between *rctt*-tetrakis(4-pyridyl)cyclobutane (4,4'-tpcb) units.

electronic effects between paramagnetic metal ions.^[56] The oxalate moiety also acts as a linker between metal centers to yield open-structures with different dimensionalities ranging from zero and three.^[57]

Amongst the oxalates, the two-dimensional honeycomb structure is the most common.^[58,59] The honeycomb structure facilitates sizeable molecular alternation and pore-functionalization.^[59] The ligating ability of the oxalate is exploited to engineer crystal structures, bischelation often giving rise to interesting physical properties, possibly due to the relatively short bonds between the metal centers.

Transition Metal Oxalates

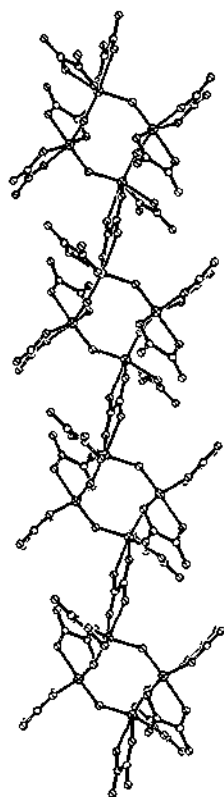
Titanium and Zirconium Oxalates: Little is known about the oxalates of zirconium and titanium.^[60] The titanyl oxalate, $(\text{NH}_4)_2\text{TiO}(\text{C}_2\text{O}_4)_2 \cdot \text{H}_2\text{O}$, possessing cyclic $[\text{Ti}_4\text{O}_4(\text{C}_2\text{O}_4)_8]$ tetrameric units was described in 1974.^[61] The one-dimensional coordination polymer, $\text{NH}_4[\text{Ti}(\text{C}_2\text{O}_4)_2] \cdot 2\text{H}_2\text{O}$, with Ti in a square-antiprismatic arrangement is also known.^[62] Hydrothermal conditions have been employed to prepare titanium oxalates in the presence of organic amines.^[63] They contain the cyclic tetranuclear anion, $[\text{Ti}_4\text{O}_4(\text{C}_2\text{O}_4)_8]^{8-}$ with the amine residing in the inter-chain locations. The structures of the one-dimensional chain formed by the basic tetrameric unit and the titanium oxalate formed in the presence of piperazine are shown in Figures 1.9a and b respectively. There are no reports of three-dimensional titanium oxalates.

Zirconium oxalates isolated from aqueous solution are well known.^[64] In these oxalates, the larger zirconium atoms, exhibit higher coordination compared to titanium,^[65] forming binuclear dimers as well as one-dimensional polymeric chains. A series of open-framework oxalates containing zirconium and cadmium or lead along with alkali or ammonium cations have been reported.^[66] They contain MO_8 (M =Zr, Cd) polyhedral units with dodecahedron or distorted square antiprism

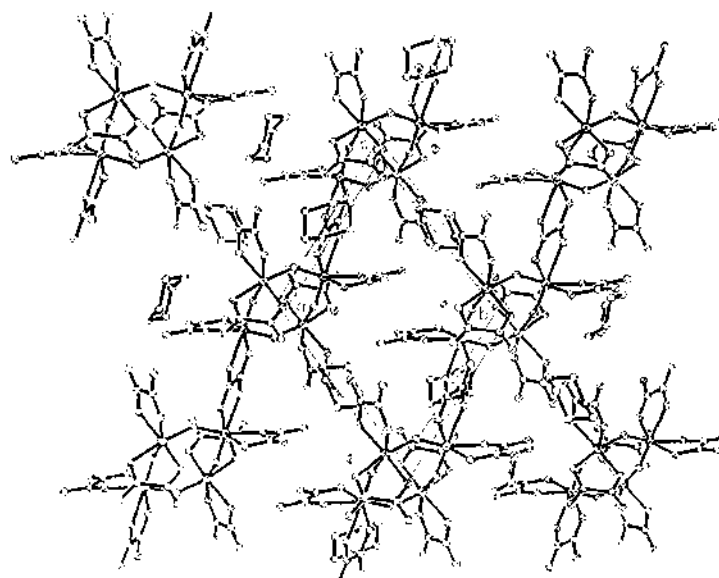
geometry linked through oxalate oxygens giving rise to three-dimensional open-frameworks. In $\text{Pb}_2\text{Zr}(\text{C}_2\text{O}_4)_4 \cdot n\text{H}_2\text{O}$, the PbO_8 and PbO_9 units form two independent chains linked through the oxalate and the isolated ZrO_8 polyhedron forming the three-dimensional structure.^[66c] The zeolitic nature of the water molecules in the channels and their influence on the lattice parameters have been studied. In $2[\text{NH}_4]^+[\text{CdZr}(\text{C}_2\text{O}_4)_4]^{2-} \cdot 3.9\text{H}_2\text{O}$ and $[\text{H}_3\text{N}(\text{CH}_2)_2\text{NH}_3]^{2+}[\text{CdZr}(\text{C}_2\text{O}_4)_4]^{2-} \cdot 4.4\text{H}_2\text{O}$, right-handed metal-oxalate helical wires are formed due to the connectivity between the oxalate and the MO_8 polyhedra ($\text{M} = \text{Cd}, \text{Zr}$).^[66a] The oxalate unit bridges the chains to yield a three-dimensional structure with channels (Fig. 1.10). It is likely that the structure-directing property of the organic amine plays a role in the formation of the helical structures.

Oxalates of Metals from Chromium to Copper: Transition metal oxalates are of special interest since they can incorporate magnetic centers with predetermined moments by availing the various coordination modes of oxalate ligand. The structures of several transition metal-oxalates are available in the literature.^[55-58,67-70] Three-dimensional mixed metal oxalates based on Cr(III) have been prepared by Tamaki et al.,^[71] availing the η^3 -complex with a D_3 symmetry. The $[\text{Cr}(\text{ox})_3]^{3-}$ anion acts as a building block by binding to three M(II) ($\text{M} = \text{Fe}, \text{Co}, \text{Ni}, \text{Cu}, \text{Zn}$) ions through the oxalate groups, thereby forming three-dimensionally extended network. These compounds have three-dimensionally ordered ferromagnetic spins and the channels occupied by NBu_4^+ or alkali metal cations, providing an example to the design and tuning of the molecular components in extended structures to attain desirable properties.

Oxalates with mixed valency and more than one metal have general formula, $\{[\text{A}][\text{M}^{\text{II}}\text{M}^{\text{III}}(\text{ox})_3]\}_n$, where A^+ is a monovalent cation; $\text{M}^{\text{II}} = \text{Mn}, \text{Fe}, \text{Co}, \text{Ni}, \text{Cu}, \text{Zn}$ and $\text{M}^{\text{III}} = \text{Cr}, \text{Fe}, \text{Co}$ and ox is $(\text{C}_2\text{O}_4)^{2-}$, possess distinct magnetic properties,



(a)



(b)

Fig. 1.9. (a) Section of the $[\text{Ti}_4\text{O}_4(\text{C}_2\text{O}_4)_7]^{6-}$ chain in $\text{Ti}_4\text{O}_4(\text{C}_2\text{O}_4)_7 \cdot 3\text{C}_4\text{N}_2\text{H}_{12} \cdot 2\text{H}_2\text{O}$. Note the presence of both bridging and terminal oxalate groups. (b) Structure of $\text{Ti}_4\text{O}_4(\text{C}_2\text{O}_4)_7 \cdot 3\text{C}_4\text{N}_2\text{H}_{12} \cdot 2\text{H}_2\text{O}$ showing the apertures occupied by piperazine.

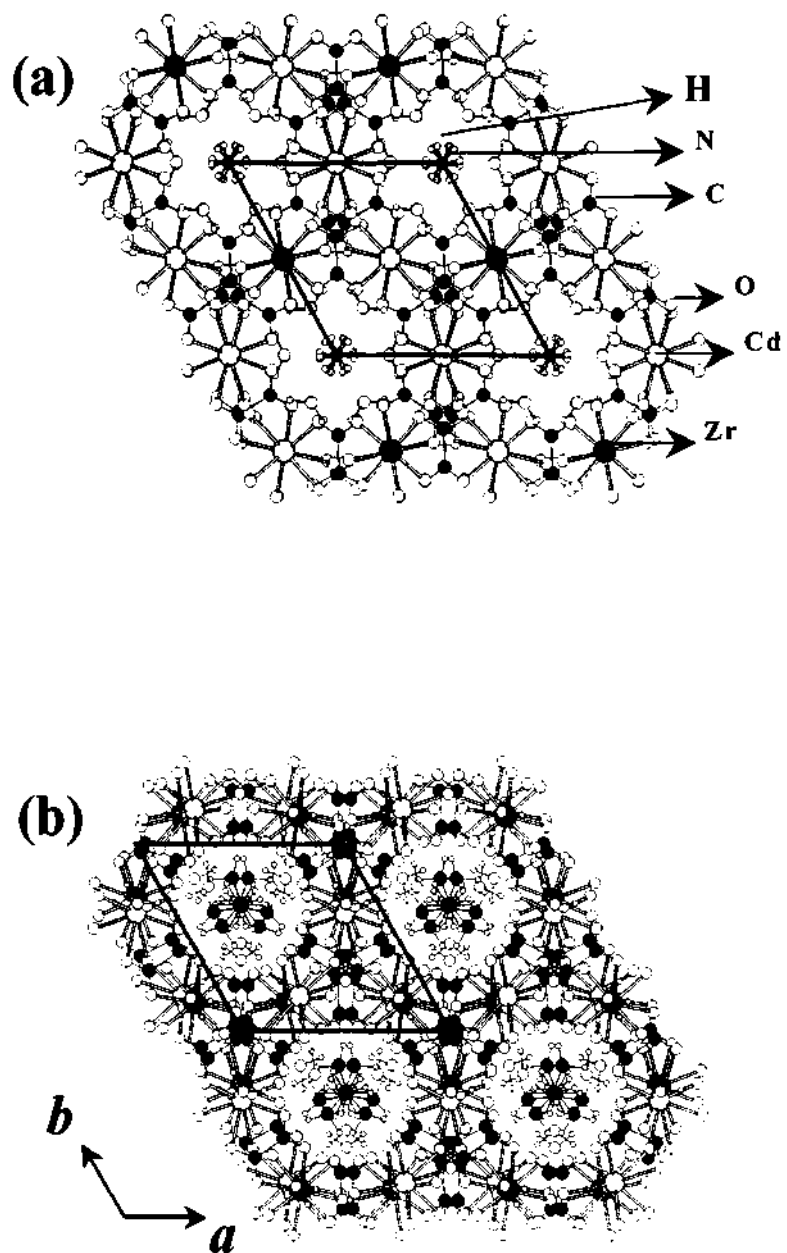


Fig. 1.10. Projection of the structures of (a) $\text{CdZr}(\text{C}_2\text{O}_4)_4(\text{NH}_4)_2 \cdot 3.9\text{H}_2\text{O}$ and (b) $\text{CdZr}(\text{C}_2\text{O}_4)_4(\text{C}_2\text{N}_2\text{H}_{10}) \cdot 4.4\text{H}_2\text{O}$.

varying from paramagnetic to ferromagnetic or antiferromagnetic.^[67c,68b,c,70a,b] Chiral metal complexes have also been used to form layered magnets with oxalate networks as in $[Z^{III}Cp^*]_2[M^II M^{III}(ox)_3]$ ($Z^{III} = Co, Fe$ or Mn ; $M^{II} = Mn, Fe, Co, Ni, Cu, Zn$; $M^{III} = Cr, Fe$), as shown in Figure 1.11, and three-dimensional anionic networks of the type $[Z^{II}(bpy)_3][M^I M^{III}(ox)_3]$ or $[[Z^{II}(bpy)_3][M^II M^{III}(ox)_3]$ ($Z^{II} = Fe, Co, Ni, Ru, Zn$; $M^{II} = Mn, Fe, Co, Cu$; $M^{III} = Cr, Fe$; $M^I = \text{alkali metal}, NH_4^+$), with cross-linking oxalate units.^[68b] An alternative way to describe these compounds would be to consider them as oxalate layers with one-dimensional channels occupied by the bulky metal complex. The interlayer separation in two-dimensional mixed metal oxalates with varying cation chain lengths, located in the interlamellar region, follows the well-known alternation effect.^[72] Magnetic properties of these materials are well understood.

Design of a chiral porous metal oxalate structure using chiral starting materials has been explored.^[69a,73] Thus, the three-dimensional chiral magnetic lattice, $[M^{z+}(C_2O_4)_3]^{(6-z)-}$, has been prepared from a pre-formed transition metal complex and oxalate units.^[69a,73] Decurtins and co-workers^[74] have elucidated the tunability of the size of the cavity in the three-dimensional metal-oxalate framework by varying the metal ions in the oxalate framework, and also investigated the magnetic properties of these materials by changing the nature of the $[M(bpy)]^{2+}$ complex incorporated in the zeolite-type cavities. A three-dimensional supramolecular complex, $\{K[Cu(\text{trans}[14]\text{dien})Cr(ox)_3]_n\}$,^[75] with large helical tunnels ($\sim 21.2 \times 9.3 \text{ \AA}$), formed by the bridging of octahedrally coordinated Cr and K centers by the oxalate ligands has been described. The Cu complex ligated to the framework via oxalate units and protruding into the channel can be chemically manipulated and exploited for potential applications. Many other transition metal oxalate frameworks, with different templates such as ammonium cation, organic

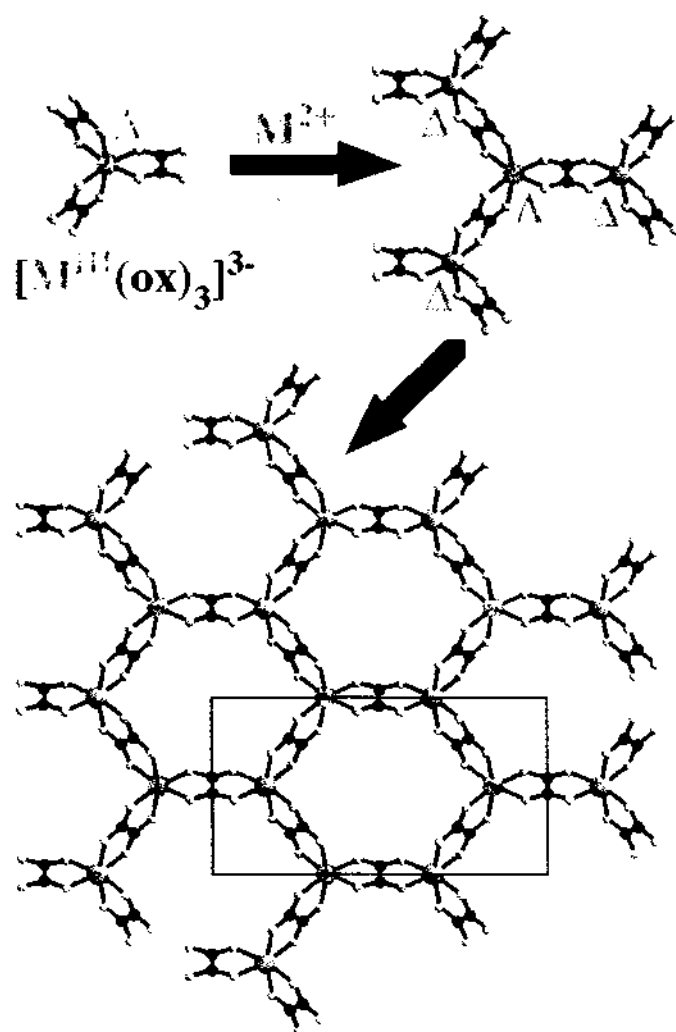


Fig. 1.11. Schematic construction of the 2-D layers by combination of alternating Λ and Δ isomers of tris(oxalato)metalate complexes in the presence of a bulky monocation.

amines and metal complexes are also known.^[57a,c,76] Thus, the iron oxalate, $\{(NH_4)_2[Fe_2O(ox)_2Cl_2] \cdot 2H_2O\}_n$, is made up of a helical motif formed by the chiral-linking of Fe atoms by the oxalate units, such motifs being bridged by a μ -oxo group to form a three-dimensional structure with helical tunnels occupied by guest species.^[77] The Fe-Fe distance of 3.384(2)Å through the oxo- ligand, and 5.496(2)Å through the bisbidentate oxalate group indicates the openness created due to the presence of the oxalate units in these structures. The templated iron oxalate framework also exhibits interesting ferromagnetic behavior with a Curie temperature, T_c , as high as 40K. A one-dimensional ladder oxalate, $Na_2Co_2(C_2O_4)_3(H_2O)_2$, prepared hydrothermally, possessing a 2-leg ladder topology, with antiferromagnetic ordering has been described.^[78] $Ba_4(C_2O_4)Cl_2[\{Fe(C_2O_4)(OH)\}_4]$ possesses two distinct channels (concave and convex), formed by the linking of vertex- sharing FeO_6 octahedra by hydroxy μ^2 - bridges and oxalate anions in monodentate fashion as shown in Figure 1.12.^[79] Type 1 channels with concave edges are occupied by barium and chloride ions, while type 2 channels with convex edges are occupied by the oxalate ions.

Zinc and Cadmium Oxalates: Zinc and cadmium oxalates with one- and two-dimensional structures have been synthesized.^[80,81] The one-dimensional structures are formed by bridging the metal polyhedra by the oxalate units, and are stabilized by cooperative, non-covalent interactions with the amine provides ancillary ligation to the Zn atom.^[80] The two- dimensional oxalates adopt the well-known honeycomb structures with 12-membered apertures.^[80,81] The honeycomb layers are stacked one over the other to create psuedo-uni-dimensional channels (Fig. 1.13).^[80] In some of the oxalates, the metal ions take ancillary coordination by bonding with water, amine etc.^[82] Recently, transformation of other dicarboxylates under reactive

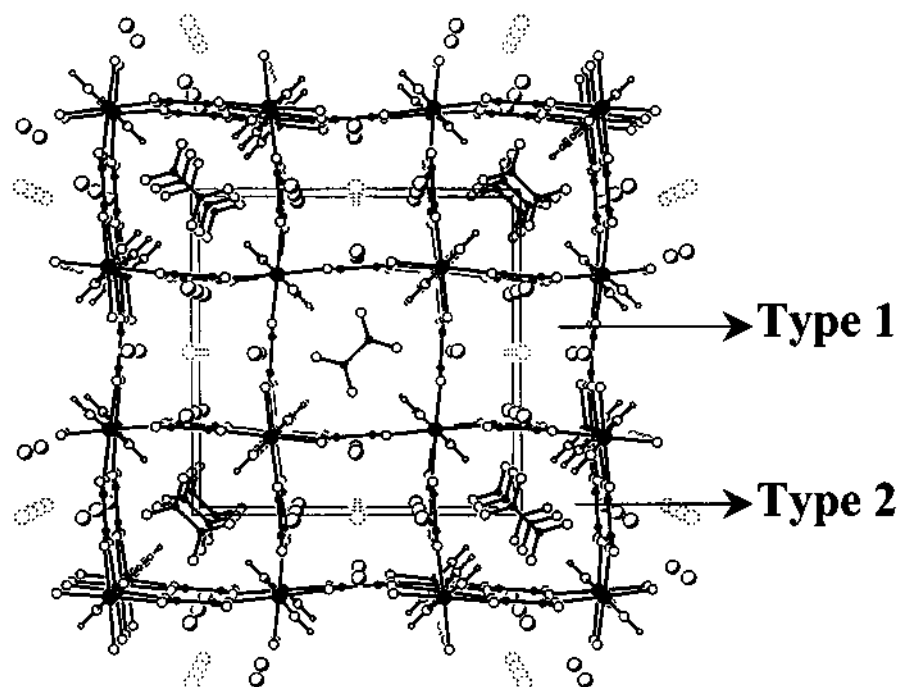


Fig. 1.12. A perspective view of the $\text{Ba}_4(\text{C}_2\text{O}_4)\text{Cl}_2[\text{Fe}(\text{C}_2\text{O}_4)(\text{OH})]_4$ showing how $\text{Fe}(\text{OH})$ chains are held together in a square lattice. Type-1 and type-2 channels contain barium and chloride ions or oxalate ions, respectively.

conditions into oxalate species, and their further reaction with the Zn^{2+} and Cd^{2+} ions to form extended metal oxalate architectures has been observed.^[83]

Rare-earth metal oxalates: Hydrated lanthanide oxalates have been prepared and characterized,^[84] and the loss of the water molecules from these invariably leads to the collapse of the structure.^[85] Several rare-earth metal oxalates have also been synthesized in the presence of alkali cations.^[86] Some of the rare-earth metal oxalates possess cavities and channels.^[87] Oxalato-carbonates of the general formula, $[\text{Ln}(\text{H}_2\text{O})]_2(\text{C}_2\text{O}_4)(\text{CO}_3)_2$ ($\text{Ln} = \text{Eu-Ho}$), exhibit two- and three-dimensional structures.^[88] Rare-earth oxalate frameworks containing ammonium cations are known.^[89,90a] Some of the mixed-metal rare-earth oxalates with two- and three-dimensional structures possess zeolite-like properties (Fig. 1.14).^[90a-e] Thermal decomposition studies of $\text{La}(\text{H}_2\text{O})_2\text{M}(\text{C}_2\text{O}_4)_2 \cdot \text{H}_2\text{O}$ ($\text{M} = \text{K}, \text{NH}_4$), show the existence of crystalline anhydrous $\text{LaM}(\text{C}_2\text{O}_4)_2$ ($\text{M} = \text{K}, \text{NH}_4$) and in some cases ion-exchange properties have also been observed.^[90d,91] A series of ammonium or amine containing uranyl oxalates exhibiting variable coordination around UO_2^{2+} has also been described.^[92]

Oxalates of main group elements, Al, Ga, In, Pb and Bi: Oxalates of the main group elements are scarce. In $[\text{Ni}(\text{bipy})][\text{NaAl}(\text{C}_2\text{O}_4)_3]$ ($\text{bpy} = 2,2'$ -bipyridine) the octahedrally coordinated Al and Na atoms have D_3 symmetry and are linked through the oxalates into a helical three-dimensional network. The tris-chelated $[\text{Ni}(\text{bipy})_3]^{2+}$ cations also have a D_3 symmetry and occupy the large voids within the anionic framework.^[93a] The mutual reflection of the symmetry of the templating cations and the framework is noteworthy. Other hydrated oxalates do not contain porous structures.^[81,93-95]

Tin(II) oxalates: Several tin oxalates with different dimensionalities have been prepared and characterized recently.^[96-100] While the zero-dimensional structure has

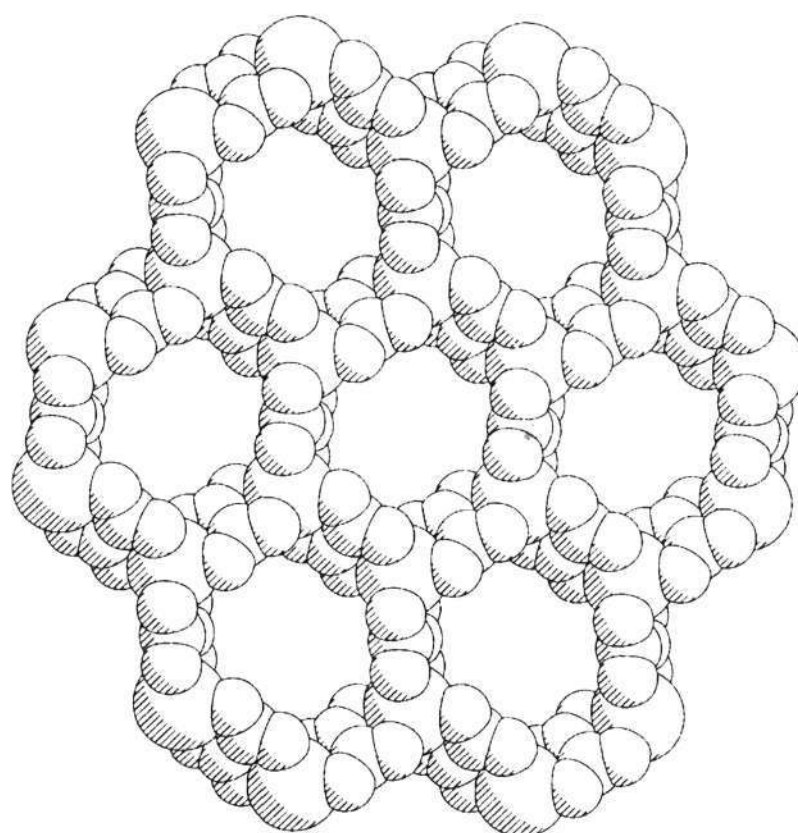
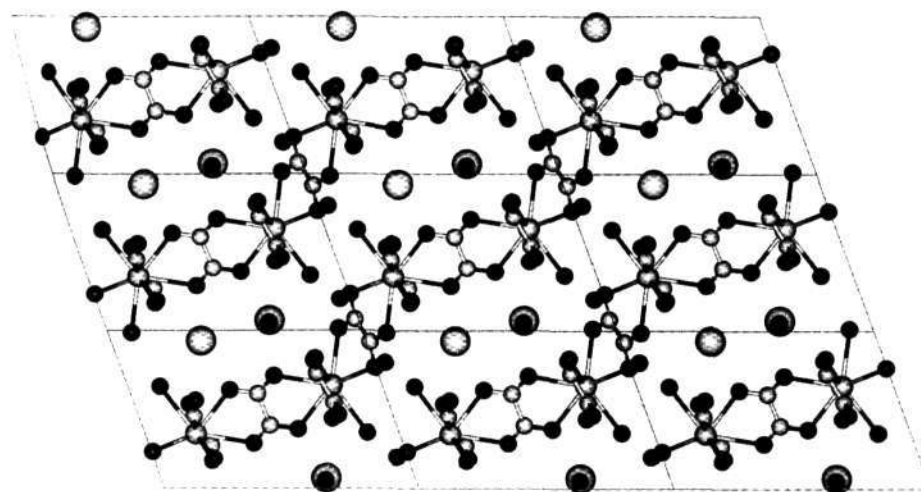
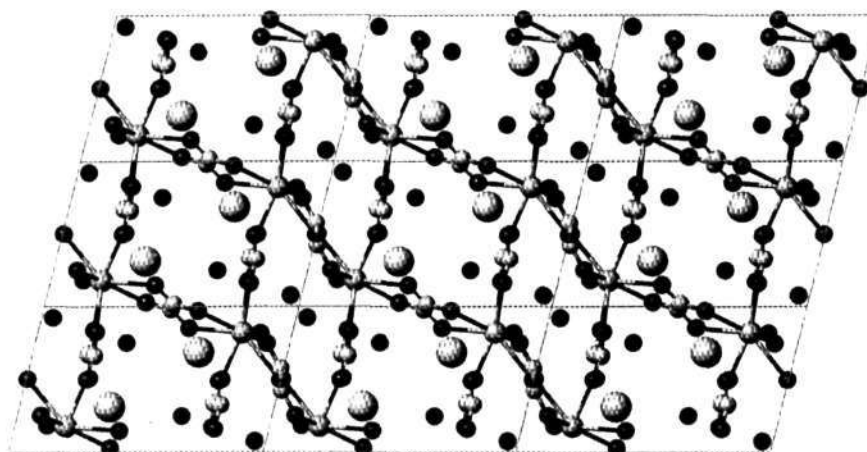


Fig. 1.13. Structure of $\text{K}[\text{C}_6\text{N}_2\text{H}_{13}][\text{Zn}_2(\text{C}_2\text{O}_4)_3] \cdot 4\text{H}_2\text{O}$ showing the AAAAA... stacking of the layers giving rise to one-dimensional channels.



(a)



(b)

Fig. 1.14. (a). Projection of the structure of $\text{La}(\text{H}_2\text{O})_2\text{K}(\text{C}_2\text{O}_4)_2 \cdot \text{H}_2\text{O}$ showing the potassium atoms and the water molecules between the layers. Large gray circles, K; small gray circles, C; small dark circle, O. (b) Projection of the structure of $\text{La}(\text{H}_2\text{O})_2\text{K}(\text{C}_2\text{O}_4)_2 \cdot \text{H}_2\text{O}$ showing the four membered rings, $[\text{La}(\text{C}_2\text{O}_4)]_4$.



the typical monomer structure stabilized by hydrogen bonding, the one-dimensional tin oxalate is similar to the corresponding zinc oxalate $\text{Zn}(\text{C}_2\text{O}_4)(\text{py})_2$,^[80] and exhibits inter-chain interdigitation. The three-dimensional $\text{Na}_4\text{Sn}_4(\text{C}_2\text{O}_4)_3\text{F}_6$ involves bonding between the fluoride ions bound to the Sn centers and the sodium ions in the interlayer regions.^[98]

1.2.3. Higher dicarboxylates

Flexible aliphatic dicarboxylates: Aliphatic dicarboxylates have greater conformational freedom, which manifests itself in the different connecting modes to give rise to novel frameworks. In general, aliphatic carboxylates possess the following features: (i) bidentate and monodentate linking modes, (ii) cis-cis or trans-trans or cis-trans orientation, (iii) three-coordinated oxygen atom connectivity, (iv) pillaring of the metal-oxygen layers or networks, (v) to give rise to secondary building units by acting as capping agents through their carboxylate ends. A large number of compounds using the $[\text{OOC}-(\text{CH}_2)_n-\text{COO}]^{2-}$ ions have been prepared and characterized.^[101-106] In some of these dicarboxylates, metal oxide dimers (0D) or chains (1D) or layers (2D) are linked or pillared by the dicarboxylates to give rise to higher dimensional frameworks as shown by Férey and co-workers.(Fig. 1.15 and 1.16).^[106d,e] The metal oxygen layers have infinite M-O-M linkages formed through edge or corner sharing of the MO_x ($x=4, 5, 6, 7$) polyhedra.

Frameworks involving infinite M-O-M type linkages are also known in the literature.^[50,107] A nickel succinate, $[\text{Ni}_7(\text{C}_4\text{H}_4\text{O}_4)_6(\text{OH})_2(\text{H}_2\text{O})_2].2\text{H}_2\text{O}$, prepared at the interface of a water-cyclohexanol mixture, containing an infinite Ni-O-Ni framework has been described by Forster and Cheetham (Fig. 1.17).^[104a,107] This compound has hydrophobic channels. Several open-framework transition metal dicarboxylates with edge/corner sharing MO_6 (M= Co, Mn, Fe) octahedra are known.^[108] The interlayer separations in these carboxylates is directly related to the

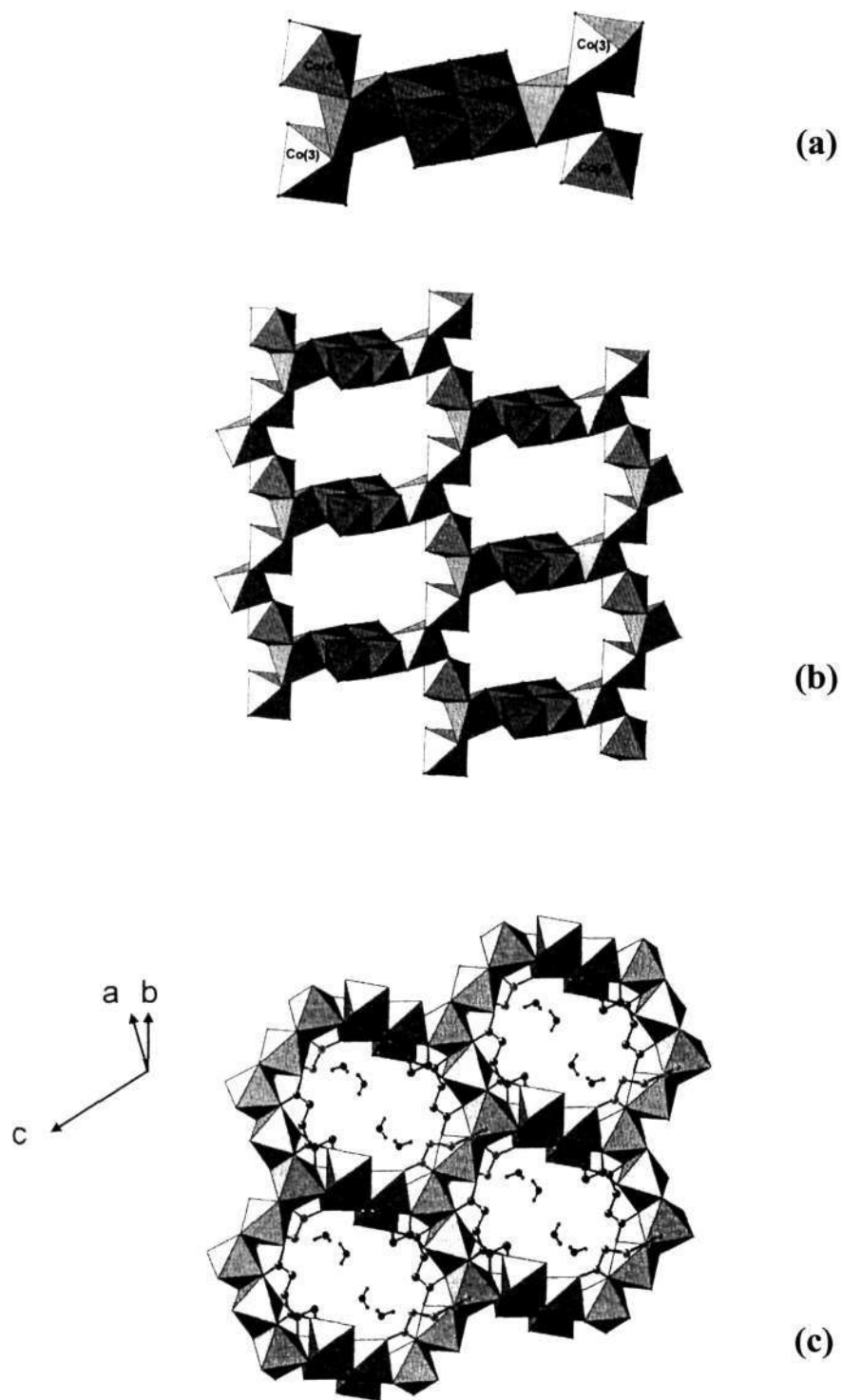


Fig. 1.15. Secondary building units observed in $\text{Co}_4(\text{OH})_2(\text{H}_2\text{O})_2(\text{C}_4\text{H}_4\text{O}_4)_3 \cdot 2\text{H}_2\text{O}$, (a) the tetrameric unit, (b) the helicoidal chain and its connectivity with the tetrameric chain, (c) projection of one layer in $\text{Co}_4(\text{OH})_2(\text{H}_2\text{O})_2(\text{C}_4\text{H}_4\text{O}_4)_3 \cdot 2\text{H}_2\text{O}$.

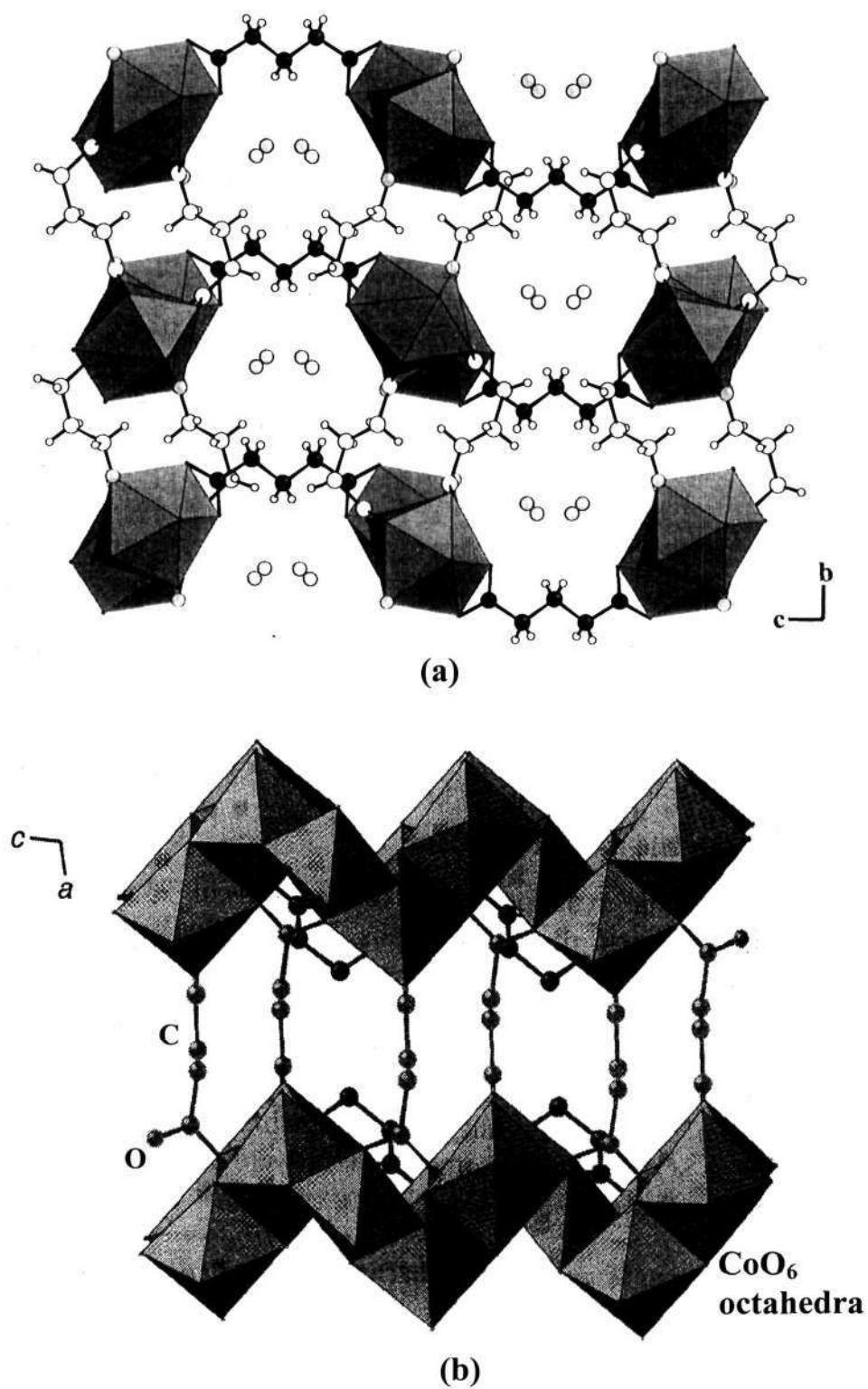


Fig. 1.16. (a) Projection of the structure of the glutarate, $[\text{Pr}(\text{H}_2\text{O})]_2[\text{O}_2\text{C}(\text{CH}_2)_3\text{CO}_2]_3 \cdot 4\text{H}_2\text{O}$, showing the water molecules in the channels. (b) Structure of the three-dimensional $\text{Co}_5(\text{OH})_2(\text{C}_4\text{H}_4\text{O}_4)_4$ (MIL-9) demonstrating the pillaring role of succinate anions.

length of the carbon backbone of the α,ω -dicarboxylic acid.

The presence of infinite M-O-M connectivities in the metal dicarboxylate structures facilitates electronic and magnetic exchanges in one-, two- and three-dimensions. In the recently reported nickel fumarate,^[106a] cobalt succinates,^[106c,e] and cobalt adipate^[105a] the possibility of braiding massive metal-organic structures with predetermined periodic M-O-M arrays with desired electronic, optical and other properties and extending such interactions to larger dimensions via the mediating carboxylate links, has been demonstrated. In the cobalt adipate compound the brucite-type $\text{Co}(\text{OH})_3$ units incorporating magnetic properties are aligned by the adipate anions.^[105a] These solids are to be distinguished from the organodiamine molybdenum oxides (MOXI-n family) based on bimetallic molybdenum oxides described by Zubietta and co-workers.^[27] Metal-dicarboxylate frameworks involving rare-earth metal ions have been shown to possess interesting properties.^[105c,f,106d,f,109] An essential feature in most of these structures is that the dicarboxylates participate in the skeleton with the inorganic species, acting both as part of the extended oxide chains or sheets and as pillars between the latter, in contrast to the Yaghi's metal organic framework (MOF) compounds, where isolated metal clusters are linked by organic links.^[24] The variety of dicarboxylate-derived three-dimensional metal-organic structures prompts to examine the different roles played by the dicarboxylate linkers in these solids. The use of long chain dicarboxylic acids in the construction of open-framework structures generally results in solids involving interpenetration. Although interpenetrated structures contribute to metal-organic structures with lattices resembling the inorganic networks, these catenated structures typically possess low porosities (<20%). This problem has been addressed by Yaghi and co-workers.^[110] Robson and Batten,^[28] in their review on interpenetrating lattices and related issues, refer to the inclusion of guest molecules

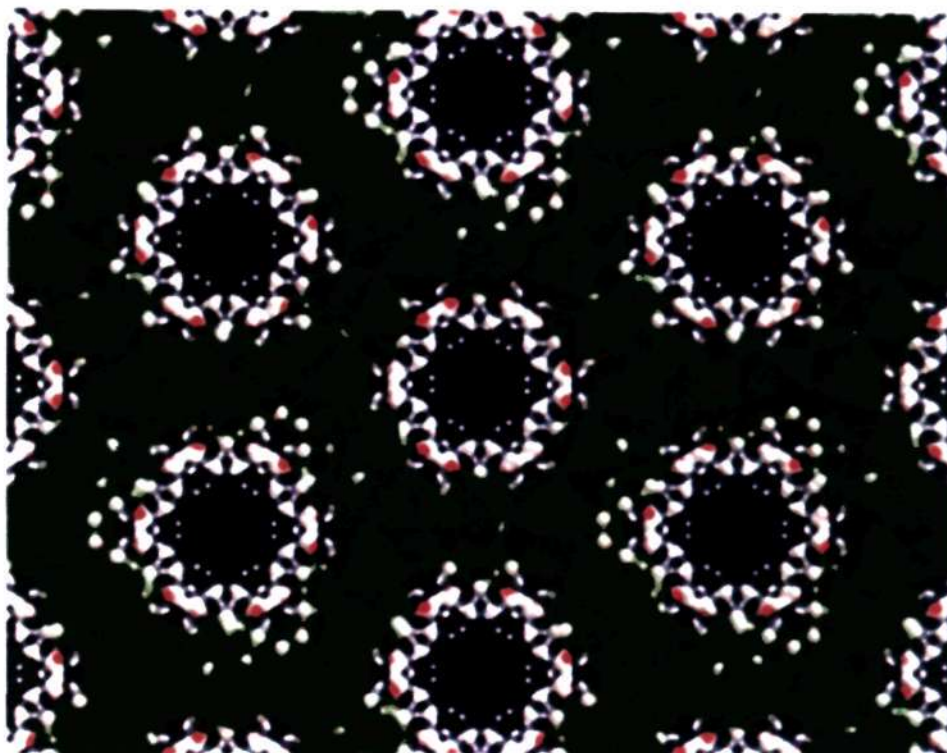


Fig. 1.17. View of the nickel succinate, $[\text{Ni}_7(\text{C}_4\text{H}_4\text{O}_4)_6(\text{OH})_2(\text{H}_2\text{O})_2] \cdot 2\text{H}_2\text{O}$, showing the hydrophobic channels.

into the framework such that they occupy the positions, where the second, independent network is found in the parent structure. The crystal engineering tool – interweaving, which involves the minimal displacement between the independent interpenetrating frameworks has been efficiently used in generating porous architectures.^[110]

Multifunctional carboxylates: A variety of open-framework solids, prepared by using carboxylic acids with two or more carboxylate arms and a rigid cyclic backbone are known. Several metal-squarates and croconates have been reported.^[111-113] In transition metal containing squarates, the metal is invariably in octahedral coordination with respect to the oxygen atoms. Molecular complexes involving squarate anions have been prepared and their magnetic properties investigated.^[111] The observed structural diversity is due to the differences in the binding mode and the orientational preferences of the squarate anion. One-dimensional squarates with chain structures are known.^[112] In some of these metal squarates, the metal take up ancillary ligations from water or DMF or hydroxyl groups.^[112] Vanadium, cobalt and cadmium squarates with two-dimensional layered structures have also been prepared and characterized.^[114a,115a] In addition, a layered iron hydroxy-squarate possessing $\text{Fe}(\text{OH})_3\text{O}_3$ double chains has also been synthesized.^[115b]

Many metal squarates with three-dimensional structures have been reported.^[114,116] In most of the 3D metal squarates, the squarate anion connects the metal through a four-fold monodentate linking mode. A neutral three-dimensional vanadium squarate, containing dimers of edge-sharing $\text{V}^{\text{III}}\text{O}_6$ octahedra and the squarate anions in μ -2 and μ -4 binding mode has been reported.^[114a] A dense manganese squarate, $\text{Mn}_2(\text{OH})_2(\text{C}_4\text{O}_4)$, showing antiferromagnetic behavior has also

been described.^[116a] A three-dimensional cobalt squarate, $[\text{Co}_3(\mu_3\text{-OH})_2(\text{C}_4\text{O}_4)_2]\cdot 3\text{H}_2\text{O}$, with brucite type $\text{Co}(\text{OH})_3$ double chains and squarate anions has been prepared.^[106b] Similar brucite-type double chains have also been observed in the cobalt adipate^[105a] and in the layered iron hydroxy-squarate.^[115b]

Some of the three-dimensional squarates comprise of cage networks entrapping solvent molecules in their cavities.^[114b-d] Metal squarates of the general formula $\text{M}(\text{H}_2\text{O})_2(\text{C}_4\text{O}_4)$ ($\text{M} = \text{Co}, \text{Mn}, \text{Zn}$), with structures related to sodalite, isolated recently, demonstrate how the four-membered square units can assemble to give rise to the sodalite-like cages.^[117] The structures of the squarates can be derived from the sodalite by replacing the Al_2Si_2 rings by the four-membered squarate C_4 rings and linking the squarate rings by the octahedral $\text{M}(\text{H}_2\text{O})_2\text{O}_4$ dianions (Fig. 1.18). A cobalt squarate with three-dimensional structure, $[\{\text{Co}_2(\text{C}_{12}\text{H}_8\text{N}_2)_4(\mu\text{-C}_4\text{O}_4)(\text{OH}_2)_2\}\text{C}_4\text{O}_4]\cdot 8\text{H}_2\text{O}$, exhibits reversible N_2 adsorption.^[114e] The transformation of one-dimensional Mn and Zn squarates into three-dimensional cage network $\text{M}(\text{C}_4\text{O}_4)(\text{OH}_2)_2$ ($\text{M} = \text{Mn}, \text{Zn}$) has been accomplished.^[118]

A series of cerium squarates showing reversible adsorption properties have been reported.^[119a] They form as layer, tunnel and 3D structures, with the common feature being the presence of infinite Ce-O-Ce chains linked via the bis-chelating squarate units. The cerium atoms exist in nine-fold coordination with respect to the oxygens. Lanthanide oxalato-squarates, wherein the oxalate bridged pairs of LnO_9 ($\text{Ln} = \text{La}, \text{Ce}, \text{Eu}$) polyhedra are linked by the squarate units into three-dimensional frameworks with tunnels, occupied by water molecules, have also been described.^[95b, 119b] A layered oxalate-squarate where the two anions are both part of the framework has been discovered recently.^[119c]

Strontium and Barium squarate trihydrates have been synthesized.^[120] Whilst

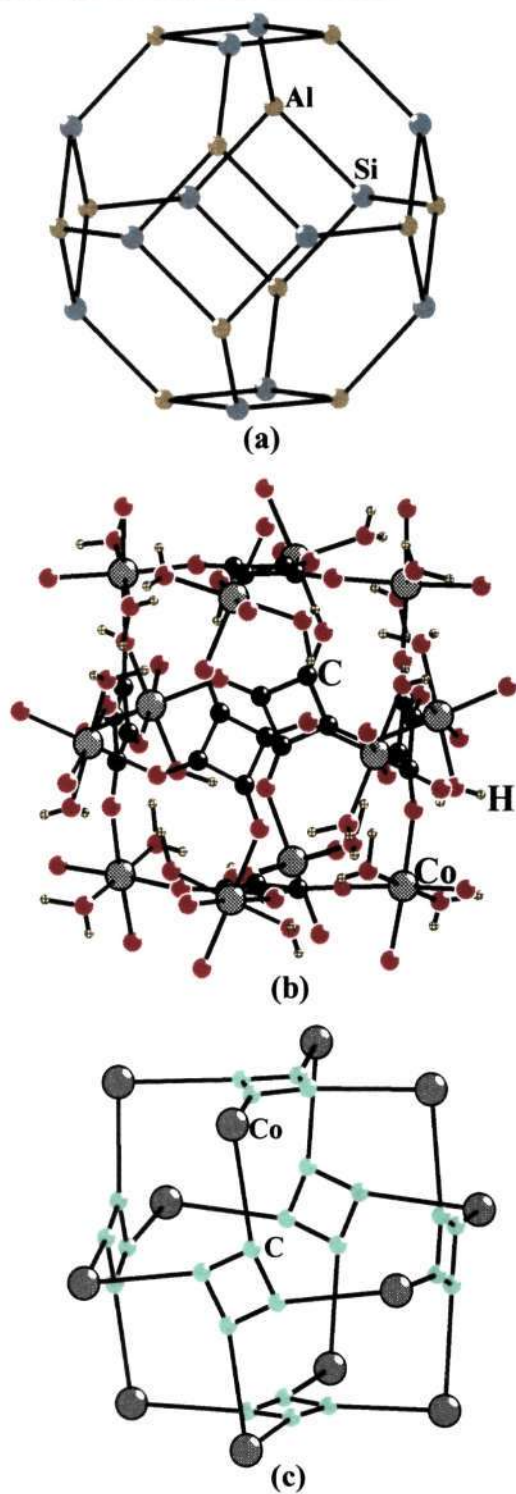


Fig. 1.18. (a) T-atom connectivity in an aluminosilicate sodalite cage. (b) The ball and stick view of analogous sodalite cage in $\text{Co}(\text{H}_2\text{O})_2(\text{C}_4\text{O}_4)$. (c) A different depiction of the sodalite cage in $\text{Co}(\text{H}_2\text{O})_2(\text{C}_4\text{O}_4)$. The oxygens have been omitted and the metal atom is linked to the carbon atoms of the squarate ring to show the analogy with sodalite cage.

the eight coordinated Sr forms a layered structure, the nine-coordinated Ba adopts a three-dimensional structure. The layered $\text{SrC}_4\text{O}_4 \cdot 3\text{H}_2\text{O}$ forms $\text{SrC}_4\text{O}_4 \cdot \text{H}_2\text{O}$ on dehydration without losing its crystalline nature. Both the structures are stabilized by extensive hydrogen bonding. The various structural relationships existing between the metal squarate networks have been discussed elaborately elsewhere.^[121]

Unlike the squarates, open-framework structures based on croconates or rhodizonates are not known hitherto. In spite of the early discovery of the croconic acid and the potassium croconate dihydrate in 1824,^[122] it is only recently that metal croconates have received attention. Thus, various alkali metal croconates stabilized by weak electrostatic interactions between the metal ion and the croconate mono or dianion have been studied.^[123] The structures possess significant π - π interactions as well as hydrogen bond interactions. Transition metal croconates of the general formula, $\text{M}(\text{C}_5\text{O}_5)(\text{H}_2\text{O})_3$ ($\text{M} = \text{Mn}, \text{Ni}, \text{Cu}, \text{Zn}$), with one-dimensional polymeric chain structures have been synthesized.^[124]

Benzene carboxylates: Many metal-organic structures comprising of aromatic carboxylates acting as linkers between metal centers have been synthesized and characterized.^[125-130] The transition metal multifunctional benzene carboxylates generally are six coordinated with an octahedral geometry. The three-dimensional vanadyl terephthalate and isophthalate structures exhibit interesting structural and physical properties.^[126a,b] They have large hydrophobic channels delimited by chains of corner-shared vanadium octahedra and the organic linkers. The terephthalate compound contains trapped terephthalic acid and water guest molecules, which can be removed without collapse of the framework structure. Similar behavior was observed in a chromium terephthalate (MIL-53) as well (Fig. 1.19).^[126c,d] In addition, the chromium terephthalate framework on dehydration shows expansion of the channels by as much as 5 Å, imparting a breathing behavior to the framework.

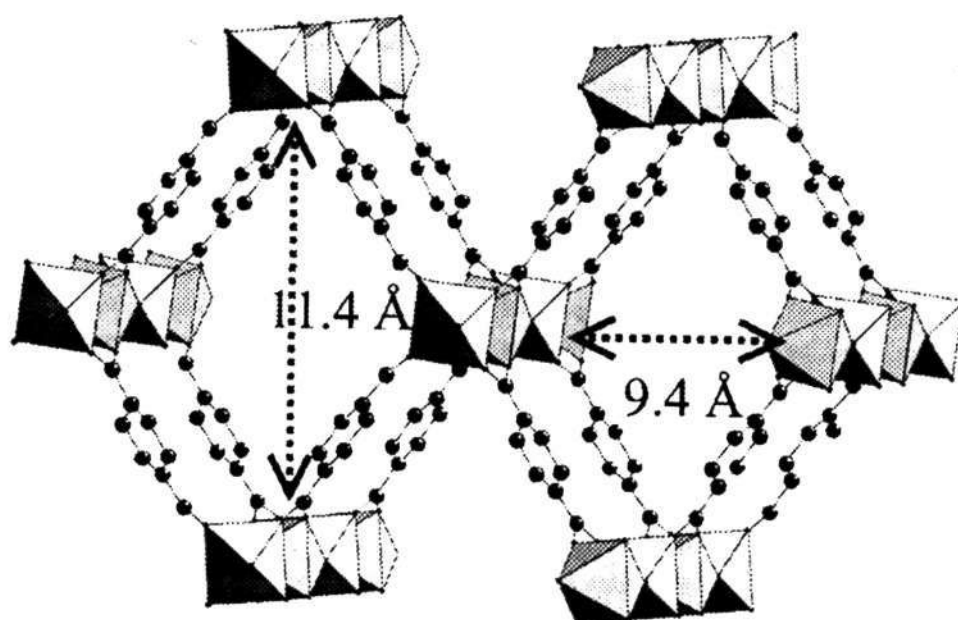


Fig. 1.19. Perspective view of the $\text{Cr}^{\text{III}}(\text{OH})\cdot(\text{O}_2\text{C}-\text{C}_6\text{H}_4-\text{CO}_2)$ (MIL-53ht), showing the channels delimited by four chains of corner-shared chromium octahedra and four terephthalate anions.

Many iron and cobalt trimesates and pyromellitates with open-structures have also been reported.^[127-129] From a structural point of view, the cobalt compounds display interesting feature, wherein the inorganic part is a zero-, one- or two-dimensional unit are connected by the carboxylate giving rise to infinite polymeric structure with channels and cavities. The cobalt pyromellitate, formed in the presence of organic amines, has the co-existence of one and two-dimensional extended polymers.^[129c] Nickel trimesates having auxiliary ligation to the metal center by alcohol molecules have been made.^[130] Ancillary ligation by the amines or macroazacycles is also observed in the copper trimesate framework compounds.^[131] The cadmium 1,3,5- benzene tricarboxylates with two- and three-dimensional structures exhibits interdigitation.^[131c,132] Some of the benzene carboxylates exhibit interesting magnetic properties.^[126a,b]

The rare-earth benzene carboxylates with framework structures have also been prepared. In most cases, the Ln atoms are nine-coordinated and occur as isolated metal polyhedra connected by the carboxylate linkers. While the Yb isophthalate^[133b] and the Gd trimesate^[134a] have two-dimensional structures, all the other lanthanide carboxylates have three-dimensional structures.

Compounds based on cyclohexane-1,3,5-tricarboxylate (ctc) are also known.^[135] In the cobalt compound one-dimensional chains formed by the Co_2O_{10} dimers and the CoO_6 octahedra are connected by the carboxylate into three-dimensions.^[135a] While in the Er compound, the Er(III)O_9 polyhedra are connected to four different ctc units forming a three-dimensional structure with one-dimensional channels occupied by the water molecules.^[135c]

1.2.4. Hybrid compounds

Phosphato- and arsenato- oxalates: One of the families of hybrid structures is formed by incorporating two anionic building units, as exemplified by oxalate-phosphates and oxalate-arsenates, a large number of which have been

synthesized.^[136-145] The phosphate-oxalates of vanadium and manganese, in general, contain the metal in octahedral coordination environment,^[136,137] while the iron and cobalt compounds with five-coordinated metal centers are also known.^[138,139] The only known three-dimensional zinc phosphate-oxalate has an unusual presence of zinc in tetrahedral, square pyramidal and trigonal bipyramidal geometry within the same structure.^[140] Thus, the transition metal phosphate-oxalates are formed as hydrated structures or in the presence of guest species like organic amines or alkali cation and have structures varying from 1- to 3-D.

The organically templated aluminium compounds exhibit two- and three-dimensional structures,^[141] the Ga and In compounds have three-dimensional structures,^[142,143] with the amine offering ancillary coordination in one of the gallium phosphate-oxalate.^[142b] Tin(II) phosphate-oxalate has a two-dimensional structure with a hybrid layer formed by the connectivity between the metal centers *via* phosphate and oxalate units.^[144] In the phosphate-oxalates, the oxalate plays two types of roles. In some of them, the layers are of the inorganic metal phosphate with the oxalate acting as pillars, while in others the oxalate unit is an integral part of the layer, linking the metal phosphate ladders to form hybrid layers. The manganese phosphate-oxalate, $[\text{H}_3\text{N}(\text{CH}_2)_3\text{NH}_3][\text{Mn}_2(\text{HPO}_4)_2(\text{C}_2\text{O}_4)(\text{H}_2\text{O})_2]$ has hybrid layers (Fig.1.20 a),^[137c] whilst the iron-phosphate-oxalate, $[\text{NH}_3(\text{CH}_2)_2\text{NH}_3]_{1.5}[(\text{Fe}_3\text{PO}_4(\text{HPO}_4)_3(\text{C}_2\text{O}_4)_{1.5})_x \cdot \text{H}_2\text{O}]$ ($x = 1.5-2.0$),^[139c] represents the former (Fig. 1.20 b). The iron phosphate-oxalate shows antiferromagnetic behavior (T_N of 46 K) and also reversible adsorption behavior. A systematic phase study of the reactions of V_2O_5 in the $\text{H}_2\text{C}_2\text{O}_4/\text{H}_3\text{PO}_4/\text{NH}_4\text{OH}$ system under hydrothermal syntheses has shown that the oxalic acid plays the role of a reducing agent.^[137a] The compounds isolated as single crystals occur in the H_3PO_4 -rich regions, while the NH_4OH - and $\text{H}_2\text{C}_2\text{O}_4$ -rich regions favor poorly crystalline phases, devoid of any

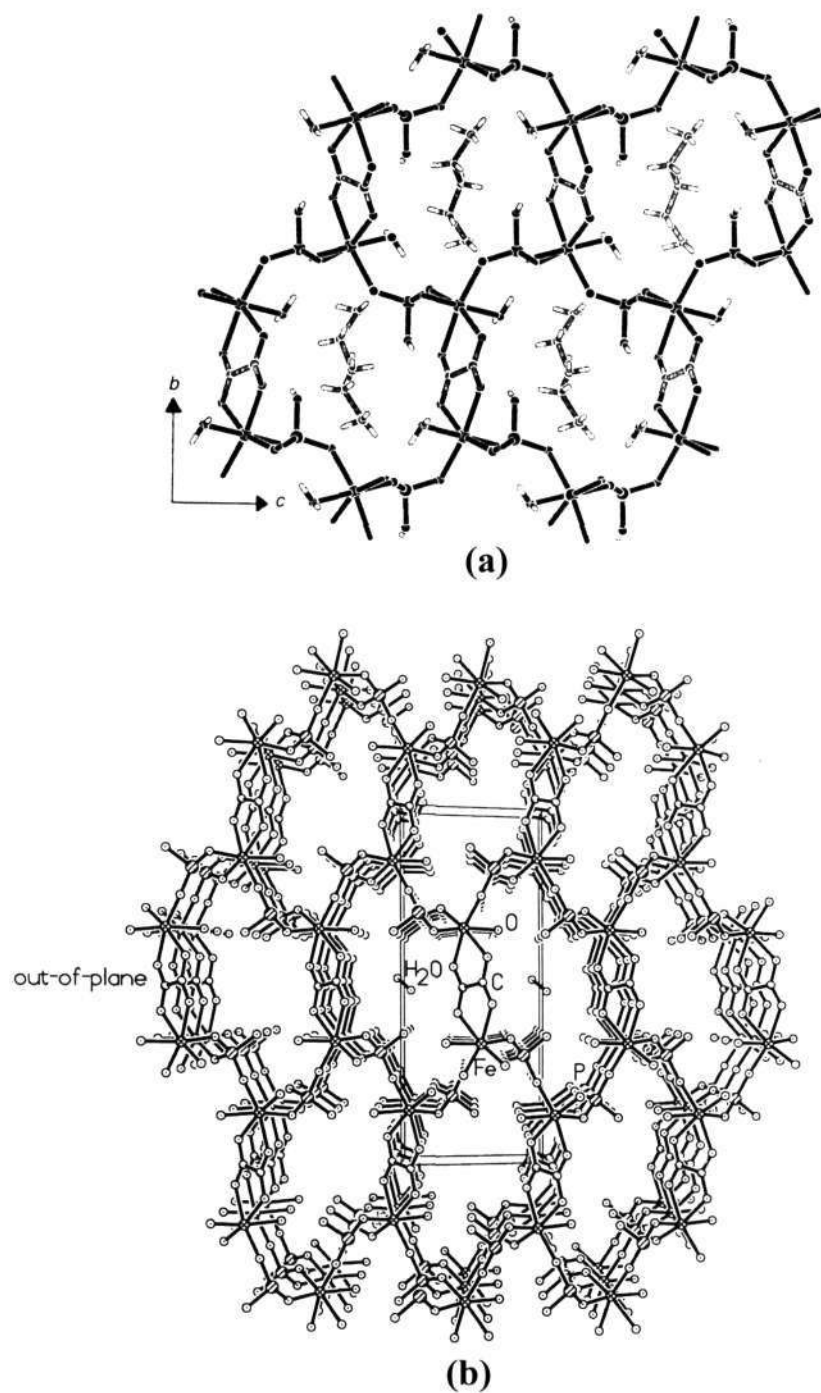


Fig. 1.20. a) Projection of the $[\text{H}_3\text{N}(\text{CH}_2)_3\text{NH}_3][\text{Mn}_2(\text{HPO}_4)_2(\text{C}_2\text{O}_4)(\text{H}_2\text{O})_2]$ showing the 12-membered apertures formed by the connectivities between the Mn centers and the *in-plane* oxalate and phosphate moieties. (b) Structure of $[\text{Fe}_2(\text{H}_2\text{O})_2(\text{HPO}_4)_2(\text{C}_2\text{O}_4)] \cdot \text{H}_2\text{O}$ showing the channels formed by the linking of the inorganic iron phosphate layers by the *out-of-plane* oxalate units.

oxalate anions.^[137a] The transformation of an one-dimensional iron arsenate-oxalate into two- and three- dimensional iron arsenates has been reported.^[145b] It appears that the phosphate- and arsenate-oxalates are intermediates between the oxalates and the phosphates (arsenates).

Other open-framework structures involving mixed anions, such as the phosphato-acetate,^[146] phosphono-oxalate,^[147,148] squarato-oxalates,^[119] carbonato-oxalates,^[88] isonicotinato-oxalate^[83b] and bipyridyl-squarates^[149] are also known. These compounds show variable dimensionality, with some of them exhibiting reversible dehydration and interesting optical properties.

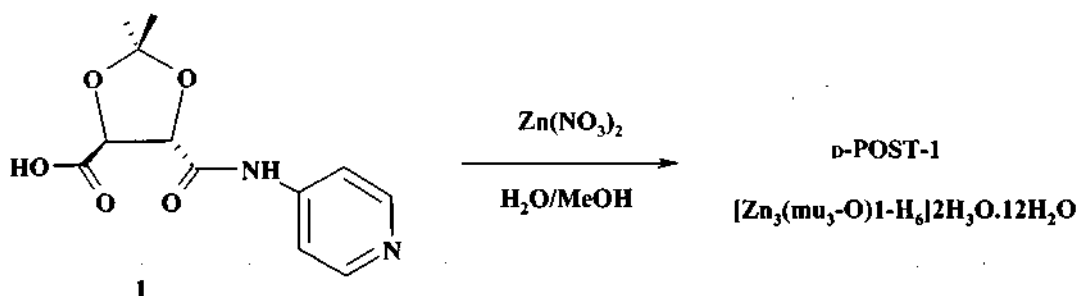
Porous hybrid architectures: Engineering new microporous structures using metal-organic frameworks is a topic of current interest. To this end, different strategies have been employed with considerable success. Some of these materials not only show openness but also exhibit interesting physical and chemical properties, making them more interesting than their pure inorganic counterparts.^[23-30] Special issues of journals dedicated to the design of hybrid nanoporous solids bear testimony to the rapid progress made in this area.^[3f,24b] One of the strategies to prepare the hybrid solids is to use appropriate inorganic building units along with a rigid organic linker to bridge the building units. The carboxylate linkers (i) can respond efficiently to chemical environments thereby enabling the tuning of the valency of the anion generated, (ii) exhibit different modes of linking, and (iii) generate the secondary building units.

The “top down” design logic, also referred as reticular synthesis, has been demonstrated recently by the arrangement of well-defined molecular building blocks into periodic frameworks by copolymerizing them with organic linkers in a polar solvent under mild conditions.^[24b,150-153] This strategy yields stable porous structures, unlike the supramolecular assemblies. This strategy is exemplified by the

preparation of the metal organic framework (MOF-n) structures, as illustrated in Figure 1.21.^[150] Another strategy is to assemble the relevant inorganic/organic building units under suitable reaction conditions to give rise to known inorganic frameworks.^[24a,b]

Large void spaces are created in these structures due to the use of long linkers. Interpenetration (maximal displacement of the catenated frameworks) and interweaving (minimal displacement of catenated frameworks) in the frameworks, often occur in frameworks containing linkers with long organic backbones. In some of the designed open-framework structures, manipulation of the steric factors and solvent molecules help in preventing interpenetration.^[110] Open-framework solids, thus prepared, show remarkable thermal stabilities and adsorption behavior (Fig. 1.22).^[150a,f,152a,153a,b] These hybrid compounds have been reviewed in detail.^[24a,b,150f,172a,c]

A copper trimesate, $[\text{Cu}_3(\text{C}_9\text{H}_3\text{O}_6)_2(\text{H}_2\text{O})_3]_n$, built up from dimeric cupric tetracarboxylate units exhibits interesting structure and properties.^[154] This compound has a neutral framework structure with square-channels (Fig. 1.23), lined by aqua ligands, which can be replaced by organic functional groups. A homochiral metal-organic compound, $[\text{Zn}_3(\mu_3\text{-O})(1\text{-H})_6] \cdot 2\text{H}_2\text{O} \cdot 12\text{H}_2\text{O}$ (D-POST-1) has been made by using an oxo-bridged trinuclear enantiopure chiral metal carboxylate as the building block, employing the below reaction.^[155]



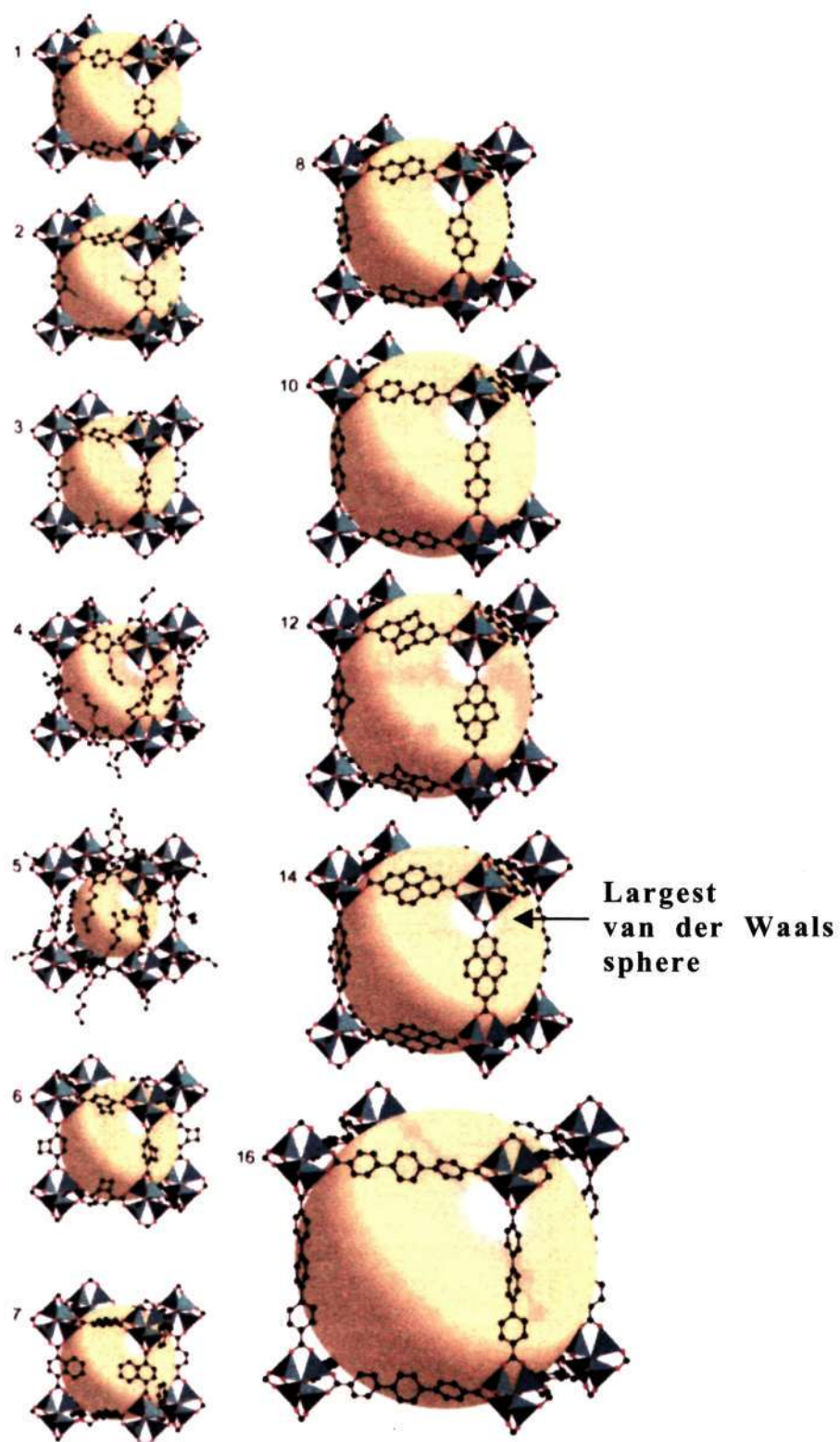


Fig. 1.21. Structures of isoreticular metal organic frameworks, IRMOF- n ($n = 1$ through 7, 8, 10, 12, 14 and 16), labeled respectively. Color scheme: ZnO_4 tetrahedra – blue; O – red; C – black; Br – green.

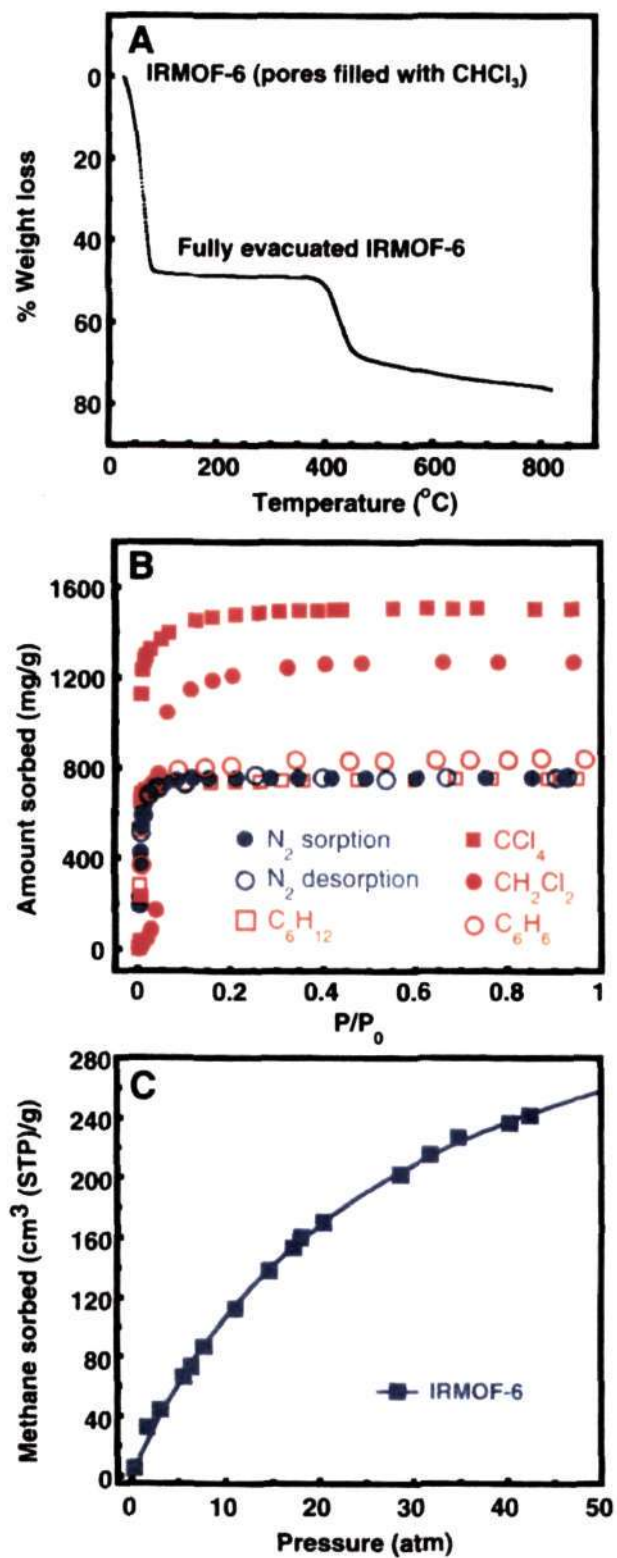


Fig. 1.22. (A) Thermogravimetric curve of IRMOF-6 including its (B) gas and organic vapor sorption isotherms and (C) its voluminous uptake of methane gas fitted at 298 K with the Langmuir equation.

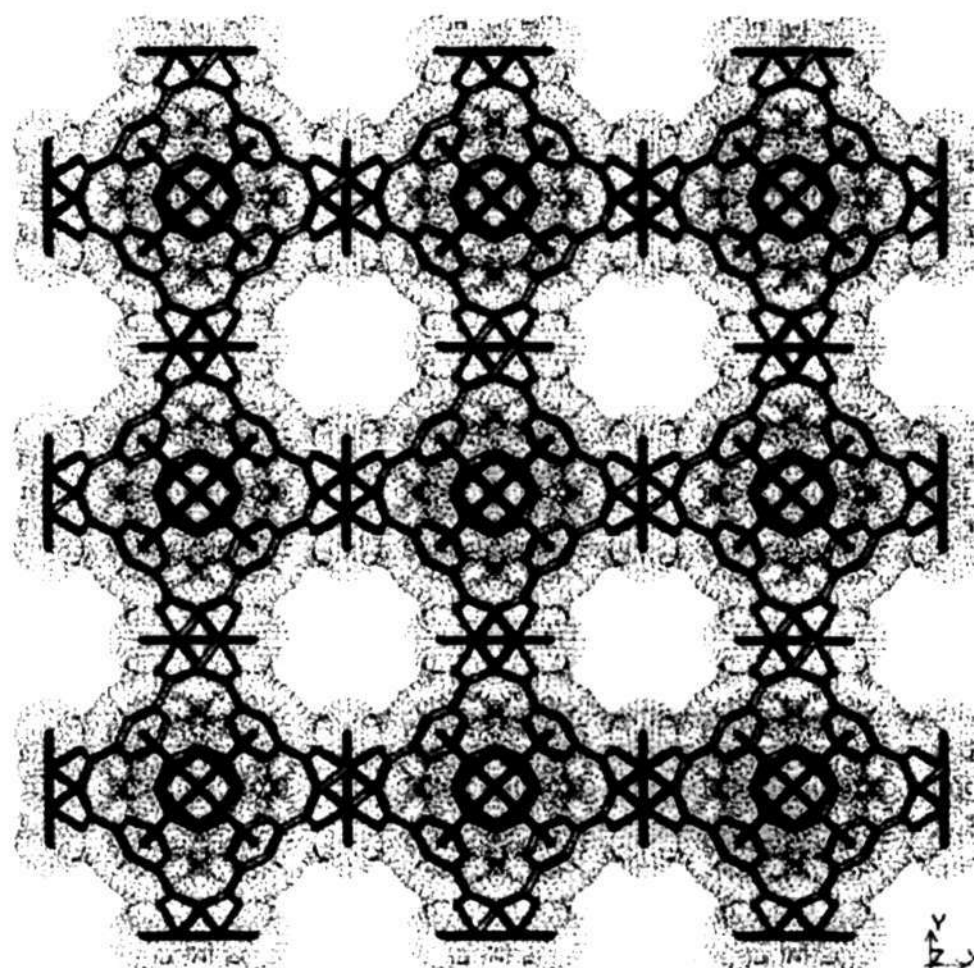


Fig. 1.23. Structure of $[\text{Cu}_3(\text{C}_9\text{H}_3\text{O}_6)_2(\text{H}_2\text{O})_3]_n$, HKUST-1 showing nanochannels with fourfold symmetry.

The three zinc ions are connected to six carboxylate units through a bridging oxygen forming a trinuclear unit which acts as the secondary building unit. The structure consists of two-dimensional layers. Stacking of these layers gives rise to chiral 1-D channels ($\sim 13.4 \text{ \AA}$). The three pyridyl groups that extrude into the interior of the channels impart ion-exchange properties. This compound also catalyzes transesterification reactions and shows remarkable enantioselectivity due to the chiral environment of the channel (Fig. 1.24).

A thermally stable material, $[\text{Zn}_8(\text{SiO}_4)(\text{C}_8\text{H}_4\text{O}_4)_6]_n$, having a $\text{Zn}_8(\text{SiO}_4)$ core, with the SiO_4 tetrahedra occupying the center and bridging eight different Zn atoms, capped by terephthalate moieties, has been prepared recently.^[156]

1.2.5. Carboxylates with additional binding sites

A family of phosphonocarboxylates ($[\text{O}_3\text{P-R-COO}]^{3-}$) wherein the end-groups can have a variety of binding modes has been isolated recently. The phosphonocarboxylates containing transition elements,^[157] zinc,^[158a] praseodymium^[158b] and main group elements^[159] are known in the literature. The use of phosphonocarboxylates with an additional N-functional group gives rise to structures wherein the channels are formed by the linking of metal centers through the O_3P and CO_2 end-groups, with the amino groups protruding into them.^[160] A three-dimensional hybrid compound, $[\text{K}_2[\text{CoO}_3\text{PCH}_2\text{N}(\text{CH}_2\text{CO}_2)_2]]_6 \cdot x\text{H}_2\text{O}$, made using (phosphonomethyl) iminodiacetic acid (PMIDA), has layers approximating to the gray arsenic structure.^[161] Compounds of PMIDA with Zn and Zr have also been made.^[162,163]

A family of nicotines and isonicotines with open-architectures possessing properties arising from the unsymmetrical nature of the ligand, has been described.^[164] The ligand has been tailored to engender acentric diamondoid coordination networks by linking tetrahedral metal clusters and tuning the push-pull

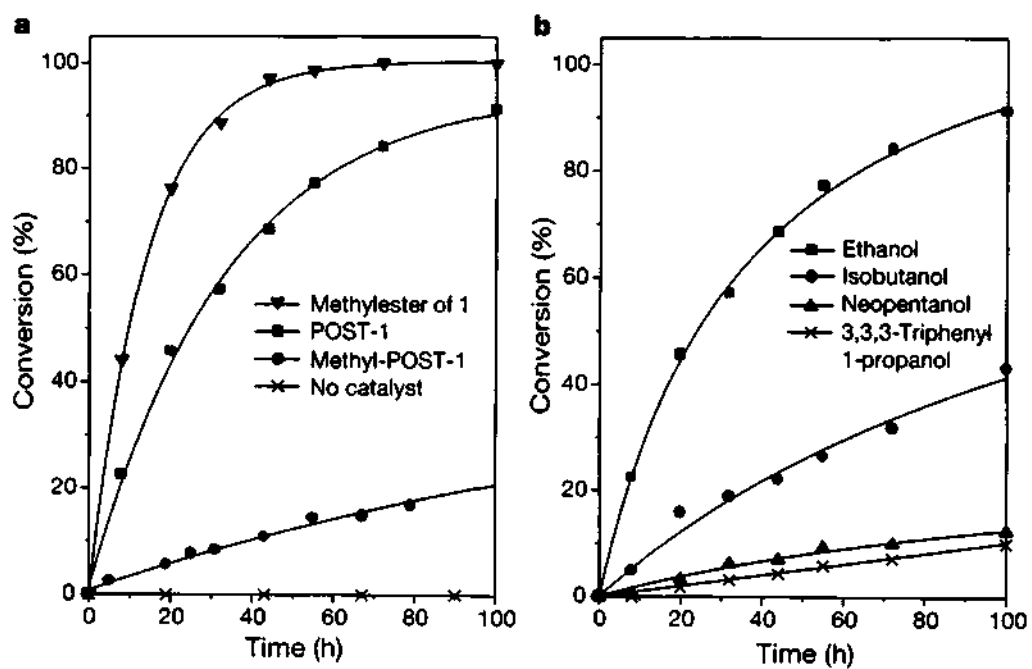


Fig. 1.24. Catalytic activity of POST-1 in transesterification reactions. (a) transesterification of 1-acetyl-2,4-dinitrobenzene with ethanol in the presence of POST-1. (b) transesterification of alcohols in the presence of POST-1. All the reactions were carried out in CCl_4 at 27°C .

effects present in the ligand to give rise to second-order non-linearity in some of the compounds.^[165] A thermally stable porous cobalt(II) nicotinate, $\text{Co}_2(\text{H}_2\text{O})(\text{C}_6\text{H}_4\text{O}_2\text{N})_4 \cdot \text{G}$ ($\text{G} = 0.5\text{EtOH}/0.5\text{H}_2\text{O}$ or $\text{C}_6\text{H}_5\text{CH}_2\text{OH}$), with channels containing ethanol, water or benzyl alcohol molecules and showing reversible adsorption behavior has been isolated.^[166] The three-dimensional open framework material, $\{[\text{Cu}(\text{isonicotinate})_2] \cdot 2\text{H}_2\text{O}\}_n$, has spiral channels and exhibits solvent selectivity comparable to that of the zeolites.^[167] $\{[\text{Zn}(\text{C}_6\text{H}_4\text{O}_2\text{N})_2] \cdot \text{MeOH} \cdot 2\text{H}_2\text{O}\}_n$ with a $4^2 \cdot 8^4$ net topology, based solely on square planar nodes, occludes naphthalene and nitrobenzene guest molecules.^[168] Use of pyrazinecarboxylate gives rise to one-dimensional chains and two-dimensional layers with Cu^{2+} ions, and a unique three-dimensional architecture with Cd^{2+} ions.^[169a] These compounds, contain one-dimensional serpentine motif (resembling inosilicates) along with the two-dimensional square grid to form the three-dimensional architecture.^[169b] A mixed metal compound, $\{[\text{ZnCu}(2,4\text{-pyridyldicarboxylate})_2(\text{H}_2\text{O})_3(\text{DMF})] \cdot \text{DMF}\}_n$, which has Zn(II) at the node of the network acting as a linker and Cu(II) in the channel wall has been synthesized and characterized.^[170] The Cu^{II} ions are amenable for guest coordination. Other framework structures of different dimensionalities with pyridyldicarboxylate anions have also been reported.^[171] 2,2'-bipyridyl-4,4'-carboxylic acid yields layered compounds with transition metal ions^[172a] and rigid three-dimensional microporous frameworks with Cd^{2+} ions.^[172b]

1.2.6. Future prospects

The discussion of various metal carboxylates with open-architectures presented in the previous sections should suffice to illustrate not only the variety of structures, but also how the carboxylate unit provides an excellent means for designing novel materials. Based on the observation of a structural hierarchy in the different dimensional phosphate structures it would be interesting to investigate the

possibility of the presence of such structures in metal-organic systems also. It should be possible to obtain different environments in the channels of the three dimensional structures, considering that even simple dicarboxylates crystallized under appropriate conditions give rise to channels with hydrophobic environments. Scheme 1.2 illustrates a possible strategy to synthesize frameworks with channels containing predetermined functionalities. In this respect hydrothermal and solvothermal routes are likely to yield several more novel materials with interesting properties.

References

1. A. F. Cronstedt, *Akad. Handl. Stockholm*, **1756**, *17*, 120.
2. R. M. Barrer, *J. Chem. Soc.* **1948**, 127.
3. (a) R. M. Barrer, "Hydrothermal Chemistry of Zeolites", Academic Press (London) 1982. (b) C. S. Cundy, P. A. Cox, *Chem. Rev.* **2003**, *103*, 663 and references therein.
4. (a) G. Férey, *Chem. Mater.* **2001**, *13*, 3084. (b) G. Férey, *J. Solid State Chem.*, **2000**, *152*, 37 and related articles in the same issue. (c) G. Férey, C. R. Acad. Sci., Paris, t. 1, *Serie II c*, **1998**, 1. (d) G. Férey, *J. Fluorine Chem.* **1995**, *72*, 187 and references therein.
5. M. E. Davis, *Nature* **2002**, *417*, 813 and references therein.
6. (a) R. Szostek, "Handbook of Molecular Sieves", Academic Press (London), 1994. (b) W. M. Meier, D. H. Olson, C. Baerlocher, *Atlas of Zeolite Structure Types*, Elsevier London, 1996. (c) Verified Syntheses of Zeolitic Materials, Eds. H. Robson, K. P. Lillerud, 2nd Ed. 2001, Elsevier Science B. V.
7. A. K. Cheetham, G. Férey, T. Loiseau, *Angew. Chem. Int. Ed. Engl.* **1999**, *38*, 3269.
8. (a) J. M. Thomas, *Angew. Chem. Int. Ed. Engl.* **1999**, *38*, 3588. (b) J. M. Thomas, *Chem. Eur. J.* **1997**, *3*, 1557.
9. F. Schuth, W. Schmidt, *Adv. Mater.* **2002**, *14*, 629.
10. W. Lowenstein, *Amer. Mineral.* **1954**, *39*, 92.
11. C. N. R. Rao, *Proc. Indian Acad. Sci. (Chem. Sci.)* **2002**, *113*, 363.
12. S. T. Wilson, B. M. Lok, C. A. Messina, T. R. Cannan, E. M. Flanigen, *J. Am. Chem. Soc.* **1982**, *104*, 1146.
13. E. M. Flanigen, R. W. Grose, "Molecular Sieves and Zeolites-1", *Amer. Chem. Soc. Adv. Chem. Series*, 1971.
14. (a) M. E. Davis et al., *J. Am. Chem. Soc.* 1989, *111*, 3919. (b) M. E. Davis, C. Saldarriga, C. Montes, J. M. Garces, C. Crowder, *Nature* **1988**, *331*, 698.
15. (a) Q. H. Huo et al., *J. Chem. Soc. Chem. Commun.* **1992**, 875. (b) G. Y. Yang, S. Sevov, *J. Am. Chem. Soc.* **1999**, *121*, 8389. (c) R. F. Lobo, M. E. Davis, *J. Am. Chem. Soc.* **1997**, *119*, 8474. (d) M. Estermann, L. B. McCusker, C. Baerlocher, A. Merrouche, H. Kessler, *Nature*, London, **1991**, 352, 320.
16. M. E. Davis, R. F. Lobo, *Chem. Mater.* **1992**, *4*, 756.

17. (a) G. D. Stucky, P. Feng, X. Bu, *Angew. Chem. Int. Ed. Engl.* **1995**, *34*, 1745. (b) G. D. Stucky, P. Feng, X. Bu, *Chem. Mater.* **1996**, *8*, 145.
18. (a) G. D. Stucky, P. Feng, X. Bu, *Nature*, **1997**, *388*, 735. (b) S. T. Wilson, *Stud. Surf. Sci. Catal.* **1991**, *58*, 137.
19. F. Ray, G. Sankar, J. M. Thomas, P. A. Barrett, D. W. Lewis, C. R. A. Catlow, *Chem. Mater.* **1995**, *7*, 1435.
20. (a) S. Neeraj, S. Natarajan, C. N. R. Rao, *Angew. Chem. Int. Ed. Engl.* **1999**, *38*, 3480. (b)
21. C. N. R. Rao, S. Natarajan, S. Neeraj, *J. Am. Chem. Soc.* **2000**, *122*, 2810.
22. (a) A. Müller, H. Reuter, S. Dillinger, *Angew. Chem. Int. Ed. Engl.* **1995**, *34*, 2328. (b) P. Y. Zavilij, M. S. Whittingham, *Acta Cryst.* **1999**, *B55*, 627.
23. (a) J. M. Lehn, *Supramolecular Chemistry, Concepts and Perspectives*, VCH, Weinheim, 1995. (b) B. Moulton, M. J. Zaworotko, *Advances in Supramolecular Chemistry*, JAI Press Inc. 2000, Vol. 7, p.235 and references therein. (c) *Supramolecular Organization and Materials Design*, eds: W. Jones and C. N. R. Rao, Cambridge Univ. Press, 2002.
24. (a) M. Eddaoudi, D. B. Moler, H. Li, B. Chen, T. M. Reineke, M. O'Keeffe, O. M. Yaghi, *Acc. Chem. Res.* **2001**, *34*, 319 and references therein. (b) M. Eddaoudi, J. Kim, D. Vodak, A. Sudik, J. Wachter, M. O'Keeffe, O. M. Yaghi, *Proc. Natl. Acad. Sci., USA* **2002**, *99*, 4900 and related articles in the same issue.
25. B. Moulton, M. J. Zaworotko, *Chem. Rev.* **2001**, *101*, 1629.
26. (a) C. J. Kepert, M. J. Rosseinsky, *Chem. Commun.* **1999**, 375. (b) E. J. Cussen, J. B. Claridge, M. J. Rosseinsky, C. J. Kepert, *J. Am. Chem. Soc.* **2002**, *124*, 9574 and references therein.
27. P. J. Hagrman, D. Hagrman, J. Zubieta, *Angew. Chem. Int. Ed. Engl.* **1999**, *38*, 2638.
28. (a) S. R. Batten, R. Robson, *Angew. Chem. Int. Ed. Engl.* **1998**, *37*, 1460 and references therein. (b) R. Robson, *J. Chem. Soc. Dalton Trans.* **2000**, 3735. (c) S. R. Batten, *Cryst. Eng. Comm.* **2001**, *18*, 1.
29. A. Clearfield, *Curr. Opin. Solid State Mater. Sci.*, **1996**, *1*, 268 and references therein.
30. C. Janiak, *Angew. Chem. Int. Ed. Engl.* **1997**, *36*, 1431.
31. (a) *Comprehensive Coordination Chemistry*, Ed. G. Wilkinson, Pergamon Press, Toronto, Canada, Vol. 5, 1987. (b) R. C. Mehrotra, R. Bohra, *Metal Carboxylates*, Academic Press, London, 1983.

32. (a) Y. Liao, W. W. Schum, S. Miller, *J. Am. Chem. Soc.* **2002**, *124*, 9336. (b) V. M. Rao, D. N. Sathyanarayana and H. Manohar, *J. Chem. Dalton Trans.* **1983**, 2167.
33. (a) G. Davey, F. S. Stephens, *J. Chem. Soc. (A)*, **1971**, 103. (b) I. Goldberg, F. H. Herbstein, *Acta Cryst.* **1973**, *B29*, 246.
34. (a) R. Kiriyaama, *Acta Cryst.* **1954**, *7*, 482. (b) H. Kiriyaama, *Bull. Chem. Soc. Japan* **1962**, *35*, 1199.
35. C. I. Stalhandske, *Acta Chemica Scandinavica* **1969**, *23*, 1525.
36. J. Hatibarua, G. S. Parry, *Acta Cryst.* **1972**, *B28*, 3099 and references therein.
37. (a) B. Kozlevkar, N. Lah, S. Makuc, P. Segedin, F. Pohleven, *Acta Chim. Slov.* **2000**, *47*, 421. (b) B. Morosin, R. C. Hughes, Z. G. Soos, *Acta Cryst.* **1975**, *B31*, 762. (c) V. J. Pickardt, *Acta Cryst.* **1981**, *B37*, 1753.
38. (a) B. K. Koo, *Bull. Korean Chem. Soc.* **2001**, *22*, 113. (b) J. E. Fiscus, S. Shotwell, R. C. Layland, M. D. Smith, H. C. zur Loye, U. H. F. Bunz, *Chem. Commun.* **2001**, 2674.
39. S. R. Batten, B. F. Hoskins, B. Moubaraki, K. S. Murray, R. Robson, *Chem. Commun.* **2000**, 1095.
40. F. A. Cotton, Y. Kim, *J. Am. Chem. Soc.* **1993**, *115*, 8511 and references therein.
41. J. Lu, W. T. A. Harrison, A. J. Jacobson, *Chem. Commun.* **1996**, 399.
42. (a) C. Cadiou, R. A. Coxell, A. Graham, A. Harrison, M. Helliwell, S. Parsons, R. E. P. Winpenny, *Chem. Commun.* **2002**, 1106 and references therein. (b) D. J. Price, S. R. Batten, B. Moubaraki, K. S. Murray, *Chem. Commun.* **2002**, 762. (c) M. Eshel, A. Bino, I. Felner, D. C. Johnston, M. Luban, L. L. Miller, *Inorg. Chem.* **2000**, *39*, 1376 and references therein. (d) J. G. Mao and A. Clearfield, *Inorg. Chem.* **2002**, *41*, 2319.
43. (a) A. J. Blake, C. M. Grant, S. Parsons, J. M. Rawsons, R. E. P. Winpenny, *J. Chem. Soc. Chem. Commun.* **1994**, 2363. (b) S. P. Watton, P. Fuhrmann, L. E. Pence, A. Caneschi, A. Cornia, G. L. Abbatic, S. J. Lippard, *Angew. Chem. Int. Ed. Engl.* **1997**, *36*, 2774.
44. (a) H. L. Li, M. Eddaoudi and O. M. Yaghi, *Angew. Chem. Int. Ed. Engl.* **1999**, *38*, 653. (b) Y. H. Liu, Y. L. Lu, H. C. Wu, J. C. Wang, K. L. Lu, *Inorg. Chem.* **2002**, *41*, 2592.
45. G. Dong, Z. Bing-guang, D. C. Ying, P. Ke-liang, M. Qing-jin, *J. Chem. Soc. Dalton Trans.* **2002**, 3783.
46. G. C. Guo, T. C. W. Mak, *Chem. Commun.* **1999**, 813.

47. (a) J. Legendziewicz, M. Borzechowska, G. Oczko, G. Meyer, *New J. Chem.* **2000**, 24, 53. (b) I. Kutlu, G. Meyer, G. Oczko, J. Legendziewicz, *Eur. J. Solid State Inorg. Chem.* **1997**, 34, 231 and references therein. (c) J. Legendziewicz, G. Oczko, G. Meyer, *Polyhedron* **1991**, 10, 1921.
48. (a) R. G. Bryant, V. P. Chacko, M. C. Etter, *Inorg. Chem.* **1984**, 23, 3580 and references therein.
49. (a) Y. Laget, C. Hornick, M. Drillon, *J. Mater. Chem.* **1999**, 9, 169. (b) S. Yamanaka, T. Sako, K. Seki, M. Hattori, *Solid State Ionics* **1992**, 53, 527. (c) S. Yamanaka, T. Sako, M. Hattori, *Chem. Lett.* **1989**, 1869.
50. R. Kuhlman, G. L. Schimek, J. W. Kolis, *Inorg. Chem.* **1999**, 38, 194.
51. I. A. Koval, P. Gamez, O. Roubeau, W. L. Driessen, M. Lutz, A. L. Spek, Reedijk, *Inorg. Chem.* **2003**, 42, 868.
52. W. Schmitt, E. Baissa, A. Mandel, C. E. Anson, A. K. Powell, *Angew. Chem. Int. Ed. Engl.*, **2001**, 40, 3578.
53. (a) L. Brammer, M. D. Burgard, M. D. Eddleston, C. S. Rodger, N. P. Rath, H. Adams, *Cryst. Engg. Commun.* **2002**, 4(44), 239. (b) L. Brammer, M. D. Burgard, C. S. Rodger, J. K. Swearingen, N. P. Rath, *Chem. Commun.* **2001**, 2468. (c) C. M. Rivas, L. Brammer, *Coord. Chem. Rev.*, **1999**, 183, 43. (d) G. R. Desiraju, *Crystal Engineering: The Design of Organic Solids*, Elsevier, New York, 1989.
54. G. S. Papaefstathiou, L. R. MacGillvray, *Angew. Chem. Int. Ed. Engl.* **2002**, 41, 2070.
55. (a) C. Sterling, *Nature* **1965**, 205, 588 and references therein. (b) C. Sterling, *Science*, **1964**, 146, 518. (c) N. Gererd, G. W. Marion, A. T. Sorel, *Bull. Soc. Chim. Fr.* **1968**, 11, 4367. (d) O. C. Pluchery, J. C. Mutin, J. Bouillot, J. C. Niepce, *Acta Cryst.* **1989**, C45, 1699. (e) I. L. Jenkins, F. H. Moore, M. J. Waterman, *J. Inorg. Nucl. Chem.* **1965**, 27, 77.
56. (a) O. Kahn, *Molecular Magnetism*; VCH: Weinheim Germany, 1993 and references therein. (b) P. Day, *Science*, **1993**, 261, 431. (c) M. Oilkington, S. Decurtins, "Magnetoscience from molecules to Materials", Chap. 10, Eds. J. S. Miller, M. Drillon, Wiley-VCH, Weinheim, 2001. (d) S. Decurtins, H. W. Schmale, R. Pellaux, P. Fischer, A. Hauser, *Mol. Cryst. Liq. Cryst.* **1997**, 305, 227. (e) S. Decurtins, H. W. Schmale, P. Schneuwly, R. Pellaux, J. Ensling, *Mol. Cryst. Liq. Cryst.* **1995**, 273, 167.
57. (a) B. Modec, J. V. Brencic, D. Dolenc, J. Zubieta, *J. Chem. Soc. Dalton Trans.* **2002**, 4582. (b) M. R. Sundberg, R. Kivekas, J. K. Koskimies, *J. Chem. Soc.*

- Chem. Commun.* **1991**, 526. (c) S. Kitagawa, T. Okubo, S. Kawata, M. Kondo, M. Katada and H. Kobayashi, *Inorg. Chem.* **1995**, *34*, 4790 and references therein. (d) G. D. Munno, R. Ruiz, F. Lloret, J. Faus, R. Sessoli, M. Julve, *Inorg. Chem.* **1995**, *34*, 408. (e) S. Decurtins, H. W. Schmalle, R. Pellaux, A. Hauser, M. E. von Arx, P. Fischer, *Syn. Met.* **1997**, *85*, 1689.
58. (a) R. P. Farrell, T. W. Hambley, P. A. Lay, *Inorg. Chem.* **1995**, *34*, 757. (b) R. Pellaux, H. W. Schmalle, S. Decurtins, P. Fischer, F. Fauth, B. Ouladdiaf, T. Hauss, *Physica B* **1997**, *234*, 783.
59. (a) Y. H. Kiang, S. Lee, Z. Xu, W. Choe, G. B. Gardner, *Adv. Mater.* **2000**, *12*, 767. (b) G. B. Gardner, D. Venkataraman, J. S. Moore, S. Lee, *Nature* **1995**, *374*, 792. (c) D. D. MacNicol, in *Inclusion Compounds*, Vol. 2, (Eds: J. L. Atwood, J. E. Davies, D. D. MacNicol), Academic, London, 1984, Ch. 1. (d) R. Bishop, I. G. Dance, in *Inclusion Compounds*, Vol. 4, (Eds: J. L. Atwood, J. E. Davies, D. D. MacNicol), Academic, London, 1991, Ch. 1.
60. (a) X. Li, Y. Lin, K. Zhou, *Chinese J. Struct. Chem.* **1984**, *3*, 45. (b) M. G. B. Drew, D. J. Eve, *Inorg. Chim. Acta* **1977**, *25*, L111. (c) G. L. Glen, J. V. Siverton, J. L. Hoard, *Inorg. Chem.* **1963**, *2*, 250. (d) B. K. Prodic, Z. R. Toros, M. Sljukic, *Acta Cryst.* **1978**, *B34*, 2001.
61. G. M. H. van de Velde, S. Harkema, P. J. Gellings, *Inorg. Chim. Acta* **1974**, *11*, 243.
62. R. B. English, D. J. Eve, *Inorg. Chim. Acta* **1993**, *203*, 219.
63. Y. Fu, Y. Liu, Z. Shi, B. Li, W. Pang, *J. Solid State Chem.* **2002**, *163*, 427.
64. (a) R. C. Fay, In *Comprehensive Coordination Chemistry*; Eds: G. Wilkinson, R. D. Gillard, J. A. McCleverty, Pergamon Press: Oxford, England, 1987; Vol. 3, p 411.
65. (a) R. Baggio, M. T. Garland, M. Perec, *Inorg. Chem.* **1997**, *36*, 737. (b) R. Baggio, M. T. Garland, M. Perec, *Inorg. Chem.* **1997**, *36*, 3198. (c) S. Morris, M. J. Almond, C. J. Cardin, M. G. B. Drew, D. A. Rice, Y. Zubavichus, *Polyhedron* **1998**, *17*, 2301 and references therein.
66. (a) E. Jeanneau, N. Audebrand and D. Louër, *Chem. Mater.* **2002**, *14*, 1187. (b) E. Jeanneau, N. Audebrand, J. P. Auffrédic and D. Louër, *J. Mater. Chem.* **2001**, *11*, 2545. (c) C. Boudaren, J. P. Auffrédic, M. Louër, and D. Louër, *Chem. Mater.* **2000**, *12*, 2324. (d) E. Jeanneau, N. Audebrand, D. Louër, *J. Mater. Chem.* **2002**, *12*, 2383.

67. (a) Z. -J. Zhong, N. Matsumoto, H. Okawa, S. Kida, *Chem. Lett.* **1990**, 87. (b) M. Clemente-Leon, E. Coronado, J. R. Galan-Mascaros, C. J. Gomez-Garcia, *Chem. Commun.* **1997**, 1727. (c) E. Coronado, J. R. Galan-Mascaros, C. J. Gomez-Garcia, J. Ensling, P. Gutlich, *Chem. Eur. J.* **2000**, *6*, 552. (d) C. Mathoniere, S. G. Carling, D. Yusheng, P. Day, *Chem. Commun.* **1994**, 1551.
68. (a) S. G. Carling, C. Mathoniere, P. Day, K.M. A. Malik, S. J. Coles, M. B. Hursthouse, *J. Chem. Soc. Dalton Trans.* **1996**, 1839. (b) E. Coronado, M. Clemente-Leon, J. R. Galan-Mascaros, C. Gomenez-Saiz, C. J. Gomez-Garcia, E. Martinez-Ferrero, *J. Chem. Soc. Dalton Trans.* **2000**, 3955 and references therein. (c) E. Coronado, J. R. Galan-Mascaros, C. J. Gomez-Garcia and J. M. Martinez-Agudo, *Adv. Mater.* **1999**, *11*, 558.
69. (a) S. Decurtins, H. W. Schmalle, R. Pellaux, R. Huber, P. Fischer, B. Ouladdiaf, *Adv. Mater.* **1996**, *8*, 647 and references therein. (b) S. Decurtins, H. W. Schmalle, P. Schneuwly, J. Ensling, P. Gutlich, *J. Am. Chem. Soc.*, **1994**, *116*, 9521.
70. (a) S. Decurtins, H. W. Schmalle, H. R. Oswald, A. Linden, J. Ensling, P. Gutlich, A. hauser, *Inorg. Chim. Acta* **1994**, *216*, 65. (b) C. J. Nuttall, P. Day, *Chem. Mater.* **1998**, *10*, 3050. (c) H. W. Schmalle, R. Pellaux, S. Decurtins, *Z. Kristall.* **1996**, *211*, 533.
71. H. Tamaki, Z. J. Zhong, N. Matsumoto, S. Kida, M. Koikawa, N. Achiwa, Y. Hashimoto, H. Okawa, *J. Am. Chem. Soc.* **1992**, *114*, 6974.
72. I. D. Watts, S. G. Carling, P. Day, *J. Chem. Soc. Dalton Trans.* **2002**, 1429.
73. (a) S. Decurtins, H. W. Schmalle, P. Schneuwly, H. R. Oswald, *Inorg. Chem.* **1993**, *32*, 1888. (b) S. Decurtins, H. W. Schmalle, R. Pellaux, P. Schneuwly, A. Hauser, *Inorg. Chem.* **1996**, *35*, 1451.
74. R. Sieber, S. Decurtins, H. S. Evans, C. Wilson, D. Yufit, J. A. K. Howard, S. C. Capelli, A. Hauser, *Chem. Eur. J.* **2000**, *6*, 361.
75. H. Y. Shen, W. M. Bu, D. Z. Liao, Z. H. Jiang, S. P. Yan and G. L. Wang, *Inorg. Chem.* **2000**, *39*, 2239.
76. (a) M. H. Molina, F. Lloret, C. R. Perez, M. Julve, *Inorg. Chem.* **1998**, *37*, 4131. (b) M. Julve, M. Verdaguer, A. Gleizes, P. Levisalles, O. Kahn, *Inorg. Chem.*, **1984**, *23*, 3808 and references therein. (c) R. E. Oughtred, E. S. Raper, H. M. M. Shearer, *Acta Cryst.* **1976**, *B32*, 82.

77. D. Armentano, G. De Munno, F. Lloret, A. V. Palii, M. Julve, *Inorg. Chem.*, **2002**, *41*, 2007.
78. D. J. Price, A. K. Powell, P. T. Wood, *J. Chem. Soc. Dalton Trans.*, **2000**, 3566.
79. D. J. Price, S. Tripp, A. K. Powell, P. T. Wood, *Chem. Eur. J.* **2001**, *7*, 200.
80. O. R. Evans, W. Lin, *Cryst. Growth Des.* **2001**, *1*, 9.
81. S. Huang, R. Wang, T. C. W. Mak, *J. Cryst. Spectros. Res.* **1990**, *20*, 99.
82. (a) M. A. Lawandy, L. Pan, X. Huang, J. Li, T. Yeun, C. L. Lin, *M. R. S. Symp. Proc.*, **2001**, Vol. 658, GG6.12.1. (b) M. C. Munoz, M. Julve, F. Lloret, J. Faus, M. Andruh, *J. Chem. Soc. Dalton Trans.* **1998**, 3125. (c) G. Marinescu, M. Andruh, R. Lescouzeze, M. C. Munoz, J. Cano, F. Lloret, M. Julve, *New. J. Chem.* **2000**, *24*, 527. (d) O. Castillo, A. Luque, P. Romàn, F. Lloret, M. Julve, *Inorg. Chem.* **2001**, *40*, 5526. (e) O. Castillo, A. Luque, J. Sertucha, P. Romàn, F. Lloret, *Inorg. Chem.* **2000**, *39*, 6142.
83. (a) P. Orioli, B. Bruni, M. D. Vaira, L. Messori, F. Piccioli, *Inorg. Chem.* **2002**, *41*, 4312. (b) J. Y. Lu, J. Macias, J. Lu, J. E. Cmaidalka, *Cryst. Growth Des.* **2002**, *2*, 485.
84. (a) W. W. Wendlandt, T. D. George, G. R. Horton, *J. Inorg. Nucl. Chem.* **1961**, *273*, 273 and references therein. (b) A. W. Wylie, *J. Chem. Soc.* **1947**, 1687. (c) I. L. Jenkins, F. H. Moore, M. J. Waterman, *J. Inorg. Nucl. Chem.* **1965**, *27*, 77. (d) R. M. Barrer, L. Ibbitson, *Trans. Faraday Soc.* **1944**, *40*, 195. (e) R. M. Barrer, *Ann. Reports* **1944**, *41*, 31.
85. V. Gilpin, W. C. McCrone, *Anal. Chem.* **1952**, *24*, 225.
86. (a) I. A. Kahwa, F. R. Fronczek, J. Selbin, *Inorg. Chim. Acta* **1984**, *82*, 167. (b) I. A. Kahwa, J. Selbin, *J. Therm. Anal.* **1983**, *28*, 359.
87. (a) E. Hansson, *Acta Chem. Scand.* **1970**, *24*, 2969. (b) F. F. Cavillou, J. C. Trombe, *Solid State Sci.* **2002**, *4*, 1199. (c) T. Bataille, D. Louër, *Acta Cryst.* **2000**, *B56*, 998. (d) P. Klaus, J. P. Sutter, S. Golhen, L. Quahab, O. Khan, *Inorg. Chem.* **2000**, *39*, 1626 and references therein.
88. (a) S. Romero, A. Mosset, J. C. Trombe, *Eur. J. Solid State Inorg. Chem.* **1997**, *34*, 209 and references therein. (b) S. Romero, A. Mosset, J. C. Trombe, *Eur. J. Solid State Inorg. Chem.* **1996**, *127*, 256.
89. T. R. R. McDonald, J. M. Spink, *Acta Cryst.* **1967**, *23*, 944.
90. (a) T. Bataille, M. Louër, J. P. Auffrédic, D. Louër, *J. Solid State Chem.* **2000**, *150*, 81. (b) T. Bataille, J. P. Auffrédic, D. Louër, *Chem. Mater.* **1999**, *11*, 1559.

- (c) T. Bataille, J. P. Auffrédic, D. Louër, *J. Mater. Chem.* **2000**, *10*, 1707. (d) T. Bataille, D. Louër, *Acta Cryst.* **1999**, *C55*, 1760. (e) O. Genecova, J. Siftar, *J. Therm. Anal.* **1997**, *48*, 321.
91. (a) M. T. V. Ganzereli, L. Maggi, V. C. Caramella, *Appl. Radiat. Isot.* **1999**, *51*, 21. (b) V. C. Caramella, L. Maggi, M. T. V. Ganzereli, *Appl. Radiat. Isot.* **1999**, *51*, 353.
92. (a) N. W. Alcock, *J. C. S. Dalton* **1973**, 1610. (b) A. E. Bradley, J. E. Hatter, M. Nieuwenhuyzen, W. R. Pitner, K. R. Seddon, R. C. Thied, *Inorg. Chem.* **2002**, *41*, 1692.
93. (a) P. Romàn, C. G. Miralles, A. Luque, *J. Chem. Soc. Dalton Trans.* **1996**, 3985. (b) N. Bulc, L. Golic, J. Siftar, *Acta Cryst.* **1984**, *C40*, 1829. (c) R. Pellaux, S. Decurtins, H. W. Schmalle, *Acta Cryst.* **1999**, *C55*, 1075.
94. (a) N. Bulc, L. Golic, *Acta Cryst.* **1983**, *C39*, 174. (b) N. Bulc, L. Golic, *Acta Cryst.* **1983**, *C39*, 176. (c) A. V. Virovets, D. Y. Naumov, E. V. Boldyreva, N. V. Podberezkaya, *Acta Cryst.* **1993**, *C49*, 1882.
95. (a) C. Boudaren, J. P. Auffrédic, P. B. Rocherullé, D. Louër, *Solid State Sci.* **2001**, *3*, 847. (b) U. Heintl, P. Hinse, R. Mattes, *Z. Anorg. Allg. Chem.* **2001**, *627*, 2173.
96. S. Ayyappan, A. K. Cheetham, S. Natarajan, C. N. R. Rao, *Chem. Mater.* **1998**, *10*, 3746.
97. T. O. Salami, K. Marouchkin, P. Y. Zavilij, S. R. J. Oliver, *Chem. Mater.* **2002**, *14*, 4851.
98. T. O. Salami, P. Y. Zavilij, S. R. J. Oliver, *Acta Cryst.* **2001**, *E57*, m111.
99. T. O. Salami, P. Y. Zavilij, S. R. J. Oliver, *Acta Cryst.* **2001**, *E57*, i49.
100. N. Audebrand, M. L. Vaillant, J. P. Auffrédic, D. Louër, *Solid State Sci.* **2001**, *3*, 483.
101. (a) Y. Q. Zheng, Z. P. Kong, *J. Solid State Chem.* **2002**, *166*, 279. (b) F. Hohn, I. Pantenburg, U. Ruschewitz, *Chem. Eur. J.* **2002**, *8*, 4536. (c) J. Sanchiz, Y. R. Martin, C. R. Perez, A. Mederos, F. Lloret, M. Julve, *New J. Chem.* **2002**, *26*, 1624. (d) A. Michaelides, V. Kiritsis, S. Skoulika, A. Aubry, *Angew. Chem. Int. Ed. Engl.* **2000**, *39*, 3470. (e) B. Benmerad, A. G. Laidoudi, F. Balegroune, H. Birkedal, G. Chapuis, *Acta Cryst.* **2000**, *C56*, 789.
102. (a) B. Benmerad, A. G. Laidoudi, G. Bernardinelli, F. Balegroune, *Acta Cryst.* **2000**, *C56*, 321. (b) E. V. Brusau, J. C. Pedregosa, G. E. Narda, G. Echeverria,

- G. Punte, *J. Solid State Chem.* **2000**, *153*, 1. (c) E. V. Brusau, G. E. Narda, J. C. Pedregosa, G. Echeverria and G. Punte, *J. Solid State Chem.* **1999**, *143*, 174.
103. (a) M. Fleck, L. Bohaty, E. Tillmanns, *Z. Kristall.* **2001**, *216*, 633. (b) P. S. Mukherjee, S. Dalai, G. Mostafa, E. Zangrando, T. H. Lu, G. Rogez, T. Mallah, N. R. Chaudhuri, *Chem. Commun.* **2001**, 1346. (c) M. R. St. J. Foreman, M. J. Plater, J. M. S. Skakle, *J. Chem. Soc. Dalton Trans.* **2001**, 1897.
104. (a) P. M. Forster, A. K. Cheetham, *Chem. Mater.*, **2002**, *14*, 17. (b) D. Chattopadhyay, S. K. Chattopadhyay, P. R. Lowe, C. H. Schwalbe, S. K. Mazumder, A. Rana, S. Ghosh, *J. Chem. Soc. Dalton Trans.* **1993**, 913. (c) I. G. de Muro, M. Insausti, L. Lezama, M. K. Urtiaga, M. I. Arriortua, T. Rojo, *J. Chem. Soc. Dalton Trans.* **2000**, 3360. (d) I. G. de Muro, F. A. Mautner, M. Insausti, L. Lezama, M. I. Arriortua, T. Rojo, *Inorg. Chem.* **1998**, *37*, 3243. (e) M. Insausti, I. G. de Muro, L. Lorente, T. Rojo, E. H. Bocanegra, M. I. Arriortua, *Therm. Acta* **1996**, *287*, 81. (f) J. Cernak, J. Chomic, C. Kappenstein, F. Robert, *J. Chem. Soc. Dalton Trans.* **1997**, 2981. (g) A. D. Burrows, R. W. Harrington, M. F. Mahon, C. E. Price, *J. Chem. Soc. Dalton Trans.* **2000**, 3845. (h) E. Suresh, M. M. Bhadbhade, K. Venkatasubramanian, *Polyhedron*, **1999**, *18*, 657.
105. (a) M. Kurmoo, *J. Mater. Chem.* **1999**, *9*, 2595. (b) E. Whelan, M. Devereux, M. McCann, V. McKee, *Chem. Commun.* **1997**, 427. (c) E. A. H. Griffith, N. G. Charles, E. L. Amma, *Acta Cryst.* **1982**, *B38*, 262. (d) K. H. Chung, E. Hong, Y. Do and C. H. Moon, *J. Chem. Soc. Chem. Commun.* **1995**, 2333. (e) A. Michaelides, S. Skoulika, V. Kiritsis, A. Aubry, *J. Chem. Soc. Chem. Commun.* **1995**, 1415. (f) A. Michaelides, V. Kiritsis, S. Skoulika, A. Aubry, *Angew. Chem. Int. Ed. Engl.* **1993**, *32*, 1495. (g) S. M. Saadeh, K. L. Trojen, J. W. Kamf, W. E. Hatfield, V. L. Pecoraro, *Inorg. Chem.* **1993**, *32*, 3034. (h) T. Glowiak, J. Legendziewicz, *Acta Cryst.* **1986**, *C42*, 1494. (i) M. Post, J. Trotter, *J. Chem. Soc. Dalton Trans.* **1974**, 1922.
106. (a) N. Guillou, S. Pastre, C. Livage, G. Férey, *Chem. Commun.* **2002**, 2358. (b) C. Livage, C. Egger, G. Férey, *Chem. Mater.* **2001**, *13*, 410 (c) C. Livage, C. Egger, G. Férey, *Chem. Mater.* **1999**, *11*, 1546. (d) F. Serpaggi, G. Férey, *J. Mater. Chem.* **1998**, *8*, 2737. (e) C. Livage, C. Egger, M. Noguès, G. Férey, *J. Mater. Chem.* **1998**, *8*, 2743. (f) F. Serpaggi, G. Férey, E. A. Fidancev, *J. Solid State Chem.* **1999**, *148*, 347. (g) F. Serpaggi, T. Luxbacher, A. K. Cheetham, G.

- Férey, *J. Solid State Chem.* **1999**, *145*, 580. (h) F. Serpaggi, G. Férey, *Microporous and Mesoporous Mater.* **1999**, *32*, 311.
107. P. M. Forster, A. K. Cheetham, *Angew. Chem. Int. Ed. Engl.* **2002**, *41*, 457.
108. Y. Kim, E. W. Lee, D. Y. Jung, *Chem. Mater.* **2001**, *13*, 2684. (b) Y. Kim, D. Y. Jung, *Bull. Korean Chem. Soc.* **2000**, *21*, 656. (c) Y. Kim, D. Y. Jung, *Bull. Korean Chem. Soc.* **1999**, *20*, 827. (d) E. W. Lee, Y. Kim, D. Y. Jung, *Inorg. Chem.* **2002**, *41*, 501. (e) Y. Kim, D. Y. Jung, *Inorg. Chem.* **2000**, *39*, 1470.
109. (a) A. Dimos, D. Tsaousis, A. Michaelides, S. Skoulika, S. Golhen, L. Ouahab, C. Didierjean, A. Aubry, *Chem. Mater.* **2002**, *14*, 2616. (b) B. Q. Ma, D. S. Zhang, S. Gao, T. Z. Jin, C. H. Yan, G. X. Xu, *Angew. Chem. Int. Ed. Engl.* **2000**, *41*, 457. (c) R. Baggio, M. T. Garland, M. Perec, D. Vega, *Inorg. Chem.* **1996**, *35*, 2396. (d) A. C. Rizzi, R. Calvo, R. Baggio, M. T. Garland, O. Pena, M. Perec, *Inorg. Chem.* **2002**, *41*, 5609.
110. N. L. Rosi, M. Eddaoudi, J. Kim, M. O' Keeffe, O. M. Yaghi, *Angew. Chem. Int. Ed.* **2002**, *41*, 284 and references therein.
111. (a) M. I. Khan, Y. D. Chang, Q. Chen, J. Salta, Y. S. Lee, C. J. O'Connor, J. Zubieta, *Inorg. Chem.* **1994**, *33*, 6340. (b) C. Castro, M. L. Calatyud, J. Sletten, F. Lloret, M. Julve, *J. Chem. Soc. Dalton Trans.* **1997**, 811 and references therein. (c) G. J. Long, *Inorg. Chem.* **1978**, *17*, 2702. (d) J. A. C. van Ooijen, J. Reedijk, A. L. Spek, *Inorg. Chem.* **1979**, *18*, 1184.
112. (a) A. Weiss, E. Riegler, I. A. H. Bohme, C. Robl, *Z. Naturforsch* **1986**, *41b*, 18. (b) C. Robl, W. F. Kuhs, *J. Solid State Chem.* **1988**, *75*, 15. (c) G. M. Frankenbach, M. A. Beno, A. M. Kini, J. M. Williams, U. Welp, J. E. Thompson, M. H. Whangbo, *Inorg. Chim. Acta* **1992**, *192*, 195. (d) M. Habenschuss, B. C. Gerstein, *J. Chem. Phys.* **1974**, *61*, 852. (e) B. D. Alleyne, L. A. Hall, H. A. Hosein, H. Jaggernauth, A. J. P. White, D. J. Williams, *J. Chem. Soc. Dalton Trans.* **1998**, 3845.
113. (a) Q. Chen, S. Liu, J. Zubieta, *Inorg. Chim. Acta* **1990**, *175*, 241. (b) N. C. Baenziger, D. G. Williams, *J. Am. Chem. Soc.* **1966**, *88*, 689. (c) I. Castro, J. Sletten, L. K. Glaerum, F. Lloret, J. Faus, M. Julve, *J. Chem. Soc. Dalton Trans.* **1994**, 2777. (d) C. C. Wang, C. H. Yang, G. H. Lee, *Inorg. Chem.* **2002**, *41*, 1015.
114. (a) K. J. Lin, K. H. Lii, *Angew. Chem. Int. Ed. Engl.* **1997**, *36*, 2076. (b) A. Weiss, E. Riegler, C. Robl, *Z. Naturforsch* **1986**, *41b*, 1329. (c) A. Weiss, E.

- Riegler, C. Robl, *Z. Naturforsch* **1986**, *41b*, 1333. (d) T. K. Maji, G. Mostafa, S. Sain, J. S. Prasad, N. R. Chaudhari, *Cryst. Engg. Comm.* **2001**, *37*, 1. (e) S. F. Lai, C. Y. Cheng, K. J. Lin, *Chem. Commun.* **2001**, 1082.
115. (a) M. Dan, K. Shivshankar, A. K. Cheetham, C. N. R. Rao (communicated). (b) J. C. Trombe, L. Sabadie, P. Millet, *Solid State Sci.* **2002**, *4*, 1209.
116. C. S. Yufit, D. J. Price, J. A. K. Howard, S. O. H. Gutschke, A. K. Powell, P. T. Wood, *Chem. Commun.* **1999**, 1561. (e) S. O. H. Gutschke, M. Molinier, A. K. Powell, P. T. Wood, *Angew. Chem. Int. Ed. Engl.* **1997**, *36*, 991.
117. S. Neeraj, M. L. Noy, C. N. R. Rao, A. K. Cheetham, *Solid State Sci.* **2002**, *10*, 1.
118. O. M. Yaghi, Guangming Li, T. L. Groy, *J. Chem. Soc. Dalton Trans.* **1995**, 727.
119. (a) J. C. Trombe, J. -F. Petit, A. Gleizes, *Inorg. Chim. Acta* **1990**, *167*, 69. (b) J. C. Trombe, J. F. Petit, A. Gleizes, *Eur. J. Solid State Inorg. Chem.* **1991**, *28*, 669. (c) M. Dan, C. N. R. Rao, *Solid State Sci.* **2003** (in press).
120. (a) C. Robl, A. Weiss, *Z. Naturforsch* **1986**, *41b*, 1490. (b) C. Robl, A. Weiss, *Z. Naturforsch* **1986**, *41b*, 1485.
121. C. R. Lee, C. C. Wang, Y. Wang, *Acta Cryst.* **1996**, *B52*, 966.
122. L. Gmelin, *Ann. Phys. (Leipzig)* **1825**, *4*, 31.
123. (a) J. D. Dunitz, P. Seifer, W. Czechtizky, *Angew. Chem. Int. Ed. Engl.* **2001**, *40*, 1779. (b) D. Braga, L. Maini, F. Grepioni, *Chem. Eur. J.* **2002**, *8*, 1804.
124. M. D. Glick, L. F. Dahl, *Inorg. Chem.* **1966**, *5*, 289. (b) M. D. Glick, G. L. Downs, L. F. Dahl, *Inorg. Chem.* **1964**, *3*, 1712.
125. M. J. Plater, A. J. Roberts, J. Marr, E. E. Lachowski, R. A. Howie, *J. Chem. Soc. Dalton Trans.* **1998**, 797.
126. (a) K. Barthelet, J. Marrot, D. Riou, G. Férey, *Angew. Chem. Int. Ed. Engl.* **2002**, *41*, 281. (b) K. Barthelet, D. Riou, G. Férey, *Chem. Commun.* **2002**, 1492. (c) F. Millange, C. Serre, G. Férey, *Chem. Commun.* **2002**, 822. (d) C. Serre, F. Millange, C. Thouvenot, M. Noguès, G. Marsolier, D. Louër, G. Férey, *J. Am. Chem. Soc.* **2002**, *124*, 13519.
127. (a) M. Sanselme, J. M. Grenèche, M. R. Cavellec, G. Férey, *Chem. Commun.* **2002**, 2172. (b) M. R. Cavellec, G. Férey, *Solid State Sci.* **2002**, *4*, 1221. (c) M. R. Cavellec, C. Albinet, C. Livage, N. Guillou, M. Noguès, J. M. Grenèche, G. Férey, *Solid State Sci.* **2002**, *4*, 267.

128. (a) R. K. Chiang, N. T. Chuang, C. S. Wur, M. F. Chong, C. R. Lin, *J. Solid State Chem.* **2002**, *166*, 158. (b) S. O. H. Gutschke, D. J. Price, A. K. Powell, P. T. Wood, *Angew. Chem. Int. Ed. Engl.* **2001**, *40*, 1920. (c) C. Livage, N. Guillou, J. Marrot, G. Férey, *Chem. Mater.* **2001**, *13*, 4387. (d) Z. L. Huang, M. Drillon, N. Masciocchi, A. Sironi, J.T. Zhao, P. Rabu, P. Panissod, *Chem. Mater.* **2000**, *12*, 2805.
129. (a) D. Cheng, M. A. Khan, R. P. Houser, *J. Chem. Soc. Dalton Trans.* **2002**, 4555. (b) Y. Li, H. Zhang, E. Wang, N. Hao, C. Hu, Y. Yan, D. Hall, *New J. Chem.* **2002**, *26*, 1619. (c) D. Cheng, M. A. Khan, R. P. Houser, *Cryst. Growth & Des.* **2002**, *2*, 415
130. (a) C. J. Kepert, T. J. Prior, M. J. Rosseinsky, *J. Am. Chem. Soc.* **2000**, *122*, 5158. (b) C. J. Kepert, M. J. Rosseinsky, *Chem. Commun.* **1998**, 31.
131. (a) D. Cheng, M. A. Khan, R. P. Houser, *Inorg. Chem.* **2001**, *40*, 6858. (b) J. W. Ko, K. S. Min, M. P. Suh, *Inorg. Chem.* **2002**, *41*, 2151. (c) J. C. Dai, X. T. Wu, Z. Y. Fu, C. P. Cui, S. M. Hu, W. X. Du, L. M. Wu, H. H. Zhang, R. Q. Sun, *Inorg. Chem.* **2002**, *41*, 1391.
132. J. C. Dai, X. T. Wu, Z. Y. Fu, S. H. Hu, W. X. Du, C. P. Cui, L. M. Wu, H. H. Zhang and R. Q. Sun, *Chem. Commun.* **2002**, 12.
133. (a) S. S. Y. Chui, A. Siu, X. Feng, Z. Y. Zhang, T. C. W. Mak, I. D. Williams, *Inorg. Chem. Commun.* **2001**, *4*, 467. (b) Y. Wan, L. Jin, K. Wang, L. Zhang, X. Zheng, S. Lu, *New J. Chem.* **2002**, *26*, 1590. (c) D. Sun, R. Cao, Y. Liang, Q. Shi and M. Hong, *J. Chem. Soc. Dalton Trans.* **2002**, 1847. (d) C. Serre, F. Millange, J. Marrot, G. Férey, *Chem. Mater.* **2002**, *14*, 2409.
134. (a) C. Daiguebonne, Y. Gerault, O. Guillou, A. Lecerf, K. Boubekeur, P. Batail, M. Kahn, O.Khan, *J. Alloys Compds.* **1998**, *275*, 50. (b) R. Cao, D. Sun, Y. Liang, M. Hong, K. Tatsumi, Q. Shi, *Inorg. Chem.* **2002**, *41*, 2087. (c) L. Pan, N. Zheng, Y. Wu, S. Han, R. Yang, X. Huang, J. Li, *Inorg. Chem.* **2001**, *40*, 828.
135. (a) H. Kumagai, M. A. Tanaka, K. Inoue, M. Kurmoo, *J. Mater. Chem.*, **2001**, *11*, 2146. (b) Kim, D. Y. Jung, *Chem. Commun.* **2002**, 908. (c) L. Pan, E. B. Woodlock, X. Wang, *Inorg. Chem.* **2000**, *39*, 4174. (d) B. G. Lor, E. G. Puebla, M. Iglesias, M. A. Monge, C. R. Valero, N. Snejko, *Inorg. Chem.* **2002**, *41*, 2429.

136. (a) J. Do, R. P. Bontchev, A. J. Jacobson, *Chem. Mater.* **2001**, *13*, 2601. (c) Y. M. Tsai, S. L. Wang, C. H. Huang, K. H. Lii, *Inorg. Chem.* **1999**, *38*, 4183.
137. (a) J. Do, R. P. Bontchev, A. J. Jacobson, *Inorg. Chem.* **2000**, *39*, 3230. (b) Z. A. D. Lethbridge, S. K. Tiwary, A. Harrison, P. Lightfoot, *J. Chem. Soc. Dalton Trans.* **2001**, 1904. (c) Z. A. D. Lethbridge, A. D. Hillier, R. Cywinski, P. Lightfoot, *J. Chem. Soc. Dalton Trans.* **2000**, 1595.
138. (a) W. J. Chang, H. M. Lin, K. H. Lii, *J. Solid State Chem.* **2001**, *157*, 233. (b) H. M. Lin, K. H. Lii, Y. C. Jiang, S. L. Wang, *Chem. Mater.* **1999**, *11*, 519. (c) Z. A. D. Lethbridge, P. Lightfoot, *J. Solid State Chem.* **1999**, *143*, 58.
139. (a) A. Choudhury, S. Natarajan, C. N. R. Rao, *Chem. Mater.* **1999**, *11*, 2316. (b) A. Choudhury, S. Natarajan, *J. Mater. Chem.* **1999**, *9*, 3113. (c) A. Choudhury, S. Natarajan, C. N. R. Rao, *Chem. Eur. J.* **2000**, *6*, 1168. (d) A. Choudhury, S. Natarajan, C. N. R. Rao, *J. Solid State Chem.* **1999**, *146*, 538. (e) N. Rajic, D. Stojakovic, D. Hanzel, N. Z. Logar, V. Kaucic, *Microporous Mesoporous Mater.* **2002**, *55*, 313. (f) A. Choudhury, S. Natarajan, *Solid State Sci.* **2000**, *2*, 365.
140. S. Neeraj, S. Natarajan, C. N. R. Rao, *J. Chem. Soc. Dalton Trans.* **2001**, 289.
141. (a) P. Lightfoot, Z. A. D. Lethbridge, R. E. Morris, D. S. Wragg, P. A. Wright, A. Kwick, G. B. M. Vaughan, *J. Solid State Chem.* **1999**, *143*, 74. (b) K. Kedarnath, A. Choudhury, S. Natarajan, *J. Solid State Chem.* **2000**, *150*, 324.
142. (a) L. C. Hung, H. M. Kao, K. H. Lii, *Chem. Mater.* **2000**, *12*, 2411. (b) C. Y. Chen, P. P. Chu, K. H. Lii, *Chem. Commun.* **1999**, 1473. (c) C. T. S. Choi, E. V. Anokhina, C. S. Day, Y. Zhao, F. Taulelle, C. Huguenard, Z. Gan, A. Lachgar, *Chem. Mater.* **2002**, *14*, 4096.
143. Y. F. Huang, K. H. Lii, *J. Chem. Soc. Dalton Trans.* **1998**, 4085.
144. S. Natarajan, *J. Solid State Chem.* **1998**, *139*, 200.
145. (a) S. Chakrabarti, M. A. Green, S. Natarajan, *Solid State Sci.* **2002**, *4*, 405. (b) S. Chakrabarti, S. Natarajan, *Angew. Chem. Int. Ed. Engl.* **2002**, *41*, 1224. (c) S. Chakrabarti, S. Natarajan, *J. Chem. Soc. Dalton Trans.* **2002**, 4156.
146. A. A. Ayi, A. Choudhury, S. Natarajan, C. N. R. Rao, *New J. Chem.* **2001**, *25*, 213.
147. B. Adair, S. Natarajan, A. K. Cheetham, *J. Mater. Chem.* **1998**, *8*, 1477.
148. N. Stock, G. D. Stucky, A. K. Cheetham, *Chem. Commun.* **2000**, 2277.
149. C. Nather, J. Greve, I. Jeß, *Chem. Mater.* **2002**, *14*, 4536.

150. (a) M. Eddaoudi, J. Kim, N. Rosi, D. Vodak, J. B. Wachter, M. O'Keeffe, O. M. Yaghi, *Science* **2002**, *295*, 469. (b) M. Eddaoudi, J. Kim, M. O'Keeffe, O. M. Yaghi, *J. Am. Chem. Soc.* **2002**, *124*, 376. (c) M. Eddaoudi, J. Kim, J. Wachter, H. K. Chae, M. O'Keeffe, O. M. Yaghi, *J. Am. Chem. Soc.* **2001**, *123*, 4368. (d) B. Chen, M. Eddaoudi, T. M. Reineke, J. W. Kampf, M. O'Keeffe, O. M. Yaghi, *J. Am. Chem. Soc.* **2000**, *122*, 11559. (e) M. Eddaoudi, H. Li, O. M. Yaghi, *J. Am. Chem. Soc.* **2000**, *122*, 1391. (f) N. L. Rosi, M. Eddaoudi, J. Kim, M. O'Keeffe, O. M. Yaghi, *Cryst. Engg. Comm.* **2002**, *4*, 401.
151. (a) B. L. Chen, M. Eddaoudi, S. T. Hyde, M. O'Keeffe, O. M. Yaghi, *Science*, **2001**, *291*, 1021. (b) O. M. Yaghi, *Chem. Innov.* October 3, **2000**. (c) T. Reineke, M. Eddaoudi, D. Moler, M. O'Keeffe, O. M. Yaghi, *J. Am. Chem. Soc.* **2000**, *122*, 1391. (d) T. J. Barton, L. M. Bull, W. G. Klemperer, D. A. Loy, B. McEnaney, M. Misono, P. A. Manson, G. Pez, G. W. Scherer, J. C. Vartuli, O. M. Yaghi, *Chem. Mater.* **1999**, *11*, 2633. (e) T. M. Reineke, M. Eddaoudi, M. O'Keeffe, O. M. Yaghi, *Angew. Chem. Int. Ed.* **1999**, *38*, 2590. (f) T. Reineke, M. Eddaoudi, M. Fehr, D. Kelley, O. M. Yaghi, *J. Am. Chem. Soc.* **1999**, *121*, 1651.
152. (a) M. Eddaoudi, H. Li, T. Reineke, M. Fehr, D. Kelley, T. L. Groy, O. M. Yaghi, in *Topics in Catalysis*, G. A. Somorjai and J. M. Thomas, Eds. **1999**, *9*, 105. (b) H. Li, M. Eddaoudi, T. L. Groy, O. M. Yaghi, *J. Am. Chem. Soc.* **1998**, *120*, 8571. (c) O. M. Yaghi, H. Li, C. Davis, D. Richardson, T. L. Groy, *Acc. Chem. Res.* **1998**, *31*, 474.
153. (a) O. M. Yaghi, C. E. Davis, G. Li, H. Li *J. Am. Chem. Soc.* **1997**, *119*, 2861. (b) O. M. Yaghi, G. Li, and H. Li, *Nature*, **1995**, *378*, 703.
154. S. S. Y. Chui, S. M. F. Lo, J. P. H. Charmant, A. G. Orpen, I. D. Williams, *Science*, **1999**, *283*, 1148.
155. J. S. Seo, D. Whang, H. Lee, S. I. Jun, J. Oh, Y. J. Jeon, K. Kim, *Nature* **2000**, *404*, 982.
156. S. Y. Yang, L. S. Long, Y. B. Jiang, R. B. Huang, L. S. Zheng, *Chem. Mater.* **2002**, *14*, 3229.
157. (a) E. M. Sabbar, M. E. de Roy, J. P. Besse, *Mater. Res. Bull.* **1999**, *34*, 1023. (b) E. M. Sabbar, M. E. de Roy, A. Ennaquadi, C. Gueho, J. P. Besse, *Chem. Mater.* **1998**, *12*, 3856. (c) B. Bujoli, A. Corilleau, P. Palvadeau, J. Rouxel, *Eur. J. Solid State Inorg. Chem.* **1992**, *29*, 171. (d) A. Distler and S. C. Sevov, *Chem.*

- Commun.* **1998**, 959. (e) S. Drumel, P. J. Janvier, M. B. Doeuff, B. Bujoli, *New J. Chem.* **1995**, *19*, 239. (d) M. R. Cavellec, M. Sanselme, M. Noguès, J. M. Grenèche, G. Férey, *Solid State Sci.* **2002**, *4*, 619. (e) D. A. Burwell and M. E. Thompson, *Chem. Mater.* **1991**, *3*, 14. (b) D. A. Burwell, K. G. Valentine, J. H. Timmermans, M. E. Thompson, *J. Am. Chem. Soc.* **1992**, *114*, 4144.
158. (a) S. Drumel, P. Janvier, P. Barboux, M. B. Doeuff, B. Bujoli, *Inorg. Chem.* **1995**, *34*, 148. (b) F. Serpaggi, G. Férey, *Inorg. Chem.* **1999**, *38*, 4741.
159. (a) G. B. Hix, D. S. Wragg, P. A. Wright, R. E. Morris, *J. Chem. Soc. Dalton Trans.* **1998**, 3359. (b) F. Fredoueil, D. Massiot, D. M. Poojary, M. B. Doueff, A. Clearfield, B. Bujoli, *Chem. Commun.* **1998**, 175. (c) (a) S. Ayyappan, G. D. de Delgado, A. K. Cheetham, G. Férey and C. N. R. Rao, *J. Chem. Soc. Dalton Trans.* **1999**, 2905. (b) N. Stock, S. A. Frey, G. D. Stucky and A. K. Cheetham, *J. Chem. Soc. Dalton Trans.* **2000**, 4292. (c) N. Stock, *Solid State Sci.* **2002**, *4*, 1089. P. Janvier, S. Drumel, P. Piffard and B. Bujoli, *C. R. Acad. Sci. Ser. II*, **1995**, 320, 29.
160. S. J. Hartman, E. Todorov, C. Cruz, S. C. Sevov, *Chem. Commun.* **2000**, 1213.
161. S. O. H. Gutschke, D. J. Price, A. K. Powell, P. T. Wood, *Angew. Chem. Int Ed. Engl.* **1999**, *38*, 1088.
162. J. G. Mao, A. Clearfield, *Inorg. Chem.* **2002**, *41*, 2319.
163. B. Zhang, D. M. Poojary, A. Clearfield, G. -Z. Peng, *Chem. Mater.* **1996**, *8*, 1333.
164. (a) R. G. Xiong, S. R. Wilson, W. Lin, *J. Chem. Soc. Dalton Trans.* **1998**, 4089. (b) W. Lin, O. R. Evans, R. G. Xiong, Z. Wang, *J. Am. Chem. Soc.* **1998**, *120*, 13272. (c) W. Lin, Z. Wang, L. Ma, *J. Am. Chem. Soc.* **1999**, *121*, 11249. (d) O. R. Evans, W. Lin, *Inorg. Chem.* **2000**, *39*, 2189. (e) O. R. Evans, R. G. Xiong, Z. Wang, G. K. Wong, W. Lin, *Angew. Chem. Int Ed. Engl.* **1999**, *38*, 536.
165. (a) O. R. Evans, W. Lin, *Chem. Mater.* **2001**, *13*, 3009. (b) O. R. Evans and W. Lin, *J. Chem. Soc. Dalton Trans.* **2000**, 3949. (c) P. Ayyappan, O. R. Evans, W. Lin, *Inorg. Chem.* **2002**, *41*, 3328.
166. Y. H. Liu, H. L. Tsai, Y. L. Lu, Y. S. Wen, J. C. Wang, K. L. Lu, *Inorg. Chem.* **2001**, *40*, 6426.
167. J. Y. Lu, A. M. Babb, *Chem. Commun.* **2002**, 1340.
168. B. Rather, B. Moulton, R. D. B. Walsh, M. J. Zaworotko, *Chem. Commun.* **2002**, 694.

-
169. (a) D. M. Ciurtin, M. D. Smith, H. C. zur Loye, *Inorg. Chim. Acta* **2001**, *324*, 46 and references therein. (b) D. M. Ciurtin, M. D. Smith, H. C. zur Loye, *Chem. Commun.* **2002**, 74.
170. S. I. Noro, S. Kitagawa, M. Yamashita and T. Wada, *Chem. Commun.* **2002**, 222.
171. (a) S. Takamizawa, W. Mori, M. Furihata, S. Takeda, K. Yamaguchi, *Inorg. Chim. Acta.* **1998**, *283*, 268. (b) Y. Liang, R. Cao, W. Su, M. Hong, W. Zhang, *Angew. Chem. Intl. Ed. Engl.* **2000**, *39*, 3304. (c) Y. Liang, M. Hong, W. Su, R. Cao, W. Zhang, *Inorg. Chem.* **2001**, *40*, 4574. (d) T. Whitfield, L. M. Zheng, X. Wang, A. J. Jacobson, *Solid State Sci.* **2001**, *3*, 829. (e) X. Haitao, Z. Nengwu, X. Hanhui, W. Yonggang, Y. Ruyi, Y. Enyi, J. Xianglin, *J. Mol. Struct.* **2001**, *597*, 1 and references therein. (f) L. A. Gerrard, P. T. Wood, *Chem. Commun.* **2000**, 2107.
172. R. C. Finn, J. Zubieta, *Solid State Sci.* **2002**, *4*, 83 and references therein. (b) Y. H. Liu, Y. L. Lu, H. C. Wu, J. C. Wang, K. L. Lu, *Inorg. Chem.* **2002**, *41*, 2592.

2.0. SCOPE OF THE PRESENT INVESTIGATIONS

The area of inorganic open-framework materials has become one of intense research activity in the past several years.^[1-6] While one of the objectives of research in open-framework solids is to find materials possessing channels and cavities which make them porous, thereby imparting potential catalytic and sorption properties, the discovery of fascinating architectures of different dimensionalities has been equally interesting. As discussed in chapter 1, the aluminosilicates and the metal phosphate structures though are studied widely,^[1-5] there has been much interest in the synthesis of new hybrid materials containing both inorganic and organic units as part of the framework.^[7,8] In the design of hybrid structures, one takes advantage of the metal-coordination as well as the flexibility and other functionalities of the organic components to give open structures.^[8,9-11] Nevertheless, the construction of organic analogues of zeolites does not necessarily mean mimicking inorganic materials, but to complement them and thereby impart properties not displayed by zeolites (for example chirality).

2.1. Organic amine oxalates

Organic crystal engineering and design has become an important area of research in the last few years.^[12-16] Crystal engineering takes advantage of the hydrogen bond interactions existing between molecules to give rise to interesting structures.^[12-15] We considered it interesting to examine the hydrogen bonding patterns present in the salts of oxalic acid. For this purpose, we have synthesized hydrogen bonded adducts between oxalic acid and several organic amines. There have been very few report of the structure of amine oxalate in the literature.^[17] The amine oxalates, examined here, exhibit different types of hydrogen bonding patterns with characteristic features. In addition, the amine-oxalates can also act as

a possible precursor for the synthesis of new metal-oxalate structures. This method of synthesis possibly offers some control of the kinetics of the reactions involved in the formation of metal oxalates.

2.2. Metal oxalates

2.2.1. Zinc oxalates

The transition metal oxalates have been studied extensively for their interesting magnetic properties.^[18] Whilst the works on bivalent metal oxalates are slowly emerging. Bivalent metal oxalates, synthesized in the presence of organic amines, are not known. Zinc oxalates with one- and two-dimensional structures have been reported.^[19] Zinc oxalates with zero to three-dimensional structures, containing structure-directing organic amines have been synthesized and characterized. The three-dimensional open-framework zinc oxalate has been investigated for its adsorption behavior.

The role of the amine phosphates as possible intermediates in the formation of metal phosphates has been established recently.^[20] Similarly, amine oxalates could also play a role in the formation of metal oxalates with open-framework architectures. The reactions of amine oxalates with Zn^{II} ions have been investigated as an alternative route to the synthesis of a variety of open-framework zinc oxalates. The investigations inferred that zinc oxalates of varying dimensionalities can be prepared by the reaction of Zn^{II} ions with amine oxalates. While the two-dimensional zinc oxalates possess layers with honeycomb-like 12-member pores, the three-dimensionally extended network have 20-membered pores with an interrupted honeycomb structure.

2.2.2. Cadmium oxalates

Cadmium oxalates have been prepared in the presence of alkali metal ions to exhibit interesting properties.^[21] Presently, cadmium oxalate frameworks have been

synthesized in the presence of alkali metal, employing hydrothermal methods. The results indicate the formation of two new cadmium oxalates, $M_4Cd_2(C_2O_4)_4 \cdot 4H_2O$, $M = Na, K$, possessing channels occupied by alkali metal ions. In addition, solvothermal conditions also facilitated the formation of a new chloro cadmium-oxalate containing cadmium chloride chains reminiscent of those observed in $Cd(OH)Cl$ and $CdCl_2$ structures.

2.2.3. Rare-earth metal oxalates

The synthesis and structure of rare-earth metal dicarboxylates have been established recently.^[21,23-26] since oxalates form interesting secondary building units in conjugation with metal ions attempts to synthesize rare-earth oxalates in the presence of organic amines. The rare-earth ions usually take large coordinations, which can facilitate more oxalate ligands to bind and thereby give rise to three-dimensional architectures with interesting properties.^[23,24] In addition, the preference to high coordination coupled with the flexibility of organic ligands can give rise to unusual structures, and in some cases can have functional groups protruding in open-channels.^[27] In this effort, two open-framework yttrium oxalates with three-dimensional structures possessing channels in all the crystallographic directions, exhibiting adsorptive properties have been prepared. Furthermore, two new open-framework neodymium oxalates, with carboxylate and amino functional groups protruding into 12-member channels have also been synthesized.

2.2.4. Tin(II) oxalates

Tin(II) compounds are interesting for the lone-pair of electrons associated with them. The stereo-active lone-pair of electrons, in some cases, direct the formation of unusual structures as shown in some of the tin(II) phosphates recently.^[28,29] Thus, the synthesis of tin(II) oxalates with open-structures seems to be an interesting possibility. The available literature clearly indicate the lack of

systematic investigations on the formation of Tin(II) oxalates. In the present study, a systematic investigation of the formation of tin(II) oxalates employing hydrothermal methods in the presence of organic amines have been carried out. A new two-dimensional layered tin(II) oxalate, containing corrugated sheets, with honeycomb like apertures occupied by the organic amine cations has been prepared and characterized.

2.3. Open-framework metal dicarboxylates, $M(O_2C(CH_2)_nCO_2$ ($M = Cd, Mn, Nd$; $n = 1, 2, 3, 4$)

The synthesis of open-framework hybrid compounds, utilizing rigid organic linkers such as carboxylates, bipyridyl and other multi-functional ligands are of contemporary interest.^[8-11] Several new materials with large porous channels have been synthesized and characterized.^[8,9] Important contributions to these materials include the syntheses and structure of a variety transition metal, rare-earth and main group carboxylate frameworks.^[30-32] In addition, open-framework metal carboxylate structures comprising of aromatic dicarboxylates have also been made. Literature survey clearly indicated the lack of systematic investigations on the formation of aliphatic dicarboxylates of Cd and Mn. In addition, it would be interesting to exploit the large hydrocarbon backbone to give rise to larger channels and novel architectures. The present study involves the use of hydro/solvothermal methods along with organic amines, to form new aliphatic dicarboxylates with novel structures. The systematic investigations yielded a family of metal-carboxylate compounds diamondoid, α -polonium networks and also three-dimensional structures with unique channels.

2.4. Hybrid Organic-inorganic structures –Cadmium oxalate host frameworks incorporating alkali metal halides

A large variety of supramolecular host-guest compounds involving metal-organic and –inorganic open-framework structures have been described.^[33-35] In many of the host-guest compounds, ions, ion-pairs, or molecules have been accommodated in cages or cavities.^[35] Recently, alkali metal halide structures have been incorporated in phosphate based frameworks, employing high temperature ion-exchange method.^[36] In the present investigations, cadmium oxalate structures have been employed as a possible host for accommodating guest alkali metal halide structures. The hybrid structures were synthesized by employing simple metathetic reactions between cadmium halide salts and alkali metal oxalates, under hydro/solvothermal conditions. The products were novel departure from the traditional host-guest chemistry in that they included alkali metal halide structures with extended lattices and of different dimensionalities. In a material point of view, the periodic alternation between the organic and inorganic structures in these solids definitely make these materials as nanocomposites capable of possessing interesting physical properties to these solids like the dielectric and optical properties.

References

1. (a) R. M. Barrer, "Hydrothermal Chemistry of Zeolites", Academic Press (London) 1982. (b) M. L. Occelli, H. C. Robson, Zeolite Synthesis, American Chemical Society, Washington D. C., 1989.
2. (a) C. S. Cundy, P. A. Cox, *Chem. Rev.* **2003** (ASAP). (b) M. T. Weller, S. E. Dann, *Curr. Opin. Solid State Mater. Sci.* **1998**, *3*, 137.
3. (a) G. Férey, *Chem. Mater.* **2001**, *13*, 3084. (b) G. Férey, *J. Solid State Chem.*, **2000**, *152*, 37 and related articles in the same issue.
4. (a) A. K. Cheetham, G. Férey, T. Loiseau, *Angew. Chem. Int. Ed. Engl.* **1999**, *38*, 3269. (b) J. M. Thomas, *Angew. Chem. Int. Ed. Engl.* **1999**, *38*, 3588. (c) J. M. Thomas, *Chem. Eur. J.* **1997**, *3*, 1557. (d) G. Férey, C. R. Acad. Sci., Paris, t. 1, *Serie II c*, **1998**, *1*. (e) F. Schuth, W. Schmidt, *Adv. Mater.* **2002**, *14*, 629. (f) C. N. R. Rao, *Proc. Indian Acad. Sci. (Chem. Sci.)* **2002**, *113*, 363.
5. (a) R. Szoystek, "Handbook of Molecular Sieves", Academic Press (London), 1994. (b) W. M. Meier, D. H. Olson, C. Baerlocher, *Atlas of Zeolite Structure Types*, Elsevier London, 1996. (c) *Verified Syntheses of Zeolitic Materials*, Eds. H. Robson, K. P. Lillerud, 2nd Ed. 2001, Elsevier Science B. V.
6. (a) A. Müller, H. Reuter, S. Dillinger, *Angew. Chem. Int. Ed. Engl.* **1995**, *34*, 2328. (b) P. Y. Zavalij, M. S. Whittingham, *Acta Cryst.* **1999**, *B55*, 627. (c) G. Férey, *J. Fluorine Chem.* **1995**, *72*, 187.
7. (a) J. M. Lehn, *Supramolecular Chemistry, Concepts and Perspectives*, VCH, Weinheim, 1995. (b) M. J. Zaworotko, *Nature* **1999**, *402*, 242. (c) M. J. Zaworotko, *Nature* **1997**, *386*, 220. (d) B. Moulton, M. J. Zaworotko, *Advances in Supramolecular Chemistry*, JAI Press Inc. 2000, Vol. 7, p.235 and references therein. (e) *Supramolecular Organization and Materials Design*, eds: W. Jones and C. N. R. Rao, Cambridge Univ. Press, 2002.
8. (a) M. Eddaoudi, D. B. Moler, H. Li, B. Chen, T. M. Reineke, M. O'Keeffe, O. M. Yaghi, *Acc. Chem. Res.* **2001**, *34*, 319 and references therein. (b) M. Eddaoudi, J. Kim, D. Vodak, A. Sudik, J. Wachter, M. O'Keeffe, O. M. Yaghi, *Proc. Natl. Acad. Sci., USA* **2002**, *99*, 4900 and related articles in the same issue.
9. (a) B. Moulton, M. J. Zaworotko, *Chem. Rev.* **2001**, *101*, 1629. (b) C. J. Kepert, M. J. Rosseinsky, *Chem. Commun.* **1999**, 375. (c) E. J. Cussen, J. B. Claridge, M. J. Rosseinsky, C. J. Kepert, *J. Am. Chem. Soc.* **2002**, *124*, 9574 and references therein.

10. (a) P. J. Hagrman, D. Hagrman, J. Zubieta, *Angew. Chem. Int. Ed. Engl.* **1999**, *38*, 2638. (b) S. R. Batten, R. Robson, *Angew. Chem. Int. Ed. Engl.* **1998**, *37*, 1460 and references therein. (c) R. Robson, *J. Chem. Soc. Dalton Trans.* **2000**, 3735. (d) S. R. Batten, *Cryst. Eng. Comm.* **2001**, *18*, 1. (e) A. Clearfield, *Curr. Opin. Solid State Mater. Sci.*, **1996**, *1*, 268 and references therein.
11. C. Janiak, *Angew. Chem. Int. Ed. Engl.* **1997**, *36*, 1431.
12. (a) G. R. Desiraju, *Angew. Chem. Int. Ed. Engl.* **1995**, *34*, 2311; (b) I. Huc, J.-M. Lehn, *Proc. Natl. Ac. Sci. USA*, **1994**, *94*, 2106; (c) J. J. Atwood, J. E. D. Davies, D. D. MacNicol, in: F. Vogtle (Ed.), *Comprehensive Supramolecular Chemistry*, Vol. 9, Pergamon, Oxford, 1996.
13. (a) G. A. Jeffrey, *An Introduction to Hydrogen Bonding*, Oxford University Press, New York, 1997; (b) G. R. Desiraju, *Crystal Engineering: The Design of Organic Solids*, Vol. 54, Elsevier, New York, 1989; (c) J. C. MacDonald, G. M. Whitesides, *Chem. Rev.*, **1994**, *94*, 2383.
14. V. R. Pedireddi, S. Chatterjee, A. Ranganathan, C. N. R. Rao, *J. Am. Chem. Soc.* **1997**, *119*, 10867; V. R. Pedireddi, A. Ranganathan, K. N. Ganesh, *Org. Lett.* **2001** 3(1), 99.
15. (a) V. R. Pedireddi, S. Chatterjee, A. Ranganathan, C. N. R. Rao, *J. Am. Chem. Soc.* **1997**, *119*, 10867; (b) V. R. Pedireddi, S. Chatterjee, A. Ranganathan, C. N. R. Rao, *Tetrahedron* **1998**, *54*, 9457.
16. J.L.Atwood, J.E.D.Davies, D.D.MacNicol, F.Vögtle, in: F.H.Herbstein (Ed.), *Comprehensive Supramolecular Chemistry*, Vol. 6, Pergamon Press, New York, 1996, Chapter 3.
17. (a) J.C.MacDonald, C.P.Doewestein, M.M.Pilley, *Cryst. Grow. Design* **2001**, *1*, 29; (b) J.A.Paixao, A.Matos Beja, M.Ramos Silva, J.Martin-Gil, *Acta Cryst.* **2000**, *C56*, 1132 and references therein.
18. (a) O. Kahn, *Molecular Magnetism*; VCH: Weinheim Germany, 1993 and references therein. (b) P. Day, *Science*, **1993**, *261*, 431. (c) O. Kahn, *Angew. Chem. Int. Eng. Ed.* **1985**, *24*, 834. (d) M. Oilkington, S. Decurtins, "Magnetoscience from molecules to Materials", Chap. 10, Eds. J. S. Miller, M. Drillon, Wiley-VCH, Weinheim, 2001. (e) S. Decurtins, H. W. Schmalle, R. Pellaux, P. Fischer, A. Hauser, *Mol. Cryst. Liq. Cryst.* **1997**, *305*, 227. (f) S. Decurtins, H. W. Schmalle, P. Schneuwly, R. Pellaux, J. Ensling, *Mol. Cryst.*

- Liq. Cryst.* **1995**, 273, 167. (g) S. Decurtins, H. W. Schmalle, P. Schneuwly, L. M. Zheng, J. Ensling, A. Hauser, *Inorg.Chem.* **1995**, 34, 5501.
19. O. R. Evans, W. Lin, *Cryst. Growth Des.* **2001**, 1,9.
20. (a) S. Neeraj, S. Natarajan, C. N. R. Rao, *Angew. Chem. Int. Ed.Engl.*, **1999**, 38, 3480. (b) C. N. R. Rao, S. Natarajan, S. Neeraj, *J. Am. Chem. Soc.* **2000**, 122, 2810.
21. (a) E. Jeanneau, N. Audebrand, D. Louër, *Chem. Mater.* **2002**, 14, 1187. (b) E. Jeanneau, N. Audebrand, J. P. Auffrédic, D. Louër, *J. Mater. Chem.* **2001**, 11, 2545. (c) C. Boudaren, J. P. Auffrédic, M. Louër, D. Louër, *Chem. Mater.* **2000**, 12, 2324. (d) E. Jeanneau, N. Audebrand, D. Louër, *J. Mater. Chem.* **2002**, 12, 2383.
22. (a) S. O. H. Gutschke, D. J. Price, A. K. Powell, P. T. Wood, *Angew. Chem. Int Ed. Engl.* **1999**, 38, 1088 and references therein.
23. (a) F. Serpaggi, G. Férey, *J. Mater. Chem.* **1998**, 8, 2749; (b) F. Serpaggi, G. Férey, *J. Mater. Chem.* **1998**, 8, 2737. (c) F. Serpaggi, T. Luxbacher, A. K. Cheetham, G. Férey, *J. Solid State Chem.* **1999**, 145, 580.
24. (a) T. M. Reineke, M. Eddaoudi, M. Fehr, D. Kelly, O. M. Yaghi, *J. Am. Chem. Soc.* **1999**, 121, 1651; (b) T. M. Reineke, M. Eddaoudi, M. O'Keeffe, O. M. Yaghi, *Angew. Chem. Int. Ed.Engl.* **1999**, 38, 2590.
25. (a) S. Distler, S. C. Sevov, *Chem. Commun.* **1998**, 959; (b) S. Ayyappan, G. D. de Delgado, A. K. Cheetham, G. Férey, C. N. R. Rao, *J. Chem. Soc. Dalton Trans.* **1999**, 2905. (c) N. Stock, S. A. Frey, G. D. Stucky, A. K. Cheetham, *J. Chem. Soc. Dalton Trans.* **2000**, 4292.
26. (a) S. J. Hartman, E. Todorov, C. Cruz, S. C. Sevov, *Chem. Commun.* **2000**, 1213. (b) S. Drumel, P. Janvier, D. Deniaud, B. Bujoli, *J. Chem. Soc., Chem. Commun.* **1995**, 1051. (c) S. Drumel, P. Janvier, P. Barboux, M. Bujoli-Doeuff, B. Bujoli, *Inorg. Chem.* **1995**, 34, 148. (d) S. Drumel, P. Janvier, P. Barboux, M. Bujoli-Doeuff, B. Bujoli, *New J. Chem.* **1995**, 19, 239. (e) G. B. Hix, D. S. Wragg, P. A. Wright, R. E. Morris, *J. Chem. Soc., Dalton Trans.* **1998**, 3359.
27. J. Zhu, X. Bu, X. P. Feng, G. D. Stucky, *J. Am. Chem. Soc.* **2000**, 122,11563.
28. (a) S. Natarajan, M.P. Attfield, A. K. Cheetham, *Angew. Chem. Int. Ed. Engl.* **1997**, 36, 978. (b) S. Natarajan, A. K. Cheetham, *Chem. Commun.* **1997**, 1089. (c) S. Natarajan, S. Ayyappan, A. K. Cheetham, C.N.R. Rao. *Chem. Mater.* **1998**, 10, 1627.

29. (a) S. Natarajan, M. Eswaramoorthy, A. K. Cheetham, C.N.R. Rao, *Chem. Commun.* **1998**, 1561. (b) S. Ayyappan, X. Bu, A. K. Cheetham, S. Natarajan, C.N.R. Rao, *Chem. Commun.* **1998**, 2181. (c) S. Natarajan, A. K. Cheetham, *J. Solid State Chem.* **1998**, *140*, 435. (d) S. Ayyappan, A. K. Cheetham, S. Natarajan, C.N.R. Rao, *J. Solid State Chem.* **1998**, *139*, 207.
30. (a) E. Lee, Y. Kim, D. -Y. Jung, *Inorg. Chem.*, **2002**, *41*, 501. (b) Y. Kim, D. -Y. Jung, *Bull. Korean Chem. Soc.*, **2000**, *21*, 656.
31. (a) Y. Kim, D. -Y. Jung, *Bull. Korean Chem. Soc.*, **1999**, *20*, 827. (b) M. Fleck, E. Tillmans, L. Bohaty, L. Z. Kristallogr., NCS, **2000**, *215*, 429.
32. (a) C. Livage, C. Egger, G. Ferey, *Chem. Mater.*, **1999**, *13*, 1546. (b) C. Livage, C. Egger, M. Nogues, G. Ferey, *J. Mater. Chem.*, **1998**, *8*, 2743. (c) C. Livage, C. Egger, G. Ferey, *Chem. Mater.*, **2001**, *13*, 410 and references therein.
33. (a) Dalton Discussion No. 3, Inorganic Crystal Engineering, *J. Chem. Soc., Dalton Trans.* **2000**, (21). (b) D. Braga, F. Grepioni, *Acc. Chem. Res.* **2000**, *33*, 601. (c) R. Kuhlman, G. L. Schemek, J. W. Kolis, *Inorg. Chem.* **1999**, *38*, 194. (d) S. S. -Y. Chui, S. M. -F. Lo, J. P. H. Charmant, A. G. Orpen, I. A. Williams, *Science.*, **1999**, *283*, 1148.
34. (a) T. M. Reineke, M. Eddaoudi, M. Fehr, D. Kelly, O. M. Yaghi, *J. Am. Chem. Soc.* **1999**, *121*, 1651. (b) T. M. Reineke, M. Eddaoudi, M. O’Keeffe, O. M. Yaghi, *Angew. Chem. Int. Ed. Engl.*, **1999**, *38*, 2590. (c) H. Li, M. Eddaoudi, M. O’Keeffe, O. M. Yaghi, *Nature* **1999**, *402*, 276. (d) T. M. Reineke, M. Eddaoudi, D. Moler, M. O’Keeffe, O. M. Yaghi, *J. Am. Chem. Soc.* **2000**, *122*, 4843.
35. (a) A. Muller, H. Reuter, S. Dillinger, *Angew. Chem. Int. Ed. Engl.* **1995**, *34*, 2328. (b) D. S. Wragg, R. E. Morris, *J. Am. Chem. Soc.* **2000**, *122*, 11246. (c) F. Taulelle, J. -M. Poble, G. Ferey, M. Benard, *J. Am. Chem. Soc.* **2000**, *122*, 0000.
36. Q. Huang, M. Ulutagay, P.A. Michener, S.-J. Hwu, *J. Am. Chem. Soc.* **1999**, *121*, 10323.

3. EXPERIMENTAL

3.1. Hydro/solvothermal synthesis

The most versatile method of making metastable solids with open structures is the hydrothermal technique.^[1-6] Thus, the hydrothermal technique has been most popular, garnering the interest from scientists and technologists of different disciplines. The term hydrothermal is purely of geological origin. It was first used by the British geologist, Sir Roderick Murchinson (1792-1871), to describe the action of water at elevated temperature and pressure in bringing about the changes in earth's crust leading to the formation of rocks and minerals.^[2] In spite of the fact that the hydrothermal technique has made tremendous progress, there is no unanimity in its definition. The term hydrothermal usually refers to any heterogeneous reaction in the presence of aqueous solvents or mineralizers under high pressure and temperature conditions to dissolve and recrystallize (recover) materials that are relatively insoluble under ordinary conditions. However, there are many other definitions for the same.^[2] Clearly, the definition can be extended further to solvothermal chemistry being the use of a sealed reaction vessel and temperature above the boiling point of the solvent used.^[3]

Water can act as a catalyst under elevated pressure-temperature conditions. The thermodynamic and transport properties of supercritical water are remarkably different from those of ambient water. The solubility of the non-polar species increases, whereas that of ionic and polar compounds decrease. Thus, a number of fundamental properties of water are greatly affected by pressure and temperature. The temperature dependence of the saturation vapor pressure is illustrated up to the critical point in Figure 3.1. In most of the hydrothermal preparations, one uses the variation in the properties of water as a function of temperature (within a confined

volume). This facilitates the migration of ions leading to enhanced reactivity giving rise to the formation of new materials.

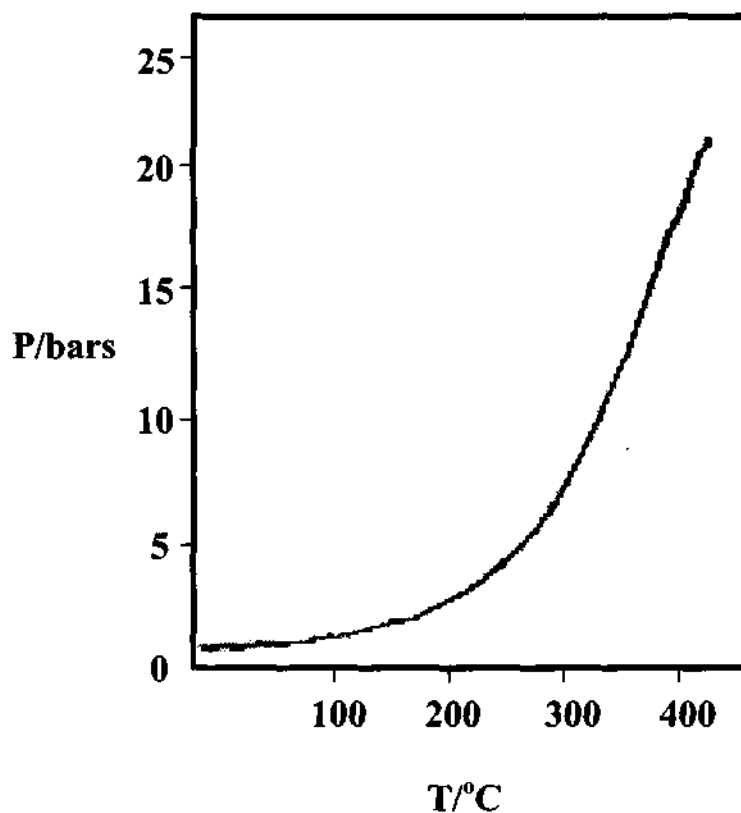


Fig. 3.1. The temperature dependence of saturation vapor pressure for water.

The relation between pressure and temperature and volume has been investigated for many solvents. In figure 3.2, the pressure, and temperature isotherms as a function of amount of water for a fixed volume is given. The figure demonstrates first dramatic rise in pressure when high percentage fill of the container is used, and second how the pressure inside the reaction container can be controlled by choice of the temperature and/or volume of the solvent used. Below the critical point of water, and even below 200 °C, a high percentage fill allows access to pressures of hundreds of atmospheres. As mentioned above, under hydrothermal conditions, the reactants, which are otherwise difficult to dissolve go

into the solution as complexes under the action of mineralizers or solvents, hence one can expect the conditions of chemical transport reactions. Therefore, some workers even define hydrothermal reaction as special cases of chemical transport reactions. Owing to specific physical properties, particularly the high solvation power, high compressibility, and high mass transport of these solvents

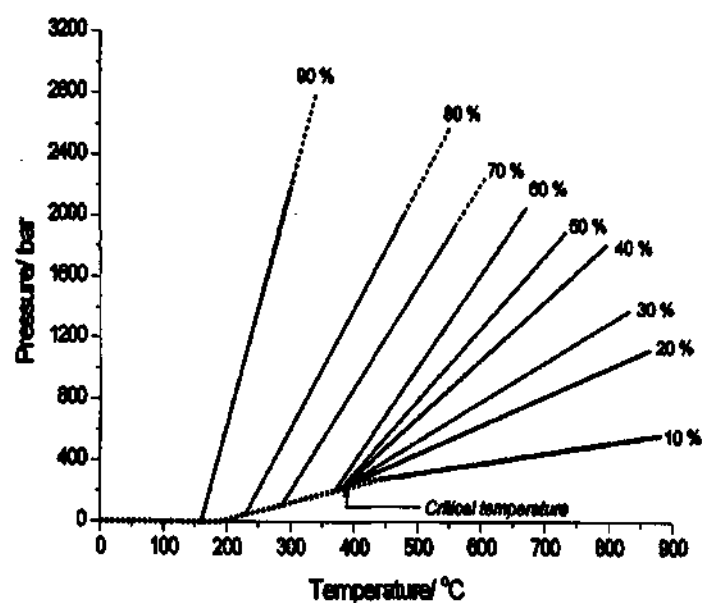


Fig. 3.2. Pressure as a function of temperature and percentage fill factor of water in a sealed vessel.

one can also expect the occurrence of different types of reactions like:

- (i) Synthesis of new phases or stabilization of new complexes.
- (ii) Crystal growth of several inorganic and/or organic compounds.
- (iii) Preparation of finely divided materials and microcrystallites with well-defined size and morphology for specific applications.

Another aspect of the hydrothermal synthesis is the use of “mineralizer”, a chemical entity that can bring about fall in free energy in a localized region enabling the formation nucleation centers. On the other hand if it is included in the

structure it adopts specific configurations preserving the structure. In many of the below mentioned synthesis, acetic acid has been used for its essentiality in the formation of the final product, but their absence in the final structure clearly suggests a mineralizing role. In fact, acetic acid has been used for a similar role in other systems too.^[7]

In a typical hydrothermal synthetic technique, the reactants are enclosed in a PTFE container (11 or 23 mL) and is sealed into a stainless steel jacket (see figure 3.3).

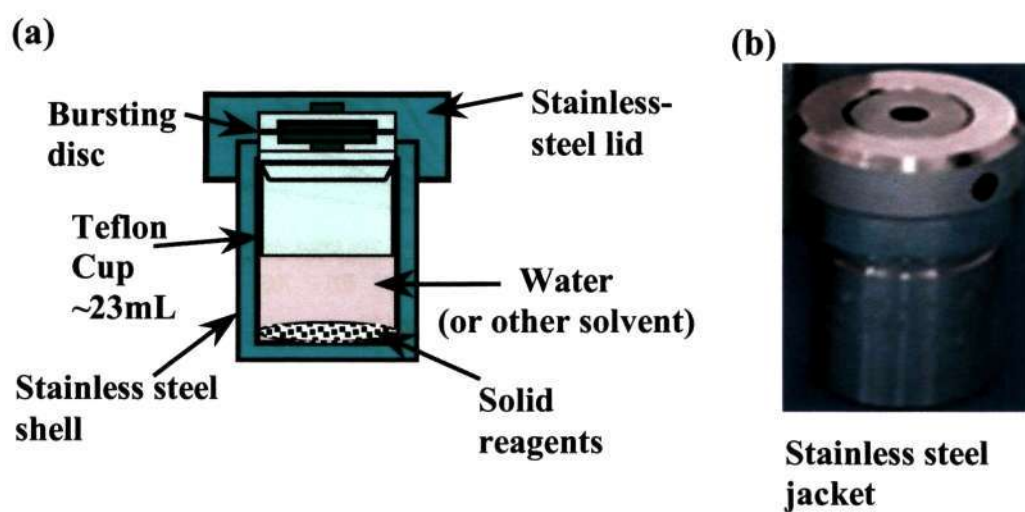


Fig. 3.3. (a) A schematic of a PTFE -lined, stainless steel autoclave typically used in the laboratory to perform subcritical hydro/solvothermal synthesis; (b) a photograph of the stainless steel jacket enclosing the PTFE liner.

This autoclave is heated in an oven in the temperature range of 70 to 250 °C for varying periods of time. In most cases, in the present study, good quality single crystals were obtained.

3.2. Synthesis

3.2.1. Synthesis of zinc oxalates

The zinc oxalates, $[\text{H}_3\text{N}(\text{CH}_2)_3\text{NH}_3]^{2+}[\text{Zn}_2(\text{C}_2\text{O}_4)_3]^{2-} \cdot 3\text{H}_2\text{O}$ (**I**) and $2[\text{C}_3\text{H}_7\text{NH}_3]^+[\text{Zn}_2(\text{C}_2\text{O}_4)_3]^{2-} \cdot 3\text{H}_2\text{O}$ (**II**), were synthesized starting from a mixture containing 1,3-diaminopropane (DAP) and n-propylamine (PA), respectively, as the structure-directing agents (SDA). In a typical synthesis, for **I**, 1.273g of oxalic acid was dissolved in 5 ml of deionized water and 0.41g of ZnO was added to the above under constant stirring. To this mixture 0.42 ml of DAP was added and homogenized for 10 min. The final composition of the mixture was ZnO: $2\text{H}_2\text{C}_2\text{O}_4$: DAP: $55\text{H}_2\text{O}$. For **II**, zinc oxide, oxalic acid, PA and water were mixed in the ratio ZnO: $\text{H}_2\text{C}_2\text{O}_4$: 2PA: $55\text{H}_2\text{O}$. The mixtures with an initial pH of 8.0 were heated in a stainless steel autoclave at 110 °C for 168 h for **I** and 65 h for **II** under autogeneous pressure. The final of the reaction mixture was 6.5. The resulting products contained large quantity of transparent plate like single crystals. The zinc oxalate, $\text{K}[\text{C}_6\text{N}_2\text{H}_{13}][\text{Zn}_2(\text{C}_2\text{O}_4)_3]_2 \cdot 4\text{H}_2\text{O}$, **III**, was synthesized in the presence of diazobicyclo[2,2,2]octane (DABCO). The mixture with a composition of ZnO: 2HCl: $2\text{K}_2\text{C}_2\text{O}_4$: $\text{C}_6\text{N}_2\text{H}_{12}$: $1.5\text{CH}_3\text{COOH}$: $200\text{H}_2\text{O}$, was heated at 150 °C for 72 h to result in large quantities of plate-like transparent crystals. The synthesis conditions for all the zinc oxalates prepared in the present study have been listed in Table 3.1.

3.2.2. Synthesis and Characterization of amine oxalates

Salts of various amines and oxalic acid were prepared in solution. Good quality single crystals were obtained by employing anyone of the following methods. Method A: Oxalic acid and the corresponding amine were dissolved in 1:1 or 2:1 ratio in water or water: n-butanol mixture. The solution was left uncovered over a water bath at 85 °C for a period of 3-4 hours. Crystals were

recovered from the solution before the solvent evaporated completely. Method B: Oxalic acid and the corresponding amine were mixed as above. The solution was then sealed in plastic bottles and was heated at 85 °C in an oven for 12 hours. On cooling good quality single crystals were isolated. Synthesis conditions and compositions for the various amine oxalates prepared during the course of the investigations are listed in Table 3.2.

Table 3.1. Compositions of the zinc oxalates made using amine oxalate route, I – VII

Starting composition of the gel	time, h	T, °C	product composition
ZnO: 2H ₂ C ₂ O ₄ : DAP: 55H ₂ O	168	110	[H ₃ N(CH ₂) ₃ NH ₃] ²⁺ [Zn ₂ (C ₂ O ₄) ₃] ²⁻ ·3H ₂ O, I
ZnO: H ₂ C ₂ O ₄ : 2PA: 55H ₂ O	65	110	[C ₃ NH ₁₀] ₂ [Zn ₂ (C ₂ O ₄) ₃].3H ₂ O, II
ZnO: 2HCl: 2K ₂ C ₂ O ₄ : C ₆ N ₂ H ₁₂ : 1.5CH ₃ COOH: 200H ₂ O	72	150	K[C ₆ N ₂ H ₁₃][Zn ₂ (C ₂ O ₄) ₃] ₂ ·4H ₂ O, III
ZnO : 5GUO : 100H ₂ O	360	85	[CN ₃ H ₆] ₂ [Zn(H ₂ O) ₂ (C ₂ O ₄) ₂], IV
ZnO : 2.04PIPO : 100H ₂ O	120	50	[C ₄ N ₂ H ₁₂] ₃ [Zn ₂ (C ₂ O ₄) ₃].8H ₂ O, V
ZnO : DABCO-O : 200H ₂ O	72	150	[C ₆ N ₂ H ₁₄][Zn(C ₂ O ₄) ₂].3H ₂ O, VI
ZnO : 5PIPO : 55H ₂ O	120	70	[C ₄ N ₂ H ₁₂][Zn ₂ (C ₂ O ₄) ₃].4H ₂ O, VII
ZnO : PRO : 25H ₂ O	72	150	[C ₃ NH ₁₀] ₂ [Zn ₂ (C ₂ O ₄) ₃].3H ₂ O, II

DAP – 1,3-diaminopropane; PA - propylamine

3.2.3. Reaction of amine oxalates with Zn^{II} ions

The amine oxalates were reacted with Zn^{II} ions under hydrothermal conditions. In a typical experiment, 0.137g of ZnO was dispersed in 3ml of water and 2g of GUO was added to it under continuous stirring. The contents were homogenized, transferred to an autoclave or plastic bottle and heated at 85°C for 15 days. The final composition of the mixture was ZnO : 5GUO : 100H₂O. The above reaction resulted in the formation of colorless rod-shaped crystals of the composition, [CN₃H₆]₂[Zn(H₂O)₂(C₂O₄)₂], **IV**.

Table 3.2. Synthesis conditions and composition of amine oxalates

Code	Starting composition*	C H N Analysis** (%)	Formula
PRO	H ₂ C ₂ O ₄ : C ₃ H ₉ N: 25 H ₂ O	N=8.58 (8.81) C=37.80 (37.74) H=7.71 (8.17)	[C ₃ NH ₁₀] ⁺ . [HC ₂ O ₄] ⁻ H ₂ O
BUO	H ₂ C ₂ O ₄ : C ₄ H ₁₁ N: 25 H ₂ O	N=7.77 (7.73) C=39.76 (37.78) H=7.82 (7.73)	[C ₄ NH ₁₂] ⁺ . [HC ₂ O ₄] ⁻ H ₂ O
ENO	H ₂ C ₂ O ₄ : C ₂ H ₈ N ₂ : 25 H ₂ O	N=10.18 (10.14) C=26.13 (26.08) H=5.85 (5.79)	0.5[C ₂ N ₂ H ₁₀] ⁺ . [HC ₂ O ₄] ⁻ H ₂ O
DABO	H ₂ C ₂ O ₄ : C ₄ H ₁₂ N ₂ : 25 H ₂ O	N=9.81 (9.79) C=33.64 (33.56) H=6.33 (6.29)	[C ₄ N ₂ H ₁₄] ⁺ . 2[HC ₂ O ₄] ⁻ H ₂ O
PIPO	2H ₂ C ₂ O ₄ : C ₄ H ₁₀ N ₂ : 25 H ₂ O	N=10.95 (10.45) C=36.48 (36.09) H=5.56 (5.26)	0.5[C ₄ N ₂ H ₁₂] ⁺ . [HC ₂ O ₄] ⁻
DCO	2H ₂ C ₂ O ₄ : C ₆ N ₂ H ₁₂ : 25 H ₂ O	N=9.84 (9.59) C=41.86 (41.09) H=5.41 (5.49)	[C ₆ N ₂ H ₁₄] ²⁺ . 2[HC ₂ O ₄] ⁻
GUO	2H ₂ C ₂ O ₄ : CN ₃ H ₆ : 25 H ₂ O	N=24.95 (25.15) C=21.17 (21.55) H=5.39 (5.39)	[CN ₃ H ₆] ⁺ . [HC ₂ O ₄] ⁻ . H ₂ O

*All syntheses were done at 85° C.

**Calculated values are given in parentheses.

A similar procedure was adopted for the preparation of other zinc oxalates, II and V – VII, by employing different amine oxalates. The summary of the synthesis conditions and the compositions of the products obtained are presented in Table 3.1.

3.2.4. Synthesis of cadmium oxalates

The compounds Na₄Cd₂(C₂O₄)₄.4H₂O, VIII and K₂Cd(C₂O₄)₂.2H₂O, IX have been synthesized under hydrothermal conditions. Typically, 0.26 g of sodium

carbonate was dispersed in a mixture of n-butanol and water (4.5ml + 1.1ml). 0.31 g of oxalic acid and 0.51 g of cadmium chloride were added to the above under continuous stirring. Finally 0.28 ml of glacial acetic acid was added and the contents stirred to homogeneity. The final gel with the composition, $\text{CdCl}_2 : \text{H}_2\text{C}_2\text{O}_4 : \text{Na}_2\text{CO}_3 : 2\text{CH}_3\text{COOH} : 20\text{C}_4\text{H}_9\text{OH} : 25\text{H}_2\text{O}$, was heated at 150 °C for 80h under autogeneous pressure. The resultant product contained needle-shaped crystals. For the synthesis of IX, a similar procedure was employed resulting in fine needle-like crystals (Table 3.3).

$\text{Cd}_2(\text{C}_2\text{O}_4)_{0.5}\text{Cl}_3\text{NaCl}\cdot 4\text{H}_2\text{O}$, X, was synthesized by reacting $\text{CdCl}_2\cdot 2\text{H}_2\text{O}$ and sodium oxalate under solvothermal conditions. Typically, 0.026g of sodium carbonate and 0.1879g of oxalic acid were dissolved in 3ml of dry n-hexanol. Contents were stirred for two hours at room temperature. 0.20g of $\text{CdCl}_2\cdot 2\text{H}_2\text{O}$ and 0.07ml of glacial acetic acid were added to the mixture and the contents were stirred to homogeneity (45 mins). The final mixture was sealed in an autoclave and heated at 150 °C for 60h. The product, colorless hexagonal plate-like and/or rod-like crystals were filtered. Both the morphologies were identified to be compound X (Table 3.3).

3.2.5. Synthesis of rare-earth metal oxalates

The yttrium oxalates, $[\text{C}_6\text{N}_2\text{H}_{16}]_{0.5}[\text{Y}(\text{H}_2\text{O})(\text{C}_2\text{O}_4)_2]2(\text{H}_2\text{O})$, XI and $[\text{C}_3\text{N}_2\text{H}_{12}][\text{Y}(\text{C}_2\text{O}_4)_2]$, XII, were synthesized hydrothermally in the presence of 1,2-diaminopropane (1,2-DAP) and 1,3-diaminopropane (1,3-DAP) respectively. For the synthesis of XI, 0.365 g of yttrium nitrate was dissolved in 1 ml of deionized water and 0.29 ml of acetic acid was added to the same under constant stirring. 0.63 g of oxalic acid and 0.43 ml of 1,2-diaminopropane (1,2-DAP) are added to the above and the mixture homogenized for 30 min. The final mixture with the composition, $\text{Y}(\text{NO}_3)_3 : 5\text{H}_2\text{C}_2\text{O}_4 : 5\text{CH}_3\text{COOH} : 51,2\text{-DAP} : 55\text{H}_2\text{O}$, was heated at

180 °C for 6 days. The resulting product contained a crop of rod-like crystals. **XI** was one of the main products of the reaction along with the condensed yttrium oxalate. For the synthesis of **XII**, a mixture of the composition, $Y(NO_3)_3 : 5H_2C_2O_4 : 5CH_3COOH : 5(1,3-DAP) : 55H_2O$ was heated at 180 °C for 5 days in the autoclave to obtain rod-like crystals.

Compounds $[NH_3CH_2CH(NH_3)CH_3][Nd(C_2O_4)_2(HCOO)].H_2O$, **XIII** and $[OC(CH_3)NCH_2CH(CH_3)NH_3][Nd(C_2O_4)_2].H_2O$, **XIV**, were synthesized hydrothermally in the presence of 1,2-DAP. Identical starting compositions were employed for both cases, but formic and acetic acids were used as mineralizer in **XIII** and **XIV**, respectively. Thus, in a typical synthesis, 1.0 $Nd(NO_3)_4 \cdot 4H_2O$ (0.33g) : 6.2DAP (0.43 ml) : 6.1 $H_2C_2O_4 \cdot 2H_2O$ (0.63g) : 6.2[HCOOH (0.19 ml)(I)/ CH_3COOH (0.29 ml)(II)] : 67.8 H_2O were taken and heated at 180 °C for 132 h. The initial pH in both the cases was close to 5.0. The final product contained large quantities of rod-shaped crystals. The conditions employed for the preparation of rare earth oxalates are listed in Table 3.3.

3.2.6. Synthesis of tin(II) oxalate

The tin(II) oxalate, $[(CH_3)_2NH(CH_2)_2NH(CH_3)_2][Sn_2(C_2O_4)_3].H_2O$, **XV**, was synthesized starting from a mixture containing N,N,N',N'-tetramethyl ethylenediamine (TMED), as the SDAs. Tin(II) oxalate, phosphoric acid (85 wt%), TMED and water were taken in the ratio $SnC_2O_4 : H_3PO_4 : TMED : 55 H_2O$ and heated at 150° C for 48h (Table 3.3). The resulting product, contained small quantity of crystals along with white powder. The single crystals could be easily separated from the white powder under an optical microscope.

Table 3.3. Synthesis conditions for compounds VIII-XV

Reactant mole ratios	Temp. ° C	Time hr	Product
CdCl ₂ : H ₂ C ₂ O ₄ : Na ₂ CO ₃ : 2CH ₃ COOH : 20C ₄ H ₉ OH : 25H ₂ O	150	80	Na ₄ Cd ₂ (C ₂ O ₄) ₄ .4H ₂ O (VIII)
CdCl ₂ : 1.5K ₂ C ₂ O ₄ : 0.84DAP : 1.93CH ₃ COOH : 44C ₄ H ₉ OH : 84H ₂ O	150	80	K ₂ Cd(C ₂ O ₄) ₂ .2H ₂ O (IX)
CdCl ₂ .2H ₂ O : 0.25 Na ₂ CO ₃ : 1.5 H ₂ C ₂ O ₄ .2H ₂ O : 1.2 CH ₃ COOH: 24 n-C ₆ H ₁₃ OH	150	60	Cd ₂ (C ₂ O ₄) _{0.5} Cl ₃ NaCl.4H ₂ O (X)
Y(NO ₃) ₃ : 5H ₂ C ₂ O ₄ : 5CH ₃ COOH : 5(1,2-DAP) : 55H ₂ O	180	120	[C ₆ N ₂ H ₁₆] _{0.5} [Y(H ₂ O)(C ₂ O ₄) ₂].2(H ₂ O) (XI)
Y(NO ₃) ₃ : 5H ₂ C ₂ O ₄ : 5CH ₃ COOH : 5(1,3-DAP) : 55H ₂ O	180	120	[C ₅ N ₂ H ₁₂][Y(C ₂ O ₄) ₂] (XII)
Nd ^(III) (NO ₃).4H ₂ O : 6.2DAP : 6.1H ₂ C ₂ O ₄ .2H ₂ O : 6.2HCOOH: 67.8H ₂ O	180	132	[NH ₃ CH ₂ CH(NH ₃)CH ₃][Nd(C ₂ O ₄) ₂ (HCOO)].H ₂ O (XIII)
Nd ^(III) (NO ₃).4H ₂ O : 6.2DAP : 6.1H ₂ C ₂ O ₄ .2H ₂ O : 6.2CH ₃ COOH: 67.8H ₂ O	180	132	[OC(CH ₃)NCH ₂ CH(CH ₃)NH ₃][Nd(C ₂ O ₄) ₂].H ₂ O (XIV)
SnC ₂ O ₄ : H ₃ PO ₄ : TMED: 55 H ₂ O	150	48	[(CH ₃) ₂ NH(CH ₂) ₂ NH(CH ₃) ₂][Sn ₂ (C ₂ O ₄) ₃].H ₂ O, XV

3.2.7. Syntheses of cadmium malonate and manganese glutarate

Compound $[\text{Cd}(\text{O}_2\text{C}-\text{CH}_2-\text{O}_2)(\text{H}_2\text{O})]\cdot\text{H}_2\text{O}$, XVI was prepared at room temperature by reacting $\text{CdCl}_2\cdot 2\text{H}_2\text{O}$ with malonic acid. Typically, 0.1g of $\text{CdCl}_2\cdot 2\text{H}_2\text{O}$ was dissolved in a n-hexanol + mixture water (1ml + 2ml). 0.16g of malonic acid and 0.1ml of 1,2-diamino propane added to the above mixture under constant stirring. The mixture was stirred to homogeneity. The final mixture with the composition $\text{CdCl}_2\cdot 2\text{H}_2\text{O}: 3.1\text{C}_3\text{O}_4\text{H}_4: 2.3\text{C}_3\text{H}_{10}\text{N}_2: 16.2\text{n-C}_6\text{H}_{13}\text{OH}: 223.6\text{H}_2\text{O}$, was allowed to crystallize at room temperature ($T=298\text{K}$) in a sealed polypropylene bottle. The product contained colorless hexagonal plate-like crystals.

Compound $[\text{Mn}(\text{O}_2\text{C}-(\text{CH}_2)_3-\text{CO}_2)]$, XVII was synthesized by reacting manganese(II) chloride with glutaric acid under solvothermal conditions. About 0.2g of $\text{MnCl}_2\cdot 4\text{H}_2\text{O}$ was dissolved in 2 ml of n-hexanol. 0.33g of glutaric acid and 0.22g of piperazine added to this and the contents were stirred to homogeneity. The final mixture with the composition $\text{MnCl}_2\cdot 4\text{H}_2\text{O}: 2.47\text{C}_5\text{H}_8\text{O}_4: 2.53\text{C}_4\text{N}_2\text{H}_{10}: 15.58\text{n-C}_6\text{H}_{13}\text{OH}$, was heated in an autoclave at $180\text{ }^\circ\text{C}$, for 72 hours. The product contained colorless hexagonal plate-like crystals. The synthesis conditions for XVI and XVII are listed in Table 3.4.

3.2.8. Synthesis of cadmium succinates

Similar to the synthesis of zinc oxalates, the reaction of amine succinates with Cd salt has been used in addition, to a direct reaction of Cd salt with succinic acid and amine. Both the methods were carried out under hydrothermal conditions. The succinates of guanidine, $3[\text{CN}_3\text{H}_6][\text{C}_4\text{H}_5\text{O}_4]$ (GUS) and piperazine, $[\text{C}_4\text{N}_2\text{H}_{12}][\text{C}_4\text{H}_4\text{O}_4]$ (PIPS) were prepared by slow evaporation from a solution of the amine and succinic acid (1:2 or 1:1 ratio) in water-n-butanol mixture over a water bath.

Compounds **XVIII-XXI** were prepared by the reaction of Cd^{2+} ions with the organoamine-succinates. Typically, for the preparation of $[\text{CN}_3\text{H}_6]_2[\text{Cd}(\text{C}_4\text{H}_4\text{O}_4)_2]$, **XIX**, 0.552g of guanidinium succinate (GUS) was dissolved in a n-butanol + water (3ml + 4ml) mixture. 0.21g of cadmium chloride and 0.15ml of piperidine were added to the above, and the contents stirred to homogeneity. The final mixture of the composition $\text{CdCl}_2: 3[\text{CN}_3\text{H}_6][\text{C}_4\text{H}_5\text{O}_4]: 1.45\text{C}_5\text{H}_{11}\text{N}: 31\text{n-C}_4\text{H}_9\text{OH}: 213\text{H}_2\text{O}$ was heated at 100 °C for 72 h. A similar procedure was employed for the synthesis of other succinates, **XVIII** and **XX - XXIII**. Piperidine was employed as the secondary base to deprotonate the succinic acid completely.

$[\text{Na}_3\text{Cd}_5(\text{C}_4\text{H}_4\text{O}_4)_6\text{Cl}]$, **XXIV**, and $[\text{Na}_3\text{Cd}_5(\text{C}_4\text{H}_4\text{O}_4)_6\text{Br}]$, **XXV** were prepared by the reaction between sodium succinate and $\text{CdCl}_2(\text{Br}_2)$ under hydrothermal conditions. In a typical synthesis of **XXIV**, 0.1053 g of Na_2CO_3 was dissolved in a mixture of 2ml n-butanol and 0.5ml water. To this 0.1173 g of succinic acid was added under continuous stirring. The contents were stirred for 20 min, followed by the addition of 0.2 g of $\text{CdCl}_2\cdot\text{H}_2\text{O}$. To this mixture, 0.11 ml of glacial acetic acid was added and the contents stirred to attain homogeneity. The final mixture of the composition $\text{CdCl}_2\cdot\text{H}_2\text{O}: \text{Na}_2\text{CO}_3: \text{H}_6\text{C}_4\text{O}_4: 1.93\text{CH}_3\text{COOH}: 22\text{n-C}_4\text{H}_9\text{OH}: 28 \text{H}_2\text{O}$ was heated at 150 °C for 72 h. The resulting product contained truncated octahedral shaped crystals. The yield was about 40%. **XXV** was obtained in 15% yield by a similar procedure using $\text{CdBr}_2\cdot 4\text{H}_2\text{O}$ in place of $\text{CdCl}_2\cdot\text{H}_2\text{O}$. The synthetic conditions employed for the synthesis of **XVIII-XXV** are presented in Table 3.4.

3.2.9. Synthesis of manganese adipate

Compound **XXVI** was synthesized by reacting manganese(II) chloride with adipic acid under solvothermal conditions. Typically, 0.2g of $\text{MnCl}_2\cdot 4\text{H}_2\text{O}$ was dissolved in 3 ml of n-hexanol and 0.295g of adipic acid, 0.1742g of piperazine and

Table 3.4. Synthesis conditions for Compound XVI-XXVI

Reactant mole ratios	Temp. ° C	Time hr	Product
CdCl ₂ .2H ₂ O: 3.1C ₃ O ₄ H ₄ : 2.3C ₃ H ₁₀ N ₃ : 16.2n-C ₆ H ₁₃ OH: 223.6H ₂ O	RT	72	[Cd(O ₂ C-CH ₂ -O ₂)(H ₂ O)].H ₂ O, XVI
MnCl ₂ .4H ₂ O: 2.47C ₃ H ₈ O ₄ : 2.53C ₄ N ₂ H ₁₀ : 15.58 n-C ₆ H ₁₃ OH	180	72	[Mn(O ₂ C-(CH ₂) ₃ -CO ₂)] ₂ , XVII
CdCl ₂ : 3.0[CN ₃ H ₆][C ₄ H ₅ O ₄]: 1.45C ₃ H ₁₀ NH: 31.0n-C ₄ H ₉ OH: 213.0H ₂ O	100	48	[CN ₃ H ₆] ₂ [Cd ₂ (C ₄ H ₄ O ₄)(Cl) ₂] (XVIII)+ [CN ₃ H ₆] ₂ [Cd(C ₄ H ₄ O ₄) ₂] (XIX)
CdCl ₂ : 3.0[CN ₃ H ₆][C ₄ H ₅ O ₄]: 1.45C ₃ H ₁₀ NH: 31.0n-C ₄ H ₉ OH: 213.0H ₂ O	100	72	[CN ₃ H ₆] ₂ [Cd(C ₄ H ₄ O ₄) ₂] (XIX)
CdCl ₂ : 1.7[C ₄ N ₂ H ₁₂][C ₄ H ₄ O ₄]: 1.6C ₃ H ₁₀ NH: 134.2H ₂ O: 35.2n-C ₄ H ₉ OH	150	80	Cd ₂ (C ₄ H ₄ O ₄) ₂ (C ₄ N ₂ H ₈)(H ₂ O) ₃ (XX)
CdCl ₂ : 2.0[C ₄ N ₂ H ₁₂][C ₄ H ₄ O ₄]: 2.0C ₃ H ₁₀ NH: 167.9H ₂ O: 22.0n-C ₄ H ₉ OH	150, 80(wb)	48 14	[C ₄ N ₂ H ₁₂][Cd ₂ (C ₄ H ₄ O ₄) ₂].4H ₂ O (XXI)
CdCl ₂ : 2.0TMEN ^b : 3.0C ₄ H ₆ O ₄ : 2.0C ₃ H ₁₀ NH: 168.0H ₂ O: 22.0n-C ₄ H ₉ OH	150	54	Cd(C ₄ H ₄ O ₄)(H ₂ O) ₂ (XXII)
CdCl ₂ : 2.1DABCO ^c : 2.0C ₄ H ₆ O ₄ : 2.0C ₃ H ₁₀ NH: 447.0H ₂ O: 44.0n-C ₄ H ₉ OH	150	78	Cd ₃ (C ₄ H ₄ O ₄)(OH) ₂ (XXIII)
CdCl ₂ .H ₂ O: Na ₂ CO ₃ : H ₆ C ₄ O ₄ : 1.93CH ₃ COOH: 22n-C ₄ H ₉ OH: 28 H ₂ O	150	72	[Na ₃ Cd ₅ (C ₄ H ₄ O ₄) ₆ Cl] (XXIV)
CdBr ₂ .H ₂ O: Na ₂ CO ₃ : H ₆ C ₄ O ₄ : 1.93CH ₃ COOH: 22n-C ₄ H ₉ OH: 28 H ₂ O	150	72	[Na ₃ Cd ₅ (C ₄ H ₄ O ₄) ₆ Br] (XXV)
MnCl ₂ .4H ₂ O: 2.0C ₃ H ₁₀ NH: 2.0C ₄ N ₂ H ₁₀ : 2.0C ₃ H ₁₁ N: 24.0n-C ₆ H ₁₃ OH	180	72	[Mn(O ₂ C-(CH ₂) ₄ -CO ₂)] ₂ (C ₄ N ₂ H ₈) (XXVI)

0.2 ml of piperidine were added to the above. The final mixture with the composition $\text{MnCl}_2 \cdot 4\text{H}_2\text{O}$: $2.0\text{C}_6\text{H}_{10}\text{O}_4$: $2.0\text{C}_4\text{N}_2\text{H}_{10}$: $2.0\text{C}_5\text{H}_{11}\text{N}$: $24.0\text{n-C}_6\text{H}_{13}\text{OH}$, has an initial pH of 8.0, was heated at 180°C , for 72 hours. The product contained colorless hexagonal plate-like crystals (Table 3.4). The yield was about ~62%.

3.2.10. Alkali halide structures incorporated in cadmium oxalate host lattices

The cadmium oxalate structures incorporating alkali halide lattices were synthesized employing simple metathetic reactions between cadmium halide salts and the alkali oxalates. Typically for the synthesis of XXVII, 0.057 g of Rb_2CO_3 was dissolved in 4 ml n-butanol and 2 ml water mixture. 0.313 g of oxalic acid and 0.1 g of CdCl_2 was added and the contents were stirred for 20 min. Finally 0.04 ml of glacial acetic acid was added and the mixture was stirred to homogeneity. The final mixture with the composition, CdCl_2 : $0.5\text{Rb}_2\text{CO}_3$: $5\text{H}_2\text{C}_2\text{O}_4$: $1.5\text{CH}_3\text{COOH}$: $90\text{C}_4\text{H}_9\text{OH}$: $220\text{H}_2\text{O}$, was heated at 150°C for 72 h. A similar synthesis procedure was employed for the preparation of compounds XXVIII – XXXIV and is presented in Table 3.5.

Table 3.5. Synthesis conditions for compounds XXVII - XXXIV

Synthetic conditions		Product	
Reactant Mole ratios	Temp. [$^\circ\text{C}$]	Time [h]	
CdCl_2 : $0.5\text{Rb}_2\text{CO}_3$: $5\text{H}_2\text{C}_2\text{O}_4$: $1.5\text{CH}_3\text{COOH}$: $88\text{n-C}_4\text{H}_9\text{OH}$: $220\text{H}_2\text{O}$	150	78	$[\text{RbCl}][\text{Cd}_6(\text{C}_2\text{O}_4)_6] \cdot 2\text{H}_2\text{O}$ (XXVII)
CdBr_2 : $0.63\text{Rb}_2\text{CO}_3$: $2.54\text{H}_2\text{C}_2\text{O}_4$: $2.41\text{CH}_3\text{COOH}$: $75\text{n-C}_4\text{H}_9\text{OH}$: $63\text{H}_2\text{O}$	150	78	$[\text{RbBr}][\text{Cd}_6(\text{C}_2\text{O}_4)_6] \cdot 2\text{H}_2\text{O}$ (XXVIII)
CdBr_2 : Cs_2CO_3 : $1.47\text{H}_6\text{C}_4\text{O}_4$: $70\text{n-C}_4\text{H}_9\text{OH}$: $150\text{H}_2\text{O}$	150	108	$2[\text{CsBr}][\text{Cd}(\text{C}_2\text{O}_4)] \cdot \text{H}_2\text{O}$ (XIX)
CdBr_2 : $(\text{COOCs})_2$: $1.95\text{CH}_3\text{COOH}$:	150	80	$2[\text{CsBr}][\text{Cd}_2(\text{C}_2\text{O}_4)(\text{Br})_2] \cdot 4\text{H}_2\text{O}$ (XXX)

40n-C ₄ H ₉ OH: 62H ₂ O				
0.8CdCl ₂ : 0.2Cd(NO ₃) ₂ :	150	78	[Rb ₂ Cd(NO ₃)(Cl)(C ₂ O ₄)(H ₂ O)] (XXXI)	
1.5Rb ₂ CO ₃ : 2.0H ₂ C ₂ O ₄ :				
1.5CH ₃ COOH: 33n-C ₄ H ₉ OH:				
33H ₂ O				
CdBr ₂ : K ₂ CO ₃ : 1.35H ₂ C ₂ O ₄ :	150	80	[K ₂ Cd ₂ (C ₂ O ₄) ₃].2KBr.2H ₂ O	
2.5CH ₃ COOH: 27C ₄ H ₉ OH:			(XXXII)	
38H ₂ O				
CdCl ₂ : Rb ₂ CO ₃ : H ₂ C ₂ O ₄ :	150	80	3[RbCl][Cd ₂ (H ₂ O)C ₂ O ₄](Cl) ₂].	
2CH ₃ COOH: 33n-C ₄ H ₉ OH:			H ₂ O (XXXIII)	
33H ₂ O				
MnCl ₂ : 1.5K ₂ C ₂ O ₄ :	150	78	K ₂ [Mn ₂ (C ₂ O ₄) ₃].2[KCl].2H ₂ O	
1.04CH ₃ COOH: 33n-C ₄ H ₉ OH			(XXXIV)	

3.3. Characterization

3.3.1. Powder X-ray diffraction

The powder X-ray diffraction (XRD) is used as a very important tool in the characterization of porous materials. Different features of a powder diffraction pattern can be exploited in the characterization of a material (see Table given below). Powder diffraction is most commonly used as a *fingerprint* in the identification of a material, however, other information can also be obtained from a diffraction pattern.

Feature	Information
Peak positions (2 theta values)	Unit cell dimensions
Non-indexable lines	Presence of a crystalline impurity (or incorrect indexing)
Systematically absent reflections	Symmetry
Background	Presence (or absence) of amorphous material
Width of the peaks	Crystallite (domain) size Stress/strain stacking faults
Peak intensities	Crystal structure

To index the powder pattern the important parameter, in addition to the peak positions (2θ), is the full-width half maximum (FWHM). The FWHM value of 0.01 or less would be an ideal value (standardized using the Si 111 reflection; 28.44° with a $\text{Cu-K}\alpha_1$ radiation). The measured 2θ values for the peaks in Si XRD pattern should agree with the literature values to within 0.01° . If the sample is off-center this will affect the 2θ zero point correction, so ideally the sample should be mixed with small amount of an internal standard so that the 2θ calibration can be done simultaneously. However, if care is taken in positioning of the sample, a 2θ calibration using an external standard is generally sufficient. For identification and structural analysis, accurate relative intensities are essential. There are three important factors that can hamper the relative peak intensities: (i) sample thickness, (ii) preferred orientation and (iii) divergence slit(s).

Most powder diffraction data analysis assume that the sample consists of millions of randomly oriented crystallites. If this is not the case, relative intensities will be distorted. For example, if the crystallites have a plate-like morphology, they are likely to lie flat. Assuming that the c-axis is parallel to the short dimension, crystallites aligned in 001 diffraction condition will be over-represented while those in the $hk0$ diffraction condition underrepresented. This will lead to bias in the relative intensities recorded. Various sample preparation techniques have been used to reduce the preferred orientation (such as back or side loading of the flatplate sample holders mixing amorphous glass beads with the sample, or spray drying, but none is foolproof. Measurements in transmission mode with the sample loosely packed in a rotating capillary are less susceptible (but not immune) to this problem. An easy way to establish whether or not preferred orientation is present is to measure the diffraction pattern in both the reflection and transmission mode. The

two measured patterns should be comparable, and if their relative intensities differ significantly (in a *hkl*-dependent manner), there is probably preferred orientation present in the sample.

In case of microporous material characterization, powder diffraction data are most commonly used to identify a newly synthesized material or to monitor the phase changes that take place as a function of changes in reaction conditions or to monitor the effects of post-synthesis treatment. In all cases, the measured pattern is compared with an existing one, whether it be a pattern in the collection of simulated XRD powder patterns for known microporous materials, the powder diffraction file (PDF) of the Inorganic Chemistry Diffraction Database (ICDD) or an in-house data file.^[8] A few practical considerations during a powder pattern recording are: (i) intensities are important so the data should be recorded keeping in mind the points discussed above; (ii) peak position information is often given in terms of *d*-values rather than 2θ values because *d*-values are independent of the X-ray wavelength (λ) used. ($d = \lambda/2\sin\theta$); (iii) the low angle lines are the ones most strongly affected by the non-framework species.^[9] In general, these lines are more intense in the calcined material than in the as synthesized form and similar materials containing different cations or different organic species may have quite different relative intensities at low angles. However, the intensities of the higher angle reflections are generally dominated by the positions of the framework atoms, so these can be compared quite well; (iv) different synthesis conditions or different post syntheses treatments can cause subtle distortions in the structure of the framework that can complicate the identification. The symmetry may be reduced and thereby produce more peaks in the pattern), although the basic framework topology remains unchanged. In such a case, indexing the powder pattern to obtain the unit cell dimensions can facilitate the identification.

In the present case, The powder X-ray diffraction patterns were recorded for all the samples on a Rich Seifert-3000TT X-ray powder diffractometer, with a flat plate sample holder with theta-theta geometry is used for the data collection. The incident X-ray is monochromated. The detector is a liq. N₂ cooled solid state detector or a simple scintillation counter. The powder XRD patterns, in most cases, indicated that the product was pure phase and new material. The XRD patterns were entirely consistent with the structures determined using the single-crystal X-ray diffraction. The simulated and the experimental powder XRD patterns for X, XX and XXIV are presented in Figures 3.4. A least squares fit (Cu-K α) of the XRD patterns of XII and XXVII, using the *hkl* indices generated from the single crystal structure, is listed in the Tables 3.6 and 3.7, respectively.

3.3.2. Determination of elemental composition

Energy dispersive X-ray analysis is carried out using a scanning electron microscope, fitted with a spectrometer, in order to determine the ratio between the different heavier elements in the compound under investigation. In some cases, the decomposition of the extra-framework organic amine under the electron beam gave rise to inconsistencies in the elemental ratio observed. In the present study, the energy dispersive analysis of X-rays (EDAX) was carried out on a Leica S440I scanning electron microscope fitted with a Link isis spectrometer. The determination of CHN is generally needed since these elements are present in the organic amine template used during the synthesis. In practice, multi-element analysis of C, H, N and S are carried out using a elemental micro-analysis instrument, which uses several alternative non-oxidative techniques with a detection limit of about 100 $\mu\text{g/g}$. The elemental compositional analyses of some of the compounds investigated in the present study are listed in Table 3.8.

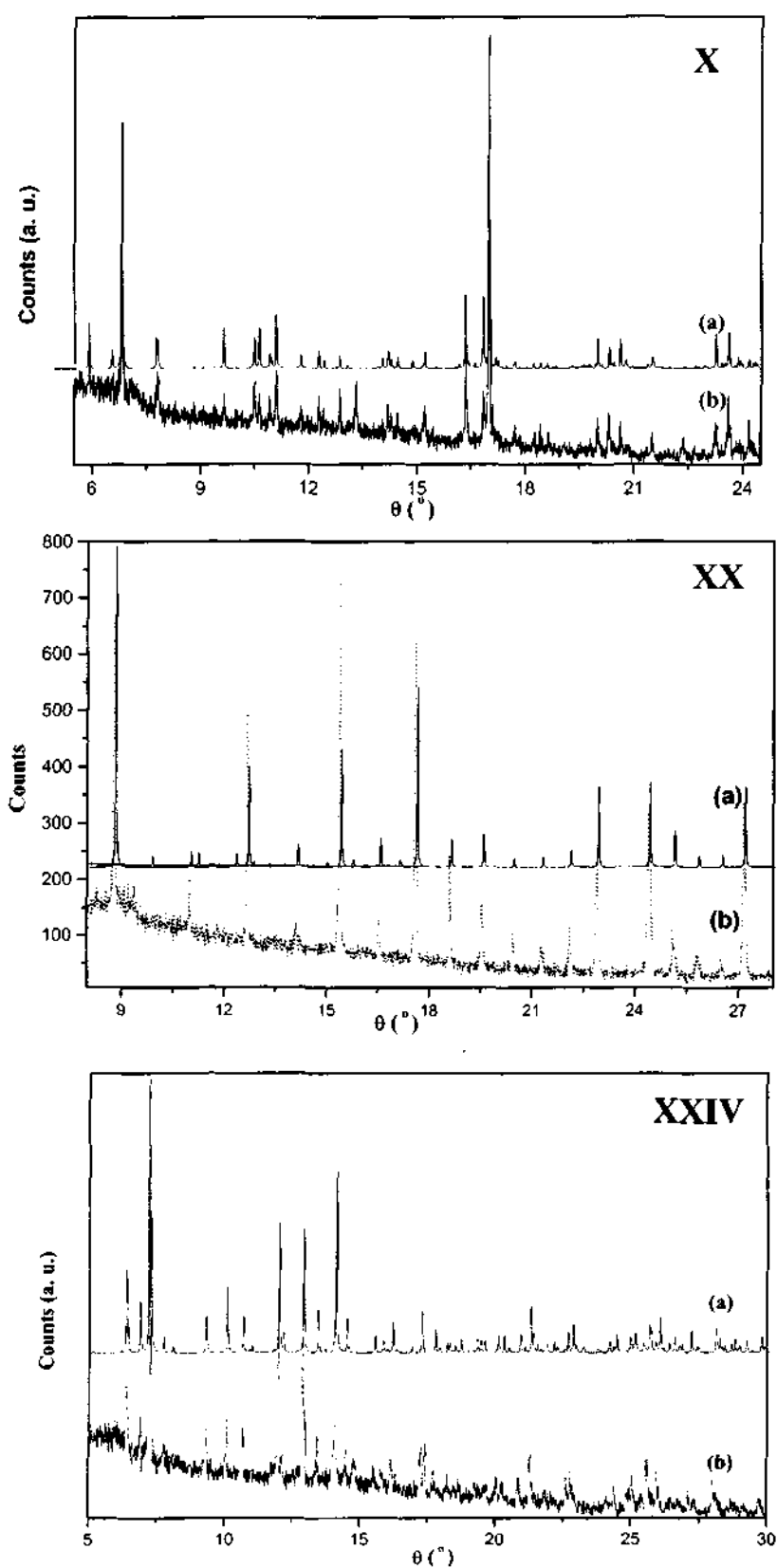


Figure 3.4. Powder XRD patterns of (1) $\text{Cd}_2(\text{C}_2\text{O}_4)_{0.5}\text{Cl}_3\text{NaCl}\cdot 4\text{H}_2\text{O}$, X, (2) $\text{Cd}_2(\text{C}_4\text{H}_4\text{O}_4)_2(\text{C}_4\text{N}_2\text{H}_8)(\text{H}_2\text{O})_3$, XX, (3) $[\text{Na}_3\text{Cd}_5(\text{C}_4\text{H}_4\text{O}_4)_6\text{Cl}]$, XXIV: (a) simulated; (b) Experimental

Table 3.6. Powder x-ray data for XIII, [H₃NCH₂CH(NH₃)CH₃][Nd(C₂O₄)₂(HCOO)].H₂O

h	K	l	2θ _{obs}	Δ(2θ) ^a	d _{calc}	Δ(d) ^b	I _{rel} ^c
1	1	0	11.196	0.004	7.905	-0.003	77
0	1	1	11.702	0.017	7.573	-0.011	100
-1	2	1	16.235	0.002	5.46	-0.001	56
1	1	1	16.92	0.009	5.243	-0.003	44
1	3	0	17.868	0.040	4.975	-0.011	50
0	3	1	18.149	0.005	4.889	-0.001	70
1	2	1	18.957	0.021	4.686	-0.005	62
2	0	0	20.066	-0.146	4.393	0.032	64
2	1	0	20.927	0.122	4.27	-0.025	69
1	3	1	21.778	-0.133	4.056	0.025	54
-2	3	1	25.418	-0.034	3.499	0.005	40
-1	3	2	26.029	-0.096	3.411	0.012	41
2	4	0	28.367	0.061	3.153	-0.007	42
-1	4	2	29.421	0.166	3.053	-0.017	56
-3	2	1	31.703	0.048	2.826	-0.004	34
-1	1	3	31.967	0.013	2.801	-0.001	40
2	1	2	33.095	0.016	2.708	-0.001	43
-3	0	2	33.191	-0.110	2.69	0.009	44
1	6	1	33.881	-0.033	2.643	0.003	48
3	3	0	33.968	-0.054	2.635	0.004	59
1	7	0	36.163	-0.035	2.481	0.003	38
-3	3	2	36.637	0.072	2.457	-0.004	35
1	3	3	39.043	0.006	2.307	0.000	28
-3	1	3	39.854	0.034	2.264	-0.002	43
0	0	4	43.327	-0.084	2.084	0.004	35
3	0	2	41.409	0.028	2.182	-0.002	33
-3	6	1	42.737	0.062	2.119	-0.003	43
2	2	3	43.508	0.170	2.088	-0.008	54
1	5	3	43.952	-0.098	2.056	0.004	44
4	1	1	45.139	-0.074	2.005	0.004	44

^a2θ_{obs} - 2θ_{calcd.} ^bd_{obs} - d_{calcd.} ^c100×I/I_{max}LSQ fitted lattice parameter (Cu-Kα): $a = 9.0065(9)$, $b = 18.1069(6)$, $c = 8.5461(9)$ Å, $\beta = 102.68(8)$.

Table 3.7. X-ray Powder Data for XXVII, [RbCl][Cd₆(C₂O₄)₆].2H₂O

H	K	L	2θ _{obs}	Δ(2θ) ^a	d _{calc}	Δ(d) ^b	I _{rel} ^c
0	0	3	11.102	0.000	7.970	0.000	11
1	0	1	11.498	0.000	7.696	0.000	9
1	0	2	13.163	0.008	6.722	0.004	52
1	0	4	18.485	-0.060	4.815	-0.015	8
1	1	0	19.007	-0.097	4.693	-0.024	20
1	1	3	21.996	-0.017	4.044	-0.003	14
0	0	6	22.369	-0.059	3.985	-0.010	11
2	0	2	23.179	-0.065	3.848	-0.011	8
2	0	4	26.560	-0.040	3.361	-0.005	100
1	0	7	28.480	-0.137	3.149	-0.015	11
2	1	1	29.384	-0.075	3.047	-0.008	17
1	1	6	29.444	-0.040	3.038	-0.004	13
2	1	2	30.135	-0.105	2.976	-0.010	9
2	1	4	32.804	-0.030	2.732	-0.002	7
0	0	9	33.739	0.000	2.657	0.000	15
2	0	7	34.395	-0.101	2.615	-0.007	6
2	1	5	34.751	-0.046	2.585	-0.003	18
3	0	3	35.045	-0.068	2.565	-0.005	7
2	0	8	37.439	-0.091	2.408	-0.006	11
1	1	9	39.086	-0.128	2.312	-0.007	6
3	1	1	40.211	-0.034	2.244	-0.002	48
3	0	6	40.248	0.001	2.241	0.000	27
3	1	2	40.703	0.024	2.215	0.001	11
3	1	5	44.424	0.002	2.039	0.000	4

^a2θ_{obs} - 2θ_{calcd.} ^bd_{obs} - d_{calcd.} ^c100×I/I_{max}

LSQ fitted lattice parameter (Cu-Kα): *a* = 9.3773(5), *b* = 9.3773(5), *c* = 23.8786(9) Å, *V* = 1818.4(3) Å³

3.3.3. Thermogravimetric analysis (TGA)

The open-framework materials are routinely characterized using TGA studies. Typically, the material under study is heated under a flow of nitrogen or air or oxygen gas and the mass loss occurring due to the step wise decomposition of the various species present in the material is measured as a function of temperature.

The temperature range at which the mass loss occurs and the amount of mass loss give a quantitative determination of the specific moiety present in the structure and this information can be used to verify the synthesis formulations. The product of calcination is identified through powder diffraction technique in order to understand the possible mode of decomposition and in some cases certain dehydrated phases can be stabilized. In the present investigations, the thermogravimetric analysis (TGA) of all the compounds were performed on a Mettler-Toledo TG850 instrument under the flow of N₂ or air, with a flow rate of 5 or 10ml/min and usually in the temperature range of 30 ° to 800 °C.

Table 3.8. Elemental composition analysis for selected compounds

Compound	CHN ratio (%) ^a	EDAX ratio
Na ₄ Cd ₂ (C ₂ O ₄) ₄ .4H ₂ O (VIII)	-	Na: Cd 3.9: 2.1
Cd ₂ (C ₂ O ₄) _{0.5} Cl ₃ NaCl.4H ₂ O (X)	2.7: 1.5 (2.4: 1.6)	Na: Cd: Cl 1.0: 1.9: 4.1
[Cd(O ₂ C-CH ₂ -O ₂)(H ₂ O)].H ₂ O (XVI)	14.8: 1.8 (14.4 : 2.4)	-
[Mn(O ₂ C-(CH ₂) ₃ -CO ₂)] (XVII)	34.3: 3.2 (32.5: 3.3)	-
[CN ₃ H ₆] ₂ [Cd(C ₄ H ₄ O ₄) ₂] (XIX)	26.1: 4.3: 18.6 (25.8: 4.3: 18.1)	-
Cd ₂ (C ₄ H ₄ O ₄) ₂ (C ₄ N ₂ H ₈)(H ₂ O) ₃ (XX)	25.9: 3.5: 3.4 (26.2: 3.7: 4.7)	-
[C ₄ N ₂ H ₁₂][Cd ₂ (C ₄ H ₄ O ₄) ₃].4H ₂ O (XXI)	26.2: 4.3: 0 (26.2: 4.4: 0)	-
Cd(C ₄ H ₄ O ₄)(H ₂ O) ₂ (XXII)	18.6: 2.1: 0 (18.2: 3.0: 0)	-
Cd ₃ (C ₄ H ₄ O ₄) ₂ (OH) ₂ (XXIII)	16.2: 1.7: 0 (15.9: 1.6: 0)	-
[Na ₃ Cd ₅ (C ₄ H ₄ O ₄) ₆ Cl] (XXIV)	21.8: 1.8 (21.1: 1.8)	-
[Na ₃ Cd ₅ (C ₄ H ₄ O ₄) ₆ Br] (XXV)	20.1: 1.8	-

	(20.5: 1.7)	
[RbCl][Cd ₆ (C ₂ O ₄) ₆].2H ₂ O (XXVIII)	-	Cd : Rb : Cl 6.5 : 1.0 : 1.1
2[CsBr][Cd(C ₂ O ₄)].H ₂ O (XXXI)	-	Cd : Cs : Br 1.1 : 1.5 : 1.5
2[CsBr][Cd ₂ (C ₂ O ₄)(Br) ₂].4H ₂ O (XXXII)	-	Cd : Cs : Br 1.1 : 1.1 : 1.8
3[RbCl][Cd ₂ (H ₂ O)C ₂ O ₄](Cl) ₂ · H ₂ O (XXXV)	-	Cd : Rb : Cl 1.0 : 1.5 : 2.5

3.3.4. Infrared spectroscopy (IR)

IR spectroscopy provides information regarding the functional groups present in the compound. The KBR pellet technique is frequently used for investigations of the vibrations of the framework.^[9] Also well-established are (i) infrared (IR) spectroscopy of self-supporting wafers (usually in transmission mode) and (ii) diffused reflectance IR Fourier transform (DRIFT) spectroscopy. Both methods enable us to investigate the cation vibrations in the Far-IR region. Thermal stability of these microporous materials against, for example, dehydration, dehydroxylation and interaction with sorbates can be characterized by (in situ) transmission IR or DRIFT.^[9]

In the far IR region (200 – 50 cm⁻¹) vibrations of cations against the framework occur. The wave numbers of the corresponding IR bands depend on the nature of the cations as well as on their coordination environment.^[9] IR spectroscopy is used to characterize microporous/adsorbate systems. Adsorption and desorption of water (hydration and dehydration) may be easily monitored by IR, since adsorbed water gives rise to typical deformation band around 1640cm⁻¹. Adsorbed or occluded template molecules are also detectable by, for example, CH and/or NH vibration bands. Two main problems encountered in IR spectroscopic

studies are (i) certain species can give rise to broad bands causing suppression of other specific bands that occur in proximity and (ii) two or more functional groups present within a compound can give rise to vibrational bands in the same range of frequencies making their distinction almost impossible. The IR- spectra of the samples synthesized were recorded on a Bruker spectrometer (IFS 66v/S). The spectra were usually recorded in the frequency range of 400 to 4000 cm^{-1} and Far-IR spectra were recorded whenever interesting metal-ligand bond characteristics were observed in the structure of the material.

3.3.5. Adsorption studies

Adsorption studies on open-structured compounds reveal several characteristic structural features of the material like the porosity, the catalytic activity etc. Several probe molecules have been routinely employed for this purpose (e.g. O_2 , N_2 , CO_2 , n-butane, alcohol). Generally adsorption of probe molecules within the materials with microporous architecture give rise to a Type I adsorption isotherm, an equilibrium process, indicating the rapid adsorption even at low concentrations of the adsorbate molecules. In addition, information on the type of pore system and the morphology of the pore structure – hydrophilicity/hydrophobicity of the interior surface of the pores can be obtained. Temperature programmed desorption (TPD) performed using ammonia as the probe enables the quantitative estimation of the number of acid sites and the strength of such sites present within the material under study. The removal of extra-framework organic amine cations usually leads to the collapse of the entire structure, however the other solvent of crystallization present in the channels can be removed reversibly and can even be exchanged for other molecules selectively. The reversible hydration/dehydration studies, in the present study, were using the adsorption set up fitted with a Cahn-2000 microbalance. In the adsorption

experiments performed in the present investigations, water and methanol were used as probe molecules.

3.3.6. Ionic conductivity

Ionic conductivity measurements have been carried out to evaluate the mobility of the alkali ions in these solids. Since the K^+ is much bigger than the Na^+ ions, the studies have been carried out only on compound VIII. Typically, cylindrical pellets of the samples (0.5 mm in thickness and 0.8 cm in diameter) were coated with silver paint on either side and pre-annealed at 90°C for 2 h before the experiment. Ionic conductivity measurements were carried out using a standard set up coupled with a impedance analyzer (Model No. HP – 4192A) in the frequency range from 10 Hz to 10 MHz. A 2-terminal capacitor configuration with silver electrode was employed in the range 298 – 493K, and the temperature was measured using Pt-Rh thermocouple positioned close to the sample. Ionic conductivity measurements were carried out using a standard set up coupled with a impedance analyzer (Model No. HP – 4192A) in the frequency range from 10 Hz to 10 MHz.

3.3.7. Single Crystal Structure Determination

Single crystal structures provide unambiguous three-dimensional molecular structures of new crystalline compounds. Besides confirming the connectivity and the stereochemistry of the molecule, crystal structures obtained can give precise bond length and angle information, absolute configuration (if appropriate) and an arrangement of molecules within the crystalline lattice. The single crystal structures were determined using a Siemens Smart-CCD diffractometer equipped with a normal focus (Fig. 3.5), 2.4 kW sealed tube x-ray source (Mo- K_{α} radiation, $\lambda = 0.71073 \text{ \AA}$) operating at 50 kV and 40mA. The diffractometer operates on a PLATFORM – three-circle goniometer for precision movement of the crystal in ω

and ϕ plus an automatic 2θ range for the detector and a two-dimensional Charge-coupled Device (CCD) detector with a 9cm diameter input imaging area.

The geometry of the diffractometer can be explained using a simple set of three-coordinate system. Smart uses the 3-circle goniometer and the geometrical alignment is briefly explained here. The three angles unique to this goniometer geometry are the χ , ϕ and ω , in addition to the 2θ angle that the detector makes with the incident X-ray beam. These angles as defined in a SMART diffractometer are represented schematically in figure 3.6. In this convention, there are two coordinate systems involved one being a three-dimensional coordinate system corresponding to the goniometer geometry (Fig. 3.7.a) and the other is the two coordinate system corresponding to the detector display geometry (Fig. 3.7.b). The direct beam propagates from $-XL$ to $+XL$, $+ZL$ is up and $+YL$ makes a right hand set (at $\omega = 0$, $\chi = 270^\circ$, the goniometer head is at $+YL$). These axes are referred to as the "laboratory axes". The goniometer setting angles 2θ and ω are right-handed rotations about ZL , χ is a left-handed rotation about XL' (XL rotated by ω), and ϕ is a left-handed rotation about ZL'' (ZL rotated by ω and χ). These are collectively called the "goniometer axes". A three-circle goniometer has the χ fixed at $+45^\circ$. The PLATFORM is fixed at $+54.74^\circ$. The 2θ goniometer setting angle is identical to the detector swing angle. The detector axes are referred to as X and Y as opposed to XL , YL and ZL or the laboratory axes. When a detector is displayed the origin of the frame is at its lower left ($X=Y=0$) and its upper right is at ($X=511$, $Y=511$), with the coordinates in pixels (Fig. 3.7b). When the goniometer setting angles are all zero, the detector X axis is parallel to $-YL$ and the detector Y axis is parallel to the ZL . This makes the viewing a displayed frame like looking from the source towards the detector.

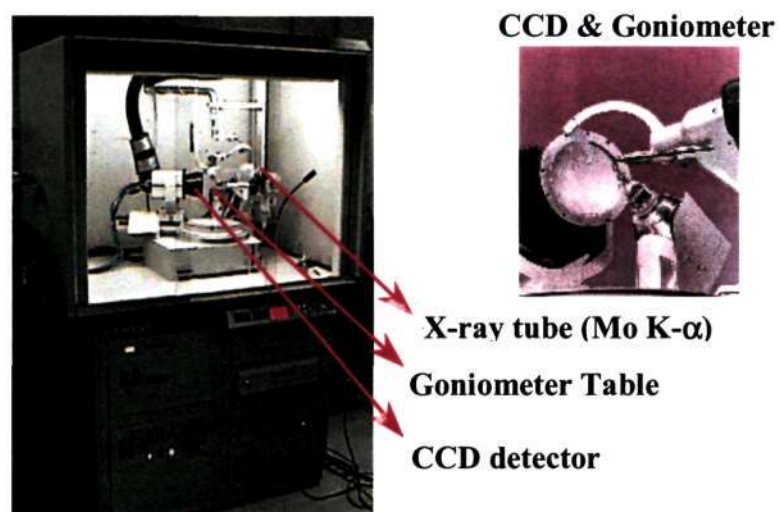


Fig. 3.5. Figure shows the photographic image of a SIEMENS SMART Single Crystal X-ray Diffractometer. Inset shows the enlarged image of the CCD and the goniometer.

The orientation matrix determined by the smart is independent of the setting angles of the frames used to determine it. As output, the matrix can be used in the standard mathematical convention to pre-multiply a column HKL vector to yield a column reciprocal lattice vector, v , with a length equal to the reciprocal interplanar spacing in the reciprocal angstroms ($|v| = d^*$). This vector can be rotated by the setting angles to obtain its XL, YL and ZL components in laboratory space for the vector in the diffracting condition.

All the compounds, **I-XXXIV**, including the amine oxalates were characterized using single crystal X-ray diffraction. For this purpose a suitable single crystal of each compound was carefully selected under a polarizing microscope and glued to a thin glass fiber with cyanoacrylate (superglue) adhesive. Single crystal structure determination by X-ray diffraction was performed on a Siemens Smart-CCD diffractometer (Fig. 3.5). In most cases, hemisphere of intensity data was collected at room temperature in 1321 frames with ω scans

(width of 0.30° and exposure time of 10 or 20s per frame). The structure was solved by direct methods using *SHELXTL-PLUS* suite of programs^[10] and difference Fourier syntheses.

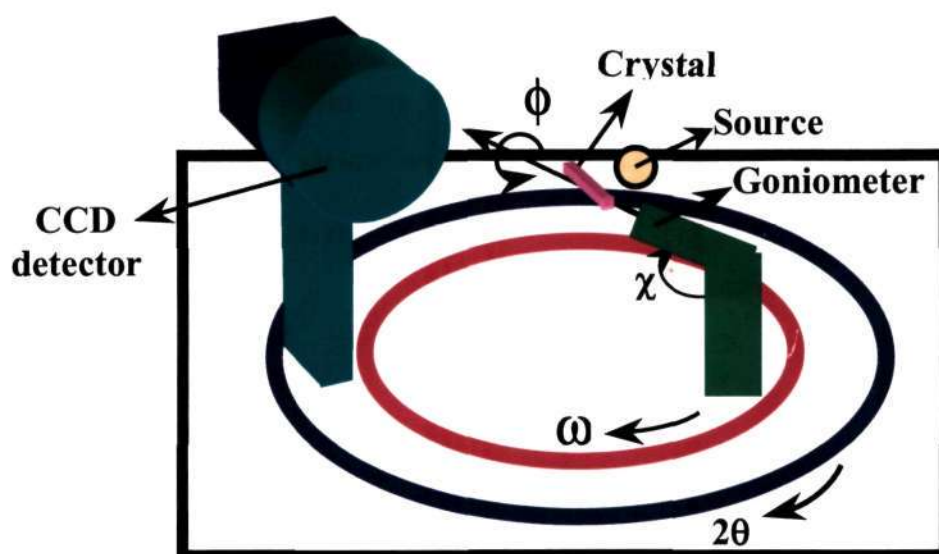
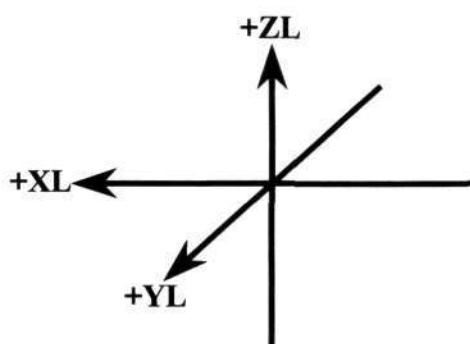


Fig. 3.6. A schematic diagram showing the different angles involved in the three-circle goniometer geometry of the SIEMENS SMART single crystal X-ray diffractometer.

**(a) SMART Goniometer
Geometry conventions**



(b) Detector geometry

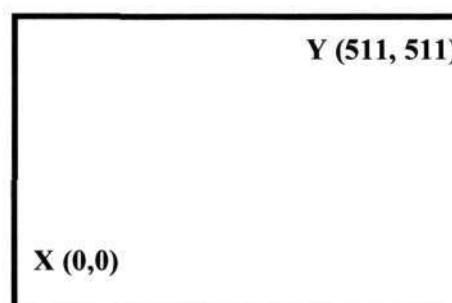


Fig. 3.7. The SMART geometry conventions, (a) goniometer axes geometry; (b) the detector geometry.

An empirical absorption correction based on symmetry equivalent reflections was applied using *SADABS* program.^[11] All the hydrogen positions are initially located in the difference Fourier maps, but for the final refinement the hydrogen atoms were placed geometrically and held in the riding mode. In case of disordered molecules, restraints for the bond distances have been used to keep the molecule intact and within reasonable limits. The last cycles of refinement included atomic positions for all the atoms, anisotropic thermal parameters for all the non-hydrogen atoms and isotropic thermal parameters for all the hydrogen atoms. Full-matrix-least-squares structure refinement against $|F^2|$ was carried out using *SHELXTL-PLUS* package of programs.^[10]

Pertinent crystallographic details for the amine oxalates in Table 3.9, for the open-framework zinc oxalates, **I**, **II** and **III**, are listed in Table 3.10, , for the zinc oxalates, **IV-VII**, in Table 3.11, for the cadmium oxalates, **VIII**, **IX** and **X** in Table 3.12, for the yttrium oxalates, **XI** and **XII**, and the neodymium oxalates, **XIII** and **XIV**, in Table 3.13, for the tin(II) oxalate, **XV**, in Table 3.14, for the cadmium malonate and manganese glutarate, **XVI** and **XVII**, in Table 3.15, for the cadmium succinates, **XVIII-XXVI**, in Table 3.16. and Table 3.17, manganese adipate, **XXVII**, in Table 3.18, for the cadmium oxalates incorporating alkali halides, **XXVIII-XXXIV**, in Table 3.19, 3.20 and 3.21. Atomic coordinates for the various compounds, **I-XXXIV**, are given in the Appendix at the end of the thesis (see Tables **AI-AXXXIV**).

Table 3.9. Crystal data and structure refinement parameters for amine oxalates

Crystal parameters	PRO	BUO	ENO	DABO	PIPO	DABCO	GUO
Empirical formula	C ₁₀ H ₂₄ N ₂ O ₉	C ₁₂ H ₂₈ N ₂ O ₉	C ₆ H ₁₄ N ₂ O ₉	C ₈ H ₁₆ N ₂ O ₉	C ₈ H ₁₄ N ₂ O ₈	C ₁₀ H ₁₆ N ₂ O ₈	C ₃ H ₉ N ₃ O ₅
Formula mass	316.32	344.36	258.2	286.24	266.23	292.25	334.26
Crystal system	Monoclinic	Monoclinic	Monoclinic	Orthorhombic	Monoclinic	Triclinic	Monoclinic
Space group	C2/c	C2/c	C2/c	Pna2(1)	C2/c	P-1	P2 ₁ /c
a (Å)	21.6428 (9)	23.238 (3)	18.025 (2)	14.6879 (6)	15.963 (6)	6.971 (7)	6.699(1)
b (Å)	5.6737 (2)	5.6590 (6)	5.6841 (6)	5.6876 (3)	5.716 (2)	9.607(10)	10.552(6)
c (Å)	14.3086 (6)	14.339 (2)	13.9913 (14)	15.6920 (7)	12.354 (4)	10.633 (11)	10.224(4)
α (°)	90	90	90	90	90	91.25(10)	90
β (°)	115.6300 (10)	99.277 (2)	126.898 (2)	90	108.07(2)	107.5(10)	103.77(3)
γ (°)	90	90	90	90	90	109.3(10)	90
Volume (Å ³)	1584.14 (9)	1861.0 (3)	1146.4 (2)	1310.89(11)	1071.5 (9)	634.8(11)	702.0(9)
Z	4	4	4	4	4	2	4
λ (MoKα) Å	0.71073	0.71073	0.71073	0.71073	0.71073	0.71073	0.71073
μ (mm ⁻¹)	0.117	0.105	0.143	0.133	0.149	0.134	0.149
Unique data	1134	1331	822	1555	760	1781	1012
R _i , wR ₂ [I > 2σ(I)]	0.0434, 0.1171	0.0548, 0.1398	0.0373, 0.0964	0.0788, 0.2088	0.0291, 0.0761	0.0492, 0.1391	0.0792, 0.2181
Goodness of fit (S)	1.141	1.163	0.999	1.134	1.112	1.062	1.089

Table 3.10. Crystal data and structure refinement parameters for **I**, $[\text{H}_3\text{N}(\text{CH}_2)_3\text{NH}_3]^{2+}[\text{Zn}_2(\text{C}_2\text{O}_4)_3]^{2-} \cdot 3\text{H}_2\text{O}$, **II**, $2[\text{C}_3\text{H}_7\text{NH}_3]^+[\text{Zn}_2(\text{C}_2\text{O}_4)_3]^{2-} \cdot 3\text{H}_2\text{O}$ and **III**, $\text{K}[\text{C}_6\text{H}_7\text{H}_{13}][\text{Zn}_2(\text{C}_2\text{O}_4)_3] \cdot 4\text{H}_2\text{O}$.

	I	II	III
Empirical formula	$\text{Zn}_2\text{O}_{15}\text{C}_9\text{N}_2\text{H}_{18}$	$\text{Zn}_2\text{O}_{15}\text{C}_{12}\text{N}_2\text{H}_{26}$	$\text{C}_{12}\text{H}_{21}\text{K}_1\text{N}_2\text{O}_{16}\text{Zn}_2$
Crystal system	Triclinic	Monoclinic	Triclinic
Space group	$P\bar{1}$	$C2/c$ (No. 15)	$P\bar{1}$ (no. 2)
a (Å)	9.261(1)	15.847(1)	7.9391 (4)
b (Å)	9.455(1)	9.685(1)	9.4382 (5)
c (Å)	12.487(1)	18.333(1)	15.4815 (8)
α (°)	83.93(1)	90.0	82.233 (2)
β (°)	88.01(1)	115.5(1)	82.868 (2)
γ (°)	61.03(1)	90.0	75.513 (2)
Volume (Å ³)	951.1(1)	2539.1(2)	1107.91 (10)
Z	2	4	2
Formula mass	524.8	569.1	618.86
ρ_{calc} (g cm ⁻³)	1.83	1.60	1.832
λ (MoK α) Å	0.71073	0.71073	0.71073
μ (mm ⁻¹)	2.60	1.97	2.433
Total data collected	3984	5142	4704
Unique data	2673	1849	3136
R indexes [$I > 2\sigma(I)$]	$R_1 = 0.03$, $wR_2 = 0.08$	$R_1 = 0.07$, $wR_2 = 0.21$	$R_1 = 0.0501$, $wR_2 = 0.1154$
Goodness of fit (S_{obs})	1.15	1.13	1.163

^a $R_1 = \sum ||F_o| - |F_c|| / \sum |F_o|$; ^b $wR_2 = \{ \sum [w(F_o^2 - F_c^2)]^2 / \sum [w(F_o^2)] \}^{1/2}$; $w = 1 / \{ \sigma^2(F_o) \}^{1/2}$; $w = 1 / \{ \sigma^2(F_o) \}^{1/2} + (aP)^2 + bP$, $P = [\max(F_o, 0) + 2(F_c)^2] / 3$, where $a = 0.0383$ and $b = 0.608$ for **I**; $a = 0.1597$ and $b = 0.0$ for **II** and $a = 0.0339$ and $b = 5.8570$ for **III**.

Table 3.11. Crystal data and structure refinement parameters for the zinc oxalates IV–VII

Structural parameter	IV	V	VI	VII
Chemical formula	Zn ₁ O ₁₀ N ₆ C ₆ H ₁₆	Zn ₁ O ₁₄ N ₃ C ₁₁ H ₁₈	Zn ₁ O ₁₁ N ₃ C ₁₀ H ₂₀	Zn ₂ O ₁₆ N ₂ C ₁₀ H ₂₀
Space group	C2/c (no. 15)	C2/c (no. 15)	P2 ₁ /n (no. 14)	C2/c (no. 15)
T (K)	293(2)	293(2)	293(2)	293(2)
a (Å)	14.170(2)	13.799(1)	9.433(1)	16.725(3)
b (Å)	10.129(1)	11.524(2)	16.860(2)	9.254(1)
c (Å)	11.324(3)	25.412(2)	9.788 (1)	31.298(2)
β (deg)	115.4(2)	105.2(1)	91.4(1)	98.59(1)
Volume (Å ³)	1468.2(3)	3897.2(2)	1556.1(2)	4789.9(3)
Z	4	8	4	4
Formula mass	397.62	481.65	409.65	555.1
ρ _{calc} (gcm ⁻³)	1.799	1.642	1.749	1.672
λ (MoKα) Å	0.71073	0.71073	0.71073	0.71073
μ (mm ⁻¹)	1.739	1.337	1.641	2.086
R (F _o ²) [I > 2σ(I)]	R ₁ = 0.044, wR ₂ = 0.098 ¹	R ₁ = 0.042, wR ₂ = 0.116 ¹	R ₁ = 0.048, wR ₂ = 0.104 ¹	R ₁ = 0.054, wR ₂ = 0.135 ¹

¹ $W = 1/[\sigma^2(F_o)^2 + (aP)^2 + bp]$ where $P = [F_o^2 + 2F_c^2]/3$,

$a = 0.0282$ and $b = 4.331$ for IV, $a = 0.0575$ and $b = 17.9514$ for V, $a = 0.0633$ and $b = 0.0$ for VI, and $a = 0.0757$ and $b = 26.3797$ for VII.

Table 3.12. Crystal data and structure refinement parameters for VIII, $\text{Na}_4\text{Cd}_2(\text{C}_2\text{O}_4)_4 \cdot 4\text{H}_2\text{O}$, IX, $\text{K}_2\text{Cd}(\text{C}_2\text{O}_4)_2 \cdot 2\text{H}_2\text{O}$ and X, $\text{Cd}_2(\text{C}_2\text{O}_4)_{0.5}\text{Cl}_3\text{NaCl}_4\text{H}_2\text{O}$

Parameters	VIII	IX	X
Empirical formula	$\text{C}_8\text{O}_{20}\text{H}_8\text{Cd}_2\text{Na}_4$	$\text{C}_4\text{O}_{10}\text{H}_4\text{CdK}_2$	$\text{Cd}_2(\text{C}_2\text{O}_4)_{0.5}\text{Cl}_3\text{NaCl}_4\text{H}_2\text{O}$
Crystal system	Monoclinic	Orthorhombic	Monoclinic
Space group	$\text{P}2_1/\text{n}$ (no. 14)	$\text{Fdd}2$ (no. 43)	$\text{C}2/\text{c}$ (No. 15)
a (Å)	12.8779(8)	14.6886(2)	12.2177 (12)
b (Å)	11.4440(7)	18.080(2)	17.2361 (12)
c (Å)	14.1301(8)	7.8162(8)	11.8314 (9)
α (°)	90	90.0	90.0
β (°)	113.01(10)	90.0	101.41 (1)
γ (°)	90	90.0	90.0
Volume (Å ³)	1916.7(2)	2075.4(4)	2442.3 (3)
Z	4	8	8
Formula mass	732.84	398.64	505.69
ρ_{calc} (g cm ⁻³)	2.54	2.552	2.750
λ (MoK α) Å	0.71073	0.71073	0.71073
μ (mm ⁻¹)	2.414	2.949	4.389
Total data collected	7810	2079	5012
Unique data	2762	750	1769
R indexes [$I > 2\sigma(I)$]	$R_1 = 0.032$, $wR_2 = 0.066$	$R_1 = 0.021$, $wR_2 = 0.054$	$R_1 = 0.0239$, $wR_2 = 0.0496$
Goodness of fit	1.067	1.127	1.027

$$^a R_1 = \frac{\sum ||F_o| - |F_c||}{\sum |F_o|}; \quad ^b wR_2 = \left\{ \frac{\sum [w(F_o^2 - F_c^2)^2]}{\sum [w(F_o^2)]} \right\}^{1/2}, \quad w = 1/[\sigma^2(F_o)^2 + (aP)^2 + bP],$$

$P = [\max.(F_o^2, 0) + 2(F_c^2)]/3$, where $a = 0.0197$ and $b = 2.3004$ for VIII and $a = 0.0321$ and $b = 0.0$ for IX and $a = 0.0103$ and $b = 0.0000$ for X.

Table 3.13. Crystal data and structure refinement parameters for XI, $[C_6N_2H_{10}]_6[Y(H_2O)(C_2O_4)_2]_2(H_2O)$, XII, $[C_5N_2H_{12}]_4[Y(C_2O_4)_2]$, XIII, $[NH_3CH_2CH(NH_3)CH_3][Nd(C_2O_4)_2(HCOO)] \cdot H_2O$ and XIV $[OC(CH_3)NCH_2CH(CH_3)NH_2][Nd(C_2O_4)_2] \cdot H_2O$

Empirical formula	XI		XII		XIII		XIV	
	$YO_{11}C_7N_7H_{14}$	$YO_8C_4N_2H_{12}$	$YO_8C_4N_2H_{12}$	$YO_8C_4N_2H_{12}$	$Nd_4O_{10}C_9N_2H_{14}$	$Nd_4O_{10}C_9N_2H_{14}$	$Nd_4O_{10}C_9N_2H_{14}$	$Nd_4O_{10}C_9N_2H_{14}$
Crystal system	Triclinic	Monoclinic	Monoclinic	Monoclinic	Monoclinic	Monoclinic	Triclinic	Triclinic
Space group	P(-1) (no. 2)	Cc (no. 9)	Cc (no. 9)	P2(1)/c (No.14)	P2(1)/c (No.14)	P2(1)/c (No.14)	P-1 (No. 2)	P-1 (No. 2)
a (Å)	8.229(3)	11.552(1)	11.552(1)	9.0279(4)	9.0279(4)	9.0279(4)	8.6222(9)	8.6222(9)
b (Å)	9.739(1)	17.168(1)	17.168(1)	18.1362(8)	18.1362(8)	18.1362(8)	9.5683(10)	9.5683(10)
c (Å)	9.754(3)	8.719(1)	8.719(1)	8.5631(4)	8.5631(4)	8.5631(4)	9.5712(10)	9.5712(10)
α (°)	60.74(1)	90.0	90.0	90.000(1)	90.000(1)	90.000(1)	109.388(2)	109.388(2)
β (°)	72.36(1)	130.64(1)	130.64(1)	102.735(10)	102.735(10)	102.735(10)	98.508(10)	98.508(10)
γ (°)	84.67(1)	90.0	90.0	90.000(1)	90.000(1)	90.000(1)	102.361(2)	102.361(2)
Volume (Å ³)	648.5(1)	1312.1(1)	1312.1(1)	1367.56(11)	1367.56(11)	1367.56(11)	706.73(13)	706.73(13)
Z	2	2	2	4	4	4	2	2
Formula mass	377.1	365.1	365.1	459.5	459.5	459.5	454.5	454.5
ρ_{calc} (g cm ⁻³)	1.931	1.848	1.848	2.080	2.080	2.080	2.220	2.220
λ (MoK α) Å	0.71073	0.71073	0.71073	0.71073	0.71073	0.71073	0.71073	0.71073
Total data collected	2760	2689	2689	5652/1782	5652/1782	5652/1782	3031/1730	3031/1730
R indexes [$I > 2\sigma(I)$]	$R_1 = 0.054^a$, $wR_2 = 0.13^b$	$R_1 = 0.023^a$, $wR_2 = 0.057^b$	$R_1 = 0.023^a$, $wR_2 = 0.057^b$	0.0229^a , 0.0599^b	0.0229^a , 0.0599^b	0.0229^a , 0.0599^b	0.0446^a , 0.1150^b	0.0446^a , 0.1150^b
Goodness of fit	1.01	1.1	1.1	1.07	1.07	1.07	1.02	1.02

^a $R_1 = \sum ||F_o| - |F_c|| / \sum |F_o|$; ^b $wR_2 = \{ \sum [w(F_o^2 - F_c^2)] / \sum [w(F_o^2)] \}^{1/2}$, $w = 1 / \{ \sigma^2(F_o) + (aP)^2 + bP \}$.

P = $[\max(F_o^2, 0) + 2(F_c^2)^3] / 3$, where $a = 0.0774$ and $b = 0.0$ for X, $a = 0.1000$ and $b = 0.0$ for XI, $a = 0.0267$ and $b = 3.6124$ for XII, $a = 0.10000$ and $b = 0.0$ for XIII

Table 3.14. Crystal data and structure refinement parameters for $[(\text{CH}_3)_2\text{NH}(\text{CH}_2)_2\text{NH}(\text{CH}_3)_2][\text{Sn}_2(\text{C}_2\text{O}_4)_3]\cdot\text{H}_2\text{O}$, XV

Parameters	$[(\text{CH}_3)_2\text{NH}(\text{CH}_2)_2\text{NH}(\text{CH}_3)_2][\text{Sn}_2(\text{C}_2\text{O}_4)_3]\cdot\text{H}_2\text{O}$
Empirical formula	$\text{Sn}_2\text{O}_{13}\text{C}_{12}\text{N}_2\text{H}_{20}$
Crystal system	Monoclinic
Space group	C2/c (No. 15)
a (Å)	16.567(8)
b (Å)	10.851(6)
c (Å)	11.652(6)
β (°)	102.62(3)
Volume (Å ³)	2038.6(2)
Z	4
Formula mass	637.4(1)
ρ_{calc} (gcm ⁻³)	2.825
λ (MoK α) Å	0.71073
μ (mm ⁻¹)	5.813
Total data collected	4180
Unique data	1466
Refinement method	Full-matrix least-squares on $ F^2 $
R indexes [$I > 2\sigma(I)$]	$R_1 = 0.043^a$, $wR_2 = 0.10^b$
Goodness of fit ($S_{\text{obs.}}$)	1.08

^a $R_1 = \Sigma ||F_0| - |F_c|| / \Sigma |F_0|$; ^b $wR_2 = \{\Sigma [w(F_0^2 - F_c^2)^2] / \Sigma [w(F_0^2)^2]\}^{1/2}$. $w = 1/[\sigma^2(F_0)^2 + (aP)^2 + bP]$, $P = [\max.(F_0^2, 0) + 2(F_c^2)]/3$, where $a=0.0433$ and $b = 0.0$ for XV.

Table 3.15. Crystal data and structure refinement parameters for [Cd(O₂C-CH₂-O₂)(H₂O)].H₂O, **XVI**, and, [Mn(O₂C-(CH₂)₃-CO₂)], **XVII**

Structural parameter	XVI	XVII
Chemical formula	CdC ₃ H ₆ O ₆	MnC ₅ H ₆ O ₄
Formula mass	250.48	185.04
Crystal symmetry	Rhombohedral	Rhombohedral
Space group	R $\bar{3}$ (No. 148)	R $\bar{3}$ (No. 148)
T/K	293 (2)	293 (2)
a /Å	17.0685 (2)	11.2944 (10)
c /Å	12.4302 (3)	29.4830 (4)
V/Å ³	3136.17 (9)	3257.08 (6)
Z	18	18
λ/Å	0.71073	0.71073
ρ _{calc} /gcm ⁻³	2.387	1.698
μ /mm ⁻¹	3.107	1.775
No. of measured/observed reflections	4504/990	4523/957
Refinement method	Full-matrix on F ²	lest-squares Full-matrix on F ²
R1, wR2 [I > 2σ(I)]	0.0336, ^a 0.0898 ^b	0.0205, ^a 0.0500 ^b

^a R₁ = ||F₀|-|F_c|| / |F₀|; ^b wR₂ = {[w(F₀² - F_c²)] / [w(F₀²)]} ^{1/2}. w = 1/[σ²(F₀)² + (aP)² + bP], P = [max.(F₀², 0) + 2(F_c²)]/3, where a = 0.0000 and b = 72.3680 for **XVI** and a = 0.0189 and b = 2.2708 for **XVII**.

Table 3.16. Crystal data and structure refinement parameters for cadmium succinates, [CN₃H₆]₂[Cd₂(C₄H₄O₄)(Cl)₂], XVIII; [CN₃H₆]₂[Cd(C₄H₄O₄)₂], XIX; Cd₂(C₄H₄O₄)₂(C₄N₂H₈)(H₂O)₃, XX; [C₄N₂H₁₂][Cd₂(C₄H₄O₄)₃].4H₂O, XXI; Cd(C₄H₄O₄)(H₂O)₂, XXII and Cd₃(C₄H₄O₄)₂(OH)₂], XXIII

Crystal parameters	XVIII	XIX	XX	XXI	XXII	XXIII
Empirical formula	C ₈ H ₁₆ N ₆ O ₄ Cl ₂ Cd	C ₁₀ H ₂₀ N ₆ O ₈ Cd	C ₁₃ H ₂₂ N ₂ O ₁₁ Cd ₂	C ₈ H ₁₂ NO ₈ Cd	C ₄ H ₈ O ₈ Cd	C ₈ H ₁₀ O ₁₀ Cd ₃
Formula mass	419.55	464.6	595.12	362.59	264.50	603.36
Crystal system	Monoclinic	Orthorhombic	Monoclinic	Triclinic	Monoclinic	Orthorhombic
Space group	P2 ₁ /n	Fddd	P2 ₁ /c	P-1	P2 ₁ /n	Pbca
a (Å)	8.3714 (2)	7.4194 (6)	9.0509 (2)	8.6967 (10)	7.1277 (7)	10.7106 (4)
b (Å)	15.0361 (3)	17.963 (2)	13.8651 (1)	8.9678 (10)	15.144 (2)	6.8922 (3)
c (Å)	12.5310 (1)	24.574 (2)	15.7025 (3)	9.2970 (10)	7.1918 (7)	17.0335 (5)
α (°)	90	90	90	64.820 (2)	90	90
β (°)	106.33 (1)	90	106.015 (1)	84.253 (2)	111.335 (2)	90
γ (°)	90	90	90	74.222 (2)	90	90
Volume (Å ³)	1514.17 (5)	3275.1 (5)	1894.05 (6)	631.35 (12)	723.12 (12)	1257.41(8)
Z	4	8	4	2	4	4
μ (mm ⁻¹)	1.813	1.389	2.304	1.761	3.001	5.078
Total data collected	6130	597	7844	2656	2925	4688
R _i , wR ₂ [I > 2σ(I)]	0.0408, 0.0984	0.0152, 0.0369	0.0304, 0.0742	0.0334, 0.0813	0.0211, 0.0497	0.0207, 0.0501
Goodness of fit (S)	1.023	1.134	1.022	1.177	1.003	1.026

Table 3.17. Crystal data and structure refinement parameters for $[\text{Na}_3\text{Cd}_5(\text{C}_4\text{H}_4\text{O}_4)_6\text{Cl}]$, XXIV and $[\text{Na}_3\text{Cd}_5(\text{C}_4\text{H}_4\text{O}_4)_6\text{Br}]$, XXV

	XXIV	XXV
Empirical formula	$[\text{Na}_3\text{Cd}_5(\text{C}_4\text{H}_4\text{O}_4)_6(\text{Cl})]$	$[\text{Na}_3\text{Cd}_5(\text{C}_4\text{H}_4\text{O}_4)_6(\text{Br})]$
Crystal system	Cubic	Cubic
Space group	I23 (No. 197)	I23 (No. 197)
a (Å)	11.8931 (10)	11.8526 (10)
Volume (Å ³)	1682.23 (2)	1665.10 (2)
Z	12	12
Formula mass	1363.09	1407.64
ρ_{calc} (gcm ⁻³)	2.691	2.807
λ (MoK α) Å	0.71073	0.71073
μ (mm ⁻¹)	3.329	4.482
Total data collected	3570	3598
Observed data ($I > 2\sigma(I)$)	408	415
Refinement method	Full-matrix least-squares on $ F^2 $	Full-matrix least-squares on $ F^2 $
R indexes [$I > 2\sigma(I)$]	$R_1 = 0.0180$, $wR_2 = 0.0448$	$R_1 = 0.0543$, $wR_2 = 0.1391$
Goodness of fit ($S_{\text{obs.}}$)	1.230	1.186

^a $R_1 = \frac{\sum ||F_o| - |F_c||}{\sum |F_o|}$; ^b $wR_2 = \left\{ \frac{\sum [w(F_o^2 - F_c^2)^2]}{\sum [w(F_o^2)^2]} \right\}^{1/2}$. $w = 1/[\sigma^2(F_o)^2 + (aP)^2 + bP]$, $P = [\max.(F_o^2, 0) + 2(F_c^2)]/3$, where $a = 0.0000$ and $b = 0.2411$ for XXIV and $a = 0.0450$ and $b = 71.7116$ for XXV.

Table 3.18. Crystal data and structure refinement parameters for $[\text{Mn}(\text{O}_2\text{C}-(\text{CH}_2)_4-\text{CO}_2)(\text{C}_4\text{N}_2\text{H}_8)]$, XXVI

Parameters	$[\text{Mn}(\text{O}_2\text{C}-(\text{CH}_2)_4-\text{CO}_2)(\text{C}_4\text{N}_2\text{H}_8)]$
Empirical formula	$\text{C}_8\text{H}_{12}\text{NO}_4\text{Mn}$
Crystal system	Monoclinic
Space group	$P2_1/c$ (No. 14)
a (Å)	10.3736(7)
b (Å)	11.7627(8)
c (Å)	8.3657(6)
β (°)	93.203(2)
Volume (Å ³)	1019.20(12)
Z	4
Formula mass	241.13
ρ_{calc} (gcm ⁻³)	1.571
λ (MoK α) Å	0.71073
μ (mm ⁻¹)	1.283
Total data collected	4160
Unique data	1464
Refinement method	Full-matrix least-squares on $ F^2 $
R indexes [$I > 2\sigma(I)$]	$R_1 = 0.0719^a$, $wR_2 = 0.1717^b$
Goodness of fit ($S_{\text{obs.}}$)	1.062

^a $R_1 = \sum ||F_0| - |F_c|| / \sum |F_0|$; ^b $wR_2 = \{ \sum [w(F_0^2 - F_c^2)^2] / \sum [w(F_0^2)^2] \}^{1/2}$. $w = 1/[\sigma^2(F_0)^2 + (aP)^2 + bP]$, $P = [\max.(F_0^2, 0) + 2(F_c^2)]/3$, where $a=0.0433$ and $b = 0.0$ for $[\text{Mn}(\text{O}_2\text{C}-(\text{CH}_2)_4-\text{CO}_2)(\text{C}_4\text{N}_2\text{H}_8)]$, XXVI.

Table 3.19. Crystal data and structure refinement parameters for RbCl][Cd₆(C₂O₄)₆].2H₂O, XXVII; [RbBr][Cd₆(C₂O₄)₆].2H₂O, XXVIII.

Parameters	XXVII	XXVIII
Empirical formula	H ₄ C ₁₂ Cd ₆ Cl ₁ O ₂₆ Rb ₁	H ₄ C ₁₂ O ₂₆ Cd ₆ BrRb
Crystal system	Rhombohedral	Rhombohedral
Space group	R-3 (no. 148)	R-3 (no. 148)
a (Å)	9.3859(3)	9.4141(2)
b (Å)	9.3859(3)	9.4141(2)
c (Å)	23.9086 (8)	23.9946 (5)
Volume (Å ³)	1824.05(10)	1841.63(10)
Z	18	6
Formula mass	1359.51	1403.85
ρ _{calc} (gcm ⁻³)	3.702	3.787
λ (MoKα) Å	0.71073	0.71073
μ (mm ⁻¹)	7.375	8.823
Total data collected	2598	2602
Unique data	589	591
R indexes [I > 2σ(I)]	R ₁ = 0.0355 ^a , wR ₂ = 0.0904 ^b	R ₁ = 0.0381 ^a , wR ₂ = 0.0972 ^b

^a $R_1 = \sum ||F_o| - |F_c|| / \sum |F_o|$; ^b $wR_2 = \{\sum [w(F_o^2 - F_c^2)^2] / \sum [w(F_o^2)^2]\}^{1/2}$, $w = 1/[\sigma^2(F_o)^2 + (aP)^2 + bP]$, $P = [\max. (F_o^2, 0) + 2(F_c^2)]/3$; where a = 0.0565, b = 9.1718 for XXVII and a = 0.0412, b = 155.4846 for XXVIII.

Table 3.20. Crystal data and structure refinement parameters for $2[\text{CsBr}][\text{Cd}(\text{C}_2\text{O}_4)] \cdot \text{H}_2\text{O}$, **XXIX**; $2[\text{CsBr}][\text{Cd}_2(\text{C}_2\text{O}_4)(\text{Br})_2] \cdot 4\text{H}_2\text{O}$, **XXX**, and $[\text{Rb}_2\text{Cd}(\text{Cl})(\text{NO}_3)(\text{C}_2\text{O}_4)(\text{H}_2\text{O})]$, **XXXI**.

Parameters	XXIX	XXX	XXXI
Empirical formula	$\text{H}_2\text{C}_2\text{Cd} \text{Br}_2\text{O}_5\text{Cs}_2$	$\text{H}_8\text{C}_2\text{Cd} \text{Br}_4\text{O}_5\text{Cs}_2$	$\text{H}_2\text{C}_2\text{O}_8\text{NCdClRb}_2$
Crystal system	Orthorhombic	Orthorhombic	Orthorhombic
Space group	Pbcm (no. 57)	Cmcm (no. 63)	Pbca (no. 56)
a (Å)	6.0854(6)	23.6251(14)	12.0600(10)
b (Å)	11.0793(11)	10.2528(6)	10.7599(2)
c (Å)	16.889(2)	7.8199 (58)	15.7905(10)
Volume (Å ³)	1138.7(2)	1894.2(2)	2049.04(4)
Z	8	16	8
Formula mass	644.06	970.33	482.84
ρ_{calc} (g cm ⁻³)	3.745	3.374	3.130
λ (MoK α) Å	0.71073	0.71073	0.71073
μ (mm ⁻¹)	15.219	14.487	11.850
Total data collected	4407	3894	8062
Unique data	855	770	1473
R indexes [$I > 2\sigma(I)$]	$R_1 = 0.0377^a$, $wR_2 = 0.0827^b$	$R_1 = 0.0334^a$, $wR_2 = 0.0744^b$	$R_1 = 0.0261^a$, $wR_2 = 0.0644^b$

^a $R_1 = \Sigma ||F_o| - |F_c|| / \Sigma |F_o|$; ^b $wR_2 = \{\Sigma [w(F_o^2 - F_c^2)^2] / \Sigma [w(F_o^2)^2]\}^{1/2}$, $w = 1/[\sigma^2(F_o^2) + (aP)^2 + bP]$, $P = [\max.(F_o^2, 0) + 2(F_o^2)^2]/3$; where $a = 0.0757$, $b = 0.0000$ for **XXIX**; $a = 0.0493$, $b = 0.0000$ for **XXX**; $a = 0.0431$, $b = 14.3797$ for **XXXI** and $a = 0.0332$, $b = 0.4837$ for **XXXII**.

Table 3.21. Crystal data and structure refinement parameters for $[\text{K}_2\text{Cd}_2(\text{C}_2\text{O}_4)_3] \cdot 2\text{KBr} \cdot 2\text{H}_2\text{O}$, XXXII; $3[\text{RbCl}][\text{Cd}_2(\text{H}_2\text{O})\text{C}_2\text{O}_4](\text{Cl})_2 \cdot \text{H}_2\text{O}$, XXXIII and $\text{K}_2[\text{Mn}_2(\text{C}_2\text{O}_4)_3]2[\text{KCl}] \cdot 2\text{H}_2\text{O}$, XXXIV.

Parameters	XXXII	XXXIII	XXXIV
Empirical formula	$[\text{K}_2\text{Cd}_2(\text{C}_2\text{O}_4)_3] \cdot 2\text{KBr} \cdot 2\text{H}_2\text{O}$	$3[\text{RbCl}][\text{Cd}_2(\text{H}_2\text{O})\text{C}_2\text{O}_4](\text{Cl})_2 \cdot \text{H}_2\text{O}$	$\text{K}_2[\text{Mn}_2(\text{C}_2\text{O}_4)_3]2[\text{KCl}] \cdot 2\text{H}_2\text{O}$
Crystal system	Orthorhombic	Monoclinic	Orthorhombic
Space group	Pbca	$P2_1/c$ (no. 14)	Pbca
a (Å)	11.898(6)	8.0648(2)	11.6912 (10)
b (Å)	10.963(1)	22.9026(4)	10.6766 (9)
c (Å)	15.503(4)	9.3967(3)	14.8912 (13)
β (°)	90.000	104.399 (10) ^o	90.000
Volume (Å ³)	1983.2(2)	1681.10(7)	1858.8 (3)
Z	4	4	8
Formula mass	841.12	782.53	152.77
ρ_{calc} (gcm ⁻³)	2.817	3.076	2.263
λ (MoK α) Å	0.71073	0.71073	0.71073
μ (mm ⁻¹)	7.077	11.961	2.608
Total data collected	7521	6939	7161
Unique data	1428	2405	1336
R indexes [$I > 2\sigma(I)$]	$R_1 = 0.0303, wR_2 = 0.0589^b$	$R_1 = 0.0409^a, wR_2 = 0.0931^b$	$R_1 = 0.0403^a, wR_2 = 0.0786^b$

^a $R_1 = \Sigma ||F_o| - |F_c|| / \Sigma |F_o|$; ^b $wR_2 = \{\Sigma [w(F_o^2 - F_c^2)^2] / \Sigma [w(F_o^2)]\}^{1/2}$, $w = 1/[\sigma^2(F_o^2) + (aP)^2 + bP]$, $P = [\max(F_o^2, 0) + 2(F_c^2)]/3$; where $a = 0.0192$, $b = 1.1216$ for XXXIII; $a = 0.0352, b = 10.3425$ for XXXIV and $a = 0.0246, b = 6.1305$ for XXXV.

References

1. R. M. Barrer, "Hydrothermal Chemistry of Zeolites", Academic Press (London) 1982.
2. K. Byrappa, M. Yoshimura, *Handbook of Hydrothermal Technology*, William Andrew Publishing, 2001, Norwich, NY.
3. (a) G. Demazeau, *J. Mater. Chem.* **1999**, *9*, 15. (b) R. I. Walton, *Chem. Soc. Rev.* **2002**, *31*, 230.
4. A. Rabenau, *Angew. Chem., Int. Ed. Engl.* **1985**, *24*, 1026.
5. S. Feng, R. Xu, *Acc. Chem. Res.* **2002**, *34*, 239.
6. A. K. Cheetham, G. Ferey, T. Loiseau, *Angew. Chem., Int. Ed. Engl.* **1999**, *38*, 3268.
7. C. W. Jones, S. J. Hwang, T. Okubo, M. E. Davis, *Chem. Mater.* **2001**, *13*, 1041-1050.
8. (a) PDF database (Sets 1-44), Copyright 1994. (b) International Centre for Diffraction Data, 12 Campus Blvd., Newton Square, PA 19073-3273, USA.
9. *Verified Synthesis of Zeolitic Materials*, H. Robson (ed.), 2001, Elsevier Science B. V. and references therein.
10. Sheldrick, M., *SHELXTL-PLUS Program for Crystal Structure solution and refinement*, University of Göttingen.
11. Sheldrick, G. M., *SADABS Siemens Area Detector Absorption Correction Programm*, University of Göttingen, Göttingen, Germany.

4. RESULTS AND DISCUSSION

4.1. Hydrogen bonded structures in amine oxalates

4.1.1. Results

The structures of the oxalates of n-propylamine (PRO), n-butylamine (BUO), ethylenediamine (ENO), 1,4-butanediamine (DABO), piperazine (PIPO), guanidine (GUO) and 1,4-diazabicyclo[2,2,2]octane (DCO) have been examined. The structures indicated three distinct types of hydrogen bond patterns: (a) involving linear chains of oxalates, (b) dimeric oxalates containing 8-membered rings and (c) layers with alternating amine and the oxalate units.

In all the amine oxalates studied by us, the oxalate unit exists as the monohydrogen oxalate anions, owing to the difference in the acidity between the two acidic hydrogen atoms of oxalic acid ($pK_{a1}=1.69$; $pK_{a2}=5.73$).^[1] In PRO, BUO, ENO, DABO and PIPO, the anionic oxalates form linear chains through hydrogen bonds. Typical linear chain structures in PRO and PIPO are shown in Figures 4.1a and 4.2a. The linear chain anions interact with the amine molecules through N-H...O hydrogen bonds. The linear oxalate chains along with the amine molecules are shown in Figure 4.1b for PRO. The water molecules, situated between the oxalate chains and the amine molecules, participate in the hydrogen bonding through O-H...O interactions. In PIPO, the interactions between the amine and the oxalate units are such as to form bifurcated N-H...O bonds (Fig. 4.2a). Similar bifurcated N-H...O bonds are found in BUO, ENO, and DABO as well. The arrangement of the anionic oxalate linear chains and its interaction with the amine molecules in PIPO is shown in Figure 4.2b. There are no water molecules in PIPO. In GUO, the oxalate units do not form a linear chain. Instead, the oxalate units are surrounded by the monoprotonated guanidinium cations forming a sheet-like structure (Fig. 4.3a). The planar propeller-like guanidinium cation interact with the

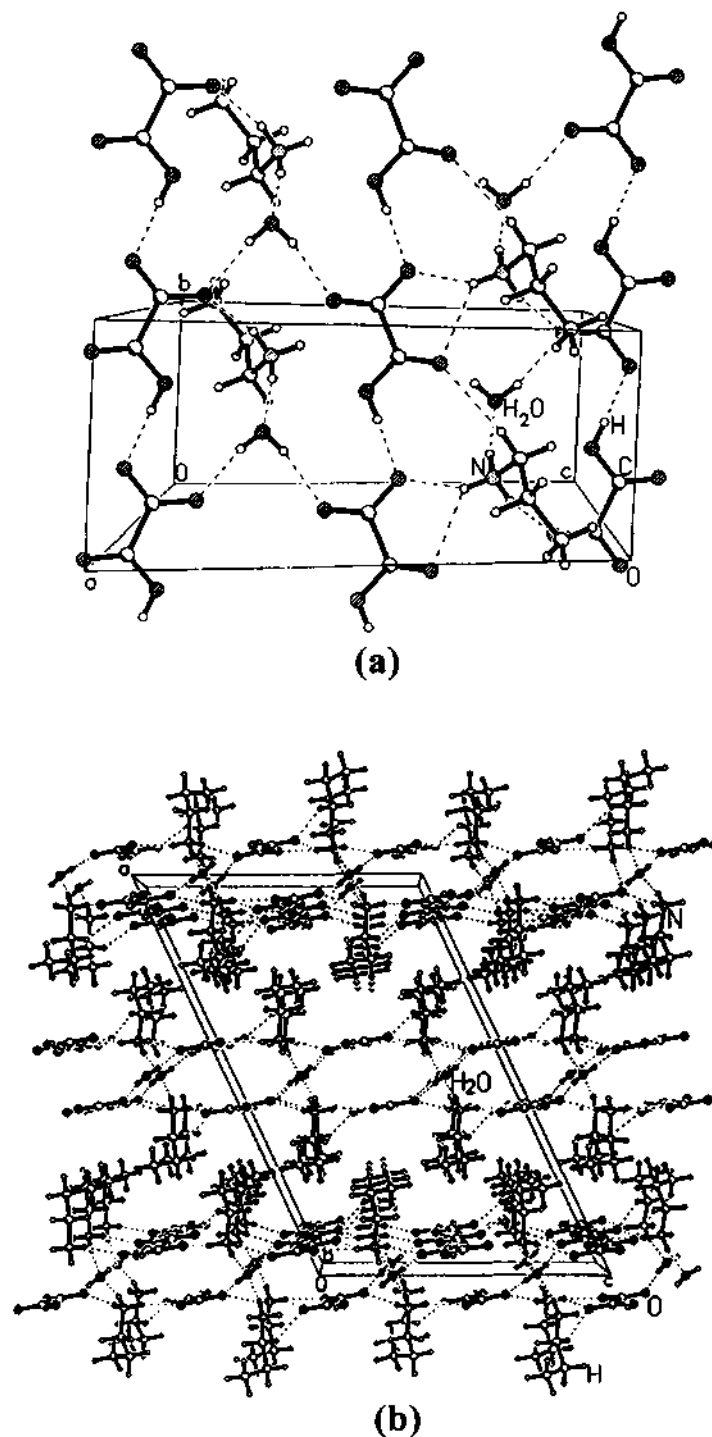


Fig. 4.1. (a) View of the PRO along the *a*-axis showing the presence of linear chain formed by the monoanionic oxalates. Note the presence of bifurcated N-H...O bonds between the amines and the linear chains. (b) Packing diagram of PRO showing the stacking of the layers formed by the linear chains and the water. Note the presence of a chain formed by the amine and water molecules.

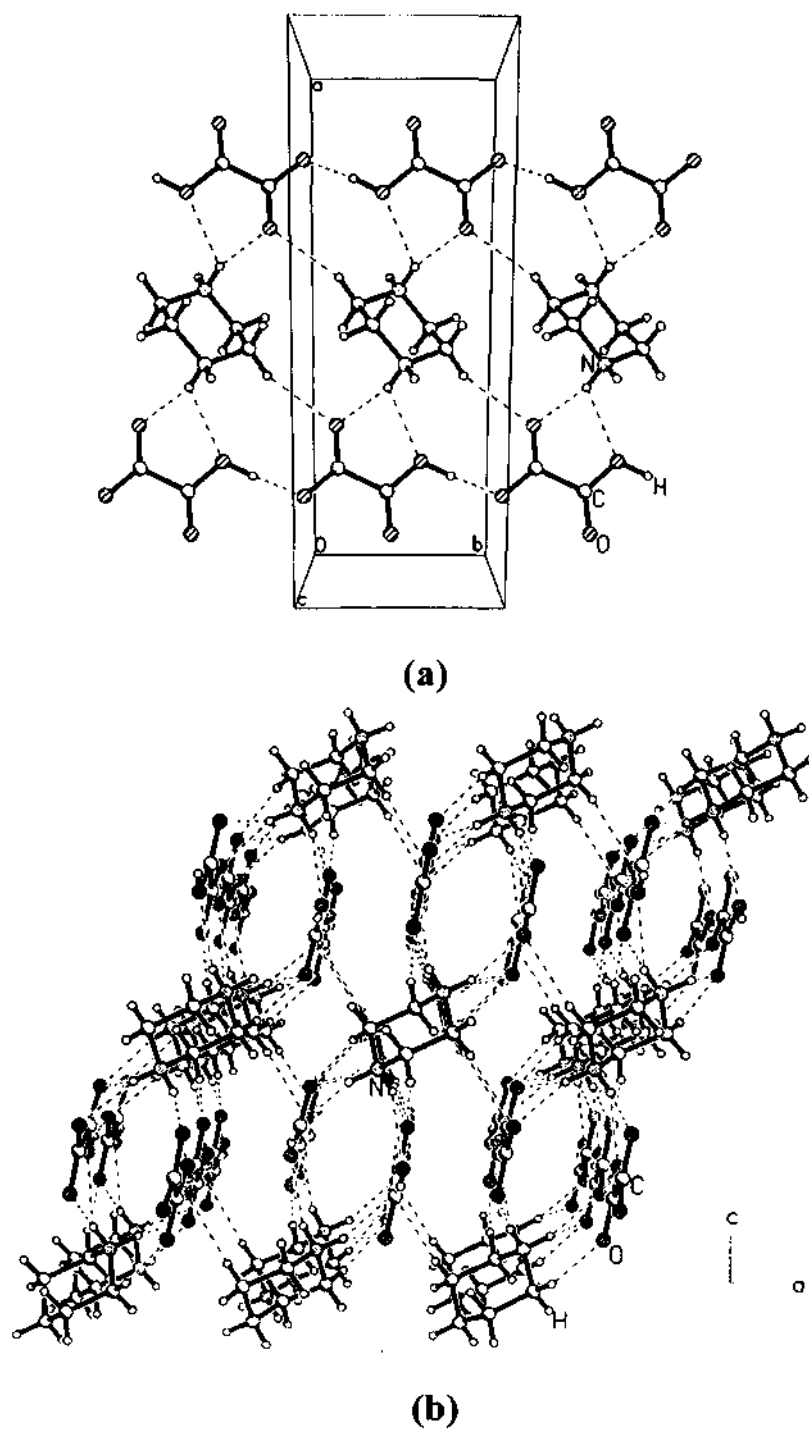


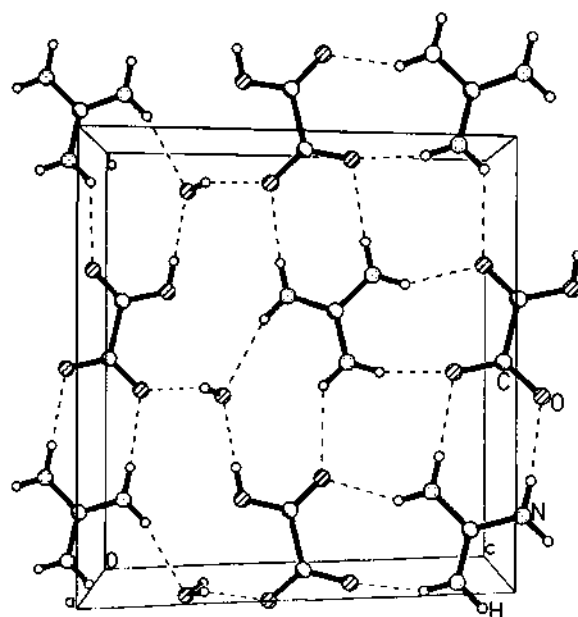
Fig. 4.2. (a) View of the PIPO along the *c*-axis showing the bifurcated N-H...O H-bonds between the amine and the monoanionic oxalate units. (b) Packing diagram of PIPO with a 3-D architecture formed by the various H-bonds between the amine and the anionic oxalate chains.

oxalate and water molecules through strong N-H...O bonds. Similar hydrogen bonded layers involving guanidinium cations have been observed also in other systems.^[2] The water molecules in GUO form hydrogen bonds with two different amine oxalate layers (Fig. 4.3b). Such *out-of-plane* O-H...O bonds facilitate stacking along the *a-axis*.

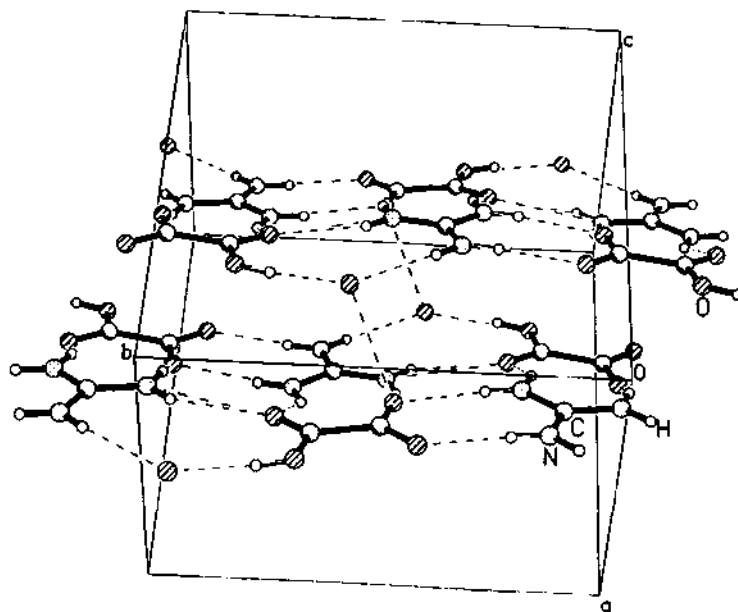
In Figure 4.4a the structure of the DABCO oxalate (DCO) is shown. The interesting feature is the presence of dimeric monohydrogen oxalate units forming 8-membered hydrogen bonded rings involving the amine molecule. The monohydrogen oxalate units form a simple dimer, which are in a *cis-* or *anti-* configuration. This is to be contrasted with the other amine oxalates where the hydrogen bond interaction between the monoprotonated oxalates forms a linear chain. The dimeric oxalate units form two distinct types of N-H...O hydrogen bonds with the neighboring amine molecules, a bifurcated one and a normal one (Fig. 4.4a). The dimer-amine layers in the *ac-plane* interact with the neighboring layer through relatively weak C-H...O bonds. This type of interaction does not extend beyond two layers (Fig. 4.4b).

Infrared spectroscopy studies

The amine oxalates show characteristic N-H stretching frequencies in the IR spectra, with a broad band in the region 3100-2800 cm^{-1} and multiple combination bands in the 2900-2000 cm^{-1} , which are characteristic IR bands of protonated amine salts.^[3] The IR spectra clearly indicate the occurrence of proton transfer from the carboxylic acid to the amine molecules through the reduction in the intensity of the carboxyl C=O stretching band in the 1675-1735 cm^{-1} region and by the appearance of the carboxylate antisymmetric and symmetric C-O stretching bands between 1600-1650 cm^{-1} and 1400 cm^{-1} regions. While the linear oxalate chains in PRO, BUO, ENO etc, in which the carbonyl groups in *trans* or *syn* position, give more to



(a)



(b)

Fig. 4.3. (a) Layer formed by the regularly alternating amine and the monohydrogen oxalate units lying in the *bc*-plane. (b) Stacking of the layers in GUO, showing O-H...O bonds between the water and the monoanionic oxalate unit of the adjacent layer.

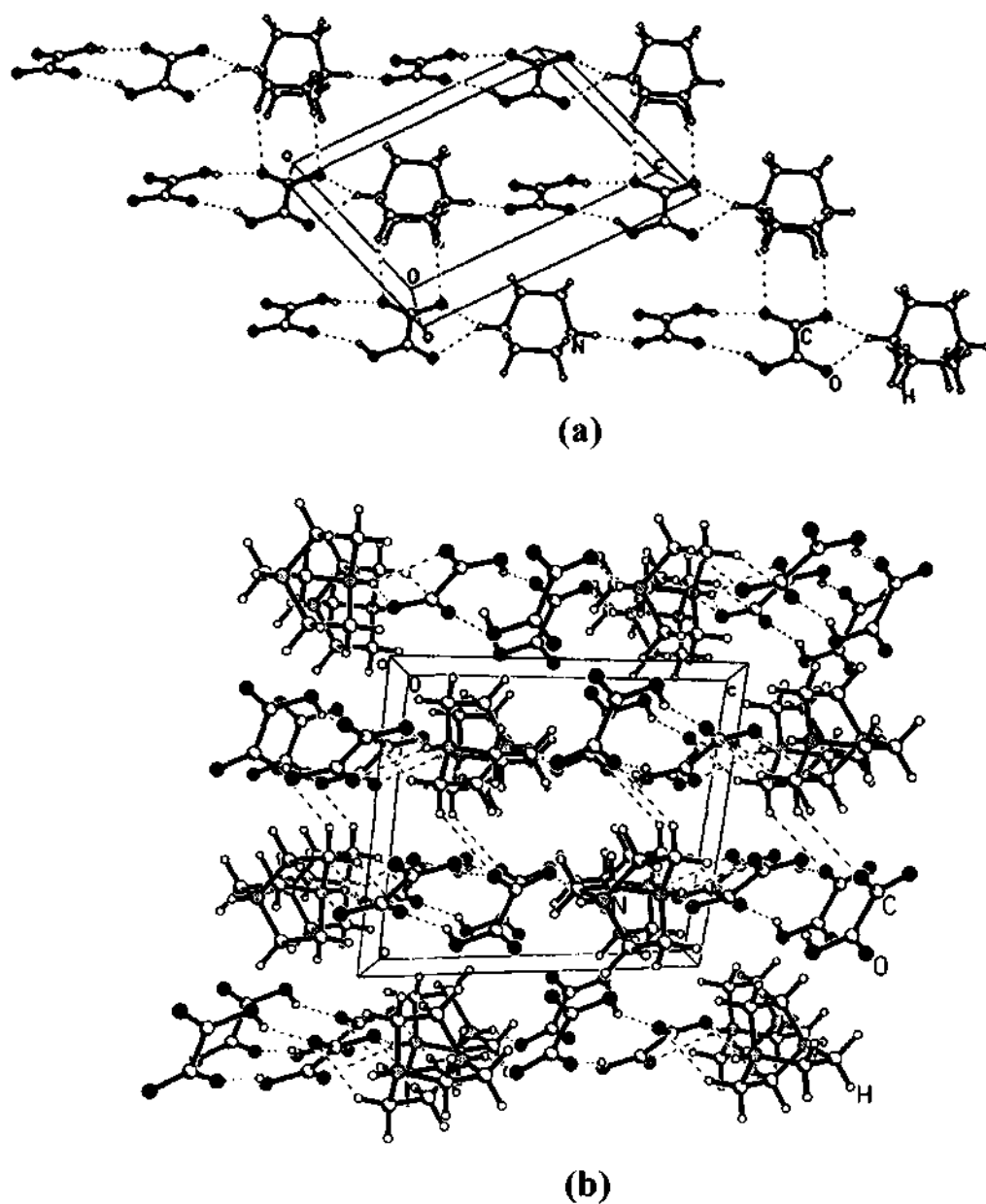


Fig. 4.4. (a) View of DCO along the b-axis showing hydrogen bonded layer formed by the cyclic dimer and the amine moieties. In-plane C-H...O interactions can be noticed. (b) Layers of DCO stacked along the b-axis with out-of-plane C-H...O interactions between the amine and the dimeric oxalate units, which does not extend beyond two layers can be seen.

the expectation, features due to the carboxylate groups, in DCO, the hydrogen bonded dimer shows high frequency carbonyl band at 1752cm^{-1} in addition to the asymmetric and symmetric C-O stretching bands of the carboxylate ion. A broad band is observed in the range $3500\text{-}3400\text{cm}^{-1}$ in all the water containing amine oxalates.

Thermal stability

Thermogravimetric analyses (TGA) of the samples show differences in the decomposition of the amine oxalates (Fig 4.5). The results indicate sharp mass

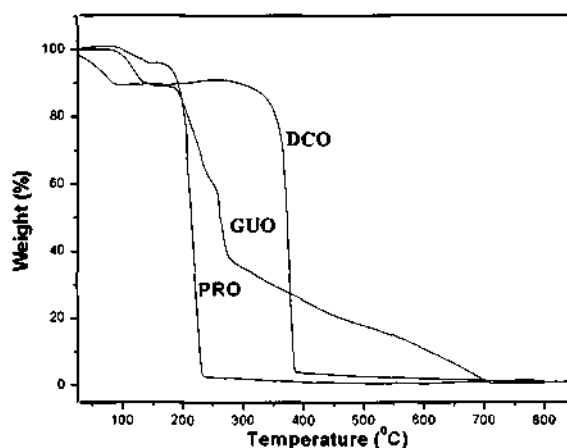


Fig. 4.5. The TGA curves of PRO, GUO and DCO, showing significant differences in their decomposition temperatures, reflecting the presence of different monoanionic oxalate motifs in them.

loss due to the decomposition of the amine and the oxalate. The differences in the decomposition temperatures appear to be related to the nature of the hydrogen bonded structures present in them. The linear chain oxalates show a sharp mass loss at $200\text{ }^{\circ}\text{C}$ while the dimeric oxalate units in DCO, shows the mass loss at $380\text{ }^{\circ}\text{C}$; GUO, which has alternating amine and oxalate units, shows the mass loss at $260\text{ }^{\circ}\text{C}$ followed by a long tail up to $450\text{ }^{\circ}\text{C}$, possibly due to the stepwise loss of the amino groups from guanidine.

4.1.2. Discussion

Hydrogen bond parameters

The hydrogen bond parameters in the amine oxalates are listed in Table 4.1. The N...O distances are in the range 2.619(2)-2.929(5)Å (av.2.816Å) and the N-H...O angles are in the range 142.0(3)-176.0(7)° (av.159.8°). In all the compounds, except GUO, O-H...O bonds are observed between the monohydrogen oxalate units. The O...O distances in such O-H...O bonds lie in the range 2.563(16)-2.741(3)Å (av. 2.604Å), while the O-H...O angles vary from 152.4(19)-178.0(6)° (av.169.4°). In the relatively weaker C-H...O hydrogen bonds, the C...O distances are generally in the range 3.328(2)-3.480(10)Å (av.3.414Å) and the C-H...O angles are in the range 141.0(18) -165.0(2)° (av.153.2°). No C-H...O hydrogen bonds are present in GUO. It is interesting that in all the amine oxalates described herein, there are no interactions between the amine molecules themselves. Of the various O-H...O bonds observed in the amine oxalates, the most significant is the one between the monoanionic oxalate units. This interaction generates linear oxalate chains, with an average O...O distance of 2.574Å and an average O-H...O angle of 174.2°. Similar interactions result in a cyclic dimer in the case of DCO with an average O...O distance of 2.680Å and an average angle of 155.0° (Table 4.1). These values are comparable to the O...O distances and O-H...O angles observed for O-H...O=C bonds in dicarboxylates, amino acids, peptides, saccharides, oligosaccharides and other related hydrogen bonded systems.^[4-7]

The linear chain oxalates with a *syn* orientation have shorter hydrogen bonds than those present in the dimeric oxalate units with an *anti* orientation. The *syn*-conformation is generally found in carboxylic acids in preference to the *anti* conformation, although some dicarboxylates crystallize in both the *syn* and the *anti* conformations.^[8] The presence of C-H...O interactions of DCO may be responsible

Table 1. Important hydrogen bond distances and angles observed in the amine oxalates

Compound	N...O (Å)	N-H...O (°)	O...O (Å)	O-H...O (°)	C...O (Å)	C-H...O (°)
PRO ^(a)	2.868(2)	142(3)	2.580(2)	176(3)	3.427(3)	147(3)
	2.862(2)	172(3)	-	-	-	-
	2.866(4)	169.0(3)	2.573(3)	178.0(6)	-	-
BUO ^(a)	2.845(3)	149.0(4)	-	-	-	-
	2.814(4)	150(2)	2.578(3)	174.0(6)	-	-
ENO ^(a)	2.832(7)	171.0(4)	-	-	-	-
	2.826(9)	153.2(6)	2.579(8)	173.0(4)	3.452(10)	146.2(9)
	2.881(8)	176.0(7)	2.569(8)	172.0(3)	3.480(10)	148.4(8)
DABO ^(a)	2.862(9)	169.7(7)	-	-	3.448(10)	151.6(8)
	2.795(9)	151.4(6)	-	-	-	-
PIPO ^(c)	2.816(19)	150.0(2)	2.563(16)	172.0(2)	3.431(2)	163.0(17)
	2.784(2)	158.0(2)	-	-	3.328(2)	159.0(18)
	-	-	-	-	3.373(2)	158.0(19)
	2.619(3)	155.0(2)	2.619(3)	158.0(3)	3.393(3)	165.0(2)
DCO ^(c)	2.677(3)	147.8(2)	2.741(3)	152.4(19)	3.359(3)	141.0(18)
	-	-	-	-	3.419(3)	153.1(18)
GUO ^(b)	2.885(5)	170.8(4)	-	-	-	-
	2.929(5)	171.0(4)	-	-	-	-

(a) Linear chains are formed by oxalate moieties.

(b) Amine and oxalate units alternate in the layer resulting in only N-H...O type H-bonds.

(c) Dimer units are formed by oxalate moieties as in oxalic acid.

for the observed *anti* conformation of the carboxylate unit. On the other hand, in 3,4-dihydroxy cinnamic acid the *anti* conformation is stabilized by O-H...O interaction between the carbonyl oxygen and the phenolic oxygen in the *meta* position.^[9] The O-H...O bonds formed by the water molecules have O...O(w) distances of 2.744Å and O-H...O(w) angles of 163.3° (Table 4.2).

It is generally recognized that the N-H...O bonds of the type N⁺...O⁻ with matching pKa values of H-bond donor and acceptor groups are stronger than the N-H...O bonds involving neutral acceptor and donors. These bonds traditionally are considered to be salt bridges^[10] and are termed low barrier H-bonds(LBHB)^[11] or +/- charge-assisted H-bonds (CAHB).^[12] Accordingly, the strongest N-H...O hydrogen bonds found in the amine oxalates possessing the linear oxalate chain or dimeric oxalate units are of the CAHB type, with an average N...O bond distance of 2.811Å and an average N-H...O bond angle of 158.2°. In GUO the average N...O distance, 2.907Å, is longer. The N...O bond distances and N-H...O angles observed in the amine oxalates are also comparable to those observed in many hydrogen bonded systems.^[6-8,13] The deviation from planarity in many of the hydrogen bonds observed in the amine oxalates may arise from conflicting packing requirements.^[14] The water molecules present in some of the amine oxalates also participate in strong H-bond interactions. Thus, strong N-H...O(w) and O-H...O(w) interactions are observed in PRO, BUO, ENO, DABO and GUO, with the N...O(w) distances generally in the range 141.1-164.0Å with an average N-H...O(w) angle of ≈170. These values are characteristic of strong hydrogen bonded systems (Table 4.2).

Table 4.2. Important hydrogen bond distances and angles in the amine oxalates involving the water molecule

Code	N...O (Å)	N-H...O (°)	O...O (Å)	O-H...O (°)
PRO	2.809(2)	164.0(2)	2.759(2)	165.0(3)
BUO	2.802(4)	161.0(4)	2.761(3)	172.0(4)
ENO	2.760(3)	160.0(3)	2.731(3)	170.0(3)
DABO	2.824(9)	159.5(7)	2.726(9)	170.0(7)
	2.828(9)	158.8(8)	2.741(9)	145.0(10)
GUO	3.313(5)	141.1(4)	2.839(5)	157.0(5)
	3.020(5)	157.7(5)	2.700(5)	154.0(6)
	-	-	2.662(4)	173.0(4)

Hydrogen bonds of the C-H...O type also play a role in the amine oxalates. We find a *zigzag* arrangement of the carbon backbone similar to that in long chain hydrocarbons^[15] and in amine phosphates^[16]. This arrangement favors C-H...O interactions between the methylene and carboxylate groups, as observed in DABO. In PIPO, the piperazine molecule is present in a boat conformation enabling C-H...O interactions. The average C...O distance in PIPO is 3.365 Å with an average C-H...O angle of 160.7°. The C-H...O hydrogen bond in DCO, has an *out-of-plane* carbon backbone. The various distances and angles of the C-H...O bonds observed here are comparable to those in other systems.^[6-8,17] Based on the Cambridge Database (1988 version), we find that the structures with *syn* and *anti* planar conformations are energetically comparable, the choice between them depending on weak, long range interactions. Here the C-H...O interaction clearly is the relevant interaction. It is noteworthy that based on a survey of carboxylic acid structures, Leiserowitz^[18] concluded that *antiplanar* conformations are, probably, induced by intermolecular forces.

Hydrogen-bond based structural motifs

A critical analysis of the structures of the amine oxalates clearly shows the presence of three types of motifs (Fig. 4.6). The monoanions of dicarboxylic acids forming hydrogen bonded linear chains can be considered as motif A (Fig. 4.6a). Similar hydrogen bonded chains of dicarboxylates have been reported in literature.^[4,19] The mono-protonated oxalate anions, in these chains, align head-to-tail and are joined by strong O-H...O hydrogen bonds. An 8-membered cyclic dimers formed by the oxalate units can be considered as the motif B (Fig. 4.6b).

The isolated monohydrogen

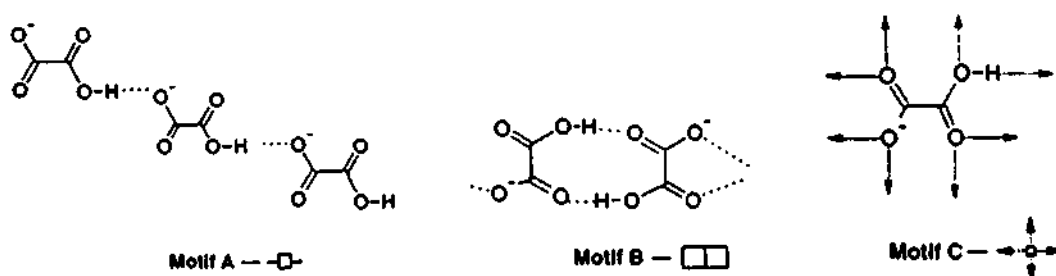


Fig. 4.6. Illustration of different motifs of the hydrogen bonds formed by the amine oxalate salts: (a) hydrogen-bonded linear chains of oxalates (motif A); (b) hydrogen-bonded cyclic dimer formed by the monoanionic oxalates (motif B); (c) Isolated monohydrogen oxalate units (motif C).

oxalate units with strong N-H...O and O-H...O type interactions within the plane is motif C (Fig. 4.6c). Motifs A-C, observed in the amine oxalates, have been observed in some of the hydrogen bonded supramolecular assemblies.^[4]

The various motifs described above can be utilized to derive insight into the possible arrangement of the motif and the amine molecules. Thus, a large number of possible arrangements can be generated by variation of the motif and the amine molecules. A comprehensive schematic of such supramolecular assembly is shown

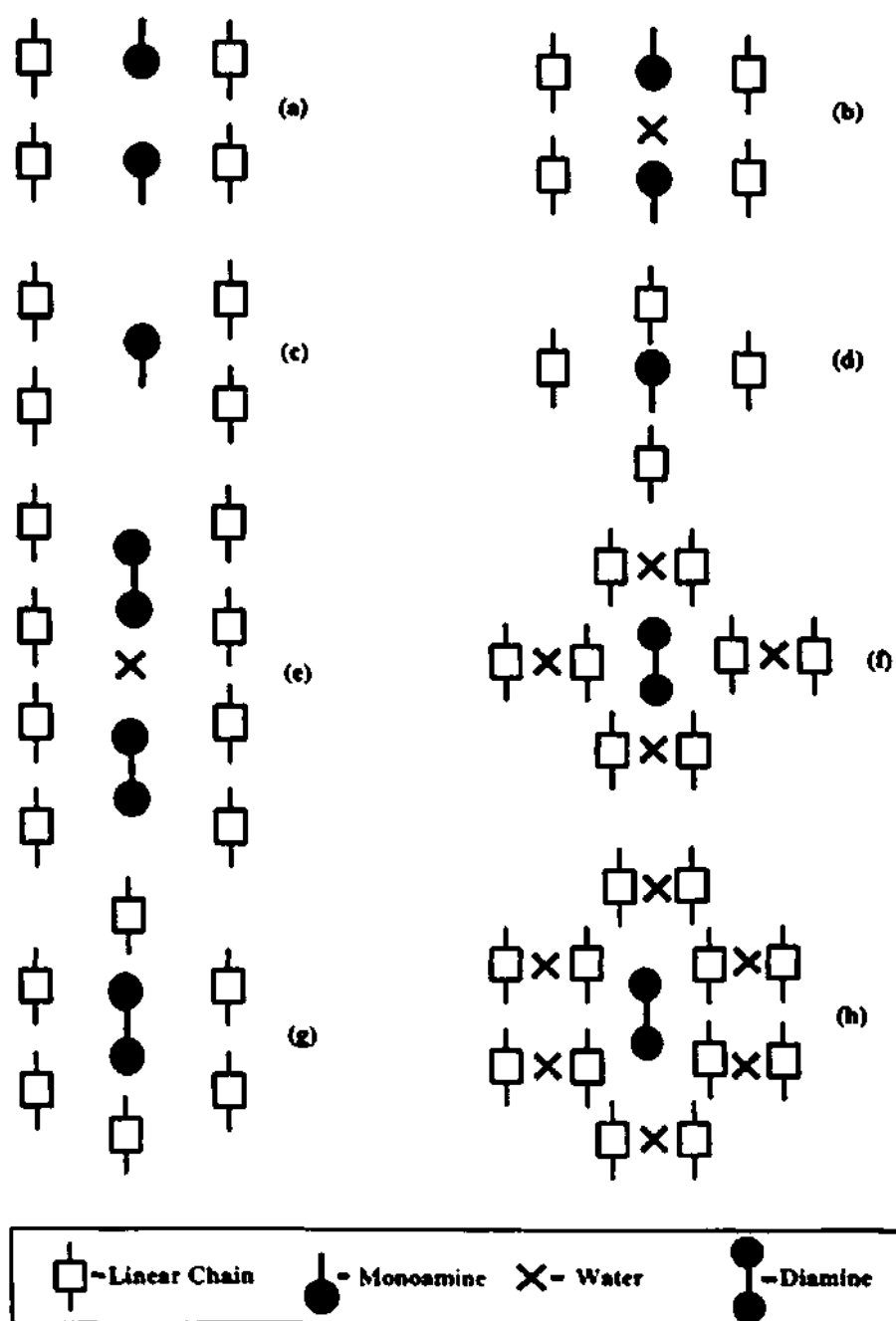


Fig. 4.7. Schematic illustration of some of the possible arrangements of the linear chain of monoanionic oxalate units around the amine molecules. Pattern b, is observed in PRO and BUO, while e, f and g are observed in ENO, DABO and PIPO respectively.

in Figure 4.7. As can be seen, some of the arrangements can be identified in present amine oxalates. By involving water of crystallization along with the motifs and amine molecules, further assemblies can be generated. Such assemblies occur in some of the amine oxalates, especially PRO and ENO (Figs. 4.7b and e). The DABO is very unique, for they have the two neighboring linear chain dicarboxylates linked through water molecules residing between them. These linear chain units arrange around the amine molecules as in Figure 4.7f.

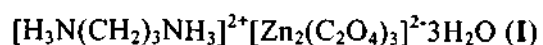
In the case of DCO, the motif B alternates with the amine molecules along both the *b*- and *c*-axis, resulting in hydrogen bonded layers lying in the *ac*-plane as seen from Figure 4.4a. The arrangement of Motif C, observed in GUO is somewhat analogous to the arrangement of motif B in DCO. In GUO, the monoanionic oxalate units replaces the dimeric unit.

4.1.3. Summary

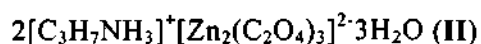
The present study of organic amine oxalates has demonstrated the occurrence of different types of supramolecular structures arising from the hydrogen bond interactions between the $[\text{HC}_2\text{O}_4]^-$ anion and the organoammonium cation. The presence of water molecules in some of them offers additional hydrogen bonding opportunities. Clearly, studies of such systems involving the organic cations and anions with hydrogen bonding donor-acceptor sites is of considerable value in supramolecular materials design. It is also interesting that the strengths of the hydrogen bonded networks in these materials is also reflected in their thermal stabilities. The study of amine oxalates, in particular, is also relevant in understanding their reactions with metal ions to yield open architectures.

4.2. Open-framework zinc oxalates with two and three-dimensional structures

4.2.1. Results



The asymmetric unit of $[\text{H}_3\text{N}(\text{CH}_2)_3\text{NH}_3]^{2+}[\text{Zn}_2(\text{C}_2\text{O}_4)_3]^{2-} \cdot 3\text{H}_2\text{O}$, **I**, contains 28 non-hydrogen atoms (Fig. 4.8). **I** consists of macroanionic sheets of formula $[\text{Zn}_2(\text{C}_2\text{O}_4)_3]^{2-}$ with interlamellar $[\text{H}_3\text{N}(\text{CH}_2)_3\text{NH}_3]^{2+}$ ions, the individual layers consists of a network of ZnO_6 octahedra and C_2O_4 units. Each Zn atoms is cross-linked to six oxalate oxygens, forming a honeycomb network as shown in Figure 4.9a. This type of network results in a 12-membered pore within the layers, which stack one over the other, along the c axis. The protonated organic amine molecules sit in the middle of the 12-membered pores. There are three water molecules occupying the pores along with the amine (Fig. 4.9b). Along the b axis the layers stack one over the other with the water molecules situated in between the layers as shown in Figure 4.10. The amine and the water molecules participate in extensive hydrogen bonding, lending additional structural stability to this material. The various hydrogen bond interactions between the sheets and the guest molecules can be seen in Figures 4.9b and 4.10. The Zn – O distances in **I** are in the range 2.068 – 2.121 Å (ave. 2.093 Å), with the longer distances being associated with the oxygens that are double-bonded to the carbon atoms. The variations in the distances are reflected in the C – O bonding as well (Table 4.3). The O – Zn – O and O – C – O bond angles are in the range 79.9 – 173.2 and 125.2 – 127.2°, respectively (Table 4.3).



The asymmetric unit of $2[\text{C}_3\text{H}_7\text{NH}_3]^+[\text{Zn}_2(\text{C}_2\text{O}_4)_3]^{2-} \cdot 3\text{H}_2\text{O}$, **II**, contains 19 non-hydrogen atoms and is shown in Figure 4.11a. **II** also consists of a network of ZnO_6 octahedra and oxalate units with the connectivity between them gives rise to a three-dimensional structure. Of the three oxalate units, two connect through an *in-plane* linkage and the third one is cross-linked to the Zn atom in an *out-of-plane* manner resulting in an interrupted honeycomb structure with a 20-member elliptical

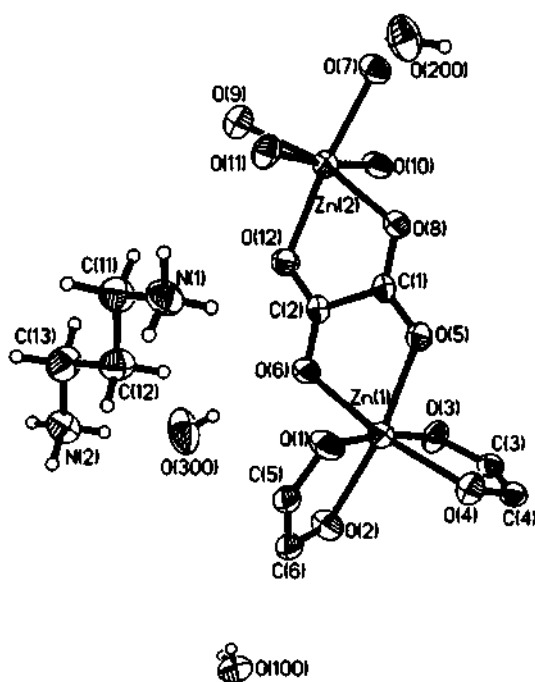


Fig. 4.8. ORTEP plot of I, $[\text{H}_3\text{N}(\text{CH}_2)_3\text{NH}_3]^{2+}[\text{Zn}_2(\text{C}_2\text{O}_4)_3]^{2-} \cdot 3\text{H}_2\text{O}$. Thermal ellipsoids are given at 50% probability.

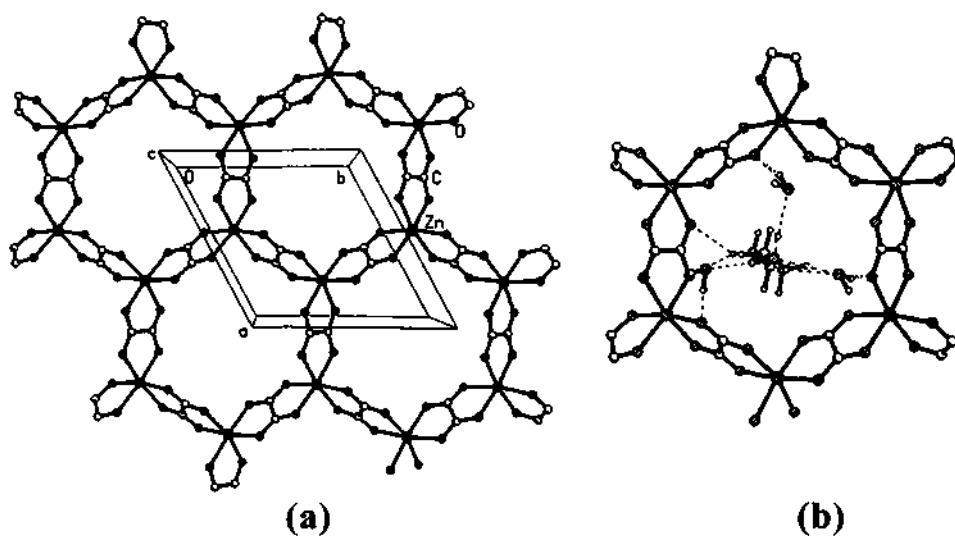


Fig. 4.9. (a) Structure of I, $[\text{H}_3\text{N}(\text{CH}_2)_3\text{NH}_3]^{2+}[\text{Zn}_2(\text{C}_2\text{O}_4)_3]^{2-} \cdot 3\text{H}_2\text{O}$ in the ab plane showing the honeycomb architecture. (b) Structure showing a single 12-membered aperture with the amine and water molecules. Dotted lines represent the hydrogen bond interactions.

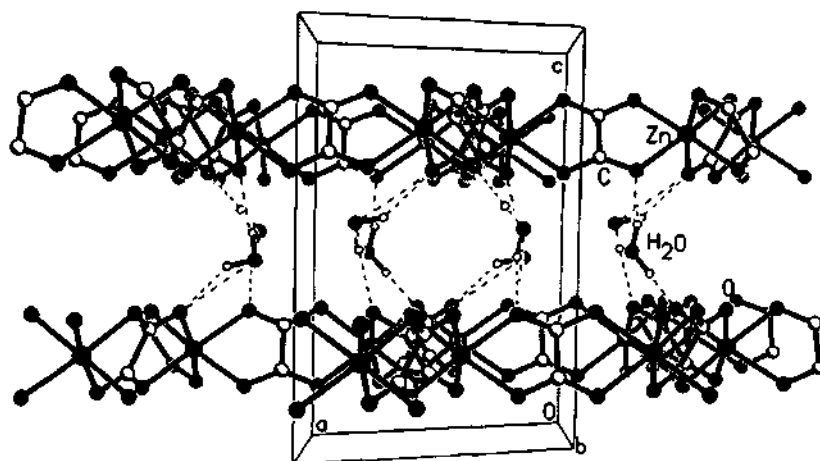


Fig. 4.10. Structure of I, $[\text{H}_3\text{N}(\text{CH}_2)_3\text{NH}_3]^{2+}[\text{Zn}_2(\text{C}_2\text{O}_4)_3]^{2-} \cdot 3\text{H}_2\text{O}$ along the *ac* plane showing the layer arrangement. Amine molecules are not shown for clarity. Note that the water molecules involve in hydrogen bonding (dotted lines).

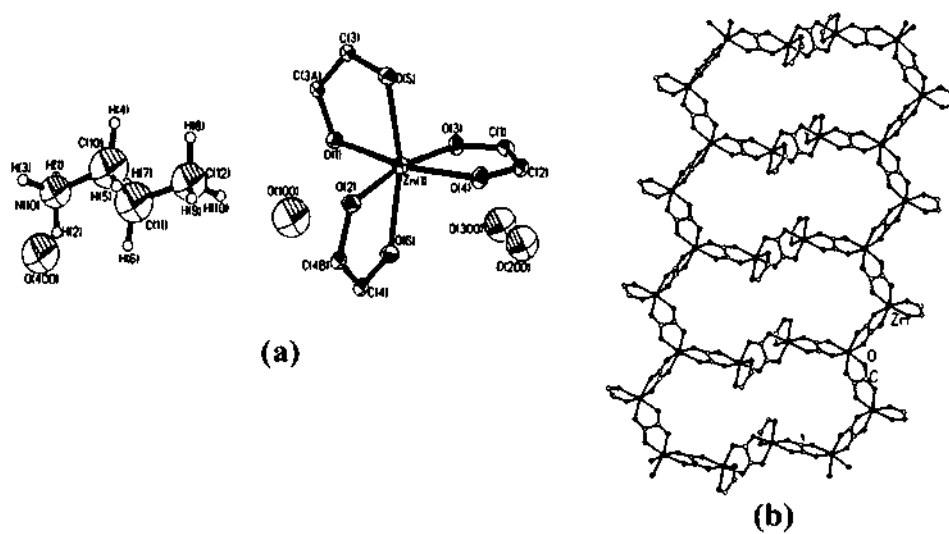


Fig. 4.11. (a) ORTEP plot of II, $2[\text{C}_3\text{H}_7\text{NH}_3]^+[\text{Zn}_2(\text{C}_2\text{O}_4)_3]^{2-} \cdot 3\text{H}_2\text{O}$. Thermal ellipsoids are given at 50% probability. (b) Structure of II, $2[\text{C}_3\text{H}_7\text{NH}_3]^+[\text{Zn}_2(\text{C}_2\text{O}_4)_3]^{2-} \cdot 3\text{H}_2\text{O}$, showing the 20-membered aperture. Note that the one of the Zn atoms is connected by out of plane oxalate unit.

ring as shown in Figure 4.11b. This type of connectivity between the Zn and oxalate units does not appear to have been encountered earlier. The elliptical pores in this 3-D zinc oxalate is formed by the linkage between 10 Zn and 10 oxalate units lying in the same plane and the other oxalate unit connect the elliptical pores such that two such rings are perpendicular to each other. Though the largest pore opening in propylamine containing zinc oxalate compound is a 20-membered one it appears smaller in projection. Thus, along the b axis, the structure has the appearance of an 12-membered square-channel made from 6 Zn and 6 oxalate units (~8.5 x 8.2 Å; longest atom-atom contact distance not including van der Waals radii) (Fig. 4.12a). The 20-member aperture has the dimensions ~17.2 x 6.9 Å. Along the c axis, there is another 12-membered channel made from 8 Zn and 4 oxalate units of 8.3 x 6.1 Å diameter (Fig. 4.12b). The organic structure-directing agent, n-propylamine, which is highly disordered, occupies these channels along with the water molecules.

Table 4.3. Selected interatomic distances in I, $[\text{H}_3\text{N}(\text{CH}_2)_3\text{NH}_3]^{2+}[\text{Zn}_2(\text{C}_2\text{O}_4)_3]^{2-} \cdot 3\text{H}_2\text{O}$

Moiety	Distance (Å)	Moiety	Distance (Å)
Zn(1) – O(1)	2.087(2)	C(1) – O(5)	1.245(3)
Zn(1) – O(2)	2.068(2)	C(1) – O(8)	1.242(3)
Zn(1) – O(3)	2.082(2)	C(2) – O(6)	1.238(4)
Zn(1) – O(4)	2.105(2)	C(2) – O(12)	1.248(4)
Zn(1) – O(5)	2.093(2)	C(3) – O(3)	1.251(3)
Zn(1) – O(6)	2.104(2)	C(3) ^b – O(9)	1.245(3)
Zn(2) – O(7)	2.080(2)	C(4) – O(4)	1.251(3)
Zn(2) – O(8)	2.084(2)	C(4) ^b – O(11)	1.242(3)
Zn(2) – O(9)	2.084(2)	C(5) – O(1)	1.248(4)
Zn(2) – O(10)	2.095(2)	C(5) ^a – O(7)	1.249(3)
Zn(2) – O(11)	2.121(2)	C(6) – O(2)	1.249(3)
Zn(2) – O(12)	2.110(2)	C(6) ^a – O(10)	1.236(4)
C(1) – C(2)	1.566(4)	C(3) – C(4)	1.558(4)

C(5) – C(6)	1.559(4)		
Organic Moiety			
N(1) – C(11)	1.484(4)	C(11) – C(12)	1.496(5)
C(12) – C(13)	1.503(4)	C(13) – N(2)	1.468(4)
Moiety	Angle (°)	Moiety	Angle (°)
O(2) – Zn(1) – O(3)	95.9(5)	O(2) – Zn(1) – O(1)	80.0(3)
O(3) – Zn(1) – O(1)	173.2(2)	O(2) – Zn(1) – O(5)	169.3(2)
O(3) – Zn(1) – O(5)	93.5(2)	O(1) – Zn(1) – O(5)	91.0(2)
O(2) – Zn(1) – O(6)	95.4(3)	O(3) – Zn(1) – O(6)	93.7(4)
O(1) – Zn(1) – O(6)	92.1(3)	O(5) – Zn(1) – O(6)	79.0(2)
O(2) – Zn(1) – O(4)	93.0(2)	O(3) – Zn(1) – O(4)	79.8(2)
O(1) – Zn(1) – O(4)	94.8(4)	O(5) – Zn(1) – O(4)	93.5(3)
O(6) – Zn(1) – O(4)	169.9(2)	O(7) – Zn(2) – O(9)	94.0(2)
O(7) – Zn(2) – O(8)	98.0(2)	O(9) – Zn(2) – O(8)	164.5(4)
O(7) – Zn(2) – O(10)	80.1(2)	O(9) – Zn(2) – O(10)	96.6(2)
O(8) – Zn(2) – O(10)	95.1(2)	O(7) – Zn(2) – O(12)	172.5(3)
O(9) – Zn(2) – O(12)	89.3(4)	O(8) – Zn(2) – O(12)	79.9(4)
O(10) – Zn(2) – O(12)	92.9(2)	O(7) – Zn(2) – O(11)	95.3(1)
O(8) – Zn(2) – O(11)	89.3(2)	O(9) – Zn(2) – O(11)	79.9(1)
O(10) – Zn(2) – O(11)	174.1(2)	O(12) – Zn(2) – O(11)	91.9(2)
O(8) – C(1) – O(5)	126.8(2)	O(6) – C(2) – O(12)	126.6(3)
O(9) ^a – C(3) – O(3)	125.2(2)	O(11) ^a – C(4) – O(4)	126.6(2)
O(1) – C(5) – O(7) ^b	125.9(3)	O(10) ^b – C(6) – O(2)	127.2(2)
O(8) – C(1) – C(2)	117.1(2)	O(5) – C(1) – C(2)	116.1(2)
O(6) – C(2) – C(1)	116.6(2)	O(12) – C(2) – C(1)	116.8(3)
O(9) ^a – C(3) – C(4)	117.5(2)	O(3) – C(3) – C(4)	117.3(2)
O(4) – C(4) – C(3)	116.3(2)	O(11) ^a – C(4) – C(3)	117.1(2)
O(1) – C(5) – C(6)	116.8(2)	O(7) ^b – C(5) – C(6)	117.2(2)
O(10) ^b – C(6) – C(5)	116.7(2)	O(2) – C(6) – C(5)	116.1(2)
Organic Moiety			
N(1) – C(11) – C(12)	112.2(3)	C(11) – C(12) – C(13)	111.6(3)
C(12) – C(13) – N(2)	113.7(3)		

^a x+1, y, z; ^b x, y+1, z

The Zn – O distances in **II** are in the range 2.068 – 2.121 Å (ave. 2.096 Å), with the longer distances being associated with the oxygens that are double-bonded to the carbon atoms. The O – Zn – O and O – C – O bond angles are in the range 79.1 – 168.4° and 126.0 – 126.5°, respectively (Table 4.4). The importance of multi-point hydrogen bonding in these materials is apparent when examining the distances and angles listed in Table 4.5.

Thermogravimetric analysis

TGA studies of **I** and **II** were carried out in static air from room temperature to 600 °C and show weight loss in three steps. For **I**, a sharp mass loss of about 9.3% occurring at 150 °C corresponds to the loss of water molecules (calcd. 10.3%) and a continuous two step mass loss of 57.2 % in the region 300-400 °C corresponds to the loss of oxalate and amine molecules (calcd. 55.6%). For **II**, a sharp mass loss of about 10.2% at 65 °C corresponds to the loss of water molecules (calcd. 9.5%) and the second mass loss of about 33.8% in the region 270-330 °C corresponds to the loss of carbon dioxide from the oxalate (calcd. 33%). The final mass loss of 24.4% in the region 360-430 °C corresponds to the loss of the amine molecules (calcd. 28%). The powder XRD patterns of the decomposed products indicated a poorly crystalline product with very weak reflections that corresponds to the mineral zincite, ZnO (JCPDS: 36-1451).

Adsorption studies

Adsorption studies, carried out gravimetrically with a Cahn electric balance, show that dehydrated $2[\text{C}_3\text{H}_7\text{NH}_3]^+[\text{Zn}_2(\text{C}_2\text{O}_4)_3]^{2-} \cdot 3\text{H}_2\text{O}$ adsorbs water reversibly exhibiting a Langmuir Type 1 adsorption isotherm (Fig. 4.13). The observed weight changes at 25 °C correspond to 3.0 water molecules per unit cell, in agreement with the framework formula derived from crystallographic investigations.

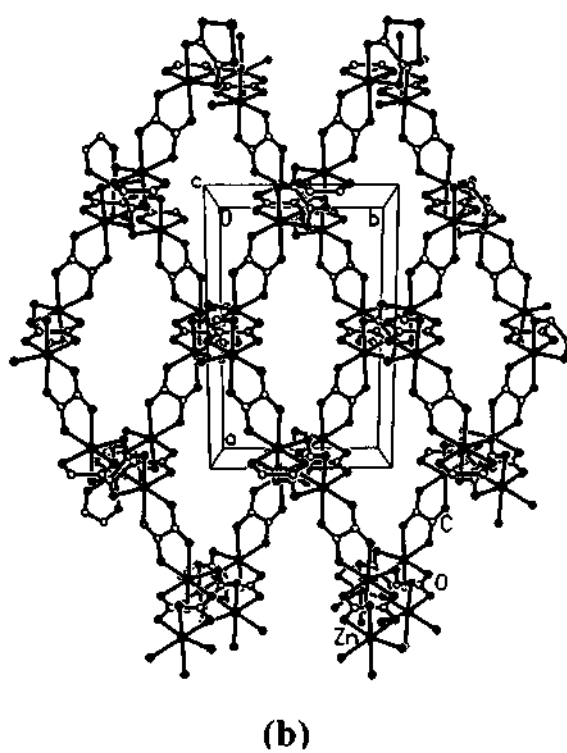
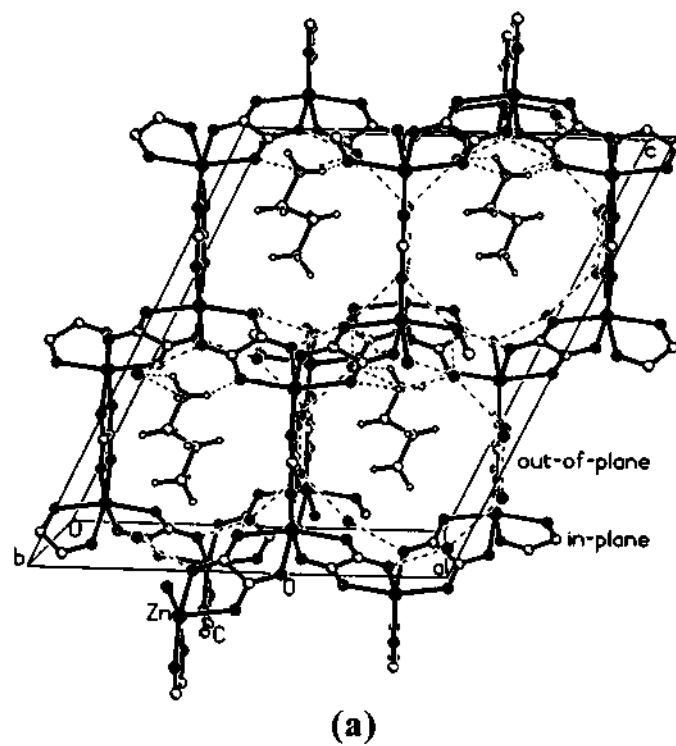


Fig. 4.12. (a) Structure of II, $2[\text{C}_3\text{H}_7\text{NH}_3]^+[\text{Zn}_2(\text{C}_2\text{O}_4)_3]^{2-} \cdot 3\text{H}_2\text{O}$, along the b axis showing the 12-membered square channels. Dotted lines represent the various hydrogen bond interactions. (b) Structure of II, $2[\text{C}_3\text{H}_7\text{NH}_3]^+[\text{Zn}_2(\text{C}_2\text{O}_4)_3]^{2-} \cdot 3\text{H}_2\text{O}$, along the c axis showing the 12-membered elliptical channels.

Table 4.4. Selected bond distances and angles in II, $2[\text{C}_3\text{H}_7\text{NH}_3]^+[\text{Zn}_2(\text{C}_2\text{O}_4)_3]^{2-} \cdot 3\text{H}_2\text{O}$

Moiety	Distance (Å)	Moiety	Distance (Å)
Zn(1) – O(1)	2.096(4)	C(1) – O(3)	1.247(5)
Zn(1) – O(2)	2.093(4)	C(2) – O(4)	1.235(5)
Zn(1) – O(3)	2.082(4)	C(3) – O(1) ^a	1.250(7)
Zn(1) – O(4)	2.099(4)	C(4) – O(6)	1.237(7)
Zn(1) – O(5)	2.099(4)	C(4) – O(2) ^b	1.246(7)
Zn(1) – O(6)	2.105(4)	C(3) – O(5)	1.233(7)
C(1) – C(2)	1.557(12)	C(3) – C(3) ^a	1.554(10)
C(4) – C(4) ^b	1.559(10)		
Moiety	Angle (°)	Moiety	Angle (°)
O(3) – Zn(1) – O(2)	168.6(2)	O(3) – Zn(1) – O(1)	92.0(2)
O(2) – Zn(1) – O(1)	97.4(2)	O(3) – Zn(1) – O(4)	79.7(2)
O(2) – Zn(1) – O(4)	92.0(2)	O(1) – Zn(1) – O(4)	168.4(2)
O(3) – Zn(1) – O(5)	98.0(2)	O(2) – Zn(1) – O(5)	90.2(2)
O(1) – Zn(1) – O(5)	79.1(2)	O(4) – Zn(1) – O(5)	94.1(2)
O(3) – Zn(1) – O(6)	93.9(2)	O(2) – Zn(1) – O(6)	79.4(2)
O(1) – Zn(1) – O(6)	90.4(2)	O(4) – Zn(1) – O(6)	98.0(2)
O(5) – Zn(1) – O(6)	164.3(2)	O(3) ^c – C(1) – O(3)	126.5(7)
O(4) ^c – C(2) – O(4)	126.0(7)	O(5) – C(3) – O(1) ^a	126.5(5)
O(6) – C(4) – O(2) ^a	126.1(5)	O(3) – C(1) – C(2)	116.7(4)
O(4) – C(2) – C(1)	117.0(4)	O(5) – C(3) – C(3) ^b	118.0(6)
O(1) ^a – C(3) – C(3) ^a	115.5(6)	O(6) – C(4) – C(4) ^b	117.4(6)
O(2) ^b – C(4) – C(4) ^b	116.4(6)		

^a $-x+1/2, -y+5/2, -z+1$; ^b $-x+1, -y+2, -z+1$ ^c $-x+1, y, -z+3/2$

Table 4.5. Important hydrogen bond distances and angles in compounds I and II.

Moiety	Distance (Å)	Moiety	Angle (°)
I			
O(3) – H(11)	2.215(1)	O(3) – H(11) – N(2)	156.0(2)
O(12) – H(12)	1.957(1)	O(12) – H(12) – N(2)	178.2(1)
O(9) – H(11)	2.345(1)	O(9) – H(11) – N(2)	142.3(1)
O(4) – H(101)	1.930(1)	O(4) – H(101) – O(100)	175.4(2)
O(1) – H(102)	2.142(1)	O(1) – H(102) – O(100)	169.7(2)
O(7) – H(201)	2.063(1)	O(7) – H(201) – O(200)	160.6(1)
O(5) – H(202)	2.101(1)	O(5) – H(202) – O(200)	149.8(1)

O(2) – H(301)	2.166(1)	O(2) – H(301) – O(300)	175.0(1)
O(6) – H(302)	2.088(1)	O(6) – H(302) – O(300)	176.1(1)
O(100) – H(2)	1.964(1)	O(100) – H(2) – N(1)	167.7(3)
O(100) – H(3)	2.158(1)	O(100) – H(3) – N(1)	142.8(1)
O(200) – H(1)	1.887(3)	O(200) – H(1) – N(1)	164.2(1)
O(300) – H(10)	1.858(1)	O(300) – H(10) – N(2)	170.5(1)
II			
O(6) – H(1)	2.342(1)	O(6) – H(1) – N(1)	132.6(1)
O(5) – H(2)	2.357(1)	O(5) – H(2) – N(1)	131.4(1)
O(100) – H(3)	2.424(1)	O(100) – H(3) – N(1)	158.2(1)

Unlike **II**, the 2-D zinc oxalate, **I**, loses crystallinity on desorption of water, indicating that the hydrogen bond interactions between the water and the framework is crucial for the structural stability of **I**.

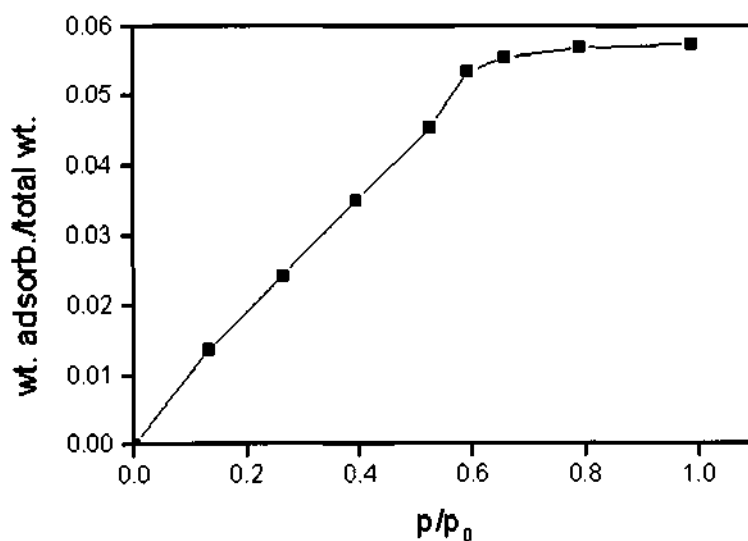
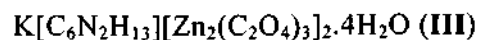


Fig. 4.13. Room-temperature adsorption isotherm for H₂O in the dehydrated sample of **II**



The asymmetric unit of $\text{K}[\text{C}_6\text{N}_2\text{H}_{13}][\text{Zn}_2(\text{C}_2\text{O}_4)_3]_2 \cdot 4\text{H}_2\text{O}$, **III**, contains 33 non-hydrogen atoms, of which 20 belong to the framework and 13 atoms to the

guest species which include one potassium ion, one amine molecule (DABCO) and four water molecules. The asymmetric unit contains two crystallographically independent Zn atoms.

The Zn atoms, in **III**, are octahedrally coordinated with respect to oxygen atoms with Zn – O distance in the range 2.074(5) – 2.131(4) Å (av. Zn(1) – O = 2.1018; Zn(2) – O = 2.1062 Å). Of the six oxygens bound to zinc, three are associated with Zn – O distances in the range 2.074(5) – 2.102(4) Å for Zn(1) and 2.075(5) – 2.089(5) Å for Zn(2), and the remaining three have distances in the range 2.105(4) – 2.131(4) for Zn(1) and 2.112(4) – 2.131(4) Å for Zn(2) (Table 4.6). Formally these correspond to the single and double bonded oxygens bound to the carbon atoms respectively. The C – O bond distances are in the range 1.236(8) – 1.272(8) Å (av. 1.255 Å) and the variations in the C – O distances are also reflected in this bonding as well (Table 4.6). The O – Zn – O angles are in the range 78.4(2) – 167.4(2)° (av. O – Zn(1) – O = 105.2; O – Zn(2) – O = 105.8°) (Table 4.6). The O – C – O bond angles are in the range 125.2(6) – 126.6(6)° (av. 125.9°) (Table 4.6). The potassium ion is coordinated to eight nearest neighbor oxygen atoms. The potassium cations coordinated to the negatively charged oxygen atoms of the oxalate ligands and to the oxygen atoms of the water molecules. Of the eight oxygens that interact with the potassium, seven oxygen atoms have distances of less than 3.1 Å, which is usually considered the upper limit for significant K ... O interaction.^[20] The K – O distances are in the range 2.758(6) – 3.305(5) Å (av. 2.907 Å) (Table 4.6). These various geometrical parameters observed in the zinc oxalate, **III**, are in the range expected for this type of bonding. Bond valence sum calculations using the methodology of Brown and Aldermatt^[21] show a valence sum of 2.048 and 2.026 for Zn(1) and Zn(2), 1.073 for K(1) and for the oxygen atom it is

Table 4.6. Selected bond distances and angles for $K[C_6N_2H_{13}][Zn_2(C_2O_4)_3] \cdot 4H_2O$, **III**

Moiety	Distance (Å)	Moiety	Distance (Å)
Zn(1)-O(1)	2.074(5)	O(1)-C(2)	1.272(8)
Zn(1)-O(2)	2.092(4)	O(2)-C(1)#4	1.242(8)
Zn(1)-O(3)	2.102(4)	O(3)-C(1)	1.264(8)
Zn(1)-O(4)	2.105(4)	O(4)-C(4)	1.267(8)
Zn(1)-O(5)	2.107(4)	O(5)-C(3)#5	1.260(7)
Zn(1)-O(6)	2.131(4)	O(6)-C(3)	1.253(7)
Zn(2)-O(7)	2.075(5)	O(7)-C(5)	1.257(8)
Zn(2)-O(8)	2.089(5)	O(8)-C(5)#6	1.256(8)
Zn(2)-O(9)	2.107(5)	O(9)-C(6)#7	1.260(8)
Zn(2)-O(10)	2.112(5)	O(10)-C(2)	1.244(8)
Zn(2)-O(11)	2.123(5)	O(11)-C(6)	1.252(8)
Zn(2)-O(12)	2.131(5)	O(12)-C(4)	1.236(8)
K(1)-O(3)	2.768(4)	C(1)-O(2)#4	1.242(8)
O(2)-K(1)#1	2.796(4)	C(3)-O(5)#5	1.260(7)
O(6)-K(1)#1	2.981(5)	C(5)-O(8)#6	1.256(8)
K(1)-O(2)#2	2.796(4)	C(6)-O(9)#7	1.260(8)
K(1)-O(4)	3.305(5)	C(1)-C(1)#4	1.555(12)
K(1)-O(6)#2	2.982(5)	C(2)-C(4)	1.547(9)
K(1)-O(100)	2.876(6)	C(3)-C(3)#5	1.543(13)
K(1)-O(300)	2.788(6)	C(5)-C(5)#6	1.538(13)
K(1)-O(300)#3	2.980(6)	C(6)-C(6)#7	1.543(13)
K(1)-O(400)	2.758(6)		
Organic moiety			
N(1)-C(11)	1.480(10)	N(2)-C(12)	1.474(10)
N(1)-C(15)	1.487(10)	C(15)-C(16)	1.531(11)
N(1)-C(14)	1.490(10)	C(11)-C(12)	1.514(11)
N(2)-C(13)	1.461(10)	C(14)-C(13)	1.527(11)
N(2)-C(16)	1.467(10)		
Moiety	Angle (°)	Moiety	Angle (°)
O(1)-Zn(1)-O(2)	94.8(2)	O(400)-K(1)-O(300)	63.3(2)
O(1)-Zn(1)-O(3)	100.8(2)	O(3)-K(1)-O(300)	79.9(2)
O(2)-Zn(1)-O(3)	79.4(2)	O(6)#2-K(1)-O(4)	100.26(12)
O(1)-Zn(1)-O(4)	79.7(2)	O(400)-K(1)-O(2)#2	84.0(2)
O(2)-Zn(1)-O(4)	167.1(2)	O(300)-K(1)-O(2)#2	76.0(2)
O(3)-Zn(1)-O(4)	90.1(2)	O(400)-K(1)-O(100)	151.7(2)

O(1)-Zn(1)-O(5)	162.4(2)	O(3)-K(1)-O(100)	76.4(2)
O(2)-Zn(1)-O(5)	99.7(2)	O(300)-K(1)-O(100)	143.6(2)
O(3)-Zn(1)-O(5)	91.6(2)	O(2)#2-K(1)-O(100)	107.9(2)
O(4)-Zn(1)-O(5)	88.0(2)	O(400)-K(1)-O(300)#3	151.0(2)
O(1)-Zn(1)-O(6)	92.1(2)	O(3)-K(1)-O(300)#3	77.2(2)
O(2)-Zn(1)-O(6)	87.1(2)	O(300)-K(1)-O(300)#3	91.6(2)
O(3)-Zn(1)-O(6)	162.0(2)	O(2)#2-K(1)-O(300)#3	75.4(2)
O(4)-Zn(1)-O(6)	104.6(2)	O(100)-K(1)-O(300)#3	56.5(2)
O(5)-Zn(1)-O(6)	78.8(2)	O(400)-K(1)-O(6)#2	76.5(2)
O(7)-Zn(2)-O(8)	80.6(2)	O(300)-K(1)-O(6)#2	122.9(2)
O(7)-Zn(2)-O(9)	168.4(2)	O(100)-K(1)-O(6)#2	87.2(2)
O(8)-Zn(2)-O(9)	95.1(2)	O(300)#3-K(1)-O(6)#2	109.3(2)
O(7)-Zn(2)-O(10)	92.6(2)	O(400)-K(1)-O(4)	84.2(2)
O(8)-Zn(2)-O(10)	166.3(2)	O(300)-K(1)-O(4)	113.3(2)
O(9)-Zn(2)-O(10)	93.8(2)	O(2)#2-K(1)-O(4)	159.30(13)
O(7)-Zn(2)-O(11)	91.2(2)	O(100)-K(1)-O(4)	76.05(14)
O(8)-Zn(2)-O(11)	95.8(2)	O(300)#3-K(1)-O(4)	121.0(2)
O(9)-Zn(2)-O(11)	78.4(2)	O(2)#4-C(1)-O(3)	126.6(6)
O(10)-Zn(2)-O(11)	96.3(2)	O(10)-C(2)-O(1)	125.5(6)
O(7)-Zn(2)-O(12)	100.6(2)	O(6)-C(3)-O(5)#5	125.7(6)
O(8)-Zn(2)-O(12)	90.5(2)	O(12)-C(4)-O(4)	126.3(6)
O(9)-Zn(2)-O(12)	90.2(2)	O(8)#6-C(5)-O(7)	125.2(6)
O(10)-Zn(2)-O(12)	79.0(2)	O(11)-C(6)-O(9)#7	126.4(6)
O(11)-Zn(2)-O(12)	167.4(2)	O(2)#4-C(1)-C(1)#4	118.0(7)
O(3)-K(1)-O(2)#2	142.60(14)	O(3)-C(1)-C(1)#4	115.4(7)
O(3)-K(1)-O(6)#2	155.08(14)	O(10)-C(2)-C(4)	118.0(6)
O(3)-K(1)-O(4)	57.92(12)	O(6)-C(3)-C(3)#5	117.4(7)
O(400)-K(1)-O(3)	109.9(2)	O(5)#5-C(3)-C(3)#5	116.9(7)
O(12)-C(4)-C(2)	117.2(6)	C(4)-O(4)-Zn(1)	113.3(4)
O(4)-C(4)-C(2)	116.4(6)	C(3)#5-O(5)-Zn(1)	113.8(4)
O(8)#6-C(5)-C(5)#6	117.2(7)	C(3)-O(6)-Zn(1)	113.0(4)
O(7)-C(5)-C(5)#6	117.6(7)	C(5)-O(7)-Zn(2)	112.4(4)
O(11)-C(6)-C(6)#7	117.3(7)	C(5)#6-O(8)-Zn(2)	112.2(4)
O(9)#7-C(6)-C(6)#7	116.2(8)	C(6)#7-O(9)-Zn(2)	114.4(4)
C(2)-O(1)-Zn(1)	114.1(4)	C(2)-O(10)-Zn(2)	112.8(4)
C(1)#4-O(2)-Zn(1)	113.4(4)	C(6)-O(11)-Zn(2)	113.6(4)
C(1)-O(3)-Zn(1)	113.7(4)	C(4)-O(12)-Zn(2)	112.9(4)

Organic moiety			
N(1)-C(15)-C(16)	107.9(6)	C(11)-N(1)-C(15)	109.6(7)
N(1)-C(11)-C(12)	108.3(6)	C(11)-N(1)-C(14)	109.1(7)
N(1)-C(14)-C(13)	107.9(6)	C(15)-N(1)-C(14)	111.0(7)
N(2)-C(13)-C(14)	111.2(6)	C(13)-N(2)-C(16)	110.0(6)
N(2)-C(16)-C(15)	111.0(6)	C(13)-N(2)-C(12)	108.4(6)
N(2)-C(12)-C(11)	111.2(6)	C(16)-N(2)-C(12)	108.1(6)

Symmetry transformations used to generate equivalent atoms:

#1 $x-1, y, z$ #2 $x+1, y, z$ #3 $-x+1, -y+1, -z+2$ #4 $-x, -y+1, -z+2$
 #5 $-x, -y, -z+2$ #6 $-x+1, -y, -z+1$ #7 $-x+1, -y+1, -z+1$

in the range 1.744 – 2.008, indicating that the valence states of the various species are as expected.

The framework structure of **III** is made up of a network of ZnO_6 and C_2O_4 moieties forming macroanionic sheets of formula $[\text{Zn}_2(\text{C}_2\text{O}_4)_3]^{2-}$ with inter-lamellar $[\text{C}_6\text{N}_2\text{H}_{13}]^+$ and K^+ ions. The connectivity between the Zn and the oxalates form layers with 12-membered apertures resembling the honeycomb architecture in the *bc* plane as shown in Figure 4.14 a and b. The mono-protonated DABCO molecule resides in the middle of such 12-membered apertures and the K^+ ion and water molecules occupy the neighboring layers (Fig. 4.15). Thus, the layers are stacked one over the other in a *AAAA*... fashion along the *ab* plane.

4.2.2. Discussion

I and **II** are members of a new family of framework solids with an identical framework composition. The difference in their structures arises from the distinct ways the oxalate units link to the Zn atoms. Whereas **II** has a three-dimensional structure arising from the covalent bonding between the oxalates and Zn, **I** has a two-dimensional architecture containing overlapping layers.

In the layered zinc oxalate, the connectivity between the Zn and the oxalate moieties results in a 12-membered honeycomb aperture within the layer. The pores

penetrate the entire structure in a direction perpendicular to the sheets, yielding a solid with unidimensional channels ($\sim 8.4 \times 8.6 \text{ \AA}$; longest atom-atom contact distance not including the van der Waals radii) containing the SDA and water molecules (Fig. 4.9a and b). **I** is the first case of a honeycomb structure in a pure zinc oxalate material. The honeycomb structure in the layered structure may be largely due to the use of the organic di-cation, $[\text{DAPH}_2]^{2+}$, in the starting synthesis mixture, as such a di-cation might be needed for neutralizing the charge on the di-anionic oxalate sheets.

The layers formed by Zn and oxalate moieties in **I** are also present in **II**, except that the layers get cross-linked by another oxalate as can be seen from Figure 4.12a. A large 20-membered aperture (Fig. 4.11b) formed by the Zn and the oxalate units is also seen. Large apertures are known to occur in other framework solids, including layered materials,^[22,23] but 20-membered rings are indeed rare, such apertures and channels being found in very few materials.^[24,25] There is three-dimensional connectivity in **II** and an examination of the connectivity patterns between the oxalates and M^{2+} ions ($\text{M} = \text{Zn}$) shows that the hexa-coordinated Zn atom has two *in-plane* connectivity and one *out-of-plane* connectivity with the oxalate units. The *out-of-plane* connectivity is responsible for the three-dimensional nature of the structure (Figs. 4.12a and b). The structure of **II** can be considered to be similar to the recently discovered oxalate-phosphates.^[26] Thus, the Fe oxalate-phosphates have iron phosphate sheets cross-linked by oxalate units. In **I**, which has a layered architecture with the organic amine at the centre of the 12-membered ring along with the water molecules, hydrogen bond interactions appear to be much stronger than in the 3-D zinc oxalate. The amine molecules participate in both inter- (involving amine and framework) as well as intra- (involving amine and water molecules) layer hydrogen bonding.

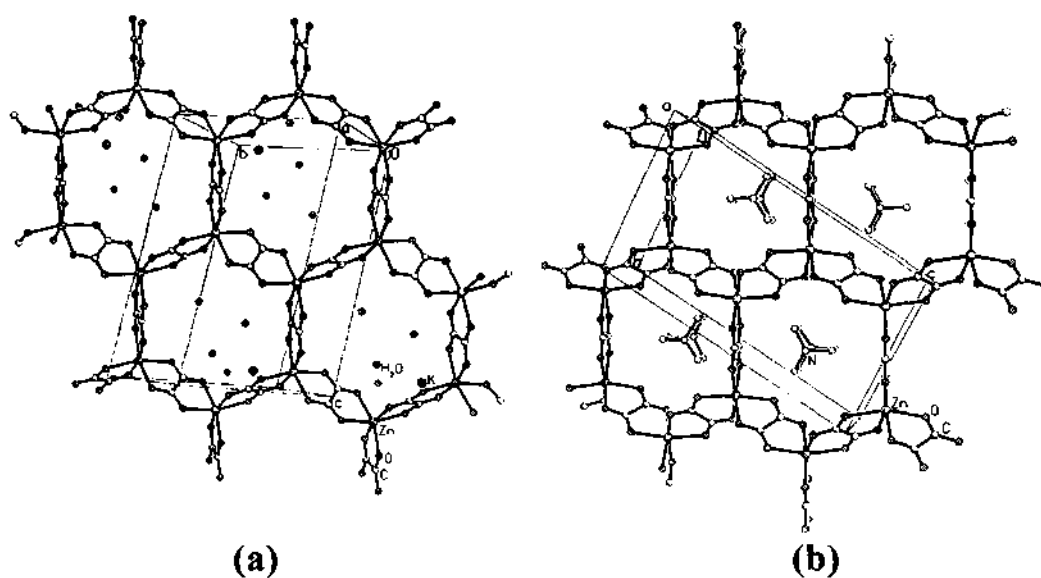


Fig. 4.14. (a) Structure of $K[C_6N_2H_{13}][Zn_2(C_2O_4)_3] \cdot 4H_2O$, III, along a axis showing the 12-membered honeycomb-like apertures. Note that the DABCO molecules occupy the center of the apertures. K^+ and water molecules are omitted for clarity. (b) Figure showing the positions of K^+ and water molecules with respect to the 12-membered aperture.

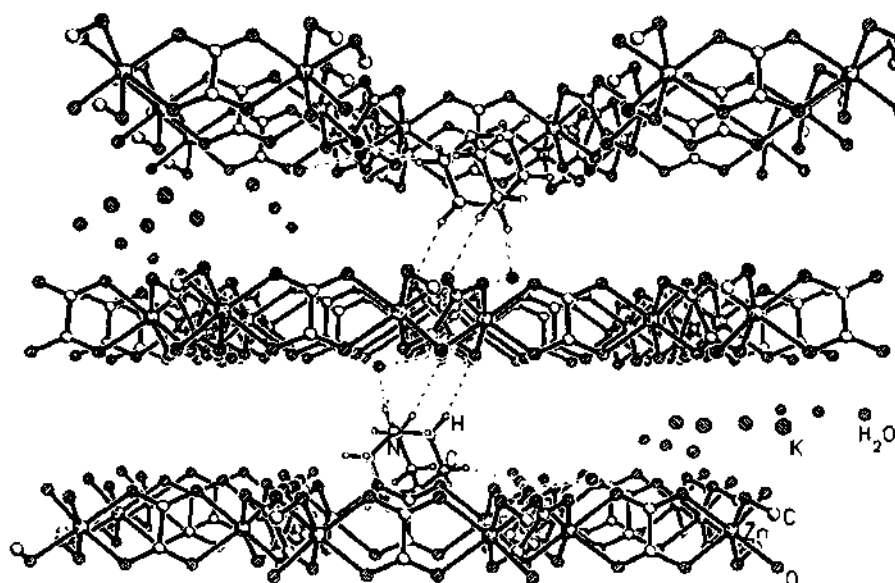


Fig. 4.15. Structure of $K[C_6N_2H_{13}][Zn_2(C_2O_4)_3] \cdot 4H_2O$ along the b axis, showing the layer arrangement. Note that K^+ and water molecules occupy inter-lamellar region and the DABCO molecules close to the framework.

Compound I, shows a dominance of hydrogen bonding with donor-acceptor (O...H) distances in the range of 1.85 – 2.35 Å and the majority of the angles above 150°. The ideal angle for a planar architecture is 180° and this 2-D oxalate network with angles above 150° indicates the importance of hydrogen bond interactions in low dimensional solids.

The remarkable feature of the structure of III, is the 12-membered apertures that penetrate the entire structure in a direction perpendicular to the sheets, yielding unidimensional channels (8.6 X 8.0 Å; longest atom-atom contact distance not including the van der Waals radii) (Figure 4.16). Similar uni-dimensional channels have been observed in aluminosilicate zeolites such as Theta-1,^[24] some detemplated microporous aluminophosphates (AlPO's),^[25] and in the recently discovered iron phosphate-oxalates.^[26] Amongst the many layered oxalates, the honeycomb architecture appears to be more common among those of transition metals. The honeycomb layers seen in I and III is well-known and identical honeycomb structures have been known for $[M(II)M(IV)(ox)_3]'$ and $[M(IV)_2(ox)_3]$, where M is a transition element.^[27,28] The honeycomb structures for the bimetallic transition metal oxalates have been made in the presence of ammonium cation.

The coordination environment of Zn atoms in open-framework phosphates and oxalates presents an interesting comparison. The Zn atoms, in most of the zinc phosphates with open architectures have a tetrahedral coordination.^[29] In the present zinc oxalates, I, II and III, the Zn atoms are octahedrally coordinated (six-fold coordination). This is likely to be because the average charge per oxygen atom on the oxalate (0.5) is less than that on the phosphate (0.75) requiring more oxalate oxygens to satisfy the valency of zinc.

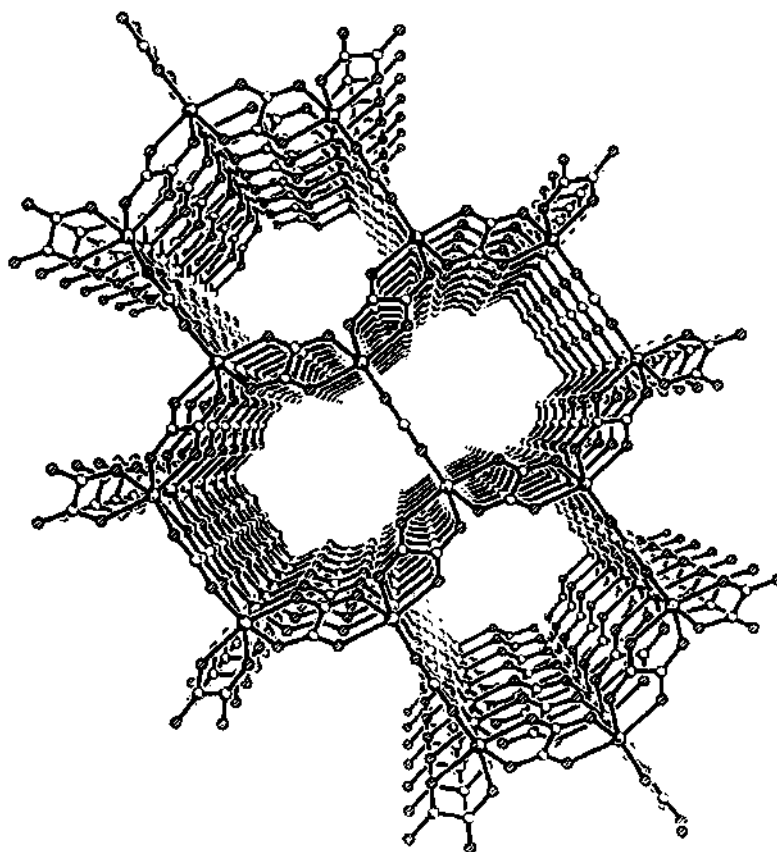


Fig. 4. 16. Structure of $\text{K}[\text{C}_6\text{N}_2\text{H}_{13}][\text{Zn}_2(\text{C}_2\text{O}_4)_3] \cdot 4\text{H}_2\text{O}$, III, along the bc plane. Note that the identical AAAAA... stacking of the layers create one-dimensional channels.

4.2.3. Summary

The present study shows that new open-framework zinc oxalates can be obtained when the synthesis is carried out in the presence of organic amines. Of the three oxalates described here, two have honeycomb layered structure and another an interrupted honeycomb with 3-D structure. While $\text{Zn}(\text{C}_2\text{O}_4) \cdot 2\text{H}_2\text{O}$ is known to possess a chain structure.^[30] The honeycomb structure observed in the present study for **I** and **III** is noteworthy as they are the first examples for Zn oxalates. This opens up the possibility of synthesizing oxalates of other divalent transition metals with honeycomb structures, which may have interesting magnetic properties. The discovery of a three-dimensional structure in **II** underscores the need for further research on open-framework oxalates prepared in the presence of structure-directing organic amines.

4.3. Reactions of Amine Oxalate with Zn^{II} ions

4.3.1. Results

The synthesis and structure of the various amine oxalates have been discussed earlier in the section 4.1. The amine oxalates were reacted with Zn^{II} ions under hydrothermal conditions.

Zero-dimensional $[\text{CN}_3\text{H}_6]_2[\text{Zn}(\text{H}_2\text{O})_2(\text{C}_2\text{O}_4)_2]$ (**IV**) and $[\text{C}_4\text{N}_2\text{H}_{12}]_3[\text{Zn}_2(\text{C}_2\text{O}_4)_5] \cdot 8\text{H}_2\text{O}$ (**V**)

The asymmetric unit of $[\text{CN}_3\text{H}_6]_2[\text{Zn}(\text{H}_2\text{O})_2(\text{C}_2\text{O}_4)_2]$, **IV**, contains 12 non-hydrogen atoms. The structure of **IV** is that of a monomer consisting of two oxalate units directly linked to Zn atoms, which are also bonded to two water molecules. The monomeric zinc oxalate units are held by strong hydrogen bonds with the monoprotonated amine (Fig. 4.17). The Zn atoms are octahedrally coordinated with the oxygens at an average Zn – O bond distance of 2.092 Å and an O – Zn – O angle of 105.4 respectively. The C – O bond distances O – C – O angles have average

values of 1.254 Å and 120.0° respectively. These values are typical for this type of bonding and similar bond distances and angles have been observed earlier in similar compounds.^[30]

The asymmetric unit of $[\text{C}_4\text{N}_2\text{H}_{12}]_3[\text{Zn}_2(\text{C}_2\text{O}_4)_5] \cdot 8\text{H}_2\text{O}$, **V** contains 29 non-hydrogen atoms. There are two Zn atoms, which are connected by one oxalate unit and possess two terminal oxalates forming a dimeric unit. The dimeric zinc oxalate is also strongly hydrogen bonded to the diprotonated amine and water molecules (Fig. 4.18). The Zn atoms are hexa-coordinated with average Zn – O distances and O – Zn – O angles of 2.104 Å and 105.3° respectively. The various other geometric parameters are as expected.

One-dimensional $[\text{C}_6\text{N}_2\text{H}_{14}][\text{Zn}(\text{C}_2\text{O}_4)_2] \cdot 3\text{H}_2\text{O}$ (**VI**)

The asymmetric unit of $[\text{C}_6\text{N}_2\text{H}_{14}][\text{Zn}(\text{C}_2\text{O}_4)_2] \cdot 3\text{H}_2\text{O}$, **VI**, contains 24 non-hydrogen atoms, of which 13 belong to the framework. Of the remaining 11 atoms, 3 belong to the water molecules and 8 to the amine. The Zn atoms are hexa-coordinated with oxygens at an average Zn – O distance of 2.099 Å. The oxygens, in turn, are connected to carbons completing the framework. The geometric parameters are in agreement with those reported earlier for similar compounds. Unlike the zero-dimensional monomeric and dimeric zinc oxalates, in **VI**, the Zn atoms and the oxalate units are connected to form a one-dimensional chain with each Zn possessing one terminal oxalate unit. The diprotonated amine is situated in between these chains and interacts with the oxygens through hydrogen bonds (Fig. 4.19). Zinc oxalate dihydrate, $[\text{Zn}(\text{C}_2\text{O}_4)(\text{H}_2\text{O})_2]$, with a chain architecture is known,^[30] but **VI** is the first example of a chain zinc oxalate synthesized in the presence of organic amine.

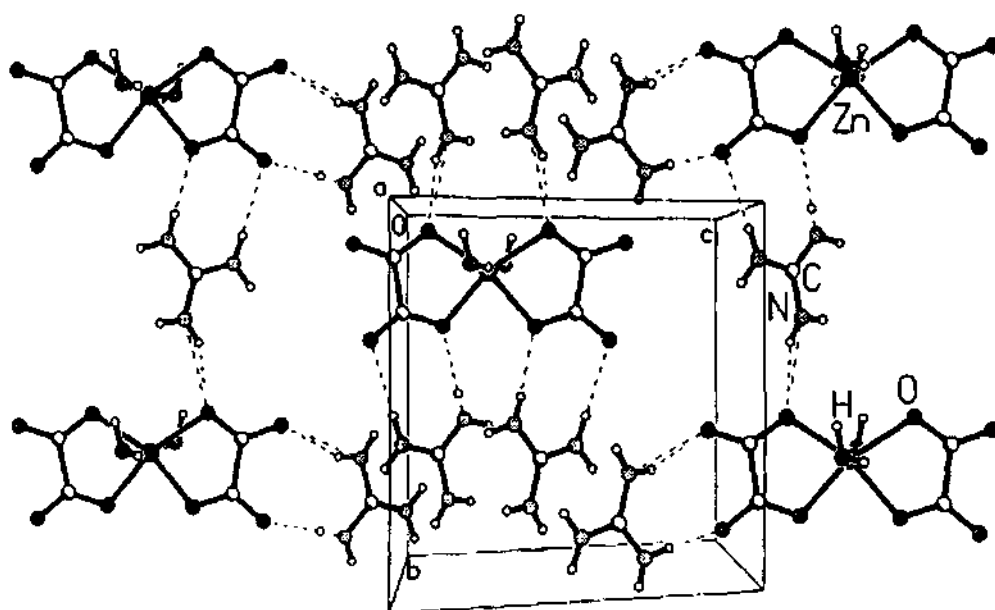


Fig. 4.17. Structure of the monomer, IV, along the $[100]$ direction. Dotted lines represent hydrogen bond interactions.

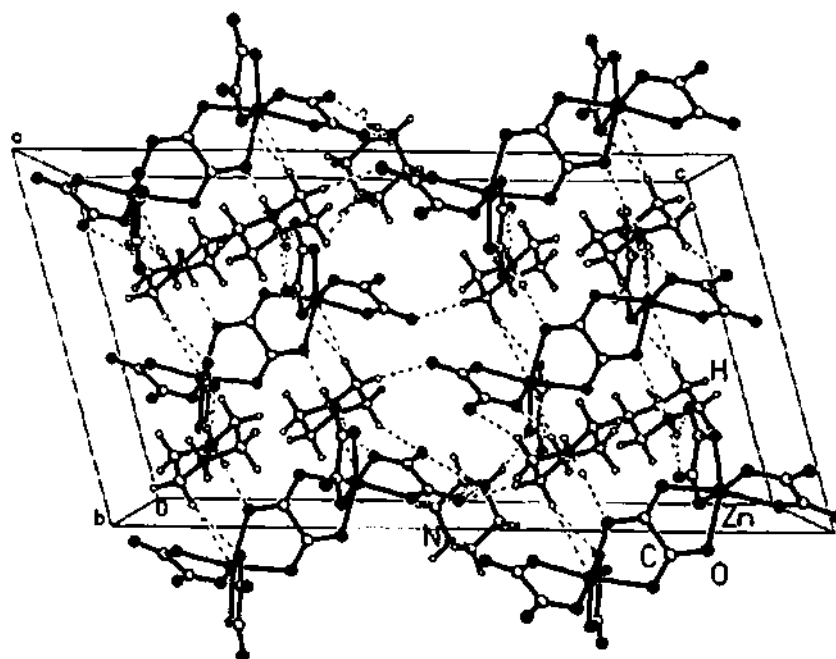


Fig. 4.18. Structure of the dimer, V, along the $[010]$ direction. The dimer and the amine alternate in a plane. Water molecules are omitted for clarity. Dotted lines are hydrogen bond interactions.

Table 4.7. Selected bond distances [Å] and angles [°] for IV, [CN₃H₆]₂[Zn(H₂O)₂(C₂O₄)₂] and V, [C₄N₂H₁₂]₃[Zn₂(C₂O₄)₅].8H₂O

IV			
Moiety	Distance	Moiety	Distance
Zn(1)-O(1)	2.082(3)	O(1)-C(1)	1.256(5)
Zn(1)-O(1) ^{#1}	2.082(3)	O(2)-C(2)	1.265(5)
Zn(1)-O(2) ^{#1}	2.102(3)	O(4)-C(1)	1.257(5)
Zn(1)-O(2)	2.102(3)	O(5)-C(2)	1.238(5)
Zn(1)-O(3)	2.154(4)	C(1)-C(2) ^{#1}	1.563(6)
Zn(1)-O(3) ^{#1}	2.154(4)		
Moiety	Angle	Moiety	Angle
O(1)-Zn(1)-O(1) ^{#1}	85.9(2)	O(1) ^{#1} -Zn(1)-O(3)	90.2(2)
O(1)-Zn(1)-O(2) ^{#1}	79.28(11)	O(2)-Zn(1)-O(3)	92.19(13)
O(1)-Zn(1)-O(2)	162.87(12)	O(2) ^{#1} -Zn(1)-O(3)	83.08(14)
O(2) ^{#1} -Zn(1)-O(2)	116.6(2)	O(3)-Zn(1)-O(3) ^{#1}	171.0(2)
O(1)-Zn(1)-O(3)	96.39(14)	O(4)-C(1)-C(2) ^{#1}	119.2(4)
C(1)-O(1)-Zn(1)	114.3(3)	O(5)-C(2)-C(1) ^{#1}	117.6(4)
C(2)-O(2)-Zn(1)	113.5(3)	O(1)-C(1)-O(4)	124.3(4)
O(1)-C(1)-C(2) ^{#1}	116.5(4)	O(5)-C(2)-O(2)	127.0(4)
O(2)-C(2)-C(1) ^{#1}	115.4(4)		
V			
Moiety	Distance	Moiety	Distance
Zn(1)-O(1)	2.042(3)	O(1)-C(1)	1.279(5)
Zn(1)-O(2)	2.069(3)	O(7)-C(1)	1.233(5)
Zn(1)-O(4)	2.093(3)	O(2)-C(2)	1.257(5)
Zn(1)-O(5)	2.097(3)	O(3)-C(2)	1.242(6)
Zn(1)-O(9)	2.160(3)	O(4)-C(3)	1.268(5)
Zn(1)-O(10)	2.164(3)	O(6)-C(3)	1.242(5)
C(1)-C(3)	1.555(6)	O(5)-C(4)	1.269(5)
C(2)-C(4)	1.569(6)	O(8)-C(4)	1.226(6)
C(5)-C(5)#1	1.544(8)	O(9)-C(5)	1.268(5)
		O(10)-C(5) ^{#1}	1.252(5)
Moiety	Angle	Moiety	Angle
O(1)-Zn(1)-O(2)	171.33(13)	O(5)-Zn(1)-O(10)	91.35(12)
O(1)-Zn(1)-O(4)	79.98(11)	O(9)-Zn(1)-O(10)	77.14(10)
O(2)-Zn(1)-O(4)	96.35(12)	C(1)-O(1)-Zn(1)	114.9(3)

O(1)-Zn(1)-O(5)	93.59 (12)	C(2)-O(2)-Zn(1)	114.5(3)
O(2)-Zn(1)-O(5)	79.64(13)	C(3)-O(4)-Zn(1)	112.9(3)
O(4)-Zn(1)-O(5)	104.41(12)	C(4)-O(5)-Zn(1)	114.0(3)
O(1)-Zn(1)-O(9)	101.35(13)	C(5)-O(9)-Zn(1)	111.6(2)
O(2)-Zn(1)-O(9)	86.41(12)	C(5) ^{#1} -O(10)-Zn(1)	111.3(3)
O(4)-Zn(1)-O(9)	89.57(12)	O(7)-C(1)-O(1)	125.9(4)
O(5)-Zn(1)-O(9)	161.16(11)	O(3)-C(2)-O(2)	125.2(4)
O(1)-Zn(1)-O(10)	90.85(12)	O(6)-C(3)-O(4)	126.2(4)
O(2)-Zn(1)-O(10)	94.69(13)	O(8)-C(4)-O(5)	126.0(4)
O(4)-Zn(1)-O(10)	162.13(12)	O(10) ^{#1} -C(5)-O(9)	125.5(4)

Symmetry transformations used to generate equivalent atoms:
 #1 $-x+1, y, -z+3/2$ for IV and #1 $-x, y, -z+3/2$ for V

Two-dimensional $[\text{C}_4\text{N}_2\text{H}_{12}]_2[\text{Zn}_2(\text{C}_2\text{O}_4)_3]_2 \cdot 8\text{H}_2\text{O}$ (VII)

The asymmetric unit of $[\text{C}_4\text{N}_2\text{H}_{12}]_2[\text{Zn}_2(\text{C}_2\text{O}_4)_3]_2 \cdot 8\text{H}_2\text{O}$, VII, contains 36 non-hydrogen atoms. VII consists of macroanionic sheets of formula $[\text{Zn}_2(\text{C}_2\text{O}_4)_3]^{2-}$ with interlamellar $[\text{C}_4\text{N}_2\text{H}_{12}]^{2+}$ ions. The individual layers involve a network of ZnO_6 octahedra and C_2O_4 units. Each Zn is cross-linked to six oxalate oxygens, forming a two-dimensional layer structure forming the honeycomb (Fig. 4.20). The honeycomb layers stack one over the other, along the *c* axis. The amine molecules occupies the middle of the 12-membered ring (6 Zn and 6 oxalate units). The four water molecules, present in VII, are present in between the layers. The geometrical parameters for IV-VII are presented in tables 4.7 and 4.8.

Three-dimensional $2[\text{C}_3\text{H}_7\text{NH}_3]^+[\text{Zn}_2(\text{C}_2\text{O}_4)_3]^{2-} \cdot 3\text{H}_2\text{O}$ (II)

The reaction of PRO and the $\text{ZnCl}_2 \cdot 2\text{H}_2\text{O}$ gives rise to the three-dimensional zinc oxalate, $2[\text{C}_3\text{H}_7\text{NH}_3]^+[\text{Zn}_2(\text{C}_2\text{O}_4)_3]^{2-} \cdot 3\text{H}_2\text{O}$, II.

Table 4.8. Selected bond distances [Å] and angles [°] for VI, $[\text{C}_6\text{N}_2\text{H}_{14}][\text{Zn}(\text{C}_2\text{O}_4)_2] \cdot 3\text{H}_2\text{O}$ and VII, $[\text{C}_4\text{N}_2\text{H}_{12}][\text{Zn}_2(\text{C}_2\text{O}_4)_3] \cdot 4\text{H}_2\text{O}$

VI			
Moiety	Distance	Moiety	Distance

Zn(1)-O(1)	2.074(4)	O(1)-C(1)	1.253(7)
Zn(1)-O(2)	2.085(4)	O(2)-C(4) ^{#1}	1.245(6)
Zn(1)-O(3)	2.089(4)	O(3)-C(2)	1.238(7)
Zn(1)-O(4)	2.103(4)	O(4)-C(3)	1.252(6)
Zn(1)-O(5)	2.112(4)	O(5)-C(4)	1.252(7)
Zn(1)-O(6)	2.134(4)	O(6)-C(1) ^{#2}	1.257(7)
C(1)-C(1) ^{#2}	1.546(11)	O(7)-C(3)	1.248(7)
C(2)-C(3)	1.549(9)	O(8)-C(2)	1.248(7)
C(4)-C(4) ^{#1}	1.550(12)		
Moiety	Angle	Moiety	Angle
O(1)-Zn(1)-O(2)	100.1(2)	O(4)-Zn(1)-O(6)	100.6(2)
O(1)-Zn(1)-O(3)	159.9(2)	O(5)-Zn(1)-O(6)	169.9(2)
O(2)-Zn(1)-O(3)	93.1(2)	C(1)-O(1)-Zn(1)	114.2(4)
O(1)-Zn(1)-O(4)	90.1(2)	C(4) ^{#1} -O(2)-Zn(1)	113.4(4)
O(2)-Zn(1)-O(4)	166.3(2)	C(2)-O(3)-Zn(1)	112.9(4)
O(3)-Zn(1)-O(4)	79.7(2)	C(3)-O(4)-Zn(1)	112.3(4)
O(1)-Zn(1)-O(5)	102.2(2)	C(4)-O(5)-Zn(1)	112.7(3)
O(2)-Zn(1)-O(5)	79.6(2)	C(1) ^{#2} -O(6)-Zn(1)	112.6(4)
O(3)-Zn(1)-O(5)	94.9(2)	O(1)-C(1)-O(6) ^{#2}	126.1(5)
O(4)-Zn(1)-O(5)	89.4(2)	O(3)-C(2)-O(8)	125.6(6)
O(1)-Zn(1)-O(6)	79.2(2)	O(7)-C(3)-O(4)	126.2(6)
O(2)-Zn(1)-O(6)	90.3(2)	O(2) ^{#1} -C(4)-O(5)	125.9(5)
O(3)-Zn(1)-O(6)	85.7(2)		

VII

Moiety	Distance	Moiety	Distance
Zn(1)-O(1)	2.079(5)	Zn(2)-O(7)	2.074(5)
Zn(1)-O(2)	2.092(5)	Zn(2)-O(8)	2.082(5)
Zn(1)-O(3)	2.100(5)	Zn(2)-O(9)	2.098(5)
Zn(1)-O(4)	2.103(5)	Zn(2)-O(10)	2.101(5)
Zn(1)-O(5)	2.107(5)	Zn(2)-O(11)	2.123(5)
Zn(1)-O(6)	2.123(5)	Zn(2)-O(12)	2.126(5)
O(1)-C(1) ^{#1}	1.257(8)	O(7)-C(3)	1.248(9)
O(2)-C(2) ^{#1}	1.264(8)	O(8)-C(1)	1.257(8)
O(3)-C(3)	1.256(9)	O(9)-C(5) ^{#2}	1.250(9)
O(4)-C(4)	1.244(8)	O(10)-C(2)	1.251(8)
O(5)-C(5)	1.259(9)	O(11)-C(6)	1.260(8)
O(6)-C(6)	1.251(8)	O(12)-C(4) ^{#2}	1.253(8)

C(1)-C(2)	1.540(11)	C(3)-C(6)	1.554(10)
C(4)-C(5)	1.548(10)		
Moiety	Angle	Moiety	Angle
O(1)-Zn(1)-O(2)	79.8(2)	O(7)-Zn(2)-O(8)	92.6(2)
O(1)-Zn(1)-O(3)	95.1(2)	O(7)-Zn(2)-O(9)	165.8(2)
O(2)-Zn(1)-O(3)	166.5(2)	O(8)-Zn(2)-O(9)	97.9(2)
O(1)-Zn(1)-O(4)	92.0(2)	O(7)-Zn(2)-O(10)	98.5(2)
O(2)-Zn(1)-O(4)	99.5(2)	O(8)-Zn(2)-O(10)	80.1(2)
O(3)-Zn(1)-O(4)	93.1(2)	O(9)-Zn(2)-O(10)	92.8(2)
O(1)-Zn(1)-O(5)	167.8(2)	O(7)-Zn(2)-O(11)	79.6(2)
O(2)-Zn(1)-O(5)	93.2(2)	O(8)-Zn(2)-O(11)	167.4(2)
O(3)-Zn(1)-O(5)	93.8(2)	O(9)-Zn(2)-O(11)	91.6(2)
O(4)-Zn(1)-O(5)	79.1(2)	O(10)-Zn(2)-O(11)	91.3(2)
O(1)-Zn(1)-O(6)	97.8(2)	O(7)-Zn(2)-O(12)	90.6(2)
O(2)-Zn(1)-O(6)	88.9(2)	O(8)-Zn(2)-O(12)	94.9(2)
O(3)-Zn(1)-O(6)	79.4(2)	O(9)-Zn(2)-O(12)	78.9(2)
O(4)-Zn(1)-O(6)	168.1(2)	O(10)-Zn(2)-O(12)	169.7(2)
O(5)-Zn(1)-O(6)	92.1(2)	O(11)-Zn(2)-O(12)	94.9(2)
C(1) ^{#1} -O(1)-Zn(1)	113.3(5)	C(3)-O(7)-Zn(2)	114.3(5)
C(2) ^{#1} -O(2)-Zn(1)	113.1(4)	C(1)-O(8)-Zn(2)	113.1(4)
C(3)-O(3)-Zn(1)	113.4(5)	C(5) ^{#2} -O(9)-Zn(2)	113.6(5)
C(4)-O(4)-Zn(1)	113.8(5)	C(2)-O(10)-Zn(2)	112.2(4)
C(5)-O(5)-Zn(1)	113.2(5)	C(6)-O(11)-Zn(2)	111.9(4)
C(6)-O(6)-Zn(1)	112.5(4)	C(4) ^{#2} -O(12)-Zn(2)	113.6(5)
O(1) ^{#3} -C(1)-O(8)	126.0(7)	O(4)-C(4)-O(12) ^{#4}	126.9(7)
O(10)-C(2)-O(2) ^{#3}	125.8(7)	O(9) ^{#4} -C(5)-O(5)	125.4(7)
O(7)-C(3)-O(3)	126.4(7)	O(6)-C(6)-O(11)	125.7(7)

Symmetry transformations used to generate equivalent atoms:

#1 $-x, -y+1, -z$; #2 $-x, -y+1, -z+1$ for VI and

#1 $x-1/2, y+1/2, z$ #2 $x, y-1, z$ #3 $x+1/2, y-1/2, z$ #4 $x, y+1, z$ for VII

4.3.2. Discussion

Thus, five zinc oxalates, $[\text{CN}_3\text{H}_6]_2[\text{Zn}(\text{H}_2\text{O})_2(\text{C}_2\text{O}_4)_2]$, IV, $[\text{C}_4\text{N}_2\text{H}_{12}]_3[\text{Zn}_2(\text{C}_2\text{O}_4)_5] \cdot 8\text{H}_2\text{O}$, V, $[\text{C}_6\text{N}_2\text{H}_{14}][\text{Zn}(\text{C}_2\text{O}_4)_2] \cdot 3\text{H}_2\text{O}$, VI, $[\text{C}_4\text{N}_2\text{H}_{12}][\text{Zn}_2(\text{C}_2\text{O}_4)_3] \cdot 4\text{H}_2\text{O}$, VII, and $[\text{C}_3\text{NH}_{10}]_2[\text{Zn}_2(\text{C}_2\text{O}_4)_3] \cdot 3\text{H}_2\text{O}$, II, possessing new structures have been synthesized by the reaction of amine oxalates with Zn^{II}

ions, the amine oxalates themselves having been synthesized and characterized for the first time. While there is no simple relation between the starting amine oxalate and the product zinc oxalates, what is significant is that zinc oxalates with one-, two- and three-dimensional architectures, in addition to the monomeric and dimeric oxalates, could be synthesized by employing mild conditions.

IV, **V** and **VI** are new members of the zinc oxalate family. Monomeric **IV** and dimeric **V** can be considered to be zero-dimensional oxalate structures, and **VI** a one-dimensional chain structure. In **IV**, the connectivity between the Zn and oxalate moieties forms a monomer, i.e., the Zn atoms have three free oxalate units, and in **V**, one oxalate joins two zinc centers with two free oxalates. In the case of **VI**, the connectivity forms a one-dimensional Zn oxalate chain and the Zn has one free oxalate group. The oxalates in **VII**, link up with Zn to form the honeycomb-like layer. The Zn atoms do not have any free oxalate groups in the layer structure.

The number of free oxalate group attached to the Zn center, probably governs the reactivity of the zinc oxalates. Thus, the monomer must be most reactive followed by the dimer, chain and the layer. In Figure 4.21, the various types of structures are presented to demonstrate the similarities and relationships. As can be seen, the structure of the dimer can be derived from that of the monomer, the chain from the dimer, and the layer from the chain. It is easy to see how the layers in **VII** get connected by oxalate units to form the three-dimensional structure of **II**. Just as the fundamental building unit, the 4-membered ring monomeric phosphate plays a crucial role in the building of framework phosphates,^[31,32] it is possible that the monomeric and dimeric oxalates are involved in the construction of the extended oxalate framework structures.

4.3.3. Summary

The present study shows that new types of zinc oxalates can be obtained by

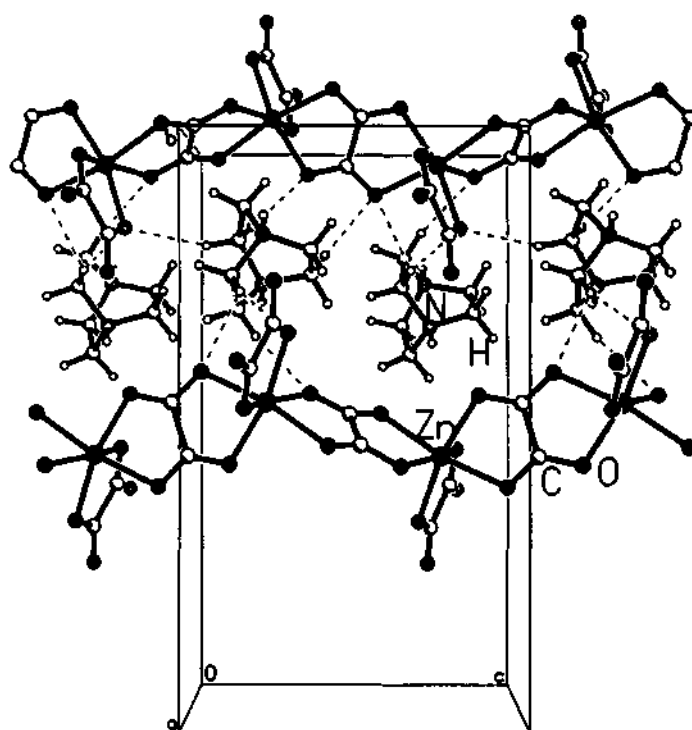


Fig. 4.19. Structure of the linear chain, VI, along the $[100]$ direction. The oxalate chains are separated by the amine.

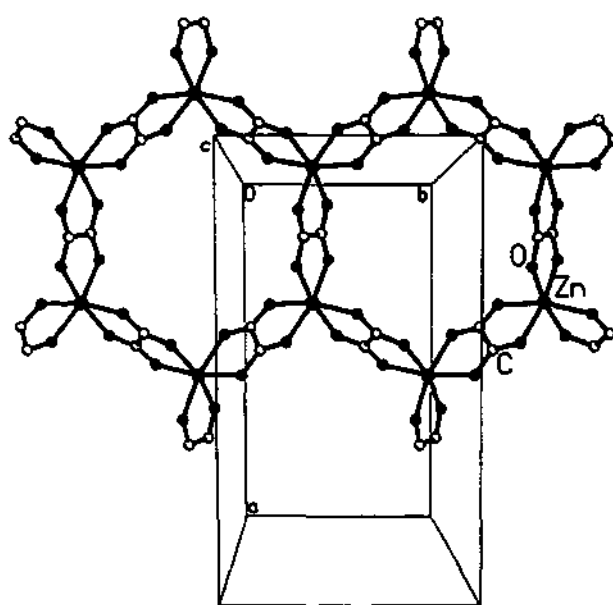


Fig. 4.20. The layer structure of VII, along the $[001]$ direction showing the honeycomb architecture. The amine molecules sit in the middle of the 12-membered aperture. The water molecules are not shown for clarity.

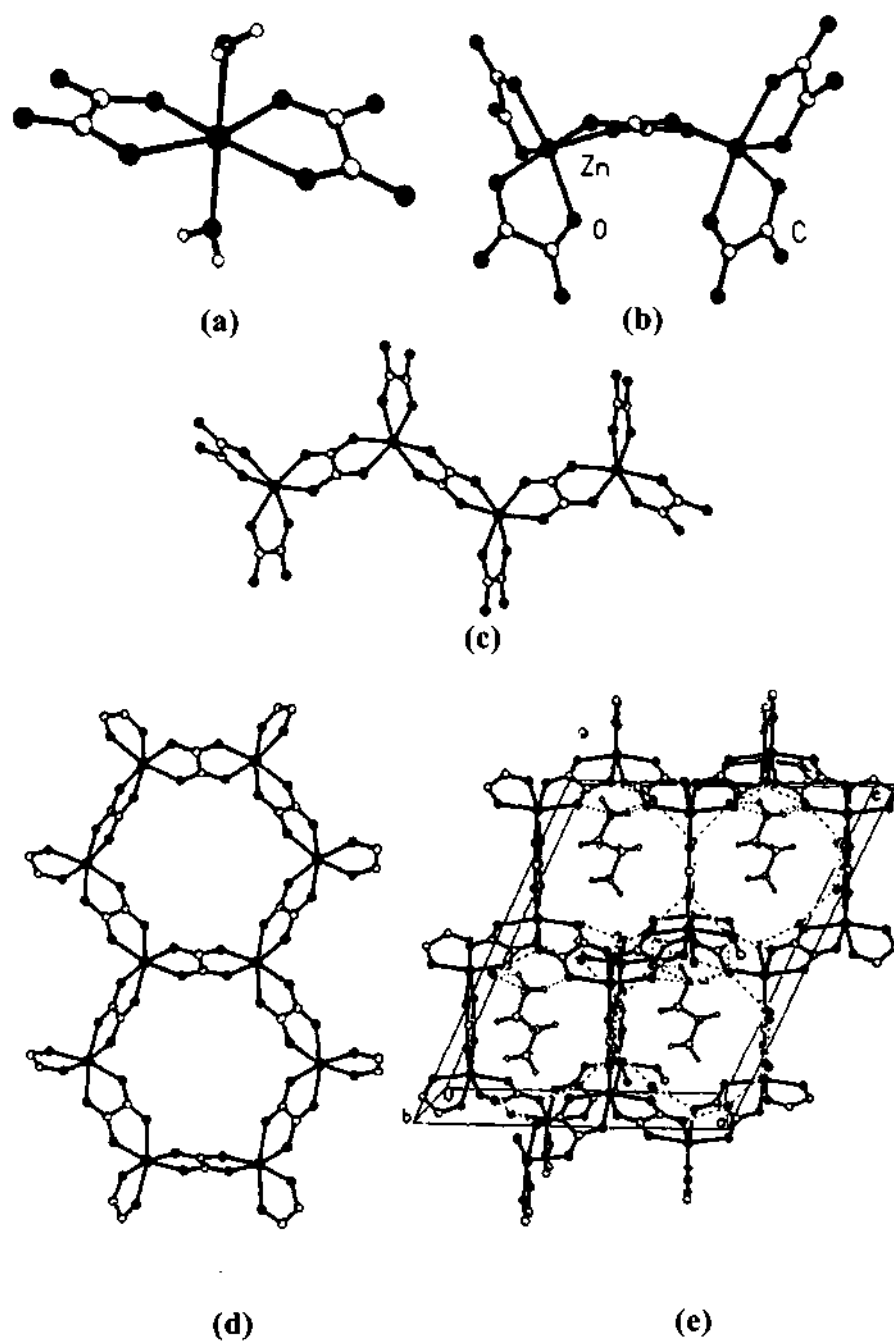


Fig. 4.21. Various types of Zn oxalate structures obtained in the present study: (a) monomer, (b) dimer, (c) one-dimensional chain, (d) two-dimensional layer and (e) three-dimensional structure. Note the close relationships amongst them.

using relatively mild conditions by the reaction of amine oxalates with Zn^{II} ions. Open-framework zinc phosphates are known to occur in four structure classes: monomers, chains, sheets and 3-D structures. In the present the oxalate analogues have been obtained for all these four structures, along with a dimer structure, which is unique to oxalates. It is possible that the zero-dimensional structures may readily transform to higher dimensional ones under hydrothermal reaction conditions, such a transformation from the zero-dimensional monomer to the linear chain structure has been shown schematically in Figure 4.22. The variety of structures obtained by the amine oxalate route suggests that it would be most worthwhile to investigate the reactions of various amine dicarboxylates with metal ions. The hierarchy of oxalates structures formed here also suggests that there is likely to be a building up principle in the formation of open-framework oxalates just as in the phosphates.^[33]

4.4. Open-framework cadmium oxalates

4.4.1. Results

$Na_4Cd_2(C_2O_4)_4 \cdot 4H_2O$ (VIII)

The asymmetric unit of **VIII** contains 35 non-hydrogen atoms (Fig. 4.23a), of which 26 belong to the framework. There are two crystallographically independent Cd atoms and five Na atoms. Of the five Na atoms, two [Na(1) and Na(4)] occupy special positions with a site occupancy of 0.5. All the Cd atoms occupy general positions. The framework structure of **VIII** is built-up by the linkages between the Cd and the oxalate units with each Cd bound to eight oxygens. The oxygens are bound to the carbon atoms forming the network structure. Conversely, the oxalate ions are connected to Cd atoms forming the architecture. The coordination environment around the cadmium is dodecahedral with respect to the oxygen atoms. The Cd – O distances in the range 2.302(4) – 2.489(4) Å (av. Cd(1) – O = 2.383 and Cd(2) – O = 2.405 Å). Of the eight oxygen atoms bound to each of the Cd

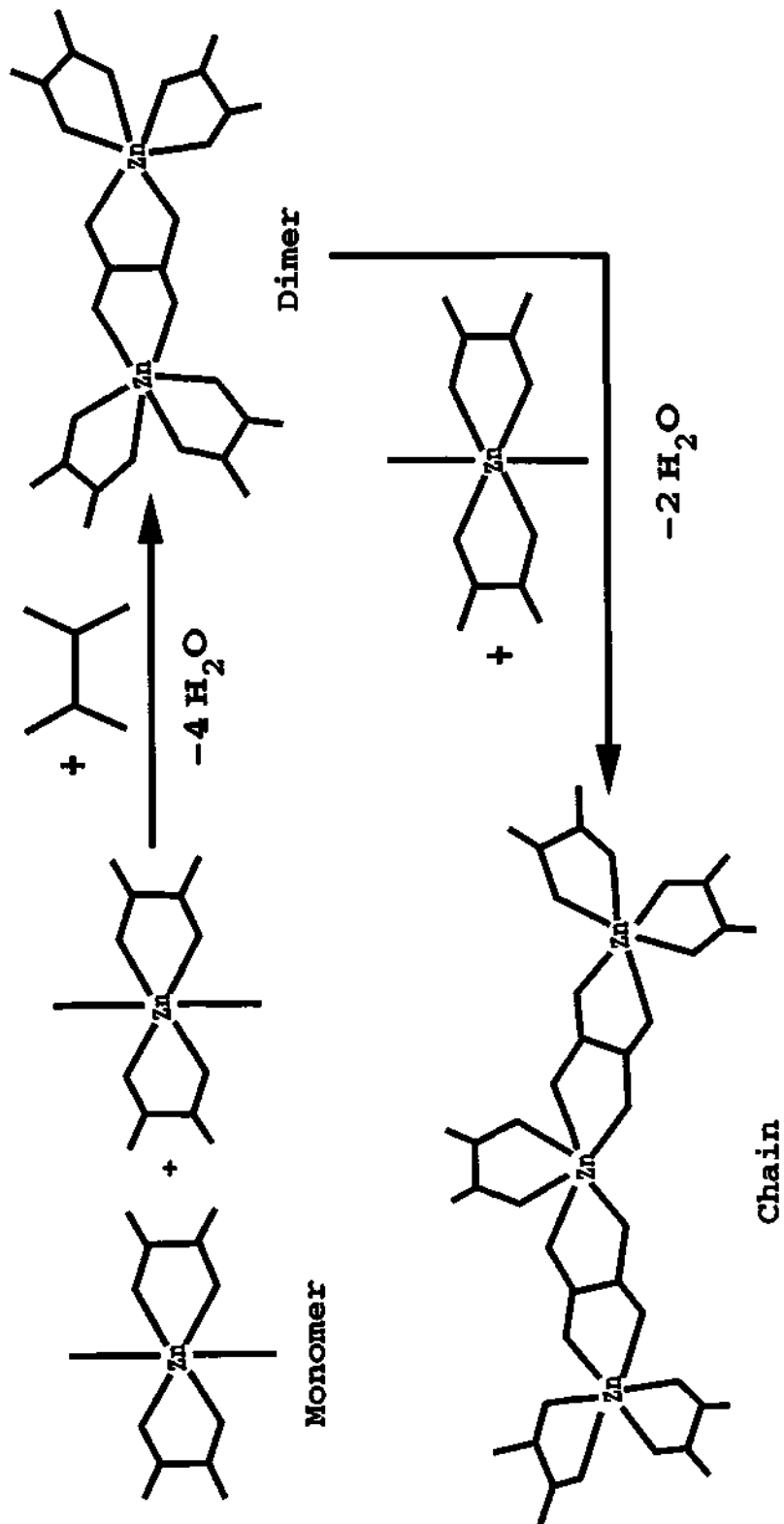


Fig. 4.22. Schematic showing the formation of chain architecture from the monomer via hydrolysis and condensation.

atoms, four are associated with Cd – O distances in the range 2.302(4) – 2.361(4) Å for Cd(1), 2.366(5) – 2.393(4) Å for Cd(2), and the other four with distances in the 2.390(4) – 2.489(4) Å for Cd(1), 2.405(5) – 2.446(4) Å for Cd(2) range. These are, in most cases, formally the single and double bonded oxygens bound to the carbon atoms, respectively. The variations in the distances are also reflected in the C – O bonding as well (Table 4.9). The O – Cd – O angles in the range 66.8(2) – 149.6(2)° (av. O – Cd(1) – O = 100.1° and O – Cd(2) – O = 100.2°) and the O – C – O bond angles are in the range 124.9(6) – 126.7(6)° (av. 125.7°) (Table 4.9). These geometrical parameters are in the range expected for this type of bonding and agree well with previously determined structures of the cadmium oxalates.^[34,35] Bond valence sum calculations^[21] indicated that the valence states of the various species forming the framework are Cd²⁺, C⁴⁺, O²⁻, as expected.

The framework structure of VIII is built up of linkages involving the Cd and the oxalate units. The structure can be understood in terms of simpler building units involving two-dimensional layers. Thus, of the four oxalate groups that connects one Cd atom, two have *in-plane* connectivity and the other two have *out-of-plane* connectivity. The *in-plane* connectivity between the oxalates and Cd atoms form a layer-like arrangement with 12-membered apertures (made of six cadmium and six oxalate units) of width 11.6 X 5.4 Å (longest O – O contact distances not including van der Waals radii). It is to be noted that, each adjacent layer is translated by half a unit-cell, and the *out-of-plane* oxalate group connects to the neighboring layer above and below. This type linkage creates inter-penetration between the layers and forms a three-dimensional structure with 8-membered channels (made of 4 cadmium and 4 oxalate units) of differing width along the *b* axis (Fig. 4.23b). The width of these channels is 4.6 x 7.0 Å and 5.1 x 7.6 Å

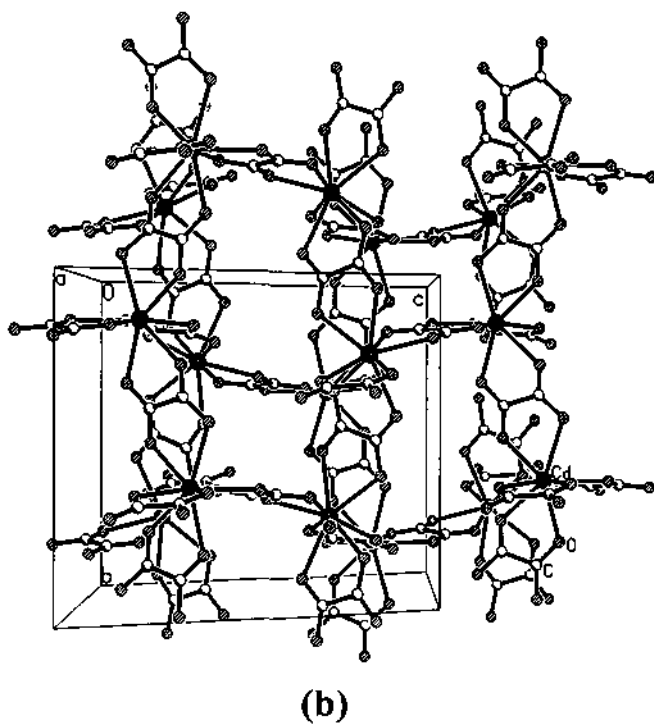
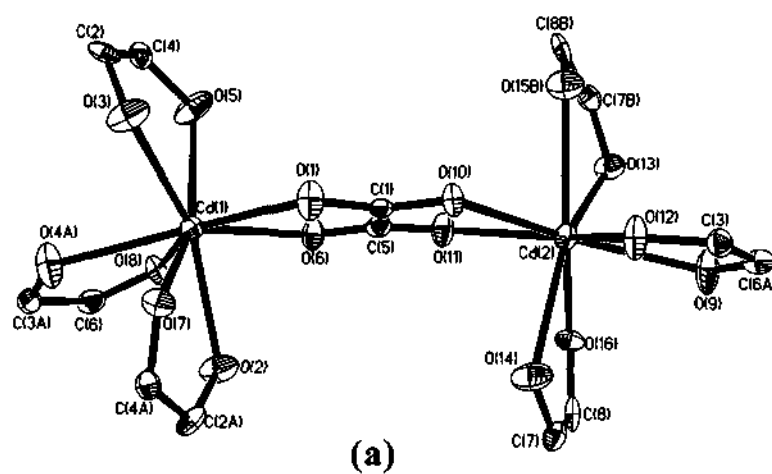


Fig. 4.23. (a) ORTEP plot of the framework of **VIII**, $\text{Na}_4\text{Cd}_2(\text{C}_2\text{O}_4)_4 \cdot 4\text{H}_2\text{O}$. Thermal ellipsoids are given at 50% probability. (b) Structure of **VIII** along the b axis showing the eight-membered channels. Na^+ ions and water molecules are omitted for clarity.

Table 4.9. Selected bond distances and angles for VIII, Na₄Cd₂(C₂O₄)₄·4H₂O

Moiety	Distance (Å)	Moiety	Distance (Å)
Cd(1)-O(1)	2.302(4)	C(6)-C(3)#1	1.547(9)
Cd(1)-O(3)	2.308(4)	C(7)-O(13)#6	1.260(8)
Cd(1)-O(2)	2.312(4)	C(7)-C(8)	1.562(9)
Cd(1)-O(4)#1	2.361(5)	Na(1)-O(5)	2.244(4)
Cd(1)-O(5)	2.390(5)	Na(1)-O(6)	2.383(4)
Cd(1)-O(6)	2.449(4)	Na(1)-O(8)	2.302(4)
Cd(1)-O(7)	2.454(4)	Na(1)-O(5)#8	2.244(5)
Cd(1)-O(8)	2.489(4)	Na(1)-O(8)#8	2.302(4)
Cd(2)-O(9)	2.366(5)	Na(1)-O(6)#8	2.383(4)
Cd(2)-O(11)	2.375(4)	Na(2)-O(13)	2.356(5)
Cd(2)-O(10)	2.383(4)	Na(2)#2-O(12)	2.366(5)
Cd(2)-O(12)	2.393(4)	Na(2)#2-O(10)	2.383(5)
Cd(2)-O(13)	2.405(5)	Na(2)-O(16)	2.509(5)
Cd(2)-O(14)	2.427(4)	Na(2)-O(12)#9	2.366(5)
Cd(2)-O(16)	2.444(4)	Na(2)-O(10)#9	2.383(5)
Cd(2)-O(15)#3	2.446(4)	Na(2)-O(300)	2.473(5)
O(4)-Cd(1)#5	2.361(5)	Na(2)-O(400)	2.487(6)
O(15)-Cd(2)#6	2.446(4)	Na(3)-O(2)	2.412(5)
O(1)-C(1)	1.252(8)	Na(3)-O(6)	2.457(5)
O(2)-C(2)#4	1.231(8)	Na(3)-O(8)	2.484(5)
O(3)-C(2)	1.263(8)	Na(3)#2-O(7)	2.609(5)
O(4)-C(3)	1.251(7)	Na(3)-O(100)	2.349(5)
O(5)-C(4)	1.252(8)	Na(3)-O(200)	2.354(5)
O(6)-C(5)	1.245(7)	Na(3)-O(7)#9	2.609(5)
O(7)-C(4)#4	1.239(7)	Na(4)-O(15)	2.320(5)
O(8)-C(6)	1.262(8)	Na(4)#3-O(10)	2.473(4)
O(9)-C(6)#5	1.251(7)	Na(4)-O(15)#10	2.320(5)
O(10)-C(1)	1.253(7)	Na(4)-O(10)#9	2.473(4)
O(11)-C(5)	1.244(8)	Na(4)-O(10)#6	2.473(4)
O(12)-C(3)	1.245(8)	Na(4)-O(300)	2.528(4)
O(13)-C(7)#3	1.260(8)	Na(4)-O(300)#10	2.528(4)
O(14)-C(7)	1.247(7)	Na(5)-O(16)	2.434(5)
O(15)-C(8)	1.241(8)	Na(5)-O(11)	2.358(5)
O(16)-C(8)	1.275(8)	Na(5)#2-O(1)	2.363(5)
C(1)-C(5)	1.563(9)	Na(5)-O(1)#9	2.363(5)

C(2)-O(2)#7	1.231(8)	Na(5)-O(7)#9	2.445(5)
C(2)-C(4)	1.567(9)	Na(5)-O(200)	2.538(6)
C(3)-C(6)#5	1.547(9)	Na(5)-O(400)	2.659(6)
C(4)-O(7)#7	1.239(7)	Na(5)#2-O(7)	2.445(5)
C(6)-O(9)#1	1.251(7)		

Moiety	Angle (°)	Moiety	Angle (°)
O(1)-Cd(1)-O(3)	84.9(2)	O(14)-Cd(2)-O(16)	68.10(14)
O(1)-Cd(1)-O(2)	94.1(2)	O(9)-Cd(2)-O(15)#2	104.5(2)
O(3)-Cd(1)-O(2)	148.8(2)	O(11)-Cd(2)-O(15)#2	89.7(2)
O(1)-Cd(1)-O(4)#1	149.6(2)	O(10)-Cd(2)-O(15)#2	71.1(2)
O(3)-Cd(1)-O(4)#1	79.2(2)	O(12)-Cd(2)-O(15)#2	84.3(2)
O(2)-Cd(1)-O(4)#1	86.7(2)	O(13)-Cd(2)-O(15)#2	66.8(2)
O(1)-Cd(1)-O(5)	98.0(2)	O(14)-Cd(2)-O(15)#2	147.2(2)
O(3)-Cd(1)-O(5)	69.1(2)	O(16)-Cd(2)-O(15)#2	143.3(2)
O(2)-Cd(1)-O(5)	141.4(2)	C(1)-O(1)-Cd(1)	120.5(4)
O(4)#1-Cd(1)-O(5)	100.2(2)	C(2)#3-O(2)-Cd(1)	116.8(4)
O(1)-Cd(1)-O(6)	69.3(2)	C(2)-O(3)-Cd(1)	118.4(4)
O(3)-Cd(1)-O(6)	131.4(2)	C(3)-O(4)-Cd(1)#4	120.1(4)
O(2)-Cd(1)-O(6)	75.8(2)	C(4)-O(5)-Cd(1)	114.1(4)
O(4)#1-Cd(1)-O(6)	139.4(2)	C(5)-O(6)-Cd(1)	115.4(4)
O(5)-Cd(1)-O(6)	74.5(2)	C(4)#3-O(7)-Cd(1)	110.4(4)
O(1)-Cd(1)-O(7)	75.3(2)	C(6)-O(8)-Cd(1)	115.2(4)
O(3)-Cd(1)-O(7)	79.1(2)	C(6)#4-O(9)-Cd(2)	117.5(4)
O(2)-Cd(1)-O(7)	70.6(2)	C(1)-O(10)-Cd(2)	116.7(4)
O(4)#1-Cd(1)-O(7)	76.4(2)	C(5)-O(11)-Cd(2)	118.1(4)
O(5)-Cd(1)-O(7)	148.0(2)	C(3)-O(12)-Cd(2)	117.2(4)
O(6)-Cd(1)-O(7)	128.5(2)	C(7)#2-O(13)-Cd(2)	117.5(4)
O(1)-Cd(1)-O(8)	141.2(2)	C(7)-O(14)-Cd(2)	116.1(4)
O(3)-Cd(1)-O(8)	125.3(2)	C(8)-O(15)-Cd(2)#5	115.7(4)
O(2)-Cd(1)-O(8)	72.3(2)	C(8)-O(16)-Cd(2)	116.2(4)
O(4)#1-Cd(1)-O(8)	67.7(2)	O(1)-C(1)-O(10)	125.3(6)
O(5)-Cd(1)-O(8)	75.3(2)	O(1)-C(1)-C(5)	116.8(6)
O(6)-Cd(1)-O(8)	72.09(14)	O(10)-C(1)-C(5)	117.9(6)
O(7)-Cd(1)-O(8)	129.04(14)	O(2)#6-C(2)-O(3)	126.0(6)
O(9)-Cd(2)-O(11)	146.3(2)	O(2)#6-C(2)-C(4)	118.5(6)
O(9)-Cd(2)-O(10)	144.3(2)	O(3)-C(2)-C(4)	115.4(6)
O(11)-Cd(2)-O(10)	69.10(14)	O(12)-C(3)-O(4)	125.7(6)

O(9)-Cd(2)-O(12)	68.8(2)	O(12)-C(3)-C(6)#4	117.1(6)
O(11)-Cd(2)-O(12)	144.1(2)	O(4)-C(3)-C(6)#4	117.1(6)
O(10)-Cd(2)-O(12)	75.5(2)	O(7)#6-C(4)-O(5)	125.2(6)
O(9)-Cd(2)-O(13)	75.9(2)	O(7)#6-C(4)-C(2)	118.7(6)
O(11)-Cd(2)-O(13)	82.3(2)	O(5)-C(4)-C(2)	116.1(6)
O(10)-Cd(2)-O(13)	128.5(2)	O(11)-C(5)-O(6)	126.3(6)
O(12)-Cd(2)-O(13)	126.4(2)	O(11)-C(5)-C(1)	116.2(6)
O(9)-Cd(2)-O(14)	91.2(2)	O(6)-C(5)-C(1)	117.5(6)
O(11)-Cd(2)-O(14)	92.8(2)	O(9)#1-C(6)-O(8)	124.9(6)
O(10)-Cd(2)-O(14)	79.3(2)	O(9)#1-C(6)-C(3)#1	117.4(6)
O(12)-Cd(2)-O(14)	74.6(2)	O(8)-C(6)-C(3)#1	117.7(6)
O(13)-Cd(2)-O(14)	146.0(2)	O(14)-C(7)-O(13)#5	125.7(6)
O(9)-Cd(2)-O(16)	75.6(2)	O(14)-C(7)-C(8)	118.5(6)
O(11)-Cd(2)-O(16)	75.0(2)	O(13)#5-C(7)-C(8)	115.8(6)
O(10)-Cd(2)-O(16)	129.6(2)	O(15)-C(8)-O(16)	126.7(6)
O(12)-Cd(2)-O(16)	127.0(2)	O(15)-C(8)-C(7)	116.7(6)
O(13)-Cd(2)-O(16)	78.1(2)	O(16)-C(8)-C(7)	116.5(6)

Symmetry transformations used to generate equivalent atoms:

#1 $x-1/2, -y+1/2, z+1/2$; #2 $x+1/2, -y+1/2, z+1/2$; #3 $-x-3/2, y+1/2, -z-7/2$; #4 $-x-3/2, y-1/2, -z-5/2$; #5 $x+1/2, -y+1/2, z-1/2$; #6 $-x-3/2, y-1/2, -z-7/2$; #7 $-x-3/2, y+1/2, -z-5/2$; #8 $-x-2, -y+1, -z-3$; #9 $x-1/2, -y+1/2, z-1/2$; #10 $-x-2, -y, -z-4$

(shortest oxygen-oxygen contact distance not including the van der Waals radii).

The Na atoms along with water molecule occupy these channels.

Impedance measurements off a sample of VIII gave typical complex plane plots with a rather broad arc at high frequencies at 298K. Lower frequency effects can be seen in the form of an inclined spike at higher temperatures (say 398K). Plots of the imaginary part of the impedance, Z'' , and the electric modulus, M'' , against log frequency, showed single peaks with an associated capacitance values of ~ 12.4 pF and 20 pF respectively for M'' and Z'' . An Arrhenius plot of the conductivity of the pellet gave a low value of the energy of activation, although the conductivities are small, in the $10^{-8} - 10^{-9} \text{ Scm}^{-1}$ range (Figure 4.24).

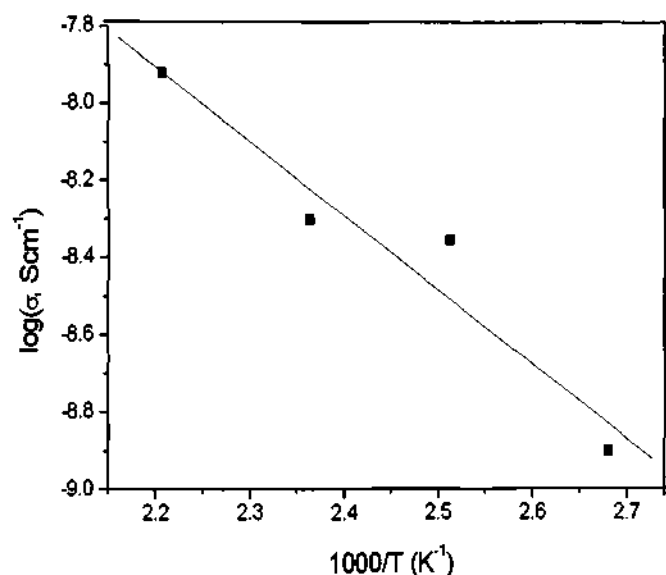


Fig. 4.24. Arrhenius plot of the overall pellet conductivity for I

$\text{K}_2\text{Cd}(\text{C}_2\text{O}_4)_2 \cdot 2\text{H}_2\text{O}$ (IX)

The asymmetric unit of $\text{K}_2\text{Cd}(\text{C}_2\text{O}_4)_2 \cdot 2\text{H}_2\text{O}$, IX, is shown in Figure 4.25a. There are eight oxygen atoms that surround the cadmium forming a dodecahedron (Fig. 4.25b). The Cd – O distances in the range 2.379(4) – 2.457(4) Å (av. Cd – O = 2.406 Å). Of the eight oxygen atoms bound to each of the Cd atoms, four have Cd – O distances in the range 2.379(4) – 2.384(4) Å and the other four in 2.404(4) – 2.457(4) Å (Table 4.10). The O – Cd – O angles are in the range 67.4(4) – 158.1(2)° (av. O – Cd(1) – O = 100.2°) and the average O – C – O bond angle is 125.5° (Table 4.10).

The framework structure of IX is built-up from linkages involving the oxalates and the Cd atoms. As in VIII, two oxalates link-up with the Cd atoms in an *in-plane* manner to give rise to a layer with 12-membered aperture and the remaining two oxalates connects these layers in an *out-of-plane* fashion forming 8-membered channels as shown in Figure 4.26. The channels in IX are uniform and

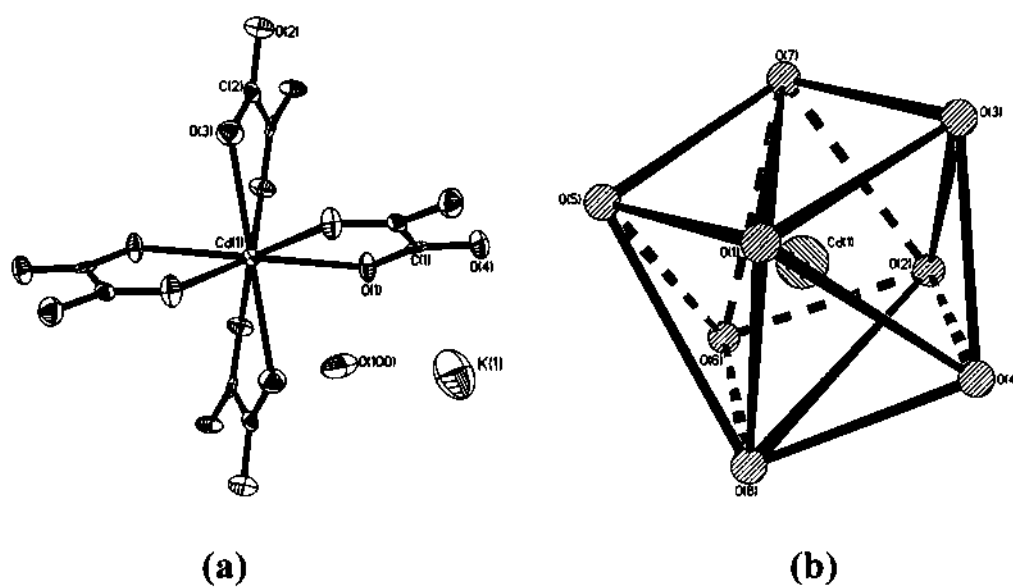


Fig. 4.25. (a) ORTEP plot of IX, $\text{K}_2\text{Cd}(\text{C}_2\text{O}_4)_2 \cdot 2\text{H}_2\text{O}$. Thermal ellipsoids are given at 50% probability. (b) The coordination environment around Cd atoms. Note the oxygens form a dodecahedral arrangement.

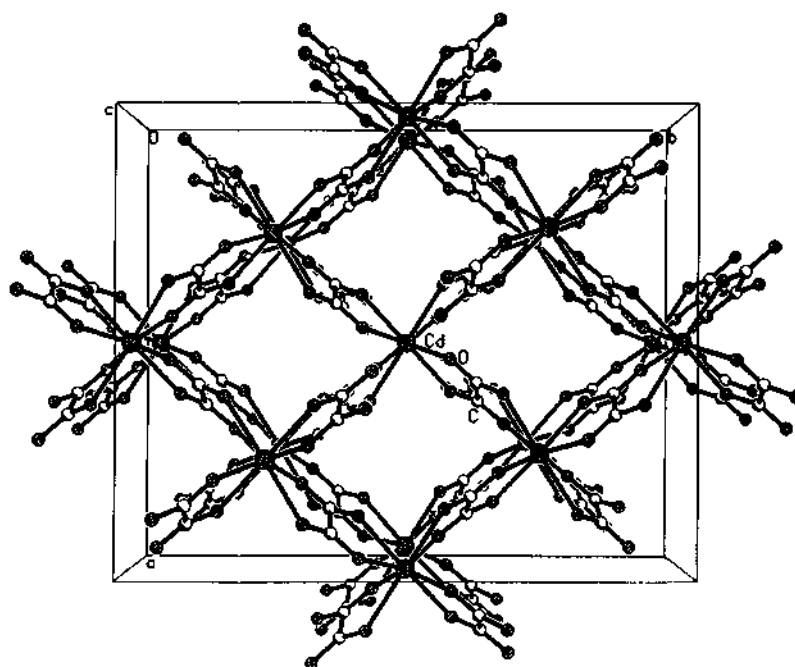


Fig. 4.26. Structure of IX along the c axis showing the uniform 8-membered channels.

Table 4.10. Selected bond distances in IX, $K_2Cd(C_2O_4)_2 \cdot 2H_2O$

Moiety	Distance (Å)	Moiety	Distance (Å)
Cd(1)-O(1)#1	2.379(4)	K(1)-O(100)	2.710(5)
Cd(1)-O(1)	2.379(4)	K(1)-O(1)	2.713(4)
Cd(1)-O(2)#2	2.384(4)	K(1)-O(4)#4	2.822(4)
Cd(1)-O(2)#3	2.384(4)	K(1)-O(4)#5	2.838(4)
Cd(1)-O(3)	2.404(4)	K(1)-O(3)#6	2.863(4)
Cd(1)-O(3)#1	2.404(4)	K(1)-O(2)#6	2.889(4)
Cd(1)-O(4)#4	2.457(4)	K(1)-O(2)#7	3.225(4)
Cd(1)-O(4)#5	2.457(4)	K(1)-O(100)#8	3.258(5)
C(1)-O(4)	1.246(6)	K(1)#9-O(2)	2.889(4)
C(1)-O(1)	1.268(6)	K(1)#10-O(2)	3.225(4)
C(1)-C(2)#3	1.557(7)	K(1)#9-O(3)	2.863(4)
C(2)-O(2)	1.233(6)	K(1)#8-O(4)	2.822(4)
C(2)-O(3)	1.257(6)	K(1)#3-O(4)	2.838(4)
C(2)-C(1)#5	1.557(7)	K(1)#4-O(100)	3.258(5)
Moiety	Angle (°)	Moiety	Angle (°)
O(1)#1-Cd(1)-O(1)	148.4(2)	O(3)-Cd(1)-O(4)#4	133.93(12)
O(1)#1-Cd(1)-O(2)#2	69.27(13)	O(3)#1-Cd(1)-O(4)#4	67.44(13)
O(1)-Cd(1)-O(2)#2	139.88(13)	O(1)#1-Cd(1)-O(4)#5	79.42(13)
O(1)#1-Cd(1)-O(2)#3	139.87(13)	O(1)-Cd(1)-O(4)#5	74.94(12)
O(1)-Cd(1)-O(2)#3	69.27(13)	O(2)#2-Cd(1)-O(4)#5	144.48(12)
O(2)#2-Cd(1)-O(2)#3	82.0(2)	O(2)#3-Cd(1)-O(4)#5	114.59(12)
O(1)#1-Cd(1)-O(3)	79.00(13)	O(3)-Cd(1)-O(4)#5	67.44(13)
O(1)-Cd(1)-O(3)	107.12(12)	O(3)#1-Cd(1)-O(4)#5	133.93(12)
O(2)#2-Cd(1)-O(3)	89.91(13)	O(4)#4-Cd(1)-O(4)#5	70.8(2)
O(2)#3-Cd(1)-O(3)	73.40(13)	O(4)-C(1)-O(1)	125.8(5)
O(1)#1-Cd(1)-O(3)#1	107.12(12)	O(4)-C(1)-C(2)#3	118.2(4)
O(1)-Cd(1)-O(3)#1	79.00(13)	O(1)-C(1)-C(2)#3	116.0(4)
O(2)#2-Cd(1)-O(3)#1	73.40(13)	O(2)-C(2)-O(3)	125.2(5)
O(2)#3-Cd(1)-O(3)#1	89.91(13)	O(2)-C(2)-C(1)#5	118.7(4)
O(3)-Cd(1)-O(3)#1	158.1(2)	O(3)-C(2)-C(1)#5	116.1(4)
O(1)#1-Cd(1)-O(4)#4	74.94(12)	C(1)-O(1)-Cd(1)	118.0(3)
O(1)-Cd(1)-O(4)#4	79.42(13)	C(2)-O(2)-Cd(1)#5	117.7(4)

Symmetry transformations used to generate equivalent atoms: ·

#1 -x, -y, z #2 -x-1/4, y-1/4, z+1/4 #3 x+1/4, -y+1/4, z+1/4 #4 -x+1/4, y-1/4, z-1/4
 #5 x-1/4, -y+1/4, z-1/4 #6 x+1/4, -y+1/4, z-3/4 #7 x+1/2, y, z-1/2 #8 -x+1/4, y+1/4, z+1/4
 #9 x-1/4, -y+1/4, z+3/4 #10 x-1/2, y, z+1/2

have width of 5.6 X 5.8 Å. The K⁺ and water molecules occupy these channels.

$\text{Cd}_2(\text{C}_2\text{O}_4)_{0.5}\text{Cl}_3\text{NaCl}\cdot 4\text{H}_2\text{O}$, X

The asymmetric unit of X consists of two crystallographically distinct octahedrally coordinated Cd atoms. Whilst Cd(1) is linked by three chlorine atoms, two oxalate oxygens and one bonded water molecule, Cd(2) is connected by six chlorine atoms. The average Cd(1)-O/Cl and Cd(2)-Cl distances are 2.459 Å and 2.631 Å, respectively (Table 4.11). The framework structure of X is formed by linkages involving Cd(1)O₃Cl₃, Cd(2)Cl₆ and oxalate units. The Cd(2) atoms are connected to each other *via* chlorine bridges giving rise to infinite one-dimensional chains and the Cd(1) atoms are connected to these chains *via* -μ₂(Cl)- and -μ₃(Cl)- types of chlorine bridges (Fig. 4.27). These one-dimensional building units are cross-linked by oxalate units giving rise to a layered architecture (Fig. 4.28).

Adjacent layers are shifted by ½ the unit cell length along the [1 0 1] direction, giving rise to ABAB... type layer stacking. Extra-framework Na⁺ ions occupy spaces in the interlamellar regions along with water molecules (Fig. 4.29). The environment around the Na⁺ ion in X can be considered to be octahedral with five water molecules (av. Na-O = 2.411 Å) and a chlorine which is also attached to two Cd atoms. The Na-Cl distance is 2.999 Å, slightly longer than the distance in bulk NaCl (2.814 Å). Selected bond distances and angles in X are presented in Table 4.11.

IR spectra (KBr pellet) of X showed characteristic features of the dicarboxylate units.^[26] The various bands are: ν_{as}(C=O) at 1646(s) cm⁻¹ and ν_s(C=O) at 1417(w) cm⁻¹; ν_s(C-O) + δ(O-C=O) at 1312(s) cm⁻¹; δ(O-C=O) + ν(MO) at 790(m) cm⁻¹; ν(MO) + ν(C-C) at 516(m) cm⁻¹; ν(MO) + ring def. at 438(w) cm⁻¹. A broad band appears in the 3550-3300 cm⁻¹ region due to the presence of water molecules.

Table 4.11. Selected bond distances and bond angles for $\text{Cd}_2(\text{C}_2\text{O}_4)_{0.5}\text{Cl}_3\text{NaCl}\cdot 4\text{H}_2\text{O}$, X

Moiety	Distance (Å)	Moiety	Distance (Å)
Cd(1)-O(1)#1	2.292(3)	Cd(2)-Cl(3)#3	2.6756(11)
Cd(1)-O(2)	2.304(3)	Na(1)-O(300)	2.322(5)
Cd(1)-O(10)	2.357(4)	Na(1)-O(100)	2.358(4)
Cd(1)-Cl(1)	2.5303(11)	Na(1)-O(200)	2.382(4)
Cd(1)-Cl(2)	2.5404(11)	Na(1)-O(200)#2	2.421(4)
Cd(1)-Cl(3)	2.7284(10)	Na(1)-O(10)	2.571(4)
Cd(2)-Cl(4)	2.5839(11)	Na(1)-Cl(2)	2.999(2)
Cd(2)-Cl(4)#2	2.5908(11)	C(1)-O(2)	1.249(5)
Cd(2)-Cl(1)#3	2.6199(11)	C(1)-O(1)	1.253(5)
Cd(2)-Cl(2)	2.6479(11)	C(1)-C(1)#1	1.569(8)
Cd(2)-Cl(3)	2.6690(11)		
Moiety	Angle (°)	Moiety	Angle (°)
O(1)#1-Cd(1)-O(2)	72.41(10)	Cl(4)-Cd(2)-Cl(2)	91.02(4)
O(1)#1-Cd(1)-O(10)	88.43(14)	Cl(4)#2-Cd(2)-Cl(2)	92.43(3)
O(2)-Cd(1)-O(10)	93.11(12)	Cl(1)#3-Cd(2)-Cl(2)	176.38(4)
O(1)#1-Cd(1)-Cl(1)	165.68(8)	Cl(4)-Cd(2)-Cl(3)	94.38(3)
O(2)-Cd(1)-Cl(1)	93.93(8)	Cl(4)#2-Cd(2)-Cl(3)	174.67(3)
O(10)-Cd(1)-Cl(1)	96.80(12)	Cl(1)#3-Cd(2)-Cl(3)	90.51(3)
O(1)#1-Cd(1)-Cl(2)	95.39(8)	Cl(2)-Cd(2)-Cl(3)	86.33(3)
O(2)-Cd(1)-Cl(2)	167.08(8)	Cl(4)-Cd(2)-Cl(3)#3	177.46(3)
O(10)-Cd(1)-Cl(2)	90.73(10)	Cl(4)#2-Cd(2)-Cl(3)#3	91.27(3)
Cl(1)-Cd(1)-Cl(2)	97.86(4)	Cl(1)#3-Cd(2)-Cl(3)#3	87.55(3)
O(1)#1-Cd(1)-Cl(3)	86.99(8)	Cl(2)-Cd(2)-Cl(3)#3	90.35(3)
O(2)-Cd(1)-Cl(3)	87.86(8)	Cl(3)-Cd(2)-Cl(3)#3	83.57(3)
O(10)-Cd(1)-Cl(3)	174.79(11)	C(1)-O(1)-Cd(1)#1	116.8(3)
Cl(1)-Cd(1)-Cl(3)	88.24(3)	C(1)-O(2)-Cd(1)	116.3(3)
Cl(2)-Cd(1)-Cl(3)	87.24(3)	O(2)-C(1)-O(1)	125.5(4)
Cl(4)-Cd(2)-Cl(4)#2	90.82(3)	O(2)-C(1)-C(1)#1	117.5(4)
Cl(4)-Cd(2)-Cl(1)#3	90.98(3)	O(1)-C(1)-C(1)#1	117.0(4)

Symmetry transformations used to generate equivalent atoms:

#1 -x+1,y,-z+1/2 #2 -x+1,-y+1,-z #3 x,-y+1,z+1/2

#4 -x+1/2,-y+1/2,-z

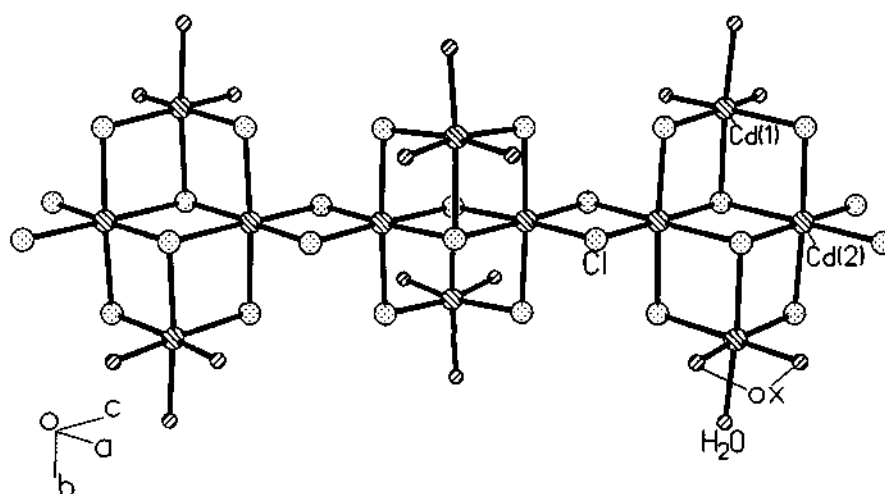


Fig. 4.27. Structure of $\text{Cd}_2(\text{C}_2\text{O}_4)_{0.5}\text{Cl}_3\text{NaCl}\cdot 4\text{H}_2\text{O}$, **X**, showing the one-dimensional cadmium chloro double chain. Note the presence of infinite $-(\mu_2\text{Cl})-$ and $-(\mu_3\text{Cl})-$ bridges.

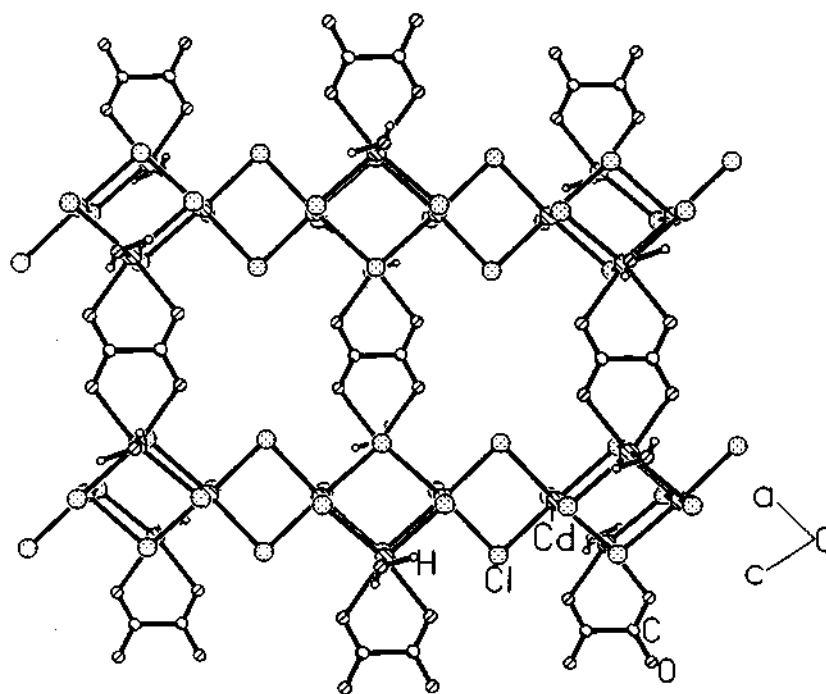


Fig. 4.28. Structure of **X**, showing the two-dimensional cadmium chloro-oxalate layer lying in the *ac*-plane.

TGA studies of **X** indicate two distinct mass losses. A gradual mass loss in the range 100-300 °C (obsd. 14.3%) due to the loss of four water molecules (14.2%). The second mass loss of 15.7% in the range of 350-450 °C is due to the loss of the oxalate moiety (calcd.17.4%). Above 500 °C, a gradual loss was observed due to the slow evaporation of the Cd compound.

4.4.2. Discussion

Two new cadmium oxalates, $\text{Na}_4\text{Cd}_2(\text{C}_2\text{O}_4)_4 \cdot 4\text{H}_2\text{O}$, **VIII**, and $\text{K}_2\text{Cd}(\text{C}_2\text{O}_4)_2 \cdot 2\text{H}_2\text{O}$, **IX**, have been synthesized hydrothermally and their structures determined by single crystal methods. **VIII** and **IX**, along with the recently described cadmium oxalate, $\text{K}[\text{C}_3\text{N}_2\text{H}_5][\text{Cd}(\text{C}_2\text{O}_4)_2]$,^[35] forms a series of compounds in a family of three-dimensional oxalates possessing channels. Though, **VIII** and **IX** have been prepared under similar conditions, subtle differences exist between the two. Thus, **IX** has been synthesized in the presence of additional amine, while **VIII** was synthesized in absence of any added amine in the synthesis mixture. The exact role of the amine molecule during the synthesis of **IX** is not yet clear, the absence of which forms a condensed phase. Glacial acetic acid in the reaction mixture probably controls the pH during the reaction. Such pH control by the acetate anions has been effected in many metal substituted aluminum phosphates (MeAlPOs).^[36] It is to be noted that both **VIII** and **IX** have similar linkages involving Cd and oxalate units, but the connectivity between Cd and oxalate units create distinct differences between the two structures. While **VIII** is formed with channels of differing dimensionalities, **IX** has uniform channels (Fig. 4.27). In both the cases, the charge compensating alkali ions along with water molecules occupy these channels.

Structures of **VIII** and **IX** along with the coordination environment of Cd

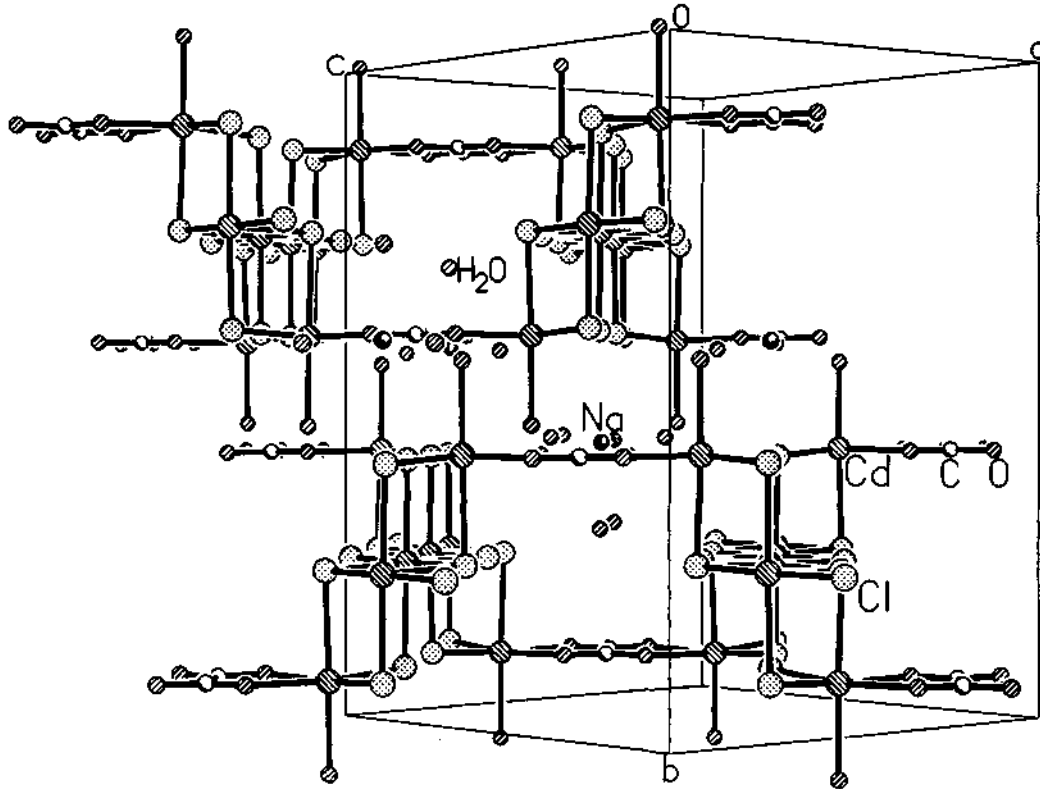
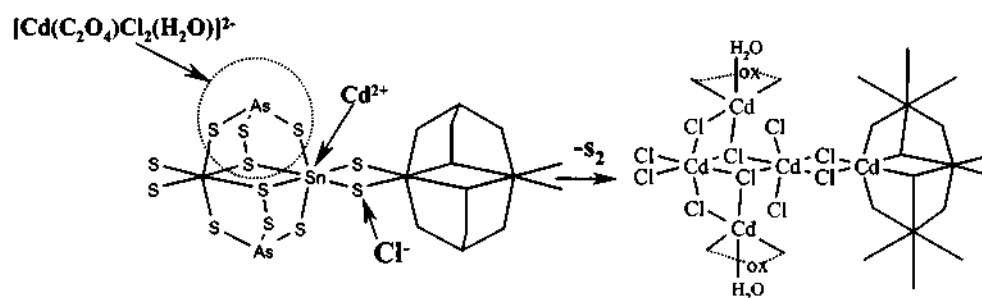


Fig. 4.29. Figure shows the stacking of the cadmium chloro-oxalate layers in X. Note that the adjacent layers are shifted by $\frac{1}{2}$ the unit cell along the $[1\ 0\ 1]$ direction. Note the presence of extra-framework Na^+ ions and water molecules in the interlamellar spaces.

merits discussion. In VIII and IX, the Cd atoms are eight-coordinated with respect to the oxygen atoms resulting in a dodecahedral arrangement (see Fig. 4.26b), unlike in the layered cadmium oxalate reported earlier, $\text{CdC}_2\text{O}_4 \cdot 3\text{H}_2\text{O}$ (15), where the Cd was only seven-coordinated. Amongst the layered oxalates, the honeycomb architecture appears to be more common, especially among the mixed-metal transition metal oxalates.^[27,28] The central metal atom in these compounds is predominantly six-coordinated with respect to the nearest neighbors (oxygen atoms). The higher coordination of the metal atom appears to favor the formation and stabilization of the three-dimensional structures, especially in the case of the cadmium oxalates. While the seven-coordination of the cadmium gives rise to the layered structure,^[34] the eight-coordinated cadmium gives rise to the three-dimensional architecture.^[35] In VIII and IX, Cd is eight coordinated forming three-dimensional structures with channels. The oxalate units perform the dual role – that of linking the cadmium within the layer and with the neighboring ones by *in-plane* and *out-of-plane* connections. Such a connectivity also gives rise to the three-dimensional architecture in the zinc oxalate, $2[\text{C}_3\text{H}_7\text{NH}_3][\text{Zn}_2(\text{C}_2\text{O}_4)_3]$, II.

The two-dimensional structure of X, has certain interesting features. The one-dimensional CdCl_2 chain in X is similar to the double-chain in ABX_3 .^[37] The structure of X can therefore be considered as originating from CdCl_2 , which under the non-aqueous conditions employed for the synthesis, can give rise to NaCdCl_3 chains. Cross-linking of the cadmium-chloro chains by the oxalate units would then yield the layer present in X, the process being somewhat similar to the assembly of molecular metal clusters by organic linkers described by Yaghi and co-workers.^[38] The cadmium chloride chains in X are related also to the infinite one dimensional chains formed by the pyramidal $\beta\text{-}[\text{AsS}_4]^{3-}$ units observed in the potassium tin

thioarsenide compound, KSnAsS_5 .^[39] One can visualize the structure of X to be arising from the replacement of the $[\text{AsS}_4]^{3-}$ units by $[\text{Cd}(\text{C}_2\text{O}_4)\text{Cl}_2(\text{H}_2\text{O})]^{2-}$ units and simultaneously replacing the Sn^{4+} by Cd^{2+} units, as represented schematically below:



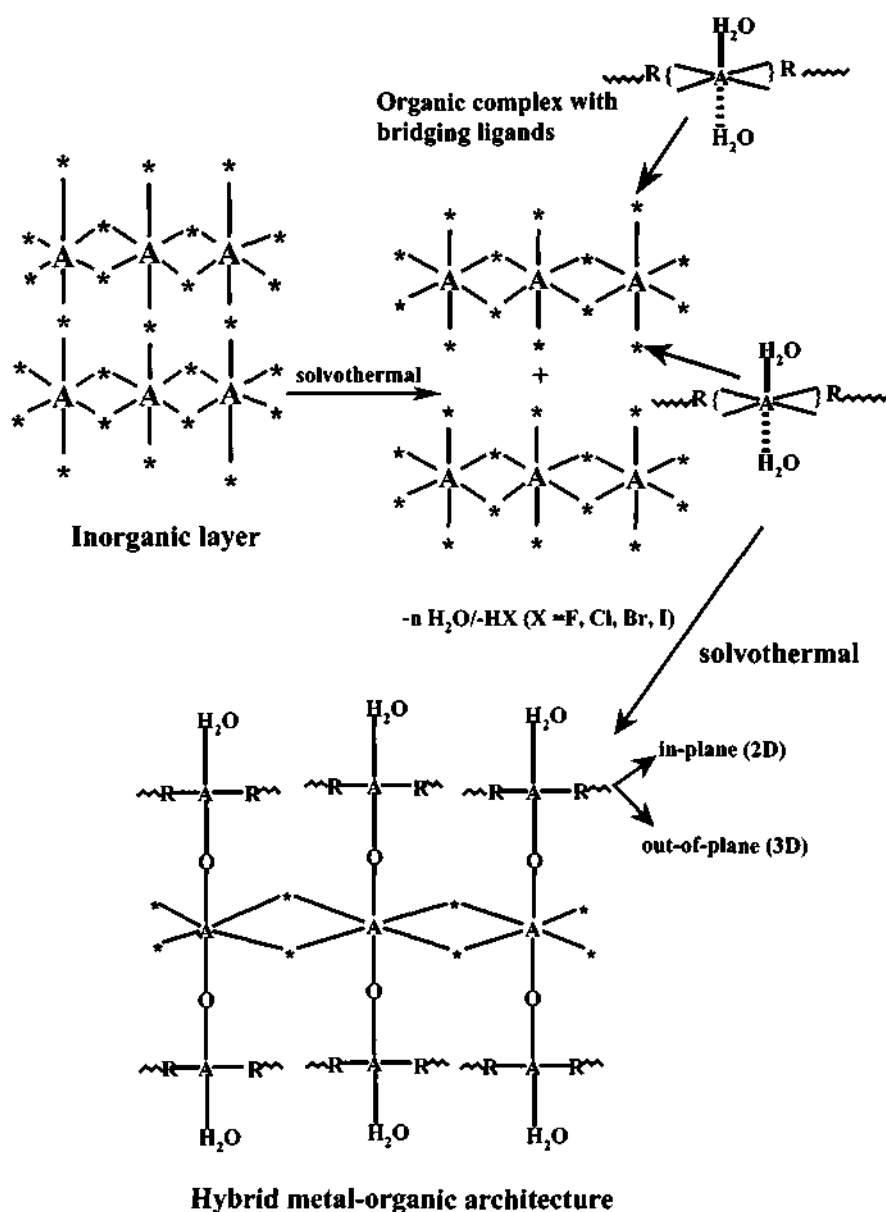
The above schematic suggests a new strategy i.e. for designing hybrid metal-organic frameworks, wherein one inorganic anion is replaced by another anion possessing an organic ligand as part of it, which in turn facilitates the extension of the structure into higher dimensions.

A more general schematic representing this notion to illustrate the building up of three-dimensional hybrid metal-organic frameworks by aligning the lower-dimensional structures of metal halides and metal hydroxides by the introduction of metal complexes with organic ligands (dicarboxylate, bipyridyl, nicotinate etc.) capable of bridging the lower dimensional inorganic structures is presented in Scheme 4.1. Depending on the mode of linking of the organic linkers, the hybrid metal-organic structures can either be two or three-dimensional. The possibility that the lower-dimensional structures can be generated by the partial disintegration of the higher dimensional parent structure under suitable reaction conditions is also indicated in Scheme 4.1. This possibility can be realized by observing the close structural relationships among some of the well-known lower-dimensional inorganic structures shown in Scheme 4.2. A similar notion has been proposed by Powell et

al.,^[40-42] to describe the possible building of the cobalt squarate framework from the parent cobalt hydroxide with a brucite structure. Notably, the structural relationship between the Cd(OH)Cl and Cu(OH)Cl to brucite has been noted recently.^[43]

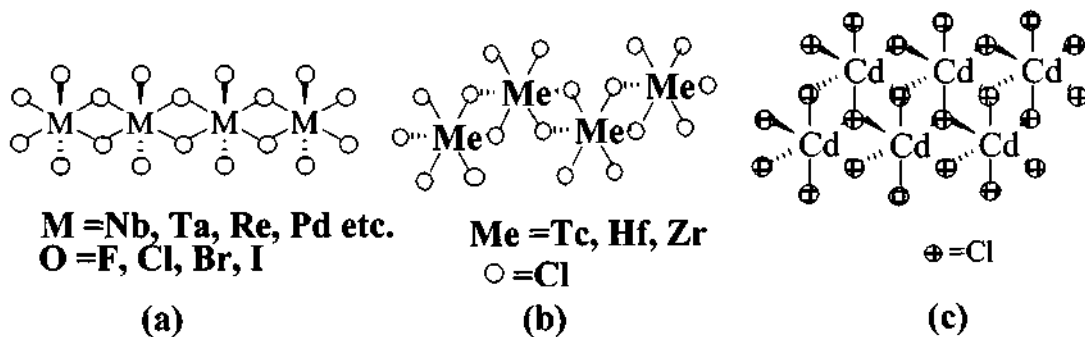
It is likely that many such hybrid metal-organic structures with open-architectures can be made by employing other different organic linkers. In this context, we should draw attention to a new three-dimensional, open-framework, neutral and anhydrous cadmium chloro compound, [CdCl₂(C₄H₈N₂)], XXXV,^[44] synthesized using solvothermal route by us, wherein the amine performs the role of linking the one-dimensional cadmium chloro chains into three-dimensions (Fig. 4.30). Interestingly, in XXXV, the channels are hydrophobic and empty. Assembling such predetermined polymeric units *via* organic pillars or linkers provides an interesting methodology to combining dimensionality of the electronic exchange pathways and the open-frameworks.^[45]

Investigations in the course of the present study have shown that large number of oxalates of Zn of varying dimensions can be synthesized under appropriate conditions, however, those of cadmium are much less studied. The present results indicate that it is possible to prepare three-dimensional cadmium oxalates by employing hydrothermal methods, with a careful choice of the reactants. The arrangement of the extra-framework Na⁺ cations gives rise to certain noteworthy features. The octahedrally coordinated sodium shares an edge with neighboring NaO₅Cl octahedra *via* bridging water molecules, forming a Na₂O₈Cl₂ dimer. These dimers are oriented in such a manner as to form strong O(w)-H...O(w) hydrogen bonds (O(w) = water oxygen) with the adjacent dimer, giving rise to a hydrogen bond stabilized one-dimensional ladder (Fig. 4.31). Such low-dimensional structures formed by the guest species, involving weak interactions contribute to the overall stability of these structures.^[10]

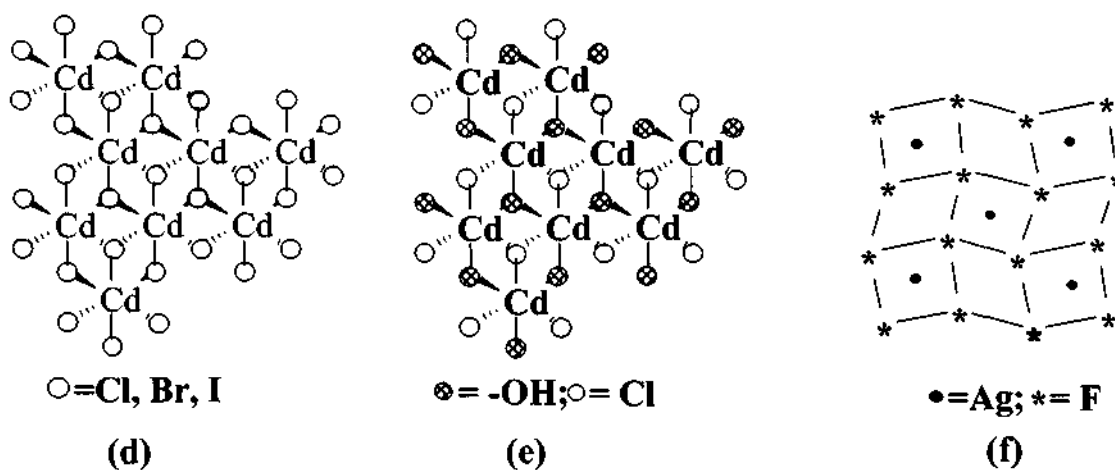


Scheme 4.1: A general scheme illustrating the building up of complex hybrid metal-organic architectures by aligning the lower-dimensional structures of metal halides/hydroxides by replacing the Cl⁻ or OH⁻ ions with metal complexes possessing organic ligands capable of bridging these lower dimensional inorganic structures. Depending on the mode of linking that the organic linkers provide the hybrid metal-organic structures can either be two or three-dimensional. The probable, generation of the low-dimensional structures by the partial disintegration of the higher dimensional parent structure under suitable reaction conditions has also been indicated. A = any metal; * = F, Cl, Br, I, -OH, H₂O; R = dicarboxylate, bipyridyl, nicotinate etc. Note that the one-dimensional inorganic chains can be introduced directly into the reaction medium.

One-dimensional chain in metal halides



Two-dimensional layers in metal halide and related compounds



Scheme 4.2: Some of the low-dimensional structures of metal halogen and related inorganic solids have been shown. (a) shows the cis-oriented 1-D chains in NbI_4 , TaCl_4 , WCl_4 ; (b) shows the trans-oriented 1-D chains in TcCl_4 , ZrCl_4 , PtCl_4 ; (c) shows the CdCl_3 double chain present in NH_4CdCl_3 ; (d) shows the structure of CdX_2 ($\text{X} = \text{Cl, Br, I}$); (e) shows a layer in $\text{Cd}(\text{OH})\text{Cl}$; (f) shows the layer in AgF . Note the similarity in the structure of the double chain in (c) and the cadmium chloride chain in X and also the structural relationship existing among the structures shown here.

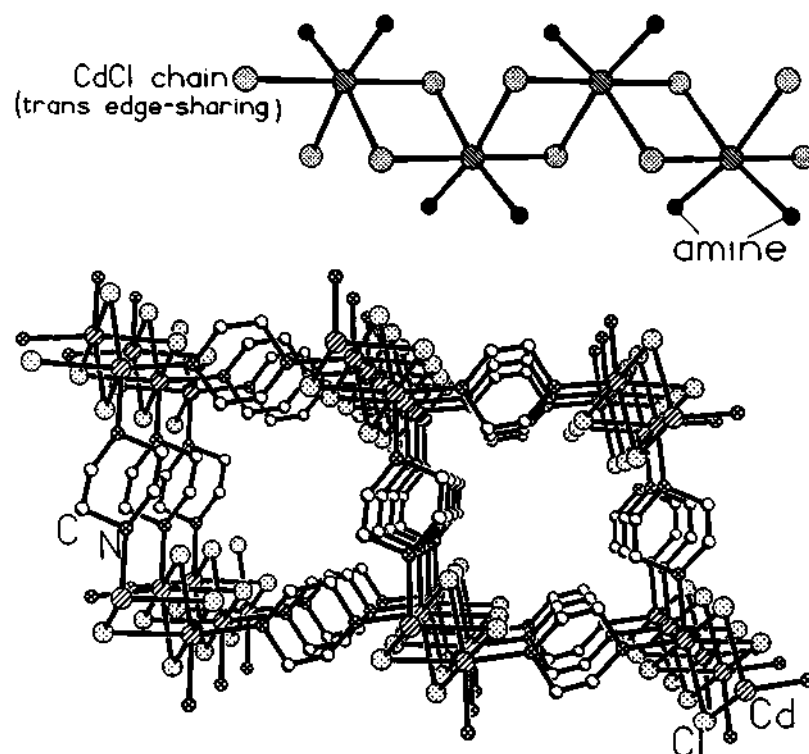


Fig. 4.30. Structure of $[\text{CdCl}_2(\text{C}_4\text{N}_2\text{H}_8)]$, XXXV, showing the square hydrophobic channels present along the *a*-axis formed by aligning of the Cd-chloro chains by the piperazine units. Inset shows the one-dimensional Cd-chloro chains formed by trans-edge sharing between the CdCl_4N_2 octahedra.

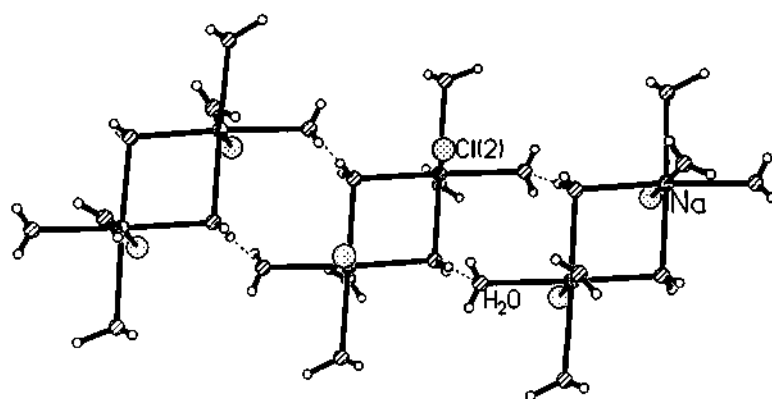
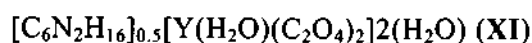


Fig. 4.31. Figure shows the one-dimensional ladder-like structure formed by the $\text{Na}_2\text{O}_8\text{Cl}_2$ dimers via $\text{O}(w)\text{-H}\dots\text{O}(w)$ hydrogen bond interactions.

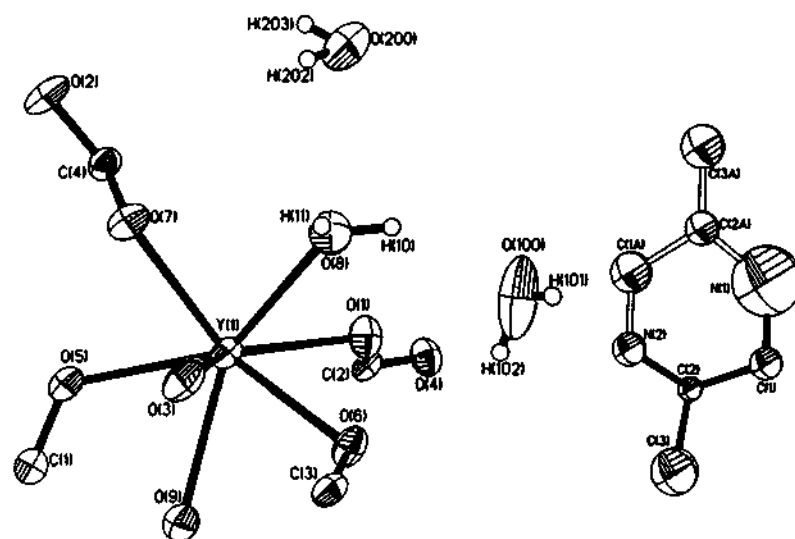
4.5. Three-dimensional rare-earth oxalates

4.5.1. Results

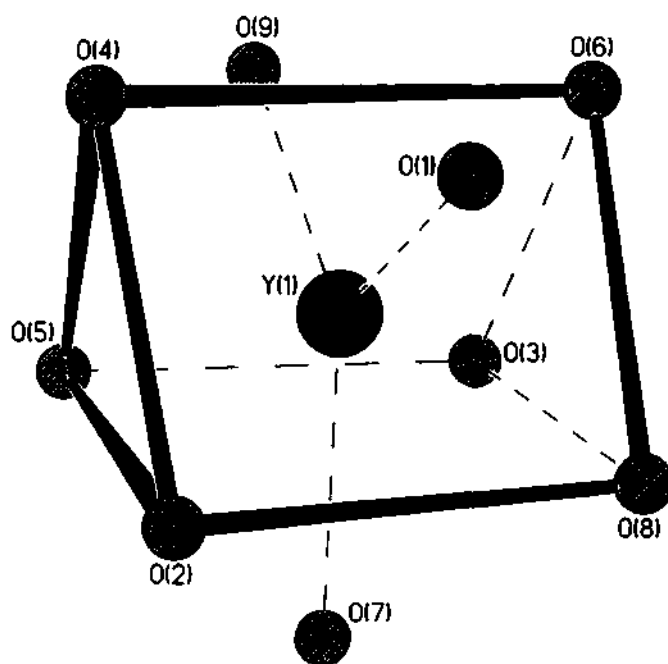


The asymmetric unit of **XI** contains 20 non-hydrogen atoms (Fig. 4.32a), of which, 14 atoms belong to the framework. The framework structure of **XI** is built-up by the linkages between the Y and the oxalate units with each Y atom bound to nine oxygens, which are, in turn, bound to carbon atoms forming network structure. Conversely, the oxalate ions are connected to the yttrium atoms forming the architecture. The coordination environment of Y atoms of a D_{3h} triply-capped trigonal prism as shown in Figure 4.32b with Y – O distances in the range 2.382 – 2.462 Å (av. 2.415 Å). Of the eight oxalate oxygens bound to yttrium, four are associated with Y – O distances in the range 2.382 – 2.400 Å and the other four with distances in the 2.406 – 2.462 Å range. The variations in the distances are also reflected in the C – O bonding as well (Table 4.12). The O – Y – O angles in the range 66.8 – 144.1° (av. 124.1°) and the O – C – O angles in the range 125.2 – 126.7° (av. 126.1°) (Table 4.12). These parameters are in the range expected for this type of bonding. The Y(1) – O(8) linkage with a distance of 2.444 Å is formally a water molecule. Two types of water molecules are present in **XI** one bound to Y and the other free water molecule present in the channels. Bond valence sum calculations^[21] indicated that the valence states of the various species forming the framework are Y^{3+} , C^{4+} , O^{2-} , as expected.

The structure of **XI** can be understood in terms of simpler building units formed by the linkages between the Y atom and the oxalate units. The connectivity between these units form layers which are linked then to one another giving rise to 3D structure three-dimensional architecture. Thus, three oxalate units $(\text{C}(1)\text{C}(1)\text{O}_4$,



(a)



(b)

Fig. 4.32. (a) ORTEP plot of XI, $[\text{C}_6\text{N}_2\text{H}_{16}]_{0.5}[\text{Y}(\text{H}_2\text{O})(\text{C}_2\text{O}_4)_2] \cdot 2\text{H}_2\text{O}$. Thermal Ellipsoids are given at 50% probability. Note the symmetry relation in the amine molecule. (b) The coordination environment around yttrium showing the D_{3h} triply capped trigonal

C(3)C(3)O₄ and C(4)C(4)O₄) connect the Y atom in an *in-plane* manner forming a honeycomb-like layer with 12-membered apertures, along the *a* axis (Fig. 4.33a), and the fourth oxalate (C(2)C(2)O₄) bridges the layers in an *out-of-plane* fashion forming the one-dimensional channels (width, 7.9 X 8.6 Å). Along the *c* axis, the connectivity between the C(2)C(2)O₄, C(3)C(3)O₄ and C(4)C(4)O₄ oxalates and the Y atom gives rise to an elliptical 12-membered channel through an *in-plane* connectivity (Fig. 4.33b), which are bridged by the C(1)C(1)O₄ oxalate forming the another one-dimensional channels of width 7.5 X 9.1 Å. Similar connectivity, along the *b* axis, gives rise to rectangular 12-membered channels of width 9.1 X 4.9 Å into which the bonded water molecule protrude (Fig. 4.34). Thus, the two types of water molecules, present in XI, are in the same channels. The amine molecules along with the water molecules occupy the channels. Thus, XI is a truly three-dimensional structure possessing channels, along all the crystallographic directions.

Table 4.12. Selected bond distances and angles for XI, [C₆N₂H₁₆]_{0.5}[Y(H₂O)(C₂O₄)₂].2H₂O

Moiety	Distance (Å)	Moiety	Distance (Å)
Y(1)-O(1)	2.393(4)	O(1)-C(2)	1.245(8)
Y(1)-O(2) ^{#1}	2.382(5)	O(2)-C(4)	1.254(8)
Y(1)-O(3)	2.405(4)	O(3)-C(3) ^{#3}	1.269(8)
Y(1)-O(4) ^{#2}	2.395(5)	O(4)-C(2)	1.269(8)
Y(1)-O(5)	2.400(5)	O(5)-C(1)	1.263(8)
Y(1)-O(6)	2.424(4)	O(6)-C(3)	1.241(8)
Y(1)-O(7)	2.430(4)	O(7)-C(4)	1.251(8)
Y(1)-O(8)	2.444(6)	O(9)-C(1) ^{#4}	1.250(8)
Y(1)-O(9)	2.462(5)	C(3)-O(3) ^{#3}	1.269(8)
C(1)-C(1) ^{#4}	1.543(13)	C(3)-C(3) ^{#3}	1.545(13)
C(2)-C(2) ^{#2}	1.532(13)	C(4)-C(4) ^{#1}	1.559(14)
Organic Moiety			
N(1)-C(11)	1.522(14)	C(12)-C(13)	1.484(13)
C(11)-C(12)	1.450(11)	N(1)-C(12) ^{#5}	1.481(12)

Moiety	Angle (°)	Moiety	Angle (°)
O(2) ^{#1} -Y(1)-O(1)	74.9(2)	O(5)-Y(1)-O(7)	70.2(2)
O(2) ^{#1} -Y(1)-O(4) ^{#2}	73.6(2)	O(3)-Y(1)-O(7)	68.7(2)
O(1)-Y(1)-O(4) ^{#2}	67.7(2)	O(6)-Y(1)-O(7)	127.9(2)
O(2) ^{#1} -Y(1)-O(5)	81.5(2)	O(2) ^{#1} -Y(1)-O(8)	85.2(2)
O(1)-Y(1)-O(5)	140.5(2)	O(1)-Y(1)-O(8)	68.8(2)
O(4) ^{#2} -Y(1)-O(5)	75.4(2)	O(4) ^{#2} -Y(1)-O(8)	135.2(2)
O(2) ^{#1} -Y(1)-O(3)	136.4(2)	O(5)-Y(1)-O(8)	140.6(2)
O(1)-Y(1)-O(3)	132.5(2)	O(3)-Y(1)-O(8)	78.5(2)
O(4) ^{#2} -Y(1)-O(3)	142.1(2)	O(6)-Y(1)-O(8)	73.8(2)
O(5)-Y(1)-O(3)	86.0(2)	O(7)-Y(1)-O(8)	70.4(2)
O(2) ^{#1} -Y(1)-O(6)	144.1(2)	O(2) ^{#1} -Y(1)-O(9)	136.8(2)
O(1)-Y(1)-O(6)	70.4(2)	O(1)-Y(1)-O(9)	111.7(2)
O(4) ^{#2} -Y(1)-O(6)	101.1(2)	O(4) ^{#2} -Y(1)-O(9)	70.6(2)
O(5)-Y(1)-O(6)	132.5(2)	O(5)-Y(1)-O(9)	66.8(2)
O(3)-Y(1)-O(6)	68.0(2)	O(3)-Y(1)-O(9)	71.8(2)
O(2) ^{#1} -Y(1)-O(7)	67.7(2)	O(6)-Y(1)-O(9)	67.6(2)
O(1)-Y(1)-O(7)	126.0(2)	O(7)-Y(1)-O(9)	122.3(2)
O(4) ^{#2} -Y(1)-O(7)	130.9(2)	O(8)-Y(1)-O(9)	137.7(2)
C(2)-O(1)-Y(1)	119.3(4)	O(5)-C(1)-C(1) ^{#4}	116.8(7)
C(4)-O(2)-Y(1) ^{#1}	119.9(4)	O(1)-C(2)-O(4)	126.2(6)
C(3) ^{#3} -O(3)-Y(1)	117.2(4)	O(1)-C(2)-C(2) ^{#2}	117.5(7)
C(2)-O(4)-Y(1) ^{#2}	118.9(4)	O(4)-C(2)-C(2) ^{#2}	116.3(7)
C(1)-O(5)-Y(1)	120.7(4)	O(6)-C(3)-O(3) ^{#3}	125.2(6)
C(3)-O(6)-Y(1)	116.0(4)	O(6)-C(3)-C(3) ^{#3}	118.7(7)
C(4)-O(7)-Y(1)	118.3(4)	O(3) ^{#3} -C(3)-C(3) ^{#3}	116.1(7)
C(1) ^{#4} -O(9)-Y(1)	118.9(4)	O(7)-C(4)-O(2)	126.7(6)
O(9) ^{#4} -C(1)-O(5)	126.4(6)	O(7)-C(4)-C(4) ^{#1}	116.6(7)
O(9) ^{#4} -C(1)-C(1) ^{#4}	116.8(7)	O(2)-C(4)-C(4) ^{#1}	116.7(7)
Organic Moiety			
C(12)#5-N(1)-C(11)	112.3(7)	C(11)-C(12)-C(13)	112.5(9)
C(12)-C(11)-N(1)	111.4(7)	N(1)#5-C(12)-C(13)	112.1(8)
C(11)-C(12)-N(1)#5	109.1(7)		

Symmetry transformations used to generate equivalent atoms:

#1 -x+1, -y+1, -z+2; #2 -x+1, -y+2, -z+2; #3 -x+2, -y+2, -z+1; #4 -x+1, -y+2, -z+1;
#5 -x+2, -y+1, -z+1

$[C_3N_2H_{12}][Y(C_2O_4)_2]$ (XII)

The asymmetric unit of XII contains 20 non-hydrogen atom (Fig. 4.35a), of which 13 belong to the framework. The structure of XII also consists of a network of Y and oxalate units. The Y atoms in XII are coordinated to eight oxalate oxygens (Table 4.13), or four oxalate units. The yttrium has a distorted square-antiprismatic coordination with respect to the oxygen atoms as depicted in Figure 4.35b.

The framework structure of XII can be understood in terms of simpler building units involving two-dimensional layers. Thus, three oxalate units link-up with the Y atom in an *in-plane* manner forming honeycomb-like layers with 12-membered apertures as shown in Figure 4.36. The fourth oxalate unit connects these layers in an *out-of-plane* manner resulting in a 12-membered one-dimensional channel of width 7.1 X 8.2 Å along the *c* axis as shown in Figure 4.37. The channels in XII occur only along one direction. The amine molecule present in the channels is 2-methyl-3,4,5,6-tetrahydro-pyrimid-1-ene resulting from the *in-situ* reaction of 1,3-DAP with acetic acid.

TGA studies of XI and XII were carried out in nitrogen atmosphere from room temperature to 700 °C using a heating rate of 10°C. The results are presented in Figure 4.38. In the case of XI the mass loss occurs in three steps, whereas in XII a single sharp mass loss is seen. In XI, the mass loss in the range 100 – 200 °C of 9.8% corresponds to the loss of free water molecules (9.6%) and a continuous two-step mass loss of 54% in the 300 – 450 °C region corresponds to the loss of the bound water and carbon dioxide and amine molecules (calcd. 58.4%). For XII, a sharp mass loss of 60% in the 425 – 550 °C range is due to the loss of carbon dioxide and the amine molecules (calcd. 66%). The powder XRD patterns of the

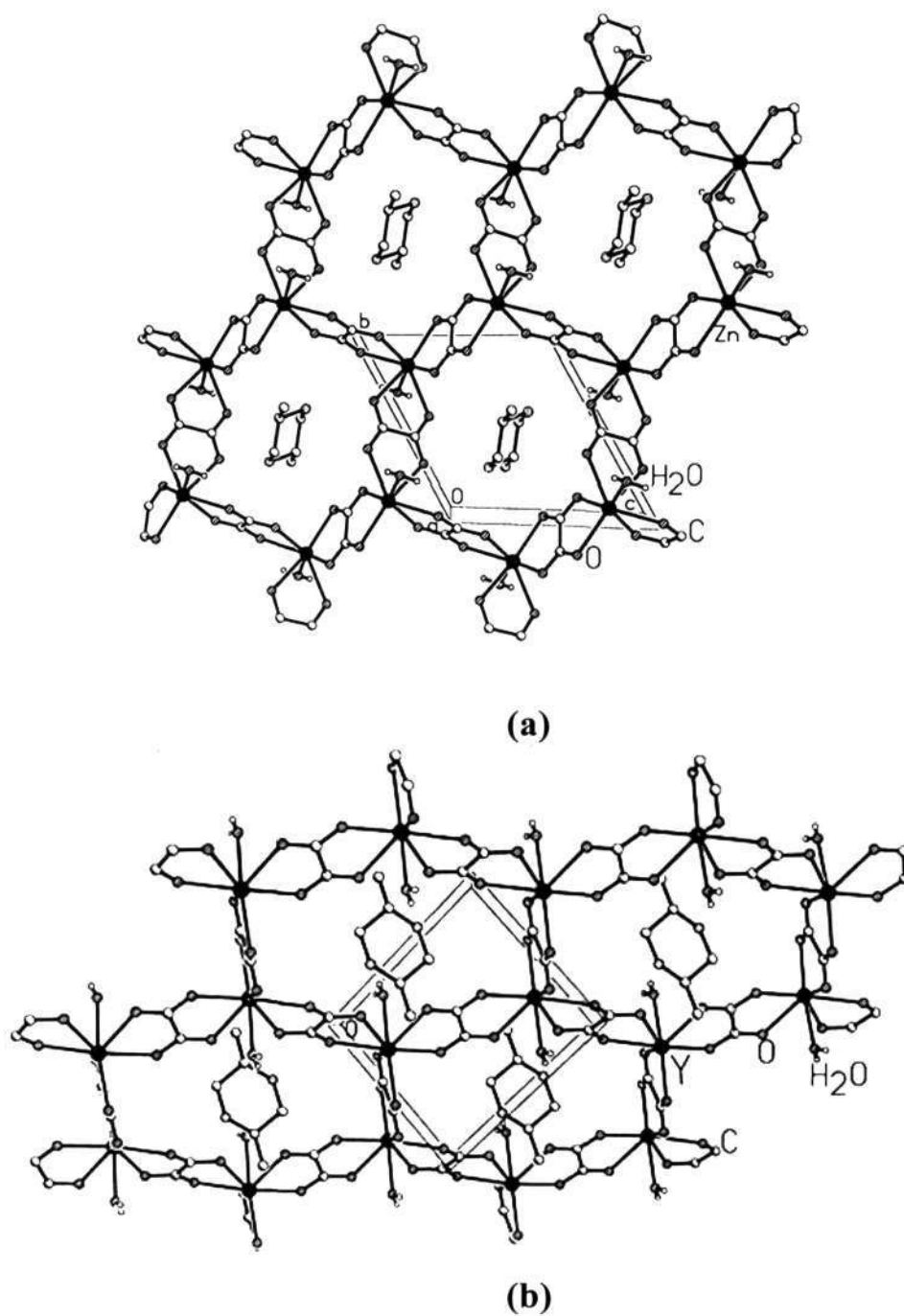


Fig. 4.33. (a) Structure of **XI** showing the honeycomb-like layers along the *a* axis. The layers are bridged by oxalate unit forming the channels. Hydrogens on the amine and the free water molecules are not shown. (b) Structure of **XI** along the *c* axis showing the layer arrangement. The bound water molecules point into the 12-membered aperture. Hydrogens on the amine and the free water molecule are not shown.

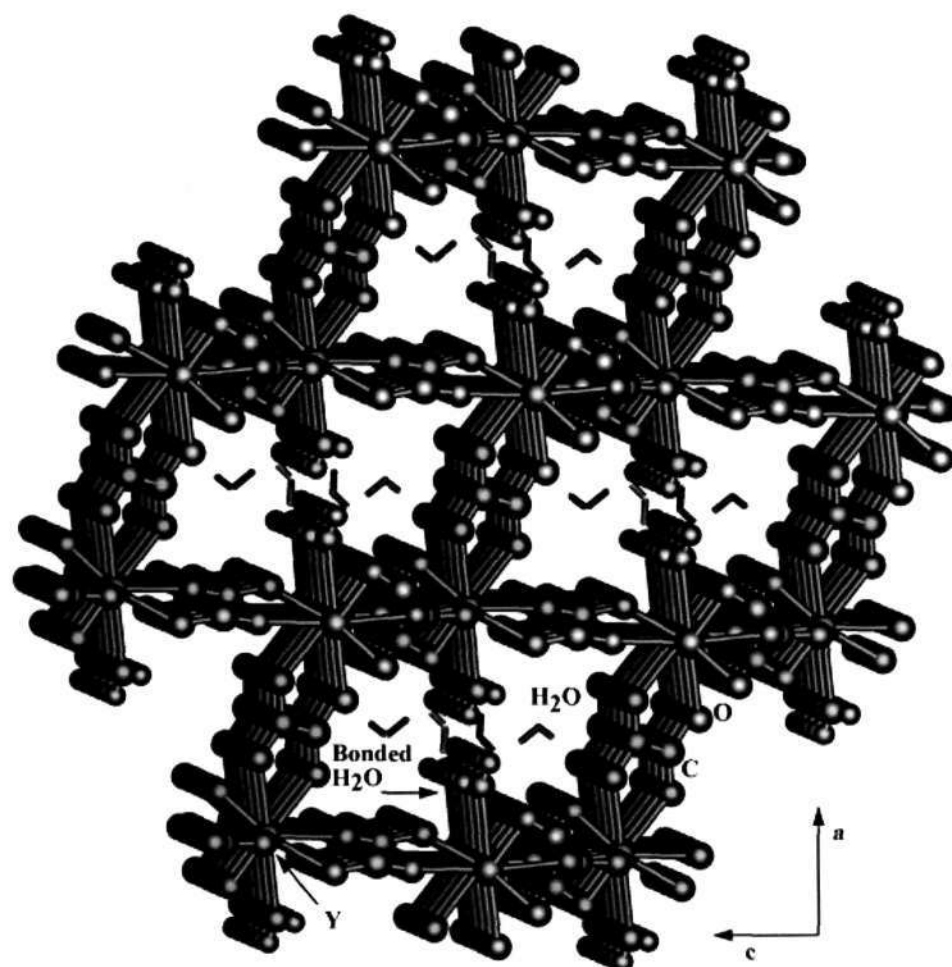


Fig. 4.34. Structure of XI along the *b* axis showing rectangular channels. The amine molecules are not shown. Note the close proximity between the bound water molecules.

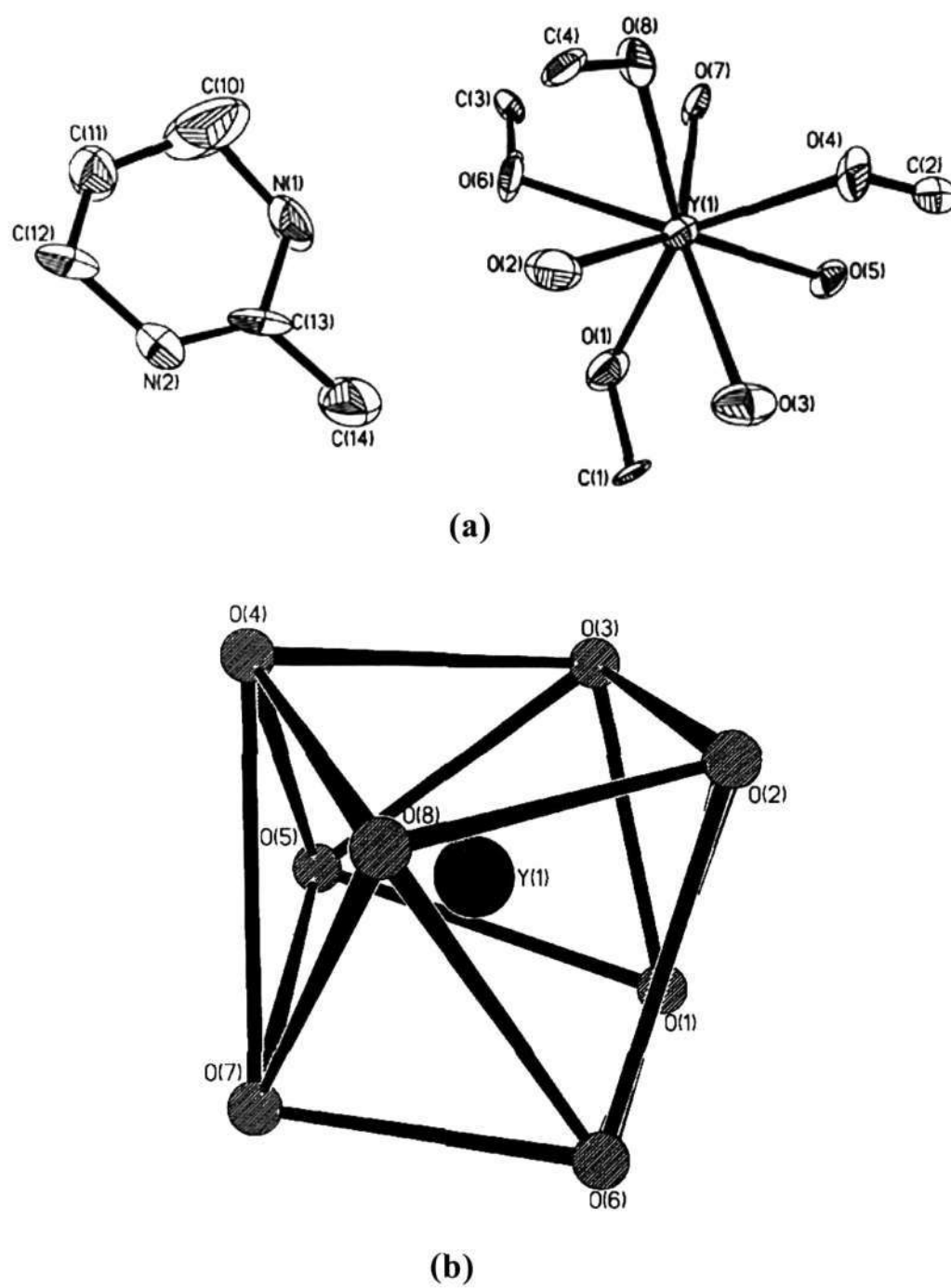


Fig. 4.35. (a) ORTEP plot of XII, $[C_5N_2H_{11}][Y(C_2O_4)_2]$. Thermal ellipsoids are given at 50% probability. (b) The coordination around yttrium atom. Note that the oxygens form square antiprismatic arrangement.

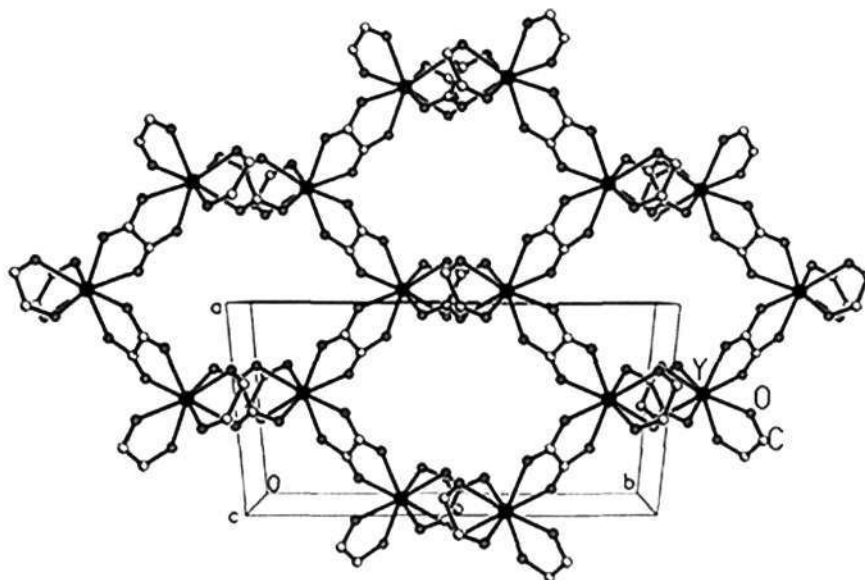


Fig. 4.36. Structure of XII, along the *c* axis showing the layer arrangement. The amine molecules are not shown.

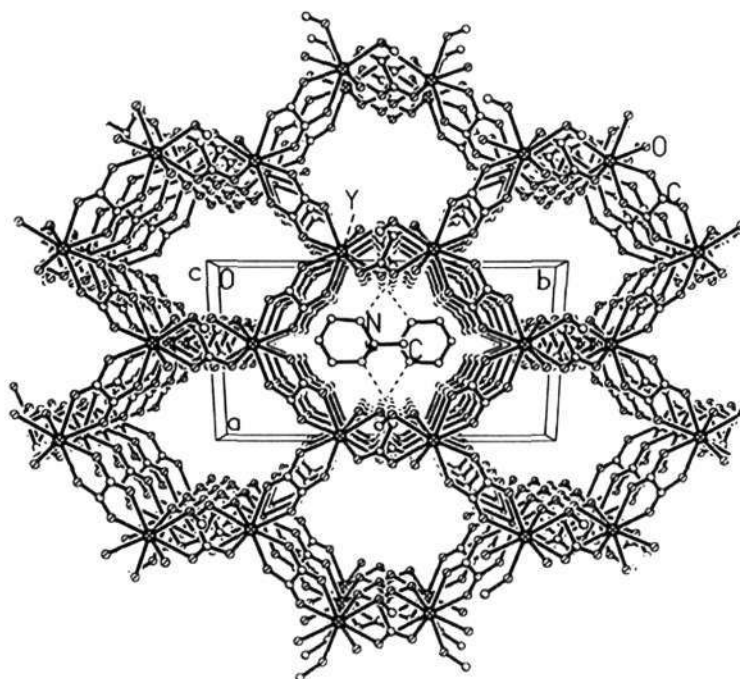


Fig. 4.37. Structure of XII, along the *c* axis showing the 12-membered channels. Amine molecules are shown in only one channels. Hydrogens on the amines are not shown.

Table 4.13. Selected bond distances and angles in **XII**, [C₅N₂H₁₁][Y(C₂O₄)₂]

Moiety	Distance (Å)	Moiety	Distance (Å)
Y(1)-O(1)	2.303(11)	O(1)-C(1)	1.36(2)
Y(1)-O(2)	2.351(10)	O(2)-C(3) ^{#1}	1.20(2)
Y(1)-O(3)	2.343(10)	O(3)-C(2) ^{#2}	1.32(2)
Y(1)-O(4)	2.340(10)	O(4)-C(2)	1.14(2)
Y(1)-O(5)	2.388(10)	O(5)-C(1) ^{#3}	1.19(2)
Y(1)-O(6)	2.407(9)	O(6)-C(3)	1.29(2)
Y(1)-O(7)	2.370(9)	O(7)-C(4) ^{#4}	1.30(2)
Y(1)-O(8)	2.405(9)	O(8)-C(4)	1.22(2)
C(1)-C(2) ^{#2}	1.551(7)	C(3)-C(4) ^{#4}	1.536(7)
Organic Moiety			
N(1)-C(10)	1.59(3)	N(2)-C(13)	1.24(2)
C(10)-C(11)	1.47(3)	N(1)-C(13)	1.37(2)
C(11)-C(12)	1.32(3)	C(13)-C(14)	1.486(10)
C(12)-N(2)	1.55(3)		
Moiety	Angle (°)	Moiety	Angle (°)
O(1)-Y(1)-O(4)	141.34(11)	O(7)-Y(1)-O(5)	72.6(3)
O(1)-Y(1)-O(3)	70.7(4)	O(1)-Y(1)-O(8)	144.2(3)
O(4)-Y(1)-O(3)	79.4(4)	O(4)-Y(1)-O(8)	73.7(3)
O(1)-Y(1)-O(2)	89.8(4)	O(3)-Y(1)-O(8)	125.0(4)
O(4)-Y(1)-O(2)	105.8(4)	O(2)-Y(1)-O(8)	67.8(3)
O(3)-Y(1)-O(2)	75.0(4)	O(7)-Y(1)-O(8)	79.2(4)
O(1)-Y(1)-O(7)	102.1(4)	O(5)-Y(1)-O(8)	131.7(3)
O(4)-Y(1)-O(7)	90.6(3)	O(1)-Y(1)-O(6)	72.3(4)
O(3)-Y(1)-O(7)	148.4(4)	O(4)-Y(1)-O(6)	145.1(4)
O(2)-Y(1)-O(7)	136.50(11)	O(3)-Y(1)-O(6)	132.8(4)
O(1)-Y(1)-O(5)	80.9(4)	O(2)-Y(1)-O(6)	76.6(4)
O(4)-Y(1)-O(5)	68.3(3)	O(7)-Y(1)-O(6)	67.9(3)
O(3)-Y(1)-O(5)	75.91(12)	O(5)-Y(1)-O(6)	125.3(4)
O(2)-Y(1)-O(5)	150.9(4)	O(8)-Y(1)-O(6)	75.39(10)
C(1)-O(1)-Y(1)	118.3(9)	O(1)-C(1)-C(2) ^{#2}	116.9(10)
C(3) ^{#1} -O(2)-Y(1)	120.3(8)	O(4)-C(2)-O(3) ^{#3}	129.6(12)
C(2) ^{#2} -O(3)-Y(1)	120.9(8)	O(4)-C(2)-C(1) ^{#3}	117.2(8)
C(2)-O(4)-Y(1)	120.0(9)	O(3) ^{#3} -C(2)-C(1) ^{#3}	113.2(8)
C(1) ^{#3} -O(5)-Y(1)	115.2(9)	O(2) ^{#4} -C(3)-O(6)	129.0(12)
C(3)-O(6)-Y(1)	120.6(7)	O(2) ^{#4} -C(3)-C(4) ^{#4}	116.7(8)

C(4) ^{#4} -O(7)-Y(1)	119.6(8)	O(6)-C(3)-C(4) ^{#4}	114.3(8)
C(4)-O(8)-Y(1)	116.6(9)	O(8)-C(4)-O(7) ^{#1}	124.2(13)
O(5) ^{#2} -C(1)-O(1)	123.9(13)	O(8)-C(4)-C(3) ^{#1}	118.4(9)
O(5) ^{#2} -C(1)-C(2) ^{#2}	119.2(8)	O(7) ^{#1} -C(4)-C(3) ^{#1}	117.4(8)
Organic Moiety			
C(13)-N(1)-C(10)	113.5(12)	C(13)-N(2)-C(12)	123.0(13)
C(11)-C(10)-N(1)	109(2)	N(2)-C(13)-N(1)	120.9(8)
C(12)-C(11)-C(10)	120(2)	N(2)-C(13)-C(14)	125(2)
C(11)-C(12)-N(2)	105(2)	N(1)-C(13)-C(14)	112(2)

Symmetry transformations used to generate equivalent atoms:

#1 $x, -y, z+1/2$; #2 $x+1/2, -y+1/2, z+1/2$; #3 $x-1/2, -y+1/2, z-1/2$; #4 $x, -y, -z+1/2$

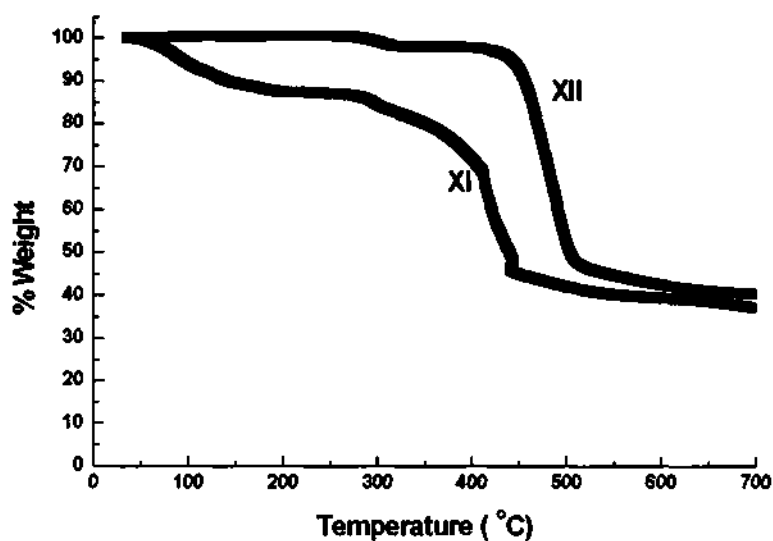


Fig. 4.38. TGA curves of XI and XII

decomposed products indicated a poorly crystalline product, Y_2O_3 (JCPDS: 25-1200).

Adsorption studies, carried out gravimetrically using a Cahn electric balance, show that a dehydrated sample of XI adsorbs water and methanol reversibly, exhibiting a Langmuir type I adsorption isotherms (Fig. 4.39). The observed weight changes at 25 °C corresponds to two and one molecules of water

and methanol per unit cell respectively. The weight change observed with water is in agreement with the framework formula derived from the crystallographic study.

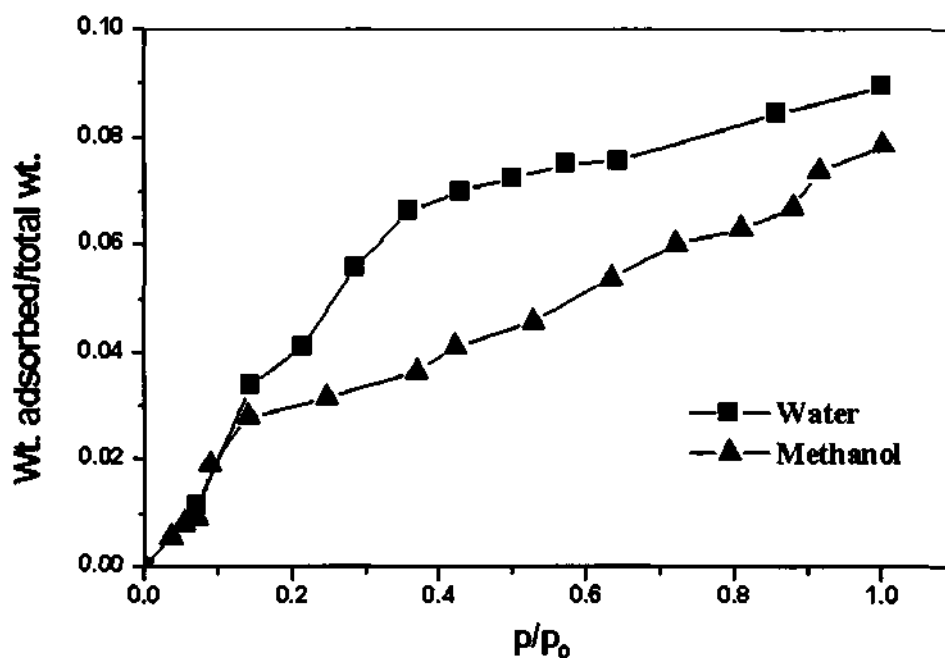


Fig. 4.39. Room-temperature adsorption isotherms for H₂O and CH₃OH in a dehydrated sample of XI.

[NH₃CH₂CH(NH₃)CH₃][Nd(C₂O₄)₂(HCOO)].H₂O (XIII) and

[OC(CH₃)NCH₂CH(CH₃)NH₃][Nd(C₂O₄)₂].H₂O (XIV)

The asymmetric units of XIII and XIV contains 24 and 23 non-hydrogen atoms (Fig. 4.40a and 4.41). The frameworks of XIII and XIV are built up of linkages between the Nd and the oxalate units, with each Nd atom bound to nine oxygens, which in turn, are bound to carbon atoms, forming a network structure. Conversely, the oxalate ions are connected to the neodymium atoms forming the architecture. The Nd atoms, in XIII, have the rare distorted square antiprism coordination capped on one square face (Fig. 4.40b). In XIV, the Nd atoms have similar coordination as the Y atoms in XI, the idealized D_{3h} triply capped trigonal prism coordination. The Nd – O distances are in the range 2.462(4) – 2.531(4) Å

(av. 2.495 Å) for XIII and in the range 2.461(6) – 2.529(7) Å (av. 2.492 Å) for XIV (Table 4.14). The O – Nd – O bond angles for XIII are in the range 65.28(12) – 143.80(14)° (av. 98.78°) and 64.2(2) – 145.4(2)° (av. 98.76°) for XIV (Table 4.14). The C – O and O – C – O distances and angles are in the expected ranges.

Table 4.14. Selected bond distances and angles for, **XIII** and **XIV**
 [NH₃CH₂CH(NH₃)CH₃][Nd(C₂O₄)₂(HCOO)].H₂O, and
 [OC(CH₃)NCH₂CH(CH₃)NH₃][Nd(C₂O₄)₂].H₂O, XIV

XIII			
Moiety	Distance (Å)	Moiety	Distance (Å)
Nd(1)-O(1)	2.462(4)	O(5)-C(2)#2	1.257(6)
Nd(1)-O(3)	2.477(4)	O(6)-C(4)	1.245(6)
Nd(1)-O(4)	2.480(4)	O(7)-C(4)#3	1.249(6)
Nd(1)-O(7)	2.488(4)	O(8)-C(3)	1.246(6)
Nd(1)-O(2)	2.498(4)	O(9)-C(5)	1.243(8)
Nd(1)-O(5)	2.500(4)	O(3)-C(1)#4	1.255(6)
Nd(1)-O(9)	2.511(4)	O(5)-C(2)#4	1.257(6)
Nd(1)-O(8)#1	2.511(4)	O(7)-C(4)#3	1.249(6)
Nd(1)-O(6)	2.531(4)	C(1)-C(2)	1.562(8)
O(1)-C(3)	1.251(6)	C(3)-C(3)#1	1.550(10)
O(2)-C(2)	1.245(6)	C(4)-C(4)#3	1.545(10)
Moiety	Angle (°)	Moiety	Angle (°)
O(1)-Nd(1)-O(3)	138.98(12)	O(3)-Nd(1)-O(6)	97.41(12)
O(1)-Nd(1)-O(4)	138.42(12)	O(4)-Nd(1)-O(6)	136.03(13)
O(3)-Nd(1)-O(4)	75.57(13)	O(7)-Nd(1)-O(6)	64.71(12)
O(1)-Nd(1)-O(7)	132.25(12)	O(2)-Nd(1)-O(6)	136.40(13)
O(3)-Nd(1)-O(7)	69.91(12)	O(5)-Nd(1)-O(6)	138.99(13)
O(4)-Nd(1)-O(7)	72.33(13)	O(9)-Nd(1)-O(6)	72.52(14)
O(1)-Nd(1)-O(2)	73.39(12)	O(8)#1-Nd(1)-O(6)	67.81(12)
O(3)-Nd(1)-O(2)	126.19(12)	C(3)-O(1)-Nd(1)	116.9(3)
O(4)-Nd(1)-O(2)	65.61(12)	C(2)-O(2)-Nd(1)	119.7(3)
O(7)-Nd(1)-O(2)	125.87(13)	C(1)#2-O(3)-Nd(1)	120.2(3)
O(1)-Nd(1)-O(5)	95.48(12)	C(1)-O(4)-Nd(1)	120.2(3)
O(3)-Nd(1)-O(5)	65.40(12)	C(2)#2-O(5)-Nd(1)	119.9(3)

O(4)-Nd(1)-O(5)	78.05(14)	C(4)-O(6)-Nd(1)	118.3(3)
O(7)-Nd(1)-O(5)	131.01(12)	C(4)#3-O(7)-Nd(1)	119.3(3)
O(2)-Nd(1)-O(5)	71.09(13)	C(3)-O(8)-Nd(1)#1	114.9(3)
O(1)-Nd(1)-O(9)	75.31(13)	C(5)-O(9)-Nd(1)	134.1(4)
O(3)-Nd(1)-O(9)	141.04(13)	O(4)-C(1)-O(3)#4	125.3(5)
O(4)-Nd(1)-O(9)	86.04(14)	O(2)-C(2)-O(5)#4	127.0(5)
O(7)-Nd(1)-O(9)	71.87(14)	O(8)-C(3)-O(1)	126.1(5)
O(2)-Nd(1)-O(9)	72.73(14)	O(6)-C(4)-O(7)#3	125.6(5)
O(5)-Nd(1)-O(9)	143.80(14)	O(9)-C(5)-N(10)	124.4(7)
O(1)-Nd(1)-O(8)#1	65.28(12)	O(4)-C(1)-C(2)	117.6(5)
O(3)-Nd(1)-O(8)#1	74.11(12)	O(3)#4-C(1)-C(2)	117.1(5)
O(4)-Nd(1)-O(8)#1	143.78(13)	O(2)-C(2)-C(1)	116.8(5)
O(7)-Nd(1)-O(8)#1	114.20(13)	O(5)#4-C(2)-C(1)	116.2(5)
O(2)-Nd(1)-O(8)#1	119.90(13)	O(8)-C(3)-C(3)#1	117.5(6)
O(5)-Nd(1)-O(8)#1	71.61(13)	O(1)-C(3)-C(3)#1	116.4(6)
O(9)-Nd(1)-O(8)#1	130.18(14)	O(6)-C(4)-C(4)#3	117.1(6)
O(1)-Nd(1)-O(6)	72.97(12)	O(7)#3-C(4)-C(4)#3	117.4(6)

XIV

Moiety	Distance (Å)	Moiety	Distance (Å)
Nd(1)-O(1)	2.471(6)	O(5)-C(13)#3	1.237(11)
Nd(1)-O(2)	2.461(6)	O(6)-C(11)	1.267(11)
Nd(1)-O(7)	2.470(8)	O(7)-C(50)	1.21(2)
Nd(1)-O(3)	2.484(6)	O(8)-C(14)	1.246(11)
Nd(1)-O(4)	2.496(7)	O(9)-C(12)#4	1.266(11)
Nd(1)-O(8)	2.494(7)	O(2)-C(14)#1	1.261(11)
Nd(1)-O(6)	2.510(7)	O(5)-C(13)#3	1.237(11)
Nd(1)-O(5)	2.521(6)	O(4)-C(11)#2	1.231(11)
Nd(1)-O(9)	2.529(7)	C(12)-C(12)#4	1.55(2)
O(1)-C(12)	1.246(12)	C(14)-C(14)#1	1.54(2)
O(2)-C(14)#1	1.261(11)	C(13)-C(13)#3	1.54(2)
O(3)-C(13)	1.239(11)	C(11)-C(11)#2	1.53(2)
O(4)-C(11)#2	1.231(11)	C(50)-C(51)	1.562(11)
Moiety	Angle (°)	Moiety	Angle (°)
O(1)-Nd(1)-O(2)	138.3(2)	O(2)-Nd(1)-O(9)	77.4(2)
O(1)-Nd(1)-O(7)	73.5(2)	O(7)-Nd(1)-O(9)	73.8(3)
O(2)-Nd(1)-O(7)	79.2(2)	O(3)-Nd(1)-O(9)	138.6(2)
O(1)-Nd(1)-O(3)	75.7(2)	O(4)-Nd(1)-O(9)	103.3(2)

O(2)-Nd(1)-O(3)	131.4(2)	O(8)-Nd(1)-O(9)	67.6(2)
O(7)-Nd(1)-O(3)	82.7(3)	O(6)-Nd(1)-O(9)	137.8(2)
O(1)-Nd(1)-O(4)	69.4(2)	O(5)-Nd(1)-O(9)	134.8(2)
O(2)-Nd(1)-O(4)	140.3(2)	C(12)-O(1)-Nd(1)	120.9(6)
O(7)-Nd(1)-O(4)	139.8(2)	C(14)#1-O(2)-Nd(1)	119.9(6)
O(3)-Nd(1)-O(4)	73.7(2)	C(13)-O(3)-Nd(1)	121.2(6)
O(1)-Nd(1)-O(8)	112.7(2)	C(11)#2-O(4)-Nd(1)	120.9(6)
O(2)-Nd(1)-O(8)	65.2(2)	C(13)#3-O(5)-Nd(1)	120.3(6)
O(7)-Nd(1)-O(8)	131.7(2)	C(11)-O(6)-Nd(1)	120.3(6)
O(3)-Nd(1)-O(8)	145.4(2)	C(50)-O(7)-Nd(1)	137.2(9)
O(4)-Nd(1)-O(8)	78.3(2)	C(14)-O(8)-Nd(1)	118.6(6)
O(1)-Nd(1)-O(6)	132.1(2)	C(12)#4-O(9)-Nd(1)	119.5(6)
O(2)-Nd(1)-O(6)	88.1(2)	O(1)-C(12)-O(9)#4	126.0(9)
O(7)-Nd(1)-O(6)	142.3(3)	O(8)-C(14)-O(2)#1	126.5(9)
O(3)-Nd(1)-O(6)	79.4(2)	O(5)#3-C(13)-O(3)	126.2(9)
O(4)-Nd(1)-O(6)	64.5(2)	O(4)#2-C(11)-O(6)	125.8(9)
O(8)-Nd(1)-O(6)	70.4(2)	O(1)-C(12)-C(12)#4	118.3(10)
O(1)-Nd(1)-O(5)	129.8(2)	O(9)#4-C(12)-C(12)#4	115.7(11)
O(2)-Nd(1)-O(5)	67.4(2)	O(8)-C(14)-C(14)#1	117.4(10)
O(7)-Nd(1)-O(5)	72.6(3)	O(2)#1-C(14)-C(14)#1	116.0(10)
O(3)-Nd(1)-O(5)	64.2(2)	O(5)#3-C(13)-C(13)#3	116.6(10)
O(4)-Nd(1)-O(5)	121.9(2)	O(3)-C(13)-C(13)#3	117.2(10)
O(8)-Nd(1)-O(5)	117.4(2)	O(4)#2-C(11)-C(11)#2	118.1(10)
O(6)-Nd(1)-O(5)	69.7(2)	O(6)-C(11)-C(11)#2	116.0(11)
O(1)-Nd(1)-O(9)	65.1(2)		

Symmetry transformations used to generate equivalent atoms:

#1 $-x+1, -y, -z$; #2 $x, -y+1/2, z-1/2$; #3 $-x, -y, -z$; #4 $x, -y+1/2, z+1/2$ for **XIII**

#1 $-x, -y, -z+1$; #2 $-x, -y+1, -z+1$; #3 $-x+1, -y+1, -z+1$; #4 $-x, -y, -z$ for **XIV**

Similar to **XI** and **XII**, the connectivity between Nd and three oxalate units gives rise to a honeycomb-like layer, with a 12-membered aperture in the *bc* plane. The layers are connected through the fourth oxalate, acting like a pillar, creating the three-dimensional structure with one-dimensional channels as shown in Figure 4.42a. The ninth coordination of Nd comes from the linkage of one of the oxygen atoms of the formate group in the case of **XIII**, and from that of N- (2- aminopropyl

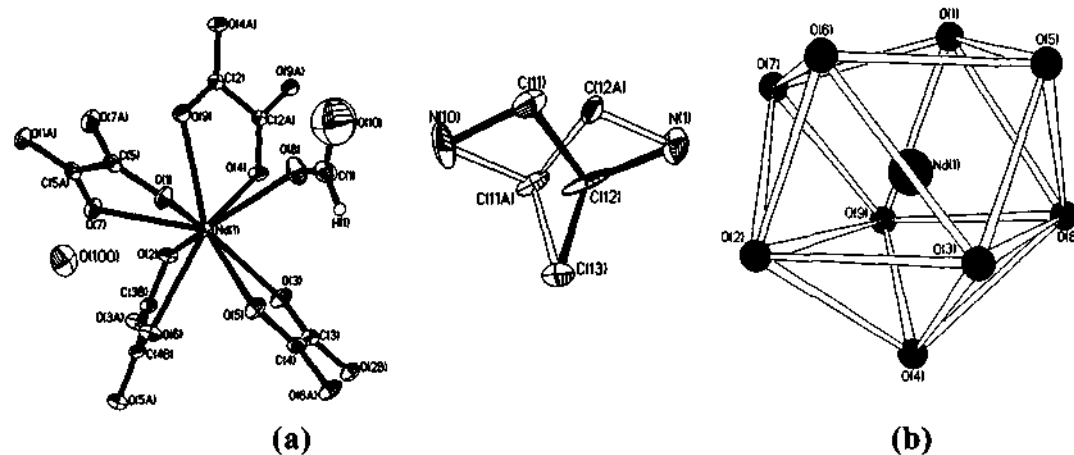


Fig. 4.40. ORTEP diagram for (a) $[\text{NH}_3\text{CH}_2\text{CH}(\text{NH}_3)\text{CH}_3][\text{Nd}(\text{C}_2\text{O}_4)_2(\text{HCOO})]\cdot\text{H}_2\text{O}$, XIII, and (b) The coordination environment around the Nd atom: mono-capped square antiprism.

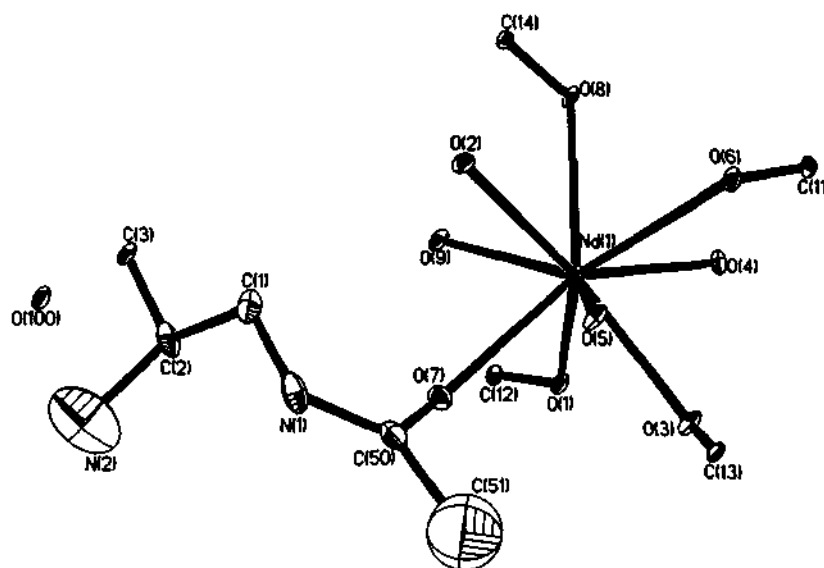
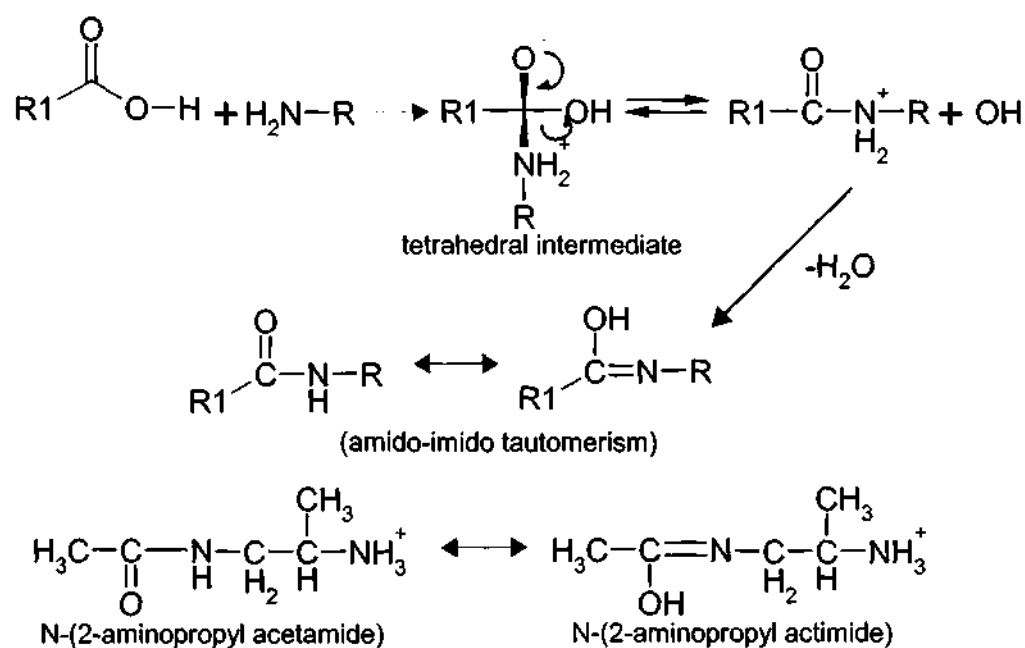


Fig. 4.41. ORTEP diagram for $[\text{OC}(\text{CH}_3)\text{NCH}_2\text{CH}(\text{CH}_3)\text{NH}_3][\text{Nd}(\text{C}_2\text{O}_4)_2]\cdot\text{H}_2\text{O}$, XIV.

acetimide) group in the case of XIV (Figs. 4.42a and b). The connectivity involves both *in-plane* and the *out-of-plane* linkages of the oxalate units (Fig. 4.43).

The organic amine, 1,2-DAP, in XIII, is diprotonated, disordered, and occupies the centre of the 12-membered channels. Such disorder of the amine molecules is observed commonly in open-framework phosphates.^[46] The formic acid in the reaction mixture occurs as formate ion in XIII and is coordinated to Nd atom.



Acetic acid in the reaction mixture reacts with 1,2-DAP, in the case of XIV, to form N-(2-aminopropyl acetamide), which occurs in the more stable tautomeric form as N-(2-aminopropyl actimide). A reaction between the acetic acid and the amine occurs through a nucleophilic attack as shown above. The imido compound is linked to Nd through the oxygen atom. The dangling formate in XIII and N-(2-aminopropyl acetimide) in XIV, have both a high positional freedom.

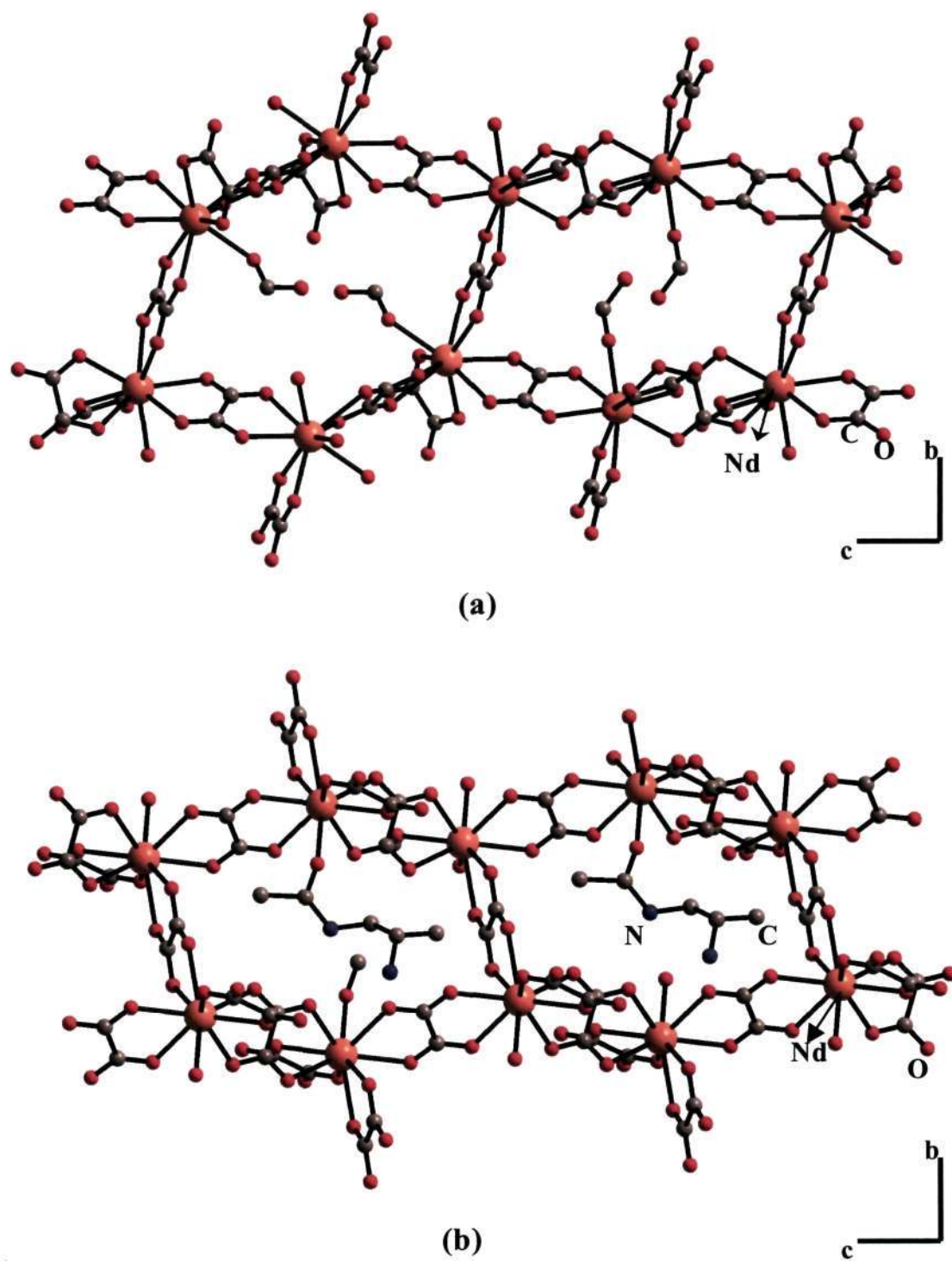


Fig. 4.42. (a) Structure of **XIII** along the *a* axis showing the 12-membered channels. Note the formate groups protrude into the channel. The amine molecules are not shown for clarity. (b) Structure of **XIV**, along the *a* axis showing the 12-membered channels. Note that the N-(2-aminopropyl acetimide) group protruding into the channel.

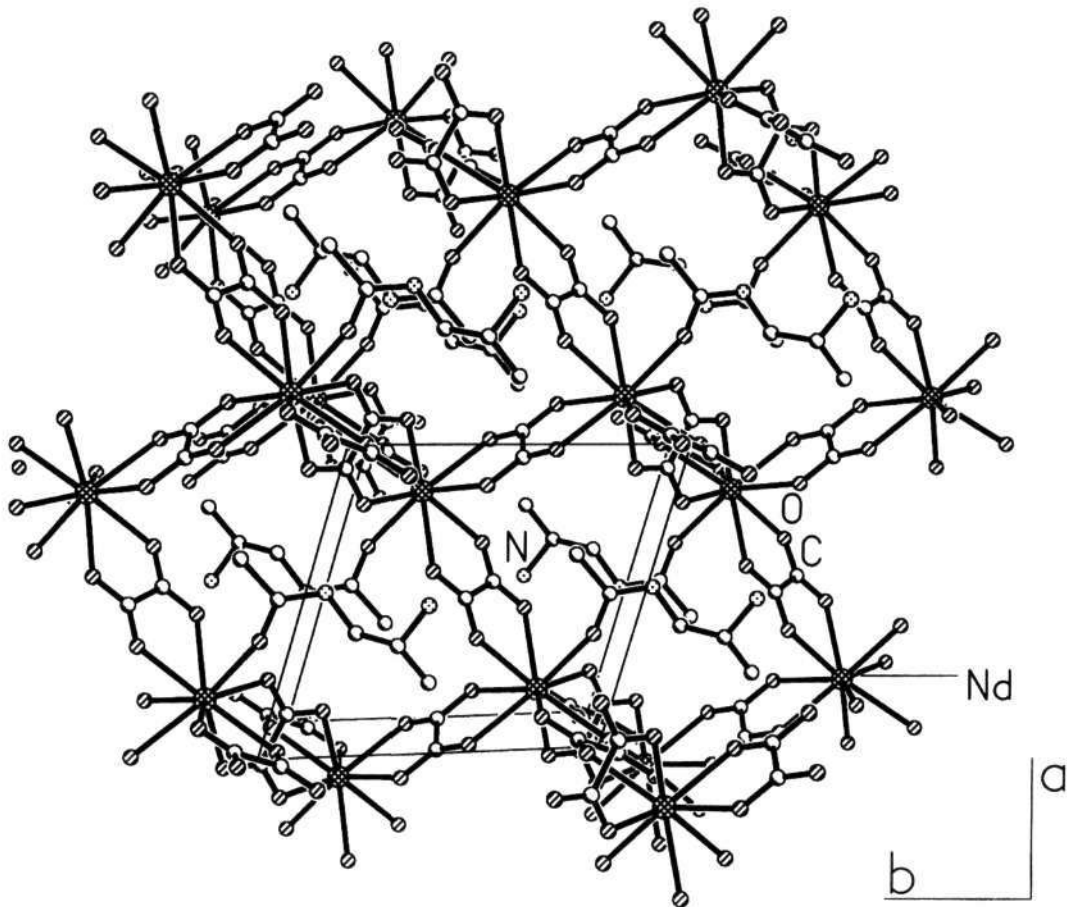
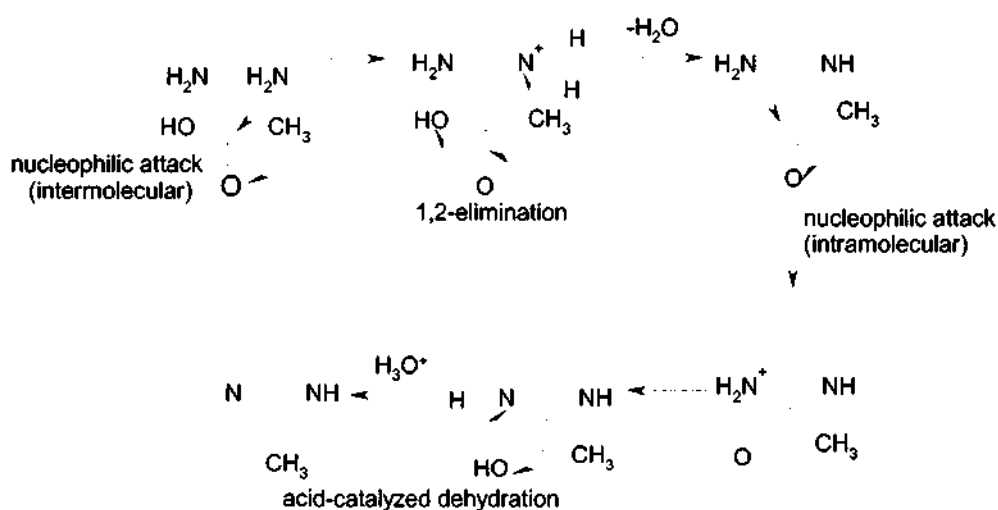


Fig. 4.43. Structure of **XIV** along the *c* axis showing the 12-membered channel. Note the in-plane and out-of-plane linkages by oxalate units.

4.5.2. Discussion

Four new open-framework rare-earth metal oxalates, $[C_6N_2H_{16}]_{0.5}[Y(H_2O)(C_2O_4)_2] \cdot 2(H_2O)$, **XI**, $[C_5N_2H_{12}][Y(C_2O_4)_2]$, **XII**, $[NH_3CH_2CH(NH_3)CH_3][Nd(C_2O_4)_2(HCOO)] \cdot H_2O$, **XIII** and $[OC(CH_3)NCH_2CH(CH_3)NH_3][Nd(C_2O_4)_2] \cdot H_2O$, **XIV**, have been obtained as good quality single crystals by hydrothermal methods. They are all members of a new family of framework solids with similar framework connectivities. Although the materials involve bonding between the oxalate units and rare-earth atoms, they exhibit distinct differences. In **XI**, **XIII** and **XIV** the connectivity leads to three-dimensional architecture with channels along all the crystallographic axes, in **XII** the channels are present in only one direction. In all the cases, the amine molecules occupy the channels. Additionally, free and bound water molecules are also present in the channels of **IX**, **XIII** and **XIV**.

It is noteworthy that the structures of **XI** and **XII** are somewhat related.



There is also a superficial similarity of the amines in **XI** and **XII** caused by the dynamic disorder of the amine in **XI**. In **XII**, the amine molecule, 2-methyl-3-4-5-

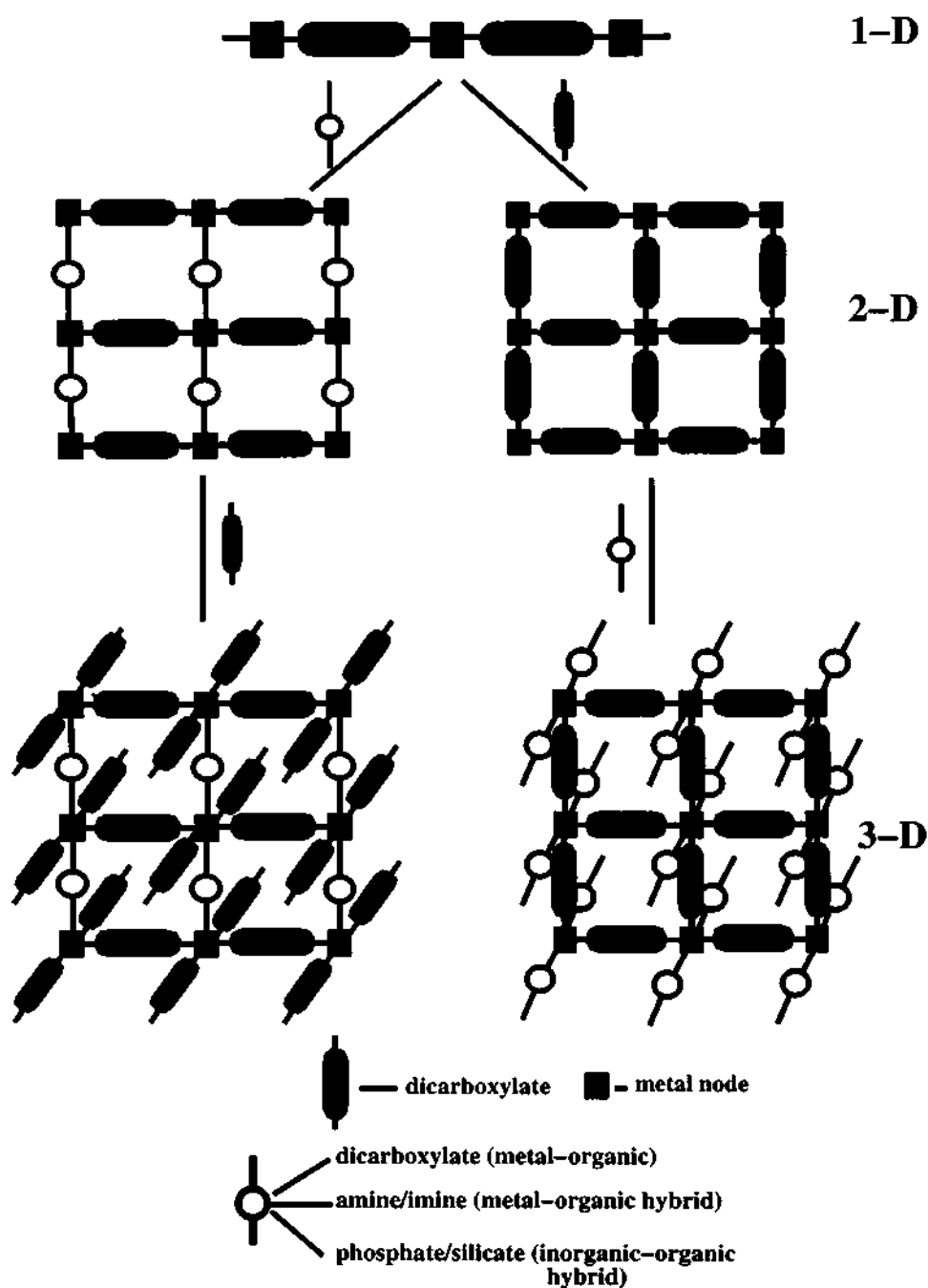
6-tetrahydro-pyrimid-1-ene, is formed *in-situ* by the reaction between 1,3-DAP and acetic acid. The formation of new types of amines under hydrothermal conditions has been observed before.^[47] The formation of 2-methyl-3-4-5-6-tetrahydro-pyrimid-1-ene can be explained on the basis of nucleophilic attack followed β -elimination as shown in the scheme above.

As in **XIII** and **XIV**, nine coordination for the rare earth atoms has been encountered in some rare earth carboxylates earlier, with the ninth coordination being provided by a water molecule.^[47] Although the structure of **XIV** is comparable to that of an yttrium oxalates, the organic species in the latter, 2-methyl-3-4-5-6-tetrahydropyrimid-1-ene, is free and occupies the channels, unlike in **XIV**, where N-(2-aminopropyl acetimide), is directly linked to neodymium.

The Y and Nd oxalates described here have features that can be compared and contrasted with those of the open-framework Zn oxalates discussed in section 4.2. In the Zn oxalates, the Zn atoms are 6-coordinated with respect to the oxalate oxygens, while in **XI** and **XII**, the Y atoms are 8-coordinated and in **XIII** and **XIV**, the Nd atoms are 9-coordinated. The framework of the Zn oxalates occur both as honeycomb layers and three-dimensional architectures. The three-dimensional Zn oxalate structure results from the *out-of-plane* connectivity of one of the oxalate units (Fig. 4.12). The commonality in the connectivity patterns among the various three-dimensional oxalates and other related hybrid structures and their possible mode of formation can be understood in terms of the Scheme 4.3.

4.5.3. Summary

The present study demonstrates the successful synthesis of rare-earth oxalates incorporating the organic amines, employing hydrothermal methods. The nature of the channels in **XI** is also reflected in its reversible adsorptive nature. Two new open- framework neodymium oxalates, having dangling organic functional

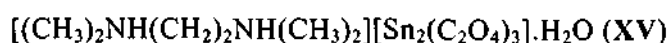


Scheme 4.3: A general schematic illustration of the possible construction of the three-dimensional structures from lower-dimensions by connecting metal centers with suitable ligands

groups uniformly distributed in the channels, has also been prepared. These Nd oxalates serve as interesting examples for the effective use of the ninth coordination of the rare-earth ion.

4.6. Open-framework tin(II) oxalate

4.6.1. Results



The asymmetric unit of the $[(\text{CH}_3)_2\text{NH}(\text{CH}_2)_2\text{NH}(\text{CH}_3)_2][\text{Sn}_2(\text{C}_2\text{O}_4)_3] \cdot \text{H}_2\text{O}$, XV, contains 15 non-hydrogen atoms (Fig. 4.44a) and the structure consists of macro-anionic sheets of formula $[\text{Sn}(\text{C}_2\text{O}_4)_{1.5}]^-$ with inter-lamellar $[(\text{CH}_3)_2\text{NH}(\text{CH}_2)_2\text{NH}(\text{CH}_3)_2]^{2+}$ ions. The framework is made up of a network of SnO_6 units [with pseudo-pentagonal bi-pyramidal geometry (Fig. 4.44b), assuming that one of the vertices is occupied by the lone-pair of electrons] and C_2O_4 moieties, which are linked to form puckered sheets that are stacked along a (Fig. 4.45-4.47). The lone pairs of electrons on Sn(II) project into the inter-lamellar spaces as shown in Figure 4.46, and the structure contains 8- (along the a axis) and 12-membered (along the b axis) apertures. The SDA (protonated N,N,N',N'-tetramethyl-1,2-diaminoethane) resides in the 12-membered pores along with water molecules (Fig. 4.45), and these pores penetrate the entire structure in a direction perpendicular to the sheets, yielding a solid with uni-dimensional channels ($\sim 4.8 \times 9.2 \text{ \AA}$; longest atom-atom contact distance not including the van der Waals radii). The various hydrogen bonding interactions between the puckered layers and the guest species are best seen in Figure 4.47.

The Sn – O distances are in the range 2.182 – 2.596 Å (av. 2.424 Å), with the oxygens that are double bonded to the carbon atoms having longer distances. These are reflected in the C – O bonding too (Table 4.15). The O – Sn – O and O – C – O bond angles are in the range 65.4 - 149.9° and 124.4 - 125.0° (Table 4.15).

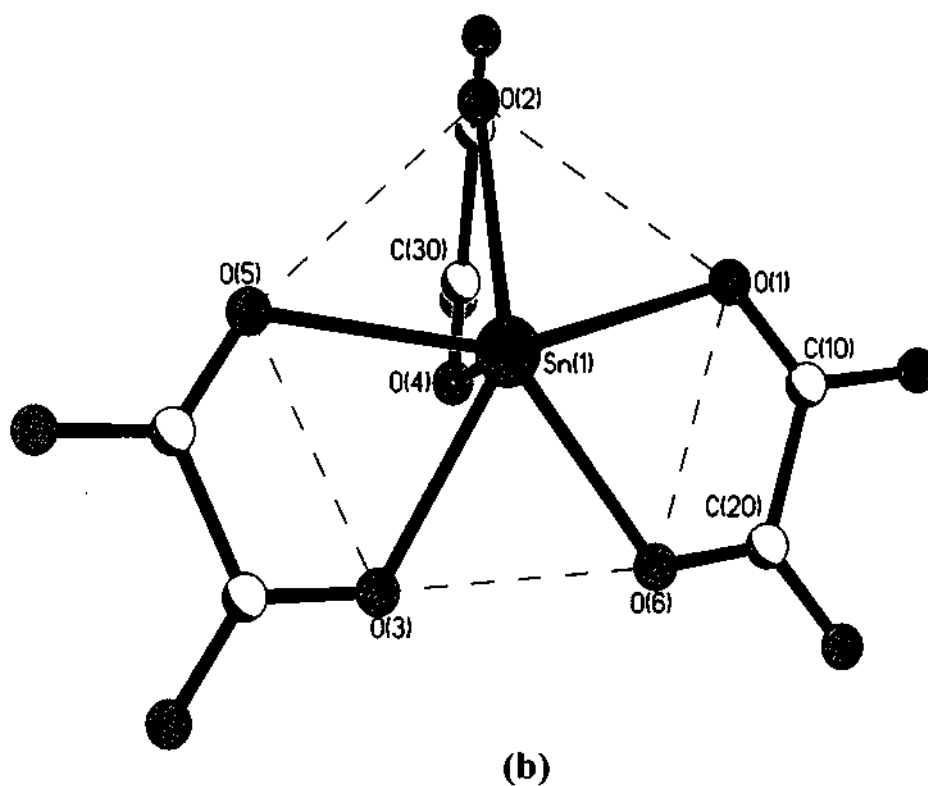
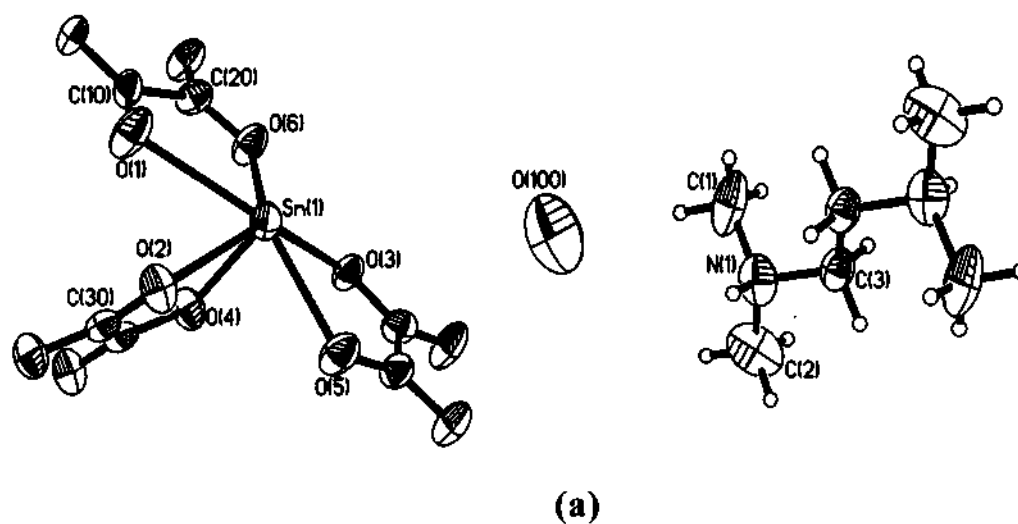


Fig. 4. 44. (a) ORTEP plot of XV, $[(\text{CH}_3)_2\text{NH}(\text{CH}_2)_2\text{NH}(\text{CH}_3)_2]^{2+}[\text{Sn}_2(\text{C}_2\text{O}_4)_3]^{2-}$ H_2O showing the connectivity (asymmetric unit is labelled). Thermal ellipsoids are given at 50% probability. (b) View showing the stereochemistry around Sn.

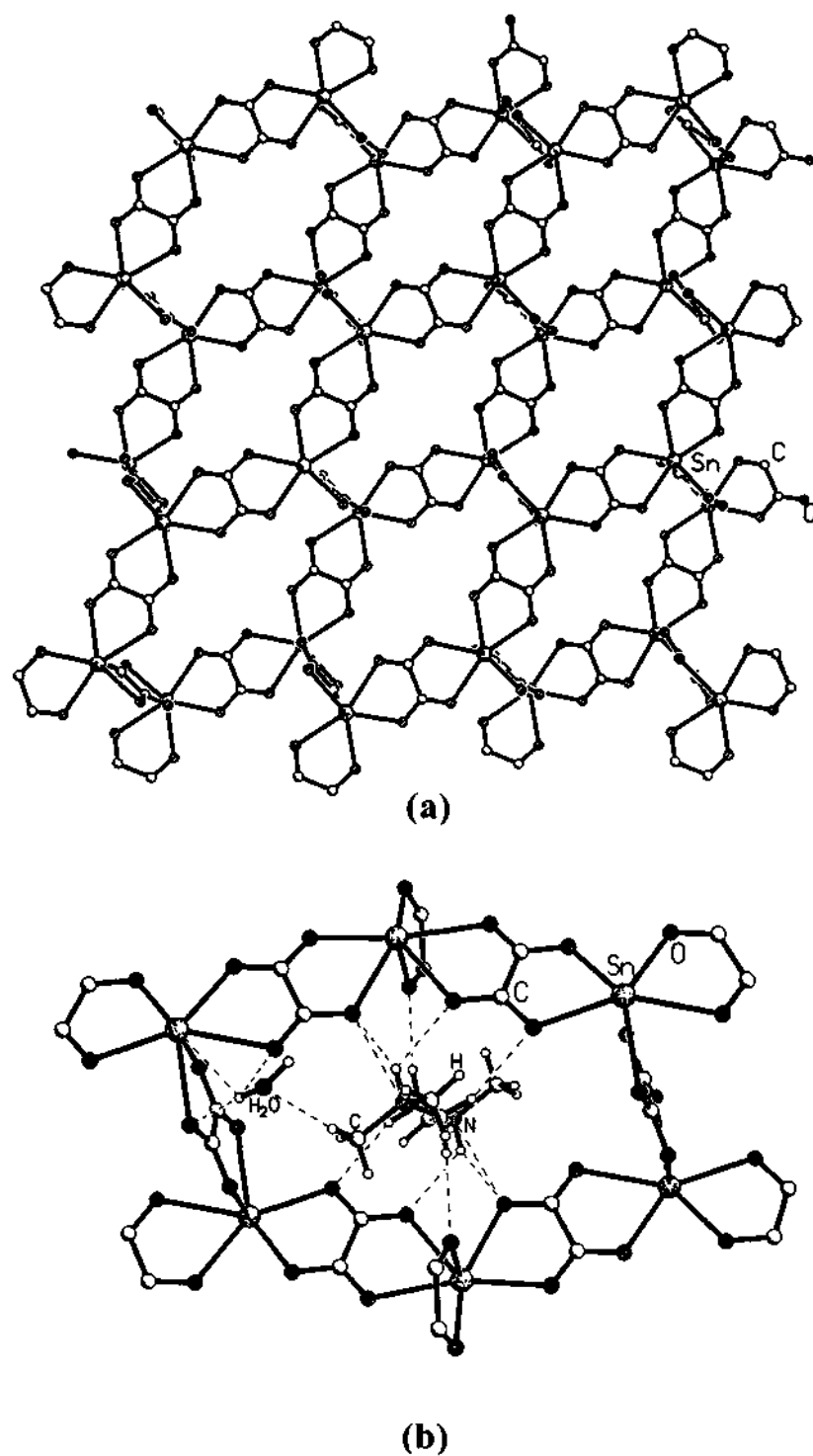


Fig. 4.45. (a) Structure of XV, $[(\text{CH}_3)_2\text{NH}(\text{CH}_2)_2\text{NH}(\text{CH}_3)_2]^{2+}[\text{Sn}_2(\text{C}_2\text{O}_4)_3]^{2-} \cdot \text{H}_2\text{O}$ along the *a* axis showing the 12-membered aperture within one single layer. (b) Figure showing the hydrogen bond interaction of the amine and water molecules with the framework within a 12-membered aperture.

TGA of **XV** was carried out in static air from room temperature to 900° C. The weight loss occurs in two steps. A sharp mass loss of about 18% at 300°C corresponds to the loss of the amine along with the hydrogen bonded water molecules (calc. 21.3%) and the loss of about 16% in the region 360-440°C corresponds to the loss of carbon from the oxalate group. The powder XRD patterns of the decomposed products indicated a poorly crystalline nature with very weak reflections corresponding to SnO (JCPDS: 13-111).

4.6.2. Discussion

The important feature of the framework is the hexa-coordinated tin atoms with a configuration similar to the classic 14-electron systems such as $[IF_6]$. This feature is observed in a previous tin(II) oxalate structure as well.³² The lone-pairs of the tin atoms play an important role in the structure. The stereoactive lone-pairs manifest themselves in the lattice by creating open spaces such as the space between the two layers in these tin oxalates. Similar lone-pair positioning have been observed in many of the layered tin(II) phosphate and related materials.^{83,84} In such an arrangement the direct interaction between the lone pairs gets avoided, enhancing the stability of the structure. This situation is reminiscent of $[XeF_5]^+$ type systems where other donor groups approach the Xe atoms obliquely to avoid the lone pair repulsions.⁷¹ The coordination environment of Sn(II) atoms in phosphates and oxalates presents an interesting comparison. Most of the tin(II) phosphates have three- or four- coordination, forming a trigonal pyramidal SnO_3 or distorted square-pyramidal SnO_4 moieties.²⁰⁻²⁴ In the tin oxalate, the Sn atoms are hexa-coordinated. This is probably because the average charge per oxygen on the oxalate (0.5) is less than that on the phosphate (0.75) and more oxalate oxygens are therefore needed to satisfy the valence of tin.

Table 4.15. Selected bond distances and angles in XV, $[(\text{CH}_3)_2\text{NH}(\text{CH}_2)_2\text{NH}(\text{CH}_3)_2]^{2+}[\text{Sn}_2(\text{C}_2\text{O}_4)_3]^{2-}\cdot\text{H}_2\text{O}$

Moiety	Distance (Å)	Moiety	Distance (Å)
Framework			
Sn(1) – O(1) ^{#1}	2.596(6)	Sn(1) – O(2)	2.513(6)
Sn(1) – O(3)	2.375(5)	Sn(1) – O(4)	2.182(5)
Sn(1) – O(5)	2.450(6)	Sn(1) – O(6)	2.427(5)
C(10) – O(1)	1.230(10)	C(10) – O(3)	1.280(10)
C(20) – O(5)	1.237(9)	C(20) ^{#1} – O(6)	1.255(9)
C(30) – O(2)	1.237(8)	C(30) ^{#2} – O(4)	1.277(9)
C(10) – C(20)	1.543(11)	C(30) – C(30) ^{#2}	1.54(2)
Organic moiety			
C(1) – N(1)	1.518(12)	C(2) – N(1)	1.494(13)
C(3) – N(1)	1.475(10)	C(3) – C(3) ^{#3}	1.53(2)
Moiety	Angle (°)	Moiety	Angle (°)
Framework			
O(1) ^{#1} – Sn(1) – O(2)	70.7(2)	O(1) ^{#1} – Sn(1) – O(3)	130.6(2)
O(1) ^{#1} – Sn(1) – O(4)	77.5(2)	O(1) ^{#1} – Sn(1) – O(5)	149.9(2)
O(1) ^{#1} – Sn(1) – O(6)	65.4(2)	O(2) – Sn(1) – O(3)	136.2(2)
O(2) – Sn(1) – O(4)	70.3(2)	O(2) – Sn(1) – O(5)	80.3(2)
O(2) – Sn(1) – O(6)	131.1(2)	O(3) – Sn(1) – O(4)	78.0(2)
O(3) – Sn(1) – O(5)	67.6(2)	O(3) – Sn(1) – O(6)	68.6(2)
O(4) – Sn(1) – O(5)	85.3(2)	O(4) – Sn(1) – O(6)	80.1(2)
O(5) – Sn(1) – O(6)	135.8(2)	O(1) – C(10) – O(3)	124.9(7)
O(5) – C(20) – O(6) ^{#3}	125.0(8)	O(2) – C(30) – O(4) ^{#2}	124.4(7)
O(1) – C(10) – C(20)	119.5(8)	O(2) – C(30) – C(30) ^{#2}	118.6(10)
O(3) – C(10) – C(20)	115.6(8)	O(4) ^{#2} – C(30) – C(30) ^{#2}	117.0(9)
O(5) – C(20) – C(10)	118.2(8)	O(6) ^{#3} – C(20) – C(10)	116.8(8)
Organic Moiety			
C(1) – N(1) – C(2)	111.4(8)	C(1) – N(1) – C(3)	111.4(8)
C(2) – N(1) – C(3)	109.8(8)	N(1) – C(3) – C(3) ^{#4}	111.9(9)

Symmetry transformations used to generate equivalent atoms:

#1 $x, -y-1, z-1/2$ #2 $-x+3/2, -y-3/2, -z$ #3 $x, -y-1, z+1/2$ #4 $-x+1/2, -y-1/2, -z+1$

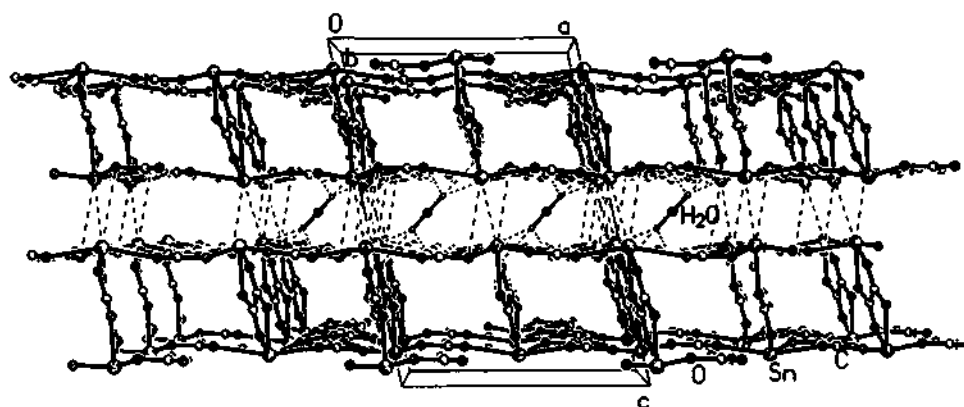


Fig. 4.46. Structure of XV, $[(\text{CH}_3)_2\text{NH}(\text{CH}_2)_2\text{NH}(\text{CH}_3)_2]^{2+}[\text{Sn}_2(\text{C}_2\text{O}_4)_3]^{2-}\cdot\text{H}_2\text{O}$ along the *b* axis showing the 8-membered aperture and the interactions between the water molecules and the framework layers. Note that the dotted lines also show the interactions between the tin atoms (lone-pair interactions) (amine molecules are not shown for clarity).

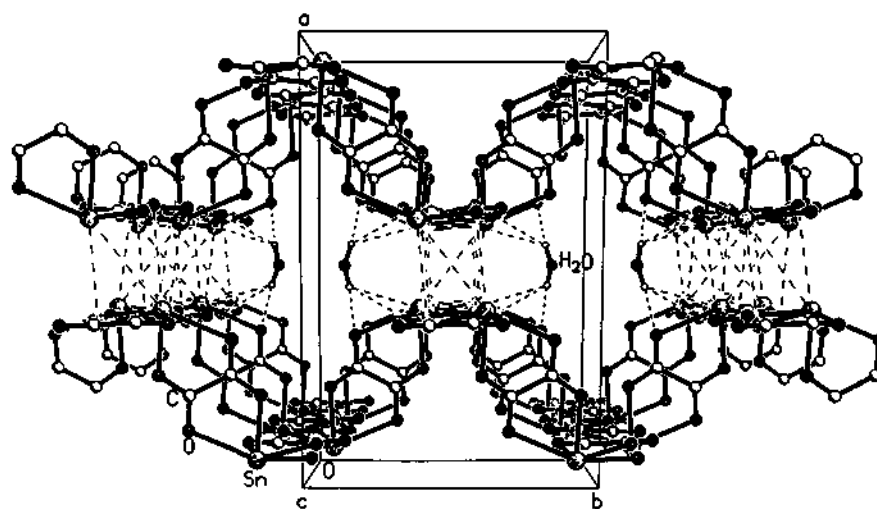


Fig. 4. 47. Structure of XV, $[(\text{CH}_3)_2\text{NH}(\text{CH}_2)_2\text{NH}(\text{CH}_3)_2]^{2+}[\text{Sn}_2(\text{C}_2\text{O}_4)_3]^{2-}\cdot\text{H}_2\text{O}$ along the *c* axis showing the layers and the water molecules. Dotted lines represent the various interactions between the layers and the guest species (see text).

It is also to be noted that **XV** was synthesized by an adjustment of the pH of the synthetic mixture (different phases are formed at lower pH^{74,24,77} and the synthesis was effected at near neutral pH. We believe that the phosphoric acid in the initial synthesis mixture essentially acts as a mineralizer, similar to F⁻ ions in some of the phosphate-based framework solids reported in the literature,^{78,85} rather than forming part of the framework (synthesis of phosphate framework materials is generally carried out under acidic conditions).

4.6.3. Summary

The present study shows that open-framework tin(II) oxalates can be synthesized by employing structure-directing amines. It is noteworthy that the oxalate, **XV**, presented has an unusual coordination for Sn resembling the classic 14 electron systems such as [IF₆]⁻. The unique coordination environment of Sn(II) described here suggests that it would be profitable to explore this lead further by investigating other Sn(II) dicarboxylates synthesized under similar conditions. Dicarboxylates of other metals are also likely to yield interesting coordination environments and new open-framework structures.

The metal oxalate structures discussed hitherto suggests the possibility of generating complex supramolecular structures with multifarious properties and functionalities, by utilizing the ability of the oxalate units to align the metal centers in two and three-dimensional assemblies. Thus, it would be meritorious to build three-dimensional structures by connecting simpler predetermined building units such as metal oxalate ladders, chains or layers and linking these through bridging oxalates to reticulate channels with the desired magnetic characteristics. At the molecular level, it is also desirable to utilize basic building units that can carry pre-coded chemical information to generate the larger framework structures.

Higher dicarboxylates

4.7. Cadmium malonate and Manganese glutarate

4.7.1. Results

$[\text{Cd}(\text{O}_2\text{C}-\text{CH}_2-\text{CO}_2)(\text{H}_2\text{O})]\cdot\text{H}_2\text{O}$ (XVI)

The asymmetric unit of the malonate, $[\text{Cd}(\text{O}_2\text{C}-\text{CH}_2-\text{CO}_2)(\text{H}_2\text{O})]\cdot\text{H}_2\text{O}$, XVI, contains 10 non-hydrogen atoms, of which 9 belong to the cadmium malonate framework and the remaining is a free water molecule. The Cd atom is seven-coordinated and has a distorted pentagonal bipyramidal arrangement. The equatorial positions are occupied by the malonate oxygen atoms and the apical positions are occupied by a water molecule and a malonate oxygen. The Cd–O distances are in the range of 2.288(7) – 2.545(5) Å (av. 2.369 Å) and the average O–Cd–O angle is 102.3°. The malonate unit has the expected bond distances and angles (Table 4.16). A similar coordination for cadmium has been observed in other cadmium dicarboxylates.^[49,50] There are two types of water molecules in XVI, one bound to the Cd atom and the other present in the channels. Bond valence sum calculations^[21] indicated the oxidation numbers of Cd, C and O to be 2+, 4+ and 2-, as expected. Ancillary ligation by water molecules has been observed in other metal carboxylates.^[49,50]

The structure of XVI can be described as a one-dimensional chain formed by corner-sharing CdO_7 pentagonal bipyramids, with the adjacent pentagonal bipyramids shifted and rotated with respect to each other, rendering the chain sinusoidal (See top of Fig.4.48). Six such chains, arranged in a hexagonal array through corner-sharing, form the three-dimensional framework. Thus, the entire structure is built up of an infinite array of corner-sharing CdO_7 pentagonal bipyramids, with unidirectional hexagonal channels (6.95 x 6.95 Å, shortest C - C contact not including the van der Waals radii) along the *c*-axis (Fig. 4.48). The inner

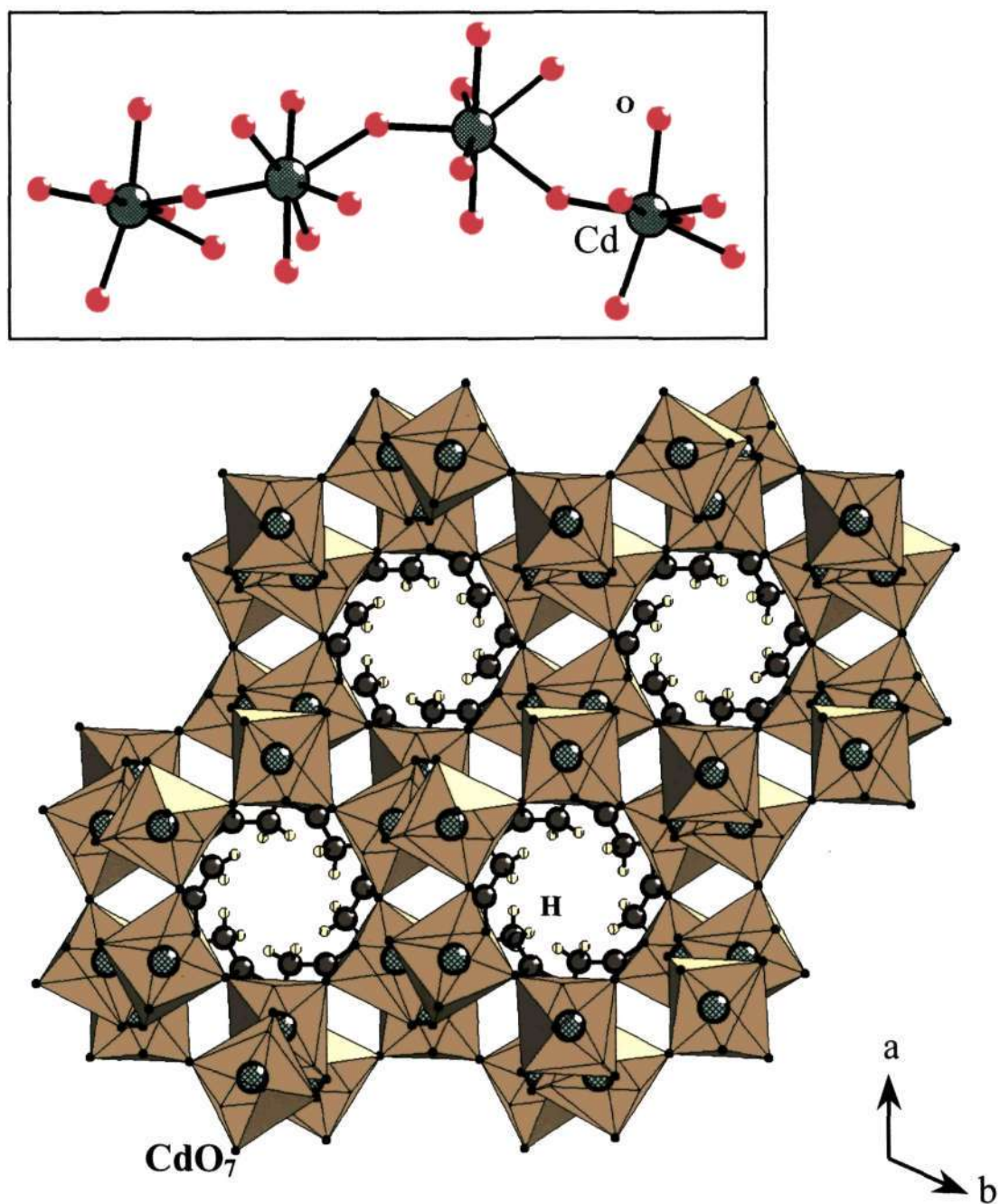


Fig. 4.48. Structure of **XVI** showing the 12-membered, methylene-lined hydrophobic channels. Note the presence of the free water molecules in the small apertures.

Table 4.16. Selected bond distances and angles for $[\text{Cd}(\text{O}_2\text{C}-\text{CH}_2-\text{CO}_2)(\text{H}_2\text{O})]\cdot\text{H}_2\text{O}$, XVI

Moiety	Distance (Å)	Moiety	Distance (Å)
Cd(1)-O(10)	2.288(7)	Cd(1)-O(2)#1	2.535(6)
Cd(1)-O(1)	2.288(5)	Cd(1)-O(1)#2	2.545(5)
Cd(1)-O(2)	2.293(6)	O(1)-Cd(1)#5	2.545(5)
Cd(1)-O(3)	2.312(6)	O(2)-Cd(1)#6	2.535(6)
Cd(1)-O(4)	2.319(6)		
Moiety	Angle(°)	Moiety	Angle(°)
O(10)-Cd(1)-O(1)	165.5(2)	O(4)-Cd(1)-O(2)#1	53.6(2)
O(10)-Cd(1)-O(2)	83.6(2)	O(10)-Cd(1)-O(1)#2	85.1(2)
O(1)-Cd(1)-O(2)	82.0(2)	O(1)-Cd(1)-O(1)#2	93.7(3)
O(10)-Cd(1)-O(3)	106.7(2)	O(2)-Cd(1)-O(1)#2	89.3(2)
O(1)-Cd(1)-O(3)	83.8(2)	O(3)-Cd(1)-O(1)#2	53.2(2)
O(2)-Cd(1)-O(3)	138.6(2)	O(4)-Cd(1)-O(1)#2	174.2(2)
O(10)-Cd(1)-O(4)	89.2(2)	O(2)#1-Cd(1)-O(1)#2	124.7(2)
O(1)-Cd(1)-O(4)	92.1(2)	C(1)#5-O(1)-Cd(1)	126.7(5)
O(2)-Cd(1)-O(4)	91.3(2)	C(1)#5-O(1)-Cd(1)#5	87.1(4)
O(3)-Cd(1)-O(4)	127.9(2)	Cd(1)-O(1)-Cd(1)#5	143.1(2)
O(10)-Cd(1)-O(2)#1	86.5(2)	C(2)#6-O(2)-Cd(1)	127.7(5)
O(1)-Cd(1)-O(2)#1	105.8(2)	C(2)#6-O(2)-Cd(1)#6	87.3(5)
O(2)-Cd(1)-O(2)#1	143.6(2)	C(1)-O(3)-Cd(1)	98.3(5)
O(3)-Cd(1)-O(2)#1	77.7(2)	C(2)-O(4)-Cd(1)	97.9(5)

Symmetry transformations used to generate equivalent atoms in I:

#1 $-x+y+2/3, -x+1/3, z+1/3$ #2 $y+1/3, -x+y+2/3, -z+5/3$ #3 $x-y, x, -z+2$

#4 $y, -x+y, -z+2$ #5 $x-y+1/3, x-1/3, -z+5/3$ #6 $-y+1/3, x-y-1/3, z-1/3$

walls of the channels are lined by the methylene groups of the malonate moiety, making them hydrophobic. The water molecule bound to Cd protrudes into the 12-membered channels along the a -axis, whilst the free water molecule reside in a smaller aperture formed due to corner-sharing between two adjacent chains.

$[\text{Mn}(\text{O}_2\text{C}-(\text{CH}_2)_3-\text{CO}_2)]$ (XVII)

The asymmetric unit of the glutarate, $[\text{Mn}(\text{O}_2\text{C}-(\text{CH}_2)_3-\text{CO}_2)]$, XVII, consists of 12 non-hydrogen atoms, of which, three are crystallographically

independent Mn atoms. Mn(1) has 1/3 occupancy, Mn(2) has 1/6 occupancy and Mn(3) has 1/2 occupancy. All three Mn atoms are octahedrally coordinated by the

Table 4.17. Selected bond distances and angles for [Mn(O₂C-(CH₂)₃-CO₂)], XVII

Moiety	Distance (Å)	Moiety	Distance (Å)
Mn(1)-O(1)#1	2.1812(13)	Mn(2)-O(3)#4	2.1483(13)
Mn(1)-O(1)	2.1812(13)	Mn(2)-O(3)#2	2.1483(13)
Mn(1)-O(1)#2	2.1813(13)	Mn(2)-O(3)#5	2.1483(13)
Mn(1)-O(2)	2.2772(13)	Mn(3)-O(4)#6	2.1118(14)
Mn(1)-O(2)#1	2.2772(13)	Mn(3)-O(4)	2.1117(14)
Mn(1)-O(2)#2	2.2773(13)	Mn(3)-O(1)#6	2.1927(13)
Mn(2)-O(3)	2.1482(13)	Mn(3)-O(1)	2.1926(13)
Mn(2)-O(3)#1	2.1483(13)	Mn(3)-O(2)	2.2122(13)
Mn(2)-O(3)#3	2.1483(13)	Mn(3)-O(2)#6	2.2122(13)
Moiety	Angle (°)	Moiety	Angle (°)
O(1)#1-Mn(1)-O(1)	105.12(4)	O(3)#1-Mn(2)-O(3)#5	180
O(1)#1-Mn(1)-O(1)#2	105.12(4)	O(3)#3-Mn(2)-O(3)#5	88.60(5)
O(1)-Mn(1)-O(1)#2	105.12(4)	O(3)#4-Mn(2)-O(3)#5	88.60(5)
O(1)#1-Mn(1)-O(2)	86.89(5)	O(3)#2-Mn(2)-O(3)#5	91.39(5)
O(1)-Mn(1)-O(2)	76.64(5)	O(4)#6-Mn(3)-O(4)	180
O(1)#2-Mn(1)-O(2)	166.64(5)	O(4)#6-Mn(3)-O(1)#6	91.17(5)
O(1)#1-Mn(1)-O(2)#1	76.64(5)	O(4)-Mn(3)-O(1)#6	88.83(5)
O(1)-Mn(1)-O(2)#1	166.64(5)	O(4)#6-Mn(3)-O(1)	88.82(5)
O(1)#2-Mn(1)-O(2)#1	86.89(5)	O(4)-Mn(3)-O(1)	91.18(5)
O(2)-Mn(1)-O(2)#1	90.33(5)	O(1)#6-Mn(3)-O(1)	180
O(1)#1-Mn(1)-O(2)#2	166.64(5)	O(4)#6-Mn(3)-O(2)	89.52(6)
O(1)-Mn(1)-O(2)#2	86.89(5)	O(4)-Mn(3)-O(2)	90.48(6)
O(1)#2-Mn(1)-O(2)#2	76.64(5)	O(1)#6-Mn(3)-O(2)	102.22(5)
O(2)-Mn(1)-O(2)#2	90.33(5)	O(1)-Mn(3)-O(2)	77.78(5)
O(2)#1-Mn(1)-O(2)#2	90.32(5)	O(4)#6-Mn(3)-O(2)#6	90.48(6)
O(3)-Mn(2)-O(3)#1	88.61(5)	O(4)-Mn(3)-O(2)#6	89.52(6)
O(3)-Mn(2)-O(3)#3	91.39(5)	O(1)#6-Mn(3)-O(2)#6	77.78(5)
O(3)#1-Mn(2)-O(3)#3	91.40(5)	O(1)-Mn(3)-O(2)#6	102.22(5)
O(3)-Mn(2)-O(3)#4	180	O(2)-Mn(3)-O(2)#6	180
O(3)#1-Mn(2)-O(3)#4	91.40(5)	C(1)-O(1)-Mn(1)	125.50(12)
O(3)#3-Mn(2)-O(3)#4	88.61(5)	C(1)-O(1)-Mn(3)	133.99(12)

O(3)-Mn(2)-O(3)#2	88.61(5)	C(2)#7-O(2)-Mn(3)	132.14(13)
O(3)#1-Mn(2)-O(3)#2	88.60(5)	C(2)#7-O(2)-Mn(1)	128.82(12)
O(3)#3-Mn(2)-O(3)#2	180	C(1)-O(3)-Mn(2)	129.01(13)
O(3)#4-Mn(2)-O(3)#2	91.39(5)	C(2)-O(4)-Mn(3)	136.86(13)
O(3)-Mn(2)-O(3)#5	91.39(5)		

Symmetry transformations used to generate equivalent atoms in **II**:

#1 -y,x-y,z #2 -x+y,-x,z #3 x-y,x,-z #4 -x,-y,-z #5 y,-x+y,-z #6 -x-1/3,-y-2/3,-z+1/3 #7 y+2/3,-x+y+1/3,-z+1/3 #8 x-y-1/3,x-2/3,-z+1/3 #9 -x+y,-x-1,z #10 -y-1,x-y-1,z

glutarate oxygens, with the average Mn-O distances of 2.229 Å, 2.148 Å and 2.172 Å for Mn(1)-O, Mn(2)-O and Mn(3)-O respectively and the average O-Mn-O angles of 105.1°, 108.0° and 108.0° for Mn(1), Mn(2) and Mn(3) respectively. Open-framework manganese dicarboxylates involving octahedrally coordinated Mn atoms have been reported recently.^[51] Bond valence sum calculations^[21] indicated that the valence states of the Mn, C and O in **XVII** were +2, +4 and -2 respectively. The glutarate moiety has the expected bond distances and angles (Table 4.17). The edge-sharing Mn(1)O₆ and Mn(3)O₆ octahedra form an infinite two-dimensional array possessing honeycomb-like apertures in the *ab*-plane, (6.642 x 6.642 Å, shortest C - C contact not including the van der Waals radii) (Fig. 4.49a). These layers are cross-linked by isolated Mn(2)O₆ octahedra and *out-of-plane* glutarate moieties to give rise to the three-dimensional architecture (Fig. 4.49b). Two-dimensional structures with open architectures are known to achieve efficient packing by the shifting of the adjacent layers.^[52] Accordingly, in **XVII** the layers formed by the edge-sharing octahedra get shifted by 1/2 the unit cell length along the *b*- and *a*- axes and thereby contribute negatively to the openness of the structure.

Thermogravimetric analysis (TGA) of **XVI** and **XVII** was carried out in a N₂ atmosphere (50 ml min⁻¹) in the 25° to 700 °C range (Fig. 4.50). **XVI** showed a mass loss of 14.8% in the range of 100-180 °C due to the loss of the lattice and the

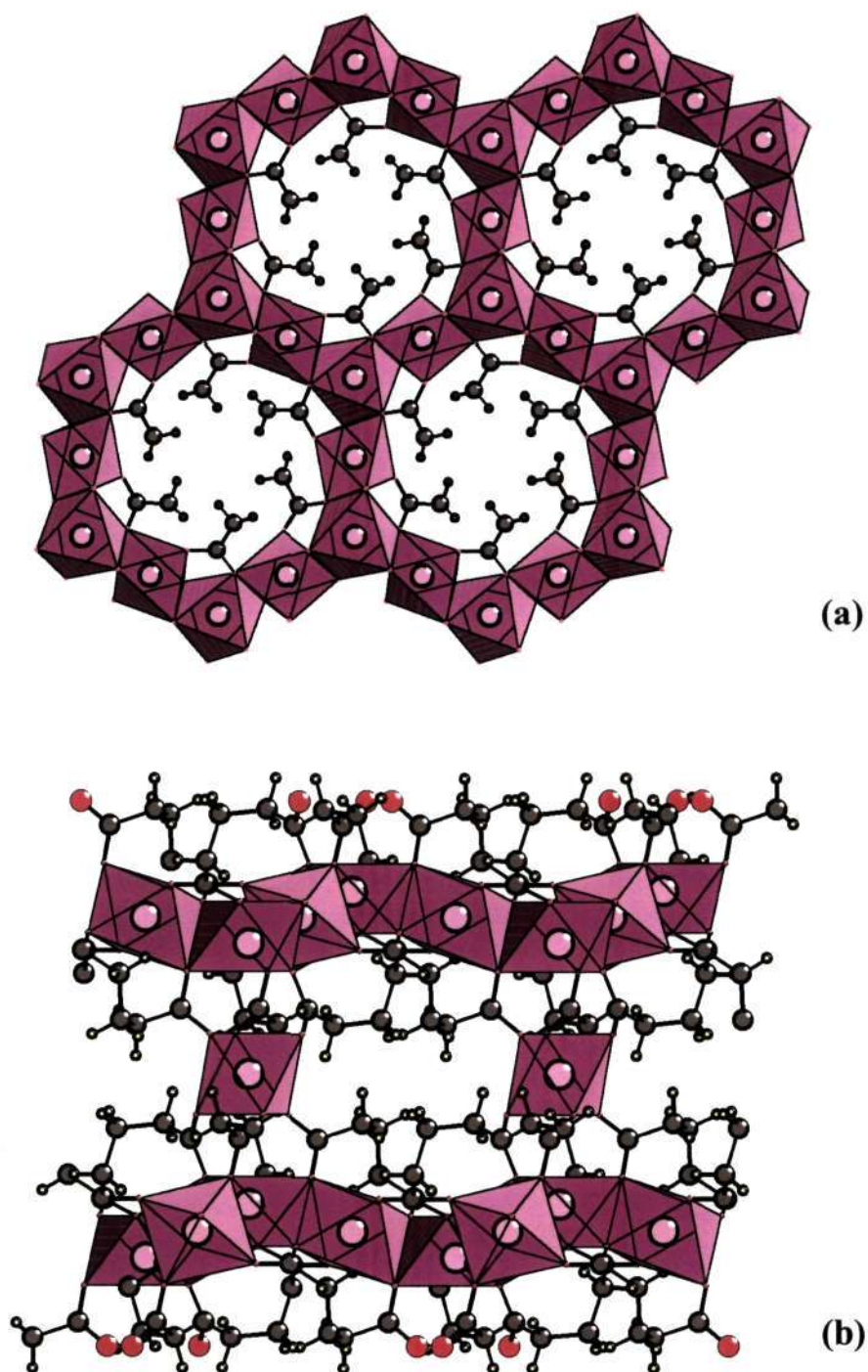


Fig. 4.49. (a) Structure of **XVII** showing the 12-membered C-backbone of glutarate-lined hydrophobic channels, formed by the edge-sharing MnO₆ octahedra. (b) Figure shows the connectivity between adjacent MnO layers *via* isolated Mn(3)O₆ octahedra in **XVII**. Note that the isolated octahedra are covalently linked by the glutarate units with the inorganic layers.

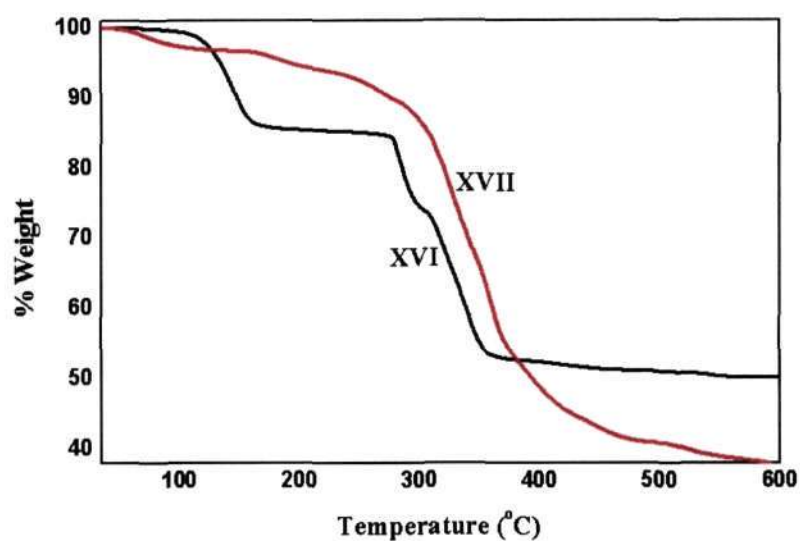


Fig. 4.50. TGA curves of **XVI** and **XVII**

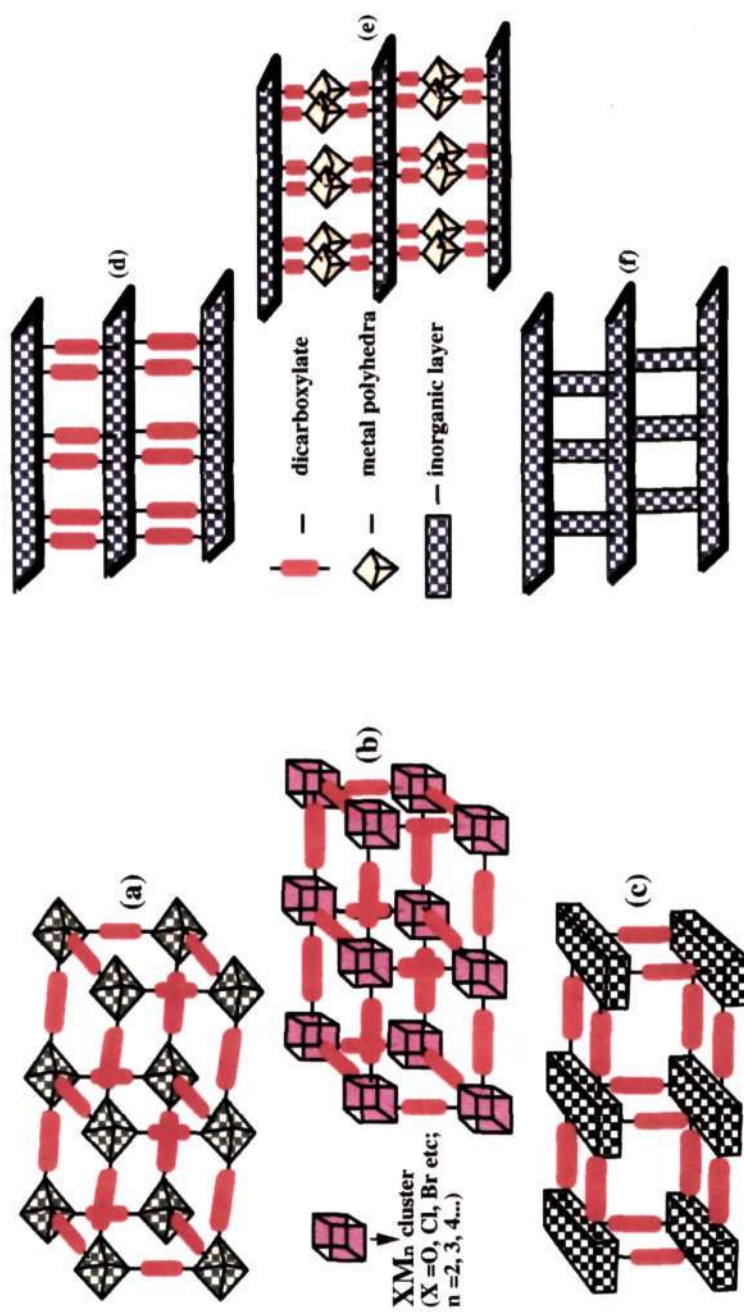
bonded water (calc. 14.3%), followed by a sharp mass loss of 35.4% in the range 220–350 °C due to the loss of the malonate moiety (calc. 34.6%). The powder XRD pattern of the product of decomposition of **XVI**, showed characteristic peaks of mineral monteporite, CdO, (JCPDS: 05-0640). **XVII** showed a gradual mass loss of 53.2% in the range 210–450 °C due to the loss of the glutarate moiety (calc. 53.0%). A very small weight loss is observed in the 50–100 °C due to the loss of some adsorbed species. The product of decomposition of **XVII**, as revealed by the powder XRD pattern, was MnO₂ (JCPDS: 44-0992).

4.7.2. Discussion

Both **XVI** and **XVII** have extended inorganic structures formed by corner- and edge-sharing of metal-oxygen polyhedra. **XVI** has a three-dimensional structure arising entirely from the infinite Cd-O-Cd connectivities while **XVII** exhibits infinite Mn-O-Mn connectivities in two dimensions. The three-dimensional nature

of **XVII** is derived through the *out-of-plane* connectivities between the Mn-O-Mn sheets and the glutarate and the isolated MnO_6 octahedral units. The M-O-M connectivity in **XVI** bears some resemblance to that in the Ni succinate reported by Foster and Cheetham.^[53] The M-O-M linkage in **XVI** occurs through corner-sharing of CdO_7 pentagonal bipyramids, whilst in the Ni succinate, it is through the edge-shared NiO_6 octahedra. The M-O-M linkages in **XVII**, are comparable to those observed in two- and three-dimensional Co succinates,^[54] but the interlayer connectivity between the two structures is different. The Co-O-Co layers in the cobalt succinate are connected by carboxylate pillars and the Mn-O-Mn layers in **XVII** are linked through isolated MnO_6 octahedra.

Several two-dimensional metal-dicarboxylate frameworks with apertures have been reported in the literature.^[54a,55] There are also examples where organic ligands link to the metal ions giving rise to 3-D structures.^[38] Some of the possible ways of building up the three-dimensional metal-dicarboxylate frameworks are illustrated in Scheme 4.4. The motif (e) in the scheme is similar to the compound **XVII** and the motif (f) is similar to compound **XVI**. There are examples available in the literature that corresponds to some of the other motifs given in scheme 4.4. Considering the structures of nickel^[53] the cobalt succinates^[54b] along with the structure of **XVI**, we notice that the common feature in these compounds under discussion is the presence of channels lined by the methylene groups of the dicarboxylate moieties, giving rise to a highly hydrophobic environment within them. It is worthy to mention that a three-dimensional vanadyl carboxylate framework possessing hydrophobic channels, exhibiting interesting adsorption properties has been reported recently.^[56] This is indeed a noteworthy feature and it is possible that such channels may show significant selectivity for non polar species. The formation of compound **XVI** at room temperature also shows the



Scheme 3: A schematic illustrating how different inorganic units can get linked through dicarboxylate units to generate three-dimensional open-framework architectures. Motif (a) represents isolated polyhedra, which could be a dimer or a trimer also, connected in all directions by dicarboxylate linkers (Ref. 17b, 30); (b) represents the metal clusters linked via dicarboxylates (Ref. 15); (c) shows the aligning of one-dimensional inorganic metal-oxygen chains by dicarboxylate linkers (Ref. 16c,31); (d) shows the classic pillaring of inorganic MO layers by the dicarboxylate units (Ref. 19b, 32); (e) represents inorganic layers pillared by isolated polyhedra through coordinating dicarboxylate linkers (e.g. Compound II); (f) shows three-dimensionality arising from the connectivities among the polyhedra (e.g. Compound I, Ref. 17a, 33). It is important to note that the dicarboxylate oxygens are directly involved in the formation of the inorganic units.

possibility of forming other open-framework structures with infinite M-O-M connectivities, under milder reaction conditions (*chimie douce*).^[54c]

4.7.3. Summary

Cadmium malonate, **XVI**, and manganese glutarate, **XVII**, with three-dimensional structures have been prepared and characterized. Both the compounds have channels lined by methylene groups providing a hydrophobic interior. In addition, **XVI**, has the three-dimensional connectivity arising entirely from the corner-sharing CdO_7 polyhedra, while the three-dimensional structure of **XVII** arises from the linking of the inorganic layers by isolated MnO_6 octahedra and the glutarate moieties. It is likely that many such metal-carboxylates with open-architectures can be made by a suitable choice of the reactants and conditions.

4.8. Open-framework cadmium succinates of different dimensionalities

4.8.1. Results

$[\text{CN}_3\text{H}_6]_2[\text{Cd}_2(\text{C}_4\text{H}_4\text{O}_4)(\text{Cl})_2]$ (**XVIII**)

The asymmetric unit of $[\text{CN}_3\text{H}_6]_2[\text{Cd}_2(\text{C}_4\text{H}_4\text{O}_4)(\text{Cl})_2]$, **XVIII** contains 19 non-hydrogen atoms, of which 11 belong to the cadmium chlorosuccinate chains and the rest to the amine molecule. The Cd atom is coordinated to four succinate oxygens and two chlorine atoms forming a distorted octahedron with an average Cd – O/Cl distance of 2.458 Å. The average O/Cl – Cd – O/Cl angle is 100.8 ° (Table 4.18). The succinate units and the amine molecules have the usual bond distances and angles. The Cd atoms are connected to two succinate units forming a one-dimensional chain with two pendant chlorine atoms (Fig. 4.51). The protonated guanidinium cations occupy the inter-chain spaces and interact with the succinate oxygens and the pendant Cl –atoms via. hydrogen bonds. A noteworthy feature in **XVIII**, is the presence of M-Cl...H interactions, which have been shown to play an important role in crystal engineering,^[10,57] being prominent in

organic/organometallic compounds.^[58] Such interactions are, however, not known in extended solids. It appears that the M-Cl...H interactions in XVIII (Fig. 4.51), with Cd-Cl(1)...H = 2.874 and Cd-Cl(2)...H = 2.734 Å distances (classified as intermediate distances),^[57] make a significant contribution in stabilizing the lower dimensional structure of XVIII. Similar interactions have been observed in a two-dimensional zinc chloro-phosphate compound, where in the chlorine atoms protrude into the inter-lamellar regions and interact with the organic guests.^[59]

Table 4.18. Selected bond distances and bond angles for XVIII, [CN₃H₆]₂[Cd₂(C₄H₄O₄)(Cl)₂]

Moiety	Distance (Å)	Moiety	Distance (Å)
Cd(1)-O(1)	2.313(3)	C(1)-O(3)	1.276(6)
Cd(1)-O(2)	2.396(4)	C(2)-O(1)	1.270(6)
Cd(1)-O(3)	2.398(4)	C(2)-O(4)	1.257(6)
Cd(1)-Cl(2)	2.484(2)	C(1)-C(4)	1.521(7)
Cd(1)-Cl(1)	2.525(2)	C(2)-C(3)	1.525(8)
Cd(1)-O(4)	2.569(4)	C(3)-C(4)#1	1.529(8)
C(1)-O(2)	1.264(6)	C(4)-C(3)#2	1.529(8)
Moiety	Angle (°)	Moiety	Angle (°)
O(1)-Cd(1)-O(2)	136.58(14)	Cl(2)-Cd(1)-Cl(1)	102.85(6)
O(1)-Cd(1)-O(3)	97.98(13)	Cl(2)-Cd(1)-O(4)	96.96(9)
O(2)-Cd(1)-O(3)	55.07(12)	Cl(1)-Cd(1)-O(4)	146.01(9)
O(1)-Cd(1)-O(4)	53.42(12)	O(2)-C(1)-O(3)	121.5(5)
O(2)-Cd(1)-O(4)	86.37(12)	O(2)-C(1)-C(4)	120.8(5)
O(3)-Cd(1)-O(4)	80.74(12)	O(3)-C(1)-C(4)	117.6(5)
O(1)-Cd(1)-Cl(2)	107.04(10)	O(4)-C(2)-O(1)	121.6(5)
O(2)-Cd(1)-Cl(2)	91.92(9)	O(4)-C(2)-C(3)	121.2(5)
O(3)-Cd(1)-Cl(2)	146.94(10)	O(1)-C(2)-C(3)	117.1(5)
O(1)-Cd(1)-Cl(1)	94.07(10)	C(2)-C(3)-C(4)#1	116.1(5)
O(2)-Cd(1)-Cl(1)	119.84(11)	C(1)-C(4)-C(3)#2	116.4(5)
O(3)-Cd(1)-Cl(1)	96.41(9)		

Symmetry transformations used to generate equivalent atoms:

#1 -x+1/4,y,-z+1/4 #2 x,-y+5/4,-z+1/4 #3 -x+1/4,-y+5/4,z
 #4 -x-1/2,-y+3/2,-z #5 -x-1/4,-y+3/4,z

[CN₃H₆]₂[Cd(C₄H₄O₄)₂] (XIX)

The asymmetric unit of [CN₃H₆]₂[Cd(C₄H₄O₄)₂], XIX, contains 8 non-hydrogen atoms. The cadmium atom sits in a special position and is coordinated with eight nearest oxygen neighbors forming a square anti-prismatic arrangement, with Cd – O distances in the range of 2.350(1) – 2.506(1) Å (av. 2.428 Å) and an average O – Cd – O angle of 90.7 ° (Table 4.19). The various distances and angles associated with the succinate and amine molecules are as expected.

Table 4.19. Selected bond distances and bond angles for XIX, [CN₃H₆]₂[Cd(C₄H₄O₄)₂]

Moiety	Distance (Å)	Moiety	Distance (Å)
Cd(1)-O(1)#1	2.3504(14)	Cd(1)-O(2)#1	2.5058(13)
Cd(1)-O(1)#2	2.3505(14)	Cd(1)-O(2)#2	2.5058(13)
Cd(1)-O(1)	2.3505(14)	C(1)-O(1)	1.266(2)
Cd(1)-O(1)#3	2.3505(14)	C(1)-O(2)#2	1.248(2)
Cd(1)-O(2)	2.5057(13)	C(1)-C(2)	1.523(3)
Cd(1)-O(2)#3	2.5057(13)	C(2)-C(2)#4	1.518(4)
Moiety	Angle (°)	Moiety	Angle (°)
O(1)#1-Cd(1)-O(1)#2	83.52(8)	O(2)-Cd(1)-O(2)#3	127.64(6)
O(1)#1-Cd(1)-O(1)	171.70(7)	O(1)#2-Cd(1)-O(2)#1	134.62(4)
O(1)#2-Cd(1)-O(1)	97.09(8)	O(1)-Cd(1)-O(2)#1	86.24(5)
O(1)#1-Cd(1)-O(1)#3	97.09(8)	O(1)#3-Cd(1)-O(2)#1	53.65(5)
O(1)#2-Cd(1)-O(1)#3	171.70(7)	O(2)-Cd(1)-O(2)#1	81.49(6)
O(1)-Cd(1)-O(1)#3	83.51(8)	O(2)#3-Cd(1)-O(2)#1	122.50(7)
O(1)#1-Cd(1)-O(2)	86.25(5)	O(1)#1-Cd(1)-O(2)#2	134.62(4)
O(1)#2-Cd(1)-O(2)	53.65(5)	O(1)#2-Cd(1)-O(2)#2	87.47(5)
O(1)-Cd(1)-O(2)	87.47(5)	O(1)-Cd(1)-O(2)#2	53.65(5)
O(1)#3-Cd(1)-O(2)	134.62(4)	O(1)#3-Cd(1)-O(2)#2	86.24(5)
O(1)#1-Cd(1)-O(2)#3	53.65(5)	O(2)-Cd(1)-O(2)#2	122.50(7)
O(1)#2-Cd(1)-O(2)#3	86.25(5)	O(2)#3-Cd(1)-O(2)#2	81.49(6)
O(1)-Cd(1)-O(2)#3	134.62(4)	O(2)#1-Cd(1)-O(2)#2	127.63(6)
O(1)#3-Cd(1)-O(2)#3	87.47(5)	O(2)#2-C(1)-O(1)	121.7(2)

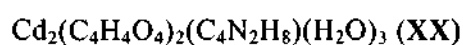
Symmetry transformations used to generate equivalent atoms:

#1 -x+1/4,y,-z+1/4 #2 x,-y+5/4,-z+1/4 #3 -x+1/4,-y+5/4,z

#4 -x-1/2,-y+3/2,-z #5 -x-1/4,-y+3/4,z

The structure of XIX consists of tetrahedral units formed by the connectivity between four succinate units and a Cd atom with an average angle of 110.6° . Four such tetrahedra surround a central one forming a supertetrahedron. The supertetrahedra get connected to give rise to the adamantane unit (Fig. 4.52). The adamantane units are linked to form the diamondoid network. An interpenetration similar to that in other diamondoid networks is observed (Fig. 4.53).^[60-63]

The structure of XIX can also be viewed as honeycomb-like layers possessing large 12-membered apertures (6Cd and 6 succinate units, $16.306 \times 12.741 \text{ \AA}$), formed by the *in-plane* connectivity between the Cd and three succinate units, cross-linked by one *out-of-plane* succinate unit (Fig. 4.54). This is somewhat similar to the connectivities observed in the three-dimensional zinc oxalate, $2[\text{C}_3\text{H}_7\text{NH}_3]^+[\text{Zn}_2(\text{C}_2\text{O}_4)_3]^{2+} \cdot 3\text{H}_2\text{O}$, II. The succinate units are connected to create catenation and interpenetration, contributing negatively to the total porosity of the solid. Such a behavior is known in many interpenetrating structures.^[60-63,64] Interpenetration in XIX reduces the 12-membered channels to smaller 8-membered channels ($\sim 5.4 \times 8.8 \text{ \AA}$, shortest O - O contact not including the van der Waals radii) along the *a*-axis (Fig. 4.55). The protonated guanidinium cations occupy the center of the channels.



The asymmetric unit of $\text{Cd}_2(\text{C}_4\text{H}_4\text{O}_4)_2(\text{C}_4\text{N}_2\text{H}_8)(\text{H}_2\text{O})_3$, XX, consists of 27 non-hydrogen atoms. There are two crystallographically independent Cd atoms. Cd(1) is octahedrally coordinated, being connected to three succinate oxygens, two bound water molecules and one nitrogen atom from the amine, at an average Cd - O/N distance of 2.362 \AA . Cd(2) is coordinated to four succinate oxygens, one water molecule and a nitrogen atom with an average Cd - O/N distance of 2.332 \AA (Table

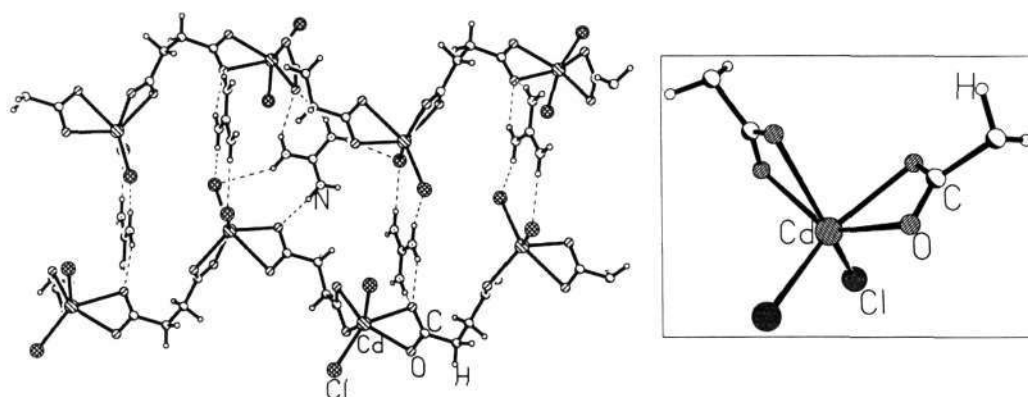


Fig. 4.51. One-dimensional chain formed by the connectivity between the Cd atoms and the succinate moieties present in $[\text{CN}_3\text{H}_6]_2[\text{Cd}_2(\text{C}_4\text{H}_4\text{O}_4)(\text{Cl})_2]$, **XVIII**. Hydrogen bonds and the weak electrostatic interactions are shown in dotted lines. Inset shows the effective tetrahedral coordination around the Cd center.

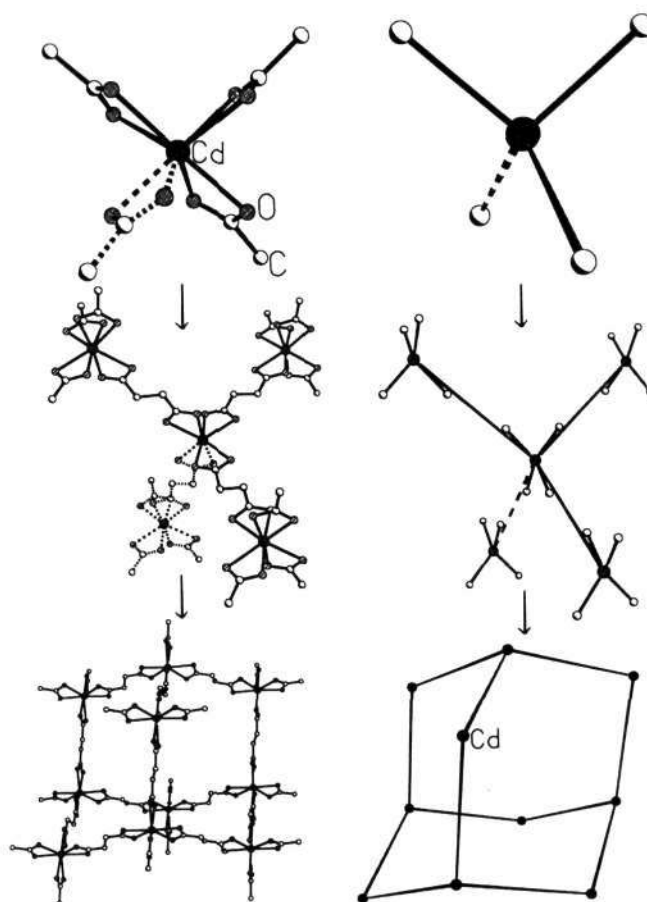


Fig. 4.52. Structure of $[\text{CN}_3\text{H}_6]_2[\text{Cd}(\text{C}_4\text{H}_4\text{O}_4)_2]$, **XIX**, showing the basic cadmium succinate tetrahedron, the supertetrahedron and the adamantane unit, demonstrating scale-up chemistry.

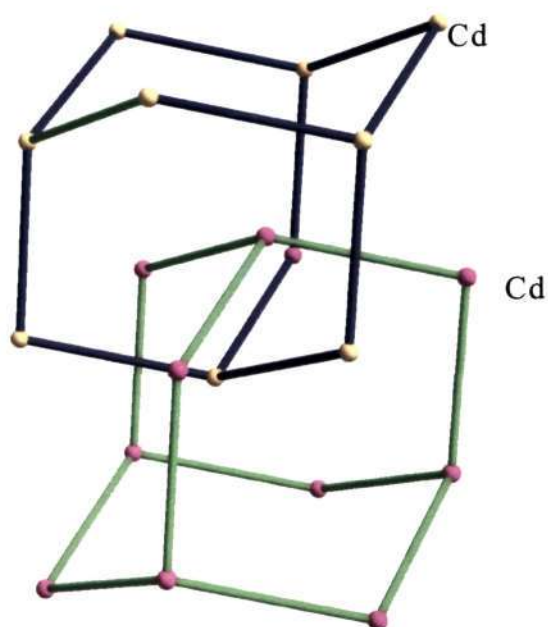


Fig. 4.53. Structure of **XIX**, showing the “normal interpenetration” present in it.

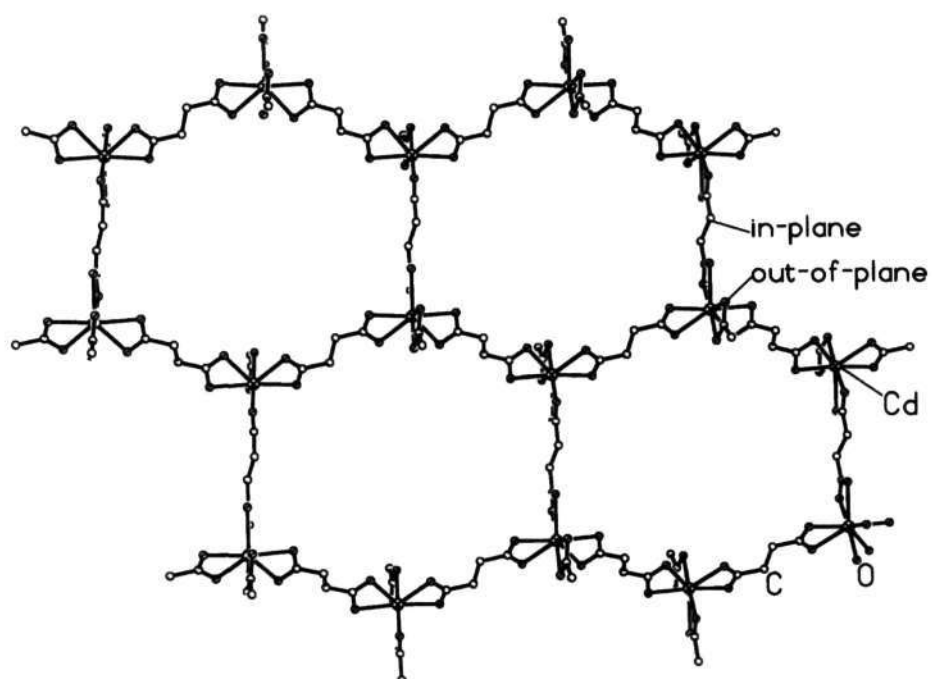


Fig. 4.54. Honeycomb-like apertures in **XIX** formed by the cadmium and the *in-plane* succinate units and their cross-linking by the *out-of-plane* succinate moieties.

4.20). The O/N – Cd – O/N angle are in the range 53.1(1) – 168.0(1) ° (av. O/N – Cd(1) – O/N =99.9 °; av. O/N – Cd(2) – O/N =103.5 °) (Table 4.20). The three-dimensional framework structure of XX consists of a hybrid layer formed by the connectivity between the Cd, two *in-plane* succinates and one piperazine molecule, giving rise to a 12 –membered rectangular aperture (11.472 x 8.220 Å, (Fig. 4.56a and b). The hybrid layers are cross-linked by an *out-of-plane* succinate unit in a monodentate fashion to form the three-dimensional structure. The structure of XX can also be viewed alternatively as having cadmium succinate layer with 10-membered apertures (11.680 x 7.027 Å) pillared by piperazine molecule as shown in Fig. 4.57. This is indeed an unusual structure wherein piperazine bonds to the Cd atom giving rise to channels along all the crystallographic axes. The channel dimensions are 11.5 x 8.2 Å along the *a*-axis (Fig. 4.57a) and 8.72 x 8.38 along the *b*-axis (Fig. 4.57b) (shortest O - O contact distance not including the van der Waals radii). Since the amine molecule is directly bound to the Cd centers, only the water molecules coordinated to the Cd protrude into the channels.

On linking the cadmium centers, a rectangular box is realized (see the inset of Fig. 4.57a), with the corners of the box occupied by the Cd₂O₂ dimers, (Cd(1)Cd(2)O(5)O(1)), O(1) and O(5) being the succinate oxygens bonded to C(4). The dimer acts as a four-connecting center and is connected by four succinate and two piperazine arms to adjacent dimers, forming a rectangular box. The rectangular box shares its faces with the neighboring ones forming the three-dimensional structure. Another independent network with identical connectivity interpenetrates this structure as shown in Fig. 58, the interpenetration being similar to that in the α - polonium related structure. Such a structure has been observed in metal nitriles,^[65,66] halides^[67,68] and seldom in other metal-organic frameworks.^[60,69,70]

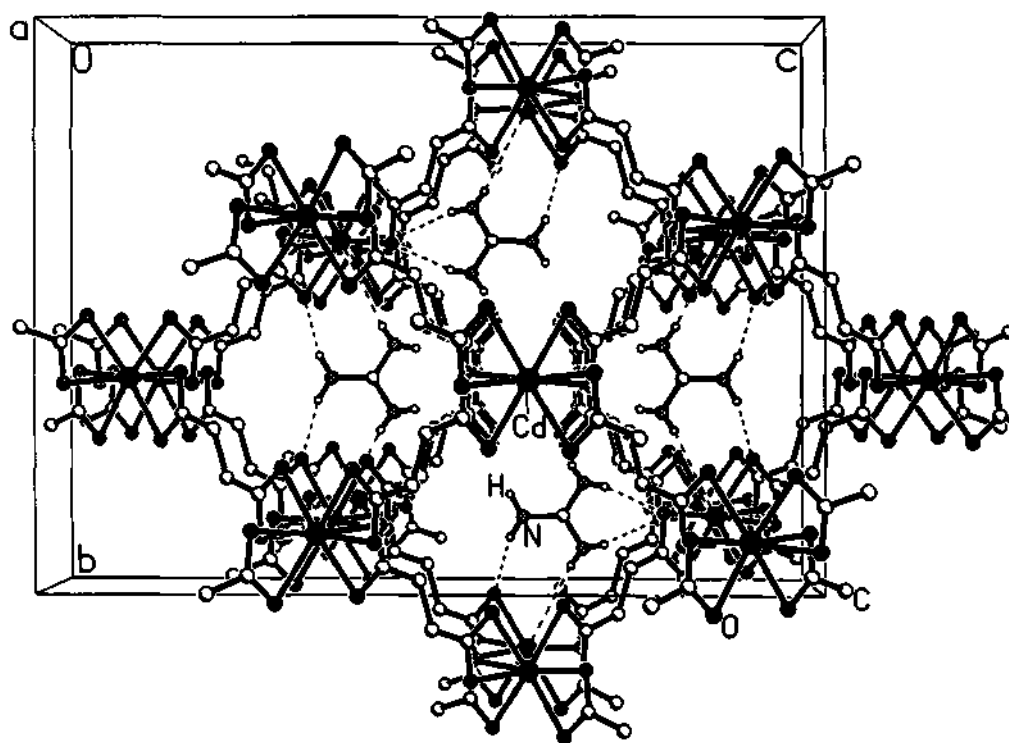


Fig. 4.55. The eight-membered channels present along the *a*-axis in XIX. Note the presence of the protonated guanidinium molecules in the channels.

Table 4.20. Selected bond distances and bond angles for XX, Cd₂(C₄H₄O₄)₂(C₄N₂H₈)(H₂O)₃

Moiety	Distance (Å)	Moiety	Distance (Å)
Cd(1)-O(1)	2.290(3)	C(5)-O(4)	1.270(6)
Cd(1)-O(100)	2.297(4)	C(5)-O(8)	1.236(6)
Cd(1)-O(200)	2.299(4)	C(6)-O(6)	1.262(6)
Cd(1)-N(1)	2.367(4)	C(6)-O(7)	1.253(6)
Cd(1)-O(2)	2.382(3)	C(1)-C(2)	1.501(7)
Cd(1)-O(3)	2.537(3)	C(1)-C(3)	1.518(7)
Cd(2)-O(4)	2.256(3)	C(3)-C(6)	1.506(7)
Cd(2)-O(5)	2.276(3)	C(4)-C(7)	1.509(6)
Cd(2)-N(2)	2.313(4)	C(5)-C(8)#3	1.524(7)
Cd(2)-O(6)	2.316(3)	C(5)-C(8)#4	1.524(7)
Cd(2)-O(300)	2.322(4)	C(7)-C(8)	1.514(7)
Cd(2)-O(7)	2.509(3)	C(50)-C(80)#5	1.506(7)
C(4)-O(1)	1.254(5)	C(50)-C(80)#6	1.506(7)
C(2)-O(2)#1	1.276(6)	C(60)-C(70)	1.518(7)
C(2)-O(2)#2	1.276(6)	N(1)-C(50)	1.474(6)
C(2)-O(3)#1	1.248(6)	N(1)-C(60)	1.476(6)
C(2)-O(3)#2	1.248(6)	N(2)-C(70)#6	1.474(6)
C(4)-O(5)	1.261(5)	N(2)-C(80)	1.484(6)
Moiety	Angle (°)	Moiety	Angle (°)
O(1)-Cd(1)-O(100)	93.0(2)	O(4)-Cd(2)-N(2)	95.51(13)
O(1)-Cd(1)-O(200)	132.34(13)	O(5)-Cd(2)-N(2)	87.98(13)
O(100)-Cd(1)-O(200)	87.2(2)	N(2)-Cd(2)-O(6)	96.98(13)
O(1)-Cd(1)-O(2)	147.53(12)	N(2)-Cd(2)-O(300)	175.57(14)
O(100)-Cd(1)-O(2)	96.08(14)	N(2)-Cd(2)-O(7)	86.71(13)
O(200)-Cd(1)-O(2)	79.31(14)	O(3)#2-C(2)-O(2)#2	121.5(4)
O(1)-Cd(1)-O(3)	97.48(11)	O(1)-C(4)-O(5)	121.3(4)
O(100)-Cd(1)-O(3)	83.2(2)	O(8)-C(5)-O(4)	123.5(4)
O(200)-Cd(1)-O(3)	129.72(13)	O(3)#2-C(2)-C(1)	122.0(5)
O(2)-Cd(1)-O(3)	53.08(12)	O(2)#2-C(2)-C(1)	116.4(4)
O(4)-Cd(2)-O(5)	89.74(11)	O(1)-C(4)-C(7)	118.7(4)
O(4)-Cd(2)-O(6)	114.38(13)	O(5)-C(4)-C(7)	120.0(4)
O(5)-Cd(2)-O(6)	154.61(12)	O(8)-C(5)-C(8)#3	121.4(4)
O(4)-Cd(2)-O(300)	86.0(2)	O(4)-C(5)-C(8)#3	115.0(4)
O(5)-Cd(2)-O(300)	87.86(13)	O(7)-C(6)-O(6)	120.6(4)
O(6)-Cd(2)-O(300)	86.16(14)	O(7)-C(6)-C(3)	119.8(5)

O(4)-Cd(2)-O(7)	168.04(11)	O(6)-C(6)-C(3)	119.5(5)
O(5)-Cd(2)-O(7)	102.10(11)	C(50)-N(1)-C(60)	108.4(4)
O(6)-Cd(2)-O(7)	53.66(12)	N(1)-C(50)-C(80)#5	112.7(4)
O(300)-Cd(2)-O(7)	92.7(2)	N(1)-C(60)-C(70)	113.0(4)
O(1)-Cd(1)-N(1)	90.77(14)	C(70)#6-N(2)-C(80)	109.7(4)
O(100)-Cd(1)-N(1)	174.7(2)	N(2)#5-C(70)-C(60)	112.9(4)
O(200)-Cd(1)-N(1)	87.5(2)	N(2)-C(80)-C(50)#6	111.8(4)
N(1)-Cd(1)-O(2)	82.58(13)	N(2)-C(80)-H(80A)	109.3(3)
N(1)-Cd(1)-O(3)	99.89(13)		

Symmetry transformations used to generate equivalent atoms:

#1 $x, y+1, z$ #2 $x, y-1, z$ #3 $x-1, y, z$
 #4 $x+1, y, z$ #5 $x, -y+3/2, z-1/2$ #6 $x, -y+3/2, z+1/2$

[C₄N₂H₁₂][Cd₂(C₄H₄O₄)₃].4H₂O (XXI)

The asymmetric unit of [C₄N₂H₁₂][Cd₂(C₄H₄O₄)₃].4H₂O, **XXI** contains 18 non-hydrogen atoms, of which 13 atoms belong to the framework and five to the amine and the water molecules. The Cd – O distances are in the range of 2.239(4) – 2.401(4) Å (av. 2.331 Å) and the O – Cd – O bond angles are in the range 55.0(1) – 146.9(2) ° (av. 101.6 °). Selected bond distances and angles in **XXI** are listed in Table 4.21.

The two-dimensional structure of **XXI** consists of macroanionic cadmium succinate sheets separated by piperazinium cations and water molecules. The individual layers are built-up from the connectivity between Cd and the succinate units. Of the three succinate units connected to the Cd atoms, two have a regular bidentate connection and while the remaining one has a monodentate connection. The monodentate succinate oxygen gets triply coordinated and connects two Cd atoms to form Cd₂O₂ dimers. Such Cd₂O₂ dimers are connected by succinate units giving rise to perforated layers with 8 – membered aperture (6.281 x 8.429 Å) in the *ac* – plane (Fig.4.59a). The doubly protonated amine molecules occupy the center of the apertures. Additionally, there are small 4 – membered apertures (4.012 x 5.220

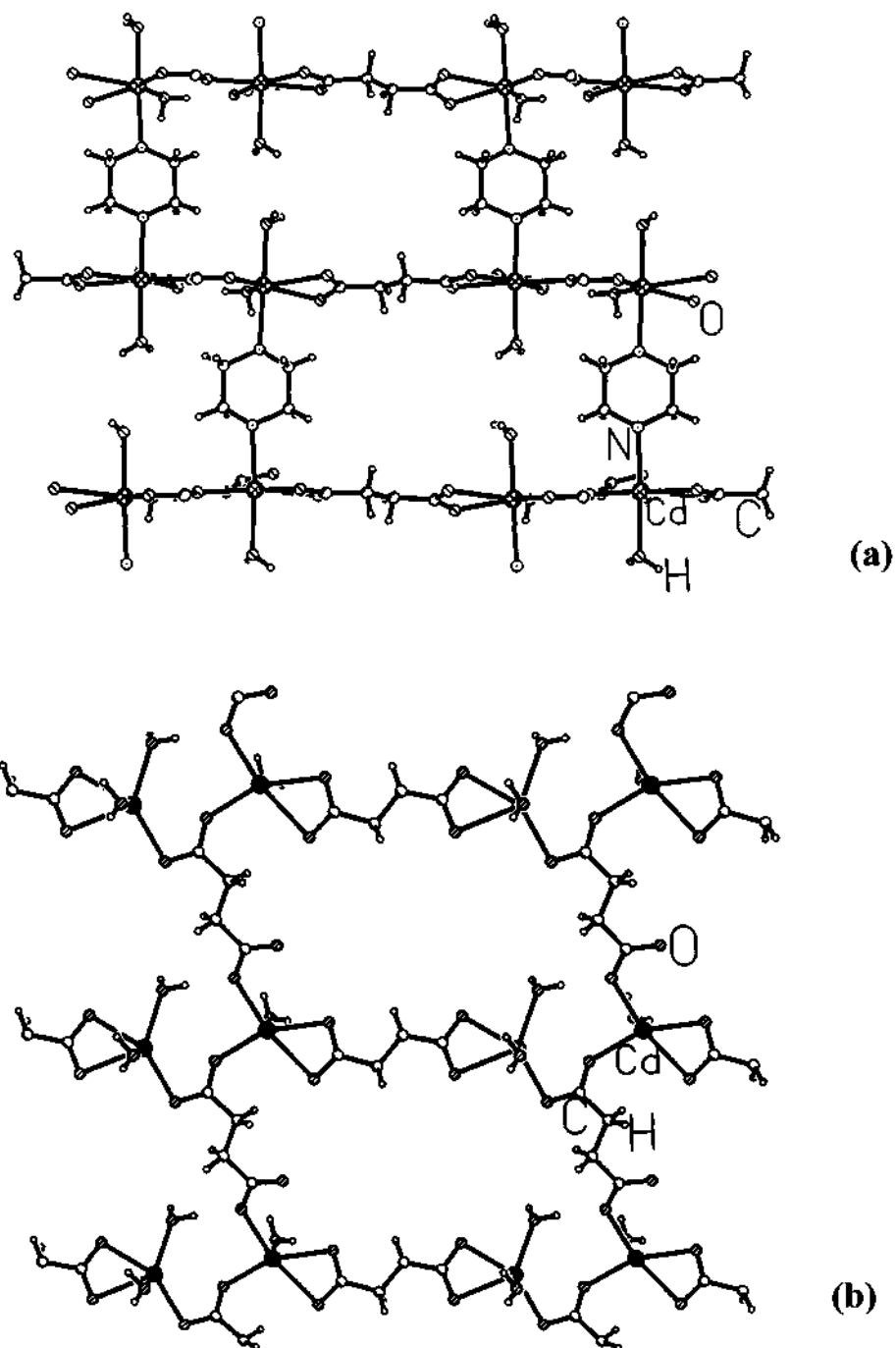


Fig. 4.56. (a) Structure of $\text{Cd}_2(\text{C}_4\text{H}_4\text{O}_4)_2(\text{C}_4\text{N}_2\text{H}_8)(\text{H}_2\text{O})_3$, **XX**, showing the hybrid metal organic layer formed by the connectivity between the Cd centers, the *in-plane* succinates and piperazine units, in the *bc*-plane. Note the presence of 12-membered apertures within the layers. (b) A perspective view of the cadmium succinate layer topology present in **XX**.

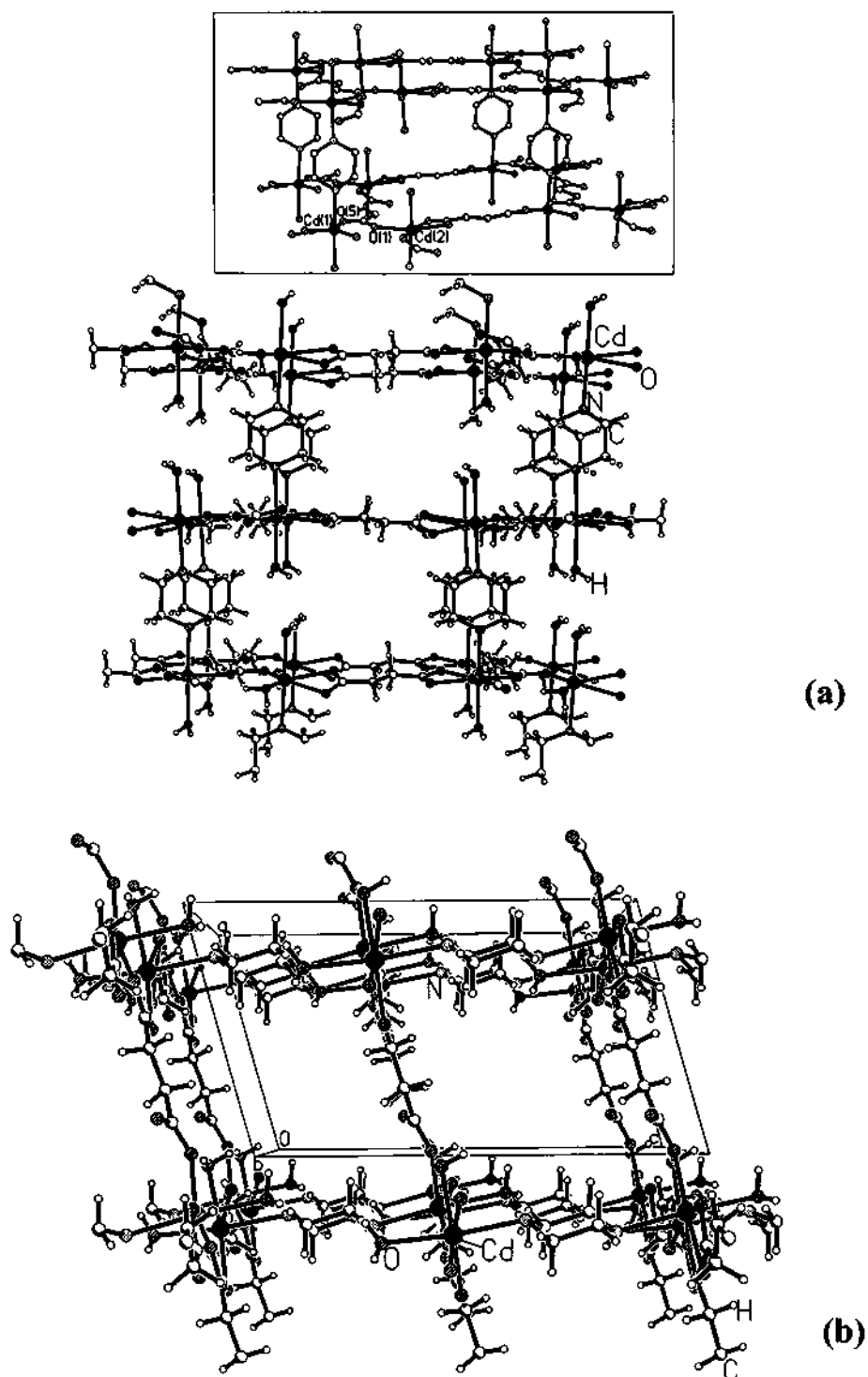


Fig. 4.57. (a) Perspective view of **XX**, along the *a*-axis, showing, 12-membered rectangular channels. Inset shows the rectangular box, which may be considered to be the basic building unit formed by the connectivity between the Cd centers via succinate units and piperazine pillars. (b) Perspective view of **XX**, along the *b*-axis, showing the 8-membered rhombic channels.

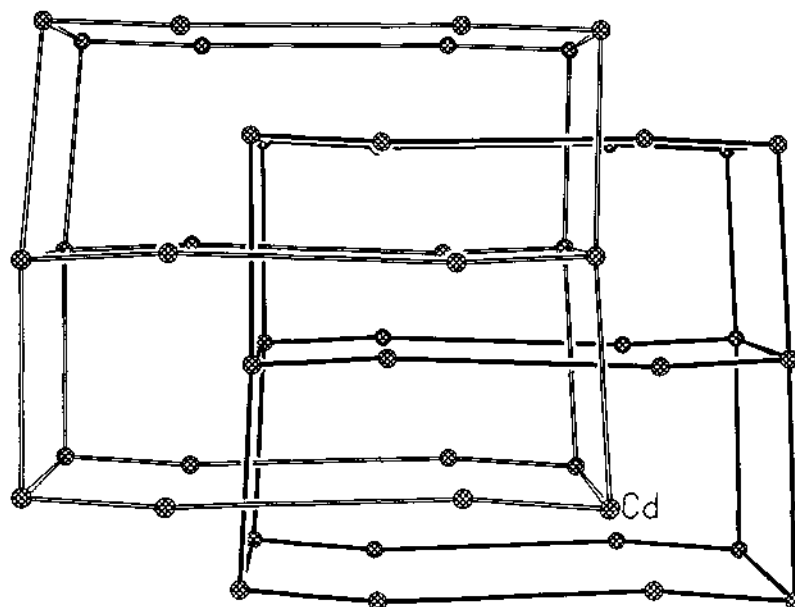


Fig. 4.58. The interpenetration present in **XX**, akin to that in the in α - polonium related network.

Table 4.21. Selected bond distances and bond angles for **XXI**,
 $[\text{C}_4\text{N}_2\text{H}_{12}][\text{Cd}_2(\text{C}_4\text{H}_4\text{O}_4)_3] \cdot 4\text{H}_2\text{O}$

Moiety	Distance (Å)	Moiety	Distance (Å)
Cd(1)-O(1)	2.239(4)	C(3)-O(4)	1.239(7)
Cd(1)-O(1)#1	2.339(3)	C(2)-O(5)	1.250(7)
Cd(1)-O(2)	2.313(4)	C(1)-O(6)	1.234(6)
Cd(1)-O(3)	2.323(4)	C(1)-C(4)	1.503(7)
Cd(1)-O(4)	2.372(4)	C(2)-C(5)	1.528(9)
Cd(1)-O(5)	2.401(4)	C(3)-C(6)	1.519(8)
C(1)-O(1)	1.283(6)	C(4)-C(4)#2	1.500(11)
C(2)-O(2)	1.259(7)	C(5)-C(6)#3	1.527(9)
C(3)-O(3)	1.262(7)		
Moiety	Angle (°)	Moiety	Angle (°)
O(1)-Cd(1)-O(2)	112.76(14)	O(4)-Cd(1)-O(5)	97.4(2)
O(1)-Cd(1)-O(3)	107.9(2)	O(6)-C(1)-O(1)	119.5(5)
O(2)-Cd(1)-O(3)	137.0(2)	O(6)-C(1)-C(4)	122.3(5)

O(1)-Cd(1)-O(1)#1	72.59(13)	O(1)-C(1)-C(4)	118.2(4)
O(2)-Cd(1)-O(1)#1	115.7(2)	O(5)-C(2)-O(2)	120.4(5)
O(3)-Cd(1)-O(1)#1	89.0(2)	O(5)-C(2)-C(5)	121.0(5)
O(1)-Cd(1)-O(4)	114.9(2)	O(2)-C(2)-C(5)	118.5(5)
O(2)-Cd(1)-O(4)	94.3(2)	O(4)-C(3)-O(3)	120.6(5)
O(3)-Cd(1)-O(4)	55.09(14)	O(4)-C(3)-C(6)	121.3(5)
O(1)#1-Cd(1)-O(4)	144.13(14)	O(3)-C(3)-C(6)	118.2(5)
O(1)-Cd(1)-O(5)	146.9(2)	C(4)#2-C(4)-C(1)	115.4(6)
O(2)-Cd(1)-O(5)	54.98(13)	C(6)#3-C(5)-C(2)	112.0(5)
O(3)-Cd(1)-O(5)	95.9(2)	C(3)-C(6)-C(5)#3	113.2(5)
O(1)#1-Cd(1)-O(5)	85.58(13)		

Symmetry transformations used to generate equivalent atoms:

#1 -x, -y+1, -z #2 -x+1, -y+1, -z #3 -x, -y, -z+1 #4 -x-1, -y, -z+1

Å) formed by the connectivity between the Cd and the bischelating succinates, which are aligned along the *a*-axis forming one-dimensional tunnels within each layer (Fig. 4.59b). Interestingly, the amine molecules in **XXI** lie in the plane of the layer and form strong N-H...O interactions with the succinate O –atoms (Fig. 4.59), in contrast to the layered zinc oxalates, **I** and **III**, where the charge-balancing organic-amine cations generally reside in the interlamellar region. The water molecules in **XXI** reside in the interlamellar region (Fig. 4.59), which is relatively less hydrophobic than the apertures within the layers.

Cd(C₄H₄O₄)(H₂O)₂ (**XXII**)

The asymmetric unit of Cd(C₄H₄O₄)(H₂O)₂, **XXII**, consists of 11 non-hydrogen atoms (Cd, succinate and two bonded water molecules). The cadmium atom is seven-coordinated with respect to the oxygen atoms, of which five are from the succinates and the other two are from the water molecules. Thus, the coordination geometry of the Cd atoms is a pentagonal bipyramid (see the inset in Fig. 4.60). Five succinate oxygens occupy equatorial positions with an average Cd – O distance and O – Cd – O angle of 2.393 Å and 107.6 °, respectively, while

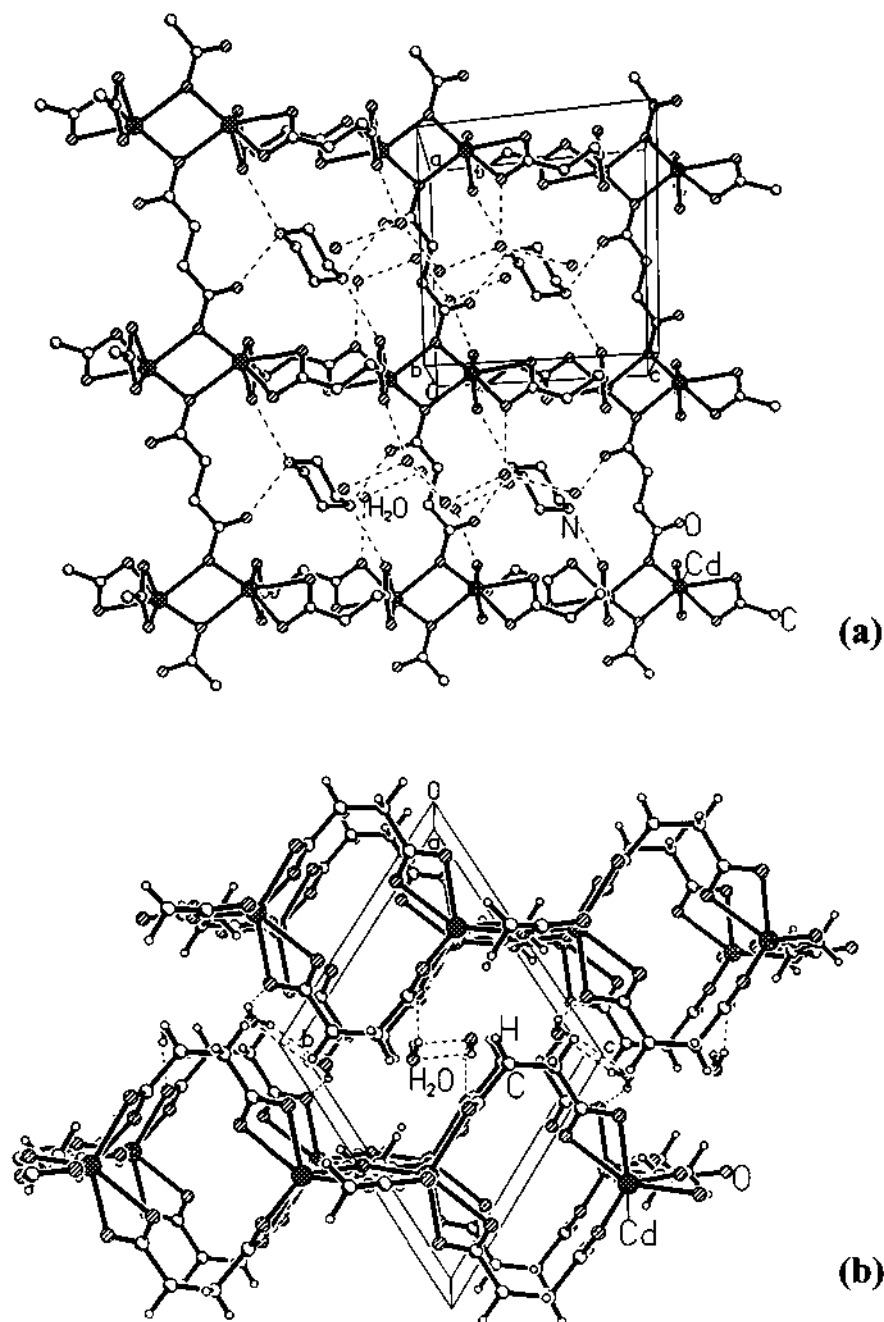


Fig. 4.59. (a) Structure of $[\text{C}_4\text{N}_2\text{H}_{12}][\text{Cd}_2(\text{C}_4\text{H}_4\text{O}_4)_3] \cdot 4\text{H}_2\text{O}$, XXI, showing the layers formed by the connectivity between the Cd_2O_{10} dimers and the succinate units. Note the piperazine and the guest water molecules in the 8-membered apertures and the monodendate binding by the succinates. (b) XXI, along the a -axis showing one-dimensional tunnels formed by the small 4-membered apertures present within the layer and also the stacking of the layers along the $[011]$ direction. (Amine molecules are not shown for clarity).

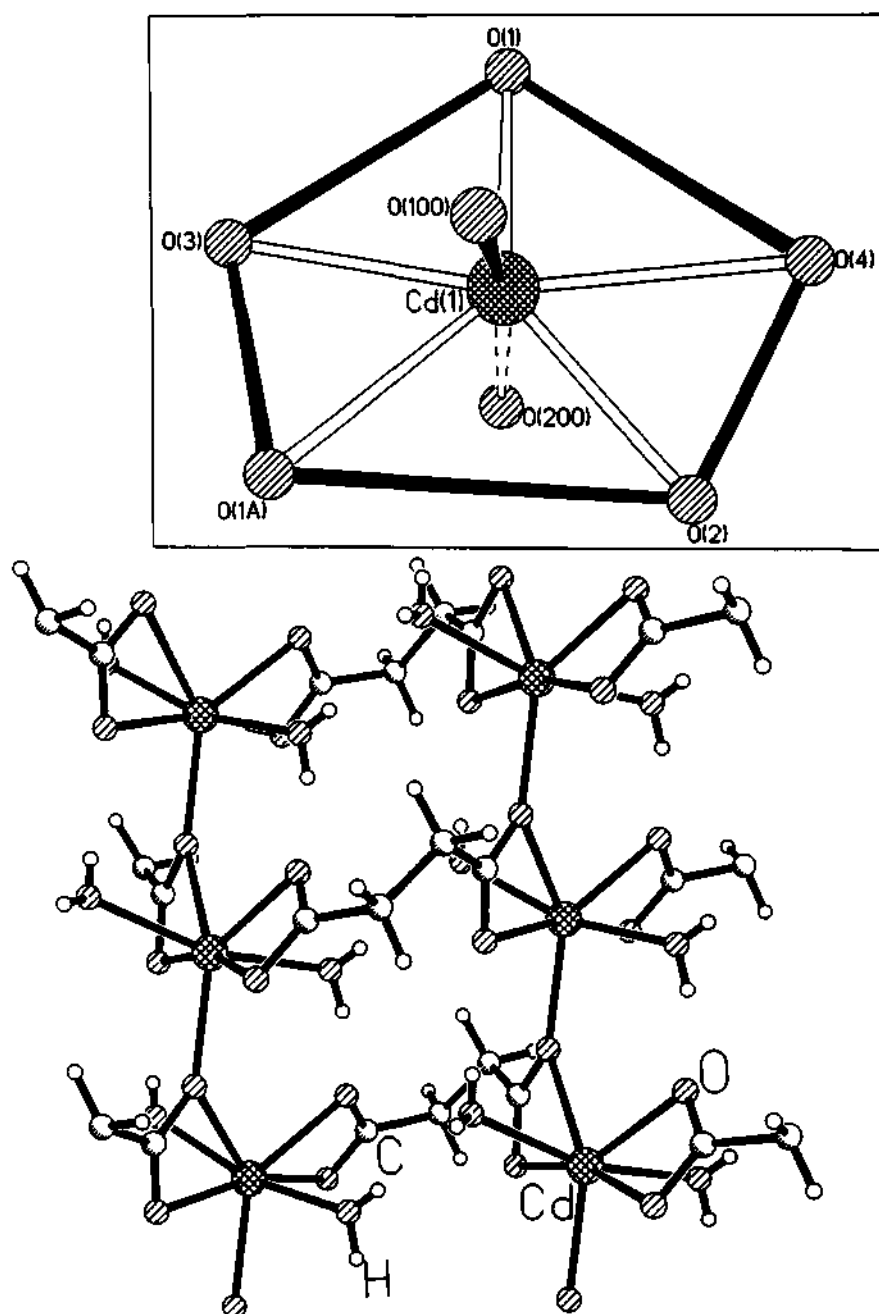


Fig. 4.60. Perspective view of the layer in the *ac*-plane in present in $\text{Cd}(\text{C}_4\text{H}_4\text{O}_4)(\text{H}_2\text{O})_2$, XXII, formed by the connectivity between the Cd atoms and the succinate units. Inset shows the pentagonal bipyramidal coordination around the Cd atom.

the bonded water molecules occupy the apical positions with an average Cd – O(w) distance of 2.296 Å and making an average O– Cd – O angle of 89.8 ° with the equatorial oxygens (see Table 4.22). The connectivity between the Cd centers and the succinate units, in **XXII**, result in perforated two-dimensional layers with 8 – membered apertures in the *ac* plane (Fig. 4.60). Such layers are stacked along the *b* – axis and are stabilized by weak interactions. The two coordinated water molecules participate in the hydrogen bonds between the layers. Similar behavior has been observed earlier in $\text{Co}_4(\text{OH})_2(\text{H}_2\text{O})_2(\text{C}_4\text{H}_4\text{O}_4)_3 \cdot 2\text{H}_2\text{O}$ ^[54] and $\text{Mn}(\text{H}_2\text{O})_4(\text{C}_4\text{H}_4\text{O}_4)$.^[71] **Cd₃(C₄H₄O₄)₂(OH)₂] (XXIII)**

The asymmetric unit of **Cd₃(C₄H₄O₄)₂(OH)₂], XXIII** contains 11 non-hydrogen atoms. There are two crystallographically independent Cd atoms, both of which are octahedrally coordinated with respect to the oxygens. The Cd – O distances are in the (Table 4.23). The three-dimensional structure of **XXIII** is made

Table 4.22. Selected bond distances and bond angles for **XXII**, $\text{Cd}(\text{C}_4\text{H}_4\text{O}_4)(\text{H}_2\text{O})_2$

Moiety	Distance (Å)	Moiety	Distance (Å)
Cd(1)-O(1)#1	2.255(3)	C(2)-O(2)	1.257(4)
Cd(1)-O(200)	2.288(4)	C(1)-O(3)	1.243(5)
Cd(1)-O(100)	2.304(3)	C(2)-O(4)	1.248(4)
Cd(1)-O(2)	2.311(2)	C(1)-C(3)	1.506(5)
Cd(1)-O(3)	2.382(3)	C(2)-C(4)	1.513(5)
Cd(1)-O(1)	2.493(3)	C(3)-C(4)#3	1.519(6)
Cd(1)-O(4)	2.523(3)	C(4)-C(3)#4	1.519(6)
C(1)-O(1)	1.276(4)		
Moiety	Angle (°)	Moiety	Angle (°)
O(1)#1-Cd(1)-O(200)	86.6(2)	O(3)-Cd(1)-O(1)	53.13(9)
O(1)#1-Cd(1)-O(100)	108.47(12)	O(1)#1-Cd(1)-O(4)	85.98(9)
O(200)-Cd(1)-O(100)	164.2(2)	O(200)-Cd(1)-O(4)	95.95(13)
O(1)#1-Cd(1)-O(2)	131.88(9)	O(100)-Cd(1)-O(4)	90.11(11)
O(200)-Cd(1)-O(2)	74.89(13)	O(2)-Cd(1)-O(4)	53.43(9)

O(100)-Cd(1)-O(2)	97.43(11)	O(3)-Cd(1)-O(4)	165.01(9)
O(1)#1-Cd(1)-O(3)	79.58(10)	O(1)-Cd(1)-O(4)	141.31(9)
O(200)-Cd(1)-O(3)	87.25(13)	O(3)-C(1)-O(1)	120.0(3)
O(100)-Cd(1)-O(3)	90.64(11)	O(3)-C(1)-C(3)	121.0(3)
O(2)-Cd(1)-O(3)	141.14(10)	O(1)-C(1)-C(3)	119.0(3)
O(1)#1-Cd(1)-O(1)	132.67(8)	O(4)-C(2)-O(2)	121.1(3)
O(200)-Cd(1)-O(1)	89.09(14)	O(4)-C(2)-C(4)	119.9(3)
O(100)-Cd(1)-O(1)	77.19(11)	O(2)-C(2)-C(4)	119.0(3)
O(2)-Cd(1)-O(1)	91.69(9)	C(1)-C(3)-C(4)#3	115.0(3)

Symmetry transformations used to generate equivalent atoms:

#1 $x+1/2, -y+1/2, z+1/2$ #2 $x-1/2, -y+1/2, z-1/2$ #3 $x+1/2, -y+1/2, z-1/2$ #4 $x-1/2, -y+1, z+1/2$

Table 4.23. Selected bond distances and bond angles for **XXIII**, $\text{Cd}_3(\text{C}_4\text{H}_4\text{O}_4)_2(\text{OH})_2$

Moiety	Distance (Å)	Moiety	Distance (Å)
Cd(1)-O(1)	2.267(3)	Cd(2)-O(5)#4	2.257(3)
Cd(1)-O(5)#1	2.284(3)	C(1)-O(2)	1.275(5)
Cd(1)-O(5)	2.300(3)	C(1)-O(4)#5	1.239(5)
Cd(1)-O(2)#2	2.321(3)	C(1)-O(4)#6	1.239(5)
Cd(1)-O(2)	2.377(3)	C(2)-O(1)	1.246(5)
Cd(1)-O(3)#3	2.393(3)	C(2)-O(3)	1.288(5)
Cd(2)-O(3)	2.351(3)	C(1)-C(4)#7	1.524(6)
Cd(2)-O(4)	2.319(3)	C(2)-C(3)	1.505(6)
Cd(2)-O(5)	2.257(3)	C(3)-C(4)	1.514(6)
Cd(2)-O(3)#4	2.351(3)	C(4)-C(1)#8	1.524(6)
Cd(2)-O(4)#4	2.319(3)		
Moiety	Angle (°)	Moiety	Angle (°)
O(1)-Cd(1)-O(5)#1	98.52(10)	O(5)-Cd(2)-O(4)#4	98.48(10)
O(1)-Cd(1)-O(5)	99.46(11)	O(5)-Cd(2)-O(4)	81.51(10)
O(5)#1-Cd(1)-O(5)	111.60(9)	O(4)#4-Cd(2)-O(4)	180
O(1)-Cd(1)-O(2)#2	164.86(11)	O(5)#4-Cd(2)-O(3)	92.30(9)
O(5)#1-Cd(1)-O(2)#2	89.92(10)	O(5)-Cd(2)-O(3)	87.71(9)
O(5)-Cd(1)-O(2)#2	88.95(10)	O(4)#4-Cd(2)-O(3)	80.18(10)
O(1)-Cd(1)-O(2)	91.83(10)	O(4)-Cd(2)-O(3)	99.82(10)
O(5)#1-Cd(1)-O(2)	89.17(10)	O(5)-Cd(2)-O(3)#4	92.29(9)
O(5)-Cd(1)-O(2)	154.32(10)	O(3)-Cd(2)-O(3)#4	179.999(1)
O(2)#2-Cd(1)-O(2)	75.66(10)	O(4)#6-C(1)-O(2)	124.1(4)

O(1)-Cd(1)-O(3)#3	83.66(10)	O(4)#6-C(1)-C(4)#7	118.3(4)
O(5)#1-Cd(1)-O(3)#3	169.19(9)	O(2)-C(1)-C(4)#7	117.6(4)
O(5)-Cd(1)-O(3)#3	78.28(10)	O(1)-C(2)-O(3)	122.8(4)
O(2)#2-Cd(1)-O(3)#3	85.78(10)	O(1)-C(2)-C(3)	119.6(4)
O(2)-Cd(1)-O(3)#3	80.16(10)	O(3)-C(2)-C(3)	117.6(4)
O(5)#4-Cd(2)-O(5)	180		

Symmetry transformations used to generate equivalent atoms:

#1 $-x+1/2, y+1/2, z$ #2 $-x, -y, -z+1$ #3 $-x+1/2, y-1/2, z$ #4 $-x+1, -y, -z+1$
 #5 $x+1/2, -y+1/2, -z+1$ #6 $x-1/2, -y+1/2, -z+1$ #7 $x-1/2, y, -z+1/2$ #8 $x+1/2, y, -z+1/2$

of dimensional Cd-O layers cross-linked by the succinate units. The Cd-O layers are formed by simpler building units. Thus, two Cd-O octahedra are joined through their edges, and by two more Cd-O octahedra above and below through their corners forming a Cd_4O_{18} tetrameric clusters. The tetrameric clusters have the appearance of SBU-4 units (see the inset in Fig. 4.61) proposed for Ga and Fe phosphates (Typically, SBU-4 is formed by two edge/corner-sharing octahedra capped by two tetrahedra on top and bottom through corner-sharing).^[72] The Cd_4O_{18} tetramers are joined together forming infinite Cd-O sheets (Fig. 4.61), which are cross-linked by succinates to give rise to the three-dimensional structure (Fig. 4.62). Similar structures have been found earlier in Co-succinates.^[54]

4.8.2. Discussion

Six cadmium succinates, XVIII-XXIII, have been synthesized hydrothermally, of which XVIII - XXI were obtained starting with the organic-amine succinate precursors. While the amines are incorporated in XVIII-XXI, they are absent in XXII and XXIII, which were prepared by the reaction of Cd salts with a mixture of succinic acid and the amine. Thus, it is only in the Cd succinates obtained from amine succinates that the amines are present in the open-framework structure. The use of organic-amine succinates also appears to facilitate the reaction to occur at lower temperatures. XVIII has a chain structure with the Cd

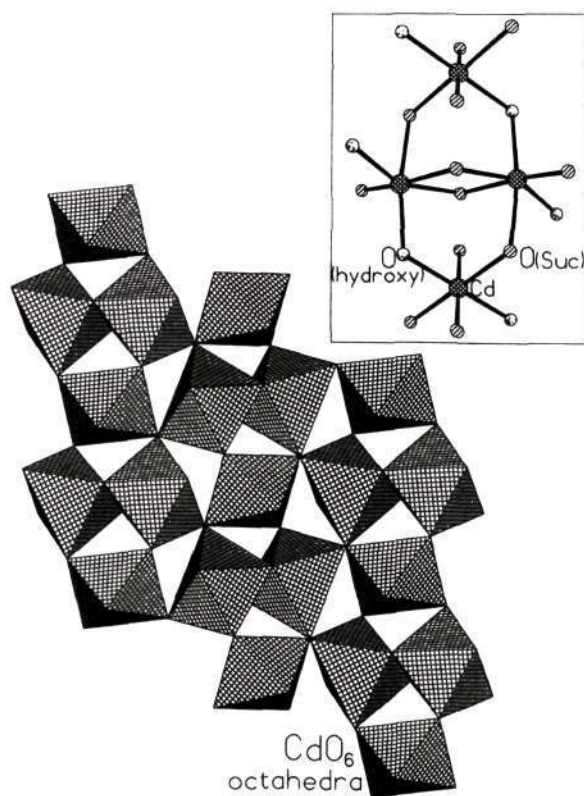


Fig. 4.61. Polyhedral view of the cadmium-oxide layers present in $\text{Cd}_3(\text{C}_4\text{H}_4\text{O}_4)_2(\text{OH})_2$, **XXIII**, formed by the corner-sharing SBU-4 type units, lying in the ab -plane. Inset shows the SBU-4 the basic building unit.

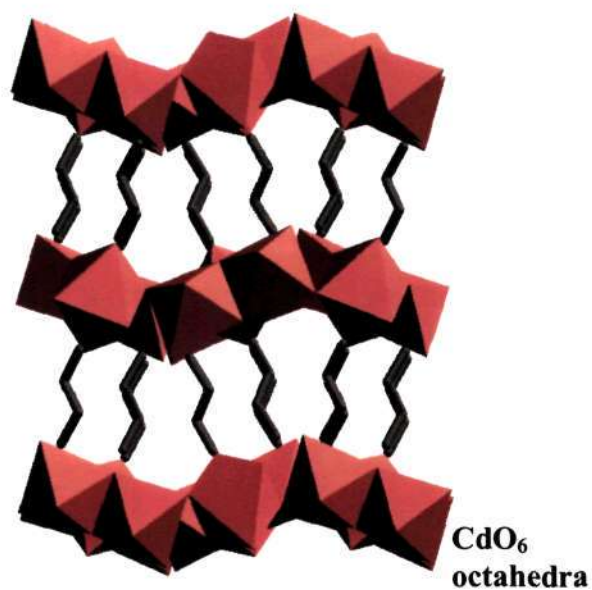


Fig. 4.62. Structure of **XXIII** showing the connectivity between the cadmium-oxide layers through the succinate linkers, forming small 8 – membered empty channels along the b -axis.

atoms linked to two succinate units; it possesses two terminal Cl atoms (Fig. 4.51). The coordination environment around Cd is tetrahedral if we consider the two succinates as two nodes and the two chlorines as the other two nodes (see the inset in Fig. 4.51). Compound **XIX** also has a four-connecting tetrahedron, but connected only by succinate units (Fig. 4.52). It appears that **XVIII** is the precursor of **XIX**, wherein the chlorine atoms in **XVIII** are replaced by the succinates, thereby forming the three-dimensional structure. This observation also gains support from the fact that **XIX** can be prepared in pure form, whilst **XVIII** always occurs as a co-product with **XIX**.

The structure of **XIX** is built up from the four-connecting Cd nodes, through the succinate linkers. This type of four-connecting nodes results in the adamantane units and thereby in diamondoid frameworks.^[60-63,73-76] The building-up process is an example of scale-up chemistry,^[77] reminiscent of self-similar structures, as shown in Figure 52. The diamondoid lattice in **XIX** can be considered as being derived from $\text{Cd}(\text{CN})_2$ ($\text{Cd} - \text{Cd} = \sim 4.46 \text{ \AA}$) by the replacement of the nitrile unit by the succinate unit thereby causing a larger aperture ($\text{Cd} - \text{Cd} = 9.43 \text{ \AA}$). The interpenetration in **XIX** (Fig. 4.53) is similar to that in $\text{Cd}(\text{CN})_2$ which is classified as normal interpenetration.^[60]

Compound **XX** also has an interpenetrated structure, but unlike in **XIX**, the three-dimensional connectivity in **XX** arises not entirely from the linking of the Cd centers by the succinate units. Instead, the connectivities in **XX** involve the piperazine moieties giving rise to a α -polonium type interpenetrated structure (Fig. 4.58) rather than a diamondoid network. The structure of **XX** is comparable to that of the other hybrid metal-organics with the α -polonium related structure, such as cadmium (hexakis(imidazolylmethyl)benzene) $\text{F}_2 \cdot 14\text{H}_2\text{O}$.^[78] If interpenetration can

be avoided in XIX and XX by the introduction of suitable guest species into the appropriate sites,^[60-64,79] they can be rendered porous.

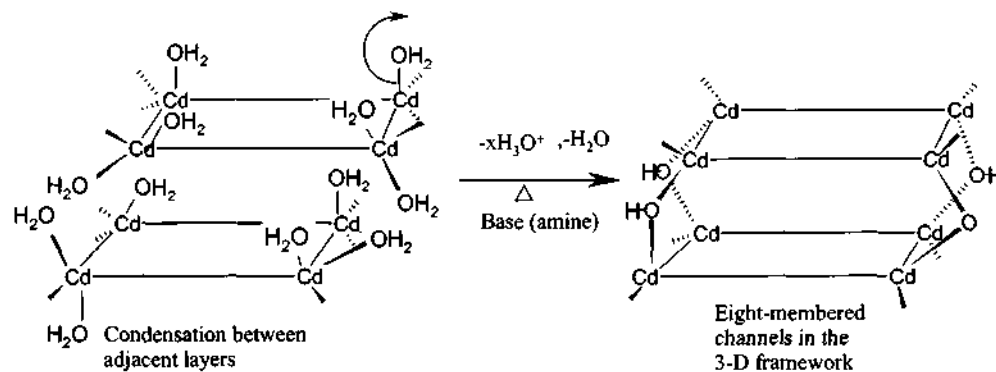
Ligation by polyfunctional amines such as 4,4'-bipyridine forming rigid networks is known to occur in oxalates and related systems.^[80,81] Ancillary ligation by water molecules has been observed in two-dimensional metal succinate architectures.^[54,71] The ligation in XX by piperazine is unusual as the amine connects Cd atoms in two different Cd succinate layers, acting as a pillar, thereby giving rise to the three-dimensional character of the structure (Fig. 4.56).

The cadmium succinate layers in XIX, XX, XXI and XXII, present an interesting comparison. In XIX, the two *in-plane* succinate units are connected to the Cd centers in a bidentate fashion, forming honeycomb-like layers (Fig. 4.54). On the other hand, the cadmium succinate layers in XX have two different types of *in-plane* succinate units, one showing a monodendate bonding and the other a bidentate bonding (Fig. 4.56b). One can also view the structure of XX in terms of the hybrid metal-organic layers, formed by the linking of the Cd atoms by the *in-plane* succinate and piperazine units (Fig. 4.56a). Similar hybrid metal-organic networks have been found in systems involving rigid bipyridyl ligands.^[80,81] The macroanionic layer in XXI with the formula $[\text{Cd}_2(\text{C}_4\text{H}_4\text{O}_4)]^{2-}$ has Cd_2O_2 dimers connected by the succinate units (Fig. 4.59a). In addition, XXI possesses unique 4-membered apertures, so aligned as to form one-dimensional tunnels along the a-axis (Fig. 4.59b), wherein the amine is located. The two-dimensional architecture in XXI is distinctly different from the honeycomb architectures observed in zinc and cadmium oxalates discussed in the earlier sections. In spite of the fact that both XXI and XXII contain layers involving three-coordinated succinate oxygens, the difference in the succinate connectivity (monodendate in XXI and bidentate in XXII) results in apertures of much smaller size (6.129 x 4.737 Å) in XXII (Fig.

4.60). Monodentate binding by the succinate units in framework metal-succinate compounds,^[54,82] appears to be more frequent than in oxalate-based compounds.^[83]

The three-dimensional architecture in **XXIII** is distinctly different from that in **XIX** or **XX**. In **XXIII**, the structure consists of two-dimensional sheets with Cd-O-Cd linkages connected by succinate pillars with no guest species. This reflects in the reduced dimensions of the channels. The structure of **XXIII** is comparable to that of the cobalt succinate, $\text{Co}_5(\text{OH})(\text{C}_4\text{H}_4\text{O}_4)_4$ described by Ferey and co-workers.^[54] **XXIII** comprises of SBU-4 like unit (see inset in Fig. 4.61), observed in the fluorinated metal phosphate frameworks.^[72] The connectivity of the cadmium-oxide layer by the succinate linkers is similar to that observed in other metal dicarboxylates.^[54]

It has been suggested recently that the complex open-framework metal phosphates may result from the transformation of lower-dimensional structures into the higher dimensional ones, involving progressive building-up.^[33] In this context, it is worth noting that the structure of **XXII** could be related to that of **XXIII**. Thus, the 2D layer of **XXII** can be condensed to yield to **XXIII**. The water molecules bound to the Cd centers in **XXII**, can condense on heating resulting in a -OH group, bridging the Cd centers of the adjacent layers ($-\mu_2-$ type bridge), forming the eight-membered channels in **XXIII**. A schematic representation of the possible mechanism of transformation is as shown below.



The structures of the amine succinates themselves merit some discussion. In GUS, the anion is the monohydrogen succinate, $C_4H_5O_4^-$, while in PIPS it is the fully deprotonated $C_4H_4O_4^{2-}$, in spite of guanidine ($pK_a \sim 12.7$) being a stronger base than the piperazine ($pK_s \sim 4.2$). It is possible that the extent of deprotonation of succinic acid depends on the different mole ratios of the amine and the acid employed in the synthesis (GUS, CN_3H_5 : 2 $C_4H_6O_4$ and PIPS, $C_4N_2H_{10}$: $C_4H_6O_4$). It would be interesting to perform a systematic study of the variation in the structure of the amine-succinate with the change in the amine: acid ratio and its effect on the structure of the open-framework material obtained. Succinic acid with a small difference between the pK_{a1} and pK_{a2} values ($pK_{a1} \sim 4.61$ and $pK_{a2} \sim 5.61$) seems to respond more sensitively to such compositional variations than oxalic acid with a large difference ($pK_{a1} \sim 1.23$ and $pK_{a2} \sim 4.19$).

4.8.3. Summary

Cadmium succinates of different dimensionalities having open-structures have been synthesized, in the presence/absence of structure directing organic amines. The one-dimensional structure, **XVIII**, possesses features suggesting its role of a possible precursor to the three-dimensional cadmium succinate, **XIX**, exhibiting a diamondoid structure. The three-dimensional structures, **XIX** and **XX**, have channels and exhibit interesting interpenetrated structures. Whilst the layered structures have apertures accommodating the guest amine and water molecules. The two-dimensional cadmium succinate, **XXII**, has terminal water molecules and their position suggests the possible formation of the three-dimensional structure of **XXIII** from the condensation reactions between the adjacent layers in **XXII**.

4.9. Cadmium succinates with XCd_4O_{24} ($X = Cl, Br$) tetrahedral clusters

4.9.1. Results

$[Na_3Cd_5(C_4H_4O_4)_6Cl]$ (**XXIV**) and $[Na_3Cd_5(C_4H_4O_4)_6Br]$, (**XXV**)

The asymmetric units of **XXIV** and **XXV** contain 8 independent non-hydrogen atoms. There are two crystallographically distinct cadmium atoms along with one sodium atom and one halogen atom. The structure of these compounds is built up of tetrahedral clusters of the composition (XCd_4O_{24}) , $X = Cl, Br$ with Cd(1)-Cl and Cd(1)-Br distances of 2.674(6) and 2.686(2) Å, respectively and an average Cd(1)-X-Cd(1) angle of 109.5° (Table 4.24). The tetrahedral cluster is constituted by four Cd atoms, each coordinated to six succinate oxygens, with the CdO_6 octahedra surrounding a central halogen atom (see inset of Fig. 4.63). The central Cl atom in **XXIV** resides in a special position with 1/12th occupancy. The CdO_6 octahedra are distorted with Cd(1)-O distances in the range 2.286(1)-2.530(4) Å [av = 2.408 Å] and an average O-Cd(1)-O angle of 83.1° (Table 4.24). The tetrahedral (XCd_4O_{24}) cluster gets cross-linked by the succinate units into three-dimensions with intersecting channels as seen in Figure 4.63.

The distance between the centers of the adjacent tetrahedral clusters is ~11.813Å. The three-dimensional architecture is comparable to the α - polonium structure, if we consider the tetrahedral cluster, $(XCd(1)_4O_{24})$, as the six-connecting node and the succinate, $[C(2)C(1)O(1)O(2)]$, arising from each cluster as the arm connecting the adjacent clusters. This three-dimensional lattice, is interpenetrated by an independent lattice (Fig. 4.64). Such an interpenetration is found in α - polonium related structures.^[60] The interpenetration reduces the size of the channel, occupied by Na and Cd(2) atoms. The Cd(2) and Na(1) occupy the same site, with 1/4th and 1/12th occupancies respectively. The Cd(2) is six-coordinated with respect to oxygen atoms forming an octahedron, with Cd(2)-O distances in the range 2.371(4)-2.450(4) [av = 2.411 Å]. The structure of **XXV** is identical to that of **XXIV** with the expected variations in the geometric parameters (Table 4.24).

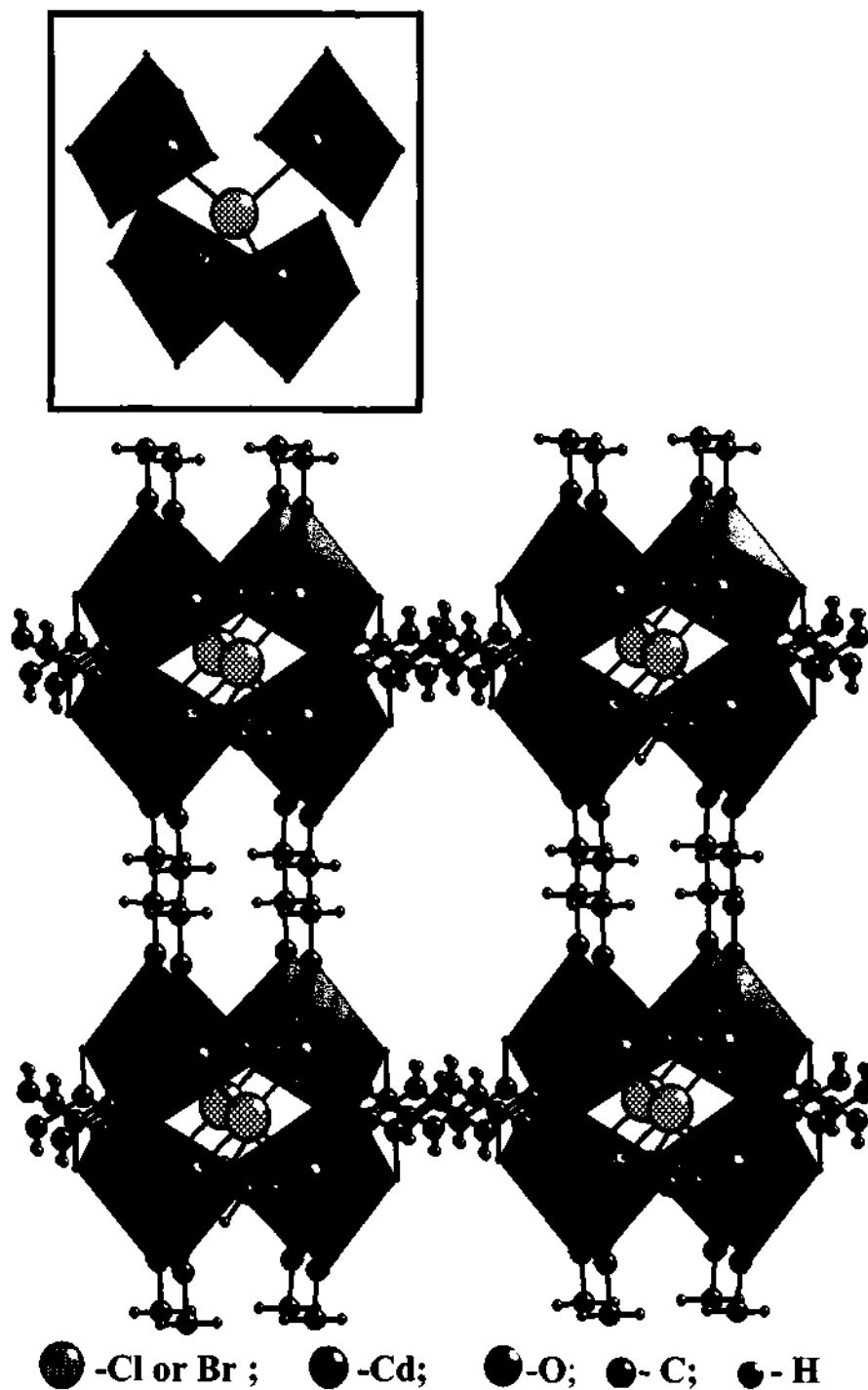


Fig. 4.63. Cube-like architecture of **XXIV** formed by connectivity between the $(\text{ClCd}_4\text{O}_{24})$ clusters and the succinate linkers (distance between the centers of the adjacent clusters is 11.831 Å). Inset shows the $(\text{Cl}(\text{Cd}(\text{Suc})_3)_4)$ cluster with Cl atom in the center. In **XXV**, the Cl is replaced by Br.

Table 4.24. Selected bond distances and bond angles for [Na₃Cd₅(C₄H₄O₄)₆Cl], XXIV and [Na₃Cd₅(C₄H₄O₄)₆Br], XXV

XXIV			
Moiety	Distance (Å)	Moiety	Distance (Å)
Cd(1)-O(1)	2.286(3)	Cd(2)-O(2)#10	2.450(4)
Cd(1)-O(1)#1	2.286(3)	Na(1)-O(1)#5	2.371(4)
Cd(1)-O(1)#2	2.286(3)	Na(1)-O(1)#6	2.371(4)
Cd(1)-O(2)#1	2.530(4)	Na(1)-O(1)#7	2.371(4)
Cd(1)-O(2)	2.530(4)	Na(1)-O(2)#8	2.450(4)
Cd(1)-O(2)#2	2.530(4)	Na(1)-O(2)#9	2.450(4)
Cd(1)-Cl(1)#3	2.6743(6)	Na(1)-O(2)#10	2.450(4)
Cd(2)-O(1)#5	2.371(4)	C(2)-C(2)#14	1.505(10)
Cd(2)-O(1)#6	2.371(4)	C(2)-C(1)	1.523(7)
Cd(2)-O(1)#7	2.371(4)	O(2)-C(1)	1.257(7)
Cd(2)-O(2)#8	2.450(4)	O(1)-C(1)	1.272(5)
Cd(2)-O(2)#9	2.450(4)		
Moiety	Angle (°)	Moiety	Angle (°)
O(1)-Cd(1)-O(1)#1	119.41(2)	O(2)-Cd(1)-C(1)#1	104.14(13)
O(1)-Cd(1)-O(1)#2	119.41(2)	O(1)#1-Cd(1)-C(1)	131.71(14)
O(1)#1-Cd(1)-O(1)#2	119.41(2)	O(1)#2-Cd(1)-C(1)	107.6(2)
O(1)-Cd(1)-O(2)#1	94.92(13)	O(2)#1-Cd(1)-C(1)	87.10(13)
O(1)#1-Cd(1)-O(2)#1	54.16(12)	O(2)-Cd(1)-C(1)	27.06(14)
O(1)#2-Cd(1)-O(2)#1	131.28(12)	O(2)#2-Cd(1)-C(1)	104.14(13)
O(1)-Cd(1)-O(2)	54.16(12)	Cl(1)#3-Cd(1)-C(1)#1	109.61(11)
O(1)#1-Cd(1)-O(2)	131.28(12)	Cl(1)#3-Cd(1)-C(1)#2	109.61(11)
O(1)#2-Cd(1)-O(2)	94.92(13)	C(1)#1-Cd(1)-C(1)#2	109.33(11)
O(2)#1-Cd(1)-O(2)	77.38(14)	Cl(1)#3-Cd(1)-C(1)	109.61(11)
O(1)-Cd(1)-O(2)#2	131.28(12)	C(1)#1-Cd(1)-C(1)	109.33(11)
O(1)#1-Cd(1)-O(2)#2	94.92(13)	C(1)#2-Cd(1)-C(1)	109.33(11)
O(1)#2-Cd(1)-O(2)#2	54.16(12)	Cd(1)#11-Cl(1)-Cd(1)#5	109.5
O(2)#1-Cd(1)-O(2)#2	77.38(14)	Cd(1)#11-Cl(1)-Cd(1)#12	109.5
O(2)-Cd(1)-O(2)#2	77.38(14)	Cd(1)#5-Cl(1)-Cd(1)#12	109.5
O(1)-Cd(1)-C(1)#1	107.6(2)	Cd(1)#11-Cl(1)-Cd(1)#13	109.5
O(1)#1-Cd(1)-C(1)#1	27.18(13)	Cd(1)#5-Cl(1)-Cd(1)#13	109.5
O(1)#2-Cd(1)-C(1)#1	131.71(14)	Cd(1)#12-Cl(1)-Cd(1)#13	109.5
O(2)#1-Cd(1)-C(1)#1	27.06(14)		

XXV			
Moiety	Distance (Å)	Moiety	Distance (Å)
Cd(1)-O(1)	2.259(10)	Moiety	Distance (Å)
Cd(1)-O(1)#1	2.259(10)	Na(1)-O(2)	2.446(13)
Cd(1)-O(1)#2	2.259(10)	Na(1)-O(2)#1	2.446(13)
Cd(1)-O(2)	2.504(11)	Na(1)-O(2)#2	2.446(13)
Cd(1)-O(2)#1	2.504(11)	Na(1)-O(1)#3	2.377(11)
Cd(1)-O(2)#2	2.504(11)	Na(1)-O(1)#4	2.377(11)
Cd(1)-Br(1)	2.686(2)	Na(1)-O(1)#5	2.377(11)
Moiety	Angle (°)	Moiety	Angle (°)
O(1)-Cd(1)-Br(1)	85.6(3)	Br(1)-Cd(1)-C(1)#2	109.3(3)
O(1)#1-Cd(1)-Br(1)	85.6(3)	Cd(1)-Br(1)-Cd(1)#6	109.5
O(1)#2-Cd(1)-Br(1)	85.6(3)	Cd(1)-Br(1)-Cd(1)#7	109.5
O(2)-Cd(1)-Br(1)	133.4(3)	Cd(1)#6-Br(1)-Cd(1)#7	109.5
O(2)#1-Cd(1)-Br(1)	133.4(3)	Cd(1)-Br(1)-Cd(1)#8	109.5
O(2)#2-Cd(1)-Br(1)	133.4(3)	Cd(1)#6-Br(1)-Cd(1)#8	109.5
Br(1)-Cd(1)-C(1)#1	109.3(3)	Cd(1)#7-Br(1)-Cd(1)#8	109.5
Br(1)-Cd(1)-C(1)	109.3(3)		

Symmetry transformations used to generate equivalent atoms in XXIV:

#1 $-z+1, -x+1, y$ #2 $-y+1, z, -x+1$ #3 $x-1, y, z$ #4 $x-1/2, -y+3/2, -z+3/2$
 #5 $-x+1, -y+2, z$ #6 $z, -x+1, -y+2$ #7 $-y+2, z, -x+1$ #8 $-y+3/2, -z+3/2, x+1/2$
 #9 $x+1/2, -y+3/2, -z+3/2$ #10 $-z+3/2, x+1/2, -y+3/2$ #11 $x+1, -y+2, -z+2$
 #12 $-x+1, y, -z+2$ #13 $x+1, y, z$ #14 $x, -y+2, -z+1$

Symmetry transformations used to generate equivalent atoms in XXV:

#1 $-y+1, z, -x+1$ #2 $-z+1, -x+1, y$ #3 $z+1/2, -x+3/2, -y+1/2$ #4 $y+1/2, -z+1/2, -x+3/2$
 #5 $x-1/2, -y+1/2, -z+1/2$ #6 $-x+2, y, -z$ #7 $-x+2, -y, z$ #8 $x, -y, -z$
 #9 $x+1/2, -y+1/2, -z+1/2$ #10 $-x+2, y, -z+1$

IR spectra (KBr pellet) showed characteristic features of the dicarboxylate units.^[3] The various bands observed were: $\nu_{as}(\text{CO}_2^-)$ at 1559(s) cm^{-1} (XXIV) and 1545(s) cm^{-1} (XXV); $\nu_s(\text{CO}_2^-)$ at 1439(s) cm^{-1} (XXIV) and 1423(s) cm^{-1} (XXV); $\nu_s(\text{CO}) + \nu(\text{CC})$ at 1323(w) cm^{-1} (XXIV) and 1324(w) cm^{-1} (XXV); $\nu_s(\text{CO}) + \delta(\text{O}-\text{C}=\text{O})$ at 1253(w) cm^{-1} (XXIV) and 1252(w) cm^{-1} (XXV); $\nu_{as}(\text{CH}_2)$ at 2974(m) cm^{-1} (XXIV) and 2938(m) cm^{-1} (XXV) and $\nu_s(\text{CH}_2)$ at 2930(m) cm^{-1} (XXIV); 2849(m) cm^{-1} (XXV). Bands due to metal-oxygen and metal-halogen vibrations are also found in the 280 - 700 cm^{-1} region.

Thermogravimetric analysis (TGA) was carried out under a flow of nitrogen (50 ml min^{-1}) from 25 to 700 °C (heating rate = 5 °C min^{-1}). Both **XXIV** and **XXV** showed two distinct mass losses. For **XXIV**, the mass loss in the range 380-500°C (53.3%) occurs due to the loss of the succinate unit (calcd.51.1%). For **XXV**, the mass loss in the range 350-500 °C (51.8%) is due to the loss of succinate units (calc.49.5%). A broad tail in the 500-600°C is observed in both cases is due to the loss of the halogen. The powder XRD pattern of the calcined samples, of **XXIV** and **XXV** was crystalline and corresponded to Na_2CdO_2 (JCPDS: 36-1199).

4.9.2. Discussion

Two new three-dimensional cadmium succinates, **XXIV** and **XXV**, made up of $\text{XCd}_4\text{O}_{24}$ ($X = \text{Cl, Br}$) tetrahedral clusters have been prepared and characterized. Considering the $(\text{XCd}_4\text{O}_{24})$ clusters to be the secondary building units in **XXIV** and **XXV**. This arrangement is reminiscent of $\text{Zn}_4\text{O}(\text{BDC})_3(\text{DMF})_8(\text{C}_6\text{H}_5\text{Cl})$, (BDC = 1,4-benzene dicarboxylate), MOF-5, where the capped Zn_4O clusters are linked via benzene dicarboxylate units.^[84] Another structure related to that of **XXIV** and **XXV**, is $\text{Rb}_3\text{Zn}_4\text{O}(\text{PO}_4)_3 \cdot 3.5\text{H}_2\text{O}$ described by Harrison et al.^[85] The XCd_4 ($X = \text{Cl, Br}$) clusters are comparable to the OZn_4 clusters observed in the zinc phosphate. Though these structures are related, certain differences between them are to be noted. The primary building unit in MOF-5 is the ZnO_4 tetrahedron. The tetrahedra form supertetrahedra based on OZn_4 clusters and these units are linked by the benzene dicarboxylate units. In the present case, the primary building unit is the CdO_6 octahedron, which forms the secondary building unit of $(\text{XCd}_4\text{O}_{24})$ clusters, which get linked by the linear succinate units.

The cadmium succinate framework, in **XXIV** and **XXV**, can be visualized based on 3-connected nets (10,3) (Fig. 4.65). The 10-gon nets form a

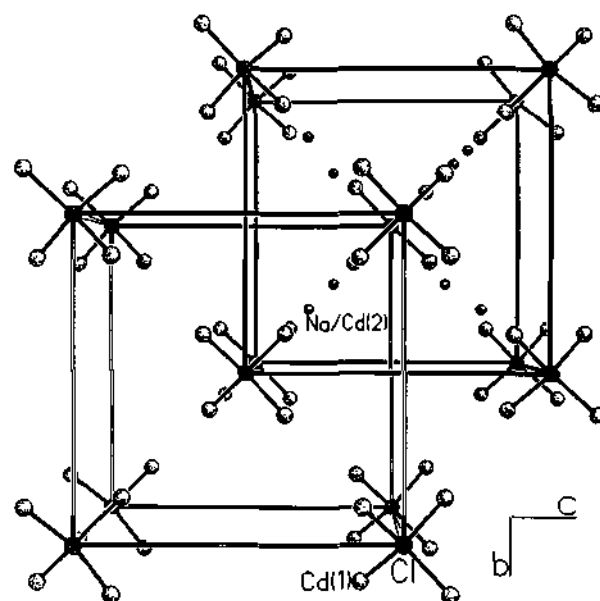


Fig. 4.64. Interpenetration of lattices in **XXIV**, comparable to that in α polonium related networks. Similar interpenetration is present in **XXV** as well.

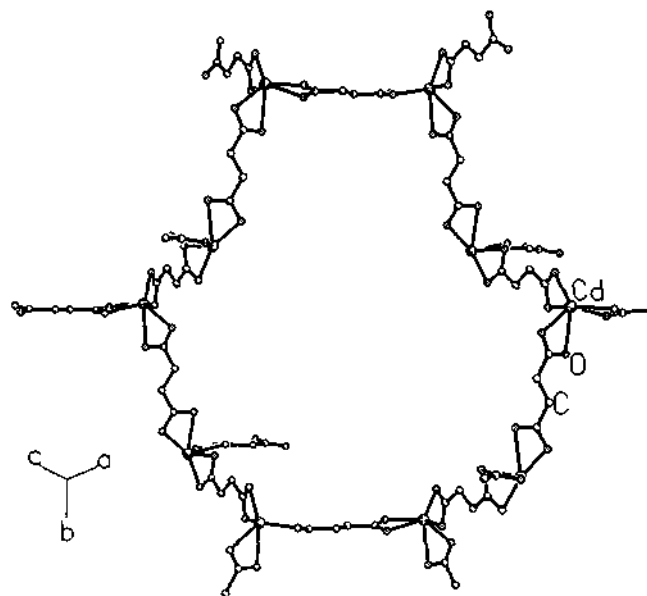


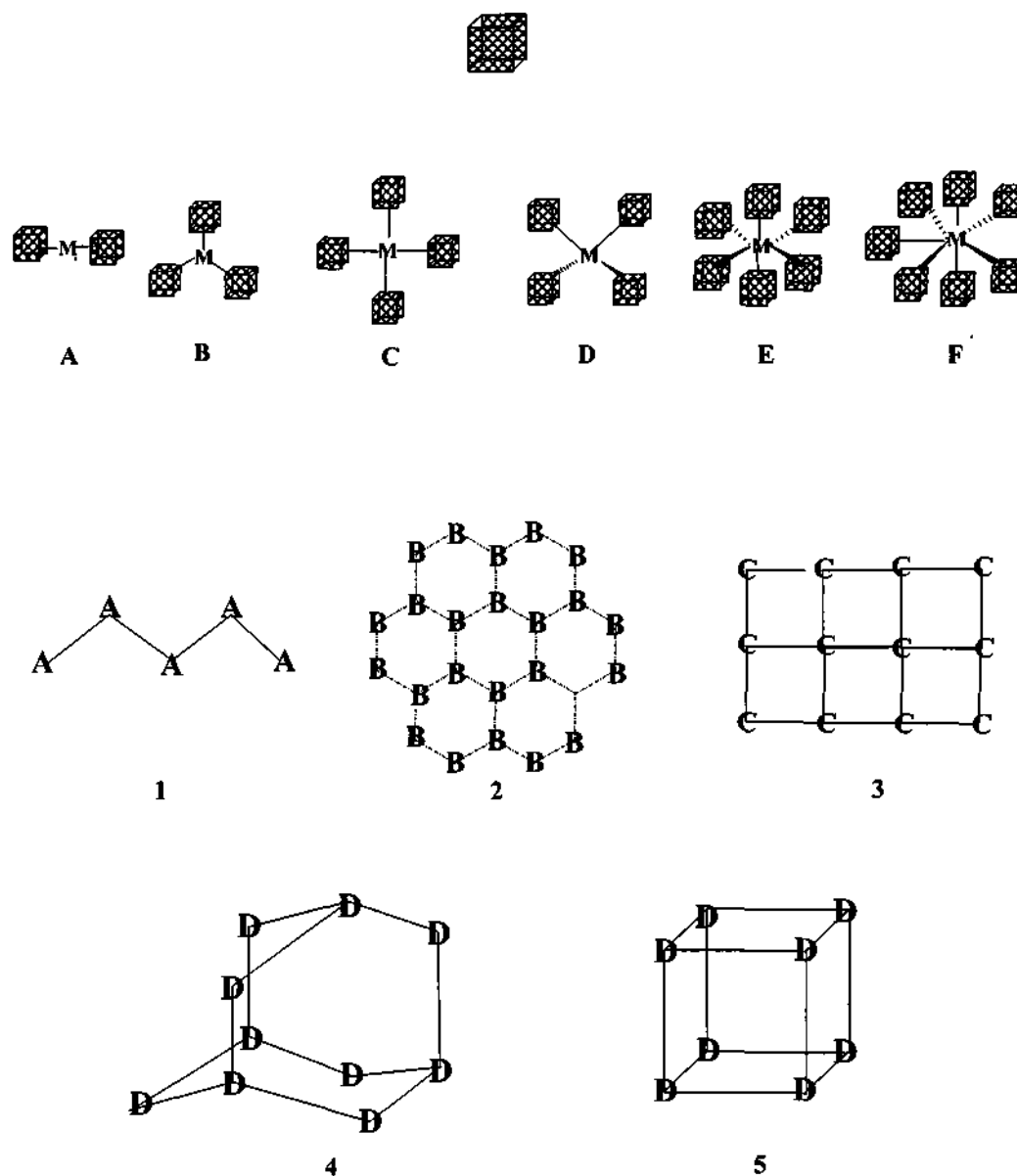
Fig. 4.65. The 3-connected 10-gon net (10,3) formed by linking of the cadmium nodes by the succinate linkers.

three-dimensional architecture with a cubic symmetry possessing intersecting channels, closely related to the (10,3)-net in the mineral eglestonite, $[(\text{Hg}_2)_3\text{O}_2\text{H}]\text{Cl}_3$.^[37,60,86,87] The similarity arises from the presence of pyramidal CdO_6 nodes in the cadmium succinates. Thus, the cadmium succinate net gives rise to a tetrahedral site occupied by the halide atom, which interact with the four nearest Cd neighbors forming $(\text{X}(\text{Cd}(\text{Suc})_3)_4)$ type tetrahedral clusters. The cubic net is a 3-connected analogue of the diamond net. Other compounds exhibiting a similar 3-connected net (10,3) topology with cubic symmetry include SrSi_2 , H_2O_2 and B_2O_3 .^[86,87]

The environment of the Na^+ ions with respect to the second nearest neighbors, namely the Cl^-/Br^- ions, presents an interesting structural feature. The Na^+ ions in XXIV and XXV are arranged in such a way that they form a XNa_4 tetrahedron ($\text{X} = \text{Cl}, \text{Br}$). The tetrahedra occupy the corners of a cube (Fig. 4.64) and are interpenetrated by another identical, but independent cube, similar to that in diamond related structures. The Na – Cl distance in XXIV is 4.242 Å compared to 2.820 Å in normal NaCl. The Na – Br distance in XXV is 4.223 Å compared 2.990 Å in normal NaBr.

4.9.3. Summary

The exchange reaction between $\text{CdCl}_2 \cdot \text{H}_2\text{O}$ or $\text{CdBr}_2 \cdot 4\text{H}_2\text{O}$ and sodium succinate yields unusual three-dimensional open-framework cadmium succinates containing tetrahedral $\text{XCd}_4\text{O}_{24}$, ($\text{X} = \text{Cl}$ or Br) clusters, linked by the succinate units. The structure of these hybrid compounds are comparable to those of the dicarboxylate linked hybrid structures.^[84] The tetrahedral cluster acts as the secondary building unit (SBU) and gives rise to a three-dimensional cubic structure. This can be visualized from Scheme 4.5 presented here. According to this scheme,



Scheme 4.5: A general scheme illustrating the building up of complex three-dimensional architectures from simpler primary and secondary building units. A-F are secondary building units (SBUs, with $M = \text{Cl}, \text{Br}, \text{O}, \text{S}, \text{Se}$ etc.) formed by the cube-like primary building unit, which could be a tetrahedron, octahedron or pentagonal bipyramid. 1-5 are tertiary building units (TBU). In XXIV and XXV, 5 is the TBU.

the primary building unit in these structures, under discussion, would be the CdO_6 octahedron, while the SBU would be the motif (D), with $M = \text{Cl}, \text{Br}$ and the TBU would be the motif (5).

4.10. Manganese adipate, $[\text{Mn}(\text{O}_2\text{C}-(\text{CH}_2)_4-\text{CO}_2)(\text{C}_4\text{N}_2\text{H}_8)]$ (XXVI)

4.10.1. Results

The asymmetric unit of the adipate, $[\text{Mn}(\text{O}_2\text{C}-(\text{CH}_2)_4-\text{CO}_2)(\text{C}_4\text{N}_2\text{H}_8)]$, XXVI, consists of 17 non-hydrogen atoms. The Mn atoms are five-coordinated by four carboxylate oxygens, and two N atoms of the amine with the average Mn-O distance of 2.229 Å and Mn-N distance of 2.14 Å. The average O/N-Mn-O/N angle is 104.5° (Table 4.25). Bond valence sum calculations^[21] indicated that the valence states of the Mn, C and O in XVII were +2, +4 and -2 respectively. The adipate moiety has the expected bond distances and angles (Table 4.25).

The connectivity between the Mn centers through the adipate units results in a three-dimensional framework with channels along the c-axis, (6.642 x 6.642 Å, shortest C - C contact not including the van der Waals radii) (Fig. 4.66). However the channel get occupied by the piperazine molecule and to satisfy the coordination requirements of the framework Mn atom the piperazine moiety bond to the Mn atom through its N atom.

4.10.2. Discussion

The piperazine, in this case, apparently performs a dual role of being a ligand as well as a template (Fig. 4.70). Interestingly, in XXVI, there are no N-H...O hydrogen bonds indicating the hydrophobic nature of the channels. The presence of five-coordinated Mn^{2+} ions in a trigonal bipyramidal arrangement in XXVI, is an unusual feature in such open-framework carboxylates, though manganese carboxylates containing Mn in an octahedral environment are known.

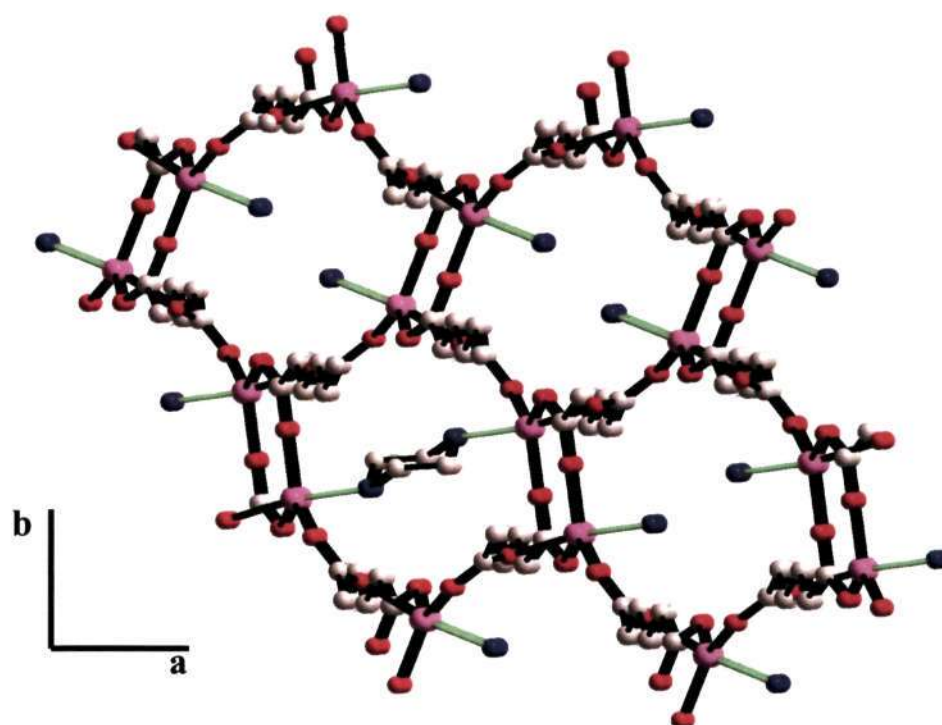


Fig. 4.66. The pseudo-channels in $[\text{Mn}(\text{O}_2\text{C}-(\text{CH}_2)_4-\text{CO}_2)(\text{C}_4\text{N}_2\text{H}_8)]$, **XXVI**, occupied by the bonded piperazine molecules, bound to the Mn atoms. Green colored bond indicates that the Mn-N bonds formed due to the coordination requirements of the Mn atoms. The position of the piperazine moieties clearly suggests their dual role of a ligand and a template. Color scheme: Mn – purple; O –red; N –blue; C –white.

Table 4.25. Selected bond distances and angles for XXVI, [Mn(O₂C-(CH₂)₄-CO₂)(C₄N₂H₈)]

Moiety	Distance (Å)	Moiety	Distance (Å)
Mn(1)-O(1)	2.072(5)	C(1)-C(6)	1.519(10)
Mn(1)-O(2)	2.122(5)	C(2)-C(4)	1.496(10)
Mn(1)-O(3)	2.134(5)	C(3)-C(4)	1.509(10)
Mn(1)-O(4)	2.143(5)	C(3)-C(5)	1.527(10)
Mn(1)-N(1)	2.275(6)	C(5)-C(6)#4	1.514(10)
O(1)-C(1)#1	1.249(8)	C(6)-C(5)#5	1.514(10)
O(2)-C(2)	1.263(9)	N(1)-C(10)	1.482(10)
O(3)-C(1)	1.257(9)	N(1)-C(20)	1.493(10)
O(4)-C(2)#2	1.260(8)	C(10)-C(20)#6	1.512(10)
O(4)-C(2)#3	1.260(8)	C(20)-C(10)#6	1.512(10)
Moiety	Angle (°)	Moiety	Angle (°)
O(1)-Mn(1)-O(2)	110.3(2)	O(1)#1-C(1)-C(6)	119.3(7)
O(1)-Mn(1)-O(3)	124.0(2)	O(3)-C(1)-C(6)	117.0(6)
O(2)-Mn(1)-O(3)	125.5(2)	O(4)#3-C(2)-C(4)	119.4(7)
O(1)-Mn(1)-O(4)	97.0(2)	O(2)-C(2)-C(4)	118.2(7)
O(2)-Mn(1)-O(4)	85.9(2)	C(4)-C(3)-C(5)	112.5(6)
O(3)-Mn(1)-O(4)	83.2(2)	C(5)#5-C(6)-C(1)	115.6(6)
O(1)-Mn(1)-N(1)	93.1(2)	C(10)-N(1)-C(20)	107.9(6)
O(2)-Mn(1)-N(1)	92.2(2)	C(10)-N(1)-Mn(1)	115.6(5)
O(3)-Mn(1)-N(1)	89.7(2)	C(20)-N(1)-Mn(1)	112.9(4)
O(4)-Mn(1)-N(1)	169.7(2)	N(1)-C(10)-C(20)#6	112.4(6)
O(1)#1-C(1)-O(3)	123.7(7)	N(1)-C(20)-C(10)#6	111.7(6)
O(4)#3-C(2)-O(2)	122.4(7)		

Symmetry transformations used to generate equivalent atoms

#1 -x+1,-y+1,-z #2 x,-y+1/2,z-1/2 #3 x,-y+1/2,z+1/2

#4 x-1,-y+1/2,z+1/2 #5 x+1,-y+1/2,z-1/2 #6 -x+1,-y+1,-z+1

4.10.3. Summary

A manganese adipate with a three-dimensional structure has been made employing solvothermal methods. The noteworthy features being the presence of a amine molecules in the one-dimensional pseudo-channels performing a dual role of a template and a ligand.

4.11. Hybrid Structures - Alkali halides incorporated in metal oxalate frameworks

4.11.1. Three-dimensional alkali halide lattices stabilized in host cadmium oxalate frameworks

[RbCl][Cd₆(C₂O₄)₆].2H₂O (XXVII) and [RbBr][Cd₆(C₂O₄)₆].2H₂O (XXVIII)

The asymmetric units of [RbCl][Cd₆(C₂O₄)₆].2H₂O, XXVII contains 10 non-hydrogen atoms, of which 7 atoms make up cadmium oxalate host framework and the remaining 3 are the guest molecules (Rb, Cl and water). [RbBr][Cd₆(C₂O₄)₆].2H₂O, XXXVIII is isostructural with XXVII, with the Cl⁻ ions replaced by the Br⁻ ions. The Cd, in both compounds, is six coordinated with respect to the oxygen atoms forming a D_{3h} trigonal prism with Cd – O distances in the range 2.292(5) – 2.384(6) Å (av. 2.339 Å) in XXVII and 2.310(7) – 2.399(7) Å (av. Cd–O = 2.355 Å) in XXVIII, with the longer Cd-O lengths probably corresponding to the double bonded oxalate oxygens. The oxygens are linked to the carbon atoms forming the oxalate unit, with average C – O distances of 1.248 and 1.251 Å, for XXVII and XXVIII, respectively (Table 4.26). The O – Cd – O bond angles are in the range 69.8(2) – 148.5(2)° (av. 102.9°), for XXVII (Table 4.26) and 69.5(2) – 147.4(2)° (av. O – Cd – O = 102.9), for XXVIII (Table 4.26). The Rb ions are coordinated by twelve oxygen atoms at a distance of ~3 Å. All the oxygen atoms interacting with rubidium are at distances less than 3.1Å, which is the upper limit for significant M...O interaction (M = Na, K, Rb etc.) (8). The Cl/Br⁻ ions are surrounded by six cadmium atoms at ~2.9/~2.92 Å (Table 4.26). These geometrical parameters are in good agreement with those reported for similar compounds.

In XXVII and XXVIII, the framework structure consists of a network of cadmium and oxalate units. The connectivity between these units is such that it forms an unusual cadmium oxide cluster of the composition [Cd₆O₂₄]. The clusters are connected

Table 4.26. Selected bond distances and bond angles for XXVII, [RbCl][Cd₆(C₂O₄)₆].2H₂O and XXVIII, [RbBr][Cd₆(C₂O₄)₆].2H₂O

XXVII			
Moiety	Distance (Å)	Moiety	Distance (Å)
Cd(1)-O(1)	2.292(5)	Rb(1)-O(3)#5	3.078(6)
Cd(1)-O(2)	2.327(6)	Rb(1)-O(3)	3.078(6)
Cd(1)-O(3)	2.341(6)	Cl(1)-Cd(1)#7	2.8919(6)
Cd(1)-O(4)	2.342(6)	Cl(1)-Cd(1)#1	2.8918(6)
Cd(1)-O(4)#1	2.348(6)	Cl(1)-Cd(1)#8	2.8918(6)
Cd(1)-O(1)#2	2.384(6)	Cl(1)-Cd(1)#7	2.8918(6)
Cd(1)-Cl(1)	2.8917(6)	Cl(1)-Cd(1)#2	2.8918(6)
Rb(1)-O(2)	2.973(6)	O(1)-C(1)	1.259(11)
Rb(1)-O(2)#3	2.973(6)	O(1)-Cd(1)#7	2.384(6)
Rb(1)-O(2)#4	2.973(6)	O(2)-C(1)#6	1.237(11)
Rb(1)-O(2)#5	2.973(6)	O(3)-C(2)	1.252(10)
Rb(1)-O(2)#6	2.973(6)	O(4)-C(2)#9	1.253(10)
Rb(1)-O(2)#4	2.973(6)	O(4)-Cd(1)#8	2.348(5)
Rb(1)-O(3)#3	3.078(6)	C(1)-O(2)#4	1.237(11)
Rb(1)-O(3)#6	3.078(6)	C(1)-C(1)#10	1.57(2)
Rb(1)-O(3)#4	3.078(6)	C(2)-O(4)#9	1.253(10)
Rb(1)-O(3)#4	3.078(6)	C(2)-C(2)#9	1.53(2)
Moiety	Angle (°)	Moiety	Angle (°)
O(1)-Cd(1)-O(2)	93.2(2)	O(2)-Cd(1)-O(1)#2	69.8(2)
O(1)-Cd(1)-O(3)	136.1(2)	O(3)-Cd(1)-O(1)#2	123.0(2)
O(2)-Cd(1)-O(3)	73.0(2)	O(4)-Cd(1)-O(1)#2	87.7(2)
O(1)-Cd(1)-O(4)	148.5(2)	O(4)#1-Cd(1)-O(1)#2	147.4(2)
O(2)-Cd(1)-O(4)	114.3(2)	O(2)#4-C(1)-O(1)	126.4(8)
O(3)-Cd(1)-O(4)	70.2(2)	O(2)#4-C(1)-C(1)#10	117.3(10)
O(1)-Cd(1)-O(4)#1	81.8(2)	O(1)-C(1)-C(1)#10	116.2(10)
O(2)-Cd(1)-O(4)#1	141.2(2)	O(3)-C(2)-O(4)#9	124.8(8)
O(3)-Cd(1)-O(4)#1	84.2(2)	O(3)-C(2)-C(2)#9	118.0(9)
O(4)-Cd(1)-O(4)#1	85.35(7)	O(4)#9-C(2)-C(2)#9	117.3(9)
O(1)-Cd(1)-O(1)#2	87.9(3)		
XXVIII			
Atom	Distance (Å)	Atom	Distance (Å)
Cd(1)-O(1)	2.310(7)	Rb(1)-O(4)#3	3.091(7)
Cd(1)-O(2)	2.323(7)	Rb(1)-O(4)#7	3.091(7)

Cd(1)-O(3)#1	2.350(7)	Rb(1)-O(4)#5	3.091(7)
Cd(1)-O(3)	2.352(7)	Cd(1)-Br(1)#1	2.917 (7)
Cd(1)-O(4)	2.358(7)	Cd(1)-Br(1)#8	2.917 (7)
Cd(1)-O(1)#2	2.399(7)	Cd(1)-Br(1)#9	2.917 (7)
Cd(1)-O(1)#8	2.399(7)	Cd(1)-Br(1)#8	2.917 (7)
Cd(1)-O(3)#9	2.350(7)	Cd(1)-Br(1)#2	2.917 (7)
Rb(1)-O(2)#3	2.983(7)	Cd(1)-Br(1)	2.917 (7)
Rb(1)-O(2)#4	2.983(7)	C(1)-O(2)	1.230(13)
Rb(1)-O(2)	2.983(7)	C(1)-O(1)#3	1.272(13)
Rb(1)-O(2)#5	2.983(7)	C(1)-O(1)#7	1.272(13)
Rb(1)-O(2)#6	2.983(7)	C(2)-O(4)#4	1.233(13)
Rb(1)-O(2)#7	2.983(7)	C(2)-O(3)	1.264(13)
Rb(1)-O(4)#6	3.091(7)	C(2)-O(4)#6	1.233(13)
Rb(1)-O(4)#4	3.091(7)	C(1)-C(1)#10	1.56(2)
Rb(1)-O(4)	3.091(7)	C(2)-C(2)#11	1.57(2)
Moiety	Angle (°)	Moiety	Angle (°)
O(1)-Cd(1)-O(2)	93.1(3)	O(2)-Cd(1)-O(1)#2	69.5(2)
O(1)-Cd(1)-O(3)#1	147.7(2)	O(3)#1-Cd(1)-O(1)#2	87.3(2)
O(2)-Cd(1)-O(3)#1	114.9(3)	O(3)-Cd(1)-O(1)#2	146.7(2)
O(1)-Cd(1)-O(3)	81.7(3)	O(4)-Cd(1)-O(1)#2	123.0(3)
O(2)-Cd(1)-O(3)	142.2(2)	O(4)#4-C(2)-O(3)	125.2(9)
O(3)#1-Cd(1)-O(3)	85.01(8)	O(2)-C(1)-O(1)#3	126.0(9)
O(1)-Cd(1)-O(4)	136.6(3)	O(2)-C(1)-C(1)#10	119.1(12)
O(2)-Cd(1)-O(4)	73.8(2)	O(1)#3-C(1)-C(1)#10	114.9(11)
O(3)#1-Cd(1)-O(4)	70.5(2)	O(4)#4-C(2)-C(2)#11	118.5(11)
O(3)-Cd(1)-O(4)	84.5(3)	O(3)-C(2)-C(2)#11	116.2(11)
O(1)-Cd(1)-O(1)#2	87.8(4)		

Symmetry transformations used to generate equivalent atoms:

For XXVII:

#1 $y-1/3, -x+y+1/3, -z+1/3$ #2 $-y+1, x-y+1, z$ #3 $-x, -y, -z$
 #4 $x-y, x, -z$ #5 $-x+y, -x, z$ #6 $y, -x+y, -z$ #7 $-x+2/3, -y+4/3, -z+1/3$
 #8 $x-y+2/3, x+1/3, -z+1/3$ #9 $-x+2/3, -y+1/3, -z+1/3$ #10 $-x, -y+1, -z$

For XXVIII:

#1 $x-y+2/3, x+1/3, -z+1/3$ #2 $-y+1, x-y+1, z$ #3 $y, -x+y, -z$
 #4 $-y, x-y, z$ #5 $-x, -y, -z$ #6 $-x+y, -x, z$ #7 $x-y, x, -z$
 #8 $-x+2/3, -y+4/3, -z+1/3$ #10 $y-1/3, -x+y+1/3, -z+1/3$
 #11 $-x+1, -y+1, z$ #12 $-x-1/3, -y+1/3, -z+1/3$

into three-dimensions by the oxalates units. The Cl⁻ ions in XXVII and Br⁻ ions in XXVIII are located inside these clusters (Fig. 4.67), with the charge compensating

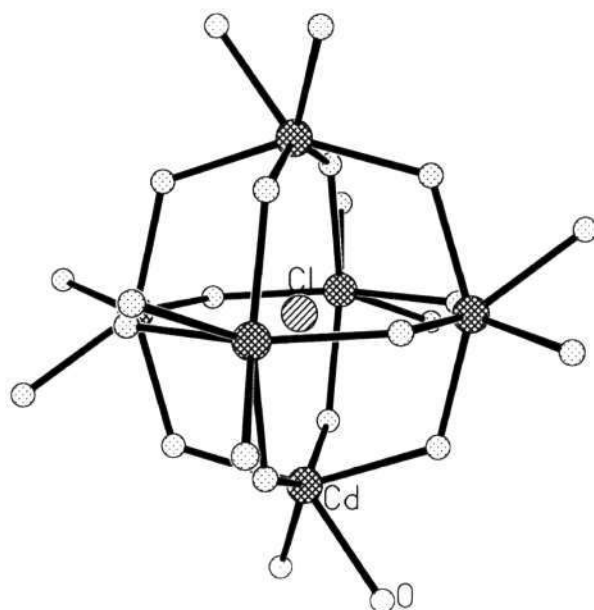


Fig. 4.67. Figure of **XXVII**, showing a single [Cd₆O₂₄] cluster with the Cl⁻ ions at the centre.

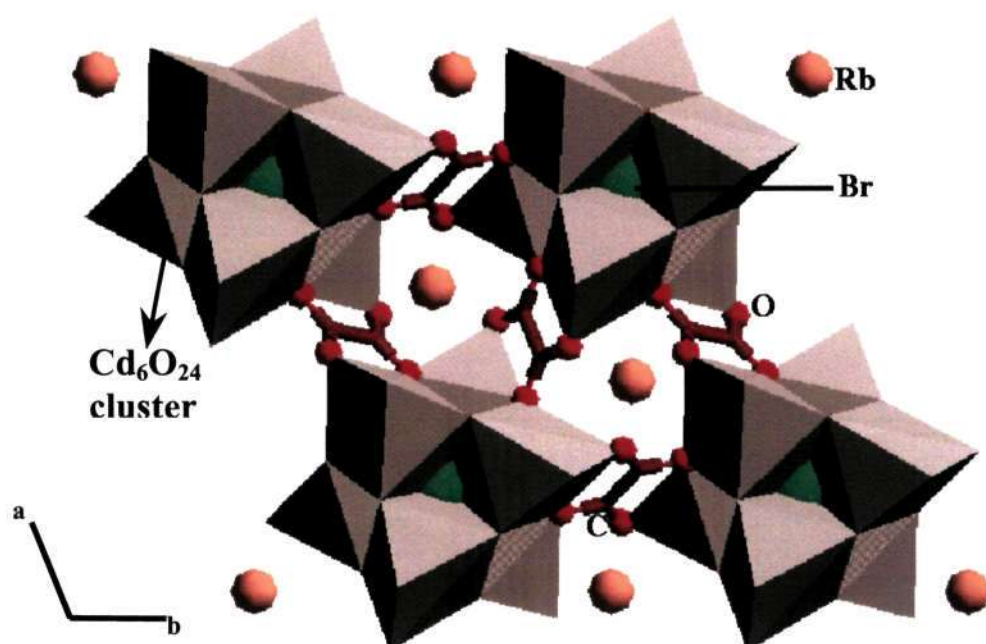


Fig. 4.68. Structure of **XXVIII** in the *ab* plane. Note that the Rb⁺ ions are positioned outside the cluster unit.

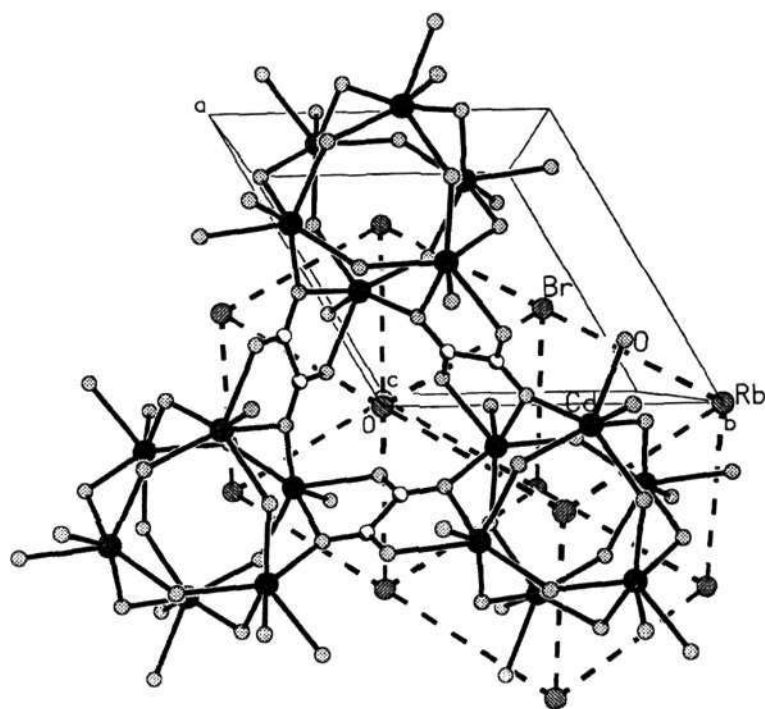


Fig. 4.69. Structure of **XXVIII**, showing the $Fm\bar{3}m$ lattice of $RbBr$ within the parent cadmium oxalate structure. The $RbCl$ in the isostructural **XXVII** is oriented in the same fashion.

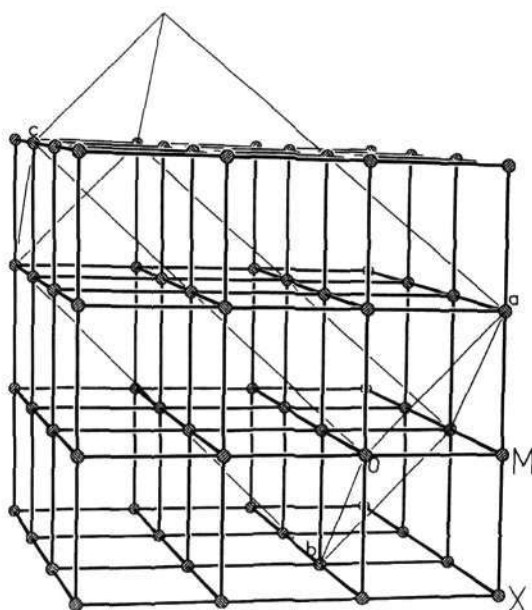


Fig. 4.70. Structure of RbX , $X = Cl, Br$ in **XXVII** and **XXVIII**, respectively. Note that RbX is along the $[111]$ lattice.

Rb⁺ ions reside in the cavities formed in between these cluster units (Fig. 4.68 and 4.69). The Rb⁺ and halide ions are perfectly ordered in three-dimensions forming an independent rock-salt (Fm3m) structure with interpenetrating *fcc* lattices (Fig. 4.70). The cubic unit cell parameter of RbCl in XXVII is 13.452 Å and that of, RbBr in XXVIII is 13.496 Å, which is roughly double that in ordinary RbCl (6.570 Å) and RbBr (6.855 Å), respectively, as shown in Fig. 4.70. The [100] RbCl and RbBr planes run along the [111] direction of XXVII and XXVIII, respectively (Fig. 4.69 and 4.70). An alternate way to describe the structure of XXVII and XXVIII would be to consider the halide ion as being at the center of a cluster of six Cd atoms arranged in such a manner that they form the six vertices of an octahedron, with the next nearest oxygen neighbors forming the trigonal prisms with Cd atoms. Accordingly, these compounds could be considered as a super rock salt arrangement of two types of clusters, [XCd₆(C₂O₄)₃]⁵⁺ (X = Cl, Br) and [Rb(H₂O)₂(C₂O₄)₃]⁵⁻. This type of arrangement is reminiscent of Chevrel phases.^[88]

Thermogravimetric analysis of compounds XXVII and XXVIII were carried out in O₂ atmosphere (50 ml min.⁻¹) in the range room temperature to 700 °C. Both XXVII and XXVIII showed two distinct mass losses. Both showed, a gradual mass loss around 100 °C followed by a sharp mass loss in the range 350 – 400 °C (42.0 (XXVII) and 43.5% (XXVIII)) was found due to the loss of the extra-framework water and oxalate (calc. 41.5 and 42.3%, for XXVII and XXVIII, respectively). A mass loss above 500 °C was found in both, due to the slow evaporation of CdO.

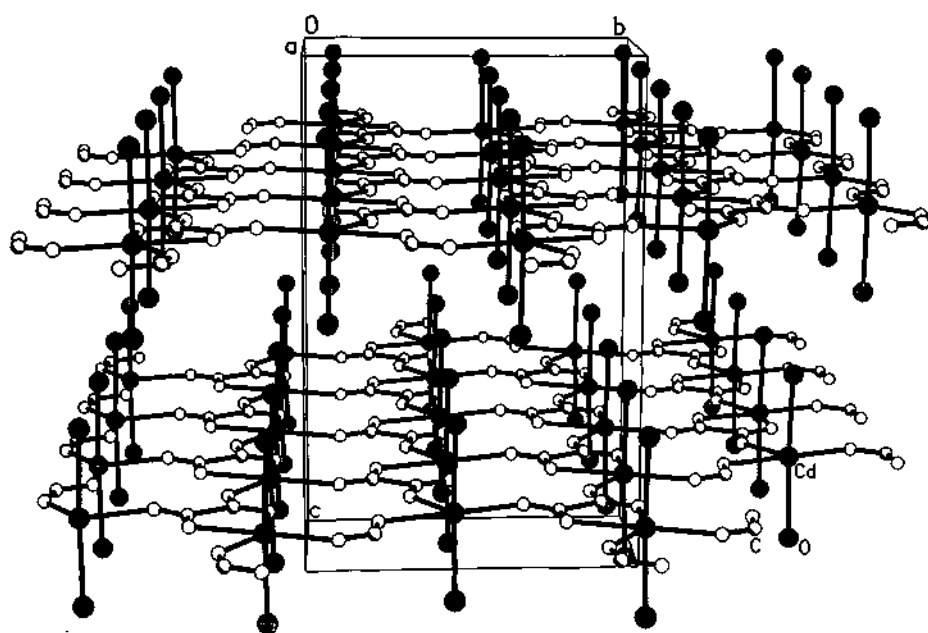
4.11.2. Cadmium oxalate hosts incorporating layered alkali halide lattices

2[CsBr][Cd(C₂O₄)]·H₂O (XXIX) 2[CsBr][Cd₂(C₂O₄)(Br)₂].2H₂O (XXX) and [Rb₂Cd(NO₃)(Cl)(C₂O₄)(H₂O)] (XXXI)

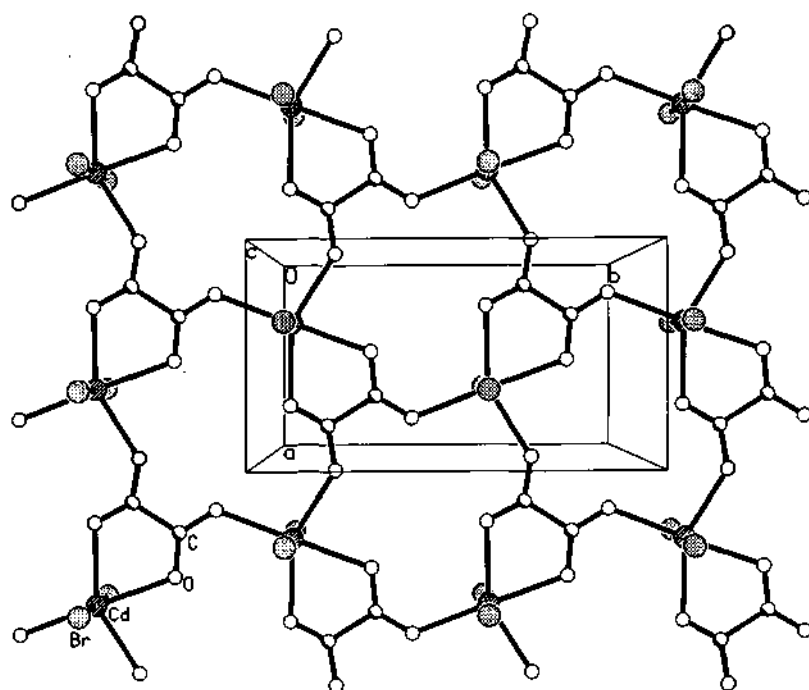
The asymmetric unit of **XXIX**, **XXX** and **XXXI** contains 10, 8 and 15 non-hydrogen atoms. The Cd atom, in all three compounds, is in an octahedral coordination. The average Cd – O distance and Cd – Br distances are 2.315 Å and 2.710 Å, for **XXIX**, 2.354 and 2.697 Å for **XXX** and 2.311Å and 2.510(2)Å, for **XXXI** (Table 4.27). The oxygens, in turn, are linked with carbon forming the oxalate unit, with average C – O distances of 1.240, 1.243 Å and 1.253 Å, for **XXIX**, **XXX** and **XXXI**, respectively. The various bond angles involved in **XXIX**, **XXX** and **XXXI** have been listed in Table 4.27. The Cs⁺ ions, in **XXIX** and **XXX**, are eight-coordinated with respect to the oxygen and bromines.

The structure of **XXXI** is different from **XXIX** and **XXX**. The extra-framework species in **XXXI** consists of two Rb and a nitrate ions, situated in the inter-lamellar regions. The average N-O bond distance and O-N-O angle in the NO₃ unit are 1.240Å and 120°, respectively. The two crystallographically distinct Rb atoms are coordinated by 10-[Rb(1)] and 12-[Rb(2)] nearest neighbors. The Rb(1) is surrounded by eight oxygens and two chlorines with average Rb(1)-O and Rb(1)-Cl distances of 2.959Å and 3.405Å, respectively (Table 4.27), while the Rb(2) is surrounded by nine oxygens and three chlorines with the average Rb(2)-O and Rb(2)-Cl distances of 3.048 and 3.637Å, respectively. The various geometrical parameters found in the compounds, **XXIX**, **XXX** and **XXXI** are in good agreement with those reported for similar compounds.

The framework structure of **XXIX** and **XXXI** consist of a network of cadmium and oxalate units forming layers (Fig. 4.71a and b), while that of **XXX** is formed of isolate cadmium oxalate units connected by the CsBr units (Fig. 72). In both **XXIX**, **XXX** and **XXXI**, the halide ions are connected to the cadmium. In **XXIX** and **XXXI** these bound halide ions and water molecules protrude into the inter-lamellar space (Fig. 4.71a).. Both in **XXIX** and **XXX**, the Cs⁺ ions along with



(a)



(b)

Fig. 4. 71. (a) Structure of **XXIX** in the bc plane showing the layer arrangement. Note that the Br atoms point into the interlamellar space. Cs and water molecules are not shown for purposes of clarity. (b) Structure of **XXIX** showing a single layer of the cadmium oxalate.

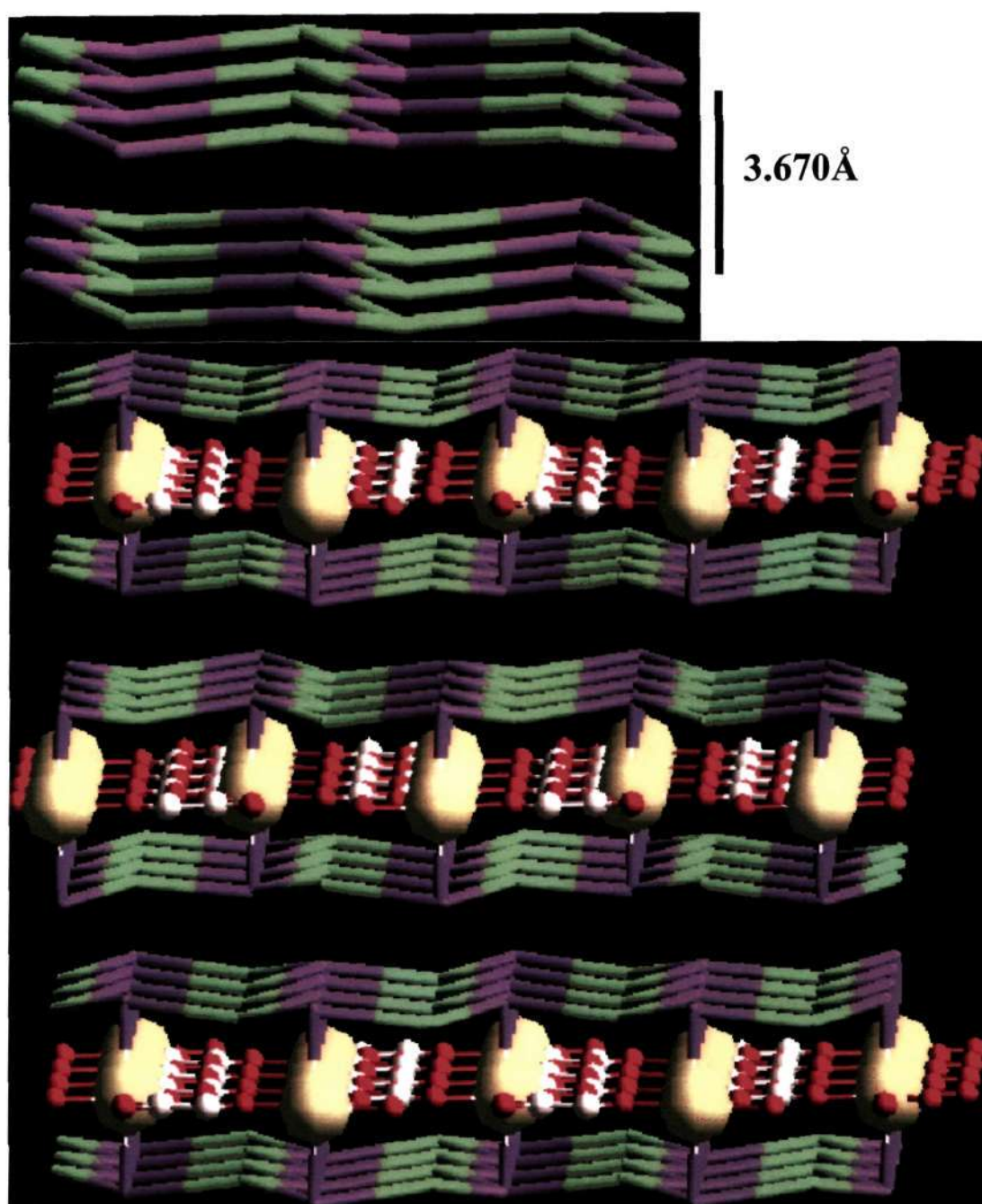


Fig. 4. 72. Structure of **XXIX** showing the CsBr lattice within the layers. Inset shows the CsBr lattice alone. Note that alternate CsBr layers have larger separation. (Color scheme: yellow – Cd, white – C, red – O, purple – Br, green – Cs).

water molecules occupy the inter-lamellar space. The relative positions between the Cs^+ and Br^- ions are such that they form a graphite-like layer (Fig. 4.72). Such arrangement creates two closely spaced CsBr layers separated by $\sim 3.7 \text{ \AA}$ in both **XXIX** and **XXX**. The thickness of the oxalate layers is 10.62 \AA in **XXIX** and 5.87 \AA in **XXX**, which is roughly half that observed in the former.

The CsBr layers are made of neutral hexagonal units of Cs_3Br_3 , with chair conformation as in cyclohexane, closely resembling that of graphite, in case of **XXIX** (Fig. 4.72), and consists of 8-membered rings that resemble the chair conformation of cyclooctane in **XXX** (Fig. 4.73a and b). What is interesting in **XXX** is that, the isolated cadmium oxalate units are situated in between these CsBr layers and act as a pillar through Cd – Br connectivity.. The unusual layered alkali halide structures in **XXIX** are stabilized by the cadmium oxalate layers, present after every two CsBr layers, by providing additional coordination for the Cs^+ ions through the oxalate oxygens. Accordingly, **XXIX** can be considered to be a genuine hetero-lattice or nano-composite with alternating organic and inorganic layers (Fig. 4.72).

The layered architecture in **XXXI** is markedly different from that of **XXIX** and **XXX**. The connectivity between the oxalate and the cadmium atoms result in a six-membered aperture within the layers, similar to the one in **XXIX**. Such layers get stacked along the *c*-axis and the Rb^+ ions and the NO_3^- ions occupy the inter-lamellar spaces and interact with the Cl^- ions and water molecules in the interlayer space (Fig. 4.74 and 4.75). The adjacent layers are shifted by nearly $1/2$ of the unit cell along the *b*-axis, resulting in a *ABABAB...* type of stacking. The Rb(1) and Rb(2) atoms appear to be at the center of the 6-membered apertures present within the cadmium oxalate layers. The interaction of the Rb(2) with the Cl^- ions results in a one-dimensional RbCl chain along the *b*-axis. The Rb(1) atom forms a dimer with

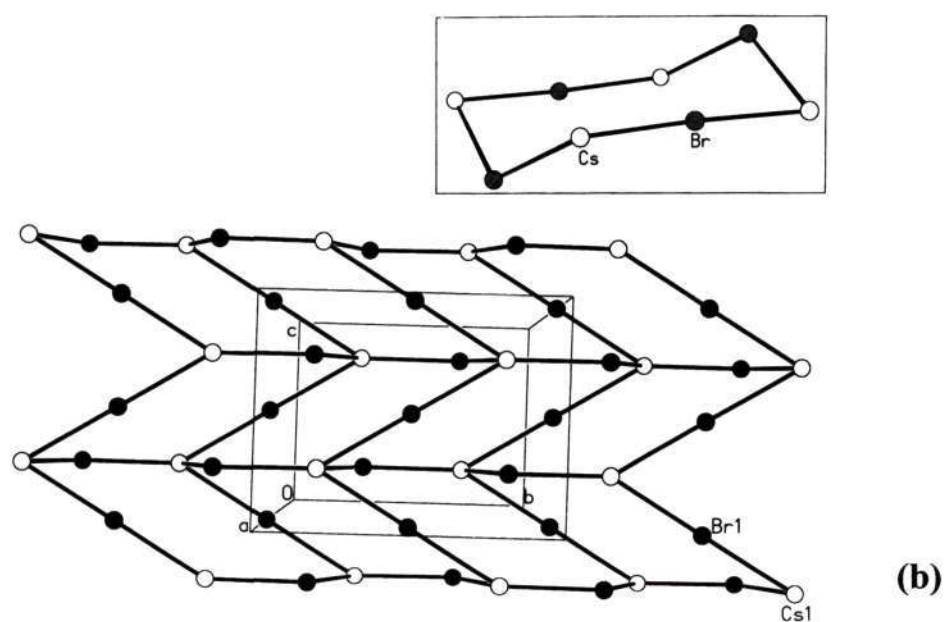
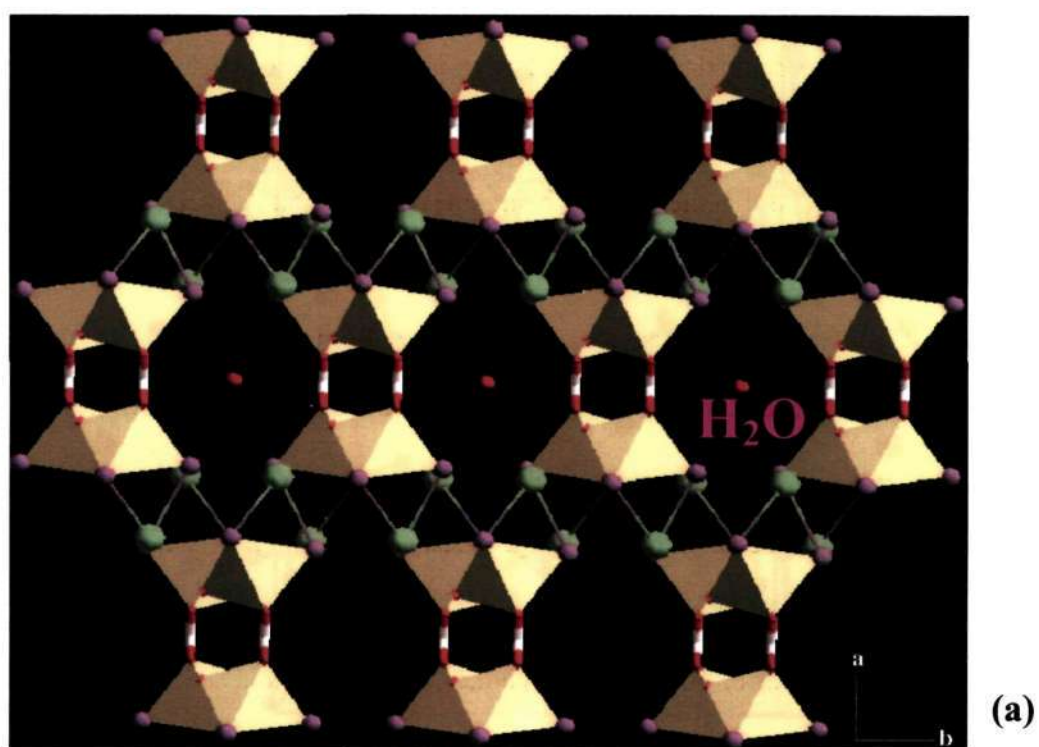


Fig. 4. 73. (a) Structure of **XXX** showing the channels formed by the connectivity between the isolated cadmium oxalate and CsBr. Note that the water molecules occupy these channels. (color scheme: yellow – Cd, white – C, red – O, purple – Br, green – Cs). (b) Layered structure of CsBr in **XXX**. Inset shows the CsBr in chair conformation.

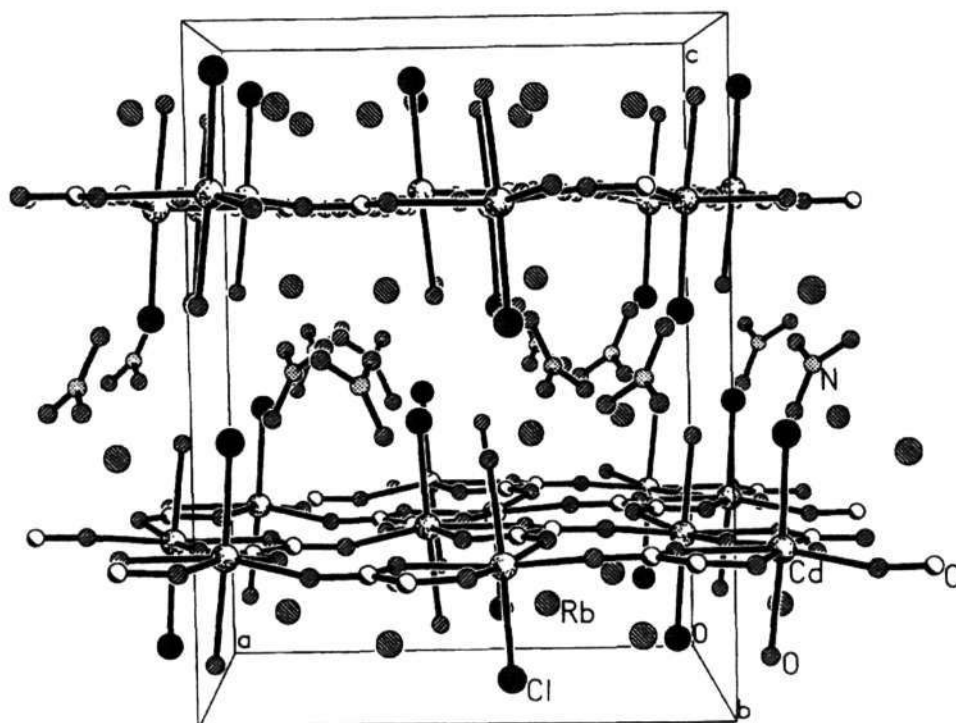


Fig. 4.74. Layer stacking of $[\text{Rb}_2\text{Cd}(\text{Cl})(\text{NO}_3)(\text{C}_2\text{O}_4)(\text{H}_2\text{O})]$ along the c -axis with the Rb^+ ions and the NO_3^- ions occupying the interlayer region, in **XXXI**. The Cl atoms protrude into the interlayer space.

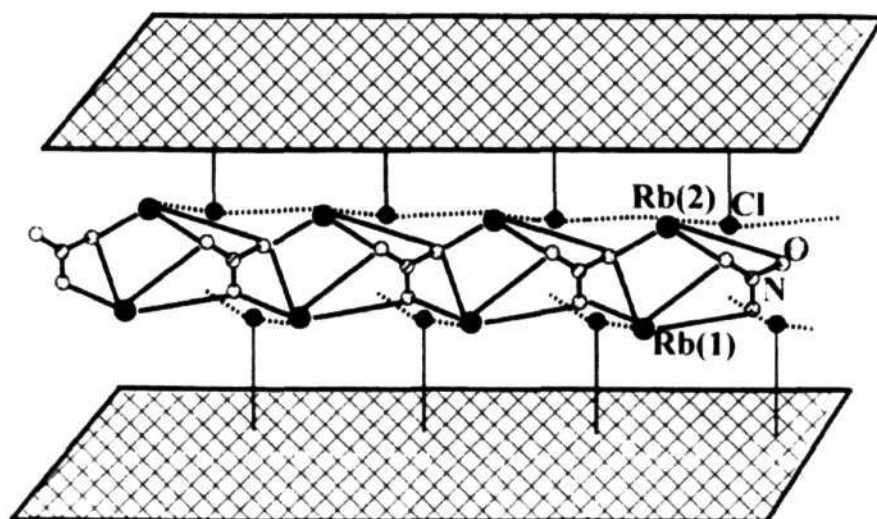


Fig. 4.75. A schematic representation showing the cation excess Rb_2NO_3 slabs sandwiched between the cadmium chloro-oxalate layers in **XXXI**. Note the Cl-atoms protruding into the inter-lamellar regions.

the Cl^- ions, which are further linked with the Rb(2) forming a layer with 12-membered aperture in the ab -plane as shown in Fig. 76a. Alternatively, Rb(1) along with Cl^- ions and NO_3^- ions, form a layer with ten-membered apertures (Fig. 76b). Such layers are reminiscent of Zn phosphate layers observed recently.^[89] The NO_3^- ions interact with the Rb atoms in both bidentate and monodentate modes within these layers. The Rb(2) on the other hand, forms a capped one-dimensional chain with both Cl^- and NO_3^- ions. The Rb atoms and the NO_3^- ions form a cation excess (Rb_2NO_3) slab (Fig. 4.75). These slabs get sandwiched between the cadmium chloro-oxalate layers. In **XXXI** one of the Rb atoms, Rb(2), forms a one-dimensional RbCl chain capped on both sides by NO_3^- ions, and Rb(1) forms a Rb_2Cl_2 dimer connected through the nitrate ion forming a layer.

Alternatively, the cation excess Rb_2NO_3 slabs in **XXXI** are linked with the Cl atoms to form Rb_2ClNO_3 type layers. A schematic presentation of such an arrangement is shown in Figure 4.75. In **XXXI**, the average RbCl distance is 3.635 Å, comparable to the distance in normal RbCl (3.291 Å).

Thermogravimetric analyses of **XXIX** and **XXXI** were carried out in O_2 atmosphere (50 ml min^{-1}) in the range room temperature to 700°C . Both showed three distinct mass losses. For **XXIX**, a sharp mass loss of 2.3% around 150°C corresponds to the loss of extra-framework water (calc. 2.8) and the second mass loss of 16% around 350°C corresponds to the loss of oxalate units. Above 600°C there was loss due to the evaporation of CdO . For **XXXI**, a gradual mass loss occurs in the range of $100\text{-}160^\circ\text{C}$ due to the bound water molecules; a relatively sharp mass loss occurs in the range of $350\text{-}450^\circ\text{C}$ due to the loss the oxalate and the decomposition of the rubidium salt. The total mass loss of 24.5% observed for compound **XXXI** is in agreement with the calculated mass loss of 22%. Mass loss

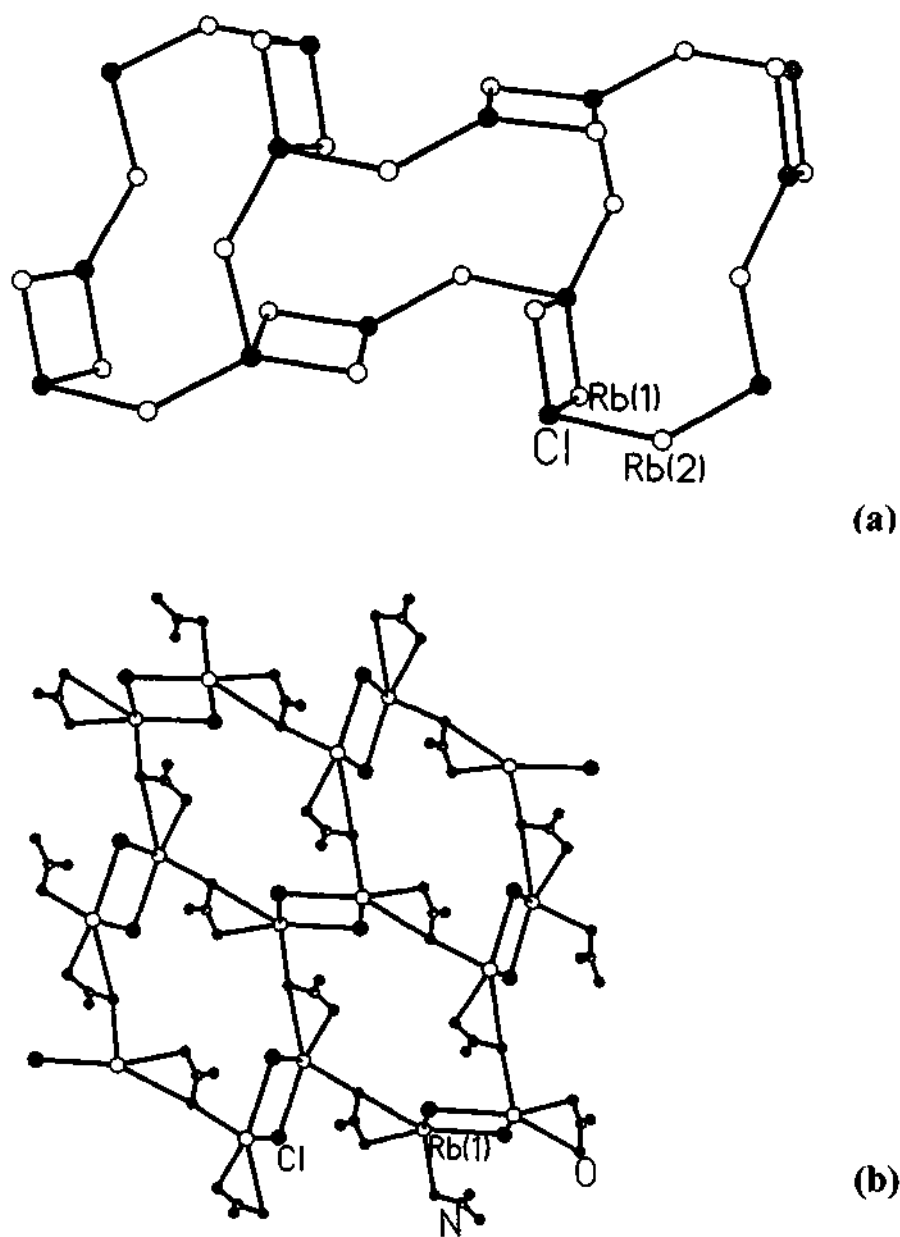


Fig. 4.76. (a) Layers in XXXI with 12-membered apertures formed by the Rb atoms and the Cl atoms. (b) Layer formed by the Rb(1), Cl and the NO_3 . Note the presence of Rb_2Cl_2 dimers connected by nitrate units.

above 500°C was observed due to the slow evaporation of CdO. In both XXIX and XXXI, the powder XRD pattern of the product of decomposition was characteristic of CdO, mineral monteporite (JCPDS: 05 – 0640).

4.11.3. Oxalate hosts incorporating one-dimensional alkali halide structures

[K₂Cd₂(C₂O₄)₃]₂KBr·2H₂O (XXXII)

[K₂Cd₂(C₂O₄)₃]₂KBr·2H₂O, XXXII, is a three-dimensional Cd oxalate (Fig. 4.77a), with oxalate layers similar to that in XXIX (Fig. 4.77b), but linked by oxalate bridges.^[9] This is also evident looking at the lattice parameters of XXIX and XXXII. One of the lattice parameter of XXXII is ~5 Å larger than XXIX, indicating that the *out-of plane* oxalate bridges the cadmium oxalate layers along that axis to form channels. Accordingly, one of the axes differs significantly in XXIX compared to XXXII. The K⁺ ions located in the channels of XXXII form linear KBr chains, with K-Br distances in the range 3.36-3.50 Å (Table 4.28). The inter-chain Br-Br distance is 3.76 Å and the K⁺ ions are coordinated by the oxalate oxygens and the Br atoms.

Table 4.27. Selected bond distances and bond angles for XXIX., 2[CsBr][Cd(C₂O₄)].H₂O, XXX, 2[CsBr][Cd₂(C₂O₄)(Br)₂].2H₂O, XXXI, [Rb₂Cd(Cl)(NO₃)(C₂O₄)(H₂O)]

XXIX			
Moiety	Distance (Å)	Moiety	Distance (Å)
Cd(1)-O(1)	2.290(8)	Br(1)-Cs(1)#10	3.6706(13)
Cd(1)-O(2)	2.293(8)	Br(1)-Cs(1)#3	3.7153(12)
Cd(1)-O(3)#1	2.310(9)	Br(1)-Cs(1)#5	3.7336(13)
Cd(1)-O(4)	2.367(9)	C(1)-O(1)	1.223(13)
O(3)-Cd(1)#11	2.310(9)	C(1)-O(4)#3	1.240(13)
Cd(1)-Br(1)	2.7099(11)	C(1)-C(2)#5	1.61(2)
Cd(1)-Br(1)#2	2.7100(11)	C(2)-O(3)	1.233(14)
Cs(1)-Br(1)#2	3.6603(13)	C(2)-O(2)	1.264(14)
Cs(1)-Br(1)#8	3.6706(13)	C(2)-C(1)#7	1.61(2)
Cs(1)-Br(1)#9	3.7153(12)	O(3)-Cs(1)#5	3.185(6)

Cs(1)-Br(1)#7	3.7336(13)	O(3)-Cs(1)#6	3.185(6)
Br(1)-Cs(1)#2	3.6602(13)	O(4)-C(1)#9	1.240(13)
Moiety	Angle (°)	Moiety	Angle (°)
O(1)-Cd(1)-O(2)	101.0(3)	O(3)#1-Cd(1)-Br(1)	90.14(3)
O(1)-Cd(1)-O(3)#1	110.0(3)	O(4)-Cd(1)-Br(1)	91.43(3)
O(2)-Cd(1)-O(3)#1	149.0(3)	O(1)-C(1)-O(4)#3	127.8(11)
O(1)-Cd(1)-O(4)	178.2(3)	O(1)-C(1)-C(2)#5	115.5(11)
O(2)-Cd(1)-O(4)	77.2(3)	O(4)#3-C(1)-C(2)#5	116.7(10)
O(3)#1-Cd(1)-O(4)	71.8(3)	O(3)-C(2)-O(2)	128.7(12)
O(1)-Cd(1)-Br(1)	88.58(3)	O(3)-C(2)-C(1)#7	118.0(11)
O(2)-Cd(1)-Br(1)	90.63(3)	O(2)-C(2)-C(1)#7	113.3(11)
XXX			
Moiety	Distance (Å)	Moiety	Distance (Å)
Cd(1)-O(1)#1	2.329(5)	Cs(1)-Br(1)	3.703(2)
Cd(1)-O(1)	2.329(5)	Br(1)-Cs(1)#6	3.610(2)
Cd(1)-O(200)#2	2.405(7)	Br(2)-Cd(1)#6	2.7332(8)
Cd(1)-Br(1)	2.6248(14)	Br(2)-Cd(1)#4	2.7332(8)
Cd(1)-Br(2)#3	2.7332(8)	C(1)-O(1)	1.243(7)
Cd(1)-Br(2)#4	2.7332(8)	C(1)-O(1)#8	1.243(7)
Cs(1)-Br(1)#2	3.610(2)	C(1)-C(1)#1	1.57(2)
Moiety	Angle (°)	Moiety	Angle (°)
O(1)#1-Cd(1)-O(1)	70.9(2)	O(1)-C(1)-C(1)#1	117.2(5)
O(1)#1-Cd(1)-O(200)#2	82.7(2)	O(1)#8-C(1)-C(1)#1	117.2(5)
O(1)-Cd(1)-O(200)#2	82.7(2)	C(1)-O(1)-Cd(1)	115.7(5)
O(1)-C(1)-O(1)#8	125.6(9)	Cd(1)#6-O(200)-Cs(1)	105.6(2)
XXXI			
Moiety	Distance (Å)	Moiety	Distance (Å)
Cd(1)-O(1)	2.248(4)	Rb(2)-O(4)#1	3.010(4)
Cd(1)-O(2)	2.266(4)	Rb(2)-O(5)#6	3.107(4)
Cd(1)-O(3)	2.311(4)	Rb(2)-O(6)#11	3.102(5)
Cd(1)-O(4)	2.372(4)	Rb(1)-Cl(1)#6	3.361(2)
Cd(1)-O(100)	2.359(4)	Rb(1)-Cl(1)	3.449(2)
Cd(1)-Cl(1)	2.510(2)	Rb(2)-Cl(1)	3.609(2)
Rb(1)-O(2)#2	2.986(4)	Rb(2)-C(1)#5	3.645(5)
Rb(1)-O(7)	2.892(4)	Rb(2)-Cl(1)#1	3.656(2)
Rb(1)-O(3)	2.955(4)	C(1)-O(1)#2	1.248(7)
Rb(1)-O(6)#4	2.956(5)	C(1)-O(4)	1.263(6)

Rb(1)-O(4)#5	2.969(3)	C(2)-O(2)	1.234(6)
Rb(1)-O(2)#5	2.986(4)	C(2)-O(3)#7	1.263(6)
Rb(1)-O(4)#2	2.970(3)	C(1)-O(1)#5	1.248(7)
Rb(1)-O(6)#10	2.956(5)	C(2)-O(3)#3	1.263(6)
Rb(2)-O(3)#7	2.981(3)	C(1)-C(2)#3	1.541(8)
Rb(2)-O(4)#8	3.010(4)	C(2)-C(1)#7	1.541(8)
Rb(2)-O(1)	3.063(4)	N(1)-O(5)	1.231(6)
Rb(2)-O(7)#6	3.076(5)	N(1)-O(6)	1.237(5)
Rb(2)-O(6)#9	3.102(5)	N(1)-O(7)	1.253(6)
Rb(2)-O(3)#3	2.981(3)		
Moiety	Angle (°)	Moiety	Angle (°)
O(1)-Cd(1)-O(2)	93.69(13)	O(4)-Cd(1)-Cl(1)	95.20(9)
O(1)-Cd(1)-O(3)	115.42(13)	O(100)-Cd(1)-Cl(1)	175.57(12)
O(2)-Cd(1)-O(3)	148.17(13)	O(2)-C(2)-O(3)#7	125.8(5)
O(1)-Cd(1)-O(100)	84.26(13)	O(1)#2-C(1)-O(4)	125.1(5)
O(2)-Cd(1)-O(100)	88.13(13)	O(1)#2-C(1)-C(2)#3	116.2(5)
O(3)-Cd(1)-O(100)	82.60(13)	O(4)-C(1)-C(2)#3	118.7(5)
O(1)-Cd(1)-O(4)	167.71(12)	O(2)-C(2)-C(1)#7	115.9(5)
O(2)-Cd(1)-O(4)	77.39(13)	O(3)#7-C(2)-C(1)#7	118.3(5)
O(3)-Cd(1)-O(4)	71.78(12)	O(5)-N(1)-O(6)	119.9(5)
O(100)-Cd(1)-O(4)	86.97(13)	O(5)-N(1)-O(7)	119.6(5)
O(3)-Cd(1)-Cl(1)	94.40(9)	O(6)-N(1)-O(7)	120.5(5)

Symmetry transformations used to generate equivalent atoms:

For XXIX:

#1 $x+1, y, z$ #2 $x, y, -z+1/2$ #3 $-x+2, y-1/2, -z+1/2$ #4 $-x+2, y-1/2, z$ #5 $-x+1, y-1/2, -z+1/2$
 #6 $-x+1, y-1/2, z$ #7 $-x+1, y+1/2, -z+1/2$ #8 $x, -y+1/2, z+1/2$ #9 $-x+2, y+1/2, -z+1/2$
 #10 $x, -y+1/2, z-1/2$ #11 $x-1, y, z$ #12 $x, -y+1/2, -z+1$

For XXX:

#1 $x, y, -z+1/2$ #2 $-x+1/2, y+1/2, -z+1/2$ #3 $-x+1/2, -y+1/2, z+1/2$ #4 $-x+1/2, -y+1/2, -z$
 #5 $-x+1/2, -y+1/2, -z+1$ #6 $-x+1/2, y-1/2, -z+1/2$ #7 $x, -y, z-1/2$ #8 $-x, y, z$ #9 $x, -y, -z+1$

For XXXI:

#1 $-x+1/2, y+1/2, z$ #2 $-x, y+1/2, -z+3/2$ #3 $x-1/2, y, -z+3/2$ #4 $-x, y-1/2, -z+3/2$
 #5 $-x, -y, -z+1$ #6 $-x-1/2, y-1/2, z$ #7 $x-1/2, -y-1/2, -z+1$ #8 $x+1/2, y, -z+3/2$
 #10 $-x+1/2, y-1/2, z$ #11 $x+1/2, -y-1/2, -z+1$ #12 $-x-1/2, y+1/2, z$

3[RbCl][Cd₂(C₂O₄)(Cl₂)]·H₂O (XXXIII)

The asymmetric unit of XXXIII contains 18 non-hydrogen atoms. There are two crystallographically independent cadmium atoms in XXXIII, both of which are octahedrally coordinated by oxygen and chlorine atoms. While Cd(1) possesses

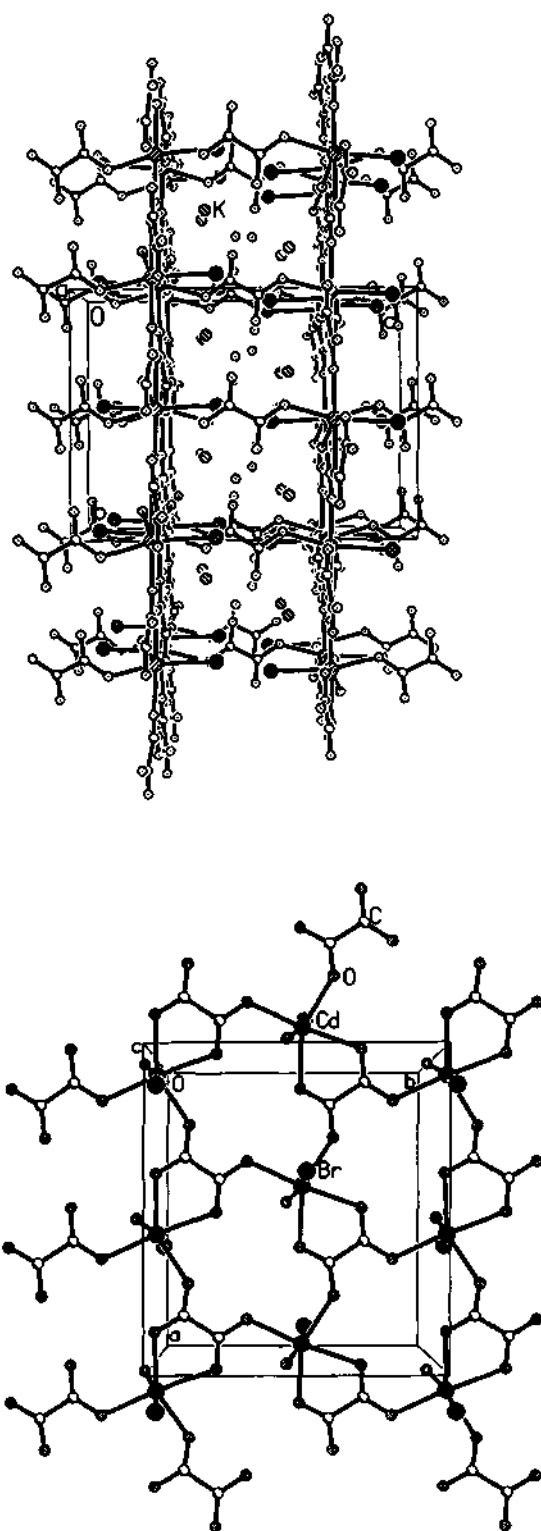


Fig. 4. 77. (a) Structure of $K_2Cd_2(C_2O_4)_3 \cdot 2KBr \cdot 2H_2O$, XXXII, along the [100] direction. Note that the oxalate connects the two layers. K and water molecules are situated inside the channels. One-dimensional KBr chains can be seen. (b) Structure of layer in XXXII.

two Cd – O (av. 2.3005 Å) and four Cd – Cl linkages (av. 2.629 Å), Cd(2) has three Cd – O (av. 2.312 Å) and Cd – Cl (av. 2.591 Å) connections. The oxygen atoms are connected to carbon atoms and form the oxalate unit with average C – O distances of 1.251 Å (Table 4.28). There are three unique Rb atoms with Rb(1) and Rb(8) being eight coordinated and Rb(3) is seven coordinated with chlorine and oxygen atoms. Thus, Rb(1) has five Rb – Cl (av. 3.390 Å) and three Rb – O (av. 2.978 Å) linkages, Rb(2) has seven Rb – Cl (av. 3.448 Å) and one Rb – O (2.914(9) Å) bonding and Rb(3) has five Rb – Cl (av. 3.457 Å) and two Rb – O (av. 2.893 Å) connectivity (Table 4.28). The average O – Cd – O, O – Cd – Cl and Cl – Cd – Cl bond angles have values of 72.3, 107.24 and 107.5° for Cd(1) and 81.7, 117.1 and 95.18° for Cd(2). These are typical values and are in agreement with those observed earlier for similar compounds.

The connectivity between the isolated oxalate units along with the chloride ions in **XXXIII** results in an interpenetrating layer-like arrangement. In **XXXIII**, the chlorine atoms connect the Cd ions of the isolated cadmium oxalate unit and form a two-dimensional layer with a right-handed helical strand with the immediate next layer having the opposite handedness, canceling the total helicity of the structure. The Rb atoms are situated between these sheets, reflect the helical nature of the cadmium chloro-oxalate layer (host), with the Rb atoms from the neighboring strand, so positioned as to cancel the helicity of the structure. Thus, there is no independent alkali halide lattice in **XXXIII** (Fig. 4.78).

K₂Mn₂(C₂O₄)₃·2KCl·2H₂O, (XXXIV)

The asymmetric unit of **XXXIV** contains 14 independent non-hydrogen atoms along with one Mn²⁺ and two K⁺ crystallographically independent cations. The Mn²⁺ ions are connected to five oxygen atoms with Mn–O distances in the range 2.150(4)–2.238(3) Å [av = 2.184 Å] and O–Mn–O angles in the range 81.6(2)

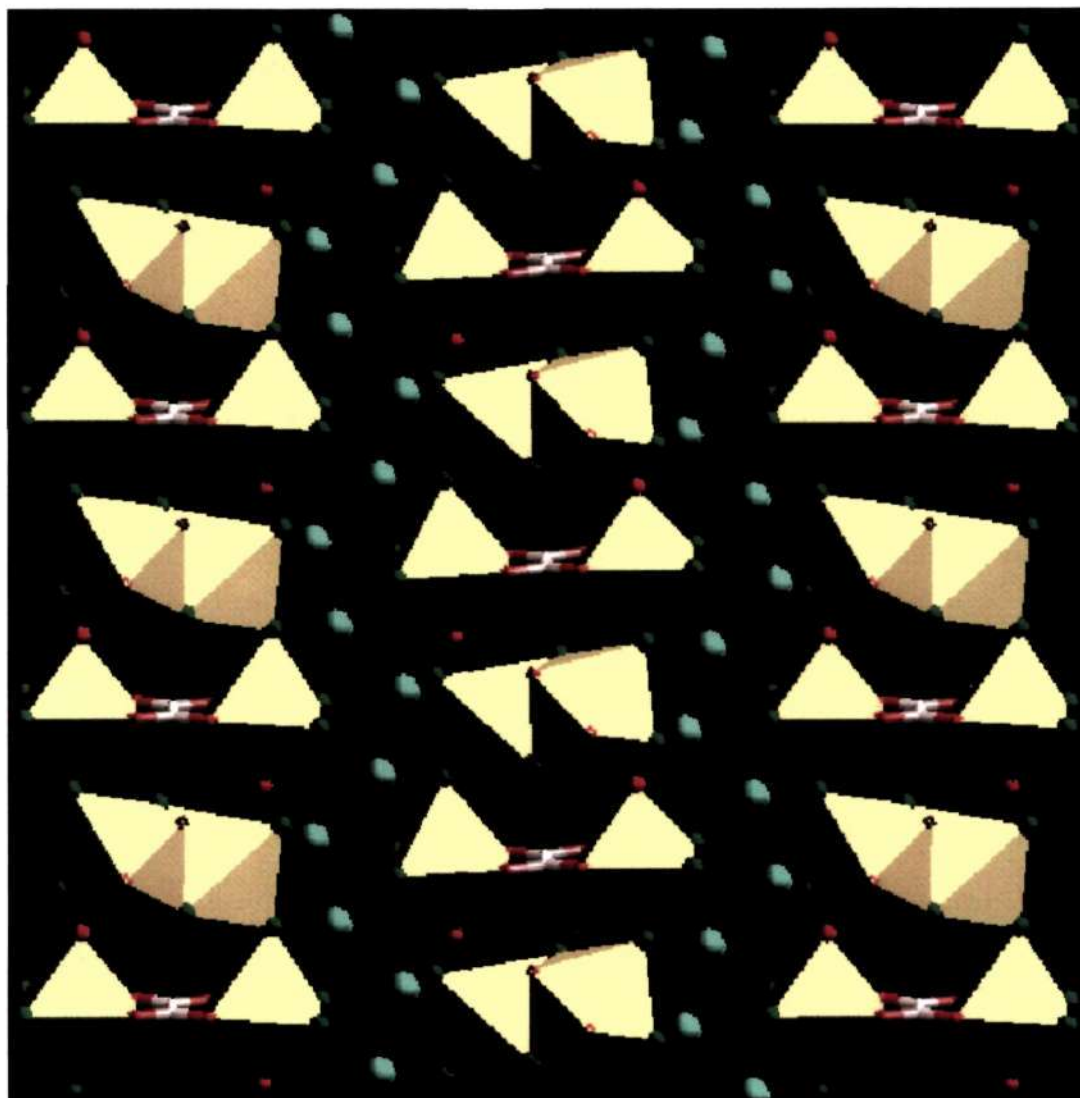


Fig. 4. 78. Structure of **XXXIII** along the *a* axis showing the cadmium chloro oxalate layers and the Rb atoms. Note that both the cadmium chloro-oxalate and the Rb atoms form a helical structure. (color scheme: yellow – Cd, white – C, red – O, green – Cl, blue –Rb).

- 178.56(13)° [av = 105.43°] (Table 4.28). The sixth coordination needed for the octahedral arrangement is provided by one Cl atom with Mn-Cl distance of 2.557(2) Å (Table 4.28). The C–O bond distances are in the range 1.225(7) – 1.264(7) Å (av. 1.245 Å), with the shortest (1.225(7) Å) and longest distance (1.264(7) Å) being associated with the monodentate oxalate units and the average O – C – O bond angles have value of 127.0° (Table 4.28). The K⁺ ions K(1) and K(2) are coordinated to eight and seven nearest neighbor atoms, respectively. Thus, K(1) is coordinated to six oxygen atoms and two chlorine atoms, and K(2) is coordinated to six oxygen atoms and one chlorine atom. The oxygen atoms have distances of less than 3.1 Å, which is usually considered the upper limit for significant K...O interaction.^[20] Whilst the coordination environment of K(1) is an idealized triangulated dodecahedron, that of the K(2) is a distorted monocapped trigonal prism. The K-Cl distances are 3.2 and 3.3 Å. Recall that the K-Cl distances in bulk material is 3.2 Å.

The framework structure of XXXIV is built up from the linkages involving Mn(O₅Cl) octahedra and oxalate units. Of the three oxalate units, two connect the Mn(O₅Cl) octahedra within the plane while the other has an *out-of-plane* connectivity. The *in-plane* connectivity between Mn and oxalate units gives rise to layer, with the adjacent layers shifted by ½ the unit cell. Thus, the layer stacking in XXXIV is of *ABABAB...* type. Similar layers have been found in XXIX and XXXII. The *out-of-plane* oxalate bridging the layers, act as a monodentate ligand (Fig. 4.79), such oxalate bridges in extended structures being rather rare.^[83] The monodentate connection of the oxalate units bridges two isolated Mn(O₅Cl) octahedra, unlike in the structure reported previously.^[83]

Table 4.28. Selected bond distances and angles for XXXII, $[\text{K}_2\text{Cd}_2(\text{C}_2\text{O}_4)_3]2\text{KBr}\cdot 2\text{H}_2\text{O}$, XXXIII, $3[\text{RbCl}][\text{Cd}_2(\text{C}_2\text{O}_4)(\text{Cl}_2)]\cdot \text{H}_2\text{O}$, XXXIV, $\text{K}_2[\text{Mn}_2(\text{C}_2\text{O}_4)_3]2[\text{KCl}]\cdot 2\text{H}_2\text{O}$

XXXII			
Moiety	Distance (Å)	Moiety	Distance (Å)
Cd(1)-O(1)	2.254(3)	O(5)-K(2)#1	2.871(3)
Cd(1)-O(2)	2.258(3)	O(5)-K(1)	2.971(3)
Cd(1)-O(3)	2.276(3)	O(6)-K(1)	2.701(4)
Cd(1)-O(4)	2.311(3)	O(6)-K(2)#5	2.834(4)
Cd(1)-O(5)	2.382(3)	K(1)-O(100)	2.758(5)
Cd(1)-Br(2)	2.70(2)	K(1)-O(4)#8	2.790(3)
Cd(1)-Br(1)	2.710(14)	K(1)-O(3)#1	2.942(3)
O(1)-C(10)	1.253(6)	K(2)-O(1)#7	2.782(4)
O(2)-C(11)	1.244(5)	K(2)-O(6)#11	2.834(4)
O(3)-C(12)#3	1.258(5)	K(2)-O(5)#4	2.871(3)
O(4)-C(11)#2	1.257(5)	K(2)-O(4)#7	2.999(3)
O(5)-C(12)	1.255(4)	K(2)-O(2)#4	3.257(4)
O(6)-C(10)	1.228(6)	K(2)-O(100)#11	3.278(6)
C(11)-O(4)#7	1.256(5)	O(100)-K(2)#5	3.277(6)
C(11)-C(12)#7	1.563(6)	K(1)-Br(1)#10	3.354(12)
C(10)-C(10)#6	1.564(9)	Br(1)-K(2)#1	3.265(13)
C(12)-O(3)#8	1.258(5)	Br(1)-K(1)#9	3.354(12)
C(12)-C(11)#2	1.563(6)	Br(1)-K(2)	3.359(13)
O(1)-K(2)#2	2.782(3)	Br(2)-K(1)#9	3.369(14)
O(2)-K(1)	2.746(3)	K(2)-Br(1)#4	3.265(13)
O(2)-K(2)#1	3.257(4)	K(2)-Br(2)#4	3.37(2)
O(3)-K(2)	2.832(3)	K(1)-Br(2)#10	3.369(14)
O(3)-K(1)#4	2.942(3)	Br(2)-K(2)#1	3.37(2)
O(4)-K(1)#3	2.790(3)	Br(2)-K(2)	3.49(2)
Moiety	Angle (°)	Moiety	Angle (°)
O(1)-Cd(1)-O(2)	99.29(12)	O(3)-Cd(1)-Br(2)	88.6(3)
O(1)-Cd(1)-O(3)	81.80(12)	O(1)-Cd(1)-Br(1)	168.8(3)
O(2)-Cd(1)-O(3)	98.50(11)	O(2)-Cd(1)-Br(1)	86.3(4)
O(1)-Cd(1)-O(4)	82.52(12)	O(3)-Cd(1)-Br(1)	87.8(2)
O(2)-Cd(1)-O(4)	149.21(11)	O(4)-Cd(1)-Br(1)	97.7(4)
O(3)-Cd(1)-O(4)	112.12(10)	O(5)-Cd(1)-Br(1)	91.2(2)
O(1)-Cd(1)-O(5)	99.48(12)	C(12)-O(5)-Cd(1)	114.4(3)
O(2)-Cd(1)-O(5)	77.31(10)	O(1)-C(10)-C(10)#6	114.8(6)

O(3)-Cd(1)-O(5)	175.75(10)	O(2)-C(11)-O(4)#7	125.7(4)
O(4)-Cd(1)-O(5)	72.11(10)	O(2)-C(11)-C(12)#7	115.3(4)
O(1)-Cd(1)-Br(2)	166.6(4)	O(4)#7-C(11)-C(12)#7	119.0(4)
O(2)-Cd(1)-Br(2)	91.3(4)	O(5)-C(12)-O(3)#8	126.5(4)

XXXIII

Moiety	Distance (Å)	Moiety	Distance (Å)
Cd(1)-O(4)#1	2.286(6)	Rb(2)-Cl(4)#9	3.646(3)
Cd(1)-O(1)	2.315(6)	Rb(3)-Cl(5)	3.343(3)
Cd(1)-Cl(3)#2	2.549(2)	Rb(3)-Cl(3)	3.365(3)
Cd(1)-Cl(1)	2.583(2)	Rb(3)-Cl(1)	3.371(3)
Cd(1)-Cl(2)	2.620(3)	Rb(3)-Cl(4)#10	3.408(3)
Cd(1)-Cl(3)	2.765(3)	Rb(3)-Cl(3)#11	3.796(3)
Cd(2)-O(2)	2.293(6)	Cl(1)-Rb(2)#5	3.418(3)
Cd(2)-O(3)	2.316(6)	Cl(2)-Cd(2)#8	2.618(2)
Cd(2)-O(10)	2.327(6)	Cl(3)-Cd(1)#2	2.549(2)
Cd(2)-Cl(4)	2.569(2)	Cl(3)-Rb(3)#11	3.796(3)
Cd(2)-Cl(5)	2.585(2)	Cl(4)-Rb(2)#12	3.281(3)
Cd(2)-Cl(2)#3	2.618(2)	Cl(4)-Rb(1)#5	3.369(3)
Rb(1)-Cl(5)#6	3.342(3)	Cl(4)-Rb(3)#4	3.408(3)
Rb(1)-Cl(4)#6	3.369(3)	Cl(4)-Rb(2)#13	3.646(3)
Rb(1)-Cl(2)	3.386(3)	Cl(5)-Rb(1)#5	3.342(3)
Rb(1)-Cl(5)	3.386(3)	Cl(5)-Rb(2)#5	3.414(2)
Rb(1)-Cl(1)	3.465(3)	Cl(5)-Rb(2)#3	3.470(3)
Rb(2)-Cl(4)#7	3.281(3)	C(1)-O(3)	1.237(11)
Rb(2)-Cl(2)	3.362(3)	C(1)-O(2)#14	1.249(11)
Rb(2)-Cl(5)#6	3.414(2)	C(1)-C(1)#14	1.58(2)
Rb(2)-Cl(1)#6	3.418(3)	C(2)-O(1)	1.258(11)
Rb(2)-Cl(5)#8	3.470(3)	C(2)-O(4)	1.259(11)
Rb(2)-Cl(1)	3.543(3)	C(2)-C(2)#1	1.54(2)

Moiety	Angle (°)	Moiety	Angle (°)
O(4)#1-Cd(1)-O(1)	72.3(2)	O(3)-C(1)-C(1)#14	118.1(9)
O(2)-Cd(2)-O(3)	72.0(2)	O(2)#14-C(1)-C(1)#14	116.1(10)
O(2)-Cd(2)-O(10)	88.2(2)	O(1)-C(2)-O(4)	124.3(8)
O(3)-Cd(2)-O(10)	84.8(2)	O(1)-C(2)-C(2)#1	118.0(10)
O(3)-C(1)-O(2)#14	125.8(8)	O(4)-C(2)-C(2)#1	117.7(10)

XXXIV

Moiety	Distance (Å)	Moiety	Distance (Å)
--------	--------------	--------	--------------

Mn(1)-O(1)	2.150(4)	K(2)-O(4)#1	2.748(4)
Mn(1)-O(2)	2.150(4)	K(2)-O(5)	3.014(4)
Mn(1)-O(3)	2.178(3)	K(2)-O(6)	2.668(4)
Mn(1)-O(4)	2.205(4)	K(2)-O(100)	2.751(5)
Mn(1)-O(5)	2.238(3)	K(2)-Cl(1)#8	3.246(5)
Mn(1)-Cl(1)	2.557(2)	C(1)-O(3)	1.253(6)
K(1)-O(1)	2.850(4)	C(1)-O(5)#1	1.242(6)
K(1)-O(3)#2	2.779(4)	C(1)-O(5)#6	1.242(6)
K(1)-O(4)	2.961(4)	C(2)-O(2)	1.248(6)
K(1)-O(5)#1	2.814(4)	C(2)-O(4)#2	1.242(6)
K(1)-O(6)#4	2.735(4)	C(2)-O(4)#5	1.242(6)
K(1)-O(100)#4	3.171(5)	C(3)-O(1)	1.264(7)
K(1)-Cl(1)#1	3.169(2)	C(3)-O(6)	1.225(7)
K(1)-Cl(1)#2	3.300(2)	C(1)-C(2)#3	1.559(7)
K(2)-O(2)	2.818(4)	C(1)-C(2)#7	1.559(7)
K(2)-O(3)#3	2.949(4)	C(3)-C(3)#4	1.593(11)

Moiety	Angle (°)	Moiety	Angle (°)
O(1)-Mn(1)-O(2)	98.1(2)	O(2)-Mn(1)-Cl(1)	87.82(11)
O(1)-Mn(1)-O(3)	81.6(2)	O(3)-Mn(1)-Cl(1)	88.27(10)
O(2)-Mn(1)-O(3)	98.99(14)	O(4)-Mn(1)-Cl(1)	94.68(11)
O(1)-Mn(1)-O(4)	84.1(2)	O(5)-Mn(1)-Cl(1)	91.79(10)
O(2)-Mn(1)-O(4)	153.58(14)	O(5)#6-C(1)-O(3)	126.7(5)
O(3)-Mn(1)-O(4)	107.36(13)	O(4)#2-C(2)-O(2)	126.3(5)
O(1)-Mn(1)-O(5)	98.4(2)	O(6)-C(3)-O(1)	127.9(5)
O(2)-Mn(1)-O(5)	79.57(13)	O(5)#6-C(1)-C(2)#3	116.6(4)
O(3)-Mn(1)-O(5)	178.56(13)	O(3)-C(1)-C(2)#3	116.7(4)
O(4)-Mn(1)-O(5)	74.07(13)	O(4)#2-C(2)-C(1)#7	116.8(4)
O(1)-Mn(1)-Cl(1)	168.94(12)	O(2)-C(2)-C(1)#7	116.9(5)

Symmetry transformations used to generate equivalent atoms:

For **XXXII**:

#1 $-x-1/2, y+1/2, z$ #2 $x-1/2, y, -z+3/2$ #3 $-x-1, y-1/2, -z+3/2$ #4 $-x-1/2, y-1/2, z$
 #5 $-x-1/2, -y, z+1/2$ #6 $-x-1, -y, -z+2$ #7 $x+1/2, y, -z+3/2$ #8 $-x-1, y+1/2, -z+3/2$
 #9 $x, -y+1/2, z-1/2$ #10 $x, -y+1/2, z+1/2$ #11 $-x-1/2, -y, z-1/2$

For **XXXIII**:

#1 $-x, -y+1, -z+1$ #2 $-x+1, -y+1, -z+1$ #3 $x, y, z+1$ #4 $x-1, y, z$ #5 $x, -y+1/2, z+1/2$
 #6 $x, -y+1/2, z-1/2$ #7 $x+1, -y+1/2, z-1/2$ #8 $x, y, z-1$ #9 $x+1, y, z-1$ #10 $x+1, y, z$
 #11 $-x+1, -y+1, -z+2$ #12 $x-1, -y+1/2, z+1/2$ #13 $x-1, y, z+1$ #14 $-x, -y+1, -z+2$

For **XXXIV**:

#1 $-x+1, y+1/2, -z+1/2$ #2 $x-1/2, y, -z+1/2$ #3 $-x+1/2, y-1/2, z$ #4 $-x+1, -y, -z+1$
 #5 $x+1/2, y, -z+1/2$ #6 $-x+1, y-1/2, -z+1/2$ #7 $-x+1/2, y+1/2, z$ #8 $x, -y+1/2, z+1/2$
 #9 $x, -y+1/2, z-1/2$

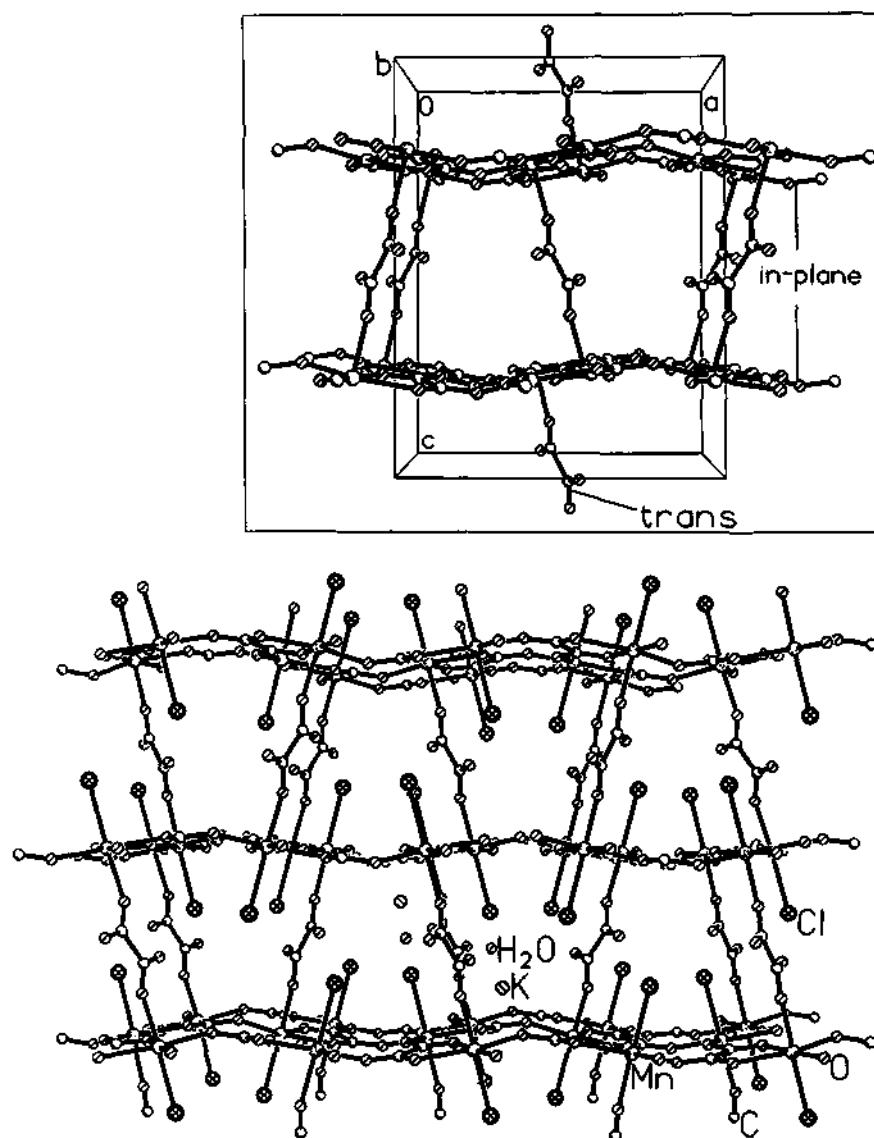


Fig. 4. 79. Structure of $K_2Mn_2(C_2O_4)_3 \cdot 2KCl \cdot 2H_2O$, XXXIV, along the *b*-axis showing the interpenetrating channels. Inset shows the linkages between the adjacent layers and the *out-of-plane*, monodentate oxalate units. Note the *trans*-orientation of the monodentate oxalate units with respect to each other.

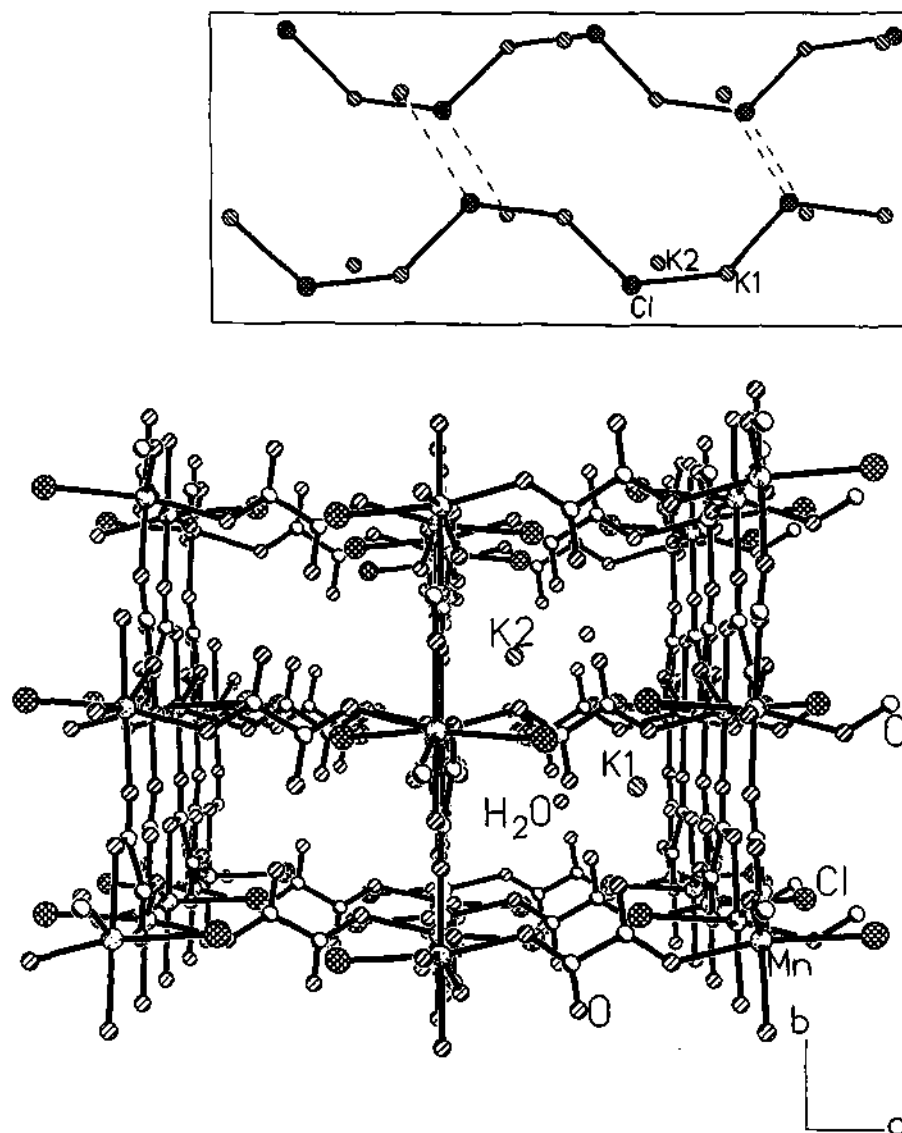


Fig. 4.80. Structure of XXXIV, viewed along the *a*-axis showing uniform rectangular channels. Note the chlorine atoms protruding in to the channels. Inset shows an one-dimensional KCl chain formed by the interaction between the bound Cl⁻ and K⁺ ions residing in the channels.

Linkages between two layers by the monodentate oxalate are in the *trans*- or *anti*- orientation with respect to each other (See inset Fig. 4.79). The framework along the *a*-axis forms uniform rectangular channels (6.3×7.5Å, shortest atom-atom contact not including the van der Waals radii) (Fig. 4.80), in which the K⁺ and water molecules reside. The chlorine atoms connected to the Mn centers protrude into these channels and interact with the K atoms in the channels. The interaction between the chlorine and the K(1) result in a one-dimensional KCl chain, with K-Cl distances close to that in bulk KCl. K(2), however, interacts weakly with the Cl atom of the chain (See inset Fig. 4.80). The KCl chains are similar to the KBr chains present in XXXII.

Thermogravimetric analysis of XXXIV, (TGA) under a flow of nitrogen (50 ml min⁻¹) from 25 to 800 °C (rate = 5 °C min⁻¹), showed two distinct mass losses. A mass loss of 7.8% in the range 100-140°C corresponding to the loss of extra-framework water (calcd.5.7%), and a mass loss of 39.7% in the range 350-700°C due to the loss of the oxalate moiety (calcd.33.9%). The powder XRD pattern of the as calcined product corresponds to a mixture of MnO (JCPDS: 07-0230, Manganosite) and Mn₂O₃ (JCPDS: 33-0900).

Infra-red spectroscopic studies as a KBr pellet showed characteristic features of the bischelating oxalate.^[3] The various bands for compounds XXVII – XXXIV are as follows: ν_{as} (C = O) in the range 1612 – 1672 vs cm⁻¹, ν_s (O – C – O) at 1372 s and 1311 s cm⁻¹ (XXVII), ν_s (O-C-O) at 1373 (m) and 1312 (s) cm⁻¹ (XXVIII), 1374 s and 1310 s cm⁻¹ (XXIX), 1372 m and 1310 s cm⁻¹ (XXX), ν_s (O-C-O) at 1373 (m) and 1312 (s) cm⁻¹ (XXXI), 1373 s and 1312 s cm⁻¹ (XXXIII), 1356.3 (m) and 1309.6 (s) cm⁻¹ (XXXIV), δ (O – C = O) at 803 m, 790 w and 774 w cm⁻¹ (XXVII), at 804(s) and 777(s) cm⁻¹ (XXVIII), 800 w and 773 s cm⁻¹ (XXIX),

773 s and 731 w cm^{-1} (XXX), 805(s) and 776(s) cm^{-1} (XXXI), 802 m and 776 m cm^{-1} (XXXIII) and 852.9(m) and 788(s) cm^{-1} (XXXIV). The extra-framework water molecules showed characteristic bands around 3550 s cm^{-1} in all the cases. The M – O (M = Cd) stretching vibrations [$\nu_s(\text{M} - \text{O})$] and $\nu_s(\text{C}-\text{C})$ are also observed at 512 s and 441 s cm^{-1} (XXVII), 512(s) (XXVIII), 513 m cm^{-1} (XXIX), 514 w cm^{-1} (XXX), 501 (s) cm^{-1} (XXXI), 512 s and 441 s cm^{-1} (XXXIII). The various infra-red bands are consistent with the structure determined by single crystal studies.

4.10.4. Discussion

The distances between the alkali metal and the halogen ions in compounds XXVII – XXXIV provide an interesting comparison. In XXVII and XXVIII, the Rb – Cl and Rb-Br distances are 6.726 and 6.855 Å, respectively, whilst in RbCl and RbBr with rock-salt structure, it is 3.285 and 3.428 Å, respectively. In the case of compounds XXIX and XXX, the average Cs – Br distance is ~3.7 Å, which is comparable to the Cs – Br distance (3.72 Å) in body-centered CsBr, similarly the Rb-Cl distance of 3.635 Å, in XXXI, comparable to the distance in normal RbCl (3.291 Å). It may be noted that in XXVII and XXVIII, the RbX (X = Cl, Br) forms a lattice identical to that of normal RbX, but with double the unit-cell dimensions, whereas in XXIX, XXX and XXXI the MX (M = Cs or Rb, X = Cl or Br) forms unusual layered architectures in spite of having nearly similar distances between M and X as in normal MX. These observations demonstrate the role of host-guest interactions in these structures.

Host – guest structures of the type observed in XXVII – XXXIV possessing expanded MX and layered MX are indeed most unusual. These structures are formed because the host structures provide the additional coordination necessary for the alkali halide ions. Thus, the expanded rock-salt structure of RbCl and RbBr is

made possible by the stability provided by the extra coordination due to the oxalate units. What is truly interesting, however, is that such beautiful structures are formed by a simple metathetic reaction carried out under hydrothermal conditions. Such a reaction under ambient conditions would clearly give a mixture of the Cd oxalate and the alkali halide. In this connection, it may be noted that the structures reported herein are different from those resulting from ion-exchange in layered solids, such as metal-anion arrays within the oxide hosts.^[90] Thus, in the layered $\text{RbLaNb}_2\text{O}_7$, the Rb^+ ions, situated in the inter-lamellar region, are exchanged topotactically by copper halide, CuX_2 ($\text{X} = \text{Cl}$ and Br), in an evacuated and sealed quartz tubes at $325\text{ }^\circ\text{C}$.^[90] This gives rise to a unique situation wherein the ability to prepare hosts at high temperatures, with varying interatomic spacings and topologies, are combined with the low-temperature ion-exchange methods to construct metal – anion arrays. The host-guest structures of **XXVII** – **XXXIV** are somewhat comparable to the KCl/CsCl structures reported in a phosphate framework.^[91] Accordingly, in $\text{A}_2[\text{M}_3(\text{X}_2\text{O}_7)_2][\text{salt}]$ ($\text{A} = \text{Rb}, \text{Cs}$; $\text{M} = \text{Mn}, \text{Cu}$; $\text{X} = \text{P}, \text{As}$), synthesized under molten salt conditions ($>600\text{ }^\circ\text{C}$), the phosphate network is formed around the alkali metal chloride salts, the salt probably acting as a structure-directing template. The super rock-salt structure formed by the clusters in **XXVII** and **XXVIII** can be considered to be a result of templating by the underlying MX lattice. This is reminiscent of organic molecules employed in conventional low-temperature hydrothermal methods for the synthesis of extended framework architectures.

In **XXXII** and **XXXIV**, the interaction between the K and the X ($\text{X} = \text{Cl}, \text{Br}$), results in zigzag one-dimensional KX chains. Whilst in **XXXIII**, the chlorine atoms connect the Cd ions of the isolated cadmium oxalate unit and form a two-

dimensional layer with a right-handed helical strand with the immediate next layer having the opposite handedness, canceling the total helicity of the structure. The Rb atoms are situated between these sheets, reflect the helical nature of the cadmium chloro-oxalate layer (host), with the Rb atoms from the neighboring strand, so positioned as to cancel the helicity of the structure. Thus, there is no independent alkali halide lattice in **XXXIII** (Fig. 4.78). However, the host layer imparting its helicity to the Rb atoms clearly suggests a host-guest interaction in this hybrid compound.

4.10.5. Summary

The new types of hybrid host-guest compounds incorporating novel alkali halide structures are likely to possess novel properties. In particular, they would be expected to exhibit interesting optical and dielectric properties. The three-dimensional organic-inorganic periodic superlattice would also bestow certain unusual properties.

References

1. S. H. Pine, *Organic Chemistry*, 5thEd., McGraw Hill International Editions, Chapter 7., P. 186.
2. (a) K. T. Holman, M. D. Ward, *Angew. Chem. Int. Ed. Engl.* **2000**, *39*, 1653. (b) J. A. Swift, M. D. Ward, *Chem. Mater.* **2000**, *12*, 1501.
3. (a) *Infrared and Raman Spectra of Inorganic and Coordination Compounds*, 5th ed.; Nakamoto, K. John Wiley, New York, 1997. (b) R.M.Silverstein and F.X.Webster, *Spectrometric Identification of Organic Compounds*, 6th Ed. John Wiley & Sons, Inc., Chapter 3., 102.
4. (a) J. C. MacDonald, C. P. Doewstein, M. M. Pilley, *Cryst. Grow. Design*, **2001**, *1*, 29. (b) J. A. Paixao, A. Matos Beja, M. Ramos Silva, J.Martin-Gil, *Acta Cryst.* **2000**, *C56*, 1132 and references therein.
5. J. Mitra, C. Ramakrishnan, *Int. J. Peptide Protein Res.* **1977**, *9*, 27.
6. R. Taylor, O. Kennard, W. Versichel, *J. Am. Chem. Soc.* **1983**, *105*, 5761.
7. (a) S. Chatterjee, V. R. Peddireddi, A. Ranganathan, C. N. R. Rao, *J. Mol. Struct.* **2000** *107*, 520; (b) M. R. St. J. Foreman, M. J. Plater, J. M. S. Skakle, *J. Chem. Soc. Dalton Trans.* **2001**, 1897.
8. (a) L. Leiserowitz, G. M. J. Schmidt, *Acta Cryst.* **1965**, *18*, 1058. (b) J. D. Dunitz, P.Strickler in: *Structural Chemistry and Molecular Biology* (Eds.) A.Rich and N.Davidson, W.H.Freeman, San Francisco, 1968, p.595.
9. S. Garcia-Granda, G. Beurskins, P. T. Buerskins, T. S. R. Krishna, G. R. Desiraju, *Acta Cryst.* **1987**, *C43*, 683.
10. G. A. Jeffrey, *An Introduction to Hydrogen Bonding*, Oxford University Press, New York, 1997.
11. (a) W. W. Cleland, M. M. Kreevoy, *Science* **1994**, *264*, 1887. (b) S. Cassidy, L. A. Reinhardt, W. W. Cleland, P. A. Frey, *J. Chem. Soc. Perkin Trans.* **1999**, *2*, 635.
12. (a) P. Gilli, V. Bertolasi, V. Ferrreti, G. Gilli, *J. Am. Chem. Soc.* **1994**, *116*, 909; (b) P. Gilli, V. Bertolasi, V. Ferrreti, G. Gilli, in: *Advances in Mol. Str. Research* (Ed.) M. Hargittai, I. Hargittai, Vol. 2, JAI press, Greenwich, CT, 1196, p.67.
13. C. Ramakrishnan, N. Prasad, *Int. J. Protein Res.* **2000**, *III*, 209.
14. J. Donhue in: *Structural Chemistry and Molecular Biology* (Eds.) A.Rich and N. Davidson, W. H. Freeman, San Francisco, 1968, p.443.

15. B. S. Green, R. A-. Yellin, M. D. Cohen in: *Topics in Stereochemistry* (Eds.) N.L.Alligner, E.L.Eliel, S.H.Wilen 16 (1986) 32.
16. C. N. R. Rao, S. Natarajan, S. Neeraj, *J. Solid State Chem.* **2000**, *152*, 302.
17. J. Bernstein, M. D. Cohen, L. Leiserowitz in: *The Chemistry of Quinonoid Compounds* (Ed.) S. Patai, Interscience, New York, 1974, p.37.
18. L. Leiserowitz, *Acta Cryst.* **1976**, *B3*,775.
19. (a) C. B. Aakeröy, M. Nieuwenhuyzen, *J. Am. Chem. Soc.* **1994**, *116*, 10983. (b) J. Emsley, *Chem. Soc. Rev.* **1980**, *9*, 91.
20. (a) W. J. Evans, R. Anwander, A. M. Ansari, J. W. Ziller, *Inorg. Chem.* **1995**, *34*, 5. (b) D. L. Clark, J.C. Gordon, J. C. Huffman, R. L. Vincent-Hollis, J. G. Watkin, B. D. Zwick, *Inorg. Chem.* **1994**, *33*, 5903.
21. I. D. Brown, D. Aldermatt, *Acta Cryst.*, **1984**, *Sect. B*, *41*, 244.
22. J. M. Thomas, R. H. Jones, J. Chen, R. Xu, A. M. Chippindale, S. Natarajan, A. K. Cheetham, *J. Chem. Soc., Chem. Commun.* **1992**, 929.
23. A. Choudhury, S. Natarajan and C.N.R. Rao, *Chem. Mater.* **1999**, *11*, 2316.
24. M. Estermann, L. B. McCusker, Ch. Baerlocher, A. Merrouche, H. Kessler, *Nature*, **1991**, *352*, 320.
25. Q. Huo, R. Xu, S. Li, Z. Ma, J. M. Thomas, R. H. Jones, A. M. Chippindale, *J. Chem. Soc., Chem. Commun.* **1992**, 875.
26. H. M. Lin, K. H. Lii, Y. C. Jiang, S. L. Wang, *Chem. Mater.*, **1999**, *11*, 519.
27. S. Decurtins, H. W. Schmalle, H. R. Oswald, A. Linden, J. Ensling, P. Gütllich, A. Hauser, *Inorg. Chem.* **1993**, *32*, 1888 and the references therein; *J. Am. Chem. Soc.* **1994**, *116*, 9521.
28. (a) H. Tamaki, Z. J. Zhong, N. Matsumoto, S. Kida, M. Koikawa, N. Achiwa, Y. Hashimoto, H. Okawa, *H. J. Am. Chem. Soc.* **1992**, *114*, 6974. (b) C. Mathoniere, S. G. Carling, P. Day, *J. Chem. Soc., Chem. Commun.* **1994**, 1551. (c) Clemente-Leon, M.; Coronado, E.; Galán-Mascarós, J.-R.; Gómez-García, C.J. *Chem. Commun.*, **1997**, 1727 and references therein.
29. S. Neeraj, S. Natarajan, S.; C. N. R. Rao, *Chem. Commun.* **1999**, 165; *New J. Chem.*, **1999**, *23*, 303; *Chem. Mater.*, **1999**, *11*, 1390.
30. R. Deyrieux, C. Bero, A. Penelous, *A. Bull. Soc. Chim. Fr.* **1973**, 25.
31. S. Oliver, A. Kuperman, G. A. Ozin, *Angew. Chem. Int. Ed.*, **1998**, *37*, 46; S. Oliver, A. Kuperman, A. Lough, G. A. Ozin, *Chem. Mater.*, **1996**, *8*, 2391.
32. S. Neeraj, S. Natarajan, C. N. R. Rao, *J. Solid State Chem.*, **2000**, *150*, 417.

33. C. N. R. Rao, S. Natarajan, A. Choudhury, S. Neeraj, A. Ayi, *Acc. Chem. Res.* **2001**, *34*, 80 and references therein.
34. S. -H. Huang, R. -J. Wang, T. C. W. Mak, *J. Cryst. Spectr. Res.* **1990**, *20*, 99.
35. P. A. Prasad, S. Neeraj, S. Natarajan, C.N.R. Rao, *Chem. Commun.* **2000**, 1251.
36. P. A. Wright, S. Natarajan, J. M. Thomas, R. G. Bell, P. L. Gai-Boyes, R. H. Jones, J. Chen, *Angew. Chem. Int. Ed. Engl.* **1992**, *31*, 1472 and references therein.
37. A. F. Wells, *Structural Inorganic Chemistry*, Oxford Press, 5th Ed., 1995, p. 450 and references therein.
38. M. Eddaoudi, D. B. Moler, H. Li, B. Chen, T. M. Reineke, M. O' Keeffe, O. M. Yaghi, *Acc. Chem. Res.* **2001**, *34*, 319 and references therein.
39. R. G. Iyer, M. G. Kanatzidis, *Inorg. Chem.*, **2002**, *41*, 3605.
40. S. O. H. Gutschke, M. Molinier, A. K. Powell, P. T. Wood, *Angew. Chem. Int. Engl. Ed.* **1997**, *36*, 991.
41. L. A. Gerrard, P. T. Wood, *Chem. Comm.* **2000**, 2107.
42. (a) S. L. Heath, A. K. Powell, *Angew. Chem. Int. Engl. Ed.* **1992**, *31*, 191. (b) S.L. Heath, P. A. Jordan, I. D. Johnson, G. R. Moore, A. K. Powell, *J. Inorg. Biochem.* **1995**, *59*, 785.
43. Y. Cudennec, A. Riou, Y. Gerault, A. Lecerf, *J. Solid State Chem.* **2001**, *162*, 150.
44. $[\text{CdCl}_2(\text{C}_4\text{N}_2\text{H}_8)]$, II, $M_r = 267.42$, Monoclinic, space group C2/c (no.15), $a = 9.5500(11)$, $b = 13.601(2)$, $c = 6.6499(8)$ Å, $\beta = 90.868(2)^\circ$; $V = 863.6(2)$ Å³, $Z = 8$, $\mu = 3.069\text{mm}^{-1}$, $D_c = 2.057\text{gcm}^{-3}$. A total of 1770 reflections were collected in the θ range 2.61 to 23.29° of which 585 with $I > 2\sigma(I)$ were considered to be observed. Final $R = 0.0513$, $S_{\text{obs}} = 1.014$ were obtained for 59 parameters. The average Cd-Cl distance and Cd-N distances are 2.682 and 2.345(4)Å respectively.
45. N. Guillou, S. Pastre, C. Livage, G. Férey, *Chem. Commun.* **2002**, 2358 and references therein.
46. S. Natarajan, *J. Solid State Chem.* **1999**, *149*, 50.
47. A. M. Chippindale, S. Natarajan, J. M. Thomas, R. H. Jones, *J. Solid State Chem.* **1994**, *111*, 18.

48. (a) M. Watanabe, K. Nagashima, *J. Inorg. Nucl. Chem.* **1971**, *33*, 3604. (b) T. R. R. McDonald, J. M. Spink, *Acta Crystallogr.* **1967**, *23*, 944.
49. (a) E. V. Brusau, J. C. Pedregosa, G. E. Narda, G. Echeverria, G. Punte, *J. Solid State Chem.* **2000**, *153*, 1. (b) E. A. H. Griffith, N. G. Charles, E. L. Amma, *Acta Cryst.* **1982**, *B38*, 262.
50. (a) E. V. Brusau, J. C. Pedregosa, G. E. Narda, G. Echeverria, G. Punte, *J. Solid State Chem.* **1999**, *143*, 174. (b) K. H. Chung, E. Hong, Y. Do, C. H. Moon, *Chem. Commun.* **1995**, 2333.
51. (a) Y.-Q. Zheng, Z.-P. Kong, *J. Solid State Chem.* **2002**, *166*, 279. (b) Y. J. Kim, D. -Y. Jung, *Inorg. Chem.* **2000**, *39*, 1470.
52. (a) E. Coronado, M. C.-L. León, J. R. Galán-Mascaros, C. Giménez-Saiz, C. J. Gómez-García, E. Martínez-Ferrero, *J. Chem. Soc. Dalton Trans.* **2000**, 3955. (b) K. Biradha, H. Hongo, M. Fujita, *Angew. Chem. Int. Ed. Engl.* **2002**, *41*, 3395.
53. (a) P. M. Forster, A. K. Cheetham, *Angew. Chem. Int. Ed. Engl.* **2002**, *41*, 457.
54. (a) C. Livage, C. Egger, G. Férey, *Chem. Mater.* **1999**, *13*, 1546. (b) C. Livage, C. Egger, M. Nogues, G. Férey, *J. Mater. Chem.* **1998**, *8*, 2743. (c) C. Livage, N. Guillou, J. Marrot, G. Férey, *Chem. Mater.* **2001**, *13*, 4387.
55. Y. Kim, D. -Y. Jung, *Bull. Korean Chem. Soc.* **1999**, *20*, 827. (b) Y. Kim, D. -Y. Jung, *Bull. Korean Chem. Soc.* **2000**, *21*, 656. (c) Y. Kim, E. W. Lee and D. -Y. Jung, *Chem. Mater.* **2001**, *13*, 2684.
56. K. Barthelet, J. Marrot, D. Riou, G. Férey, *Angew. Chem. Int. Ed. Engl.* **2002**, *41*, 281.
57. G. Aullon, D. Bellamy, L. Brammer, E. A. Bruton, A. G. Orpen, *Chem. Commun.* **1998**, 653 and references therein.
58. (a) D. Braga, F. Grepionni, P. Sabatino, G. R. Desiraju, *Organometallics* **1994**, *13*, 3532. (b) D. Braga, F. Grepionni, E. Tedesco, K. Biradha, G. R. Desiraju, *Organometallics* **1996**, *15*, 2962 and references therein.
59. S. Neeraj, S. Natarajan, *J. Mater. Chem.*, **2000**, *10*, 1171.
60. (a) S. R. Batten, R. Robson, *Angew. Chem. Int. Ed. Engl.* **1998**, *37*, 1460 and references therein; (b) S. R. Batten, *Cryst. Eng. Comm.* **2001**, *18*, 1.
61. (a) B. F. Hoskins, R. Robson, *J. Am. Chem. Soc.* **1990**, *112*, 1546. (b) L. Carlucci, G. Ciani, D. M. Proserpio, A. Sironi, *J. Chem. Soc. Chem. Commun.* **1994**, 2755. (c) C. L. Cahill, Y. Ko, J. B. Parise, *Chem. Mater.* **1998**, *10*, 19.

62. (a) S. R. Batten, *Cryst. Eng. Comm.* **2001**, *18*, 1. (b) S. R. Batten, A. R. Harris, P. Jensen, K. S. Murray, A. Ziebell, *J. Chem. Soc. Dalton Trans.* **2000**, 3829. (c) Z. F. Chen, R. G. Xiong, B. F. Abrahams, X. Z. You, C. M. Che, *J. Chem. Soc. Dalton Trans.* **2001**, 2453.
63. (a) T. Kitazawa, S. Nishikiori, R. Kuroda, T. Iwamoto, *J. Chem. Soc. Dalton Trans.* **1994**, 1029; (b) T. Kitazawa, S. Nishikiori, R. Kuroda, T. Iwamoto, *J. Chem. Soc. Chem. Commun.* **1992**, 413; (c) O. R. Evans, R. G. Xiong, Z. Wang, G. K. Wong, W. Lin, *Angew. Chem. Int. Ed. Engl.* **1999**, *38*, 536.
64. N. L. Rosi, J. Kim, M. Eddaoudi, M. O'Keeffe, O. M. Yaghi, *Angew. Chem. Int. Ed. Engl.* **2002**, *41*, 284.
65. B. F. Abrahams, S. R. Batten, H. Hamit, B. F. Hoskins, R. Robson, *Angew. Chem. Int. Ed. Engl.* **1996**, *35*, 1690.
66. T. Soma, H. Yuge, T. Iwamoto, *Angew. Chem. Int. Ed. Engl.* **1994**, *33*, 1665.
67. H. Schafer, H. G. Schnering, K. Niehues, H. G. Nieder-Vahrenholz, *J. Less-Common Met.* **1965**, *9*, 95.
68. J. Zhang, J. D. Corbett, *Inorg. Chem.* **1991**, *30*, 431.
69. P. G. Desmartin, A. F. Williams, G. Bernardinelli, *New. J. Chem.* **1995**, *19*, 1109.
70. P. C. M. Duncan, D. M. L. Goodgame, S. Menzer, D. Williams, *J. Chem. Commun.* **1996**, 2127.
71. M. Fleck, E. Tillmans, L. Bohaty, *Z. Kristallogr. Ncs.* **2000**, *215*, 429.
72. (a) G. Ferey, *J. Fluorine Chem.* **1995**, *72*, 187 and references therein; (b) G. Ferey, *C. R. Acad. Sci. Paris*, t. 1, Serie II, **1998**, p. 1- 13.
73. (a) L. R. MacGillivray, S. Subramaniam, M. J. Zaworotko, *J. Chem. Soc. Chem. Commun.* **1994**, 1325; (b) L. Carlucci, G. Ciani, D. M. Proserpio, A. J. Sironi, *J. Chem. Soc. Chem. Commun.* **1994**, 2755.
74. (a) O. M. Yaghi, H. Li, *Angew. Chem. Int. Ed. Engl.* **1995**, *34*, 207. (b) O. M. Yaghi, H. Li, T. L. Groy, *Inorg. Chem.* **1997**, *36*, 4292.
75. M. O'Keeffe, M. Eddaoudi, H. Li, T. M. Reineke, O. M. Yaghi, *J. Solid State Chem.* **2000**, *152*, 3.
76. B. Moulton, M. J. Zaworotko, *Advances in Supramolecular Chemistry*, JAI Press Inc., **2000**, Vol. 7, p.235 and references therein.
77. G. Ferey, *J. Solid State Chem.* **2000**, *152*, 37.

-
78. B. F. Hoskins, R. Robson, D. A. Slizys, *Angew. Chem. Int. Ed. Engl.* **1997**, *36*, 2752.
79. B. Chen, M. Eddaoudi, T. M. Reineke, J. W. Kampf, M. O'Keeffe, O. M. Yaghi, *J. Am. Chem. Soc.* **2000**, *122*, 11559.
80. H. Li, J. Kim, T. L. Groy, M. O'Keeffe, O. M. Yaghi, *J. Am. Chem. Soc.* **2001**, *123*, 4867 and referenced therein.
81. J. Y. Lu, M. A. Lawandy, J. Li, *Inorg. Chem.* **1999**, *38*, 2695 and references therein.
82. Y. J. Kim, E. W. Lee, D. Y. Jung, *Chem. Mater.* **2001**, *13*, 2684 and references therein.
83. O. Castillo, A. Luque, J. Sertucha, P. Roman, F. Lloret, *Inorg. Chem.* **2000**, *39*, 6142 and references therein.
84. H. Li, M. Eddaoudi, M. O'Keeffe, O. M. Yaghi, *Nature* **1999**, *402*, 276.
85. W. T. A. Harrison, R. W. Broach, R. A. Bedard, T. E. Gier, X. Bu, G. D. Stucky, *Chem. Mater.* **1996**, *8*, 691.
86. K. Mereiter, J. Zemman, W. Hewat, *Am. Miner.* **1992**, *77*, 839.
87. A. F. Wells, *Three-dimensional Nets and Polyhedra*, Wiley-Interscience, New York, 1997.
88. (a) R. Chevrel, M. Sergent, and J. Prigent, *J. Solid State Chem.* **1971**, *3*, 515. (b) Subba Rao, G. V. Balakrishnan, *G. Bull. Mater. Sci (India)*. **1984**, *6*, 283 and the references therein; (c) G. V. Subba Rao, *Proc. Ind. National Sci. Acad.* **1986**, *52A*, 292.
89. D. Chidambaram, S. Neeraj, S. Natarajan, C. N. R. Rao, *J. Solid State Chem.* **1999**, *147*, 154.
90. T. A. Kodenkandath, J. N. Lalena, W. I. Zhou, E. E. Carpenter, A. U. Sangregorio, A. U. Falster, J. R. Simmons, C. J. O'Connor, J. B. Wiley, *J. Am. Chem. Soc.* **1999**, *121*, 10743.
91. Q. Huang, M. Ulutagy, P. A. Michener, S. J. Hwu, *J. Am. Chem. Soc.* **1999**, *121*, 10323.

APPENDIX

Table A1. Atomic coordinates [$\times 10^4$] and equivalent isotropic displacement parameters [$\text{\AA}^2 \times 10^3$] for propylamine oxalate (PRO)

Atom	x	y	z	U(eq) [#]
O(100)	0	770(5)	2500	43(1)
O(2)	-831(1)	-7195(3)	-427(1)	58(1)
O(4)	-941(1)	-2801(3)	-1204(1)	56(1)
O(3)	-771(1)	-1348(3)	332(1)	58(1)
O(1)	-641(1)	-5672(3)	1101(1)	56(1)
C(5)	-763(1)	-5525(4)	176(2)	38(1)
C(4)	-834(1)	-3051(4)	-311(2)	37(1)
N(1)	-904(1)	-2753(5)	2522(2)	45(1)
C(2)	-2163(2)	-3326(7)	1850(3)	73(1)
C(3)	-1590(1)	-1647(6)	2017(2)	55(1)
C(1)	-2257(2)	-5285(8)	1103(4)	83(1)

Table A2. Atomic coordinates [$\times 10^4$] and equivalent isotropic displacement parameters [$\text{\AA}^2 \times 10^3$] for butylamine oxalate (BUO)

Atom	x	y	z	U(eq) [#]
O(1)	4377(1)	1236(4)	9000(1)	57(1)
O(2)	4209(1)	2672(4)	10375(1)	63(1)
C(1)	4303(1)	2935(5)	9582(2)	42(1)
O(3)	4325(1)	7085(3)	9714(1)	58(1)
O(4)	4412(1)	5582(4)	8318(1)	65(1)
C(2)	4348(1)	5415(5)	9159(2)	42(1)
N(1)	5748(1)	2627(6)	8327(2)	54(1)
C(3)	6353(1)	1778(7)	8386(2)	66(1)
C(4)	6787(2)	3800(10)	8603(3)	96(1)
C(6)	7813(3)	5212(15)	8929(4)	180(4)
C(5)	7404(2)	3120(14)	8659(4)	140(3)
O(100)	5000	9054(5)	7500	51(1)

Table A3. Atomic coordinates [$\times 10^4$] and equivalent isotropic displacement parameters [$\text{\AA}^2 \times 10^3$] for ethylenediamine oxalate (ENO)

Atom	x	y	z	U(eq) [#]
O(1)	1106(1)	8652(3)	1699(2)	59(1)
O(2)	1015(1)	4351(3)	2345(1)	56(1)
O(3)	1149(1)	2808(3)	997(2)	60(1)
O(4)	1296(1)	7193(3)	380(2)	59(1)
C(1)	1189(1)	6943(3)	1143(2)	38(1)
C(2)	1113(2)	4494(3)	1543(2)	38(1)
N(1)	-1199(1)	7537(4)	970(2)	41(1)
C(10)	-2154(2)	8485(4)	298(2)	40(1)
O(100)	0	11021(4)	2500	42(1)

Table A4. Atomic coordinates [$\times 10^4$] and equivalent isotropic displacement parameters [$\text{\AA}^2 \times 10^3$] for 1,4-diaminobutane oxalate (DABO)

Atom	x	y	z	U(eq) [#]
C(1)	4428(6)	-2544(13)	1569(6)	31(2)
C(2)	4474(5)	-83(12)	2000(6)	30(2)
C(3)	1999(6)	-263(12)	2250(6)	32(2)
C(4)	1844(6)	2223(13)	2650(6)	31(2)
O(1)	4527(5)	127(9)	2749(4)	61(2)
O(2)	4477(4)	1607(9)	1440(4)	45(2)
O(3)	4544(5)	-4226(9)	2085(4)	51(2)
O(4)	4252(4)	-2704(9)	811(4)	37(2)
O(5)	2259(5)	-490(10)	1533(4)	57(2)
O(6)	1805(4)	-1954(9)	2775(4)	42(2)
O(7)	2057(5)	3897(9)	2172(4)	47(2)
O(8)	1560(5)	2313(9)	3384(4)	44(2)
C(10)	2935(6)	36(13)	5057(6)	35(2)
C(11)	3729(5)	-1609(14)	4919(6)	39(2)
C(12)	3523(6)	-3652(14)	4335(6)	36(2)
C(13)	4322(5)	-5322(12)	4219(6)	36(2)
N(1)	2170(4)	-1105(11)	5523(4)	31(2)

N(2)	5104(5)	-4152(11)	3787(5)	34(2)
O(100)	3872(4)	589(10)	-400(5)	35(1)

Table A5. Atomic coordinates [$\times 10^4$] and equivalent isotropic displacement parameters [$\text{\AA}^2 \times 10^3$] for piperazine oxalate (PIPO)

Atom	x	y	z	U(eq) [#]
N(1)	4287(1)	-4833(3)	8958(1)	27(1)
C(2)	5041(1)	-6451(3)	9056(2)	29(1)
C(1)	4571(1)	-2761(3)	9723(2)	32(1)
O(1)	1106(1)	-15513(2)	7886(1)	43(1)
O(2)	2436(1)	-14005(2)	8814(1)	29(1)
O(3)	1800(1)	-19882(2)	8325(1)	28(1)
O(4)	3125(1)	-18282(2)	9194(1)	28(1)
C(11)	1880(1)	-15728(3)	8417(1)	23(1)
C(10)	2321(1)	-18178(3)	8677(1)	21(1)

Table A6. Atomic coordinates [$\times 10^4$] and equivalent isotropic displacement parameters [$\text{\AA}^2 \times 10^3$] for DABCO oxalate (DCO)

Atom	x	y	z	U(eq) [#]
O(1)	2374(3)	3233(2)	4916(2)	55(1)
O(2)	894(3)	3177(2)	6492(2)	57(1)
O(3)	1934(3)	851(2)	7360(2)	65(1)
O(4)	3043(4)	662(2)	5651(2)	78(1)
O(5)	-3319(4)	3684(3)	-900(2)	101(1)
O(6)	-1790(4)	3635(3)	-2422(2)	80(1)
O(7)	432(3)	2089(2)	-969(2)	58(1)
O(8)	-1135(3)	2101(2)	569(2)	61(1)
C(7)	1811(3)	2701(2)	5855(2)	39(1)
C(8)	2322(4)	1301(3)	6270(2)	49(1)
C(9)	-2086(4)	3311(3)	-1286(2)	54(1)
C(10)	-804(3)	2411(3)	-491(2)	40(1)
N(1)	-5707(3)	2549(2)	3351(2)	41(1)

N(2)	-3834(3)	2619(2)	1694(2)	40(1)
C(1)	-5951(4)	3756(3)	2529(2)	43(1)
C(2)	-4795(4)	3807(3)	1519(2)	44(1)
C(3)	-2254(4)	2868(3)	3063(2)	47(1)
C(4)	-3398(4)	2831(3)	4065(2)	49(1)
C(5)	-6708(4)	1092(3)	2475(2)	51(1)
C(6)	-5569(4)	1140(3)	1460(2)	47(1)

Table A7. Atomic coordinates [$\times 10^4$] and equivalent isotropic displacement parameters [$\text{\AA}^2 \times 10^3$] for guanidine oxalate (GUO)

Atom	x	y	z	U(eq) [#]
O(1)	3588(5)	4770(3)	1258(3)	44(1)
O(2)	1849(5)	4244(3)	-799(3)	47(1)
O(3)	1445(5)	6676(3)	-1503(3)	48(1)
O(4)	3202(5)	7240(3)	540(3)	51(1)
C(1)	2634(6)	5020(4)	85(5)	33(1)
C(2)	2456(6)	6447(4)	-272(4)	34(1)
O(100)	8684(6)	846(3)	2002(3)	42(1)
N(3)	6328(6)	7045(3)	3187(4)	43(1)
N(2)	8034(6)	6546(4)	5333(4)	48(1)
N(1)	6806(6)	4973(3)	3818(4)	50(1)
C(3)	7049(6)	6190(4)	4121(4)	35(1)

Table A8. Atomic coordinates [$\times 10^4$] and equivalent isotropic displacement parameters [$\text{\AA}^2 \times 10^3$] for the non-hydrogen atoms in I, $[\text{H}_3\text{N}(\text{CH}_2)_3\text{NH}_3][\text{Zn}_2(\text{C}_2\text{O}_4)_3] \cdot 3\text{H}_2\text{O}$

Atom	x	y	z	U(eq) [#]
Zn(1)	5730(1)	-1446(1)	-2376(1)	30(1)
Zn(2)	2432(1)	-4895(1)	-2418(1)	30(1)
O(1)	3918(3)	603(2)	-3275(2)	38(1)
O(2)	5574(2)	353(2)	-1493(2)	36(1)
O(3)	7713(2)	-3357(2)	-1501(2)	36(1)
O(4)	7710(2)	-1502(2)	-3286(2)	32(1)

O(5)	5418(3)	-2980(2)	-3323(2)	36(1)
O(6)	3955(3)	-1833(3)	-1493(2)	38(1)
O(7)	2523(3)	-6710(2)	-3272(2)	35(1)
O(8)	4082(3)	-4397(3)	-3342(2)	37(1)
O(9)	447(2)	-4715(2)	-1492(2)	35(1)
O(10)	4264(3)	-6951(2)	-1520(2)	36(1)
O(11)	450(2)	-2954(2)	-3340(2)	34(1)
O(12)	2650(3)	-3282(3)	-1475(2)	35(1)
C(1)	4443(3)	-3452(3)	-2950(2)	27(1)
C(2)	3603(3)	-2791(3)	-1869(2)	27(1)
C(3)	9086(3)	-3650(3)	-1882(2)	27(1)
C(4)	9089(3)	-2610(3)	-2936(2)	27(1)
C(5)	3575(3)	1898(3)	-2898(2)	28(1)
C(6)	4561(3)	1761(3)	-1870(2)	28(1)
O(100)	7953(3)	-41(3)	4724(2)	43(1)
O(200)	1786(4)	-5377(3)	-5443(2)	52(1)
O(300)	2055(4)	577(4)	-175(3)	69(1)
N(2)	-1064(3)	3145(3)	-536(2)	38(1)
N(1)	-1312(3)	2251(3)	-4350(2)	43(1)
C(11)	-1915(4)	2160(4)	-3242(2)	43(1)
C(12)	-1069(4)	2591(4)	-2439(2)	41(1)
C(13)	-1851(4)	2722(4)	-1353(2)	44(1)

Table A9. Atomic coordinates [$\times 10^4$] and equivalent isotropic displacement parameters [$\text{\AA}^2 \times 10^3$] for the non-hydrogen atoms in **II**, $2[\text{C}_3\text{H}_7\text{NH}_3][\text{Zn}_2(\text{C}_2\text{O}_4)_3] \cdot 3\text{H}_2\text{O}$

Atom	x	y	z	U(eq) [#]
Zn(1)	4180(1)	11249(1)	5861(1)	69(1)
O(1)	3584(3)	12847(5)	5024(3)	83(1)
O(2)	3936(3)	9650(5)	5025(2)	81(1)
O(3)	4669(3)	12626(4)	6827(2)	75(1)
O(4)	4662(3)	9861(4)	6835(2)	75(1)
O(5)	2783(3)	11145(4)	5688(3)	79(1)
O(6)	5408(3)	11355(4)	5687(3)	79(1)

C(1)	5000	12047(8)	7500	66(2)
C(2)	5000	10440(8)	7500	61(2)
C(3)	2273(4)	11993(6)	5192(3)	62(1)
C(4)	5425(3)	10499(6)	5193(3)	64(1)
O(100) ^a	4703(16)	14278(20)	4407(13)	394(10)
O(200) ^{a,1}	4644(14)	5548(18)	6795(11)	182(6)
O(300) ^{a,1}	4673(14)	6993(19)	6726(12)	189(6)
O(400) ^a	2801(13)	13183(19)	529(12)	360(9)
N(10) ^a	1721(12)	11247(10)	947(10)	222(6)
C(10) ^a	1738(18)	10745(28)	1735(12)	329(13)
C(11) ^a	2583(19)	11696(29)	2030(16)	347(13)
C(12) ^a	2645(18)	11158(19)	2833(15)	284(11)

^a refined isotropically; ¹ Site Occupancy Factor (SOF) = 0.5

Table A10. Atomic coordinates [$\times 10^4$] and equivalent isotropic displacement parameters [$\text{\AA}^2 \times 10^3$] for **III**, $\text{K}[\text{C}_6\text{N}_2\text{H}_{13}][\text{Zn}_2(\text{C}_2\text{O}_4)_3] \cdot 4\text{H}_2\text{O}$

Atom	x	y	z	U(eq) [#]
Zn(1)	806(1)	2534(1)	9142(1)	25(1)
Zn(2)	4122(1)	2467(1)	5824(1)	31(1)
K(1)	5643(2)	3205(2)	9350(1)	43(1)
O(1)	419(6)	3490(5)	7873(3)	33(1)
O(2)	-1361(5)	3971(5)	9720(3)	31(1)
O(3)	2029(5)	4002(5)	9582(3)	31(1)
O(4)	3191(6)	1520(5)	8479(3)	35(1)
O(5)	1462(6)	979(5)	10232(3)	31(1)
O(6)	-879(6)	1116(5)	9090(3)	30(1)
O(7)	2936(6)	1030(5)	5362(3)	33(1)
O(8)	6347(6)	992(5)	5331(3)	34(1)
O(9)	5459(7)	4047(5)	6022(3)	38(1)
O(10)	1775(6)	3506(5)	6518(3)	38(1)
O(11)	3795(6)	3909(5)	4648(3)	36(1)
O(12)	4508(6)	1436(5)	7119(3)	35(1)
C(1)	980(8)	5018(7)	9966(4)	24(1)
C(2)	1698(9)	3065(7)	7312(4)	29(2)

C(3)	-673(8)	43(7)	9672(4)	24(1)
C(4)	3287(9)	1909(7)	7662(4)	27(2)
C(5)	4027(9)	2(7)	5019(4)	28(2)
C(6)	4516(9)	4957(8)	4606(4)	30(2)
N(1)	11521(8)	1861(8)	2899(4)	47(2)
N(2)	8327(8)	1955(7)	2909(4)	40(2)
C(15)	11302(11)	338(9)	2916(7)	58(2)
C(11)	10860(10)	2761(10)	2098(5)	50(2)
C(14)	10551(11)	2557(11)	3681(6)	60(3)
C(13)	8620(10)	2592(9)	3671(5)	47(2)
C(16)	9350(10)	426(9)	2918(6)	49(2)
C(12)	8938(11)	2801(10)	2113(5)	53(2)
O(100)	4779(7)	1102(6)	10752(4)	56(2)
O(200)	4675(7)	2271(7)	3168(4)	62(2)
O(300)	5063(8)	6203(6)	8781(4)	60(2)
O(400)	6781(8)	3962(8)	7633(4)	67(2)

Table A11. Atomic coordinates [$\times 10^4$] and equivalent isotropic displacement parameters [$\text{\AA}^2 \times 10^3$] for IV, $[\text{CN}_3\text{H}_6]_2[\text{Zn}(\text{H}_2\text{O})_2(\text{C}_2\text{O}_4)_2]$

Atom	x	y	z	U(eq) [#]
Zn(1)	5000(4)	8287(1)	7500(2)	28(1)
O(1)	4236(3)	6782(3)	6182(3)	34(1)
O(2)	5775(2)	9379(3)	9231(3)	32(1)
O(3)	6304(3)	8454(4)	7005(4)	32(1)
C(1)	3767(3)	7156(4)	5016(5)	27(1)
O(4)	3273(3)	6400(3)	4070(3)	38(1)
C(2)	6190(3)	8667(5)	10242(5)	28(1)
O(5)	6550(3)	9039(3)	11393(3)	41(1)
C(10)	3769(3)	3251(4)	6037(4)	31(1)
N(1)	3946(4)	3563(5)	5017(5)	43(1)
N(2)	3648(4)	4191(5)	6779(5)	43(1)
N(3)	3690(4)	1997(4)	6327(5)	43(1)

Table A12. Atomic coordinates [$\times 10^4$] and equivalent isotropic displacement parameters [$\text{\AA}^2 \times 10^3$] for V, $[\text{C}_4\text{N}_2\text{H}_{12}]_3[\text{Zn}_2(\text{C}_2\text{O}_4)_5] \cdot 8\text{H}_2\text{O}$

Atom	x	y	z	U(eq) [#]
Zn(1)	1164(1)	10949(1)	8537(1)	27(1)
O(1)	1770(2)	12488(3)	8864(1)	39(1)
O(2)	706(2)	9275(3)	8303(1)	36(1)
O(3)	1310(3)	7523(3)	8211(2)	65(1)
C(1)	1575(3)	12766(4)	9313(2)	31(1)
C(2)	1413(3)	8564(4)	8341(2)	36(1)
O(4)	750(2)	10925(3)	9273(1)	35(1)
O(5)	2557(2)	10100(3)	8716(1)	36(1)
O(6)	616(2)	12164(3)	9928(1)	40(1)
O(7)	1849(3)	13662(3)	9575(1)	47(1)
O(8)	3224(3)	8410(3)	8573(2)	57(1)
C(3)	922(3)	11879(4)	9529(2)	28(1)
C(4)	2508(3)	9048(4)	8563(2)	34(1)
O(9)	-345(2)	11474(3)	8117(1)	30(1)
O(10)	1312(2)	11460(3)	7742(1)	34(1)
C(5)	-478(3)	11468(3)	7604(2)	26(1)
C(6)	8144(5)	10271(5)	8899(2)	57(2)
C(7)	7236(4)	10132(5)	7927(2)	50(1)
N(1)	7838(3)	10899(3)	8369(2)	49(1)
C(8)	7828(4)	9068(4)	7873(2)	42(1)
C(9)	8734(4)	9211(5)	8847(2)	50(1)
N(2)	8159(3)	8439(3)	8403(2)	36(1)
C(10)	10143(4)	5663(5)	9543(2)	42(1)
C(11)	9061(4)	4391(4)	9914(2)	43(1)
N(3)	9132(3)	5498(3)	9627(2)	38(1)
O(100)	1074(3)	8706(4)	9789(2)	71(1)
O(200)	9409(3)	6772(4)	8146(3)	94(2)
O(300)	4780(4)	9326(4)	8114(3)	114(2)
O(400)	2210(9)	7183(10)	9434(4)	216(5)

Table A13. Atomic coordinates [$\times 10^4$] and equivalent isotropic displacement parameters [$\text{\AA}^2 \times 10^3$] for VI, $[\text{C}_6\text{N}_2\text{H}_{14}][\text{Zn}(\text{C}_2\text{O}_4)_2] \cdot 3\text{H}_2\text{O}$

Atom	x	y	z	U(eq) [#]
Zn(1)	993(1)	4542(1)	2514(1)	36(1)
O(1)	-780(4)	4417(2)	3710(4)	41(1)
O(2)	441(4)	5568(2)	1437(4)	37(1)
O(3)	3119(4)	4614(2)	1978(4)	39(1)
O(4)	1712(4)	3416(2)	3144(4)	42(1)
O(5)	293(4)	4046(2)	634(4)	38(1)
O(6)	1604(4)	5239(2)	4250(4)	42(1)
C(1)	-682(6)	4758(4)	4844(6)	34(2)
C(2)	3768(7)	3983(4)	2159(6)	41(2)
C(3)	2945(7)	3275(4)	2764(6)	39(2)
C(4)	-39(6)	4562(4)	-237(6)	30(1)
O(7)	3554(5)	2618(3)	2802(5)	67(2)
O(8)	5035(5)	3863(3)	1887(6)	76(2)
O(100)	4397(8)	5834(6)	4865(10)	86(2)
O(200)	1533(7)	1396(5)	3152(8)	67(2)
O(300)	6779(7)	5027(4)	873(7)	77(2)
N(2)	-1201(5)	1749(3)	2341(5)	42(1)
N(1)	-3396(5)	2545(3)	2220(5)	44(1)
C(10)	-2237(7)	2990(4)	1552(7)	46(2)
C(9)	-983(7)	2448(4)	1436(7)	50(2)
C(8)	-2383(7)	1251(4)	1736(7)	47(2)
C(7)	-3660(7)	1777(4)	1507(6)	46(2)
C(6)	-1553(8)	2004(5)	3715(6)	60(2)
C(5)	-3007(7)	2394(5)	3682(6)	55(2)

Table A14. Atomic coordinates [$\times 10^4$] and equivalent isotropic displacement parameters [$\text{\AA}^2 \times 10^3$] for VII, $[\text{C}_4\text{N}_2\text{H}_{12}][\text{Zn}_2(\text{C}_2\text{O}_4)_3] \cdot 4\text{H}_2\text{O}$

Atom	x	y	z	U(eq)
Zn(1)	4770(1)	1345(1)	3612(1)	30(1)
Zn(2)	6513(1)	-3641(1)	3596(1)	28(1)

O(1)	3911(3)	692(5)	3988(2)	33(1)
O(2)	3709(3)	1951(6)	3210(2)	34(1)
O(3)	5736(3)	245(6)	3978(2)	38(1)
O(4)	5003(3)	3267(5)	3967(2)	36(1)
O(5)	5519(3)	2440(5)	3234(2)	37(1)
O(6)	4793(3)	-575(5)	3243(2)	34(1)
O(7)	6467(3)	-1768(5)	3955(2)	35(1)
O(8)	7569(3)	-4337(6)	3977(2)	34(1)
O(9)	6252(3)	-5545(5)	3239(2)	33(1)
O(10)	7371(3)	-2969(6)	3211(2)	33(1)
O(11)	5580(3)	-2504(5)	3199(2)	33(1)
O(12)	5724(3)	-4700(5)	3968(2)	33(1)
C(1)	8198(4)	-4028(7)	3821(2)	28(2)
C(2)	8078(5)	-3263(7)	3379(2)	26(2)
C(3)	5913(4)	-920(8)	3809(2)	30(2)
C(4)	5472(4)	4104(8)	3816(2)	27(2)
C(5)	5779(4)	3628(8)	3395(2)	29(2)
C(6)	5384(4)	-1364(8)	3378(2)	28(2)
O(100)	3702(4)	693(7)	2321(2)	59(2)
O(200)	6662(4)	-5685(9)	905(2)	78(2)
O(300)	5124(9)	1273(18)	4938(8)	294(11)
O(400)	4874(8)	-3950(14)	4677(4)	173(5)
C(7)	6203(5)	-4451(9)	1891(3)	42(2)
C(8)	6204(5)	-3811(9)	2332(3)	42(2)
C(9)	7109(5)	-1903(9)	2140(3)	44(2)
C(10)	7060(6)	-2580(10)	1701(3)	52(2)
C(11)	6879(7)	-3585(10)	4949(3)	66(3)
C(12)	7368(5)	-1110(8)	4806(2)	33(2)
C(13)	6984(9)	2204(14)	5313(4)	92(4)
C(14)	7123(9)	2577(13)	4572(4)	94(4)
N(1)	6361(4)	-2232(7)	2326(2)	36(2)
N(2)	6938(4)	-4139(8)	1711(2)	44(2)
N(3)	6690(7)	-1939(12)	4954(3)	108(4)
N(4)	6819(6)	1634(10)	4884(3)	83(3)

Table A15. Atomic coordinates [$\times 10^4$] and equivalent isotropic displacement parameters [$\text{\AA}^2 \times 10^3$] for VIII, $\text{Na}_4\text{Cd}_2(\text{C}_2\text{O}_4)_4 \cdot 4\text{H}_2\text{O}$

Atom	x	y	z	U(eq) [#]
Cd(1)	2130(1)	3631(1)	6803(1)	16(1)
Cd(2)	3225(1)	2638(1)	3058(1)	16(1)
O(1)	3531(3)	3462(4)	6182(4)	24(1)
O(2)	1512(4)	1728(4)	6399(4)	27(1)
O(3)	3340(4)	4936(4)	7956(4)	29(1)
O(4)	6537(4)	1523(4)	3182(4)	32(1)
O(5)	1589(4)	5602(4)	6279(4)	32(1)
O(6)	1325(3)	3591(4)	4920(3)	20(1)
O(7)	3510(3)	2290(4)	8000(4)	22(1)
O(8)	38(4)	3637(4)	6211(3)	23(1)
O(9)	3651(4)	1808(4)	1718(4)	31(1)
O(10)	3983(3)	3129(4)	4838(3)	19(1)
O(11)	1788(3)	3325(4)	3576(4)	23(1)
O(12)	5155(4)	2028(4)	3668(4)	26(1)
O(13)	2271(4)	3884(4)	1606(4)	25(1)
O(14)	3272(4)	728(4)	3821(4)	29(1)
O(15)	983(4)	-390(4)	1734(4)	27(1)
O(16)	1561(3)	1475(4)	2071(4)	22(1)
C(1)	3287(5)	3320(5)	5240(5)	16(2)
C(2)	3012(5)	5976(6)	7954(5)	17(2)
C(3)	5529(5)	1746(5)	3010(5)	17(2)
C(4)	1931(5)	6329(6)	6998(5)	18(2)
C(5)	2013(5)	3419(5)	4513(5)	16(2)
C(6)	-333(6)	3361(6)	6886(5)	22(2)
C(7)	2640(5)	-28(6)	3246(5)	20(2)
C(8)	1631(5)	381(6)	2258(5)	20(2)
Na(1)	0	5000	5000	20(1)
Na(2)	830(2)	2694(2)	468(2)	26(1)
Na(3)	-125(2)	2167(2)	4867(2)	29(1)
Na(4)	0	0	0	30(1)
Na(5)	99(2)	2416(2)	2489(2)	31(1)

O(100)	-1641(4)	1216(4)	5071(4)	32(1)
O(200)	459(4)	876(4)	3874(4)	30(1)
O(300)	1766(4)	1005(4)	43(4)	33(1)
O(400)	-268(4)	4075(4)	1077(5)	46(2)

Table A16. Atomic coordinates [$\times 10^4$] and equivalent isotropic displacement parameters [$\text{\AA}^2 \times 10^3$] for IX, $\text{K}_2\text{Cd}(\text{C}_2\text{O}_4)_2 \cdot 2\text{H}_2\text{O}$

Atom	x	y	z	U(eq) [#]
Cd(1)	0	0	300(1)	12(1)
K(1)	1091(1)	703(1)	-3978(2)	32(1)
C(1)	1356(3)	1366(3)	523(7)	15(1)
C(2)	-1595(3)	1183(3)	-178(6)	14(1)
O(1)	1144(3)	860(2)	-527(5)	21(1)
O(2)	-2143(3)	1685(2)	103(6)	23(1)
O(3)	-1358(3)	698(2)	886(5)	25(1)
O(4)	1891(2)	1887(2)	239(6)	23(1)
O(100)	2123(4)	-96(3)	-6180(7)	53(1)

Table A17. Atomic coordinates [$\times 10^4$] and equivalent isotropic displacement parameters [$\text{\AA}^2 \times 10^3$] for X, $\text{Cd}_2(\text{C}_2\text{O}_4)_{0.5}\text{Cl}_3\text{NaCl} \cdot 4\text{H}_2\text{O}$

Atom	x	y	z	U(eq) [#]
Cd(1)	6603(1)	882(1)	917(1)	24(1)
Cd(2)	8793(1)	2512(1)	1324(1)	25(1)
Na(1)	8811(2)	-762(1)	1333(2)	41(1)
Cl(1)	6258(1)	969(1)	-1260(1)	31(1)
Cl(2)	8720(1)	977(1)	1300(1)	29(1)
Cl(3)	6569(1)	2464(1)	982(1)	25(1)
Cl(4)	9065(1)	2527(1)	3546(1)	30(1)
C(1)	4501(3)	902(2)	1969(4)	20(1)
O(1)	3536(2)	910(2)	2179(3)	29(1)
O(2)	4732(2)	903(2)	987(2)	28(1)
O(10)	6706(3)	-481(2)	1042(4)	32(1)

O(100)	8540(4)	-693(2)	-694(3)	38(1)
O(200)	9174(3)	-695(3)	3384(3)	41(1)
O(300)	8736(5)	-2108(3)	1275(5)	72(2)

Table A18. Atomic coordinates [$\times 10^4$] and equivalent isotropic displacement parameters [$\text{\AA}^2 \times 10^3$] for **XI**, $[\text{C}_6\text{N}_2\text{H}_{16}]_{0.5}[\text{Y}(\text{H}_2\text{O})(\text{C}_2\text{O}_4)_2] \cdot 2\text{H}_2\text{O}$

Atom	x	y	z	U(eq) [#]
Y(1)	6704(1)	8413(1)	7868(1)	20(1)
O(1)	6902(6)	9068(6)	9881(6)	29(1)
O(2)	5300(7)	3395(5)	9631(6)	33(1)
O(3)	8817(6)	8284(5)	5614(5)	28(1)
O(4)	5602(6)	10082(6)	11532(6)	31(1)
O(5)	4632(6)	8120(5)	6732(6)	29(1)
O(6)	9131(6)	10280(5)	6711(5)	25(1)
O(7)	6702(6)	5777(5)	8189(5)	28(1)
O(8)	8874(8)	6948(7)	9171(9)	34(1)
O(9)	6596(6)	10783(6)	5298(6)	32(1)
C(1)	4430(8)	9235(8)	5411(8)	22(2)
C(2)	5729(9)	9760(7)	10392(8)	21(2)
C(3)	10071(8)	10565(8)	5326(8)	21(2)
C(4)	5581(9)	4760(8)	9365(8)	24(2)
O(100)	10826(13)	8857(14)	9462(12)	77(3)
O(200)	8149(10)	4174(8)	12251(10)	49(2)
N(1)	9878(14)	3655(10)	6533(11)	81(3)
C(11)	8338(12)	4221(11)	5892(11)	54(2)
C(12)	8496(10)	5914(9)	4816(9)	32(2)
C(13)	7001(17)	6500(16)	4186(18)	96(5)

Table A19. Atomic coordinates [$\times 10^4$] and equivalent isotropic displacement parameters [$\text{\AA}^2 \times 10^3$] for **XII**, $[\text{C}_3\text{N}_2\text{H}_{11}][\text{Y}(\text{C}_2\text{O}_4)_2]$

Atom	x	y	z	U(eq) [#]
Y(1)	4410(4)	1280(1)	2605(5)	24(1)

O(1)	6706(11)	1705(6)	3615(15)	33(3)
O(2)	5685(11)	759(7)	5843(14)	40(3)
O(3)	5238(11)	2365(7)	4722(15)	40(3)
O(4)	2081(11)	1750(6)	1524(14)	29(2)
O(5)	3523(11)	2369(5)	384(14)	28(2)
O(6)	5722(11)	166(4)	2700(13)	37(3)
O(7)	3185(11)	784(6)	-670(12)	27(2)
O(8)	3093(10)	176(5)	2530(12)	32(2)
C(1)	7371(16)	2343(7)	4842(18)	26(3)
C(2)	1529(13)	2283(8)	495(18)	23(3)
C(3)	5190(14)	-194(7)	1056(17)	22(3)
C(4)	3714(17)	-156(7)	4130(20)	28(3)
N(1)	8332(16)	-724(9)	5908(20)	56(4)
C(10)	8142(33)	-1629(14)	6103(33)	117(9)
C(11)	9639(23)	-1954(4)	7806(29)	51(4)
C(12)	10483(27)	-1605(15)	9582(41)	176(18)
N(2)	10570(15)	-742(9)	9154(22)	52(4)
C(13)	9446(22)	-371(3)	7728(28)	41(2)
C(14)	9390(31)	491(4)	7523(41)	72(3)

Table A20. Atomic coordinates [$\times 10^4$] and equivalent isotropic displacement parameters [$\text{\AA}^2 \times 10^3$] for XIII, $[\text{NH}_3\text{CH}_2\text{CH}(\text{NH}_3)\text{CH}_3][\text{Nd}(\text{C}_2\text{O}_4)_2(\text{HCOO})]\cdot\text{H}_2\text{O}$

Atom	x	y	z	U(eq) [#]
Nd(1)	2685(1)	1192(1)	643(1)	21(1)
O(1)	4879(4)	409(2)	1806(4)	30(1)
O(2)	4164(4)	1866(2)	3027(4)	33(1)
O(3)	1476(4)	1745(2)	-1972(4)	30(1)
O(4)	1433(4)	2324(2)	1346(5)	38(1)
O(5)	4207(4)	2186(2)	-288(5)	32(1)
O(6)	1899(4)	-129(2)	-41(5)	33(1)
O(7)	-99(4)	960(2)	38(5)	31(1)
O(8)	5969(4)	-647(2)	1357(4)	32(1)
O(9)	2022(5)	627(3)	3077(5)	46(1)

C(1)	2036(6)	2690(3)	2536(6)	25(1)
C(2)	3621(6)	2430(3)	3512(6)	26(1)
C(3)	5249(6)	-70(3)	913(6)	23(1)
C(4)	574(6)	-313(3)	-27(6)	23(1)
C(5)	2723(8)	537(4)	4485(8)	49(2)
O(100)	-2705(6)	1904(3)	-208(7)	69(2)
N(10)	2946(10)	-100(4)	5197(7)	92(3)
C(11)	3087(15)	-752(7)	4168(17)	62(6)
C(11A)	1789(16)	-742(7)	4693(14)	52(6)
C(12)	1637(19)	-1187(8)	4248(15)	87(8)
C(12A)	2629(17)	-1205(7)	3663(20)	58(6)
N(11)	1659(7)	-1864(3)	3168(9)	67(2)
C(13)	1365(11)	-1259(5)	5976(10)	72(3)

Table A21. Atomic coordinates [$\times 10^4$] and equivalent isotropic displacement parameters [$\text{\AA}^2 \times 10^3$] for XIV, $[\text{OC}(\text{CH}_3)\text{NCH}_2\text{CH}(\text{CH}_3)\text{NH}_3][\text{Nd}(\text{C}_2\text{O}_4)_2]\cdot\text{H}_2\text{O}$

Atom	x	y	z	U(eq) [#]
Nd(1)	1614(1)	2283(1)	3498(1)	23(1)
O(1)	976(9)	1989(8)	795(7)	34(2)
O(2)	2039(8)	678(8)	4985(8)	33(2)
O(3)	3440(8)	4651(8)	3453(8)	35(2)
O(4)	-176(9)	3920(8)	3103(7)	35(2)
O(5)	4315(8)	3403(8)	5440(8)	34(2)
O(6)	1382(8)	4280(8)	5882(7)	32(2)
O(7)	3597(10)	1068(10)	2318(9)	49(2)
O(8)	-836(8)	1220(8)	4320(8)	33(2)
O(9)	-13(9)	-400(8)	1653(7)	35(2)
C(12)	286(12)	699(11)	-233(11)	27(2)
C(14)	-826(11)	164(10)	4807(10)	24(2)
C(13)	4749(11)	5356(11)	4420(11)	25(2)
C(11)	448(12)	5123(11)	5805(11)	28(2)
O(100)	808(11)	-6552(9)	-1680(8)	49(2)
N(2)	4789(34)	-3630(43)	654(34)	264(17)

C(3)	2187(14)	-4283(12)	1285(11)	31(2)
C(2)	3447(20)	-3045(18)	1298(14)	65(4)
C(1)	3754(19)	-1656(16)	2794(15)	58(4)
N(1)	5113(14)	-403(14)	3011(13)	67(3)
C(50)	4923(17)	917(17)	2740(17)	64(4)
C(2A)	3374(37)	-2869(36)	-145(34)	161(10)
C(51)	6277(39)	2325(35)	2797(52)	291(17)

Table A22. Atomic coordinates [$\times 10^4$] and equivalent isotropic displacement parameters [$\text{\AA}^2 \times 10^3$] for XV, $[(\text{CH}_3)_2\text{NH}(\text{CH}_2)_2\text{NH}(\text{CH}_3)_2][\text{Sn}_2(\text{C}_2\text{O}_4)_3] \cdot \text{H}_2\text{O}$

Atom	x	y	z	U(eq) [#]
Sn(1)	5941(1)	-6076(1)	-15(1)	33(1)
O(1)	6205(4)	-3441(5)	2910(5)	51(2)
O(2)	6551(3)	-8197(5)	-5(5)	39(1)
O(3)	6224(3)	-4276(5)	1167(5)	35(1)
O(4)	7285(3)	-5947(5)	276(5)	36(1)
O(5)	6187(4)	-6533(5)	2097(5)	45(2)
O(6)	6062(4)	-4273(5)	-1203(5)	42(2)
O(100)	5000	-1337(12)	2500	141(6)
C(10)	6199(5)	-4336(8)	2259(8)	35(2)
C(20)	6139(5)	-5647(8)	2749(8)	34(2)
C(30)	7284(5)	-8133(7)	-79(7)	29(2)
N(1)	3548(5)	-1912(8)	4837(8)	51(2)
C(1)	3345(7)	-1182(9)	3695(9)	74(3)
C(2)	4236(7)	-1327(9)	5714(11)	80(4)
C(3)	2816(5)	-2051(7)	5354(8)	41(2)

Table A23. Atomic coordinates [$\times 10^4$] and equivalent isotropic displacement parameters [$\text{\AA}^2 \times 10^3$] for XVI, $[\text{Cd}(\text{O}_2\text{C}-\text{CH}_2-\text{CO}_2)(\text{H}_2\text{O})] \cdot \text{H}_2\text{O}$

Atom	x	y	z	U(eq) [#]
Cd(1)	3998(1)	651(1)	8495(1)	25(1)
C(1)	4718(5)	2272(5)	9622(6)	21(2)

C(2)	3431(5)	-1068(5)	9312(7)	27(2)
C(3)	3100(6)	-2042(5)	9667(7)	29(2)
O(1)	5425(4)	1043(4)	7936(5)	31(1)
O(2)	3797(4)	764(4)	6690(5)	33(1)
O(3)	4750(4)	1593(4)	9929(4)	30(1)
O(4)	3504(4)	-880(4)	8331(4)	34(1)
O(10)	2523(4)	311(5)	8606(6)	32(1)
O(100)	1435(5)	-1290(6)	9555(6)	63(2)

Table A24. Atomic coordinates [$\times 10^4$] and equivalent isotropic displacement parameters [$\text{\AA}^2 \times 10^3$] for **XVII**, $[\text{Mn}(\text{O}_2\text{C}-(\text{CH}_2)_3-\text{CO}_2)]$

Atom	x	y	z	U(eq) [#]
Mn(1)	0	0	1387(1)	21(1)
Mn(2)	0	0	0	20(1)
Mn(3)	-1667	-3333	1667	22(1)
O(1)	-1398(1)	-1991(1)	1091(1)	27(1)
O(2)	299(1)	-1481(1)	1830(1)	28(1)
O(3)	-1709(1)	-1258(2)	431(1)	30(1)
O(4)	-622(2)	-4173(1)	1320(1)	39(1)
C(1)	-1875(2)	-2196(2)	687(1)	27(1)
C(2)	-621(2)	-5272(2)	1318(1)	29(1)
C(3)	-2739(3)	-3650(3)	523(1)	53(1)
C(4)	532(3)	-5295(3)	1068(1)	49(1)
C(5)	-4253(3)	-4115(3)	576(1)	69(1)

Table A25. Atomic coordinates [$\times 10^4$] and equivalent isotropic displacement parameters [$\text{\AA}^2 \times 10^3$] for **XVIII**, $[\text{CN}_3\text{H}_6]_2[\text{Cd}_2(\text{C}_4\text{H}_4\text{O}_4)(\text{Cl})_2]$

Atom	x	y	z	U(eq) [#]
Cd(1)	605(1)	6069(1)	2450(1)	35(1)
Cl(1)	-45(2)	4538(1)	1612(1)	50(1)
Cl(2)	3219(2)	6462(1)	1994(1)	58(1)
C(1)	-2090(6)	7181(4)	1785(4)	32(1)

C(2)	1387(6)	6299(4)	4751(5)	34(1)
C(3)	1727(7)	6282(3)	6012(5)	37(1)
C(4)	-3525(7)	7839(4)	1558(5)	34(1)
O(1)	1351(5)	5556(3)	4263(3)	43(1)
O(2)	-809(4)	7341(3)	1473(3)	47(1)
O(3)	-2212(4)	6476(2)	2323(3)	42(1)
O(4)	1120(5)	7018(2)	4219(3)	41(1)
C(10)	3555(7)	3547(4)	4957(5)	38(1)
C(20)	-100(7)	9158(4)	3865(5)	40(1)
N(1)	2812(7)	4026(3)	5539(4)	55(2)
N(2)	3293(7)	3685(4)	3875(4)	57(1)
N(3)	4570(6)	2888(3)	5439(4)	61(2)
N(4)	1428(6)	8950(3)	3934(5)	60(2)
N(5)	-674(7)	9967(3)	3578(4)	65(2)
N(6)	-1089(6)	8541(3)	4098(4)	51(1)

Table A26. Atomic coordinates [$\times 10^4$] and equivalent isotropic displacement parameters [$\text{\AA}^2 \times 10^3$] for XIX, $[\text{CN}_3\text{H}_6]_2[\text{Cd}(\text{C}_4\text{H}_4\text{O}_4)_2]$

Atom	x	y	z	U(eq) [#]
Cd(1)	1250	6250	1250	17(1)
O(1)	-847(2)	6155(1)	536(1)	27(1)
O(2)	-374(2)	5193(1)	1700(1)	29(1)
C(1)	-1163(2)	6846(1)	503(1)	22(1)
C(2)	-2543(3)	7093(1)	81(1)	28(1)
C(10)	-1250	3750	779(1)	26(1)
N(1)	-1250	3750	1312(1)	39(1)
N(2)	-769(3)	4352(1)	506(1)	38(1)

Table A27. Atomic coordinates [$\times 10^4$] and equivalent isotropic displacement parameters [$\text{\AA}^2 \times 10^3$] for XX, $\text{Cd}_2(\text{C}_4\text{H}_4\text{O}_4)_2(\text{C}_4\text{N}_2\text{H}_8)(\text{H}_2\text{O})_3$

Atom	x	y	z	U(eq) [#]
Cd(1)	2732(1)	9238(1)	1133(1)	22(1)

Cd(2)	1963(1)	5936(1)	1262(1)	21(1)
O(1)	5016(4)	8446(2)	1308(2)	30(1)
O(2)	1333(4)	10708(2)	787(2)	31(1)
O(3)	3812(4)	10935(2)	1383(3)	35(1)
O(100)	3011(6)	9294(3)	2631(3)	34(1)
O(200)	268(4)	8699(3)	973(3)	34(1)
O(4)	-236(4)	6777(2)	1080(2)	29(1)
O(5)	3268(4)	7342(2)	1280(2)	25(1)
O(6)	1630(4)	4281(2)	1126(3)	34(1)
O(7)	4044(4)	4701(2)	1409(3)	36(1)
O(300)	1409(5)	5961(3)	-272(3)	35(1)
O(8)	-1574(4)	5594(2)	1446(3)	44(1)
C(1)	2138(6)	2318(3)	1127(4)	31(1)
C(2)	2480(6)	1261(3)	1104(3)	23(1)
C(3)	3485(6)	3013(3)	1292(3)	30(1)
C(4)	4623(5)	7577(3)	1301(3)	21(1)
C(5)	-1420(5)	6449(3)	1265(3)	24(1)
C(6)	3028(7)	4060(3)	1261(3)	27(1)
C(7)	5806(5)	6807(3)	1311(4)	28(1)
C(8)	7352(6)	7197(4)	1277(4)	27(1)
N(1)	2208(5)	9141(3)	-427(3)	24(1)
C(50)	2916(6)	9920(3)	-818(3)	29(1)
C(60)	2518(7)	8214(4)	-808(3)	36(1)
N(2)	2669(5)	5992(3)	2794(3)	25(1)
C(70)	2011(6)	8206(3)	-1814(3)	34(1)
C(80)	2364(6)	5064(3)	3185(3)	28(1)

Table A28. Atomic coordinates [$\times 10^4$] and equivalent isotropic displacement parameters [$\text{\AA}^2 \times 10^3$] for XXI, $[\text{C}_4\text{N}_2\text{H}_{12}][\text{Cd}_2(\text{C}_4\text{H}_4\text{O}_4)_3] \cdot 4\text{H}_2\text{O}$

Atom	x	y	z	U(eq) ^a
Cd(1)	226(1)	3049(1)	1865(1)	28(1)
O(1)	1499(4)	5007(5)	276(4)	36(1)
O(2)	1343(5)	396(5)	1862(5)	40(1)

O(3)	-1415(5)	4138(6)	3507(5)	55(1)
O(4)	688(5)	2096(6)	4624(5)	45(1)
O(5)	-1246(5)	1060(5)	2068(5)	41(1)
O(6)	3405(4)	3009(5)	1843(5)	45(1)
C(1)	2979(6)	4401(7)	698(6)	25(1)
C(2)	30(7)	1(7)	2063(6)	33(1)
C(3)	-559(7)	3117(7)	4725(6)	30(1)
C(4)	4137(6)	5423(8)	-236(7)	28(1)
C(5)	36(8)	-1792(8)	2292(7)	36(1)
C(6)	-1107(7)	3166(7)	6311(7)	35(1)
N(1)	-4025(5)	637(6)	3666(6)	38(1)
C(10)	-4032(7)	1051(8)	5041(7)	39(1)
C(20)	-4382(7)	-1033(8)	4137(8)	42(1)
O(100)	4122(6)	-1187(7)	759(7)	69(2)
O(200)	-4572(6)	5739(7)	3419(7)	71(2)

Table A29. Atomic coordinates [$\times 10^4$] and equivalent isotropic displacement parameters [$\text{\AA}^2 \times 10^3$] for XXII, $\text{Cd}(\text{C}_4\text{H}_4\text{O}_4)(\text{H}_2\text{O})_2$

Atom	x	y	z	U(eq) [#]
Cd(1)	-95(1)	1969(1)	801(1)	23(1)
O(1)	-1949(4)	3034(2)	-1882(4)	28(1)
O(2)	-3069(4)	1350(2)	774(4)	31(1)
O(3)	1193(4)	3296(2)	-54(4)	37(1)
O(4)	-499(4)	485(2)	2206(4)	35(1)
O(100)	-20(6)	1292(2)	-2041(5)	37(1)
O(200)	-989(7)	2790(3)	3017(7)	56(1)
C(1)	-397(6)	3529(2)	-1399(5)	22(1)
C(2)	-2285(6)	699(2)	1863(5)	23(1)
C(3)	-540(6)	4401(3)	-2450(6)	25(1)
C(4)	-3533(6)	177(2)	2788(7)	26(1)

Table A30. Atomic coordinates [$\times 10^4$] and equivalent isotropic displacement parameters [$\text{\AA}^2 \times 10^3$] for XXIII, $\text{Cd}_3(\text{C}_4\text{H}_4\text{O}_4)_2(\text{OH})_2$

Atom	x	y	z	U(eq) [#]
Cd(1)	1642(1)	137(1)	4658(1)	16(1)
Cd(2)	5000	0	5000	16(1)
O(1)	2370(3)	693(4)	3428(2)	31(1)
O(2)	-449(3)	753(4)	4263(2)	25(1)
O(3)	3892(3)	2024(4)	4135(2)	24(1)
O(4)	4323(3)	1248(4)	6191(2)	32(1)
O(5)	3238(2)	-1767(4)	5131(2)	17(1)
C(1)	-801(3)	1972(6)	3745(2)	20(1)
C(2)	3399(4)	1526(6)	3475(3)	21(1)
C(3)	4097(4)	2039(7)	2737(2)	19(1)
C(4)	3566(4)	1182(7)	1990(3)	22(1)

Table A31. Atomic coordinates [$\times 10^4$] and equivalent isotropic displacement parameters [$\text{\AA}^2 \times 10^3$] for XXIV, $[\text{Na}_3\text{Cd}_5(\text{C}_4\text{H}_4\text{O}_4)_6\text{Cl}]$

Atom	x	y	z	U(eq) [#]
Cd(1)	1298(1)	8702(1)	8702(1)	26(1)
Cd(2)	7941(1)	7941(1)	7941(1)	25(1)
Na(1)	7941(1)	7941(1)	7941(1)	25(1)
Cl(1)	10000	10000	10000	22(1)
C(2)	1528(4)	10354(4)	5524(4)	26(1)
O(2)	1704(3)	8645(3)	6615(3)	38(1)
O(1)	1395(3)	10224(3)	7533(3)	33(1)
C(1)	1554(4)	9692(5)	6619(4)	26(1)

Table A32. Atomic coordinates [$\times 10^4$] and equivalent isotropic displacement parameters [$\text{\AA}^2 \times 10^3$] for XXV, $[\text{Na}_3\text{Cd}_5(\text{C}_4\text{H}_4\text{O}_4)_6\text{Br}]$

Atom	x	y	z	U(eq) [#]
Cd(1)	8691(1)	1308(1)	1308(1)	22(1)
Cd(2)	7057(2)	2943(2)	2943(2)	21(1)

Na(1)	7057(2)	2943(2)	2943(2)	21(1)
Br(1)	10000	0	0	59(2)
O(1)	10202(9)	1412(11)	2466(9)	26(3)
O(2)	8662(11)	1721(10)	3380(9)	33(3)
C(1)	9688(13)	1563(12)	3367(13)	20(3)
C(2)	10351(14)	1536(14)	4472(13)	24(4)

Table A33. Atomic coordinates [$\times 10^4$] and equivalent isotropic displacement parameters [$\text{\AA}^2 \times 10^3$] for XXVI, $[\text{Mn}(\text{O}_2\text{C}-(\text{CH}_2)_4-\text{CO}_2)(\text{C}_4\text{N}_2\text{H}_8)]$

Atom	x	y	z	U(eq) [#]
Mn(1)	3982(1)	3773(1)	1081(1)	28(1)
O(1)	3507(5)	5434(4)	476(7)	46(2)
O(2)	2347(5)	2908(5)	1896(6)	46(2)
O(3)	5814(5)	3019(4)	717(6)	36(1)
O(4)	3470(5)	3031(4)	-1207(6)	37(1)
C(1)	6609(7)	3544(6)	-89(9)	29(2)
C(2)	2434(7)	2159(6)	2978(9)	30(2)
C(3)	78(7)	2165(7)	3574(9)	36(2)
C(4)	1261(7)	1467(6)	3276(10)	35(2)
C(5)	-1064(7)	1434(6)	4022(10)	37(2)
C(6)	7755(7)	2872(6)	-635(10)	38(2)
N(1)	4684(6)	4250(5)	3617(7)	32(2)
C(10)	5871(8)	4953(7)	3756(10)	41(2)
C(20)	3675(8)	4833(7)	4522(9)	37(2)

Table A34. Atomic coordinates [$\times 10^4$] and equivalent isotropic displacement parameters [$\text{\AA}^2 \times 10^3$] for XXVII, $[\text{RbCl}][\text{Cd}_6(\text{C}_2\text{O}_4)_6] \cdot 2\text{H}_2\text{O}$

Atom	x	y	z	U(eq) [#]
Cd(1)	2567(1)	3862(1)	966(1)	15(1)
Rb(1)	0	0	0	18(1)
Cl(1)	3333	6667	1667	15(1)
O(1)	1121(7)	5001(7)	587(2)	19(1)

O(2)	3151(8)	3164(8)	96(2)	24(2)
O(3)	2194(8)	1212(8)	1048(2)	25(2)
O(4)	4191(8)	3795(7)	1697(2)	19(1)
C(1)	342(11)	4467(11)	136(4)	19(2)
C(2)	2770(11)	934(10)	1481(4)	15(2)
O(100)	6667	3333	767(20)	232(18)

Table A35. Atomic coordinates [$\times 10^4$] and equivalent isotropic displacement parameters [$\text{\AA}^2 \times 10^3$] for XXVIII, $[\text{RbBr}][\text{Cd}_6(\text{C}_2\text{O}_4)_6] \cdot 2\text{H}_2\text{O}$

Atom	x	y	z	U(eq) [#]
Cd(1)	2558(1)	3845(1)	962(1)	10(1)
Rb(1)	0	0	0	14(1)
Br(1)	3333	6667	1667	35(1)
C(1)	4444(12)	4143(12)	-135(4)	12(2)
C(2)	-920(12)	1822(13)	1479(4)	11(2)
O(1)	1110(9)	4999(9)	584(3)	14(2)
O(2)	3146(9)	3173(9)	94(3)	16(2)
O(3)	472(8)	2949(8)	1637(3)	13(2)
O(4)	2190(9)	1187(9)	1051(3)	17(2)
O(100)	6667	3333	762(20)	246(30)

Table A36. Atomic coordinates [$\times 10^4$] and equivalent isotropic displacement parameters [$\text{\AA}^2 \times 10^3$] for XXIX, $2[\text{CsBr}][\text{Cd}(\text{C}_2\text{O}_4)] \cdot \text{H}_2\text{O}$

Atom	x	y	z	U(eq) [#]
Cd(1)	8496(2)	871(1)	2500	21(1)
Cs(1)	6536(1)	3910(1)	3847(1)	32(1)
Br(1)	8483(2)	809(1)	896(1)	40(1)
C(1)	8168(20)	-1994(10)	2500	15(3)
C(2)	3271(21)	1789(12)	2500	23(3)
O(1)	7119(15)	-1053(8)	2500	28(2)
O(2)	5319(13)	1983(8)	2500	30(2)
O(3)	2291(15)	816(7)	2500	29(2)

O(4)	9807(13)	2882(8)	2500	29(2)
O(100)	2733(18)	2500	5000	93(5)

Table A37. Atomic coordinates [$\times 10^4$] and equivalent isotropic displacement parameters [$\text{\AA}^2 \times 10^3$] for XXX, $2[\text{CsBr}][\text{Cd}_2(\text{C}_2\text{O}_4)(\text{Br})_2] \cdot 2\text{H}_2\text{O}$

Atom	x	y	z	U(eq) [#]
Cd(1)	1243(1)	4005(1)	2500	28(1)
Cs(1)	3116(1)	3170(1)	2500	47(1)
Br(1)	1692(1)	1663(1)	2500	52(1)
Br(2)	3074(1)	0	0	33(1)
C(1)	0	3522(9)	1499(13)	22(2)
O(1)	468(2)	3522(5)	772(6)	32(1)
O(200)	4173(3)	1145(7)	2500	33(2)
O(100)	101(69)	118(72)	6151(186)	739(227)

Table A38. Atomic coordinates [$\times 10^4$] and equivalent isotropic displacement parameters [$\text{\AA}^2 \times 10^3$] for XXXI, $[\text{Rb}_2\text{Cd}(\text{Cl})(\text{NO}_3)(\text{C}_2\text{O}_4)(\text{H}_2\text{O})]$

Atom	x	y	z	U(eq) [#]
Cd(1)	692(1)	1568(1)	7410(1)	16(1)
Rb(1)	-1433(1)	-464(1)	6139(1)	27(1)
Rb(2)	3296(1)	-348(1)	6214(1)	30(1)
Cl(1)	823(1)	1452(2)	5826(1)	36(1)
C(1)	-1019(4)	3735(5)	7402(3)	15(1)
C(2)	3279(4)	2538(5)	7595(3)	15(1)
O(1)	1543(3)	-265(4)	7617(2)	22(1)
O(2)	2264(3)	2687(3)	7601(2)	21(1)
O(3)	-1223(3)	1507(3)	7433(2)	19(1)
O(4)	24(3)	3642(3)	7444(2)	22(1)
O(100)	470(3)	1550(4)	8894(2)	36(1)
N(1)	-1796(4)	2438(5)	4987(3)	28(1)
O(5)	-1385(4)	2128(4)	4305(3)	44(1)

O(6)	-1602(4)	3481(4)	5281(3)	47(1)
O(7)	-2428(3)	1703(4)	5368(3)	43(1)

Table A39. Atomic coordinates [$\times 10^4$] and equivalent isotropic displacement parameters [$\text{\AA}^2 \times 10^3$] for **XXXII**, $[\text{K}_2\text{Cd}_2(\text{C}_2\text{O}_4)_3] \cdot 2\text{KBr} \cdot 2\text{H}_2\text{O}$

Atom	x	y	z	U(eq) [#]
Cd(1)	-4245(1)	211(1)	7529(1)	17(1)
O(1)	-4741(3)	-333(3)	8905(2)	36(1)
O(2)	-2688(2)	1306(3)	7840(2)	31(1)
O(3)	-3463(2)	-1683(3)	7542(2)	22(1)
O(4)	-6165(3)	145(3)	7305(2)	25(1)
O(5)	-4926(2)	2255(3)	7521(2)	23(1)
O(6)	-4376(3)	1355(3)	9662(2)	42(1)
C(10)	-4734(4)	310(5)	9586(3)	22(1)
C(11)	-1664(3)	1155(4)	7715(3)	18(1)
C(12)	-5972(3)	2347(4)	7438(3)	16(1)
Br(1)	-3615(17)	390(10)	5821(9)	41(2)
Br(2)	-3812(17)	333(12)	5788(10)	49(3)
K(1)	-3349(1)	3247(1)	8857(1)	28(1)
K(2)	-1675(1)	-1728(1)	6313(1)	29(1)
O(100)	-1512(5)	2347(6)	9753(4)	72(2)

Table A40. Atomic coordinates [$\times 10^4$] and equivalent isotropic displacement parameters [$\text{\AA}^2 \times 10^3$] for **XXXIII**, $3[\text{RbCl}][\text{Cd}_2(\text{C}_2\text{O}_4)(\text{Cl}_2)] \cdot \text{H}_2\text{O}$

Atom	x	y	z	U(eq) [#]
Cd(1)	3176(1)	4425(1)	4647(1)	24(1)
Cd(2)	-62(1)	3703(1)	9969(1)	22(1)
Rb(1)	393(1)	3103(1)	5741(1)	33(1)
Rb(2)	4892(1)	2793(1)	2861(1)	36(1)
Rb(3)	4799(1)	4150(1)	9398(1)	36(1)
Cl(1)	4605(3)	3526(1)	6111(3)	30(1)
Cl(2)	1497(3)	3657(1)	2765(3)	35(1)

Cl(3)	4832(3)	5177(1)	6845(3)	33(1)
Cl(4)	-2435(3)	3006(1)	10294(3)	32(1)
Cl(5)	2212(3)	3009(1)	9392(3)	28(1)
C(1)	-902(11)	5002(4)	10186(10)	22(2)
C(2)	47(12)	5220(4)	4394(10)	23(2)
O(1)	1282(8)	5181(3)	3804(7)	30(2)
O(2)	1511(8)	4507(3)	9666(7)	28(2)
O(3)	-1605(8)	4528(3)	10268(7)	29(2)
O(4)	-1083(8)	5612(3)	4100(7)	29(2)
O(10)	-1496(8)	3782(3)	7500(7)	28(2)
O(100)	7572(10)	3677(4)	3508(9)	51(2)

Table A41. Atomic coordinates [$\times 10^4$] and equivalent isotropic displacement parameters [$\text{\AA}^2 \times 10^3$] for XXXIV, $\text{K}_2[\text{Mn}_2(\text{C}_2\text{O}_4)_3]2[\text{KCl}] \cdot 2\text{H}_2\text{O}$

Atom	x	y	z	U(eq) [#]
Mn(1)	4210(1)	246(1)	2528(1)	17(1)
K(1)	6706(1)	-1720(1)	3670(1)	27(1)
K(2)	3249(1)	3305(1)	3920(1)	29(1)
Cl(1)	3665(2)	411(1)	868(1)	44(1)
C(1)	4092(4)	-2658(4)	2555(3)	17(1)
C(2)	1608(4)	1120(5)	2722(3)	18(1)
C(3)	4713(5)	360(5)	4590(4)	23(1)
O(1)	4673(4)	-274(4)	3874(2)	35(1)
O(2)	2660(3)	1241(3)	2835(3)	28(1)
O(3)	3535(3)	-1656(3)	2521(2)	22(1)
O(4)	6064(3)	121(3)	2271(3)	26(1)
O(5)	4860(3)	2218(3)	2546(2)	21(1)
O(6)	4370(4)	1430(4)	4713(3)	35(1)
O(100)	1449(4)	2199(4)	4807(4)	58(1)

[#] U_{eq} is defined as one-third of the orthogonalized tensor U_{ij}